

This PDF was created from the British Library's microfilm copy of the original thesis. As such the images are greyscale and no colour was captured.

Due to the scanning process, an area greater than the page area is recorded and extraneous details can be captured.

This is the best available copy

D43422'82

Attention is drawn to the fact that the copyright of this thesis rests with its author.

This copy of the thesis has been supplied on condition that anyone who consults it is understood to recognise that its copyright rests with its author and that no quotation from the thesis and no information derived from it may be published without the author's prior written consent.

I

*

D 43422/82

SHAW L.S.

pp

487

Some double pages

Back

X-RAY CRYSTALLOGRAPHIC STUDIES ON THE SELF-CONDENSATION PRODUCTS
OF o-AMINOBENZALDEHYDE AND ANTHRANILIC ACID AND OF THE METAL
COMPLEXES OF SOME RELATED TETRA-AZAMACROCYCLES

A thesis submitted to the
Council for National Academic Awards
in partial fulfilment of the requirements for the degree of
Doctor of Philosophy

by

Leylâ Süheylâ Shaw (née Gözen)

The research described in this thesis was carried out in the Department
of Chemistry, The Polytechnic of North London

May 1982

ACKNOWLEDGEMENTS

The author is grateful to her supervisor, Dr. P. G. Owston, Head of the Department of Chemistry, The Polytechnic of North London, for his wise counsel, his unfailing courtesy in matters great and small, and for the excellent research facilities made available to her.

She wishes to thank Dr. M. McPartlin and Dr. K. Henrick for helping her to find her feet in crystallography. Some helpful discussions with Dr. P. A. Tasker are also acknowledged. She is grateful to the staff of the Computing Service for advice in the printing of her Thesis.

Above all, she wishes to acknowledge her deep indebtedness to her husband for his unfailing encouragement, understanding, and help, emotional, physical, intellectual, and scientific, during a demanding but challenging period of her life.

To

MY HUSBAND

STATEMENT

While registered as a candidate for the degree for which submission is made, the author has not been a registered candidate for another award of the CNA A or of a University. The results and conclusions presented in this thesis represent original work by the author, unless otherwise stated.

X-ray crystallographic studies on the self-condensation products of ortho-aminobenzaldehyde and anthranilic acid and of the metal complexes of some related tetra-azamacrocycles. Leylâ Süheylâ Shaw (née Gözen)

ABSTRACT

This Thesis describes X-ray crystallographic investigations on twelve compounds. The first three are the products of the acid condensation of ortho-aminobenzaldehyde, OAB, the so-called TAAB salts, based on the tetra-anhydro tetramer of OAB. Although known since 1926, their structures have remained controversial. Of the three salts, $\text{TAABH}_2(\text{X})_2$, investigated, that of $\text{X} = \text{picrate}$ was found to be ordered, whilst those of $\text{X} = \text{HSO}_4$ and BF_4 were disordered. The structure of the TAABH_2 cation is saddle-shaped and based on a fused heptacyclic framework. In all the three salts the anion appears to be doubly hydrogen bonded to the cation, through hydrogen donors NH and CH. The results enable a controversy in the literature regarding the structures of these compounds to be resolved.

The self-condensation products of anthranilic acid, AA, also somewhat controversial in nature, have been investigated. The formation of a trimeric, and minor yields of a tetrameric derivative, is confirmed. The crystal structures of the tetramer and of two solvates of the trimer (CHCl_3 and $\text{CH}_3\text{CN}\cdot\text{H}_2\text{O}$) were determined. These two compounds, also, have a fused heptacyclic double saddle-shape overall structure. Their structures are compared with those of the TAAB salts.

Related types of hydrogen bonding are surveyed, and the results found in this Thesis are put in a wider context.

The structure of the copper complex $\text{Cu}(\text{TAABH}_2)$ of the reduced TAAB derivative TAABH_4 , a 16-membered tetra-azamacrocyclic has been investigated. It, too, has an overall saddle-shape, but this is considerably flatter than those of the TAAB salts and AA derivatives.

Two metal complexes (CuII and FeIII) of a 14-membered tribenzotetra-azamacrocyclic were investigated. In the case of the iron compound, X-ray crystallography showed that an unexpected, novel oxygenation reaction of the ethylene bridge had taken place to give an α,β -diketo group. The purpose-made copper diketo-analogue was examined for comparative purposes. This derivative, in contrast to that based on TAABH_4 , has an almost square planar co-ordination around the copper atom. A compound, thought to have been the free parent ligand of these metal complexes, was also investigated. The data set was poor, but it could be shown that the compound was acyclic, contained an extra ortho-phenylene diamine residue, and was probably hydrogen bonded.

The crystal structures of two metal complexes based on CuII and FeIII of two dibrominated Schiff bases were investigated. The dibrominated copper salen derivative is monomeric, in contrast to the unbrominated compound, which is dimeric. The FeIII derivative, like the earlier-mentioned oxidised tetra-azamacrocyclic iron derivative, has a dimeric structure, with the iron atoms linked by a μ -oxo-bridge.

The structures of the three copper and two iron derivatives are discussed and compared.

Three themes emerge from the twelve structures described in this Thesis: (i) the structural importance of hydrogen bonding, (ii) the inadequacy of a single valence bond formulation to explain the observed X-ray crystallographic results, and the need to invoke resonance forms, mainly ortho-quinonoid, and (iii) the versatile role of nitrogen in organic and metal organic heterocyclic structures.

CONTENTS

CHAPTER 1. CHEMISTRY

1.1 Self-condensation Products of <u>o</u> -Aminobenzaldehyde and Anthranilic Acid.....	1
1.1.1 Self-condensation Products of <u>o</u> -Aminobenzaldehyde.....	1
1.1.2 Self-condensation Products of Anthranilic Acid.....	9
1.2 Metal Complexes of Tetra-azamacrocycles and of Schiff Bases.....	12
1.2.1 Reduction Products of TAAB and Derivatives.....	12
1.2.2 Summary of Metal Complexes of TAAB and its Reduction Products with Co-ordination Number 4.....	14
1.2.3 Summary of Metal Complexes of TAAB and its Reduction Products with Co-ordination Number greater than 4.....	19
1.2.4 Metal Complexes of 14-Membered Tetra-azamacrocycles and of Schiff Bases.....	21
1.3 Hydrogen Bonding.....	27
References.....	44

CHAPTER 2. CRYSTALLOGRAPHY

2.1 Theory.....	51
2.1.1 Introduction.....	51
2.1.2 X-ray Diffraction from Crystals.....	53
2.1.3 Determination of Cell Parameters.....	57
2.1.4 Data collection.....	58
2.1.5 Structure Solution.....	61
2.1.6 Electron Density Synthesis and the Determination of Phases.....	67

2.2 Technique.....	76
References.....	82

CHAPTER 3. STRUCTURAL INVESTIGATIONS OF TAAB SALTS

3.1 Methods of Preparation.....	83
3.2 Data Collection and Structure Determinations of TAAB salts.....	84
3.2.1 Data Collection and Structure Solution of TAABH ₂ (PICRATE) ₂	84
3.2.2 Data Collection and Structure Solution of TAABH ₂ (HSO ₄) ₂	88
3.2.3 Data Collection and Structure Solution of TAABH ₂ (BF ₄) ₂	93
3.3 Discussion of TAAB Salts.....	95
3.3.1 TAABH ₂ (PICRATE) ₂	96
3.3.2 TAABH ₂ (HSO ₄) ₂	115
3.3.3 TAABH ₂ (BF ₄) ₂	132
3.4 A Comparison of the Structures of the TAAB Salts (PICRATE, HSO ₄ , and BF ₄).....	149
References.....	156

CHAPTER 4. STRUCTURAL INVESTIGATIONS OF THE SELF-CONDENSATION

PRODUCTS OF ANTHRANILIC ACID

4.1 Method of Preparation.....	160
4.2 Data Collection and Structure Solution of Anthranilic Acid (AA) Derivatives.....	161

4.2.1 Data Collection and Structure Solution of AA TETRAMER.....	161
4.2.2 Data Collection and Structure Solution of AA TRIMER. CHCl ₃	165
4.2.3 Data Collection and Structure Solution of AA TRIMER. CH ₃ CN.H ₂ O.....	166
4.3 Discussion of AA Derivatives.....	169
4.3.1 AA TETRAMER.....	169
4.3.2 AA TRIMER.CHCl ₃	178
4.3.3 AA TRIMER.CH ₃ CN.H ₂ O.....	187
4.4 Comparison of AA Structures.....	195
4.5 Comparison of AA Derivatives with TAABH ₂ (PICRATE) ₂	197
References.....	204
 CHAPTER 5. STRUCTURAL INVESTIGATIONS OF Cu(TAABH ₂)	
5.1 Method of Preparation.....	205
5.2 Data Collection and Structure Solution.....	205
5.3 Discussion of Cu(TAABH ₂).....	210
5.3.1 Description of Cu(TAABH ₂).....	210
5.3.2 Comparison of the Structure of the Copper and Related TAABH ₄ Derivatives.....	221
References.....	231
 CHAPTER 6. STRUCTURAL INVESTIGATIONS OF METAL COMPLEXES OF LIGAND OXIDISED TETRA-AZAMACROCYCLES	
6.1 Method of Preparation.....	232
6.2 Data Collection and Structure Solution of Metal Complexes of Ligand Oxidised Tetra-azamacrocycles.....	233

6.2.1 Data Collection and Structure Solution of FeDIKETO....	233
6.2.2 Data Collection and Structure Solution of CuDIKETO....	242
6.2.3 Data Collection and Structure Solution of FREE LIGAND.	245
6.3 Discussion.....	247
6.3.1 FeDIKETO.....	247
6.3.2 CuDIKETO.....	257
6.3.3 FREE LIGAND.....	266
6.3.4 Comparison between Metal Complexes of Ligand Oxidised Tetra-azamacrocycles.....	268
References.....	277

CHAPTER 7. STRUCTURAL INVESTIGATIONS OF METAL COMPLEXES OF
DIBROMINATED SCHIFF BASES

7.1 Methods of Preparation.....	278
7.2 Data Collection and Structure Solution of Copper and Iron Complexes of Dibrominated Schiff Bases.....	278
7.2.1 Data Collection and Structure Solution of Cu(DIBrSALEN)	278
7.2.2 Data Collection and Structure Solution of Fe(DIBrSALOF)	288
7.3 Description of Structures.....	298
7.3.1 Cu(DIBrSALEN).....	298
7.3.2 Fe(DIBrSALOF).....	306
References.....	322

CHAPTER 8. A COMPARISON OF THE METAL COMPLEXES DESCRIBED

IN THIS THESIS.....	323
References.....	337

CHAPTER 9. SUMMARY, CONCLUSIONS AND SCOPE FOR FUTURE WORK.....	338
References.....	345
APPENDIX 1: FRACTIONAL ATOMIC CO-ORDINATES, TEMPERATURE FACTORS, AND INTRA- AND INTER-MOLECULAR DISTANCES FOR TAAB SALTS.....	
APPENDIX 2: FRACTIONAL ATOMIC CO-ORDINATES, TEMPERATURE FACTORS, AND INTRA- AND INTER-MOLECULAR DISTANCES FOR AA DERIVATIVES.....	
APPENDIX 3: FRACTIONAL ATOMIC CO-ORDINATES, TEMPERATURE FACTORS, AND INTRA- AND INTER-MOLECULAR DISTANCES FOR Cu(TAABH ₂).....	
APPENDIX 4: FRACTIONAL ATOMIC CO-ORDINATES, TEMPERATURE FACTORS, AND INTRA- AND INTER-MOLECULAR DISTANCES FOR FeDIKETO and CuDIKETO.....	
APPENDIX 5: FRACTIONAL ATOMIC CO-ORDINATES, TEMPERATURE FACTORS, AND INTRA- AND INTER-MOLECULAR DISTANCES FOR Cu(DIBrSALEN) and Fe(DIBrSALOF).....	
SUPPLEMENTARY MATERIAL.....	

CHAPTER 1

CHEMISTRY

1.1 SELF-CONDENSATION PRODUCTS OF o-AMINOBENZALDEHYDE AND ANTHRANILIC

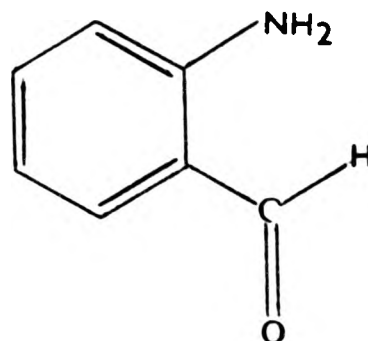
ACID

1.1.1 SELF-CONDENSATION PRODUCTS OF o-AMINOBENZALDEHYDE

Tetra-azamacrocycles and their metal complexes, naturally occurring (the prosthetic groups in haemoglobin, chlorophyll and vitamin B₁₂ are based on such structures) and synthetic derivatives, have aroused considerable interest for a number of years. One aspect of these studies is the use of metal ions as templates for the formation of macrocycles from acyclic precursors. In particular, the self-condensation of o-aminobenzaldehyde, OAB, in the presence of metal ions has received considerable attention. This reaction was first reported by Pfeiffer et al.¹ Subsequently, in 1954, Eichhorn and Latif² reported the same type of reaction, but omitted ammonia from the reaction mixture. More recently Busch and his co-workers³⁻⁵ have investigated these reactions in considerable detail by using different metal ions. Metal complexes based on trimeric and tetrameric derivatives of OAB were isolated and some of these have been characterized, relatively recently, by X-ray crystallography.⁶⁻⁸ The

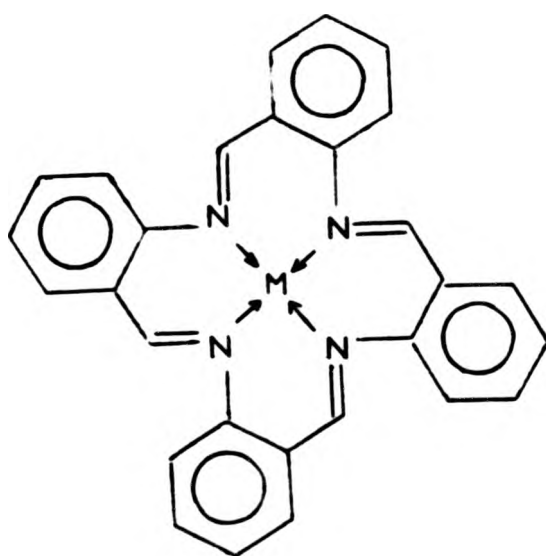
self-condensation of OAB under acidic conditions was first investigated in the 1920's by Seidel⁹ and by Bamberger.¹⁰ Despite these extensive studies, the structures of the acid condensation products have remained controversial.

Part of this Thesis will deal with the structures of the acid condensation products of OAB and of some related metal complexes. A review of the current knowledge of these products will be given here.

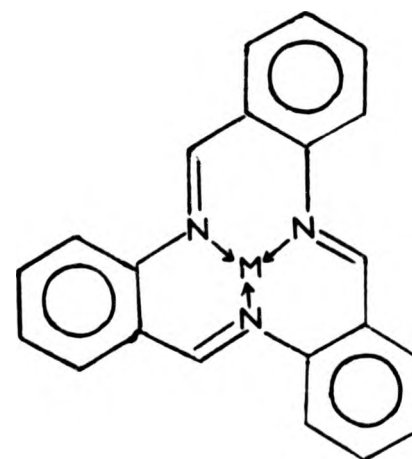


(1)

The condensation of OAB (1) in the presence of metal ions [e.g. Ni(II), Cu(II)] gives rise to metal complexes of two different types (2,3).

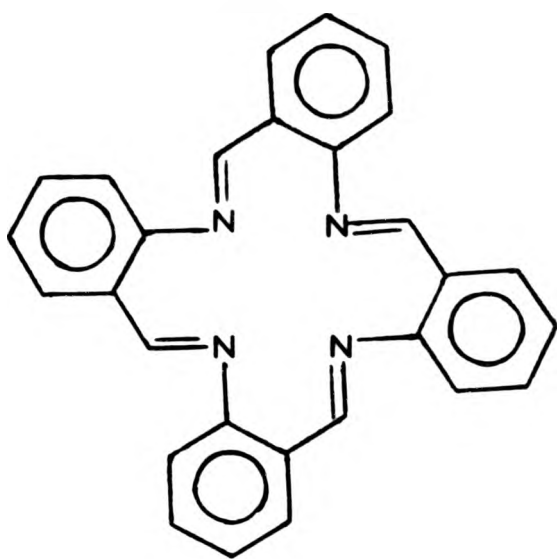


(2)

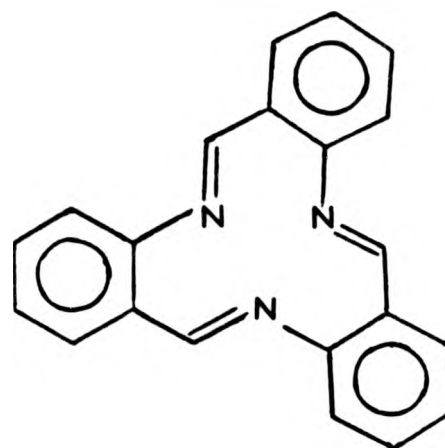


(3)

These are based on the tetra-anhydro tetramer of the starting compound, where the ligand is usually designated TAAB (4), and those based on the tri-anhydro trimer, where the macrocycle is conventionally called TRI (5).



(4)



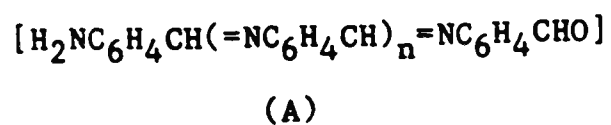
(5)

The free macrocycles TAAB (4) and TRI (5) from which these metal complexes are derived have not yet been isolated.

By contrast, the isolation of species whose analytical values indicated that the elements of one molecule of water had been added to TAAB and TRI, were reported as early as 1926 by Seidel. These species have been referred to as TAAB, H₂O and TRI, H₂O or alternatively as tri-anhydro tetramer and di-anhydro trimer of OAB. Both types of names will be used in this Thesis. Throughout the discussion the term TAAB, H₂O or hydrate etc. refers to composition and is without prejudice regarding to the real nature of the structure.

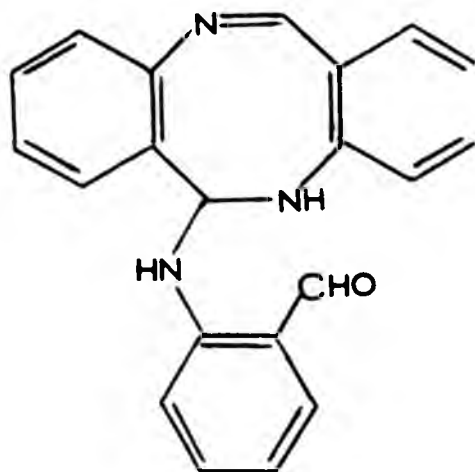
According to Seidel⁹ the di-anhydro trimer is prepared by weakly acidifying an aqueous solution of OAB from which it precipitates in a

crystalline form. This product was characterized as (A) ($n = 1$) by chemical evidence and elemental analysis.



The second self-condensation product, the tri-anhydro tetramer was also prepared by Seidel,⁹ by the action of 50% sulphuric or hydrochloric acid on OAB, as red crystalline salts. Tri-anhydro tetramer was liberated by treatment of the red salts with water. Seidel initially formulated this product as (A) ($n = 2$).

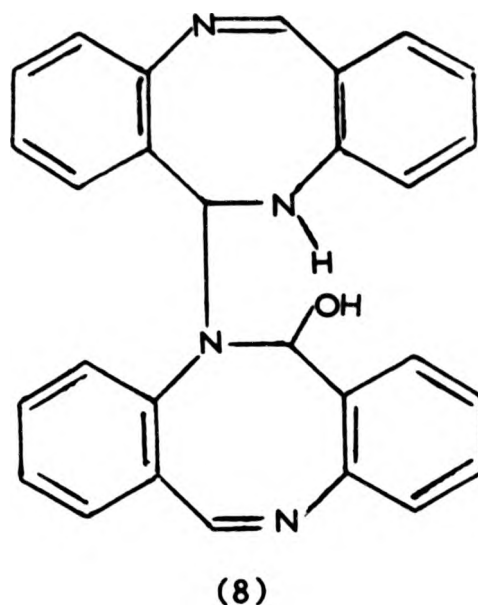
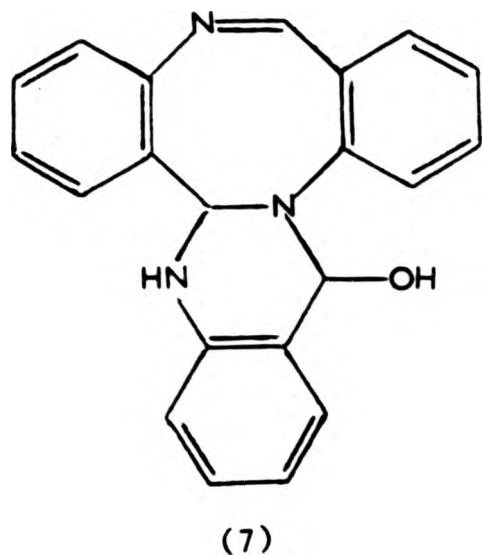
Bamberger¹⁰ first suggested structure (6) for the di-anhydro trimer, [cf. (A) ($n = 1$) of Seidel] based on the molecular weight (measured ebullioscopically in pyridine) and elemental analysis. As Bamberger himself admitted in the paper, he had no experimental evidence for this structure and just liked to speculate.



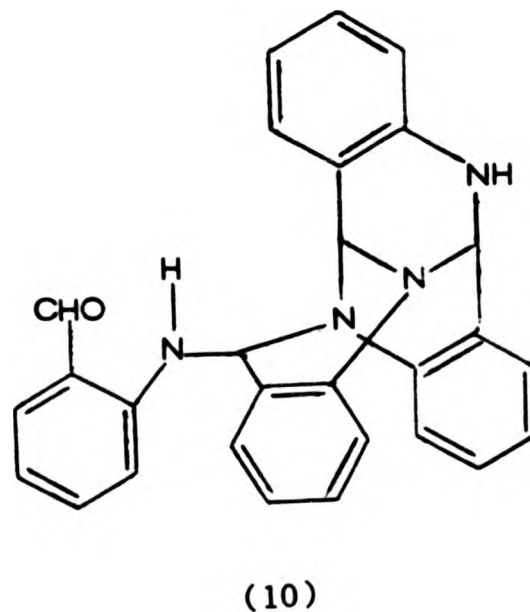
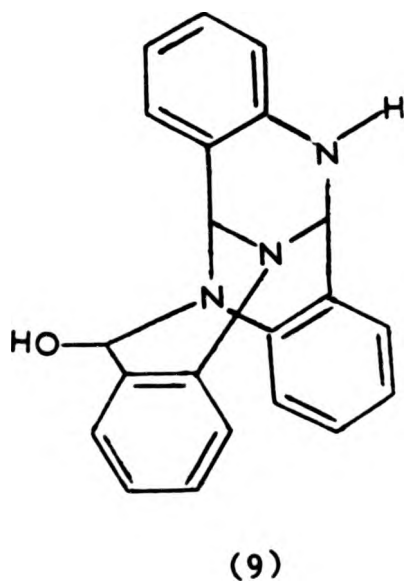
(6)

Subsequently Seidel¹¹ amended the structure (A) (based on characterisation of further derivatives) of the di-anhydro trimer $n = 1$

and the tri-anhydro tetramer $n = 2$ to (7) and (8) respectively.

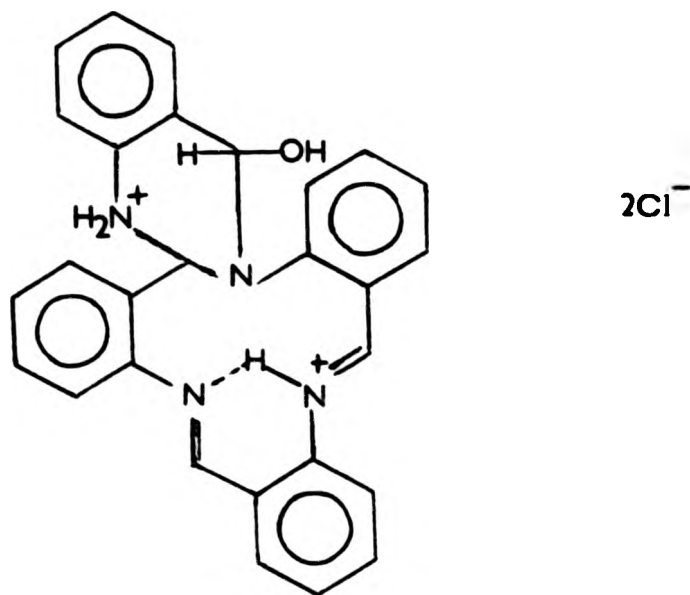


McGeachin¹² in 1966 repeated the two reactions using Seidel's procedures and assigned new structures (9) and (10) to the two products. He based his evidence on infrared, ultraviolet and ¹H N.M.R. spectroscopy, as well as the preparation and characterization of derivatives. In particular, he observed NH and OH groups in the infrared spectrum of compound (9) and by the same technique two NH and a carbonyl band for compound (10).



Albert and Yamamoto¹³ independently repeated Seidel's work and came to the same conclusion as McGeachin. The red tetramer hydrochloride,

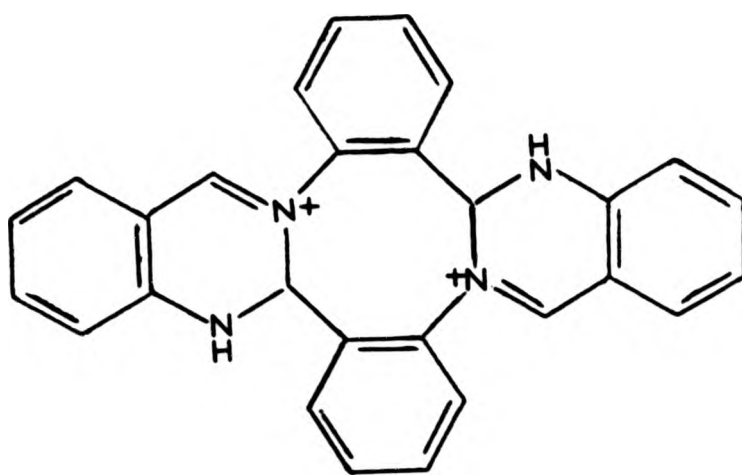
obtained as an intermediate in the preparation of the tetramer had been isolated by Seidel, who, however, had not proposed a structure for it. Albert and Yamamoto assigned structure (11) to this $\text{TAAB} \cdot \text{H}_2\text{O}(\text{HCl})_2$. The formulation was based on elemental analysis and the structural proposal was derived from a combination of infrared, ultraviolet and ^1H N.M.R. evidence. The infrared spectrum indicated either the presence of $-\text{OH}$ or water. Based on its elemental composition, it can be called a $\text{TAAB} \cdot \text{H}_2\text{O}$ salt without prejudice to its actual structure.



(11)

Whilst $\text{TAAB} \cdot \text{H}_2\text{O}$ and $\text{TRI} \cdot \text{H}_2\text{O}$ are structurally related, as indeed are TAAB and TRI , there are clearly very significant structural differences between the anhydrous and the hydrated derivatives.

In 1977 Busch and co-workers¹⁴ prepared a series of salts, $\text{TAABH}_2(\text{X})_2$ ($\text{X} = \text{BF}_4, \text{ClO}_4, \text{CF}_3\text{SO}_3, \text{HSO}_4$) which could be described as anhydrous TAAB salts. Based on infrared spectroscopy, by which NH and $\text{C}=\text{N}$ vibrations were observed, structure (12) was proposed for the TAABH_2 cation.

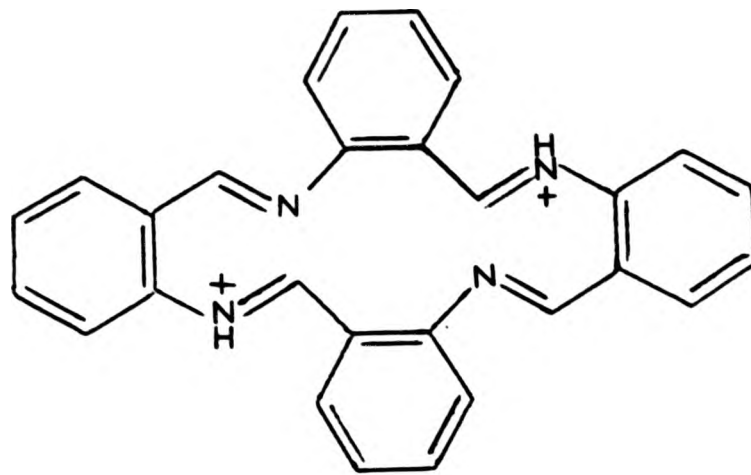


(12)

In this paper,¹⁴ reference was made to an unpublished X-ray crystallographic study of the trifluoromethylsulfonate salt ($X = CF_3SO_3$). Disorder problems prevented these authors from reaching a definite conclusion about the bond orders within the structure. The general outline, however, agreed with the structure proposed. These workers also obtained the hydrated salts, $TAABH_2(Br)_2(H_2O)$ and $TAABH_2(Cl)_2(H_2O)_2$. With the second hydrated salt, they first obtained $TAAB(HCl)_{2.5}(H_2O)_{3.5}$. When this sample was ground and heated to 130-135 °C in vacuo, it analysed for $TAABH_2(Cl)_2(H_2O)_2$. This hydrated salt was similar to the one reported by Albert and Yamamoto¹³, $TAABH_2(Cl)_2(H_2O)$, (11) (obtained by heating at 150 °C/0.01 mm for one hour). (11) Busch and co-workers¹⁴, however, preferred to consider it to have a structure analogous to that of the anhydrous salt (12), the water being present as lattice water and not as an alcoholic hydroxyl group as suggested by Albert and Yamamoto.¹³

Subsequently to Busch's work, Goddard and Norris¹⁵ carried out the condensation of OAB in acetic acid in the presence of boron trifluoride diethyl etherate and obtained a red salt, $TAABH_2(BF_4)_2$, which they stated to be identical (elemental analysis, infrared, and mass spectra) to the one isolated by Busch, (12), but they preferred the valence bond

isomeric structure (13) without, however, giving any evidence for this point of view.



(13)

In view of the variety of structures which had been proposed for apparently related compounds accurate structural data was essential.

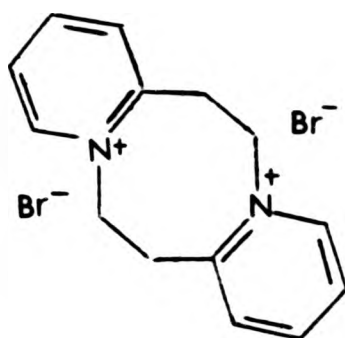
The present knowledge of TAAB and its derivatives is summarised in Table 1.1.

Table 1.1: Summary of the present knowledge on TAAB derivatives

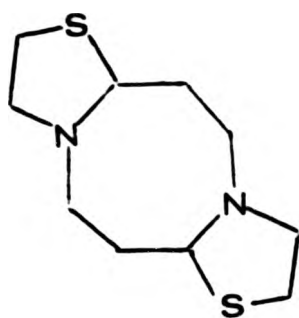
Formula	Compound	Structure proposed	Evidence for structure
$C_{28}H_{20}N_4$	TAAB	4	Never isolated or observed
$C_{28}H_{22}N_4O$	TAAB.H ₂ O	10	Spectroscopic (U.V., I.R., ¹ H N.M.R.)
$C_{28}H_{24}N_4OC_2$	TAAB.H ₂ O.2HCl	11	Spectroscopic (U.V.)
$C_{28}H_{20}N_4M$	TAABM	2	X-ray crystallographic
$C_{28}H_{22}N_4X_2$	TAAB.2HX	12,13	Spectroscopic (U.V., I.R., ¹ H N.M.R.) (Two valence bond isomeric structures proposed)

1.1.2 SELF-CONDENSATION PRODUCTS OF ANTHRANILIC ACID

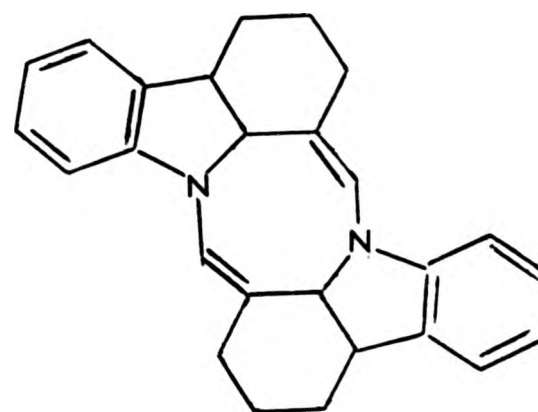
The valence bond isomeric structure preferred by Busch¹⁴ (12) contains an inner eight-membered heterocyclic ring with nitrogen atoms in the 1,5-positions. Katritzky and co-workers¹⁶ have summarised compounds of this type, where these two nitrogen atoms are additionally part of other heterocyclic rings fused to the central one. The number of such systems is small. They are given below: (14)-(18).



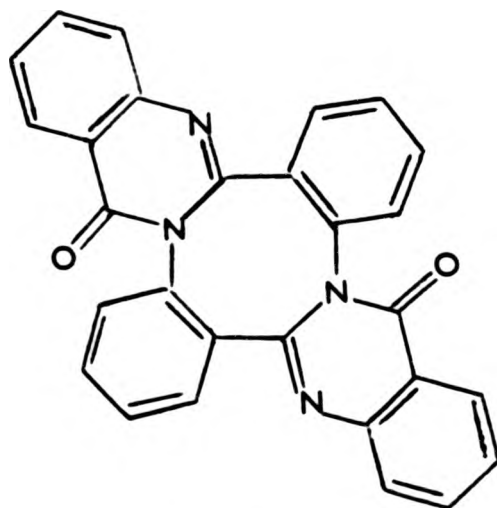
(14)



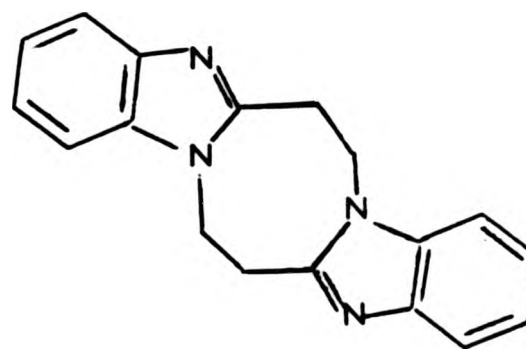
(15)



(16)



(17)



(18)

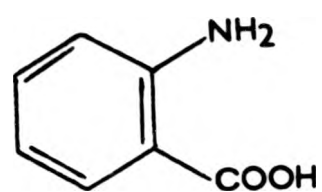
These authors reported the synthesis and X-ray crystallographic structure determination of (18), which revealed that the inner eight-membered heterocyclic ring adopted a chair conformation.

One of the systems discussed by Katritzky was the tetrameric

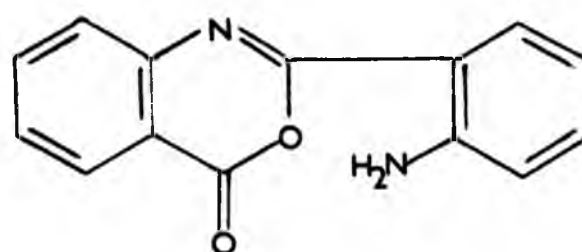
self-condensation product (17) of anthranilic acid, AA, (19), reported by Chatterjee and Ganguly.¹⁷ The structures proposed for these compounds seem to be closely related to the valence bond isomeric form of the TAAB salts preferred by Busch: (12). A comparison between these two structures seemed therefore to be desirable, particularly as in the AA product, (17), valence bond isomerisation to give a structure analogous to (13) is not possible. The literature on the self-condensation of AA is, however, not clear. Whilst condensation reactions of AA with other compounds have been widely studied,^{17,19} the self-condensation of this acid was reported for the first time in 1967 by Kurihara.¹⁸ This worker used polyphosphoric acid as a condensing agent. The major product of the reaction was the dimeric species (20) in 59% yield. Later work by Chatterjee and Ganguly¹⁷ reported the isolation of the trimeric species (21) in 74% yield, with only about a 3% yield of the tetrameric derivative (17). However, somewhat different conditions were used with phosphorus pentoxide as the condensing agent.

(The AA tetramer is, strictly speaking, a hexa-anhydro tetramer, the trimer a tetra-anhydro trimer and the dimer a di-anhydro dimer. For convenience the abbreviated forms AA TETRAMER, AA TRIMER and AA DIMER will be used throughout this Thesis).

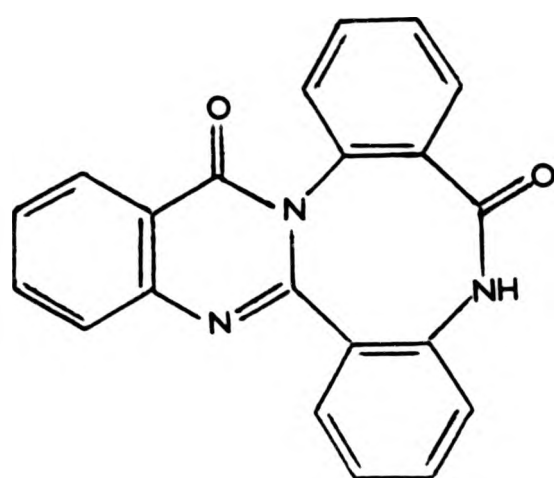
In 1977 Rhee and White,¹⁹ using yet again different conditions, with N,N'-dicyclohexylcarbodi-imide as the condensing agent, again isolated only the dimeric product (20), and in a foot-note to their paper they appeared to cast doubt on Chatterjee's and Ganguly's work. Hence, the self-condensation of AA appeared worthy of re-investigation if the AA TETRAMER (17) was to be used as a model to assist the interpretation of



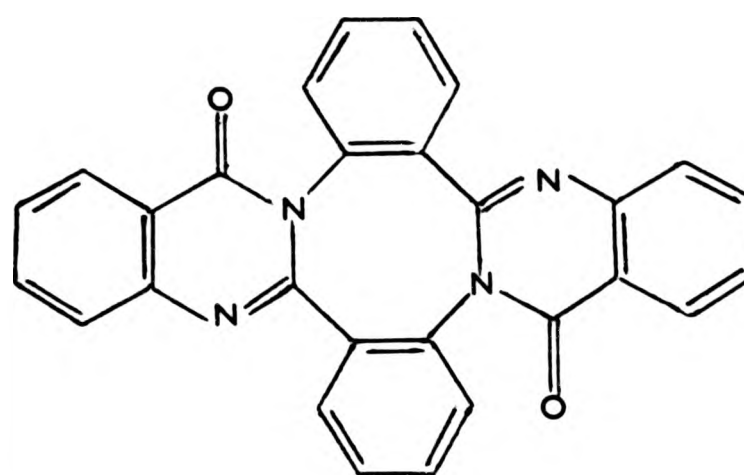
(19)



(20)



(21)



(17)

the structure of the TAAB salt (12).

The trimeric and tetrameric products as formulated by Chatterjee and Ganguly (elemental analysis, U.V., I.R., ^1H N.M.R. and mass spectra) both had structures similar to those proposed by Busch for the TAAB salts (12). The tetramer, (17), in particular, was suggested to have an almost identical heptacyclic frame-work.

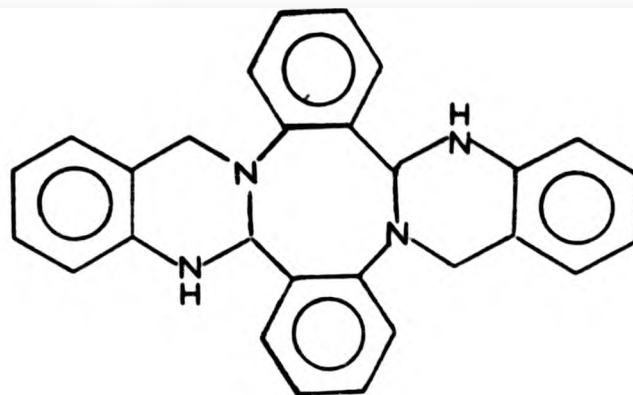
1.2 METAL COMPLEXES OF TETRA-AZAMACROCYCLES AND OF SCHIFF BASES

1.2.1 REDUCTION PRODUCTS OF TAAB AND DERIVATIVES

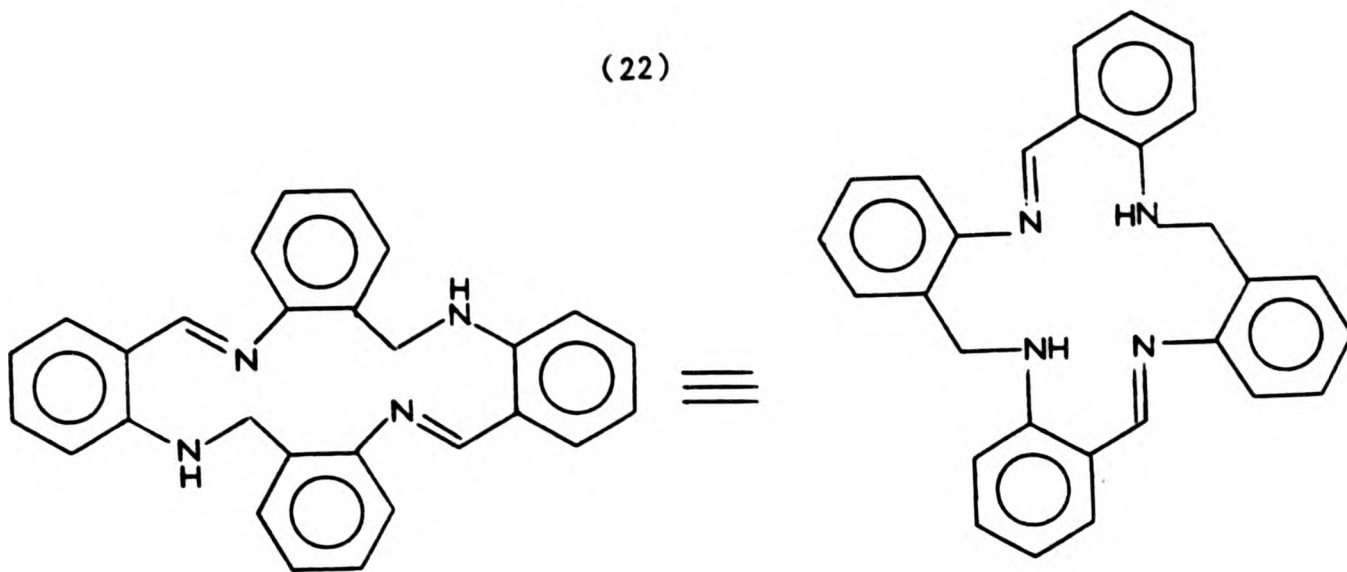
From the preceding discussion it can be seen that OAB and AA undergo condensation reactions to give products for which a range of diverse structures have been proposed.

Busch and co-workers¹⁴ reduced the $\text{TAABH}_2(\text{BF}_4)_2$ salt with sodium borohydride to yield a crystalline yellow compound, TAABH_4 . This yellow product, on repeated recrystallisation from hot acetonitrile, gave a colourless isomer. The two compounds were found from chemical analysis to be isomers of $\text{C}_{28}\text{H}_{24}\text{N}_4$ each giving the same molecular ion in their mass-spectra ($m/e = 416$). Based on a study of the ultra-violet, infra-red, and ^1H N.M.R. spectra of the yellow, and the infra-red and ^1H N.M.R. spectra of the colourless isomer, structures (23) and (22), were proposed respectively.

Goddard and Norris¹⁵ were only able to isolate the yellow isomer (23) from this reaction. However, they isolated the colourless isomer (22) by catalytic hydrogenation of the $\text{TAABH}_2(\text{BF}_4)_2$ salt (ethanol/dimethylformamide solution, PtO_2 on charcoal, 50°C , 60 psi hydrogen pressure). The evidence cited for the structure of the two isomers appears to be reasonable. However, neither of these two groups of workers reported melting points and hence this criterion of purity is lacking. Goddard and Norris also found that the yellow isomer (23) was not reduced under conditions of catalytic hydrogenation (THF solution, PtO_2 on charcoal, 50°C , 1500 psi hydrogen pressure). Busch and his co-workers¹⁴, however, successfully reduced the isomer (23) by treatment



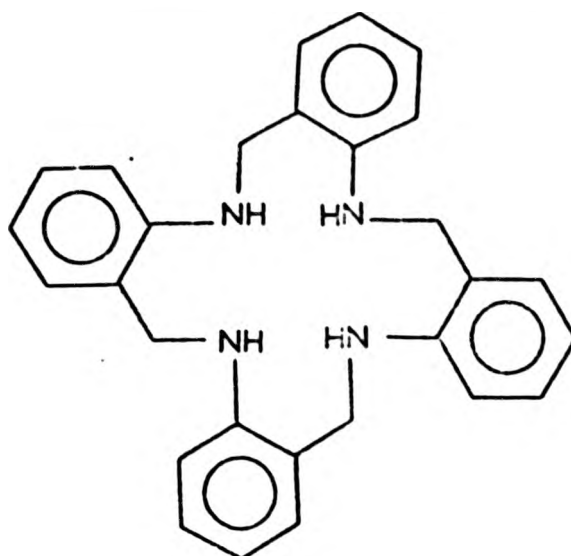
(22)



(23)

with lithium aluminium hydride to TAABH_8 (24). The fully saturated compound (24) was shown to give a nickel complex with an infra-red spectrum identical to that of a sample prepared by catalytic reduction of $\text{TAABH}_2(\text{BF}_4)_2$ in methanol (PtO_2 catalyst, 60 psi hydrogen pressure). Based on infra-red and mass spectra they proposed structure (24) for TAABH_8 ; again no melting point was reported.

Busch and his co-workers prepared several metal complexes of TAAB and of its reduction products. These are listed below.

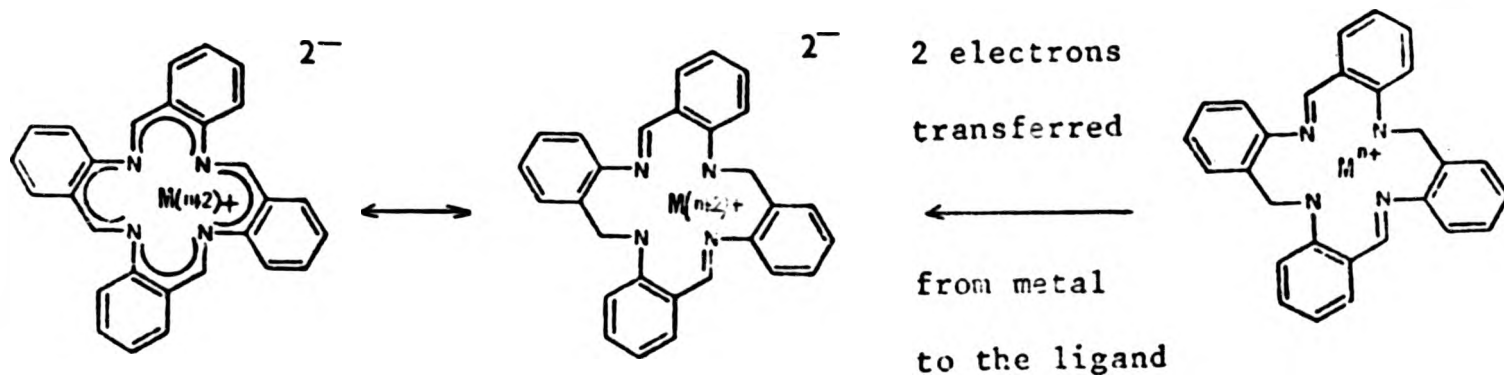
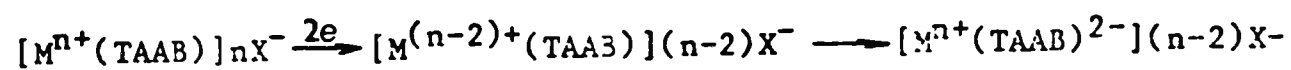


(24)

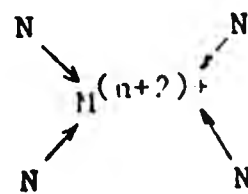
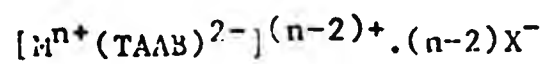
1.2.2 SUMMARY OF METAL COMPLEXES OF TAAB AND ITS REDUCTION

PRODUCTS WITH CO-ORDINATION NUMBER 4

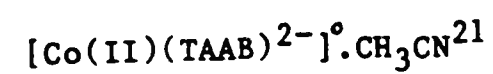
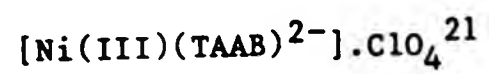
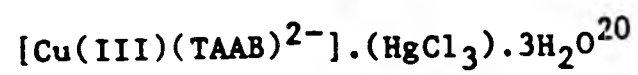
The compounds have been classified using as criterion the number of π -electrons in the inner great ring.

1) 18 π -electrons

Structure possible in principle:

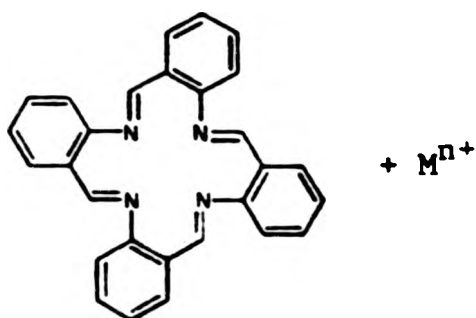


Examples:



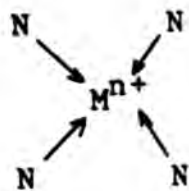
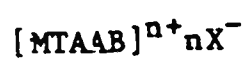
No X-ray crystallographic investigations have been reported for the above class of compounds.

2) 16 π -electrons

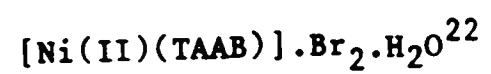
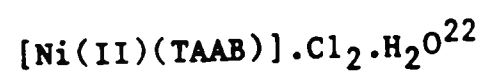
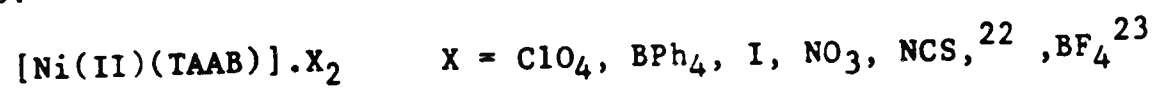


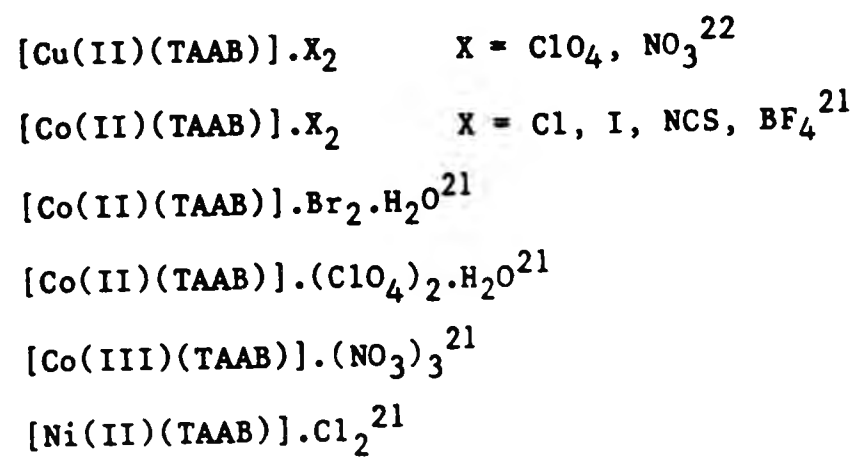
TAAB (4 imine bonds)

Structure possible in principle



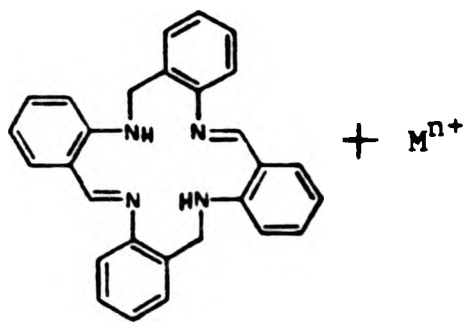
Examples:





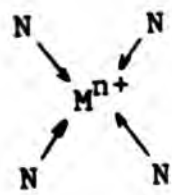
An X-ray crystal structure determination for $[\text{Ni(II)(TAAB)}](\text{BF}_4)_2$ has been reported, (25).⁶

3) 12 π -electrons

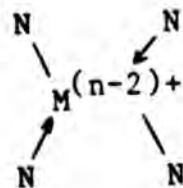


TAABH₄ (2 imine bonds)

Structures possible in principle



No example reported.

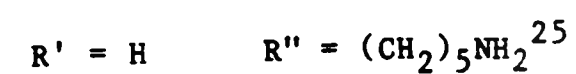
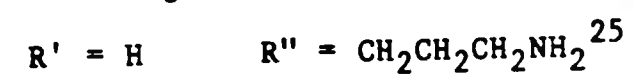
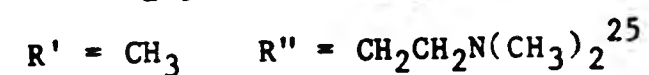
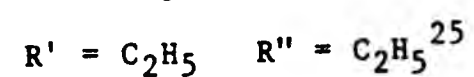
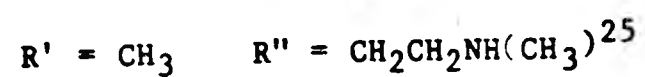
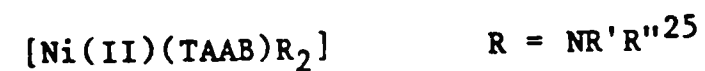
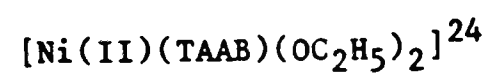
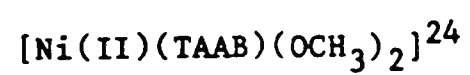
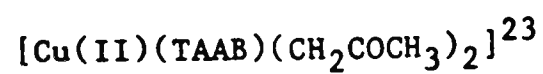
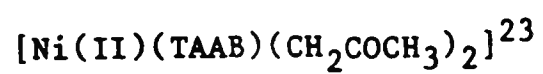


No example previously reported.



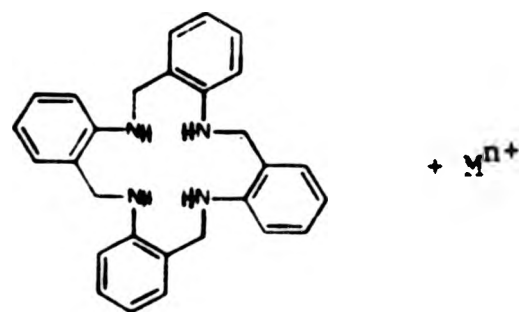
When one hydrogen on each of the two saturated carbon atoms in (b) is replaced by R groups

Examples:



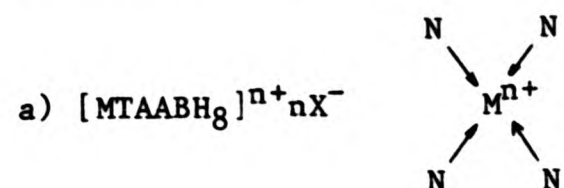
An X-ray crystal structure determination of the compound $[Ni(II)(TAAB)(CH_2COCH_3)_2]$ (26) has been reported.²³

4) 8 π -electron system

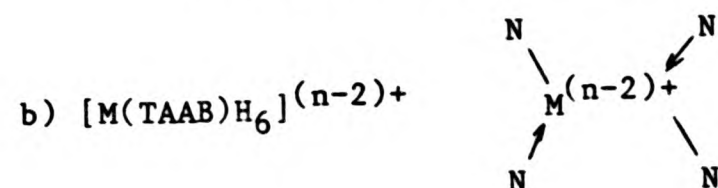
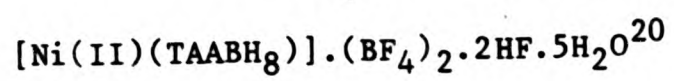
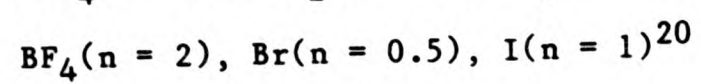
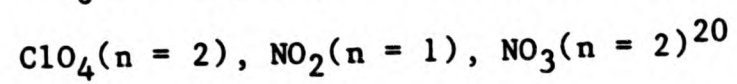
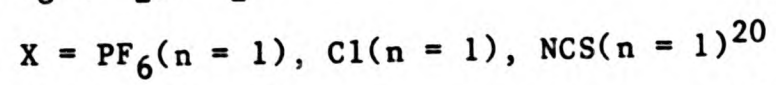
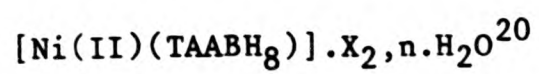


TAABH₈ (no imine bonds)

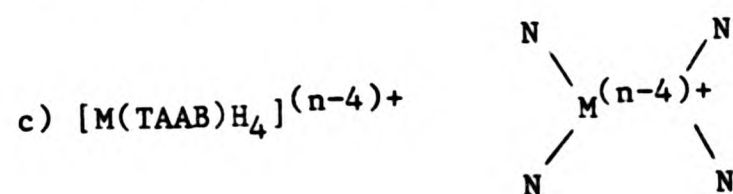
Structures possible in principle:



Examples:



No example reported.



No example reported.

No X-ray crystallographic investigations have been reported for the above class of compounds.

1.2.3 SUMMARY OF METAL COMPLEXES OF TAAB AND ITS REDUCTION PRODUCTS

WITH CO-ORDINATION NUMBER GREATER THAN 4

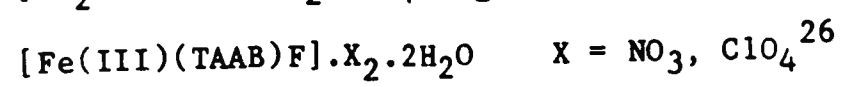
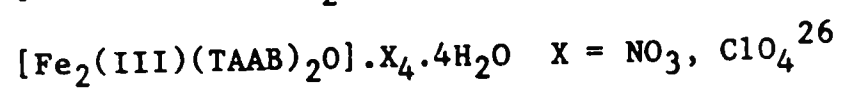
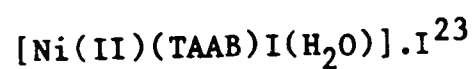
1) 16 π -electrons

4 imine bonds

Y or X = univalent anion or equivalent

Z = neutral ligand

Examples:



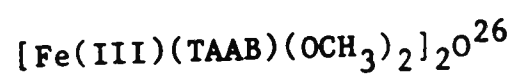
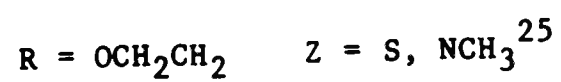
An X-ray structure determination of $[\text{Ni(II)(TAAB)I(H}_2\text{O)}] \cdot \text{I}$ has been reported.⁶ It will be discussed later.

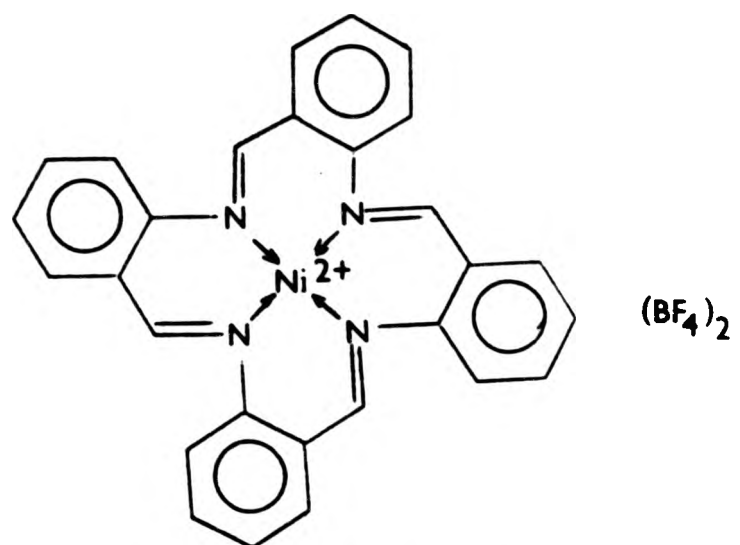
2) 12 π -electrons

2 imine bonds

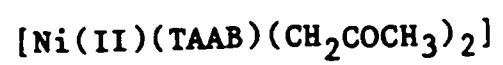
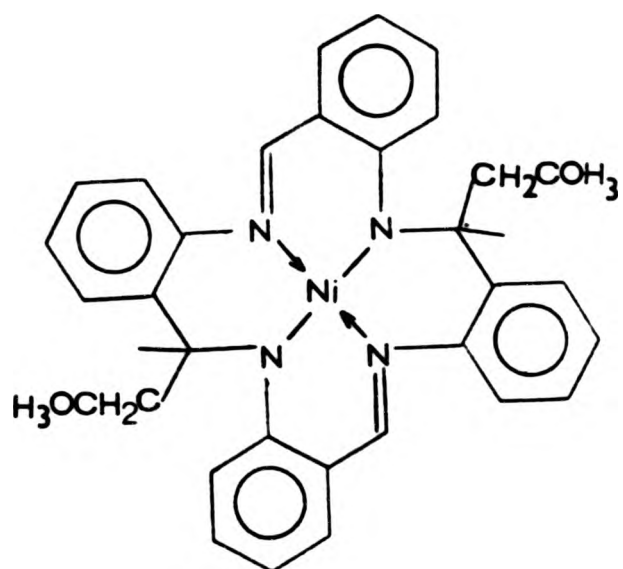
X and Z are the same as in the above section.

Examples:

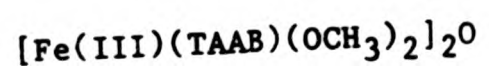
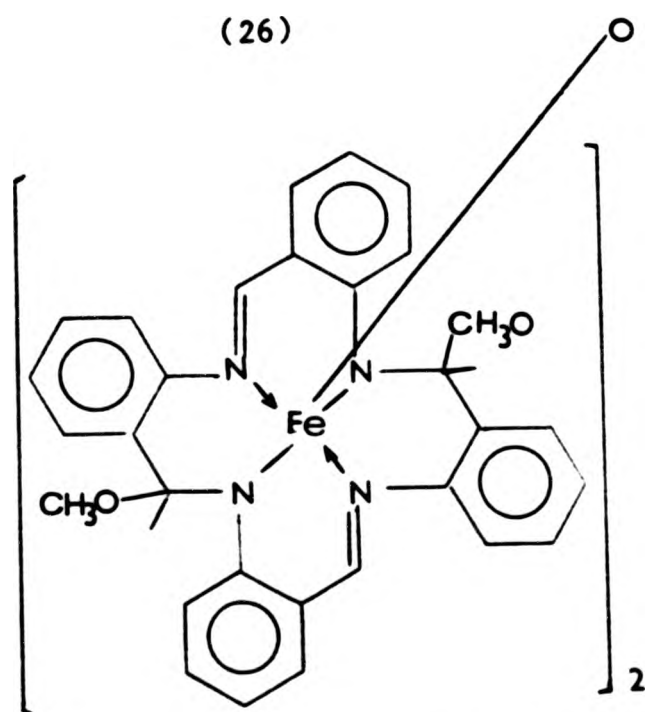




(25)



(26)



(27)

An X-ray structure determination of $[\text{Fe}(\text{III})(\text{TAAB})(\text{OCH}_3)_2]_2\text{O}$ (27) has been reported.²⁸ The structures of (25), (26), (27) previously reported are discussed in section 5.2.

1.2.4 METAL COMPLEXES OF 14-MEMBERED TETRA-AZAMACROCYCLES AND

OF SCHIFF BASES

In the previous section, metal complexes based on tetra-azamacrocycles were discussed, whose inner great rings of the free ligands are 16-membered. The conformation/configuration and the stability of related macrocyclic rings will be expected to differ markedly as the size of this inner great ring is varied. An example in point are 14-membered tetra-azamacrocycles. These have been reviewed by Lindoy.²⁹ A series of these have been reported where four, two, or no azomethine (imine) linkages are present. Tautomeric changes have been observed. In particular, iron and nickel complexes have been investigated and their oxidations have been studied (see Diagram 1.1).

These compounds contain ethylene diamine residues which on oxidation give rise to azomethine linkages. Some of these reactions were studied because of an interest in template syntheses, others because of a desire to understand the reactions of the co-ordinated ligands.

As a series of tribenzo-analogues of such metal complexes were available in this laboratory, structural studies seemed to be rewarding and were carried out on selected examples (see chapter 6).

An X-ray structure determination of $[\text{Fe}(\text{III})(\text{TAAB})(\text{OCH}_3)_2]_2\text{O}$ (27) has been reported.²⁸ The structures of (25), (26), (27) previously reported are discussed in section 5.2.

1.2.4 METAL COMPLEXES OF 14-MEMBERED TETRA-AZAMACROCYCLES AND

OF SCHIFF BASES

In the previous section, metal complexes based on tetra-azamacrocycles were discussed, whose inner great rings of the free ligands are 16-membered. The conformation/configuration and the stability of related macrocyclic rings will be expected to differ markedly as the size of this inner great ring is varied. An example in point are 14-membered tetra-azamacrocycles. These have been reviewed by Lindoy.²⁹ A series of these have been reported where four, two, or no azomethine (imine) linkages are present. Tautomeric changes have been observed. In particular, iron and nickel complexes have been investigated and their oxidations have been studied (see Diagram 1.1).

These compounds contain ethylene diamine residues which on oxidation give rise to azomethine linkages. Some of these reactions were studied because of an interest in template syntheses, others because of a desire to understand the reactions of the co-ordinated ligands.

As a series of tribenzo-analogues of such metal complexes were available in this laboratory, structural studies seemed to be rewarding and were carried out on selected examples (see chapter 6).

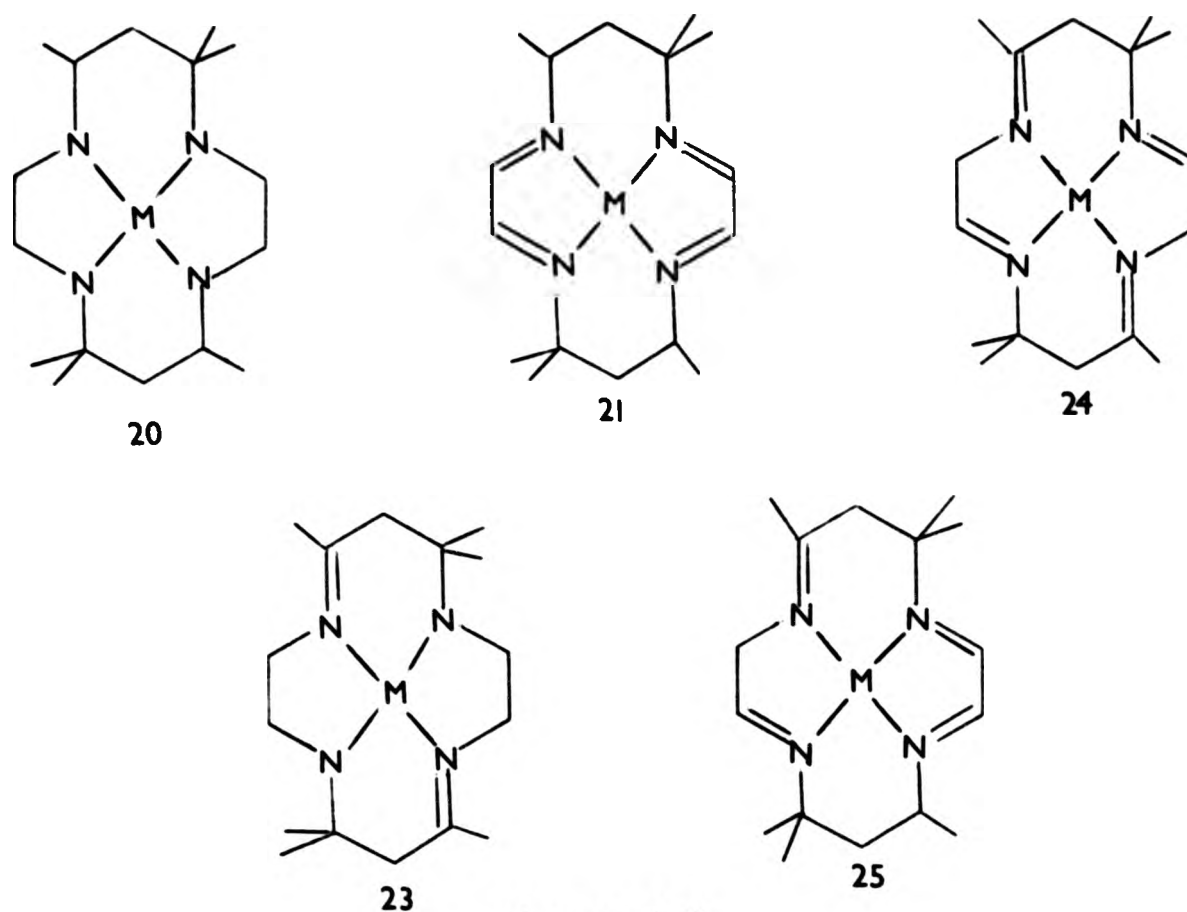


Diagram 1.1

In the literature there are a number of examples of X-ray crystallographic structure determinations of 4-³⁰⁻⁴⁵, 5-^{46,47}, and 6-co-ordinate Cu(salen) and related derivatives. Many of these have square planar or distorted tetragonal main ligand structures, with the Schiff base in equatorial positions. The axial bonds in 5- or 6-co-ordinate species are usually considerably longer than the equatorial ones.

In those of the above complexes, where the Schiff base represents one tetradentate ligand, the two nitrogen atoms, as well as the two oxygen atoms, of the resulting complex have a cis-relationship.³⁰⁻³⁸ When the ligand consists of two independent bidentate Schiff bases, in general the pair of nitrogen atoms, as well as the pair of oxygen atoms, have a trans-disposition.³⁹⁻⁴⁵ In the absence of steric effects, the copper atom adopts, in general, with the above Schiff bases a square planar configuration, or nearly so, regardless of whether the metal atom

is 4-, 5-, or 6-co-ordinate, i.e. the $\text{Cu}(\text{N}_2\text{O}_2)$ or $\text{Cu}(\text{NO})_2$ unit is nearly planar.

When bulky groups such as the $t\text{-Bu}^{43}$ are attached to the nitrogen atoms, or if a larger bridging group than the ethylene is introduced between the two nitrogen atoms,³⁷ the configuration around the metal atom tends to be distorted towards a tetrahedral structure. This is regardless of whether the nitrogen atoms are cis or trans to each other.

$\text{Cu}(\text{salen})$ itself has received considerable attention. The unsolvated complex³⁰ forms dimer units via two copper phenolic oxygen intermolecular contacts, these bonds forming the 5th, i.e. the apical co-ordination position, the co-ordination of copper with the other ligand atoms remaining essentially the same. The length of the copper oxygen bond involved in the dimer formation is 2.41 Å. The same compound with chloroform³⁵ in the crystal lattice retains the same overall stereochemistry as the unsolvated complex, but the oxygen apical bond is considerably longer at 2.79 Å. The chloroform forms a hydrogen bond $\text{C}\cdots\text{O} = 3.03$ Å with the other phenolic oxygen atom. This structure is somewhat reminiscent of the one reported in this Thesis for the chloroform solvated AA TRIMER, where one carbonyl oxygen is involved with the NH group of another molecule in dimer formation and the other carbonyl oxygen is involved in hydrogen bonding with chloroform (see section 4.3.2).

The *p*-nitrophenol adduct of the above $\text{Cu}(\text{salen})^{34}$ complex shows no tendency towards dimer formation; a rather strong hydrogen bond ($\text{O}\cdots\text{O} = 2.66$ Å) is formed between the phenolic group of the solvate

and one of the co-ordinated oxygen atoms of the ligand.

Hall and Waters³⁵ suggested that there might well be some relationship between dimer formation and hydrogen bonding. They point out, however, that this cannot be the only effect as bis(N-methyl-salicylidene-iminato) copper(II) exists as a similar dimer in one of its crystalline modifications, but not in the other two, suggesting that the associating metal oxygen bond is by no means sufficiently strong to dominate the structure. Dimer formation has thus far only been reported when the substituents on the imine nitrogen atoms are the least sterically demanding, i.e. either two methyl groups or an ethylene bridge.

In the thiourea complex of Cu(salen), [Cu(salen)tu],³⁶ the copper atom is again square planar and there are no signs of dimerisation. Hydrogen bonding again occurs from the nitrogen atoms of the thiourea towards the phenolic oxygen atoms, N-H...O = 2.89 and 2.94 Å, and nitrogen-sulphur hydrogen bonds are observed amongst the thioureas, N-H...S = 3.46 and 3.49 Å.

The thiourea complex of Cu(salof), [Cu(salof)tu],³⁶ is again monomeric with a square planar configuration of the copper atom and it exhibits similar hydrogen bonding to the above, N-H...O = 2.96 and 2.97 Å and N-H...S = 3.43 and 3.57 Å.

The only significant difference between the two complexes is that the salof ligand shows only small distortions from complete planarity, whilst the salen ligand, due to the presence of the ethylene bridge

which adopts a gauche conformation, causes a somewhat greater distortion from planarity. A square planar configuration in Cu(salen) has also been observed for the complex which it forms with sodium perchlorate and p-xylene.³²

Salen and related derivatives of Fe(III) are not as well documented crystallographically as those of Cu(II), and those structure investigations are usually less accurate, as many of the compounds are dimerised via a μ -oxo-bridge. Hence the ratio of the number of data points to parameters is small. The salen derivative of Fe(III) has been the one most thoroughly investigated.⁴⁸⁻⁵⁰ Data are available on the unsolvated complex,⁴⁹ as well as on its pyridine⁴⁸ and methylene chloride adducts.⁵⁰ Again here, as in the copper compounds, one tetradentate ligand usually gives rise to nitrogen atoms cis to one another,⁴⁸⁻⁵⁰ whilst two bidentate Schiff base ligands give rise to trans-structures.⁵¹⁻⁵³ Examples of the latter are when the ethylene bridge in salen is replaced by p-chlorophenyl⁵¹ or n-propyl groups⁵² on nitrogen.

All Fe(salen) and related derivatives so far studied have the iron atom 5-co-ordinate as a square pyramid, with the Schiff base as the basal plane and the 5th ligand at the apical position. Fe-N bond lengths are generally longer than Fe-O (phenolic) distances and the Fe atom is 0.53 to 0.58 Å above the four-atom basal plane towards the apical site. Unlike (in) the Cu(salen) derivatives the presence or absence of solvent molecules does not appear to alter the nature of the complex. Whilst all Fe-O(bridge) bond lengths fall within the same region (1.76 to 1.82 Å), the bond angles at the μ -oxo-bridge vary

significantly (see Table 8.4). Those relating to the salen derivatives, solvated or unsolvated, are considerably smaller ($139-145^\circ$) than those derived from Schiff bases without a bridge between the two nitrogen atoms ($164-175^\circ$).

Murray has surveyed μ -oxo-bridged metal complexes⁵⁴ (Table 1.2). This type of compound occurs with quite a number of metals and in the majority of cases the M-O-M arrangement is linear or nearly so. Iron appears to be an exception to this, in that the Fe-O-Fe bond angles span a range from 142.2 to 178° ⁵⁵⁻⁶³, with the linear arrangement being the exception rather than the rule. The Fe-O(μ) bonds are generally substantially shorter than the other Fe-O bonds in these complexes. This has been associated with π -bonding from the lone pairs of electrons of the μ -oxo atom towards the iron atoms.⁵⁴ The range of Fe-O-Fe bond angles appears to be somewhat larger than the range of the Fe-O(μ) bond lengths. No satisfactory explanation of this variation, or indeed why these deviations from linearity occur at all, has so far been offered (see Table 8.1).

Table 1.2: M-O-M geometry in some oxo-bridged dimers⁵⁴

Complex	M-O μ (Å)	Co-ord. of M	M-O-M $^\circ$	M-M (Å)
{[Cr(NH ₃) ₅] ₂ O}Cl ₄ .H ₂ O	1.82	6	180	3.64
(MnPc) ₂ O.Py ₂	1.71	6	178	3.42
K ₄ [(ReCl ₅) ₂ O].H ₂ O	1.86	6	180	3.72
K ₄ [(RuCl ₅) ₂ O].H ₂ O	1.80	6	180	3.60
[Al(2-Me-oxine) ₂] ₂ O	1.68	5	180	3.34

It has been suggested as a generalisation, that Fe-N bond lengths and the stereochemistry of the iron atom are affected by the spin state

of the latter.²⁸ It has been stated that, in general, in high spin iron complexes the Fe-N bond length is longer than in low spin ones (see Table 8.2), and that, in high spin complexes, the iron atom is higher above the plane of the set of nitrogen atoms than in low spin ones. A similar variation in nickel-nitrogen bond lengths has been observed for high and low spin nickel derivatives (Table 1.3).²⁸

Table 1.3: Nickel-nitrogen bond lengths in some nickel tetra-azamacrocycles

Complex	Co-ord. of M	M-N (Å)	Spin state
Ni(TAAB)(BF ₄) ₂	4	1.90	low
Ni(TAAB)(CH ₂ COCH ₃) ₂	4	1.902	low
NiEtioI	4	1.96	
NiDeut	4	1.96	
Ni(TAAB)I ₂ .H ₂ O	6	2.09	high

1.3 HYDROGEN BONDING

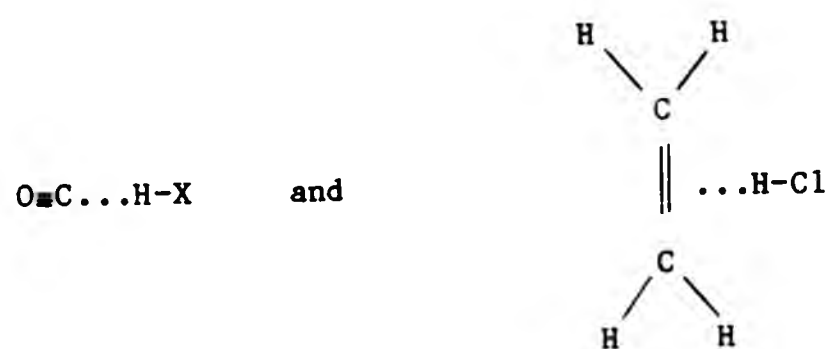
It has been found convenient to discuss interatomic forces in three classes.

- 1) Chemical bonds, generally in the range 50-200 kcal/mol (209-837 kJ/mol).⁶³
- 2) "Classical" hydrogen bonds, 2-7 kcal/mol (8-29 kJ/mol).⁶⁴
- 3) Van der Waal's forces < 1 kcal/mol (< 4 kJ/mol).⁶⁵

These three classes as defined above differ greatly from each other.

Recent experimental and theoretical work, however, has shown that very strong hydrogen bonds exist, approaching the bond strengths of covalent bonds,^{66,67} e.g. $[F-H...F]^-$ 51 kcal/mol (219 kJ/mol), $H_2O...OH^-$ 41 kcal/mol (172 kJ/mol), and $HC(O)NH_2...F^-$ 35 kcal/mol (148 kJ/mol).

Improved instrumentation (e.g. N.M.R. and microwave spectroscopy) has demonstrated the existence of very weak hydrogen bonds, some only marginally stronger than van der Waal's forces. Examples are the self-association of chloroform observed by 1H N.M.R. spectroscopy⁶⁸ and the association as 1:1 complexes of CO, Ar, Kr with HX (X = F, Cl, Br) and of C_2H_4 with HCl observed by microwave spectroscopy. The geometries are e.g.



Energies range from 2.8-0.2 kcal/mol (12-1 kJ/mol).^{69,70} Similarly, theoretical calculations⁷¹ suggest the possibility of very weak interactions, e.g. He, HF 0.11-0.15 kcal/mol (0.46-0.63 kJ/mol) and H_2, H_2O 0.75-1.05 kcal/mol (3.1-4.4 kJ/mol), which might be described as very weak hydrogen bonds.

Early publications dealing with some, as yet not completely

formalised, hydrogen interactions have been summarised.^{63,71-73} The first clear definition of a hydrogen bond was put forward by Maurice Huggins in 1919.⁷⁴ The first publication (1920) dealing with this topic is by Latimer and Rodebusch.⁷⁵ Hydrogen bonds are formed when a hydrogen finds itself in the close proximity of two or more electronegative groups. These were originally observed with F, O, and N containing compounds though this range has considerably widened in recent years. The hydrogen bond is frequently written as X-H...Y, where X and Y can be the same or different, and are based on the above mentioned negative centres. X is often described as the hydrogen donor and Y as the electron donor. Hydrogen attached to such an electronegative group is generally called active,⁷² as it is capable, given the right structural parameters, of participating in hydrogen bonding. Various combinations, in which X can be neutral or positively charged and Y can be neutral or negatively charged, have been reported.

Hydrogen bonding has been postulated from a variety of physical properties such as: molecular weights, boiling and melting points, but probably the most convincing and widespread proof of its existence comes from I.R., Raman, and N.M.R. spectroscopy.^{63,73} A book has been devoted to C-H hydrogen bonding,⁷⁶ where the evidence cited is based mainly on physical methods other than diffraction.

The detailed nature of the hydrogen bond is even now subject to discussion. It is generally agreed that electrostatic forces make a major contribution to its bonding. Delocalisation effects, repulsive forces, and dispersion forces have all been considered by Coulson.^{64,77} He pointed out that the uncertainties in theoretical calculations are

likely to lead to errors in energy larger than those involved in the hydrogen bonds themselves. In view of these, and as most geometric characteristics of the hydrogen bond can be explained from the Coulomb energy alone,⁷² the electrostatic model will be accepted for any subsequent discussion.

Crystallographic investigations of hydrogen bonds fall into two types:

- 1) Neutron diffraction
- 2) X-ray diffraction

Advances in X-ray crystallographic techniques have allowed in recent years more frequent direct observations of the hydrogen atoms involved in hydrogen bonding. In addition the greater availability of neutron diffraction has allowed the accurate determination of hydrogen positions in a number of structures.^{72,78,79} The bond lengths X-H involving hydrogen atoms have been found to be systematically longer by neutron than by X-ray diffraction. The reason for this is that neutrons are scattered by atomic nuclei whilst X-rays are by electrons.⁷² In the case of hydrogen the centroid of electron density is a considerable distance removed from the hydrogen nucleus in the direction towards its bonding partner X, and therefore such bonds when determined by X-ray diffraction give smaller values than those from neutron diffraction. A table of comparison of N-H and C-H distances in α -glycine as determined by neutron and by X-ray diffraction is given in Table 1.4.⁷²

Table 1.4: Comparison of X-H distances derived from neutron and X-ray for α -glycine ($\text{H}_3\text{NCH}_2\text{CO}_2^-$).

Covalent bond	X-Hn (Å)	X-Hx (Å)	Δ (Å)
N-H(1)	1.054(2)	0.996(19)	0.066
N-H(2)	1.037(2)	0.982(18)	0.067
N-H(3)	1.025(2)	0.959(16)	0.070
C(2)-H(4)	1.090(2)	0.963(16)	0.130
C(2)-H(5)	1.089(2)	0.966(18)	0.133

Wells⁸⁰ gives the values of 1.00 and 0.85 Å for the O-H bond when determined by neutron and X-ray diffraction respectively.

1) Neutron diffraction deals with α , as yet, much more limited group of examples. This technique allows the accurate determination of the position of the hydrogen atom. Two very recent surveys^{81,82} quote only the H...Y distances; a slightly older one, however, gives the X.....Y distances as well.⁷²

The generally accepted criterion for a hydrogen bond in crystals is that of Hamilton and Ibers,⁸³ which postulates the existence of a hydrogen bond if $d > 0.3$ Å, where $d = v(\text{H}) + v(\text{Y}) - r(\text{H}...Y)$ and $v(\text{H})$ and $v(\text{Y})$ are the respective van der Waal's radii of H and Y, and $r(\text{H}...Y)$ is the actual distance observed between H and Y.

The use of this criterion is, however, complicated by the different values for van der Waal's radii given to the atoms in question (see

Table 1.5).

Table 1.5: Van der Waals' radii (Å).

H	O	N	ref.
1.0	1.4		72
1.2	1.5	1.55	81
1.5	1.65	1.7	82
1.2	1.4	1.5	84

Use of different van der Waal's radii leads of course to some difference in interpretation of finer details, nevertheless a surprisingly good, broad concensus emerges.

A survey by Jeffrey and Maluszynska⁸² of hydrogen bond geometries in crystal structures of amino-acids gives a distribution of hydrogen bond lengths in this class of compounds (see Figure 1.1). Another survey by Taylor and Kennard⁸¹ of 113 organic compounds accurately determined by neutron diffraction, focussing only on C-H hydrogen bonds, gives H...O contacts between 2.045 and 2.399 Å, H...N distances between 2.522 and 2.721 Å and H...Cl distances between 2.569 and 2.944 Å, all of which are considered as hydrogen bonds. Taylor and Kennard consider that, particularly for these C-H...Y interactions, the electrostatic energy is the determining factor. They mention that a neutral or positively charged nitrogen atom immediately adjacent to a C-H bond gives a favourable environment for C-H hydrogen bonding. The same authors conclude that almost any type of oxygen atom, e.g. in sulphonate,

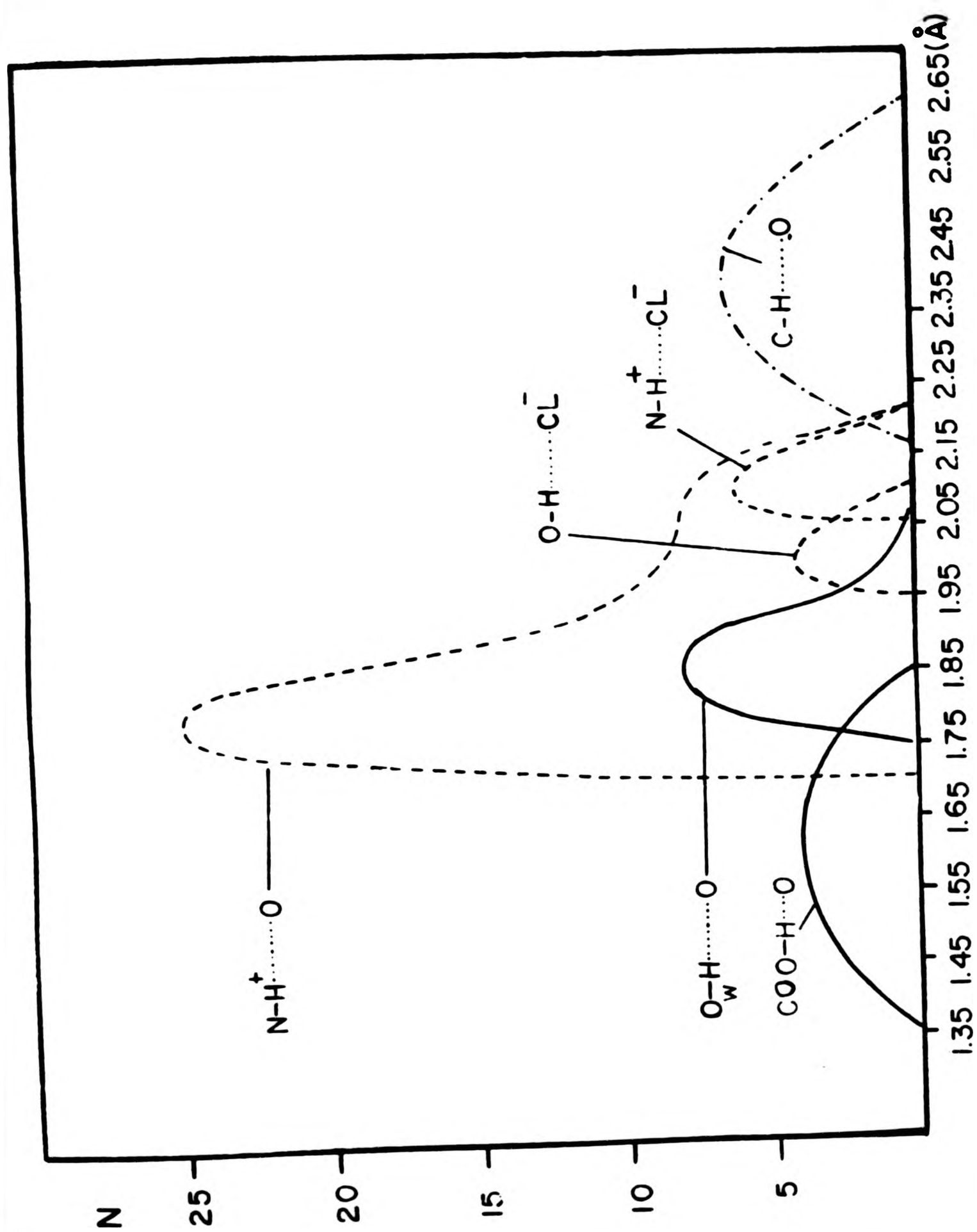


Fig. 1. Distribution of hydrogen-bond lengths in amino acid crystal structures from neutron diffraction data.

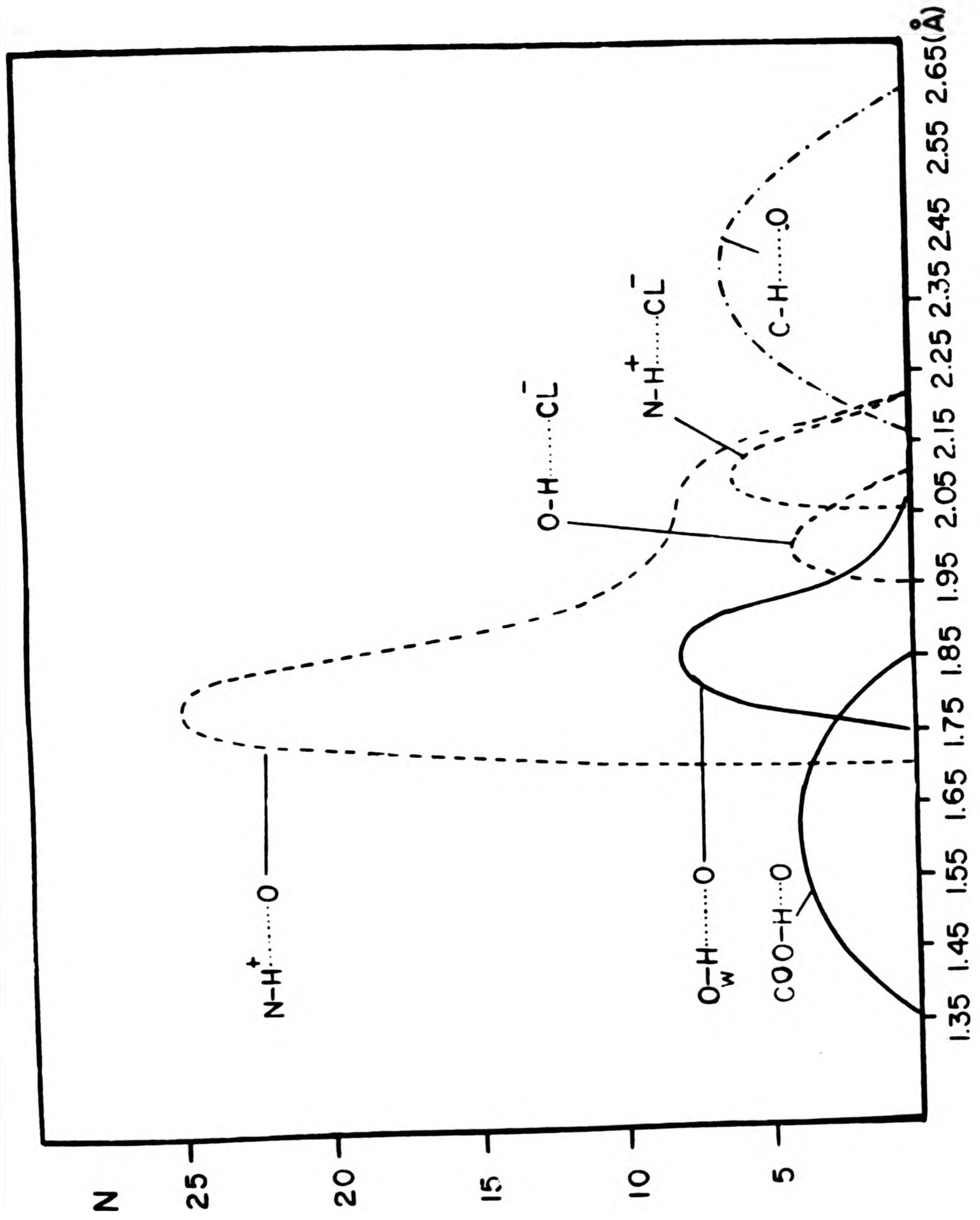


Fig. 1. Distribution of hydrogen-bond lengths in amino acid crystal structures from neutron diffraction data.

carboxylate, nitro, carbonyl, ether, etc., can act as an electron donor. They conclude that the C-H...O hydrogen bond is very sensitive to the immediate environment of the C-H group, but insensitive to the nature of the oxygen atom. Both groups of investigators^{81,82} agree that the proton of the hydrogen bond prefers to lie in or near the plane containing the lone pair orbitals of the electron donor atom. There is, however, a divergence of opinion of whether the hydrogen atom points preferentially towards the lone pairs or not. As far as the C-H...O bond is concerned, Taylor and Kennard⁸¹ conclude that the hydrogen is attracted rather than repelled by the lone pairs of the oxygen atom and that the optimum C-H...O arrangement is probably linear.

The above work^{81,82} places the existence of C-H hydrogen bonds now beyond all reasonable doubt.

2.) X-ray diffraction accounts for the vast majority of hydrogen bond observations/postulates in crystals. In many cases the hydrogen atom was not, or at least not accurately, located. The criterion used in this work was the approach of the atoms X and Y to a distance closer than that expected from the van der Waal's radii of the H and Y atoms and the bonding distance X-H as shown in Diagram 1.2. This would be meaningful only if X-H...Y was linear. If the angle (see Diagram 1.2) differs substantially from 180° , this can lead to errors, particularly if the hydrogen atom has not been observed and the deductions are based solely on the distance R.

The danger of this is brought out in Diagram 1.3,⁷² where close

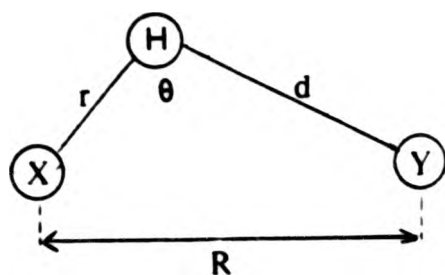
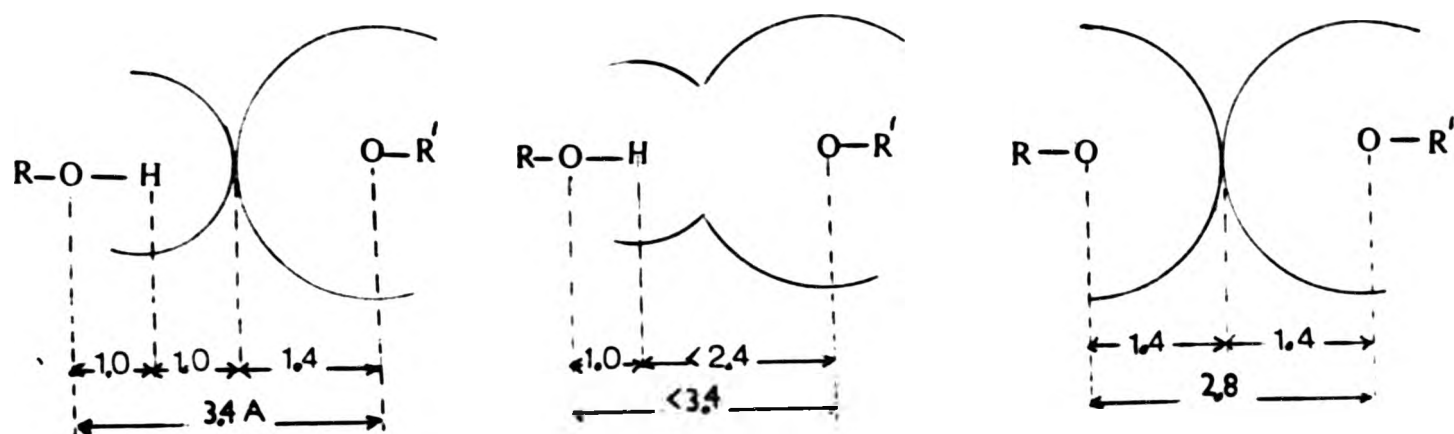


Diagram 1.2

approach between X and Y (in this case both of them oxygen atoms) in 2(c) could lead to the erroneous postulate of a hydrogen bond, when in fact no hydrogen is involved.



Van der Waal's contact
distance

Hydrogen bonding
shortens this
distance

Van der Waal's contacts
with no hydrogen
involved

(a)

(b)

(c)

Diagram 1.3

Sterically crowded molecules can give rise to surprisingly short contacts without the intervention of hydrogen bonds. Examples of this come from the work of Ferguson and Sim⁸⁵ on *o*-chlorobenzoic acid ($R = H$) [and 2-chloro-5-nitrobenzoic acid ($R = NO_2$)]. The Cl.....O and Cl.....C intramolecular contacts are as shown in Diagram 1.4, 2.892(2.896) and 3.217(3.173) Å respectively, whereas the sums of the appropriate van der Waal's radii are 3.20 and 3.80 Å respectively.

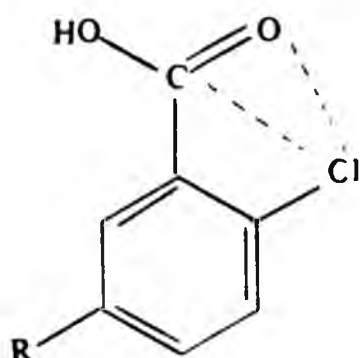
R=H or NO₂

Diagram 1.4

Bearing all the above reservations in mind, it is still nevertheless useful to consider the X...Y distances, even when the hydrogen atom has not been crystallographically observed, if there is good reason to suppose that hydrogen bonding may be involved.

Divergence from linearity has been documented. For instance O-H...O angles vary from 110 to 180°, with the bulk between 165 and 180° and N-H...O angles from 150 to 180° with bulk between 150 and 180°.72

Much data is available on hydrogen bonds by X-ray diffraction, but it suffers from the above mentioned disadvantage regarding the accurate location of the hydrogen atoms. It will be seen that in a number of cases this bond X-H...Y is not linear. Thus a short R = X...Y distance need not necessarily mean a short H...Y distance, and hence a strong hydrogen bond (see Diagrams 1.2-1.4).

Most examples of hydrogen bonding even when X and Y are identical give rise to asymmetric hydrogen bonds. Examples of symmetric hydrogen bonds are known, and these are confined to the strongest hydrogen bonds, e.g. [F...H...F]⁻, e.g. reference 80.

Hydrogen bonds O-H...O, N-H...O have been exceedingly well

documented by X-ray crystallography, 63,73,80,83,84

Amongst very short O-H...O distances reported in recent years are those of pyridine-2,3-dicarboxylic acid⁸⁶ O.....O 2.398 Å, Cs⁺ (O₂FSO.H.OSFO₂)⁻ ⁸⁷ O.....O 2.41 Å where the hydrogen bonds are symmetrical, and trans-[RhCl₄(Me₂SO)₂]⁻ (Me₂SO.H.OSMe₂)⁺ ⁸⁸ O.....O 2.42 Å, where a disorder was observed in two slightly asymmetric hydrogen positions.

The shorter O-H...O distances are generally associated with acids, the longer ones with water and hydrates⁸⁰. A possible explanation for this observation is that in acids the proton has a more pronounced fractional positive charge and this contributes to a stronger hydrogen bond. Similarly in the system X-H...Y, an increase of negative charge on Y should lead to a stronger hydrogen bond. An excellent example of this is given by the H-F system. F.....F distances decrease with an increase of the negative charge on Y. Crystalline (H-F)_n 2.49 Å, KH₄F₅ 2.45 Å, KH₂F₃ 2.33 Å, NaHF₂ 2.27 Å.⁸⁰

It has been observed that as a general rule, all active hydrogen atoms participate, in crystals, in hydrogen bonding, even when this may involve more proton donors than electron donors,^{72,82} e.g. the structure of solid ammonia.⁷² (Diagram 1.5).

A survey of the literature, not necessarily comprehensive, reveals a number of other structures for which C-H...O (as well as some C-H...N) hydrogen bonds have been postulated. The suggestion that C-H...O hydrogen bonds might exist was put forward by June Sutor⁸⁹ in 1962.

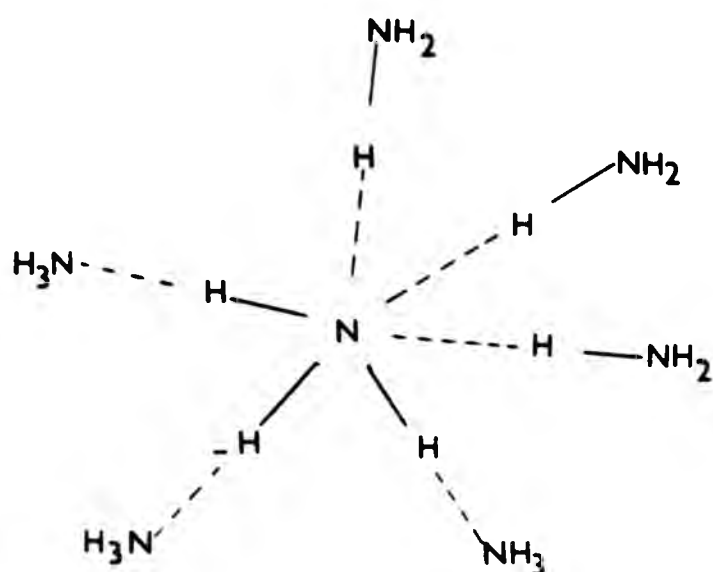


Diagram 1.5

The basis for her arguments, were close carbon-oxygen contacts, as observed by X-ray crystallography.

A selection of structures where such bonds have been postulated are given below.

1) o-Halogenobenzoylacetylene^{90,91}

	a) X = Cl	b) X = Br
C-H...O	3.212 Å	3.260 Å
<u>o</u> -X-C ₆ H ₄ C(O)C≡C-H...O=C(<u>o</u> -X-C ₆ H ₄)(C≡CH)		
C-H...O	161.9°	
C=O...H	145.3°	
H...O	2.19 Å	

2) Propargyl 2-Bromo-3-nitrobenzoate⁹²

2-Br-3-NO ₂ -C ₆ H ₃ -C(O)-OCH ₂ -C≡C-H...O=C(OCH ₂ C≡CH)(C ₆ H ₃ -2-Br-3NO ₂)		
C-H...O	3.39 Å	
C-H...O	156°	
H...O	2.39 Å	

3) Triethylprop-2-ynylammonium p-Bromobenzenesulphonate⁹³

	C-H...O	3.36 Å
<u>p</u> -Br-C ₆ H ₄ SO ₂ O ⁻ ...	H...O	2.38 Å
	C-H...O	154

4) p-Bromophenacyl Dichloroacetate (a) and Difluoroacetate (b)⁹⁴

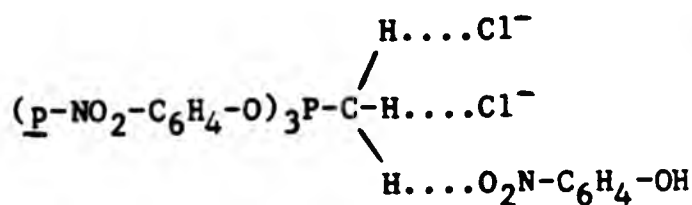
	a) X = Cl	b) X = F
<u>p</u> -Br-C ₆ H ₄ -C(=O)-C(H)-O-C(=O)-CHX ₂	C-H...O	3.21 Å
	C-H...O	162°
	H...O	2.27 Å
X ₂ CH-C(=O)-O-H ₂ C-C(=O)-C ₆ H ₄ - <u>p</u> -Br		3.31 Å
		168°
		2.26 Å

5) Methylenebis(phosphonic dichloride)⁹⁵

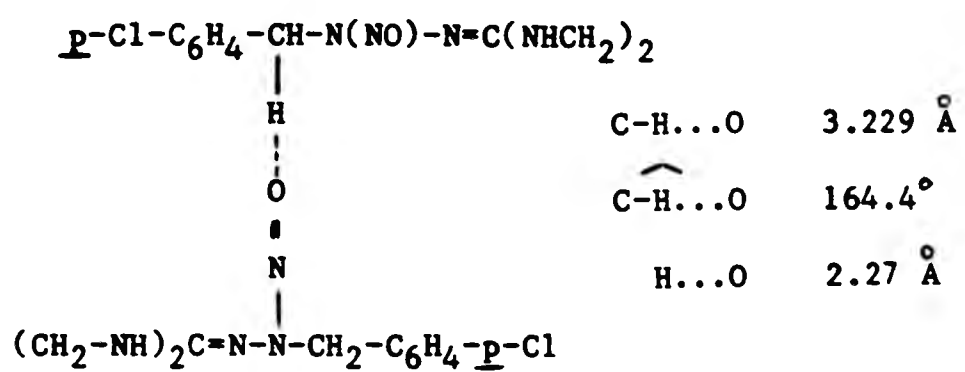
	C-H...O	3.23 Å
	C-H...O	Deviation from linearity
[Cl ₂ P(O)] ₂ CH ₂ ...		is small.
	H...O	2.42 Å

6) Methyltri(p-nitrophenoxy)phosphonium Chloride . p-nitrophenol . 1/2 benzene⁹⁶

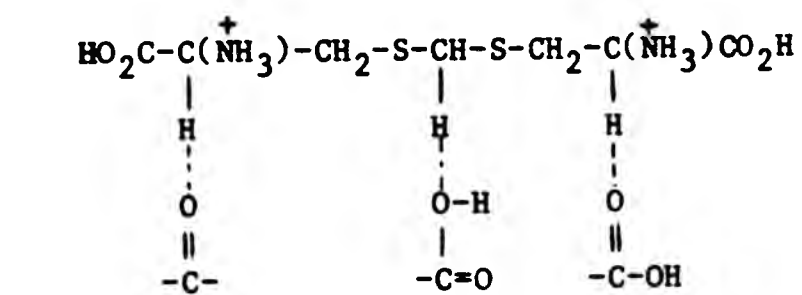
	C-H...O	3.312 Å
	C-H...Cl	3.44 and 3.490 Å
	H...O	2.39 Å
	C-H...O	Nearly linear
	C-H...Cl	" "



7) 1-(4-Chlorobenzyl)-1-nitroso-2-(4,5-dihydro-2-imidazolyl)hydrazine-Monohydrate⁹⁷



8) S,S'-Methylenebis(L-Cysteine) Monohydrochloride⁹⁸

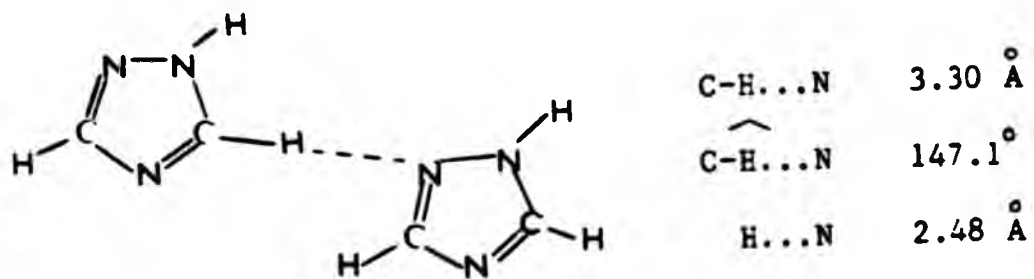


	a	b	c
C-H...O	3.165	3.377	3.267 Å
$\widehat{\text{C-H...O}}$	136	131	136°
H...O	2.27	2.48	2.41 Å

9) Hydrogen Cyanide⁹⁹

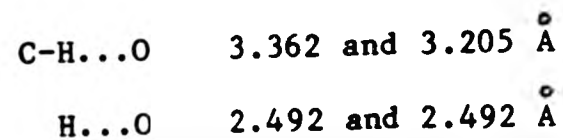
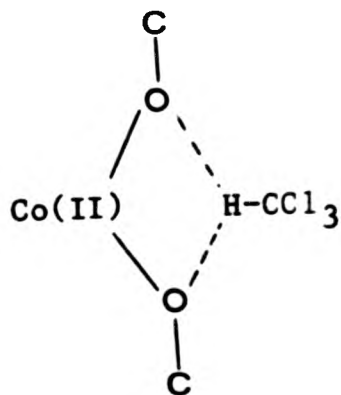
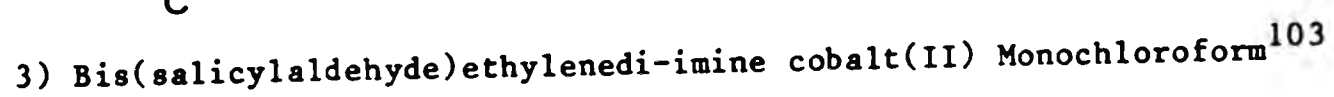
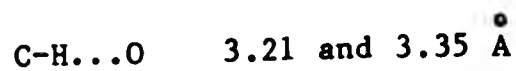
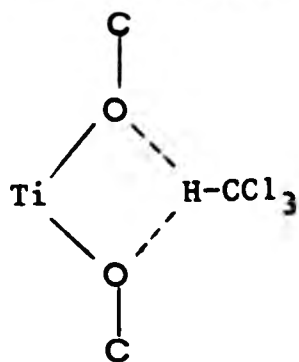
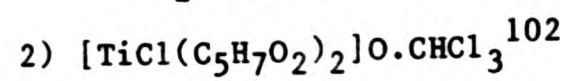
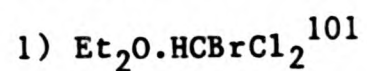


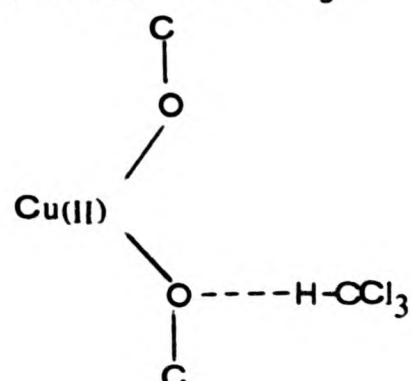
10) 1,2,4-Triazole¹⁰⁰



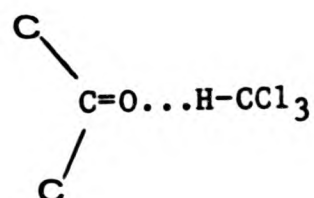
A special case of C-H...O hydrogen bonding is represented by the interaction of chloroform with molecules capable of acting as electron donors. Such hydrogen bonding, mainly based on spectroscopic evidence, has been postulated for many years.^{63,73,76} Although the number of such examples obtained by crystallographic investigations is, as yet, not very large, some examples from the literature are appended below (The last two examples provide evidence for C-H...Cl bonding). The fact that the chloroform molecule is a separate, relatively small (in relation to the host molecule) entity with a considerable degree of freedom to orientate itself in the crystal lattice, makes it likely that it will lead to more conclusive information about C-H...O interactions.

Examples:



4) Cu(salen).CHCl₃³⁵

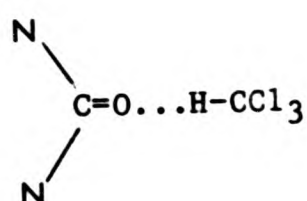
C-H...O 3.03 Å

5) 4,6-dianilino-2-phenylquinoline-5,8-quinone.CHCl₃¹⁰⁴

C-H...O 136°

H...O 2.34 Å

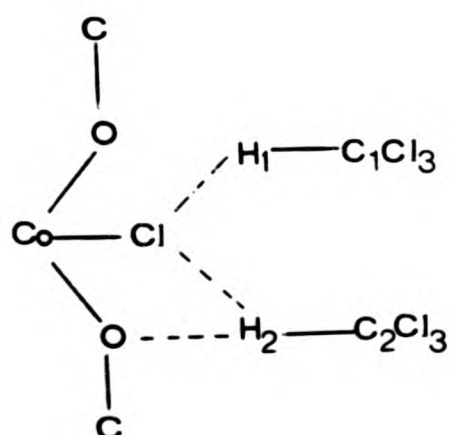
C-H 0.99 Å

6) 5'-Acetamido-3'-acetyl-5'-deoxythymidine.CHCl₃¹⁰⁵

C-H...O 3.05 and 3.05 Å

H...O 2.13 and 2.15 Å

The chloroform molecule is disordered.

7) Bis[-bis(salicylaldehyde)ethylenedi-imine]-dicobalt(III)
Dichloride chloroform¹⁰⁶

C(1)-H...Cl 3.59 Å

H(1)...Cl 2.67 Å

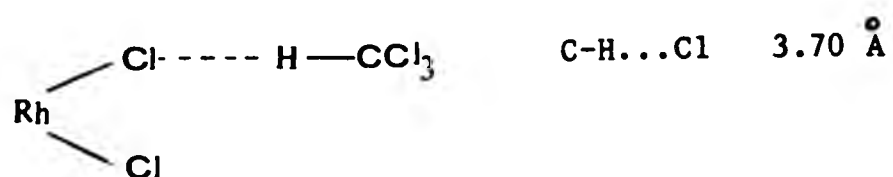
C(2)-H...O 3.41 Å

C(2)-H...Cl 3.52 Å

H(2)...Cl 2.72 Å

H(2)...O 2.61 Å

8) $\{\text{Rh}(\text{CO})\text{RhCl}_2[(\text{PhO})_2\text{PN}(\text{Et})-\text{P}(\text{OPh})_2]_2\} \cdot \text{CHCl}_3$ ¹⁰⁷



Since the early observations of hydrogen bonds, publications dealing with these have multiplied enormously and the great importance this interaction plays in chemistry and biology has been realized.

Hydrogen bonding plays an important part in the structures reported and discussed in this Thesis, and the work described here will deal with the following types of interactions which are given in Table 1.6, together with reported literature ranges for X...Y and, where available, H...Y distances (in Å), as well as X-H...Y (in °).

Table 1.6: Some hydrogen bond geometries from the literature

Segment	Distance Å	Bond	Distance Å	Angle ° X-H...Y
X-H...Y		H...Y		
O-H...O	2.40-3.17 ⁷²	H...O	1.21-2.30 ^{72, a}	140-180 ⁷²
N-H...O	2.63-3.25 ⁷²	H...O	1.60-2.40 ^{72, a}	110-180 ⁷²
N-H...F	2.57-3.45 ^b	H...F	1.88-2.51 ^b	122-172 ^b
C-H...O	3.17-3.39 ^c	H...O	2.05-2.65 ^{81, 82, a}	90-176 ^{81, 82, a}
C-H...Cl	3.52-3.70 ^{106, 107}	H...Cl	2.57-2.94 ^{81, a}	119-169 ^{81, a}
C-H...F				

^a By neutron diffraction; ^b see section 3.3.3; ^c see above

REFERENCES

1. P. Pfeiffer, T. Hesse, R. Pfitzner, W. Scholl, and H. Thielert, J. prakt. Chem., 1937, 149, 217.
2. G. L. Eichhorn and R.A. Latif, J. Am. Chem. Soc., 1954, 76, 5180.
3. N. E. Tokel, V. Katovic, K. Farmery, L. B. Anderson, and D. H. Busch, J. Am. Chem. Soc., 1970, 92, 400.
4. S. C. Cummings and D. H. Busch, J. Am. Chem. Soc., 1970, 92, 1924.
5. G. A. Melson and D. H. Busch, J. Am. Chem. Soc., 1965, 87, 1706, and references there-in.
6. S. W. Hawkinson and E. B. Fleischer, Inorg. Chem., 1969, 8, 2402.
7. E. B. Fleischer and E. Klem, Inorg. Chem., 1965, 4, 637.
8. R. M. Wing and R. Eiss, J. Am. Chem. Soc., 1970, 92, 1929.
9. F. Seidel, Ber., 1926, 59, 1894.
10. E. Bamberger, Ber., 1927, 60, 314.
11. F. Seidel and W. Dick, Ber., 1927, 60, 2018.
12. S. G. McGeachin, Can. J. Chem., 1966, 44, 2323.
13. A. Albert and H. Yamamoto, J. Chem. Soc. (B), 1966, 956.
14. J. S. Skuratovicz, I. L. Madden, and D. H. Busch, Inorg. Chem., 1977, 16, 1721.
15. J. D. Goddard and T. Norris, Inorg. Nucl. Chem. Letts., 1978, 14, 211.
16. J. Elguero, A. R. Katritzky, B. S. El-Osta, R. L. Harlow, and S. H. Simonsen, J. Chem. Soc. Perkin I, 1976, 312.
17. A. Chatterjee and M. Ganguly, J. Org. Chem., 1968, 33, 3358.
18. M. Kurihara, Makromol. Chem., 1967, 105, 84.
19. R. P. Rhee and J. D. White, J. Org. Chem., 1977, 42, 3650.
20. V. Katovic, L. T. Taylor, F. L. Urbach, W. H. White, and D. H. Busch, Inorg. Chem., 1972, 11, 479.

21. N. Takvoryan, K. Farmery, V. Katovic, F. V. Lovecchio, E. S. Gore, L. B. Anderson, and D. H. Busch, J. Am. Chem. Soc., 1974, 96, 731.
22. G. A. Melson and D. H. Busch, J. Am. Chem. Soc., 1964, 86, 4834.
23. B. Kamenar, B. Kaitner, V. Katovic, and D. H. Busch, Inorg. Chem., 1979, 18, 815.
24. L. T. Taylor, F. L. Urbach, and D. H. Busch, J. Am. Chem. Soc., 1969, 91, 1072.
25. V. Katovic, L. T. Taylor, and D. H. Busch, Inorg. Chem., 1971, 10, 458.
26. V. Katovic, S. C. Vergez, and D. H. Busch, Inorg. Chem., 1977, 16, 1716.
27. S. C. Cummings and D. H. Busch, Inorg. Chem., 1971, 10, 1220.
28. B. Kamenar and B. Kaitner, in "Structural Studies on Molecules of Biological Interest", G. Dodson, J. Glusker, and D. Sayre, Edts., Oxford University Press, 1981, p. 123.
29. L. F. Lindoy, Chem. Soc. Rev., 1975, 4, 421.
30. D. Hall and T. N. Waters, J. Chem. Soc., 1960, 2644.
31. D. Hall, A. D. Rae, and T. N. Waters, J. Chem. Soc., 1963, 5897.
32. G. H. W. Milburn, M. R. Truter, and B. L. Vickery, Chem. Comm., 1968, 1188; J. Chem. Soc. Dalton, 1974, 841.
33. G. R. Clark, D. Hall, and T. N. Waters, J. Chem. Soc. (A), 1968, 223.
34. E. N. Baker, D. Hall, and T. N. Waters, J. Chem. Soc. (A), 1970, 400.
35. Idem, ibid., p. 406.
36. M. B. Ferrari, G. G. Fava, and C. Pelizzi, Acta Cryst., 1976, B32, 901.

37. R. C. Elder and M. C. Hill, Inorg. Chem., 1979, 18, 729.
38. D. E. Fenton, J. Chem. Soc. Chem. Comm., 1979, 39.
39. E. N. Baker, D. Hall, and T. N. Waters, J. Chem. Soc. (A), 1966, 680.
40. T. P. Cheeseman, D. Hall, and T. N. Waters, J. Chem. Soc. (A), 1966, 685.
41. D. Hall, S. V. Sheat, and T. N. Waters, J. Chem. Soc. (A), 1968, 460.
42. D. Hall, R. H. Summer, and T. N. Waters, J. Chem. Soc. (A), 1969, 420.
43. E. E. Castellano, O. J. R. Hodder, C. K. Prout, and P. J. Saddler, J. Chem. Soc. (A), 1971, 2620.
44. T. G. Fawcett, M. Ushay, J. P. Rose, R. H. Lalancett, J. A. Potenza, and H. J. Schugar, Inorg. Chem., 1979, 18, 327.
45. E. D. McKenzie and S. J. Selvey, Inorg. Chim. Acta, 1976, 18, L1.
46. F. J. Llewellyn and T. N. Waters, J. Chem. Soc., 1960, 2639.
47. G. R. Clark, D. Hall, and T. N. Waters, J. Chem. Soc. (A), 1969, 823.
48. M. Gerloch, E. D. McKenzie, and A. D. C. Towl, J. Chem. Soc., 1969, 2850.
49. J. E. Davies and B. M. Gatehouse, Acta Cryst., 1973, B29, 1934.
50. P. Coggon, A. T. McPhail, F. E. Mabbs, and V. N. McLachlan, J. Chem. Soc. (A), 1971, 1014.
51. J. E. Davies and B. M. Gatehouse, Acta Cryst., 1973, B29, 2651.
52. Idem, Cryst. Struct. Commun., 1972, 1, 115.
53. Idem, Acta Cryst., 1972, B28, 3541.
54. K. S. Murray, Coord. Chem. Rev., 1974, 12, 1.
55. M. G. B. Drew, V. McKee, and S. M. Nelson, J. Chem. Soc. Dalton,

- 1978, 80.
56. A. B. Hoffman, D. M. Collins, V. W. Day, E. B. Fleischer, T. S. Srivastava, and J. L. Hoard, J. Am. Chem. Soc., 1972, 94, 3620.
57. F. E. Mabbs, V. N. McLachlan, D. McFadden, and A. T. McPhail, J. Chem. Soc. Dalton, 1973, 2016.
58. M. C. Weiss and V. L. Goedken, Inorg. Chem., 1979, 18, 819.
59. C. C. Ou, R. G. Wollmann, D. N. Hendrickson, J. A. Potenza, and H. J. Schugar, J. Am. Chem. Soc., 1978, 100, 4717.
60. A. Coda, B. Kamenar, C. K. Prout, J. R. Carruthers, and J. S. Rollett, Acta Cryst., 1975, B31, 1438.
61. J. Lippard, H. J. Schugar, and C. Walling, Inorg. Chem., 1967, 6, 1825.
62. E. B. Fleischer and S. Hawkinson, J. Am. Chem. Soc., 1967, 89, 720.
63. S. N. Vinogradov and R. H. Linnell, "Hydrogen Bonding", Van Nostrand Reinhold Company, New York, Cincinnati, Toronto, London, Melbourne, 1971.
64. C. A. Coulson, "Valence", Clarendon Press, Oxford, 1952.
65. Although the statement that van der Waal's forces are weak occurs in every text-book, numerical data is very elusive. P. W. Atkins, "Physical Chemistry", Oxford University Press, 1978, pp. 760-764, and E. A. Colbourn and A. E. Douglas, J. Chem. Phys., 1976, 65, 1741, give values to substantiate the < 1 kcal/mol (< 4 kJ/mol) generalisation.
66. P. Schuster, in "The Hydrogen Bond", Edts. P. Schuster, G. Zundel, and C. Sandorfy, North Holland, Amsterdam, New York, Oxford, 1976, Ch. 2.
67. J. Emsley, D. Jones, M. Miller, R.J. E. Overill, and R. A.

- Waddilove, J. Am. Chem. Soc., 1981, 103, 24.
68. L. W. Reeves and W. G. Schneider, Can. J. Chem., 1957, 35, 251;
G. J. Korinek and W. G. Schneider, ibid., p. 1157.
69. A. C. Legon, P. D. Soper, and W. H. Flygare, J. Chem. Phys.,
1981, 74, 4944.
70. P. D. Aldrich, A. C. Legon, and W. H. Flygare, J. Chem. Phys.,
1981, 75, 2126.
71. E. Lippert, ref. 4, Ch. 1.
72. I. Olovsson and P.-G. Jonsson, ref. 4, Ch. 9.
73. G. C. Pimentel and A. L. McClellan, "The Hydrogen Bond",
W. H. Freeman and Co., San Francisco, London, 1960.
74. M. L. Huggins, Laboratory Report, Inorganic Chemistry, University
of California, 1919 (as referred to by G. N. Lewis, "Valence and
the Structure of Atoms and Molecules", Chemical Catalog Co.,
New York, 1923; M. L. Huggins, Chemtech., 1980, 10, 422.;
and in ref. 11.)
75. W. M. Latimer and W. H. Rodebusch, J. Am. Chem. Soc., 1920, 42,
1419.
76. R. D. Green, "Hydrogen Bonding by C-H Groups", MacMillan, London,
1974.
77. C. A. Coulson, in "Hydrogen Bonding", Edts. D. Hadzi and
H. W. Thompson, Pergamon, London, New York, Paris, Los Angeles,
1959, p. 339.
78. Th. Koetzle and M. S. Lehmann, ref. 4, Ch. 9.
79. J.-O. Lundgren and I. Olovsson, ref. 4, Ch. 10.
80. A. F. Wells, "Structural Inorganic Chemistry", 4th Edn., Clarendon
Press, Oxford, 1975, pp. 301-321.
81. R. Taylor and O. Kennard, J. Am. Chem. Soc., 1982, in the press

and personal communication.

82. G. A. Jeffrey and H. Maluszynska, Int. J. Biol. Macromol., 1982, in the press and personal communication.
83. W. C. Hamilton and J. A. Ibers, "Hydrogen Bonding in Solids", Benjamin, New York, 1968.
84. L. Pauling, "The Nature of the Chemical Bond", 3rd Edn., Cornell University Press, Ithaca, New York, 1960, p. 260.
85. G. Ferguson and G. A. Sim, Acta Cryst., 1961, 14, 1262; J. Chem. Soc., 1962, 1767.
86. A. Kvik and M. Backeus, Acta Cryst., 1974, B30, 474.
87. C. Belin, M. Charbonnel, and J. Potier, J. Chem. Soc. Chem. Comm., 1981, 1036.
88. B. R. James, R. H. Morris, F. W. B. Einslen, and A. Willis, J. Chem. Soc. Chem. Comm., 1980, 31.
89. D. J. Sutor, Nature, 1962, 195, 68; J. Chem. Soc., 1963, 1105.
90. G. Ferguson and K. M. S. Islam, J. Chem. Soc. (B), 1966, 593.
91. G. Ferguson and J. Tyrrell, Chem. Comm., 1965, 195.
92. J. C. Calabrese, A. T. McPhail and G. A. Sim, J. Chem. Soc. (B), 1966, 1235.
93. Idem, ibid., 1970, 282.
94. Idem, ibid., 1970, 285.
95. W. S. Sheldrick, J. Chem. Soc. Dalton, 1975, 943.
96. D. Schomburg, J. Am. Chem. Soc., 1980, 102, 1055.
97. G. J. Palenik, Acta Cryst., 1965, 19, 47.
98. F. Bigoli, M. Lanfranchi, E. Leporati, M. Nardelli, and M. A. Pellinghelli, Acta Cryst., 1982, B38, 498.
99. W. J. Dulmage and W. N. Lipscomb, Acta Cryst., 1951, 4, 330.
100. P. Goldstein, J. Ladell, and G. Abowitz, Acta Cryst., 1969,

B25, 135.

101. P. Andersen and T. Thurmann-Moe, Acta Chem. Scand., 1964, 18, 433.

102. K. Watenpaugh and C. N. Caughlan, Inorg. Chem., 1967, 6, 963.

103. W. P. Schaefer and R. E. Marsh, Acta Cryst., 1969, B25, 167.

104. A. Gieren and F. Schanda, Acta Cryst., 1977, B33, 2554.

105. C.-H. Chang, J. Pletcher, W. Furey, Jr., and M. Sax,

Acta Cryst., 1980, B36, 2655.

106. B.-C. Wang, B. T. Huie, and W. P. Schaefer, Acta Cryst., 1979,

B35, 1232.

107. R. J. Haines, E. Meintjies, and M. Lang, Inorg. Chim. Acta, 1979,

36, L403.

CHAPTER 2

CRYSTALLOGRAPHY

2.1 THEORY

2.1.1 INTRODUCTION^{1,2}

The fundamental characteristic of crystalline materials is their inherent periodicity. A crystal contains atoms, ions, or molecules arranged in a repetitive three-dimensional pattern in such a way as to give the system the lowest potential energy. Most well-formed crystals have their faces arranged in groups of two or more with respect to certain directions in the crystal. This is an indication of a very high degree of internal order. When each smallest repeating unit is considered as a point, then a three-dimensional lattice is defined. The smallest repeating unit in space is defined as the unit cell. The successive distances to translate this unit in the three non-coplanar directions define the unit cell dimensions a , b , and c , with the corresponding angles between them α , β and γ .

Unit cells in crystals can be chosen in various ways, either primitive, with one lattice point in the cell, or centred, with more than one lattice point in the cell. It is conventional to choose a unit cell which exhibits the highest symmetry present.

The possible symmetry elements are: a) rotational symmetry (order 2,3,4, and 6), b) reflection symmetry, c) inversion axes (order 1,2,3,4, and 6). There are seven three-dimensional co-ordinate systems which are useful in describing crystals and which are the basis for their classification. They are derived from a combination of the various symmetry elements with primitive cells, and are called crystal systems. When non-primitive unit cells are also taken into consideration, then 14 Bravais lattices can be formed. Table 2.1 summarises the seven crystal systems, relations between unit cell parameters, lattice symmetries, and the Bravais lattices associated with each of them.

Table 2.1: Classification of crystals

Crystal system	Unit cell parameters	Lattice symm.	Bravais lattice
Triclinic	$a \neq b \neq c$ $\alpha \neq \beta \neq \gamma$	$\bar{1}$	P
Monoclinic	$a \neq b \neq c$ $\alpha = \gamma = 90^\circ$ $\beta \neq 90^\circ$	2/m	P, C
Orthorhombic	$a \neq b \neq c$ $\alpha = \beta = \gamma = 90^\circ$	mmm	P, C, I, F
Tetragonal	$a = b \neq c$ $\alpha = \beta = \gamma = 90^\circ$	4/mmm	P, I
Rhombohedral	$a = b = c$ $\alpha = \beta = \gamma \neq 90^\circ$	$\bar{3}m$	R
Hexagonal	$a = b \neq c$ $\alpha = \beta = 90^\circ$ $\gamma = 120^\circ$	6/mmm	P
Cubic	$a = b = c$ $\alpha = \beta = \gamma = 90^\circ$	m3m	P, I, F

P=Primitive F=All face centred R=A doubly centred
 C=C face-centred I=Body centred

It can be shown from Group Theory that there are only 32 possible ways of combining the various crystallographic angular symmetry

elements. These 32 combinations constitute the crystal classes or point groups. It can also be shown that when the 32 point groups are combined with the 14 Bravais lattices, there are 230 unique ways of arranging identical objects in three-dimensional space. These 230 unique ways, called space groups, can also be obtained when the 32 point groups are combined with 2 new kinds of symmetry operations: screw axes and glide planes. A rotation axis followed by a translation parallel to that axis produces a screw axis. The combination of a mirror plane and a translation parallel to the reflecting plane form a glide plane.

2.1.2 X-RAY DIFFRACTION FROM CRYSTALS

(i) X-RAYS AND BRAGGS LAW: X-rays which have an approximate range of wave-lengths of 0.1 to 100 Å are usually produced when a target material is bombarded by a stream of fast electrons. The electrons are accelerated by an electric field and directed against a metal target, which rapidly decelerates them by multiple collisions. As a result of these collisions the system loses energy either by a) the emission of radiation or b) ejection of one or more photo-electrons from the target atom.

a) The energy, E , lost in the emission of the photon of radiation of frequency ν is given by Planck's relation $E = h\nu$. Under the usual conditions most of the electrons are not brought to a full stop by a single collision. The electron, after the first collision, may still have some energy left for further collisions with the emission of more radiation of lower frequencies, with a sharp upper limit corresponding to the maximum energy of the incident electron. Hence a continuum of

radiation is formed. This energy is determined by the accelerating potential of the X-ray tube, and is given by

$$E_{\max} = h\nu_{\max} = eV = hc/\lambda_{\min}$$

E_{\max} = Max. energy of the photon e = charge of the electron

h = Planck's constant

V_{acc} = Accelerating potential

ν_{\max} = Upper frequency limit

c = Velocity of light

λ_{\min} = Minimum wavelength

Hence the minimum wavelength of this continuum white radiation from the above equation is

$$\lambda_{\min} = 12.4/V_{\text{acc}} \text{ \AA}$$

b) In the second process, the incident electron displaces an electron of the target atom, let us say from the K-shell, if the former has an energy greater than the ionization energy of the latter. Then one electron from the K-shell is emitted as a photo-electron leaving the ionized atom in an excited state. When this happens, another electron from an outer shell will drop into the K-shell, a region of lower energy, and a photon will be emitted, in the form of an X-ray, with a frequency equivalent to the energy change of that electron. Hence the spectrum of this emitted radiation has a maximum intensity at a few wave-lengths characteristic of the target material.

The wave-lengths of the X-rays required for the observation of diffraction effects from crystals are of the same order as the interatomic distances. In 1912 Max von Laue showed that the

diffraction of X-rays by crystal lattices is analogous to the diffraction of visible light by a three-dimensional diffraction grating, where the electrons of the atoms replace the edges of the slits. In the same year W. L. Bragg deduced a simple equation (see below) treating diffraction as reflections from the planes in the lattice passing through unit cells and cutting unit cell dimensions at several points. The lattice planes are expressed by their Miller indices (h,k,l) , where a/h , b/k , c/l are proportional to the intercepts made on a, b, c respectively. Figure 2.1 shows θ_{hkl} , the angle of incidence and reflection for hkl planes, P_1 and P_2 , and d_{hkl} , the interplanar spacing between 2 parallel planes.

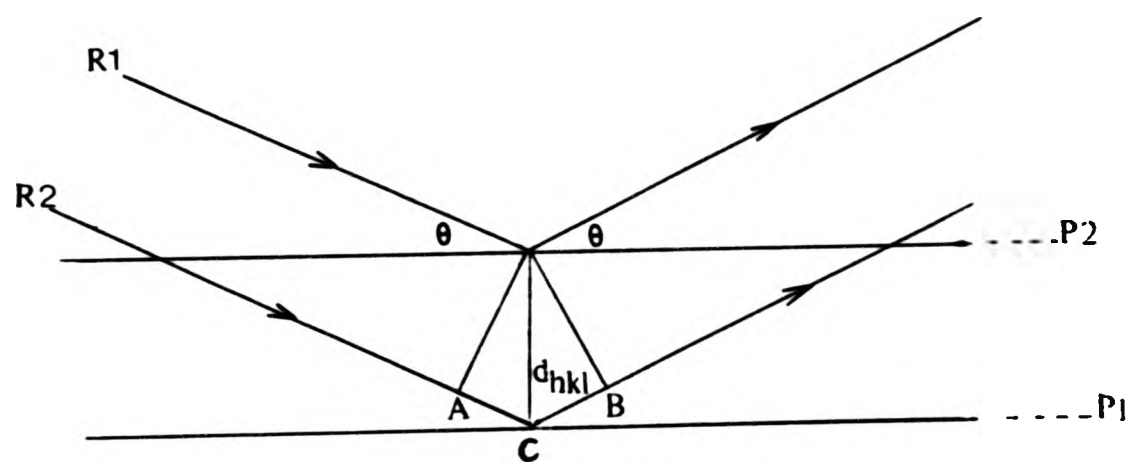


Figure 2.1

A diffracted beam of maximum intensity will result if the waves represented by rays R_1 and R_2 are in phase, i.e. when the path difference between these two rays is equal to λ or an integer number of λ , then diffraction maxima will occur. Therefore we can write:

$$AC + CB = n\lambda, AC = CB, 2AC = n\lambda$$

$$\text{Since } \sin\theta = AC/d$$

$$n\lambda = 2d\sin\theta$$

This is the Bragg equation. From this equation $\sin\theta = \lambda/2d \leq 1$. It follows that $d \geq \lambda/2$, so that for a given wave-length, λ , the smallest spacing which will give rise to diffraction is $\lambda/2$.

(ii) RECIPROCAL LATTICE: The concept of the reciprocal lattice was used by P. P. Ewald and extended by Max von Laue in 1913 to describe the relationship between crystal structures and their diffraction spectra. The laws of optical reflection require that the incident beam, the reflected beam, and the normal to the reflecting surface should lie in one plane. This condition, together with the magnitude of d , required by Bragg's law, suffices to define the directions of the diffracted beams relative to that of the incident beam and the orientation of the crystal. From Bragg's Law

$$\sin\theta = (n\lambda/2) \cdot 1/d$$

It can be seen that $\sin\theta$ is inversely proportional to the interplanar spacing d . Since $\sin\theta$ is a measure of the deviation of the diffracted from the incident beam, it is obvious that structures with large d -values will give compressed diffraction patterns and the converse holds for small d -values. A reciprocal lattice has the same symmetry as the direct one and is based on $1/d$ which varies directly with $\sin\theta$.

The reciprocal lattice is constructed in the following manner. Along the normals to the various planes of the direct lattice, points are marked off at distances $K(1/d)$ from the origin, where d is the spacing of the planes. Because all the planes nh, nk, nl have the same normal, every line will be divided at intervals of K/d_{hkl} . It is

generally convenient to make $K = \lambda$, the wave-length of the radiation. Therefore reciprocal lattice units are dimensionless. It can be shown that the set of reciprocal points form a true lattice, in which each point corresponds to a reflecting plane.

2.1.3 DETERMINATION OF CELL PARAMETERS

The unit cell dimensions can be determined directly using Bragg's Law, because at a particular value of n and for monochromatic radiation (constant wave-length), the angle of incidence or diffraction of the X-ray beam is dependent only on the separation of the diffracting lattice planes, which are directly related to the cell parameters. By measurement of the diffraction angles from known planes all the cell constants can be calculated.

Having determined the cell dimensions, it is a simple matter to calculate the volume, and if the density and molecular weight of the compound under investigation are known, the number of molecules in the unit cell can be found using the equation

$$Z = D_m \cdot V \cdot N / M$$

where z is the number of molecules per unit cell, D_m is the measured density (g/cm^3), V is the unit cell volume (cm^3) and N is Avogadro's number (6.023×10^{23}). A knowledge of the value of z considerably simplifies the solution of a structure.

2.1.4 DATA COLLECTION

(i) INTENSITY MEASUREMENTS: The intensity data provide basic information from which crystal structures are derived. As with all types of wave-motion, the intensities of the diffracted beams are directly proportional to the squares of their amplitudes.

$$|F_{hkl}| \propto (I_{hkl})^{1/2}$$

where I_{hkl} is the measured intensity of the beam diffracted by the (hkl) set of planes. The exact relationship between $|F_{hkl}|$ and I_{hkl} is dependent on a number of geometric factors which relate to each reflection and to the method used to measure the intensity, and may be written

$$|F_{hkl}| = [K \cdot I_{hkl} / Lp \cdot A]^{1/2}$$

where K is a scale factor, dependent on crystal size, the beam intensity, and a number of fundamental constants, and is used to set the relative scaled intensities on an absolute scale. L is the Lorentz, p the polarization, and A the transmission factor.

(ii) THE LORENTZ FACTOR (L): This is dependent on the exact technique used in the measuring intensities, as the time required for a reciprocal lattice point to pass through the sphere of reflection is not constant but varies with the position in reciprocal space and the direction in which it approaches the sphere. For four-circle diffractometer measurements, L has the simple form:

$$L = 1/(\sin^2\theta_{hkl}) \quad (\theta \text{ is the angle of incidence})$$

(iii) THE POLARIZATION FACTOR (p): This term arises because the reflection efficiency of the X-ray beam varies with the reflection angle, and so it is a simple function of 2θ , but it is not dependent on the method used to collect the data. The incident beam is unpolarized, that is, the electric vectors associated with its photons can point in any direction perpendicular to the direction of propagation. If each vector is considered in terms of its components in two directions: one parallel to the surface of the reflecting plane (w_1) and the other at right angles to it (w_2), the waves having their electric vectors parallel to the reflecting plane are reflected by an extent determined only by the electron density in the plane and not the reflection angle. The other vector is dependent on the electron density and $\cos^2 2\theta$, and will consequently decrease at higher 2θ angles. Because of this greater efficiency of reflection w_1 over w_2 , the reflected beam becomes partially polarized. The expression for the polarization factor is

$$p = [1 + (\cos^2 2\theta)]/2$$

(iv) ABSORPTION: when a photon of electromagnetic radiation hits a target material and imparts the whole of its energy to the atom, it emits a photo-electron. The attenuation of a beam of X-rays passing through a layer of matter is a function of the thickness of the layer, the number of atoms per unit area in the layer, their atomic numbers, and the wave-length of the X-rays.

When a beam of initial intensity I_0 passes through a layer of

thickness t

$$\text{then } dI/dx = -I\mu$$

where μ is called the linear absorption co-efficient and is a function of the material and of the wave-length. The emergent beam I is then expressed as $I = I_0 e^{-\mu x}$. The absorption is additive for all the different kinds of atoms in the material regardless of their state of aggregation, so that the linear absorption co-efficient may be calculated from a knowledge of the density of the material, the elements composing it, and the mass absorption co-efficients (μ/ρ) of the various elements.

$$\mu = d \sum_a P_a (\mu/\rho)_a$$

where d is the density of the material, P_a is the fraction by weight of the element A in the material, $(\mu/\rho)_a$ its mass absorption co-efficient at the particular wave-length.

To obtain the total intensity of scattering from whole crystal, the intensities of radiation scattered from different regions of the crystal are summed. For each reflection from planes (hkl) the absorption correction is calculated by evaluating the amount by which the incident and diffracted beams are reduced in intensity, and is expressed as

$$A_{hkl} = 1/V \int \exp[-\mu(x_i - x_d)] dV$$

where A_{hkl} is the transmission factor for each reflection, x_i is the

path-length of the incident beam before being scattered by the volume element, dV , and x_d is the path length after scattering.

Generally absorption increases with increasing wave-length. It is a continuous curve (the variation is roughly proportional to λ^3) with a number of discontinuities when there is a pronounced fall in absorption. These discontinuities correspond to the ionization energies of the various electronic levels of the atom. When the energy of the photon is not enough to ionize the electrons in the various shells, for example the K-shell, then the K-photo-electric process ceases and the absorption falls.

2.1.5 STRUCTURE SOLUTION

(i) SIGNIFICANT INTENSITIES: Intensity data obtained by automatic diffractometers consist of a gross intensity, measured at $2\theta_{hkl}$, and a background generally recorded on either side of the intensity maxima. A reflection is considered significant if

$$I_{hkl} \geq 3\sigma(I)$$

where I_{hkl} refers to the net intensity (gross minus background), and $\sigma(I)$ is the standard deviation of the intensity. $\sigma(I)$ is calculated using the equation

$$\sigma(I_{hkl}) = [I_{hkl} + 2B + (0.04I_{hkl})^2]^{1/2} \times \text{scale}$$

where B is the background. The 0.04 multiplicative term is introduced to prevent excessive weight being given to high intensity reflections. Scale includes the Lorentz factor L, and the polarization factor p.

$$\text{Then as } F_{hkl} = (I_{hkl})^{1/2}$$

$$\sigma(F_{hkl}) = \sigma(I_{hkl}) / 2F_{hkl}$$

path-length of the incident beam before being scattered by the volume element, dV , and x_d is the path length after scattering.

Generally absorption increases with increasing wave-length. It is a continuous curve (the variation is roughly proportional to λ^3) with a number of discontinuities when there is a pronounced fall in absorption. These discontinuities correspond to the ionization energies of the various electronic levels of the atom. When the energy of the photon is not enough to ionize the electrons in the various shells, for example the K-shell, then the K-photo-electric process ceases and the absorption falls.

2.1.5 STRUCTURE SOLUTION

(i) SIGNIFICANT INTENSITIES: Intensity data obtained by automatic diffractometers consist of a gross intensity, measured at $2\theta_{hkl}$, and a background generally recorded on either side of the intensity maxima. A reflection is considered significant if

$$I_{hkl} \geq 3\sigma(I)$$

where I_{hkl} refers to the net intensity (gross minus background), and $\sigma(I)$ is the standard deviation of the intensity. $\sigma(I)$ is calculated using the equation

$$\sigma(I_{hkl}) = [I_{hkl} + 2B + (0.04I_{hkl})^2]^{1/2} \times \text{scale}$$

where B is the background. The 0.04 multiplicative term is introduced to prevent excessive weight being given to high intensity reflections. Scale includes the Lorentz factor L , and the polarization factor p .

$$\text{Then as } F_{hkl} = (I_{hkl})^{1/2}$$

$$\sigma(F_{hkl}) = \sigma(I_{hkl}) / 2F_{hkl}$$

(ii) STRUCTURE FACTOR: When X-rays are diffracted by a crystal, the intensity of scattering at any angle can be calculated by considering the combination of the waves scattered from different atoms to give constructive or destructive interference.

When monochromatic radiation is used, the resultant wave scattered in a particular direction may be obtained by superimposing the individual waves, all of which have the same frequency, and this resultant can then be expressed in terms of its phase, θ_r , where

$$\theta_r = \tan^{-1} \left[\frac{\sum_j a_j \sin \theta_j}{\sum_j a_j \cos \theta_j} \right]$$

and its amplitude, a_r , where

$$a_r = \left[\left(\sum_j a_j \cos \theta_j \right)^2 + \left(\sum_j a_j \sin \theta_j \right)^2 \right]^{1/2}$$

a_j is the amplitude of the j th wave, and θ_j is the phase associated with it relative to some arbitrary origin.

An alternative expression for the resultant scattered beam can be derived by use of complex numbers, where a complex number, C , is defined as

$$C = x + iy$$

where x and y are real numbers, and i is $\sqrt{-1}$. Then the magnitude (amplitude) of C , $|C|$, is defined as the square root of the product of C with its complex conjugate, C^* , defined as $x - iy$, so that

$$|c| = |cc^*|^{1/2} = [(x+iy)(x-iy)]^{1/2} = (x^2 - i^2y^2)^{1/2} = (x^2 + y^2)^{1/2}$$

The similarity between this result and the amplitude equation is clear, so letting $A = \sum_j a_j \cos \theta_j$ and $B = \sum_j a_j \sin \theta_j$, this equation becomes

$$a_r = (A^2 + B^2)^{1/2}$$

Then, by using a power-series expansion on the identity

$$e^{i\theta} = \cos \theta + i \sin \theta$$

the expression for the total scattering can be written

$$A + iB = a_r \cos \theta_r + i a_r \sin \theta_r = a_r e^{i\theta_r}$$

and $\theta_r = \tan^{-1}(B/A)$

The electrons are the only part of the atom that scatter X-rays significantly, and as they are distributed over atomic volumes with dimensions comparable to the wave-lengths of X-rays, so X-rays scattered from one part of an atom will interfere with those scattered from another part at all scattering angles greater than 0° . At 0° in 2θ , all the electrons in the atom scatter in phase, and the scattering power of an atom at this angle, expressed relative to the scattering power of a free electron, is equal to the number of electrons present (the atomic number for neutral atoms).

The amplitude of scattering for an atom is called the atomic

scattering factor, and is denoted by f . If, for an atom assumed to have spherical symmetry, f is plotted against $(\sin\theta)/\lambda$, a fairly smooth curve results, showing the increase in destructive interference with increasing θ , and this can be used to interpolate the value of the atomic scattering factor at any angle of incidence.

The radiation scattered by one unit cell of a structure in any direction where there is a diffraction maximum has a particular combination of amplitude and phase, known as the structure factor $F(hkl)$. It is measured relative to the scattering by a single electron. The intensity of the scattered radiation is proportional to the square of the amplitude, $|F|^2$, and so the structure factor may be written

$$F(hkl) = |F(hkl)| e^{i\theta(hkl)} = A(hkl) + iB(hkl)$$

with $|F(hkl)|$ representing the amplitude of the scattered wave, and $\theta(hkl)$ its phase relative to the origin of the unit cell. It may also be defined in terms of the sum of the amplitudes and phases of the radiation scattered by the individual atoms in that direction, making use of the atomic scattering factors, thus

$$F(hkl) = \sum_j f_j e^{i\theta_j}$$

where f_j is the scattering factor of the j th atom, θ_j is the phase associated with it, and the summation is over all the atoms in the unit cell.

The phase of the wave scattered by an atom located at the position

x, y, z in the unit cell (in fractional co-ordinates) is equal to $2\pi(hx + ky + lz)$ radians, and so the above equation becomes

$$F(hkl) = \sum_j f_j e^{2\pi i(hx_j + ky_j + lz_j)}$$

or

$$F(hkl) = \sum_j f_j \cos 2\pi(hx_j + ky_j + lz_j) + i \sum_j f_j \sin 2\pi(hx_j + ky_j + lz_j).$$

(iii) THE TEMPERATURE FACTOR: In real crystals the atoms are not stationary but vibrate about their mean positions, and the magnitude of these vibrations depends on the temperature, the mass of the atom, and the strength of the bonding which holds it in position. In general, the higher the temperature, the greater the vibration, and this thermal motion spreads the electron cloud over a larger volume, causing the scattering power of the real atom to fall off more rapidly than in the ideal model. The change in scattering power is given by the expression

$$e^{-U_j(\sin^2\theta)/\lambda^2}$$

where U_j is the isotropic temperature factor for the j th atom, and represents the mean square displacement of the atom, in angstroms, from its mean position in a direction normal to the reflecting plane.

Hence, the complete expression for the structure factor for a particular reflection, (hkl) , is

$$F(hkl) = \sum_j f_j e^{i\theta_j} e^{-U_j(\sin^2\theta)/\lambda^2}$$

This isotropic correction, where the amplitude of vibration is equal in all directions, is a useful approximation in the early stages of structure refinement, but a more accurate representation can be obtained if anisotropic temperature factors are introduced. Here the assumption of spherical symmetry is abandoned, and the size and orientation of the thermal ellipsoid is described in terms of six parameters, defined in the expression

$$\exp[-2\pi^2(U_{11}h^2a^{*2}+U_{22}k^2b^{*2}+U_{33}l^2c^{*2}+2U_{12}hka^*b^*+2U_{13}hla^*c^*+2U_{23}klb^*c^*)]$$

Here the first three temperature factors (U_{ii}) define the dimensions of the tri-axial vibrational ellipsoid, and the final three (U_{ij}) its orientation referred to the reciprocal cell axes.

(iv) SPACE GROUP DETERMINATION: Intensity data collected, either as they are or converted to structure factors, give the information needed about the space group. If symmetry elements involving translation, such as glide planes, screw axes, are present, systematic absences will occur. These are reflections which are systematically zero because of space-group considerations rather than accidentally zero due to the particular arrangements of atoms in an asymmetric unit.

For example, if an n-glide, perpendicular to b, is present as a symmetry element, the atoms occur in pairs with co-ordinates (x, y, z,) and (x + 1/2, -y, z + 1/2). The structure factor equation may be written

$$F_{hkl} = \sum_{j=1}^{1/2N} f_j \{ \exp[2\pi i(hx_j + ky_j + lz_j)] + \exp\{2\pi i[h(x_j + 1/2) - ky_j + l(z_j + 1/2)]\} \}.$$

Then

$$F_{hkl} = \sum_{j=1}^{1/2N} f_j \{ \exp[2\pi i(hx_j + ky_j + lz_j)] + \exp[2\pi i(hx_j - ky_j + lz_j) + \pi i(h+1)] \}$$

For the special case, $k = 0$

$$F_{h0l} = \sum_{j=1}^{1/2N} f_j \{ \exp[2\pi i(hx_j + lz_j)] [1 + \exp \pi i(h+1)] \}$$

$$F_{h0l} = \sum_{j=1}^{1/2N} f_j \{ \exp[2\pi i(hx_j + lz_j)] [1 + (-1)^{h+1}] \}$$

$$= 0 \quad \text{for } (h+1) \text{ odd}$$

$$F_{h0l} = \sum_{j=1}^{1/2N} 2f_j \{ \exp[2\pi i(hx_j + lz_j)] \} \quad \text{for } (h+1) \text{ even.}$$

Hence, reflections of the type $h0l$ will be missing unless the sum of h and l is even, and this is the characteristic absence for an n -glide. Table 2.2 gives a list of the lattice information derived from the more commonly observed systematic absences, odd reflections being absent.

Unfortunately only a few space groups have unique diffraction patterns, so complete determination of the systematic absences may not uniquely define the space group, but it will limit it to one of a few possibilities. The actual space group can be determined by successful refinement of the structure.

2.1.6 ELECTRON DENSITY SYNTHESIS AND THE DETERMINATION OF PHASES

An image of the scattering matter in the unit cell, the electron distribution, may be obtained by describing the electron density, $\rho(x,y,z)$, at any point (x,y,z) in terms of some function of the

Table 2.2: Some common limiting conditions for reflections

Diffracting plane	Condition	Symmetry element present
h00	$h=2n$	2_1 screw axis along a
0k0	$k=2n$	2_1 screw axis along b
00l	$l=2n$	2_1 screw axis along c
hk0	$h=2n$	a glide perpendicular to c
hk0	$k=2n$	b glide perpendicular to c
hk0	$h+k=2n$	n glide perpendicular to c
h0l	$h=2n$	a glide perpendicular to b
h0l	$l=2n$	c glide perpendicular to b
h0l	$h+l=2n$	n glide perpendicular to b
0kl	$k=2n$	b glide perpendicular to a
0kl	$l=2n$	c glide perpendicular to a
0kl	$k+l=2n$	n glide perpendicular to a
hkl	$k+l=2n$	A centred lattice
hkl	$h+l=2n$	B centred lattice
hkl	$h+k=2n$	C centred lattice
hkl	$h+k=2n$ $h+l=2n$ $k+l=2n$	All face centred lattice
hkl	$h+k+l=2n$	Body centred lattice

diffraction. As crystals are periodic in three dimensions, ρ can be calculated using a three-dimensional Fourier series:

$$\rho(x,y,z) = 1/V \sum_h \sum_k \sum_l F_{hkl} \exp[-2\pi i(hx + ky + lz)]$$

where V is the volume of the unit cell, and F_{hkl} is the structure factor for the set of indices h, k and l . So, in theory, the electron density at all points in a three-dimensional asymmetric unit could be calculated and the molecular structure identified, regions of high electron density corresponding to the atom positions.

Unfortunately the structure factor is composed of two parts, as shown in section 2.1.5(ii), and only the structure factor amplitudes $|F_{hkl}|$, and not their phases, θ_{hkl} , can be obtained directly from intensity measurements. Therefore, by expanding the three-dimensional Fourier series equation in terms of sine and cosine, and assuming that Friedel's law holds, so that the sine terms cancel for pairs of F_{hkl} and $F_{\bar{h}\bar{k}\bar{l}}$, it can be rewritten as

$$\rho(x,y,z) = 1/V \sum_h \sum_k \sum_l |F_{hkl}| \cos 2\pi(hx + ky + lz - \theta_{hkl}).$$

It becomes clear that to evaluate the electron distribution, the phase of each reflection must be known, and consequently structural analysis becomes essentially a problem of determining these phases.

(i) PATTERSON METHOD: Patterson showed that, while the Fourier synthesis with $|F|$'s as the coefficients gives the distribution of atoms in the cell, a synthesis calculated with $|F|^2$'s as coefficients has

peaks corresponding to all the interatomic vectors. As the square of the structure factor amplitude has no associated phase, direct evaluation of the function P , at a point (u,v,w) , can be calculated from the measured intensities.

$$P(u,v,w) = 1/V \sum_h \sum_k \sum_l |F_{hkl}|^2 \cos 2\pi(hu + kv + lw)$$

The vector map produced is as if each atom in the molecule was, in turn, placed on an arbitrary origin and vectors drawn to all the other atoms, the peaks corresponding to the atom positions relative to this origin. If a vector is drawn from atom A to atom B, there will be another vector from B to A, equal in magnitude but opposite in direction, and, consequently, all Patterson syntheses are centrosymmetric.

For a molecule containing N atoms in the unit cell the Patterson will show N^2 peaks, of which N will be vectors of zero length from each atom to itself, resulting in a very large peak at the origin. The remaining $N^2 - N$ peaks will be distributed throughout the unit cell and for a structure of any size will be densely packed, resulting in considerable overlap, particularly as Patterson peaks are inherently wider than Fourier peaks. The resulting map would give an almost featureless distribution of vector density. Fortunately, the weight of a Patterson peak is proportional to the product of the atomic numbers of the atoms between which the vector occurs, and if there are a few atoms in the molecule that are significantly heavier (higher atomic numbers) than the rest, the vector peaks between them will stand out above the

background and make determination of their positions relatively simple. This is the "heavy atom method".

Having obtained the heavy atom positions from the vector analysis, a structure factor calculation for all (hkl) reflections on these positions should produce a set of phases in reasonably good agreement with the true ones. By combining these phases with the corresponding observed structure factor amplitudes an electron density synthesis can be computed, from which at least some of the light atom positions may be determined, despite inaccurate phases. Inclusion of these atoms in further structure factor calculations yields a better set of phases, and an iterative analysis follows until all the atomic positions are located.

(ii) DIRECT METHOD: Direct methods form a very powerful tool in structure solution when all the atoms have about the same atomic number. The structure is extracted from the intensity data by direct phase determination using analytical methods only. For centrosymmetric space groups the phases are either 0 or π , so the structure factors are simply obtained by assigning a plus or minus sign to each observed structure amplitude.

The electron density, in the unit cell, can never be negative but it will be close to zero except for the peaks at atom positions. From these facts certain relationships can be derived among the indices and among the structure amplitudes of the stronger reflections. For centrosymmetric structures the two simplest relationships are the Harker-Kasper inequality

$$U_{hkl}^2 < 1/2 + 1/2 U_{2h2k2l}$$

where $U_{hkl} = F_{hkl}/F_{000}$, so that the sign and magnitude of U_{hkl}^2 are known, while the phase of U_{2h2k2l} remains the only unknown, and secondly the Sayre probability equation

$$S(F_{hkl}) \sim S(F_{h'k'l'}) \cdot S(F_{-h',-k',-l'})$$

where S means 'the sign of' and \sim means 'is probably equal to', so that any structure factor F_{hkl} is determined by the products of all the pairs of structure factors whose indices sum to give (hkl) . If the magnitudes of U_{hkl} and U_{2h2k2l} are very large, the sign of the latter has to be positive for the inequality to hold, and so the sign of the reflection $(2h, 2k, 2l)$ has been determined. The above equation has a wider application, as it still probably holds for reflections whose intensities are too small for the inequalities, but are nevertheless relatively large. By use of both equations a sign expansion pathway can be set up and phases of sufficient reflections derived for the structure to be solved.

A problem in applying inequalities to $|F|$'s is that $|F|$ falls off with increasing $\sin\theta$ and rapidly lowers the $|F|/F_{000}$ ratios below the level where any phase information can be obtained. As the information content of a reflection is determined by its intensity relative to the average of its neighbours, more phase data may be obtained from relatively strong reflections at high $\sin\theta$, although they are much weaker than many at low $\sin\theta$ on an absolute scale. Thus, allowing for these factors, direct method calculations are carried out using

normalized structure factors, F_{hkl} , where all classes of reflections are normalized to a common basis, rather than F 's.

In practice, the whole process of centrosymmetric direct methods has become automatic with the computer programmes now available. For a simple light atom structure all the atom positions can usually be determined from the first "E-map" (a synthesis in which the coefficients are E 's, normalized structure factors, rather than F 's); in more complex situations some of the atoms can be located from the E-map and the rest by repeated use of Fourier techniques.

(iii) FOURIER DIFFERENCE SYNTHESIS: Once the position of one or more atoms has been located, Fourier difference syntheses can be used to find the rest. Structure factors calculated from the known positions are compared with the observed ones, F_o , and the difference in electron density is expressed by the equation

$$\Delta\rho = \frac{1}{V} \sum_{hkl} \sum_{-\infty}^{\infty} (|F_o| - |F_c|) e^{i\theta_c} e^{-2\pi i(hx+ky+lz)}$$

where θ_c is the phase of the calculated structure factor F_c . Therefore a Fourier synthesis calculation using $(|F_o| - |F_c|)$ as the coefficients will only give peaks where there is insufficient electron density in the trial structure, and troughs in positions where there is too much electron density. The result is a much clearer difference map with much less risk of peak overlap, and for a completely correct structure the map will have a practically flat topography.

The difference synthesis also overcomes the problem of series

termination errors experienced in electron density syntheses where the Fourier series require summation to infinity of h , k , and l . These errors cause spurious Fourier peaks and small ripples around the true maxima. In the difference synthesis, for a complete structure, the termination effects for both series will become identical, and their difference zero.

(iv) STRUCTURE REFINEMENT: Once all the approximate atom parameters have been derived, they can be improved until a best fit between the observed and the calculated structure factor amplitudes is obtained by an iterative process. There are two common refinement techniques, one involving Fourier syntheses and the other a least squares process. These methods are nearly equivalent, differing in the weighting attached to the experimental observations and in manipulative details. In crystallographic least squares routines, the observed diffraction intensities are fitted to the calculated ones so that the sum of the squares of the deviations is a minimum. This method is only applicable if there are many more observations than parameters, and, if it is felt that some measurements are more accurate than others, different "weights" can be applied to them, where the weight associated with a measurement is inversely proportional to the square of the standard deviation. Then, if ΔF is the difference in the amplitudes of the observed and calculated structure factors, $|F_o| - |F_c|$, and the standard deviation of $F_o(hkl)$ is $[w(hkl)]^{-1/2}$, the best parameters of the structure are those which correspond to the minimum values of the equation

$$M = \sum w(hkl) [\Delta |F(hkl)|]^2$$

where the sum is taken over all unique reflections. By analysing the equations for $|F_c|$, the effects of small changes in the parameters are considered, and the changes made which reduce M to a minimum.

For all the parameters to be refined, the minimisation of the above equation involves setting the derivatives of M with respect to each of the parameters equal to zero, giving a set of independent simultaneous equations. Unfortunately, these equations are far from linear, involving trigonometric and exponential functions, whereas the straightforward application of the method of least squares requires a set of linear equations. However, if the model structure is nearly complete, a set of linear equations can be derived in which the variables are the shifts from the model structure and not the parameters themselves. This is computed by expanding in a Taylor's series about the model parameters, and, as the shifts are small, all terms higher than the first derivative are neglected, so that

$$\Delta F_c = (\delta|F_c|/\delta x_1)\Delta x_1 + (\delta|F_c|/\delta y_1)\Delta y_1 + \dots \\ \dots + (\delta|F_c|/\delta U_{33,n})\Delta U_{33,n}$$

As the linearisation of the equations makes them only approximate, several cycles of refinement are required before they converge to a minimum. The linear approximation becomes better as the solution is approached, and as the higher derivative terms become negligible.

The degree of accuracy of a structure, at any stage of solution or refinement, may be expressed in terms of the residual or R-factor

$$R = \frac{\sum \left| |F_o| - |F_c| \right|}{\sum |F_o|},$$

thus giving the reflection-by-reflection agreement between the observed and calculated structure factor amplitudes. The corresponding weighted R-factor is

$$R_w = \left[\frac{\sum w (|F_o| - |F_c|)^2}{\sum w |F_o|^2} \right]^{1/2}.$$

The R-value should not be taken as conclusive proof of a good structure, because it is possible to have a few reflections with bad agreement which are masked by fair overall agreement. A correct structure should have no large, unexplained differences between F_o and F_c , give a flat Fourier difference map, a flat analysis of variance, and atom and bond parameters with low standard deviations.

2.2 TECHNIQUE

(i) DATA COLLECTION: A crystal suitable for X-ray analysis (less than 0.5 mm in the longest dimension, clean, with well-shaped faces, and not showing double growth) was selected under the microscope. It was mounted arbitrarily, on a thin quartz/glass fibre, using Araldite. A brass pin, to hold the fibre was placed on the PW1100 automated Philips diffractometer's goniometer. The crystal was then carefully centred using the x/y arcs.

The unit cell dimensions for each crystal were obtained using the powerful PW1100 diffractometer peak search routine without recourse to preliminary photographic techniques. This technique allowed an

arbitrarily mounted crystal to be used to collect 25 diffraction points in a predefined area of reciprocal space, for low values of θ . Analysis of a reduced matrix, $\tilde{UB}.UB$, where UB = machine orientation matrix, together with associated Dirichlet reduction transformation matrices, allowed the direct lattice constants to be derived. Accurate unit cell determinations were carried out by a least squares fit of the angular parameters of 25 reflections, with $\sim 16^\circ < 2\theta < 32^\circ$. Estimated standard deviations for unit cell dimensions were calculated from 15 successive refinements of 25 reflections. Intensity data were collected at room temperature with the $\omega - 2\theta$ scan mode and graphite monochromatised Mo- K_α radiation ($\lambda = 0.71069 \text{ \AA}$).

Depending on the diffracting power of the crystal and its believed chemical composition, different scan and background modes were used.

Scan mode 1 (SMO 1): This mode scans until an assigned count or an assigned number of scans is reached to increase the accuracy of weak reflections. This mode is being used for organic compounds, since the weak reflections would be needed in direct method solutions.

Scan mode 2 (SMO 2): This mode operates like SMO 1; however, preliminary scan and background measurements of 5 sec. at each side of the reflection were used as a criterion of rejection, while those reflections were ignored, for which

$$I_{\text{top}} - 2\sqrt{I_{\text{top}}} < I_{\text{bck}}$$

where I_{top} = the top intensity in counts/sec. measured at the top of

the reflection, I_{bck} = background intensity. This mode was used for compounds containing heavy atoms, since Patterson syntheses were used for their solution.

Background mode 1 (BMO 1): The background measuring time at each side of the scan is scan-time/2. The total background time is equal to the scan time.

Background mode 2 (BMO 2): The background measuring time at each side of the scan is scan-time/ $2\sqrt{I_{bck}/I_{int}}$, where I_{int} = total number of counts gathered during scans divided by the total scan-time.

After the first scan, preliminary background measurements of 5 sec. at each side of the peak were done. The mean of these two measurements determines the background intensity I_{bck} (count/sec.).

For all crystals a constant scan-speed of 0.05 sec^{-1} and a variable scan-width (SWD) of $(\text{SWD} + 0.01 \tan\theta)^c$ were used. Three reflections for each sample were measured every 3 to 6 hours during data collection to check crystal alignment and for possible crystal decomposition.

The appropriate portion of the reciprocal sphere for the particular crystal system under study was collected. For the triclinic, 1/2 of the reciprocal sphere ($\pm h, \pm k, \pm l$), for the monoclinic, 1/4 of that sphere ($\pm h, k, l$), and for the orthorhombic, 1/8 of the reciprocal sphere (h, k, l) was scanned.

For those crystals whose absorption (μ) was greater than 20cm^{-1} ,

absorption correction data were collected. This was done by the semi-empirical psi-scan method using programs supplied by Professor G. M. Sheldrick³. Selected reflections were measured at 10 intervals of rotation about their diffraction vector. A pseudo-ellipsoid model, in which the direction cosines were fitted to a 6-parameter equation to optimise the agreement between equivalent reflections (which were measured at the azimuthal angles), was used.

(ii) STRUCTURE SOLUTION: The raw data (peak intensity and background measurements) were converted to intensities using the data reduction program DRED⁴, written for the PW1100 Philips diffractometer. The intensity was given by $I = CT - tB$, where CT = total number of counts recorded during the peak scan, B = the total of the two background counts either side of the peak, t = the ratio of peak to background measuring times.

Estimated errors $[\sigma(I)]$ were calculated from the expression

$$\sigma(I) = [\sigma_c^2(I) + (0.04I)^2]^{1/2}$$

where $\sigma_c^2(I)$ = the variance due to counting statistics. The term $(0.04 I)^2$ was introduced to allow for other sources of errors.⁵

$$\sigma I = Lp[(scalexspeed)/(NSCXATT)][\sigma_c^2 + (0.04I)^2]^{1/2}$$

$$\sigma_c^2 = \text{total scan} + (B1+B2)[(NSCXSWD)/(SPEXBackground \text{ time})]$$

$$(0.04I)^2 = \text{total scan} - (B1+B2)[(NSCXSWD)/(SPEXBackground \text{ time})]$$

where $B1, B2$ = Background 1,2 SWD = Scan width
 NSC = Number of scans ATT = Attenuation factor

SPE = Speed.

The I and $\sigma(I)$ values were corrected for Lorentz and polarization factors. The reflections, which were measured twice to increase the accuracy, were averaged. From the systematic absences the space group was deduced and a unique data set obtained.

For all non-hydrogen atoms, the atomic scattering factors were taken from ref. 6, and for hydrogen atoms from ref. 7. The weighting scheme used for least squares refinement and analysis of variance was based on $\sigma(F)$ (estimated standard deviations of structure factors).

$$\sigma(F) = [\sigma(I)/2]^{1/2}$$

$$w = k/(\sigma^2 F + gF^2)$$

k was determined after each structure factor calculation and, if there were no systematic errors, it was not much greater than unity. Varying g, a fixed weighting scheme was applied to try to minimise the function $w.(F_o - F_c)^2$ as a function of the magnitude of F_o (observed structure factors).

For those crystals which contained heavy atoms, the Patterson synthesis was used; to others, direct methods were applied using normalized structure factors (E), where the sign expansion is based on the equation

$$S(h) = \text{Sign of} [E(k).E(h-k)].$$

For the direct method synthesis, the reflections with $F < \sigma F$ were set with $F = 1/2\sigma F$ in the data reduction program to aid in the normalization procedure.

The R-indices calculated for every structure are given in section 2.1.6(iv).

Detailed structure solution and refinement data are given with every structure.

(iii) DENSITY MEASUREMENTS: All the density measurements were carried out by the flotation method. For crystals with calculated densities less than 1.6 g/cm^3 , mixtures of carbon tetrachloride ($D = 1.595 \text{ g/cm}^3$) and chlorobenzene ($D = 1.10 \text{ g/cm}^3$) were used. For crystals with calculated densities greater than 1.6 g/cm^3 , mixtures of methyl iodide ($D = 2.28 \text{ g/cm}^3$) and carbon tetrachloride were used.

The specimen was immersed in the denser liquid and the less dense liquid (which is miscible with the former) was added until the sample neither sank nor rose in the solvent mixture. The density of the immersion medium was then determined by weighing a known volume of the liquid. The agreement between the measured and the calculated densities was ± 0.02 .

REFERENCES

1. G. H. Stout and L. H. Jensen, "X-Ray Structure Determination", MacMillan Publishing Co., Inc., New York, 1968.
2. M. F. C. Ladd and R. A. Palmer, "Structure Determination by X-Ray Crystallography", Plenum Press, New York and London, 1978.
3. G. M. Sheldrick, University of Cambridge, 1978, EMPABS, program for semi-empirical psi-scan absorption corrections.
4. J. Hornstra and B. Stubbe, PW1100 Data Processing Program, 1972, Philips Research Laboratories, Eindhoven, The Netherlands.
5. P. W. R. Corfield, R. J. Doedens, and J. A. Ibers, Inorg. Chem., 1967, 6, 197.
6. D. T. Cromer and J. B. Mann, Acta Cryst., 1968, A24, 321.
7. R. F. Stewart, J. Chem. Phys., 1965, 42, 3177.

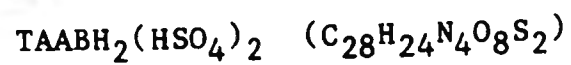
CHAPTER 3

STRUCTURAL INVESTIGATIONS OF TAAB SALTS

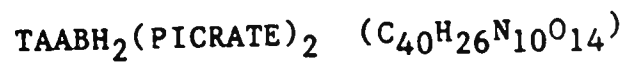
3.1 METHOD OF PREPARATION

20 Grams of crude o-aminobenzaldehyde, OAB, was dissolved in 50 ml of acetonitrile. To the yellow solution thus obtained, 10 ml of 48% tetrafluoroboric acid was added. The solution almost immediately deposited $\text{TAABH}_2(\text{BF}_4)_2$ as red crystals. The crystals and the solution were set aside overnight, filtered, and then washed with ethanol.¹

The same method on a smaller scale (1g OAB) was used to obtain crystals of $\text{TAABH}_2(\text{HSO}_4)_2$, $\text{TAABH}_2(\text{PICRATE})_2$, and $\text{TAABH}_2(\text{p-tolSO}_3)_2 \cdot 2\text{p-tolSO}_3\text{H} \cdot 4\text{H}_2\text{O}$, using sulphuric, picric, and p-toluenesulfonic acid respectively.



	C	H	N	S
Analysis: Found	55.2	3.85	9.4	10.8
Calculated	55.3	3.9	9.2	10.5



	C	H	N
Analysis: Found	55.0	3.0	16.45
Calculated	55.2	3.0	16.1

	TAABH ₂ (<u>p</u> -tolSO ₃) ₂ , 2 <u>p</u> -tolSO ₃ H, 4H ₂ O (C ₅₆ H ₅₈ N ₄ O ₁₆ S ₄)				
	C	H	N	S	O
Analysis: Found	57.1	5.1	5.0	11.2	22.3
Calculated	57.4	4.95	4.8	10.9	21.8

The crystals of TAABH₂(p-tolSO₃)₂, 2p-tolSO₃H, 4H₂O were not of very good quality, and were not investigated further. It is however worth noting that both forms (orthorhombic and monoclinic)² of p-tolSO₃H, H₂O contain H₃O⁺ and p-tolSO₃⁻ ions. It is likely that similar species are present in the above crystals, in which ample possibilities for hydrogen bonding should exist.

Crystals of the other three compounds, namely TAABH₂(BF₄)₂, TAABH₂(HSO₄)₂, and TAABH₂(PICRATE)₂, were found to be of very good quality for X-ray crystallography. One crystal from each compound was selected for X-ray structure determination.

3.2 DATA COLLECTION AND STRUCTURE DETERMINATIONS OF TAAB SALTS

3.2.1 DATA COLLECTION AND STRUCTURE SOLUTION OF TAABH₂(PICRATE)₂

Details of the data collection and of the crystal data are summarized in Tables 3.1 and 3.2.

Data reduction applied to the raw data consisting of 5758 reflections resulted in 1801 unique reflections with $I > 3\sigma(I)$. The following systematic absences were observed.

Table 3.1: Crystal data of o-aminobenzaldehyde condensation products

	TAABH ₂ (BF ₄) ₂	TAABH ₂ (HSO ₄) ₂	TAABH ₂ (PICRATE) ₂
Formula	C ₂₈ H ₂₂ N ₄ B ₂ F ₈	C ₂₈ H ₂₄ N ₄ S ₂ O ₈	C ₄₀ H ₂₆ N ₁₀ O ₁₄
Molecular weight	588	608	870
Crystal system	Monoclinic	Orthorhombic	Monoclinic
Space group	C2/c	Pmmm	P2/n
a (Å)	19.372(5)	14.100(3)	22.694(6)
b (Å)	8.877(2)	10.789(3)	9.344(3)
c (Å)	17.962(4)	8.876(2)	9.765(3)
α (°)	90.00	90.00	90.00
β (°)	116.72(2)	90.00	107.48(9)
γ (°)	90.00	90.00	90.00
Volume (Å ³)	2759.0	1340.7	1907.0
D _c (g/cm ³)	1.421	1.505	1.462
D _m (g/cm ³)	1.414	1.503	1.471
Z	4	2	2
F(000)	1200	632	900
μ(Mo-Kα)(cm ⁻¹)	0.82	2.10	0.72

Table 3.2: Data collection and structure solution details of
o-aminobenzaldehyde condensation products

	TAABH ₂ (BF ₄) ₂	TAABH ₂ (HSO ₄) ₂	TAABH ₂ (PICRATE) ₂
Crystal size (mm)	0.31x0.42x0.35	0.35x0.35x0.48	0.41x0.42x0.23
Crystal colour	Bright red	Bright red	Bright red
Shape	Chunky blocks	Cubic	Thick plates
BMO	1	1	1
SMO	2	1	1
Scan width (°)	1.20	1.30	1.30
θ-range (°)	3-30	3-30	3-30
Reflections	1262	2141	5758
measured			
Unique data set	1177	928	1801
Least-squares	267	148	290
parameters			
Data/parameter	5.4	6.2	6.2
Shift/e.s.d.	0.001	0.001	0.5
Weighting scheme	1/[σ ² (F)]	1/[σ ² (F)]	1/[σ ² (F)]
Max. electron			
dens. residue e/Å ³	0.45	0.20	0.20
R	0.065	0.057	0.050
R _w	0.071	0.053	0.049

h00	h=2n+1	h0l	h+l=2n+1
0k0	N.C.	hk0	N.C.
00l	l=2n+1	0kl	N.C.

The calculated density, $D_c = 1.462 \text{ g/cm}^3$, based on two molecules in the unit cell, using the volume of the unit cell, agreed with the measured density. ($D_m = 1.471 \text{ g/cm}^3$). From the above conditions the space group was deduced as the nonstandard one $P2/n$. Equivalent positions for $P2/n$,

1)	x	y	z
2)	-x	-y	-z
3)	1/2-x	y	1/2-z
4)	1/2+x	-y	1/2+z.

A centrosymmetric direct method was applied with E -values ≥ 1.2 and the 2 pathway was expanded to 576 signs using 5085 relations. From the E -map of highest combined figure of merit, 16 peaks (selected from the 34 highest ones) were used to locate all the non-hydrogen atoms in the cation. Successive difference Fourier and full matrix least-squares refinement calculations led to the location of the picrate anion. At this stage the refinement converged at $R = 0.20$ and it was not possible to refine it further. It was concluded that the molecule has the correct orientation, but the wrong position. To find the real positions of the atoms a tangent map was calculated with $E \geq 1.3$. The origins were selected manually taking care that they had the same parity as in the E -map. Several multisolutions were introduced manually. With $E \geq 1.6$, there were 1656 unique phase relations. The tangent map with

the highest value of R_0 gave the correct solution. From the 34 highest peaks 25 non-hydrogen atoms were located. When these atoms were used in blocked least-squares refinement calculations an R-value of 0.30 was obtained. The atoms were blocked as follows: block 1 picrate ion, block 2 cation. Successive difference Fourier and least-squares refinement calculations led to the location of all the remaining non-hydrogen atoms; at this stage $R = 0.09$. When all the non-hydrogen atoms were refined with anisotropic thermal parameters, all hydrogen atoms were located, $R = 0.075$. All observed hydrogen atom co-ordinates were included, and for refinement allowed to ride on their respective carbon and nitrogen atom co-ordinates with site occupation factors free and the temperature factors common. The final values of R and R_w were 0.050 and 0.049 respectively. The refinement was stopped when the calculated parameter shift/ e.s.d. ratio fell to a maximum of 0.001. The highest residual electron density of $0.45 \text{ e}/\text{\AA}^3$ was observed near the H(8) atom.

$$0.45 < \Delta\rho < 0.48$$

3.2.2 DATA COLLECTION AND STRUCTURE SOLUTION OF $\text{TAABH}_2(\text{HSO}_4)_2$

Details of data collection and of crystal data are summarised in Tables 3.1 and 3.2.

Data reduction applied to the raw data, consisting of 2141 reflections, resulted in 928 unique ones with $I > 3\sigma(I)$. The following systematic absences were observed:

h00	h=2n+1	hk0	h+k=2n+1
0k0	k=2n+1	0k1	N.C.
001	N.C.	h01	N.C.

Assuming that there are two molecules in the unit cell, the density was calculated, $D_c = 1.505 \text{ g/cm}^3$. It agrees very well with the measured density, $D_m = 1.503 \text{ g/cm}^3$. From the above conditions two space groups were possible.

These are:

- (i) the centric space group $Pm\bar{m}n$
- and (ii) the non-centric one $Pmn2_1$
- (when the k and l axes are exchanged).

Both space groups were investigated. Using a Patterson synthesis for the $Pmn2_1$ space group, the sulphur atom was located. Seven cycles of difference Fourier and full matrix least squares refinement calculations led to the location of 12 non-hydrogen atoms, $R = 0.57$. When the 12 non-hydrogen atoms were included in the refinement after 5 cycles, the refinement converged at $R = 0.34$, and 7 more non-hydrogen atoms were located. The newly found non-hydrogen atoms were included and after 5 cycles of full matrix least squares refinement calculations gave $R = 0.15$. When the HSO_4 counter-ion was refined with anisotropic thermal parameters the refinement converged at $R = 0.13$. 8 Hydrogen atoms were located geometrically and 9 further cycles of full matrix least squares refinement led to $R = 0.12$. A further 9 cycles with all the non-hydrogen atoms refined with anisotropic thermal parameters reduced the R-value to 0.083. It was not possible to refine the structure further, and, in addition, there were high correlations

h00	h=2n+1	hk0	h+k=2n+1
0k0	k=2n+1	0k1	N.C.
001	N.C.	h01	N.C.

Assuming that there are two molecules in the unit cell, the density was calculated, $D_c = 1.505 \text{ g/cm}^3$. It agrees very well with the measured density, $D_m = 1.503 \text{ g/cm}^3$. From the above conditions two space groups were possible.

These are:

- (i) the centric space group $Pmmn$
- and (ii) the non-centric one $Pmn2_1$
- (when the k and l axes are exchanged).

Both space groups were investigated. Using a Patterson synthesis for the $Pmn2_1$ space group, the sulphur atom was located. Seven cycles of difference Fourier and full matrix least squares refinement calculations led to the location of 12 non-hydrogen atoms, $R = 0.57$. When the 12 non-hydrogen atoms were included in the refinement after 5 cycles, the refinement converged at $R = 0.34$, and 7 more non-hydrogen atoms were located. The newly found non-hydrogen atoms were included and after 5 cycles of full matrix least squares refinement calculations gave $R = 0.15$. When the HSO_4 counter-ion was refined with anisotropic thermal parameters the refinement converged at $R = 0.13$. 8 Hydrogen atoms were located geometrically and 9 further cycles of full matrix least squares refinement led to $R = 0.12$. A further 9 cycles with all the non-hydrogen atoms refined with anisotropic thermal parameters reduced the R-value to 0.083. It was not possible to refine the structure further, and, in addition, there were high correlations

between the co-ordinates of the atoms shown in Diagram 3.1, on each side of mirror plane 2, which appears to exist.

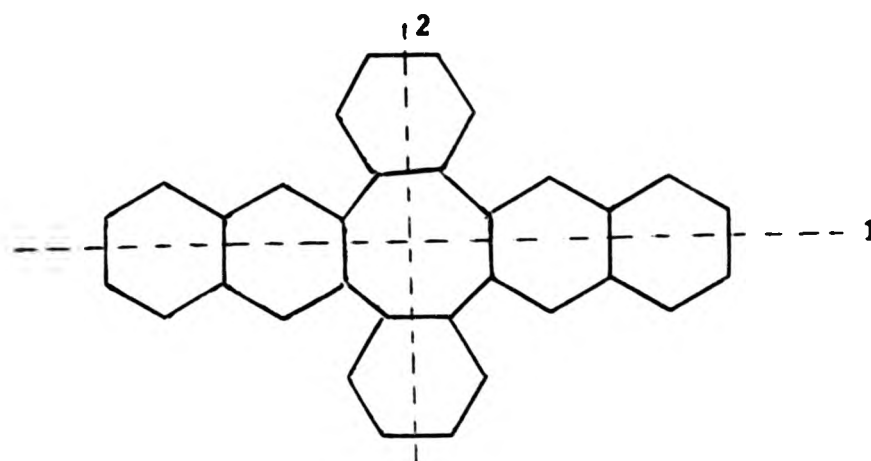


Diagram 3.1

At this stage it was considered that the space group $Pm\bar{m}n$ was the more likely one. Because of the mirror planes, which the space group $Pm\bar{m}n$ enforces to be present in the molecule, the asymmetric unit contains half of the HSO_4 ion. Hence the sulphur atom and two of the oxygen atoms have to lie on one of the mirror planes with half site occupancy factors. That was indeed what was found. The sulphur and oxygen atoms lying on the mirror plane are designated as S, O(2), and O(3) with half occupancy, the third one on one side of the mirror plane, O(1), with full occupancy. The Patterson map was solved for the sulphur atom for the $Pm\bar{m}n$ space group, where it was on a special position on the mirror plane with half occupancy and $y = 1/4$. Inclusion of the sulphur atom into the Fourier difference map led to the location of 10 non-hydrogen atoms with $R = 0.56$. When these were included, 6 cycles of difference Fourier and full matrix least squares refinement led to $R = 0.25$. One more oxygen atom O(2), lying on the mirror plane, was located. The observed oxygen atom was included, the sulphur and all carbon and nitrogen atoms were refined with anisotropic thermal parameters. 6 Cycles of refinement led to $R = 0.22$. The second oxygen atom, O(3), lying on the mirror plane was located. 6 Cycles of full

matrix least squares refinement with the last oxygen atom found also included, and the full occupancy oxygen atom refined with anisotropic thermal parameters, gave $R = 0.14$. When the half occupancy oxygen atoms were also refined with anisotropic thermal parameters, 10 cycles of refinement led to $R = 0.09$. 5 Hydrogen atoms, except that on the C(1) atom, were located at this stage. The 5 hydrogen atoms were included, and 8 cycles of blocked full matrix refinement gave $R = 0.081$. The atoms were blocked as follows: Block 1 all non-hydrogen atoms, block 2 all the hydrogen atoms. A high thermal vibration was observed for the O(1) atom along the z-axis. Disorder of this atom was considered. The O(1) atom was deleted from the atom list and a difference Fourier map was calculated. In the three-dimensional difference Fourier map, two maxima were observed along the z-axis. The O(1) atom was resolved into two components, O(1a) and O(1b), each having one of these maxima as z-co-ordinate, which gave on refinement site occupancy factors of 0.45 and 0.55 respectively. This vibration along the z-axis (because of the nature of the tetrahedron, and also the vibration being perpendicular to the S-O bond) would automatically cause vibration of the other oxygen atoms, O(2) and O(3), along the x-axis. As a result the O(2) and O(3) atoms would be respectively on and off the mirror plane. Therefore, the half hydrogen atom which one would expect to find on one of the oxygen atoms, O(2) or O(3), will produce a second image, appearing to belong to the other oxygen atom. This was observed. When all the non-hydrogen atoms were refined with anisotropic thermal parameters, and all the located hydrogen atoms were included, 6 cycles of refinement led to $R = 0.066$, $R_w = 0.061$. Three high electron density points were observed near C(1) and near the two oxygen atoms with half occupancy, O(2) and O(3), which could be considered as half hydrogen atoms at the first

point, and two quarter hydrogen atoms at the other two positions, at distances of 1.20, 0.91, and 1.31 Å from C(1), O(2), and O(3) respectively. It was assumed that C(1) has H(1) at a distance of 1.20 Å with half occupancy, and the two oxygen atoms, O(2) and O(3), have the last two hydrogen atoms with 1/4 occupancy at a distance of 0.91 Å each, caused by the disorder in the HSO₄ ion (see section 3.3.2.). When these 3 hydrogen atoms were included, 8 cycles of full matrix refinement converged at R = 0.062, R_w = 0.058. When the statistical disorder model was assumed (see section 3.3.2.) [the N(1), N(2), C(1), and C(8) atom positions were assumed to be simultaneously occupied by 1/2 N and 1/2 C atoms], the R-factor dropped to 0.057, and R_w = 0.053. The refinement was stopped when the calculated parameter shift/e.s.d. ratio fell to a maximum of 0.001. The highest residual electron density of 0.20 e/Å³ was observed near the H(N1) atom.

$$0.20 < \Delta\rho < -0.22$$

point, and two quarter hydrogen atoms at the other two positions, at distances of 1.20, 0.91, and 1.31 Å from C(1), O(2), and O(3) respectively. It was assumed that C(1) has H(1) at a distance of 1.20 Å with half occupancy, and the two oxygen atoms, O(2) and O(3), have the last two hydrogen atoms with 1/4 occupancy at a distance of 0.91 Å each, caused by the disorder in the HSO₄ ion (see section 3.3.2.). When these 3 hydrogen atoms were included, 8 cycles of full matrix refinement converged at R = 0.062, R_w = 0.058. When the statistical disorder model was assumed (see section 3.3.2.) [the N(1), N(2), C(1), and C(8) atom positions were assumed to be simultaneously occupied by 1/2 N and 1/2 C atoms], the R-factor dropped to 0.057, and R_w = 0.053. The refinement was stopped when the calculated parameter shift/e.s.d. ratio fell to a maximum of 0.001. The highest residual electron density of 0.20 e/Å³ was observed near the H(N1) atom.

$$0.20 < \Delta\rho < -0.22$$

3.2.3 DATA COLLECTION AND STRUCTURE SOLUTION OF $\text{TAABH}_2(\text{BF}_4)_2$

Details of the data collection and of the crystal data are summarised in Tables 3.1 and 3.2.

Data reduction applied to the raw data, consisting of 1262 reflections, resulted in 1177 unique reflections with $I > 3\sigma(I)$. The following systematic absences were observed:

hkl	$h + k = 2n$		
h0l	$l = 2n$ ($h = n$)	h00	N.C.
0kl	N.C.	0k0	$k = 2n$
hk0	N.C.	00l	N.C.

Assuming that there are 4 molecules in the unit cell, the density was calculated, $D_c = 1.414 \text{ g/cm}^3$. It was in good agreement with the measured one, $D_m = 1.407 \text{ g/cm}^3$. The two possible space groups are Cc and C2/c. Direct methods were applied to both space groups. Only the centrosymmetric one, C2/c, gave the solution. A centrosymmetric direct method was applied with E-values ≥ 1.4 , and the $\Sigma 2$ pathway was expanded to 290 signs using 2436 relations. The first E-map gave the positions of all the 21 non-hydrogen atoms. Successive difference Fourier and full matrix least squares refinement calculations led to $R = 0.205$. In further cycles of refinement, the C(1) and C(8) atoms (See Diagram 3.2) and the BF_4 ion were refined with anisotropic thermal parameters. At this stage refinement converged at $R = 0.135$. Disorder was observed in the BF_4 ion. In the next cycle the remaining non-hydrogen atoms were refined with anisotropic thermal parameters and the refinement converged at $R = 0.121$. At this stage all the hydrogen atoms were located

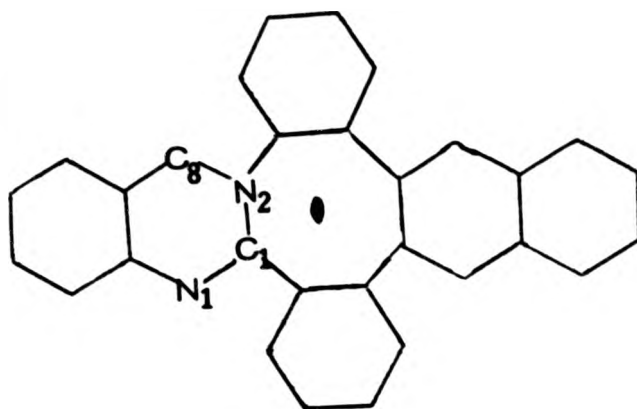


Diagram 3.2

[including H(8) and H(N1)]. All hydrogen atom co-ordinates were estimated geometrically (assuming C-H = 1.08 Å), and for refinement allowed to ride on their respective carbon atom co-ordinates. The refinement converged at R = 0.101.

To resolve the disorder observed in the BF_4 ion, the 4 fluorine atoms were deleted, and difference Fourier and full matrix least squares refinement calculations were carried out. The 4 fluorine atoms were observed with each having two maxima in the difference Fourier map along the x-, y-, and z-directions. Hence each fluorine atom was treated as if it consisted of two half atoms. These are labelled as F(1a), F(1b), F(2a), F(2b), F(3a), F(3b), F(4a), and F(4b), each having half occupancy. One further cycle with bond instructions permitted the correct tetrahedral pairs to be selected. In the next 5 cycles the site occupancy factors of each tetrahedral pair of 4 fluorine atoms were refined. The site occupancy factors of the (a)- and (b)-components were found to be 0.617 and 0.383 respectively. The R-factor converged at 0.090.

In the next 5 cycles, blocked full matrix least squares refinement was applied. Each pair of BF_4 ions (a- and b-components) was refined using separate blocks, and the cation as the third block. For this

refinement a $\lambda/\sin^2\theta$ cut-off value of 0.3 was used. At the same time the C(1) and C(8) atoms were exchanged with the N(2) and N(1) atoms respectively. The refinement converged at 0.077. Two possible hydrogen peaks near C(1) (1.14 Å) and N(2) (1.46 Å) were observed. For the reasons given in the following discussion section, a statistical disorder model was introduced (see section 3.3.2) and the N(1), N(2), C(1), and C(8) atom positions were assumed to be occupied by half nitrogen and half carbon atoms. A further 6 cycles of full matrix least squares refinement led to $R = 0.067$, $R_w = 0.071$. The atoms were blocked as follows: the cation and the boron atom (block 1), the (a)-component of the 4 fluorine atoms (block 2), and the (b)-component of the 4 fluorine atoms (block 3), and all the hydrogen atoms including H(1) and H(N1), located from an earlier difference map at 1.27 and 1.41 Å respectively with half occupancy (block 4). The refinement was stopped when the calculated parameter shift/e.s.d. ratio fell to a maximum of 0.5. The highest residual electron density of $0.2 \text{ e}/\text{Å}^3$ was observed near the F(1b) atom.

$$0.20 > \Delta\rho > -0.20$$

3.3 DISCUSSION OF TAAB SALTS

Chronologically the investigations of the TAAB salts started with the tetrafluoroborate; this was followed by the bisulphate; and then the picrate. As the last of these was an ordered structure, whilst the first two were disordered, it will be more meaningful to discuss the structures in the reverse order to the chronological one.

3.3.1 TAABH₂(PICRATE)₂

The compound TAABH₂(PICRATE)₂ has the structure (with a crystallographic two-fold symmetry imposed on the molecule) shown in Figure 3.1, which also shows the numbering scheme used together with the important bond lengths and angles. The bond length and angle data for the complete structure is in Tables 3.3 and 3.4. The ORTEP drawings of the structure are in Drawing 3.1.

The data set for the compound was good and no disorder was observed either in the cation or in the anionic counter-ion. The X-ray results show clearly that the heterocyclic skeleton proposed by Busch and co-workers¹ (structure A) is correct, and the structure B (Diagram 3.3), suggested for this cation by Goddard and Norris³ is definitely ruled out.

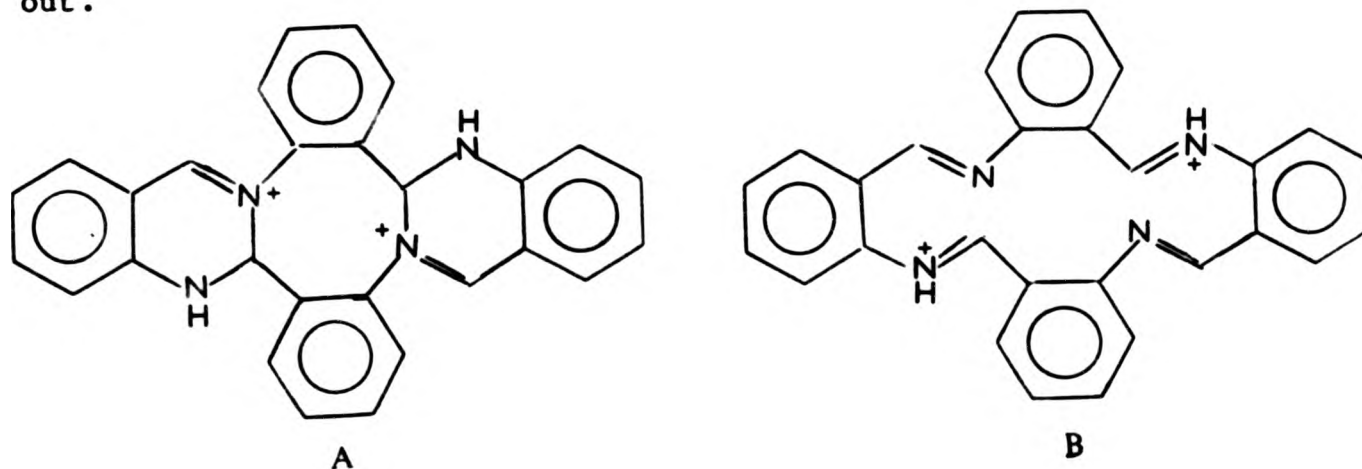


Diagram 3.3

The bond lengths C(1)-N(2), C(9)-N(2), and C(1)-C(14') are 1.484(5), 1.464(5), and 1.491(5) Å respectively; these have single bond character. The comparison between these bond lengths and some examples reported in the literature for similar bonds is given below.

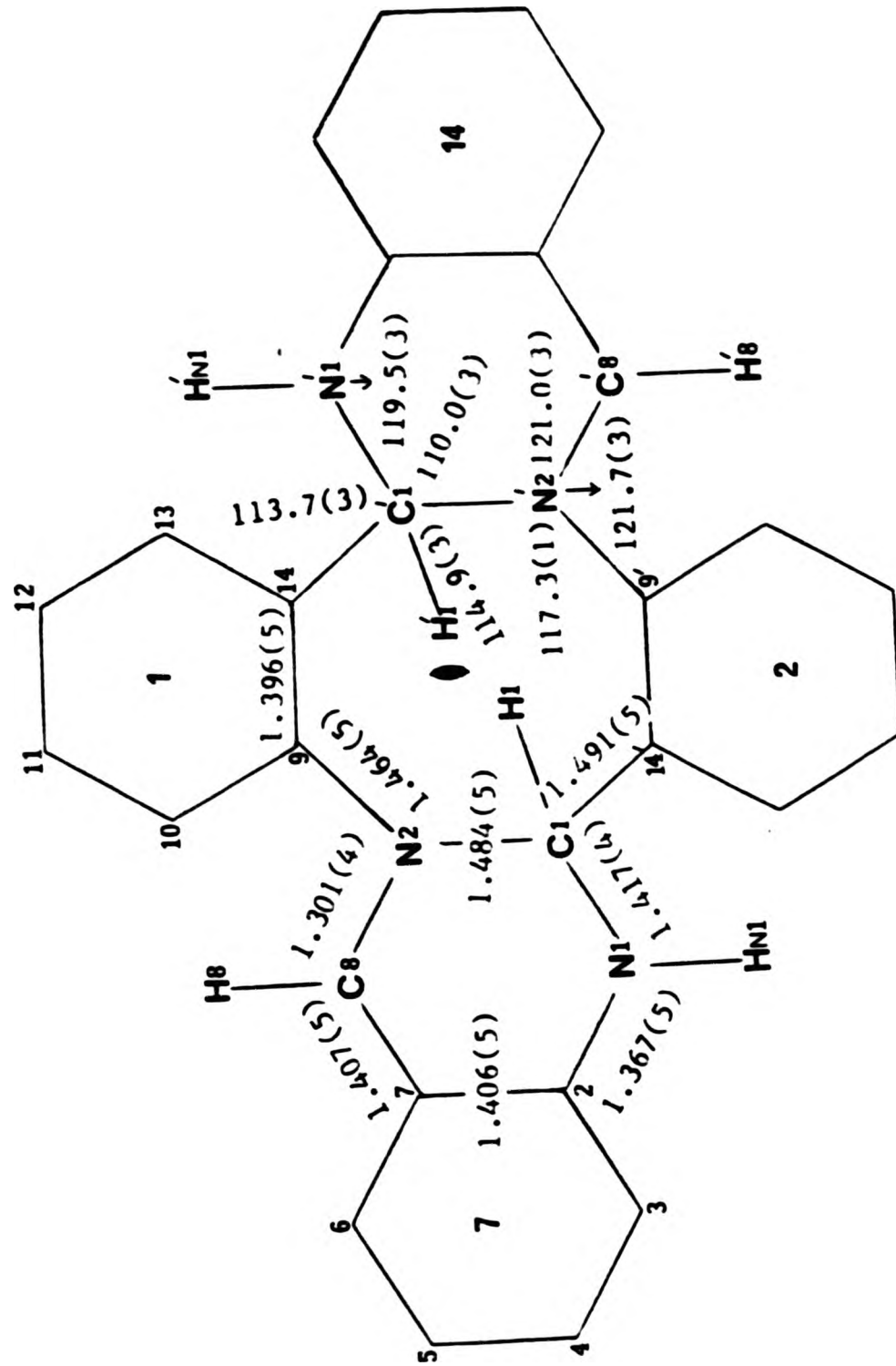


Figure 3.1

Table 3.3 Bond lengths (Å) for TAABH₂(PICRATE)₂

N(1) -C(1)	1.417(4)	N(1) -C(2)	1.367(5)
N(2) -C(1)	1.484(5)	N(2) -C(8)	1.301(4)
C(1) -C(14)	1.491(5)	C(2) -C(3)	1.402(5)
C(2) -C(7)	1.406(5)	C(3) -C(4)	1.375(6)
C(4) -C(5)	1.405(6)	C(5) -C(6)	1.363(6)
C(6) -C(7)	1.412(5)	C(7) -C(8)	1.407(5)
C(9) -C(10)	1.362(5)	C(9) -C(14)	1.396(5)
C(10) -C(11)	1.389(6)	C(11) -C(12)	1.380(6)
C(12) -C(13)	1.399(5)	C(13) -C(14)	1.380(5)
Cp(1) -Cp(2)	1.368(5)	Cp(1) -Cp(6)	1.464(5)
Cp(1) -Np(a)	1.457(5)	Cp(2) -Cp(3)	1.392(5)
Cp(3) -Cp(4)	1.382(5)	Cp(3) -Np(b)	1.457(5)
Cp(4) -Cp(5)	1.367(5)	Cp(5) -Cp(6)	1.461(5)
Cp(5) -Np(c)	1.453(5)	Cp(6) -O(7)	1.243(4)
Np(a) -O(1)	1.206(4)	Np(a) -O(2)	1.223(4)
Np(b) -O(3)	1.226(4)	Np(b) -O(4)	1.240(5)
Np(c) -O(5)	1.231(4)	Np(c) -O(6)	1.226(4)
N(2) -C(9)	1.464(5)		

Table 3.3 continued

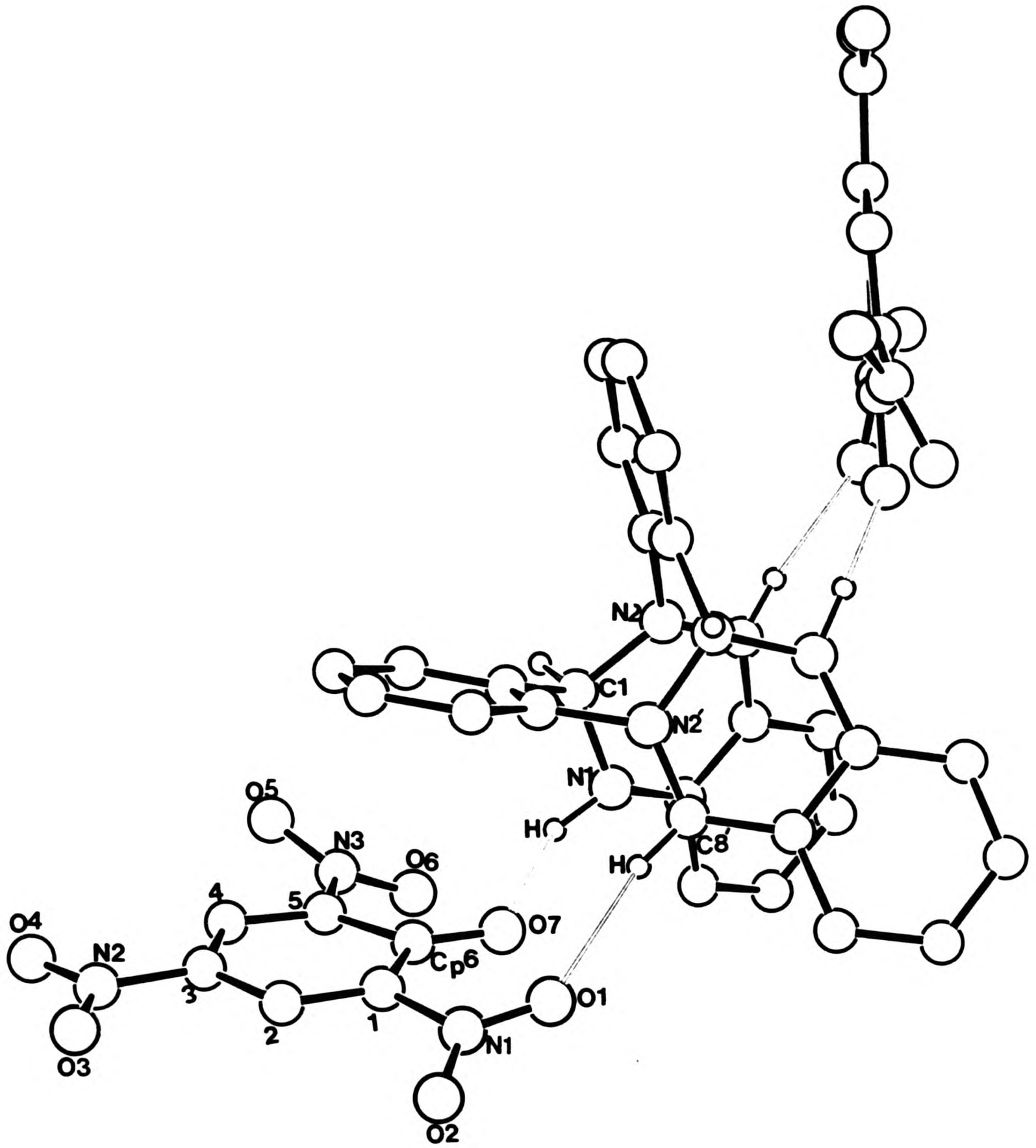
N(1) -Hn(1)	.979(1)	C(1) -H(1)	1.041(1)
C(3) -H(3)	1.080	C(4) -H(4)	1.080
C(5) -H(5)	1.080	C(6) -H(6)	1.080
C(8) -H(8)	.948(1)	C(10) -H(10)	1.080
C(11) -H(11)	1.080	C(12) -H(12)	1.080
C(13) -H(13)	1.080	Cp(2) -Hp(2)	1.080
Cp(4) -Hp(4)	1.080		

Table 3.4 Bond angles ($^{\circ}$) for $\text{TAABH}_2(\text{PICRATE})_2$

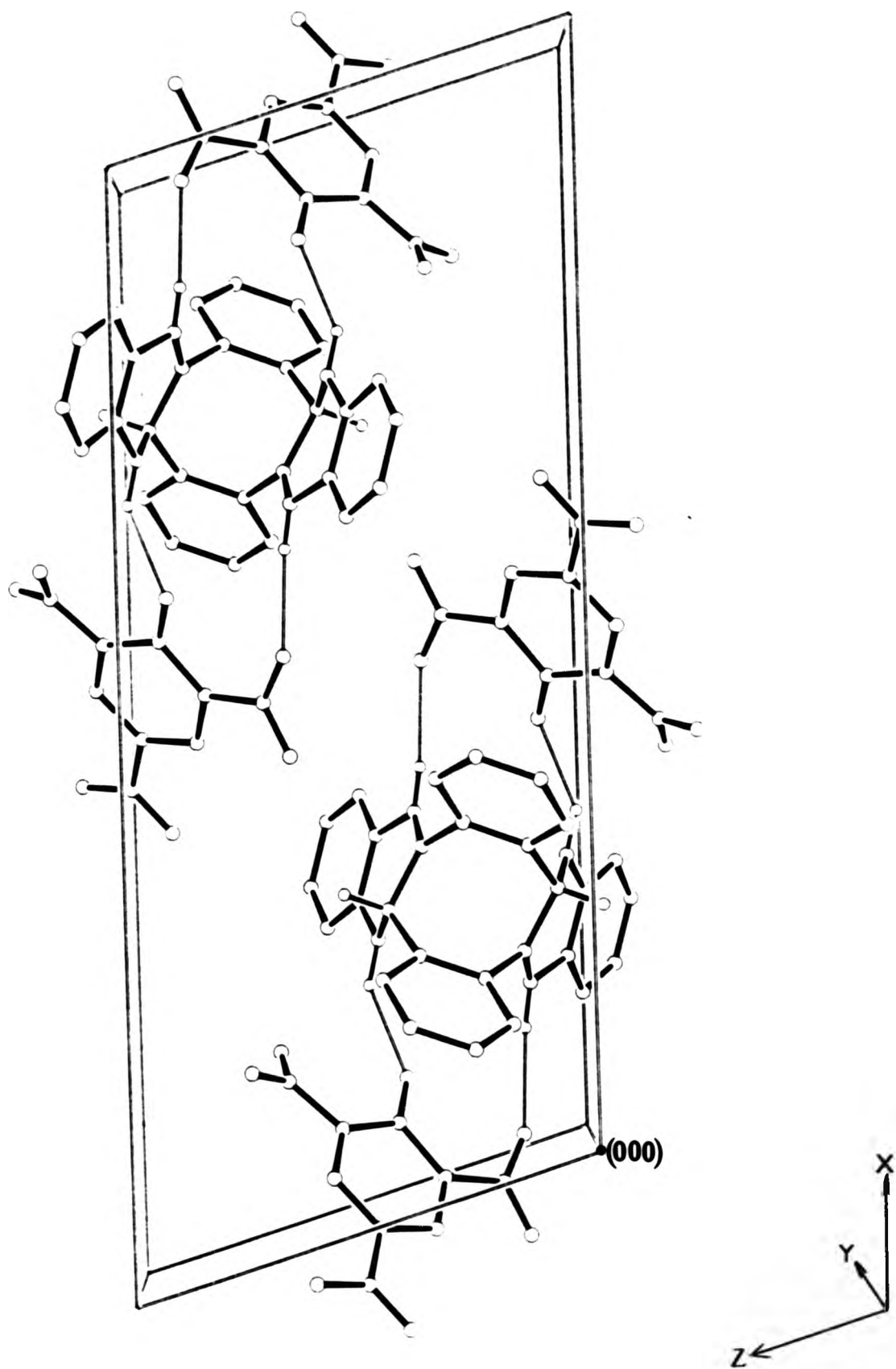
C(2) -N(1) -C(1)	119.5(3)	C(8) -N(2) -C(1)	121.0(3)
C(9) -N(2) -C(1)	117.3(1)	C(9) -N(2) -C(8)	121.7(3)
N(2) -C(1) -N(1)	110.0(3)	C(14) -C(1) -N(1)	113.7(3)
C(14) -C(1) -N(2)	114.9(3)	C(3) -C(2) -N(1)	121.9(4)
C(7) -C(2) -N(1)	118.3(4)	C(7) -C(2) -C(3)	119.7(4)
C(4) -C(3) -C(2)	119.0(4)	C(5) -C(4) -C(3)	121.5(4)
C(6) -C(5) -C(4)	120.0(4)	C(7) -C(6) -C(5)	119.8(4)
C(6) -C(7) -C(2)	119.9(4)	C(8) -C(7) -C(2)	117.8(4)
C(8) -C(7) -C(6)	122.1(4)	C(7) -C(8) -N(2)	121.0(4)
C(14) -C(9) -C(10)	122.1(4)	C(11) -C(10) -C(9)	119.1(4)
C(12) -C(11) -C(10)	120.5(4)	C(13) -C(12) -C(11)	119.5(4)
C(14) -C(13) -C(12)	120.5(4)	C(9) -C(14) -C(1)	121.8(3)
C(13) -C(14) -C(1)	119.8(3)	C(13) -C(14) -C(9)	118.3(4)
Cp(6) -Cp(1) -Cp(2)	124.9(4)	Np(a) -Cp(1) -Cp(2)	115.6(4)
Np(a) -Cp(1) -Cp(6)	119.4(3)	Cp(3) -Cp(2) -Cp(1)	118.5(4)
Cp(4) -Cp(3) -Cp(2)	121.6(4)	Np(b) -Cp(3) -Cp(2)	118.9(4)
Np(b) -Cp(3) -Cp(4)	119.5(4)	Cp(5) -Cp(4) -Cp(3)	119.5(4)
Cp(6) -Cp(5) -Cp(4)	124.3(4)	Np(c) -Cp(5) -Cp(4)	115.1(4)
Np(c) -Cp(5) -Cp(6)	120.6(4)	Cp(5) -Cp(6) -Cp(1)	111.1(3)
O(7) -Cp(6) -Cp(1)	124.6(4)	O(7) -Cp(6) -Cp(5)	124.3(4)
O(1) -Np(a) -Cp(1)	120.3(3)	O(2) -Np(a) -Cp(1)	118.8(4)
O(2) -Np(a) -O(1)	120.9(4)	O(3) -Np(b) -Cp(3)	119.1(4)

Table 3.4 continued

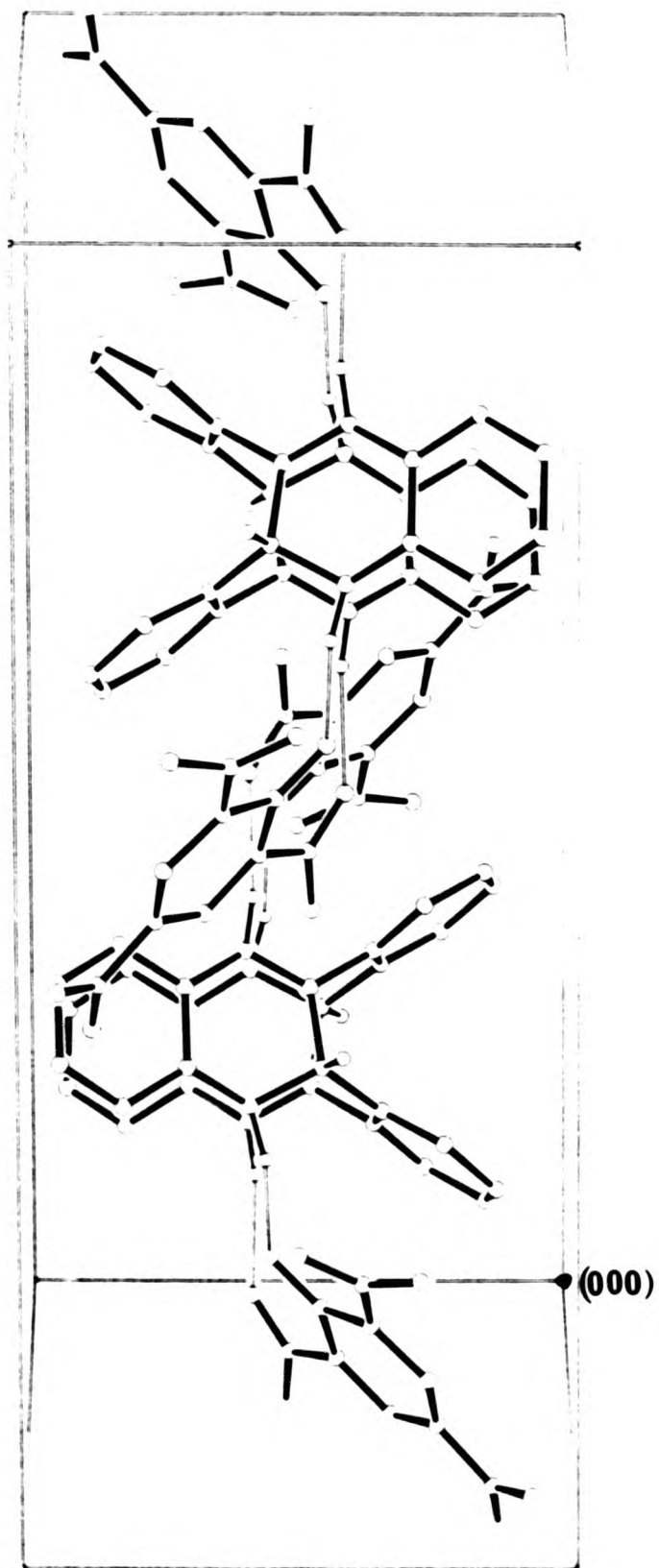
O(4)	-Np(b)	-Cp(3)	117.0(4)	O(4)	-Np(b)	-O(3)	124.0(4)
O(5)	-Np(c)	-Cp(5)	118.4(4)	O(6)	-Np(c)	-Cp(5)	118.4(4)
O(6)	-Np(c)	-O(5)	123.2(4)				
C(1)	-N(1)	-Hn(1)	103.0(2)	C(2)	-N(1)	-Hn(1)	131.5(2)
H(1)	-C(1)	-N(1)	107.8(2)	H(1)	-C(1)	-N(2)	100.7(2)
C(14)	-C(1)	-H(1)	108.7(2)	H(3)	-C(3)	-C(2)	120.5(2)
C(4)	-C(3)	-H(3)	120.5(3)	H(4)	-C(4)	-C(3)	119.3(3)
C(5)	-C(4)	-H(4)	119.3(3)	H(5)	-C(5)	-C(4)	120.0(3)
C(6)	-C(5)	-H(5)	120.0(3)	H(6)	-C(6)	-C(5)	120.1(3)
C(7)	-C(6)	-H(6)	120.1(3)	H(8)	-C(8)	-N(2)	112.0(2)
H(8)	-C(8)	-C(7)	121.2(2)	H(10)	-C(10)	-C(9)	120.5(3)
C(11)	-C(10)	-H(10)	120.5(2)	H(11)	-C(11)	-C(10)	119.7(2)
C(12)	-C(11)	-H(11)	119.7(3)	H(12)	-C(12)	-C(11)	120.3(3)
C(13)	-C(12)	-H(12)	120.3(3)	H(13)	-C(13)	-C(12)	119.7(3)
C(14)	-C(13)	-H(13)	119.7(2)	Hp(2)	-Cp(2)	-Cp(1)	120.7(2)
Cp(3)	-Cp(2)	-Hp(2)	120.7(2)	Hp(4)	-Cp(4)	-Cp(3)	120.3(3)
Cp(5)	-Cp(4)	-Hp(4)	120.3(2)				



Drawing 3.1a



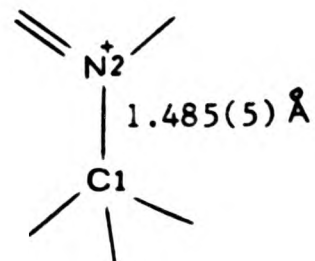
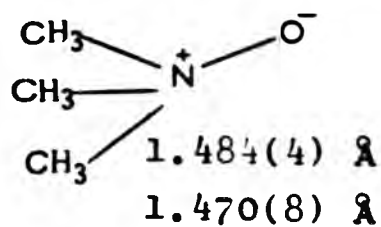
Drawing 3.1b



Drawing 3.1c

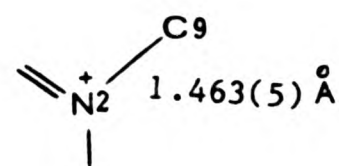
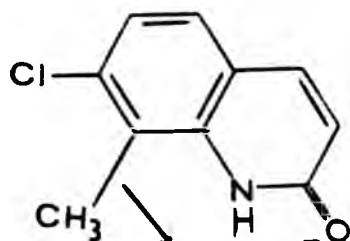
Examples:

Present structure

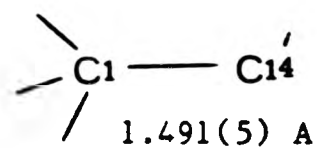
1) Trimethylamine Oxide $(\text{CH}_3)_3\text{NO}^+$ 2) Ni(TAAB) $(\text{CH}_2\text{COCH}_3)_2^5$

see section 5.3.2

1.431(9) Å
 1.430(9) Å

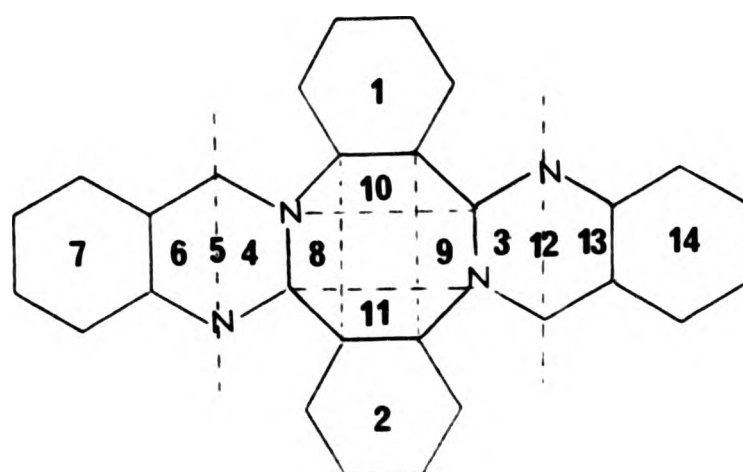
3) 7-Chloro-8-methylcarbostyryl⁶

1.495(5) Å



The above are some fairly recent examples from the literature. Dewar⁷ gives a value of 1.485 Å for an sp^2 - sp^2 carbon-carbon bond with zero π -bond order. He also quotes a value of 1.483 Å for the central bond in butadiene. The angle between the benzo ring (2) and the segment (4) of the heterocyclic ring is 89° (see Figure 3.1 and Table 3.5). The benzo ring is thus orthogonal with the segment (4), and hence no conjugation or hyperconjugation between C(1) and C(14') is possible. A value comparable in accuracy to the above (Csp^2 - Csp^2) for a pure C-C single bond between sp^3 - and sp^2 -hybridized carbon atoms is not available. The value of 1.491 Å between C(1) and C(14') is hardly

Table 3.5: Angles between the planes in the TAAB salts



planes	BF_4 angles	HSO_4 angles	picrate angles
1-2	68	65	68
3-4	27	23	16
6-13	72	69	60
4-8, 3-9	22	24	27
7-14	61	61	52
8-9	71	71	70
10-11	68	67	63
1-10	3	1	3
2-11	3	1	3
4-6	22	23	22
1-4	80	84	82
2-4	95	96	89

The atoms forming each plane are lying in that plane.

significantly longer than the value quoted by Dewar for the sp^2-sp^2 single bond.

A similar geometrical relationship holds between benzo ring (1) and segment (4). The angle is 82° , again preventing any π -bonding interaction between these two segments. The bond length of 1.463 \AA between N(2)-C(9) can thus be taken as an sp^2-sp^2 single bond between carbon and nitrogen without any π -bond character.

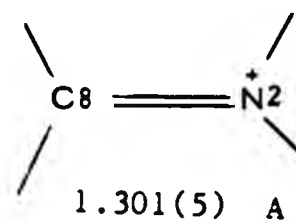
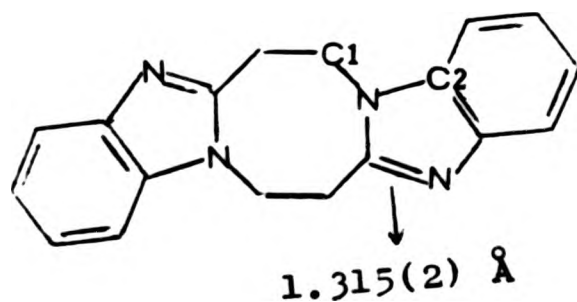
The bond length of 1.485 \AA between C(1) and N(2) which is 0.022 \AA longer than that between N(2) and C(9) is an eminently reasonable bond length passing from an sp^2 - to an sp^3 -hybridized carbon atom in an otherwise analogous bond.

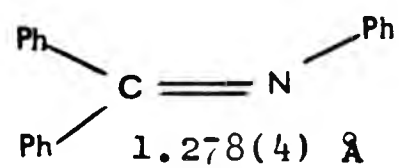
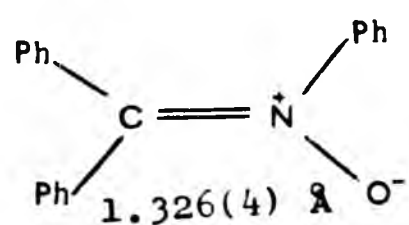
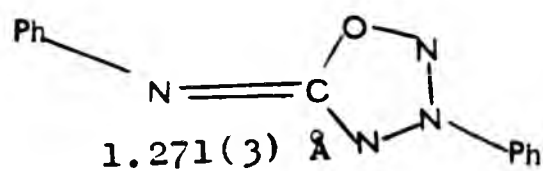
The N(2)-C(8) bond length of $1.301(5) \text{ \AA}$ is in the range of a carbon-nitrogen double bond.

Examples:

Present structure

- 1) 6,7,14,15-Tetrahydrobisbenzimidazo
[1,2-a;1',2'-e][1,5]diazocine⁸



2) N-(diphenylmethylene)aniline⁹3) Triphenylnitron¹⁰4) N-[3-Phenyl-5-(1,2,3,4-oxatriazolio)]-phenylamide¹¹

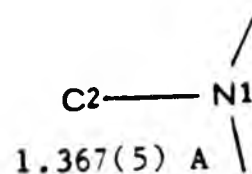
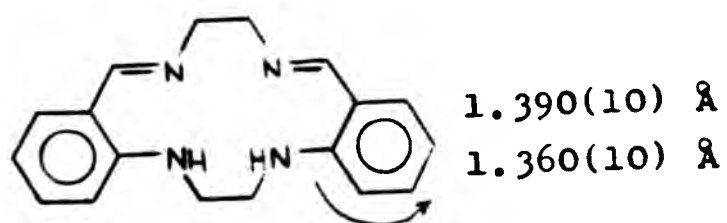
The bond lengths C(8)-C(7) and C(1)-N(1) are 1.406(5) and 1.418(5) Å respectively. These are somewhat short for single bonds.

The bond length N(1)-C(2) = 1.367(5) Å is intermediate between that of a single and of a double carbon-nitrogen bond.

Examples:

Present structure

1) 5,6,7,8,15,16,17,18-Octahydrodibenzo
[e,o][1,4,8,13]tetra-azacyclohexadecene¹²



2) Ref. 8 (see earlier)

$$\text{C-N} = 1.386(2) \text{ \AA}$$

Much of the above can be rationalised by assuming a contribution from an ortho-quinonoid resonance form (Diagram 3.4), arising from back-donation of the lone-pair of electrons on N(1).

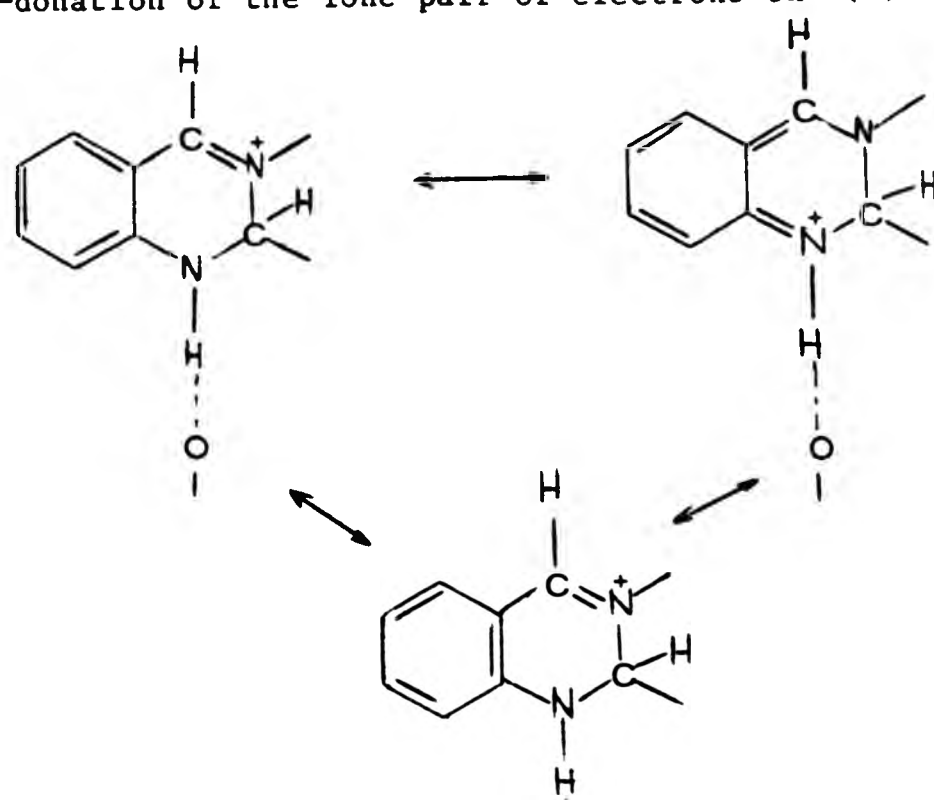
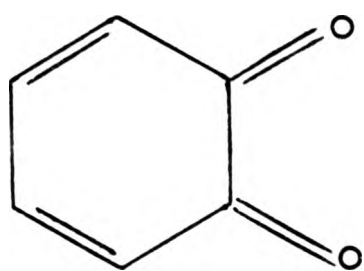


Diagram 3.4

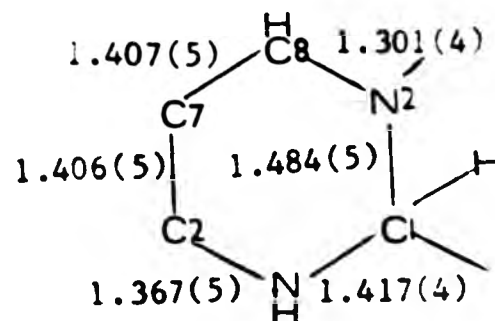
This back-donation of the lone-pair of electrons on N(1) is further strengthened by the hydrogen bonding of the NH group (see sections 4.2 and 4.3). Similar structural types, where such back-donation is also possible, show bond lengths of a similar magnitude. Contributions from this ortho-quinonoid resonance form would account for the observed shortening of the N(1)-C(2) and the C(7)-C(8) bonds from values expected for single bonds.

Regardless which route this mesomeric effect takes through the benzene ring, a shortening of the bonds C(3)-C(4) and C(5)-C(6) would be expected. A tendency for this to occur is observed. The C(3)-C(4) and

C(5)-C(6) bonds are marginally shorter than the two bonds flanking them. In the former this shortening is just over, in the latter just under, 3 e.s.d.'s (see Diagram 3.5).



ortho-quinone



Relevant segment of TAABH₂(PICRATE)₂

Diagram 3.5

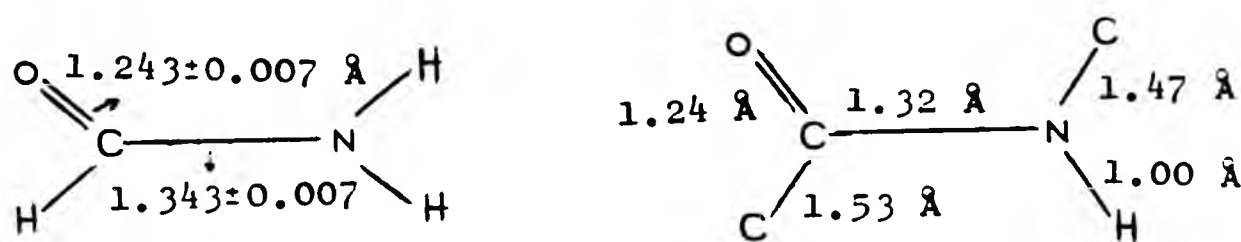
By reasoning similar to the above, one might expect the double bond between C(8) and N(2) to be somewhat lengthened. Some carbon-nitrogen double bonds slightly shorter than the one observed here are reported (see above and section 3.4).

It may well be, however, that the bond lengthening of a double bond caused by such a resonance contribution is rather less than the bond shortening of the single bonds; a given percentage change in bond character is likely to lead to greater bond length changes in weaker rather than in stronger bonds.

Support for this argument comes from the calculations on bond lengths made by Pauling¹³ for resonance between single and double carbon-carbon bonds. It is clear from these calculations that the double bond is much less affected (i.e. lengthened) than the single bond (i.e. shortened). This is persuasively demonstrated by the dimensions of the amide group. The principal resonance structures for an amide are (a) and (b) (see Diagram 3.6).



Accurate data for formamide by micro-wave spectroscopy obtained by Kurland and Wilson¹⁴, together with mean distances assembled by Pauling¹⁵ from the X-ray crystallographic structure determinations of amino-acids and simple peptides, show that, whilst the C-O bond is only marginally lengthened from a double bond, the C-N bond is drastically shortened from the value for a single bond (see Diagram 3.7).



As the C=N length in $\text{TAABH}_2(\text{PICRATE})_2$ is little affected by the above-mentioned resonance, it is not surprising that the bonding around this atom is virtually planar. The sum of the bond angles around this nitrogen atom is 360.0° , and this atom is only 0.012 \AA above the plane through its three bonding partners.

The whole molecule can be described as having a double saddle-shape. One pair of opposite benzene rings are folding down with respect to the central eight-membered ring, and the other pair are folding up with respect to the same reference feature. Hence this gives to the eight-membered ring a boat conformation. There is also a fold of 22° along the N(1),C(8) line. The sum of the bond angles around N(1) and C(8) are 354.0° and 354.2° respectively, indicating deviation of both

atoms from a trigonal planar bonding arrangement. This probably accounts for the fold along the N(1),C(8) line.

The bond lengths and angles for the picrate counter-ion are given in Tables 3.3 and 3.4. These values are closely similar to those in other structures reported.

Tables 3.6 and 3.7 are summaries of bond lengths and angles of picrates reported in the literature. These values can be compared with the present structure. Good agreement with the literature values is observed. The last two lines in these Tables give values for the picric acid molecule. It can be seen that the carbon atom C(p6) bound to the phenolic oxygen atom has a short C-O- bond-length (1.243 Å) in the picrate, much shorter than the corresponding bond in the picric acid molecule (1.327 Å). The bond lengths C(p1)-C(p6) = 1.462 Å and C(p5)-C(p6) = 1.464 Å, on the other hand, are longer than in picric acid, but similar to those in the picrate ions reported (1.404 Å). The C(p5)-C(p6)-C(p1) angle of 111.1° is smaller than that in picric acid (115.4°). Hence the bond lengths and angles data of the present structure show definitely the presence of a picrate ion, not of a picric acid molecule.

The picrate anion is bonded to the (TAABH₂)²⁺ cation by relatively strong hydrogen bonds: O(7)...H(N1)-N(1) with O.....N 2.89, O.....H 2.04 Å and an O...H-N angle of 154°, and there is also a close inter-ionic contact O(1)...H(8')-C(8') with O.....C 3.12, O...H 2.18 Å, and an O...H-C angle of 169° (see Diagram 3.8 and Section 3.4).

Table 3.6: Bond lengths in picrate ions and picric acid

Compound	[C(p1)-C(p6) C(p5)-C(p6)] _{av}	[C(p4)-C(p5) C(p2)-C(p1)] _{av}	[C(p4)-C(p3) C(p2)-C(p3)] _{av}	[C(p)-N] _{av}	(N-O) _{av}	C(p6)-O7
TAABH ₂ (PICRATE) ₂	1.462(3)	1.367(3)	1.387(3)	1.455(3)	1.225(2)	1.243(5)
Ref.16	1.440(6)	1.395(6)	1.380(6)	1.451(5)	1.212(4)	1.240(9)
Ref.17	1.464(5)	1.365(5)	1.390(5)	1.454(5)	1.223(3)	1.234(5)
Ref.18(a)	1.452(3)	1.372(4)	1.382(3)	1.446(5)	1.229(2)	1.243(7)
Ref.19	1.454(2)	1.370(2)	1.383(2)	1.452(2)	1.229(1)	1.240(4)
Ref.18(b)	1.450(3)	1.372(4)	1.368(3)	1.459(3)	1.218(2)	1.239(6)
Ref.20	1.448(5)	1.358(6)	1.382(6)	1.450(4)	1.218(3)	1.249(7)
Ref.21(a)	1.449(3)	1.371(3)	1.384(3)	1.450(3)	1.222(2)	1.237(4)
Ref.21(b)	1.403(3)	1.378(4)	1.370(4)	1.473(3)	1.217(2)	1.321(4)
Ref.22	1.404(3)	1.374(3)	1.383(3)	1.464(3)	1.219(2)	1.327(3)

Ref.16, The ternary charge transfer salt pyridinium-1-naphthylamine-picrate; ref.17, succinylcholine picrate, ref. 18(a), potassium picrate; ref.18(b), ammonium picrate; ref.19, serotonin picrate monohydrate; ref. 20, 2,2'-di-o-carboxymethoxyphenoxy-diethyl ether potassium picrate; ref. 21(a), 1:1 complex carbomylcholine picrate, picric acid; ref.21(b), picric acid of ref. 21(a); ref. 22, picric acid in anthracene:picric acid complex.

Table 3.7: Bond angles of picrate ions and of picric acid

Compound	C(p1)-C(p6)-C(p5)	[C(p4)-C(p5)-C(p6) C(p2)-C(p1)-C(p6)] _{av}	[C(p3)-C(p4)-C(p5) C(p3)-C(p2)-C(p1)] _{av}	C(p4)-C(p3)-C(p2)
TAABH ₂ (PICRATE) ₂	111.1(3)	124.6(3)	119.0(3)	121.6(4)
Ref. 16	113.3(6)	123.9(4)	117.5(4)	123.6(6)
Ref. 17	110.4(4)	125.1(3)	118.9(4)	121.3(4)
Ref. 18(a)	111.1(5)	124.9(3)	118.5(3)	122.0(5)
Ref. 19	111.1	124.6	119.3	120.8
Ref. 18(b)	111.5(4)	124.2(2)	119.1(2)	121.9(3)
Ref. 20	111.6(5)	124.4(3)	119.3(3)	120.9(5)
Ref. 21(a)	111.2(2)	124.7(2)	118.9(2)	121.3(3)
Ref. 21(b)	115.6(3)	122.8(2)	118.1(2)	122.5(3)
Ref. 22	115.3(3)	123.3(2)	118.0(2)	122.0(3)

References and compounds as in Table 3.3.

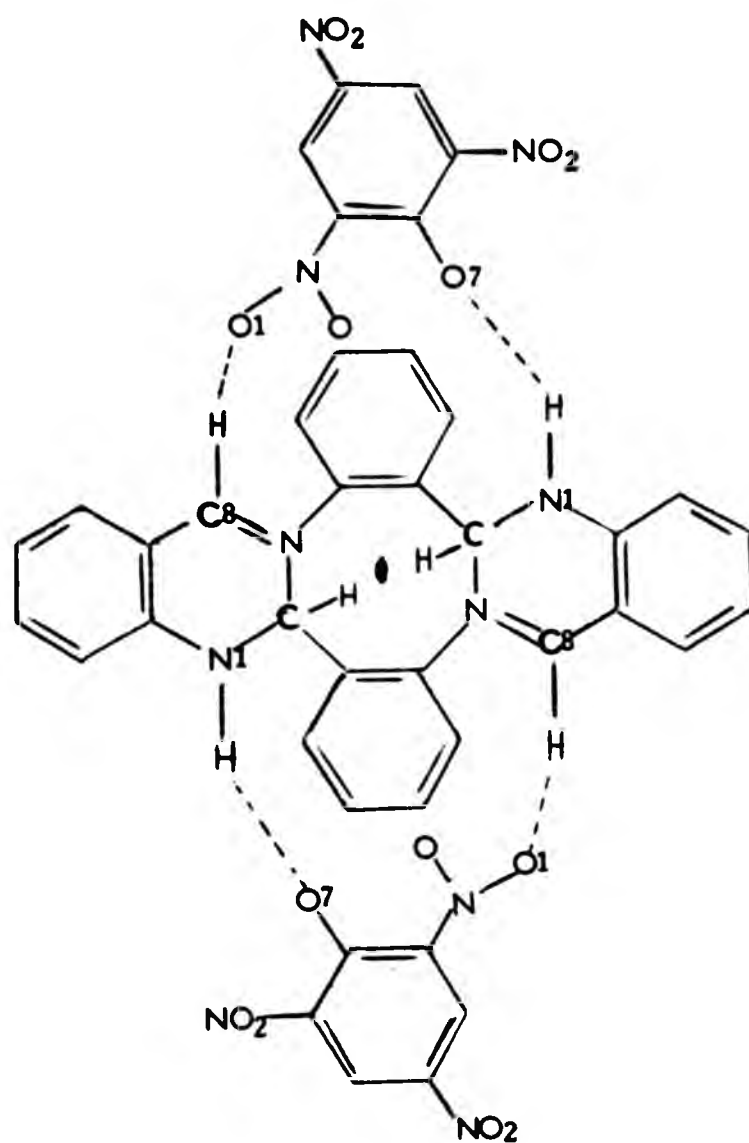


Diagram 3.8

3.3.2 $\text{TAABH}_2(\text{HSO}_4)_2$

The bisulphate and chloride salts were amongst the first salts of TAAB to be investigated by Seidel²³. The former was also used by McGeachin²⁴ in his structural studies using spectroscopic techniques. As it was one of a limited number of counter-ions still containing a hydrogen capable of further hydrogen bonding, it was hoped that this might induce an ordered structure, and hence overcome some of the difficulties encountered with the earlier-investigated BF_4 (section 3.3.3) and CF_3SO_3 ¹ salts.

The $\text{TAABH}_2(\text{HSO}_4)_2$ salt was prepared as explained in section 3.1. Attempts to recrystallize it from various solvents were unsuccessful, and the crystals used were those obtained from the reaction mixture.

The compound was totally insoluble in every solvent investigated (e.g. CHCl_3 , CH_3CN , Et_2O , PhH). From this total insolubility (the crystals have a deep red colour which allows the detection of even small amounts in solution), it was suspected that the compound has a macromolecular structure, through intermolecular hydrogen bonding. The result of the X-ray crystallographic investigation showed that the compound $\text{TAABH}_2(\text{HSO}_4)_2$ has the structure given in Figure 3.2, where the numbering scheme and important bond lengths and angles are also shown. (The same numbering scheme is used as in the picrate salt for purposes of comparison.) The bond length and angle data for complete structure is given in Tables 3.8 and 3.9. The ORTEP drawings of the structure are in Drawing 3.2.

The compound crystallizes in space group Pmmn , which requires the molecule to have two mirror planes and the asymmetric unit to be $1/4$ of the molecule. Hence a statistical disorder model (as explained below) is required for this salt, as the cation cannot have any mirror symmetry.

If we assume that an ordered structure would pack as shown in Diagram 3.9, in the xy -plane, and in the same manner along the z -axis, equivalent carbon atoms $\text{C}(a)$'s and $\text{C}(b)$'s would be superimposed on each other, and equivalent nitrogen atoms $\text{N}(a)$'s and $\text{N}(b)$'s would do the same.

Then, if we take a cross-section along the z -axis cutting the x,y -plane through the $\text{N}(b)$, $\text{C}(b)$ line and looking down from the X -axis, we would observe the following pattern (Diagram 3.10).

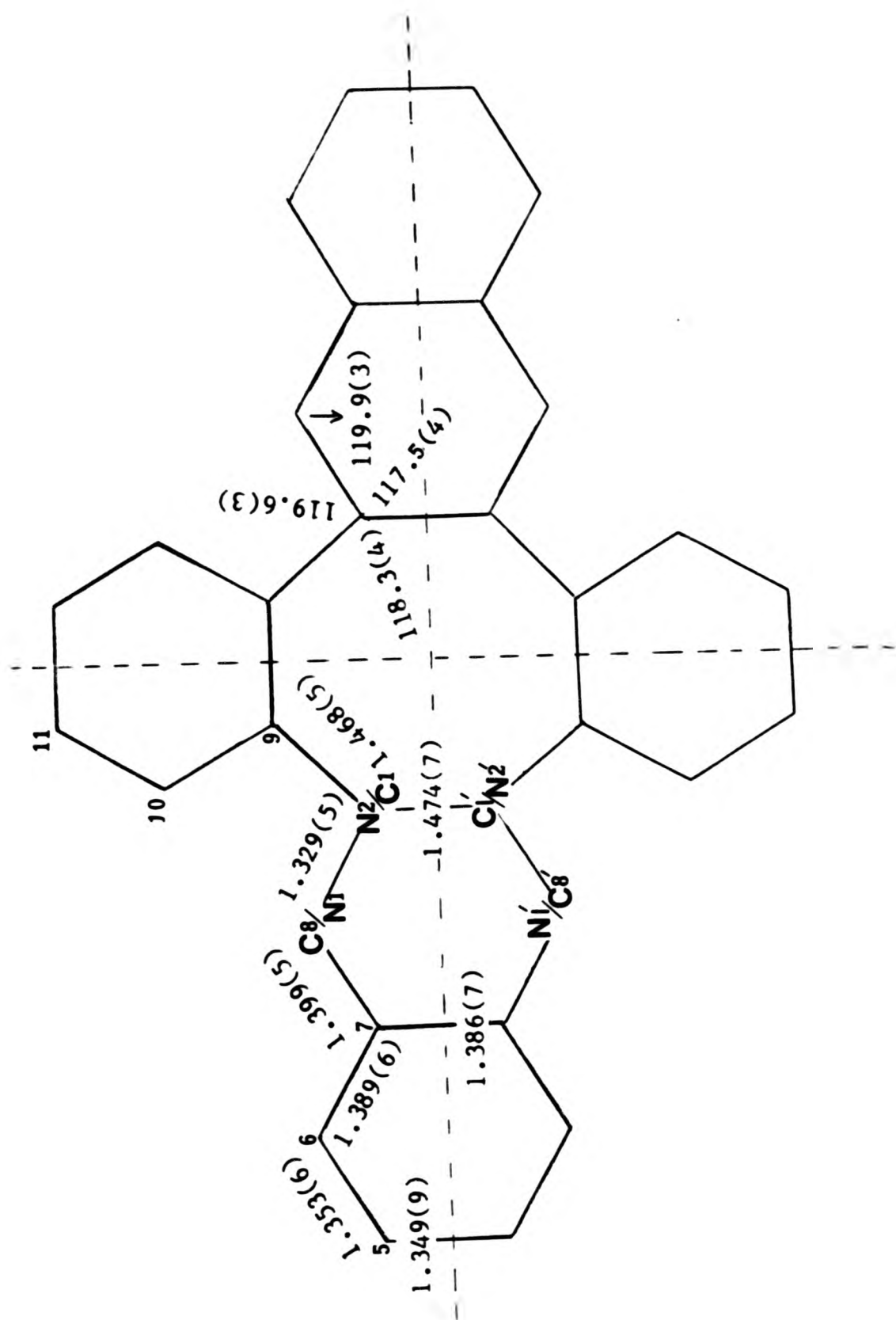


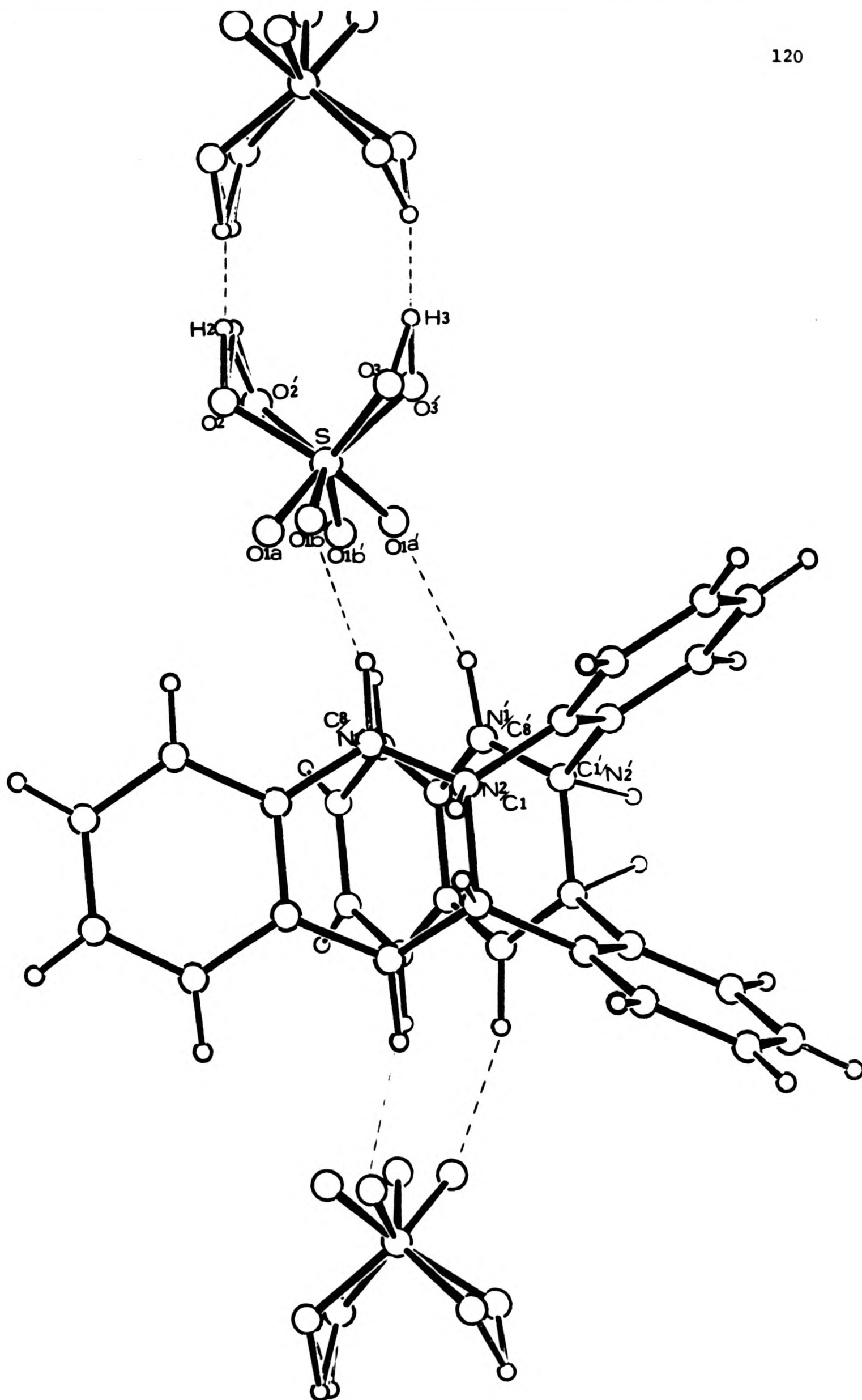
Figure 3.2

Table 3.8: Bond lengths (Å) for TAABH₂(HSO₄)₂

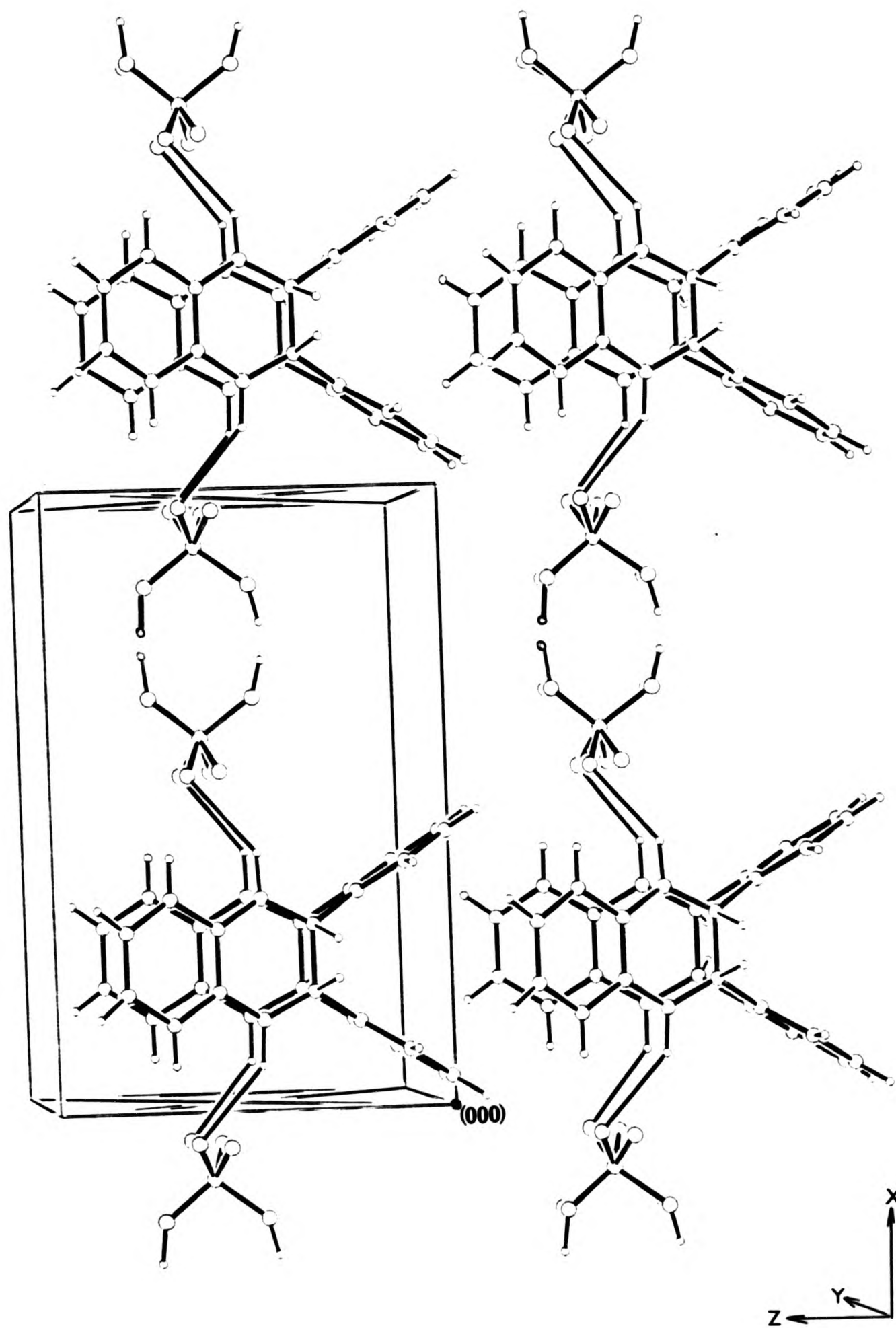
C(11) -C(10)	1.381(6)	C(11) -C(11)	1.366(8)
C(10) -C(9)	1.376(5)	C(9) -C(1)	1.468(5)
C(9) -N(2c1)	1.468(5)	C(9) -C(9)	1.384(7)
C(1) -N(1)	1.329(5)	C(1) -C(8n1)	1.329(5)
C(1) -C(1)	1.474(7)	N(2c1)-N(1)	1.329(5)
N(2c1)-C(8n1)	1.329(5)	N(2c1)-N(2c1)	1.474(7)
N(1) -C(7)	1.399(5)	C(8n1)-C(7)	1.399(5)
C(7) -C(6)	1.389(6)	C(7) -C(7)	1.386(7)
C(6) -C(5)	1.353(6)	C(5) -C(5)	1.349(9)
S -O(1a)	1.386(19)	S -O(1b)	1.457(14)
S -O(2)	1.475(5)	S -O(3)	1.515(5)
O(1a) -O(1b)	.721(16)	O(2) -O(2)	.707(17)
O(3) -O(3)	.917(12)		

Table 3.9: Bond angles ($^{\circ}$) for $\text{TAABH}_2(\text{HSO}_4)_2$

C(9) -C(10) -C(11)	120.4(4)	C(1) -C(9) -C(10)	119.5(3)
N(2c1)-C(9) -C(10)	119.5(3)	N(2c1)-C(9) -C(1)	0.0(1)
N(1) -C(1) -C(9)	119.6(3)	C(8n1)-C(1) -C(9)	119.6(3)
C(8n1)-C(1) -N(1)	0.0(1)	N(1) -N(2c1)-C(9)	119.6(3)
C(8n1)-N(2c1)-C(9)	119.6(3)	C(8n1)-N(2c1)-N(1)	0.0(1)
N(2c1)-N(1) -C(1)	0.0(1)	C(7) -N(1) -C(1)	119.9(3)
C(7) -N(1) -N(2c1)	119.9(3)	N(2c1)-C(8n1)-C(1)	0.0(1)
C(7) -C(8n1)-C(1)	119.9(3)	C(7) -C(8n1)-N(2c1)	119.9(3)
C(8n1)-C(7) -N(1)	0.0(1)	C(6) -C(7) -N(1)	123.0(3)
C(6) -C(7) -C(8n1)	123.0(3)	C(5) -C(6) -C(7)	120.8(4)
O(1b) -S -O(1a)	29.2(7)	O(2) -S -O(1a)	112.9(7)
O(2) -S -O(1b)	86.5(5)	O(3) -S -O(1a)	85.1(7)
O(3) -S -O(1b)	101.7(5)	O(3) -S -O(2)	99.1(3)
O(1b) -O(1a) -S	81(2)	O(1a) -S -O(1a)	97(2)
O(1a) -O(1b) -S	70(2)	O(1b) -S -O(1b)	113(1)
O(2) -S -O(2)	27.8(6)	O(3) -S -O(3)	35.3(4)



Drawing 3.2a



Drawing 3.2b

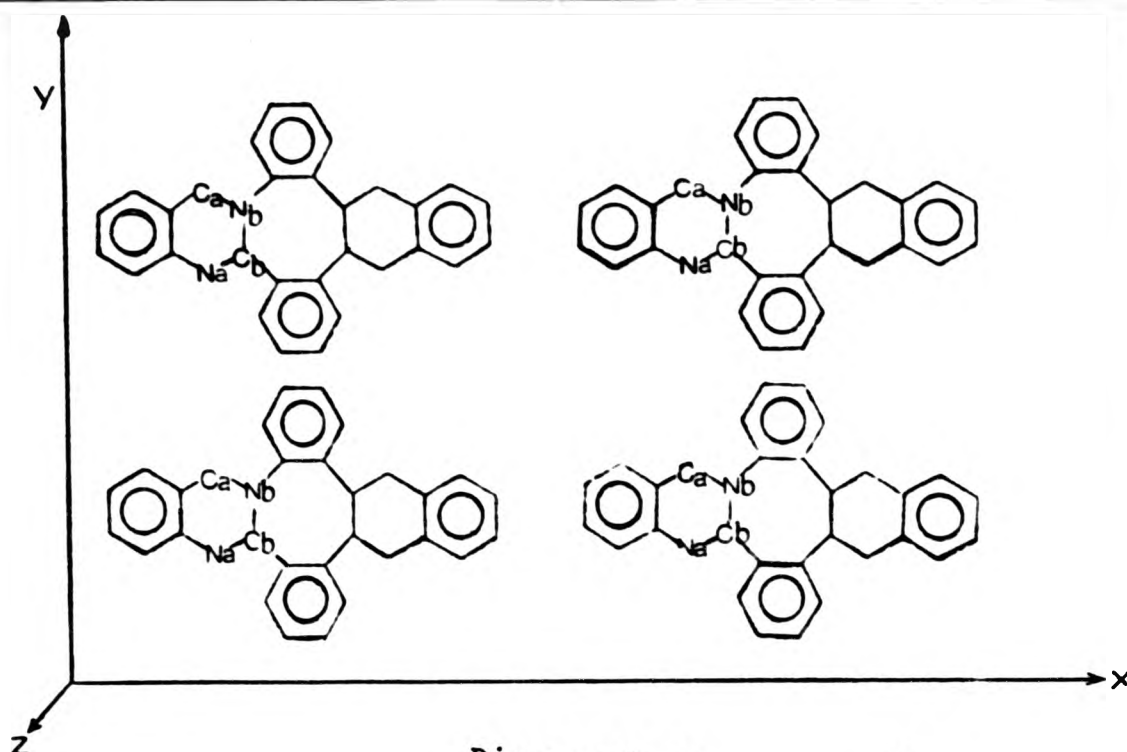


Diagram 3.9

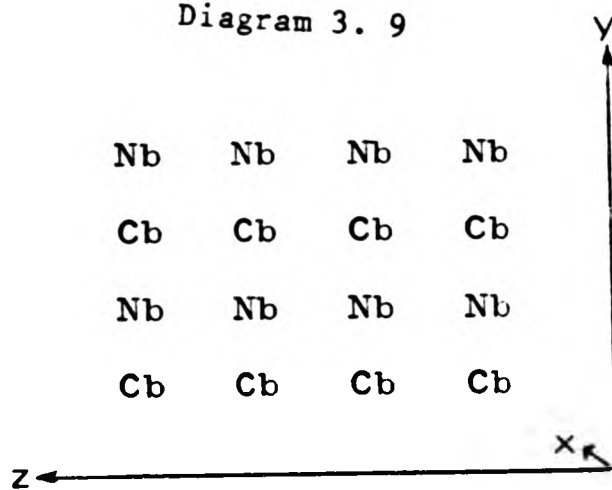


Diagram 3.10

This would keep the tetrahedral character of C(b) and the trigonal planar character of N(b).

Now, if we assume that the molecules pack randomly, we get a pattern as shown in (Diagram 3.11).

Then if we take a cross-section in the same manner as we did for an ordered model we would observe the following pattern (Diagram 3.12).

This would result in an averaged structure of (a) and (b) (Diagram 3.13). Hence, if we take molecules (a) and (b) from the disordered model (Diagram 3.13) and place them on top of each other (using the numbering scheme of Figure 3.2) we will observe the following (Diagram

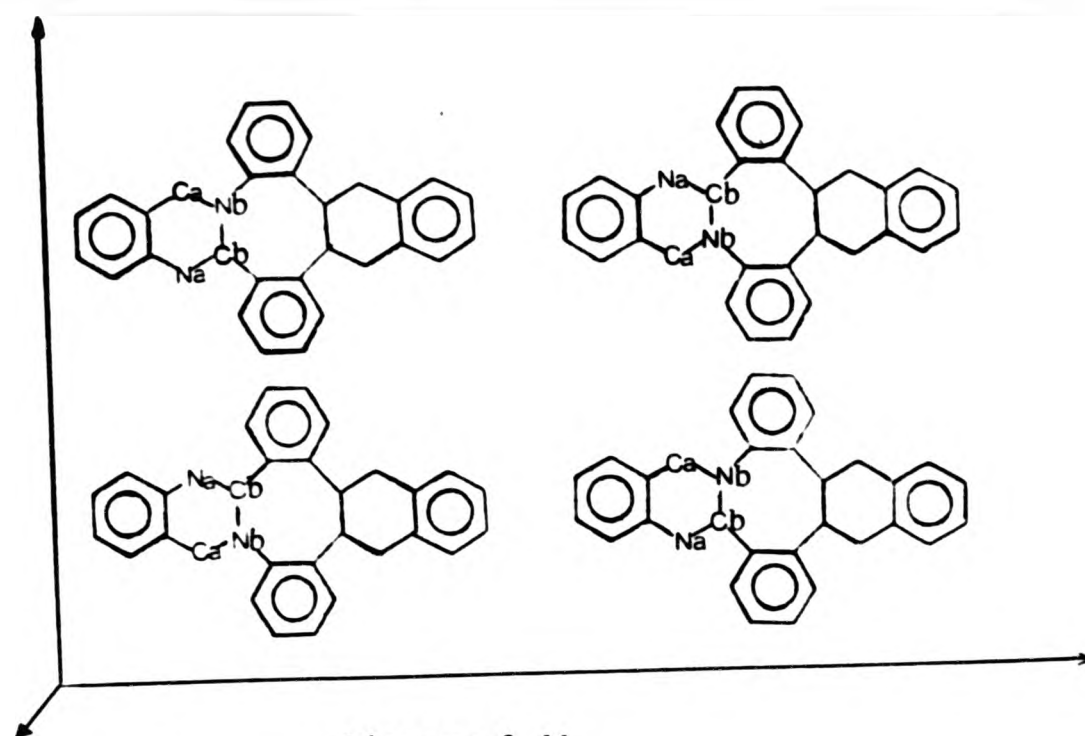


Diagram 3.11

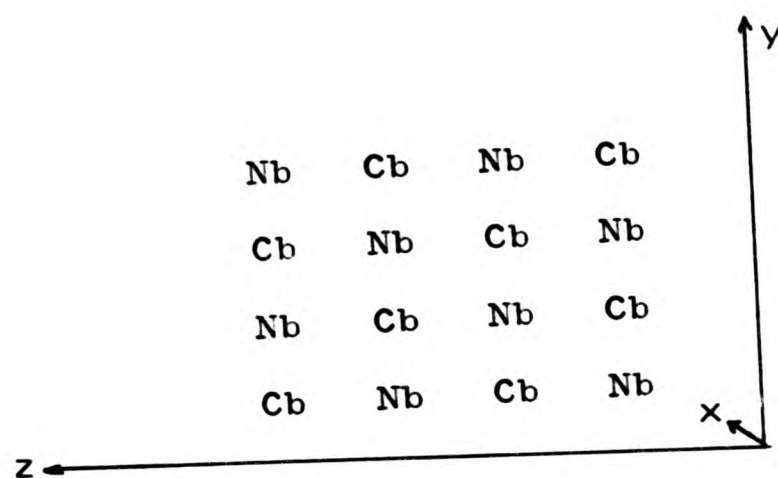


Diagram 3.12

3.14), where dashed lines indicate half double, half single bonds.

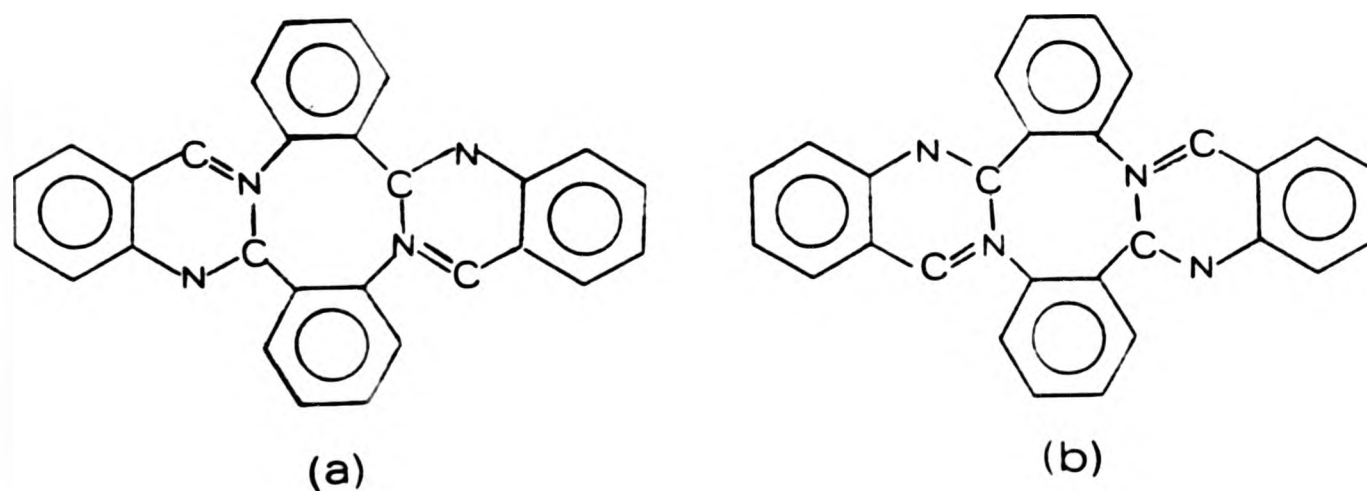


Diagram 3.13

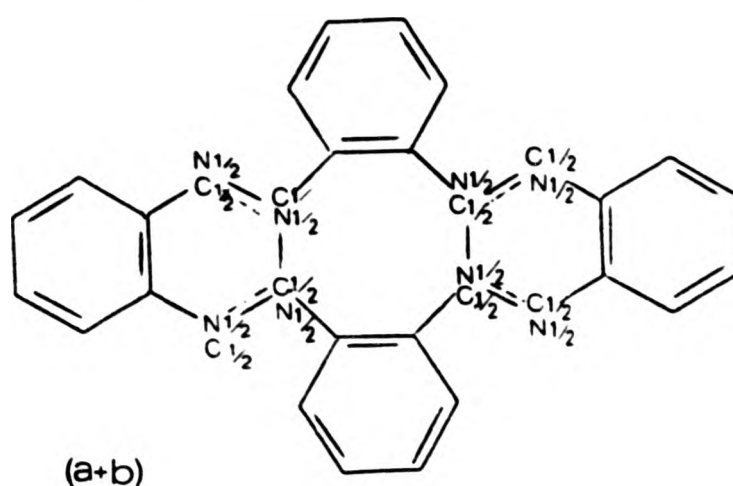
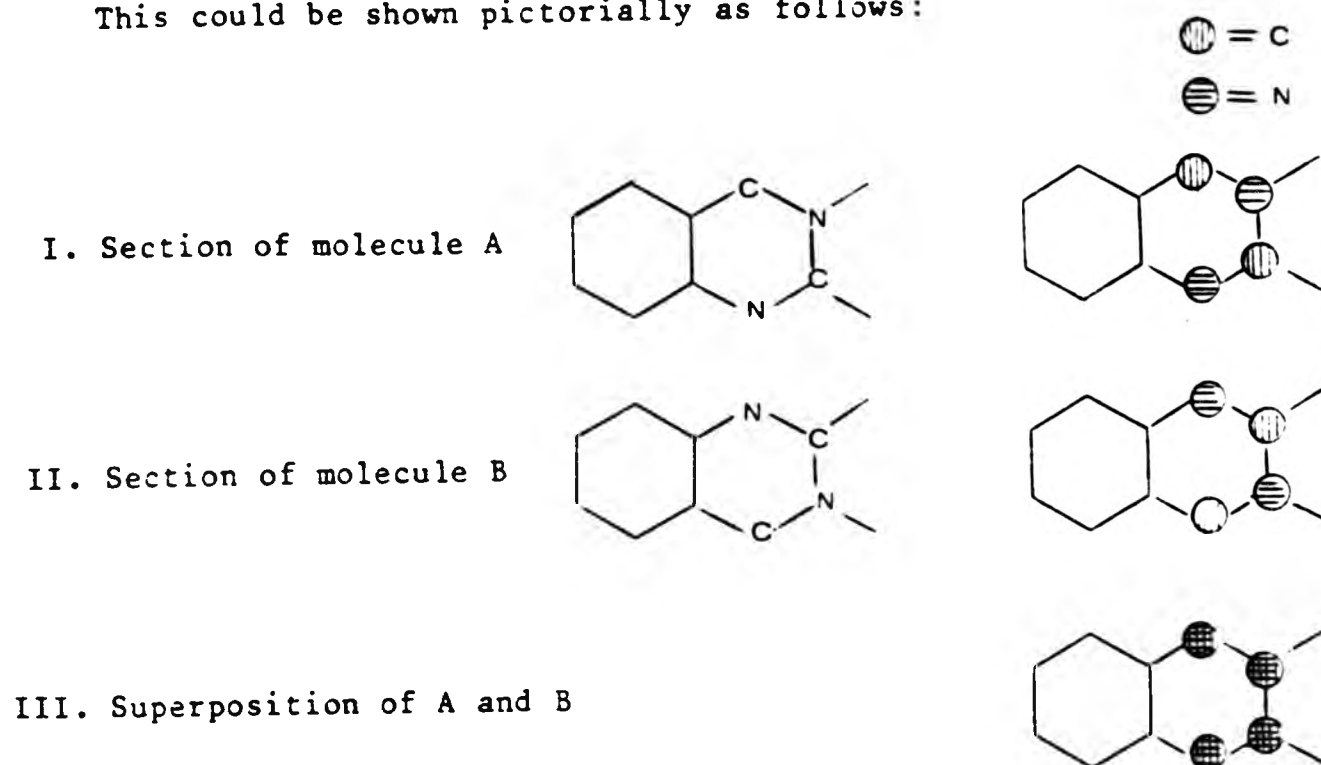


Diagram 3.14

This could be shown pictorially as follows:



As can be seen from model (III) or (a+b), [using the numbering scheme in Diagram 3.13(a)], the N(2)-C(1), N(2)-C(9), and C(1)-C(14') bond lengths would remain as single bonds, as they were in (a) and (b), and the last two bond lengths in the (a+b) model would appear to be equal. The C(8)-N(2) and C(1)-N(1) bond lengths, however, whilst having double and single bond character respectively in (a), would now in this model have a character intermediate between that of a double and of a single bond, and should be equal to each other. The C(7)-C(8) and N(1)-C(2) bonds would also be expected to be equal to each other. One

would also expect to observe a peak near N(2), as well as near C(1), and the angles around C(1) and N(2) would be intermediate between tetrahedral and trigonal planar configurations.

When the statistical disordered model (which is required by the space group) was assumed the structure refined further and the R-factor dropped from 0.062 to 0.057, $R_w = 0.053$.

All the bond lengths and angles agree very well with the statistical disorder model, based on data taken from the ordered picrate salt (see section 3.3.1). The distance between the N(2)/C(1) and C(1)/N(2) atom sites is $1.473(6) \text{ \AA}$, which proves the existence of a bond between these two points and eliminates (as in the picrate salt) the possibility of the structure proposed by Goddard and Norris³ (see section 3.3.1). The sum of the bond angles around the N(2)/C(1) site is 355.4° , which is expected from the above disordered model.

At a distance of 1.334 and 1.510 \AA from the C(1)/N(2) site two electron density points were observed. A half hydrogen atom was assumed to be present at the distance of 1.334 \AA and it was included in the refinement. The refinement converged at 5.7%. The distance of 1.334 \AA for the hydrogen atom at the C(1)/N(2) is as expected, if we compare the pyramidality of this site with that of the C(1) site in the ordered picrate salt. The C(1)/N(2) and C(1) sites are 0.175 and 0.398 \AA respectively above the plane of the three connected atoms. Hence one would expect to observe the C(1)/N(2) hydrogen distance at $0.398 - 0.175 + 1.080 = 1.303 \text{ \AA}$. The value which is observed (1.334 \AA) is very near to that. The peak at 1.510 \AA remains unexplained.

The bond lengths and angles for the disordered HSO_4 ion (see section 3.2.2) are given in Tables 3.8 and 3.9. As the insolubility suggested, a macromolecular structure due to intermolecular hydrogen bonding was observed. Very close intermolecular distances were found between the pairs of HSO_4 ions and between the HSO_4 counter-ion and the cation, forming three different types of hydrogen bonds.

The HSO_4 ion in relation to the cation is shown in Diagram 3.15.

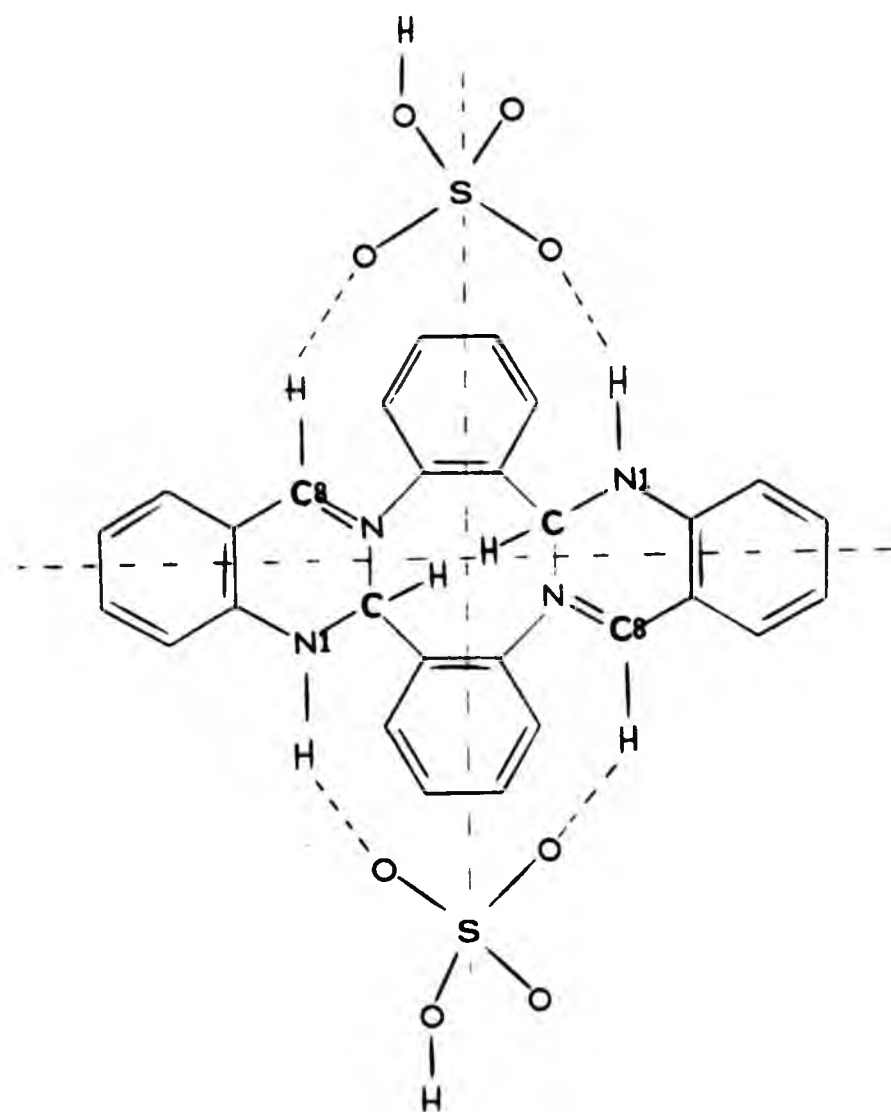


Diagram 3.15

Whilst the crystallographic literature contains numerous examples of inorganic and organic chloride salts, data on corresponding HSO_4 salts are rather scarce. Sulphuric acid and its acid salts can give rise to various hydrogen bonding patterns, which can be classified according to

the number of hydrogen atoms and the number of formal negative charges in the sulphuric acid moiety.

1) Anhydrous sulphuric acid, H_2SO_4 : This is a neutral covalent molecule, which forms 4 hydrogen bonds per molecule, using 2 hydrogen donors from the SOH groups and 2 electron donors from the other 2 SO units. This gives rise to an infinite 2-dimensional layer structure.²⁵

2) Bisulphates, $MHSO_4$: These can be divided into two sub-groups where a) M is a cation not capable of hydrogen bonding, e.g. Na,^{26,27} K,²⁸⁻³⁰ Rb,³¹ and b) M is a cation capable of forming hydrogen bonds to the bisulphate ion, e.g. NH_4 ,³² H_3O ,³³ etc. Thus in this sub-group, 2(b), in addition to O-H...O hydrogen bonds between HSO_4 units, there may be other O-H...O bonds arising from interactions with the cation, water of hydration,^{34,35} as well as N-H...O bonds with the cation.³²

3) A third class is when there are three HSO_4 and one SO_4 ion present in the structure. This is represented by $[Co_2(NH_3)_{10}O_2](HSO_4)_3(SO_4)$. As Schaefer and Marsh^{36,37} point out, the hydrogen bonding pattern is extremely complex. Somewhat simplified, it can be described as two HSO_4 ions forming an acyclic dimer; the other HSO_4 and the SO_4 ion form another acyclic dimer, and both these dimer units form numerous N-H...O hydrogen bonds with the ammonia molecules of the cation. The structure is somewhat unusual as the above pair of HSO_4 ions form an acyclic dimer, whilst, in general, cyclic dimers or infinite chains are preferred.

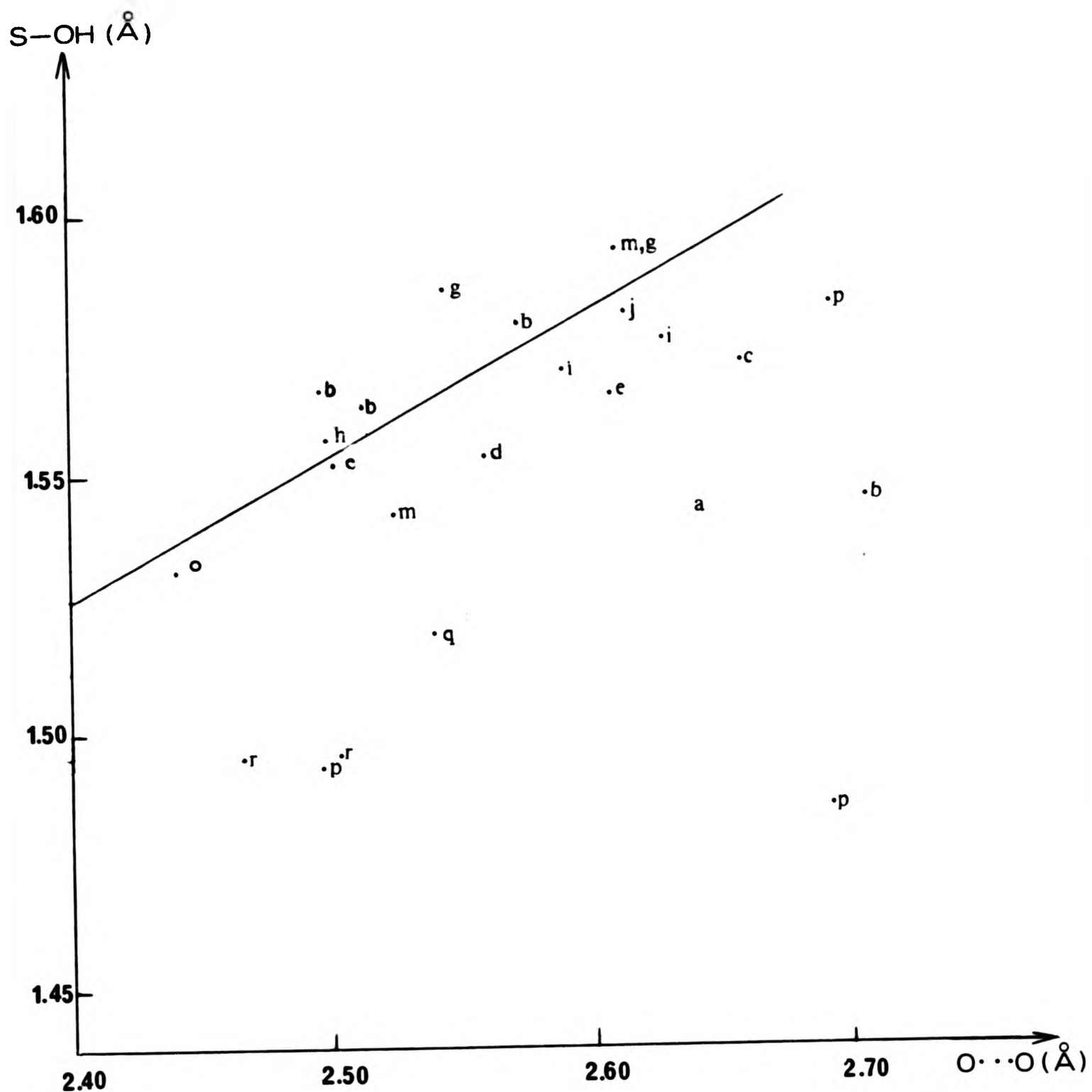
4) The fourth class consists of compounds such as $M_3H(SO_4)_2$ where

the ratio of HSO_4 to SO_4 is 1:1. Here again, as in class 2, the cation a) may not be capable of hydrogen bonding, e.g. $\text{M} = \text{Na}$,³⁸ while b) is capable of hydrogen bonding, e.g. $\text{M} = \text{NH}_4$.³⁹ The same remarks pertain as in class 2, regarding cation-anion hydrogen bonding. In this class the anions form acyclic dimer units.

In class 2 the HSO_4 moieties form, either acyclic dimers, or, more frequently, infinite chains. The potassium salt, which has been investigated three times,²⁸⁻³⁰ has both structural units present in the same unit cell. In the case of the sodium salt, the α -form²⁷ has chains, the β -form²⁶ cyclic dimers. A plot of the S-OH against the O.....O distances has been given by Catti, Ferraris, and Ivaldi³⁸ for all four classes. This, together with the most recent data, is presented in Figure 3.3. Some slight trends can be observed when one considers the shortest hydrogen bond in each of the different compounds. Thus for the alkali metal bisulphates (except the α -Na salt), S-OH and O.....O distances decrease with increasing size of the cation. There is also a general trend towards stronger hydrogen bonds as the ratio of the number of negative charges to SOH groups increases. This trend is in keeping with observations from the HF system, where the strongest hydrogen bond is observed when X and Y are both F^- , i.e. in the $[\text{F}...\text{H}...\text{F}]^-$ ion (see section 1.3). In the bisulphate system, X and Y are the same and represent the oxygen atoms of the SO_4^{2-} groups.

Examples of all four classes, together with the present structure are detailed in Table 3.10.

In $\text{TAABH}_2(\text{HSO}_4)_2$, the HSO_4 anions form cyclic dimers. The O.....O



- (a) H_2SO_4 ; (b) $[\text{Co}_2(\text{NH}_3)_{10}\text{O}_2](\text{HSO}_4)_3(\text{SO}_4)$; (c) $(\text{H}_3\text{O})(\text{HSO}_4)$;
 (d) $(\text{CH}_3\text{CO}_2\text{H}_2)(\text{HSO}_4)$; (e) NH_4HSO_4 ; (f, f', f'') $\text{NaHSO}_4 \cdot \text{H}_2\text{O}$;
 (g) $\text{K}_{0.55}\text{Rb}_{0.45}(\text{HSO}_4)$; (h) $[\text{Ag}(\text{C}_6\text{H}_{16}\text{N}_{10})]\text{SO}_4 \cdot \text{HSO}_4 \cdot \text{H}_2\text{O}$;
 (i) KHSO_4 ; (l) trans- $[\text{CoCl}_2(\text{NH}_3)_4]\text{HSO}_4$; (m) RbHSO_4 ;
 (n) $\beta\text{-NaHSO}_4$; (o) $\text{Na}_3\text{H}(\text{SO}_4)_2$; (p) $\alpha\text{-NaHSO}_4$; (q) $(\text{NH}_4)_3\text{H}(\text{SO}_4)_2$;
 (r) present structure.
 (a-o) taken from ref. 38; (p) ref. 27; (q) ref. 39; (r) this Thesis.

Figure 3.3

Table 3.10: Hydrogen bonding in bisulphates

Example	Type	S-OH (Å)	S-O (Å)	O-H...O (Å)	H...O (Å)	O-H...O (°)
Present structure	Cyclic dimers(i)	1.495(av)	1.416(av)	2.506	1.703	149.0
				2.466	1.621	139.1
H_2SO_4 ²⁵	Infinite two-dimensional layers	1.535	1.426	2.63		
$\alpha-NaHSO_4$ ²⁷	a) Chains	1.582(6)	1.442(3)	2.690(8)		
	b) Dimers(i)	1.486(6)	1.435(6)	2.692(8)		
		1.493(6)	1.452(6)	2.497(11)		
$\beta-NaHSO_4$ ²⁶	Cyclic dimers	1.58(2)	1.46(2)	2.67(3)		
$KHSO_4$ ²⁸⁻³⁰	a) Polymeric chain	1.564(4)	1.448(2)	2.630(5)	1.907	173(5)
	b) Cyclic dimers	1.561(3)	1.444(2)	2.583(5)	1.894	158(7)
$RbHSO_4$ ³¹	Two chains a)	1.54(2)	1.44(1)	2.53	1.54	174
	b)	1.58(1)	1.43(1)	2.62	1.59	169
NH_4HSO_4 ³²	Two chains a)	1.546(3)	1.430(1)	2.514	1.790	160
	b)	1.557(2)	1.440(1)	2.598	1.920	172
$NaHSO_4 \cdot H_2O$ ^{34, 35}	Zigzag chains	1.599	1.450	2.65		
$(H_3O)HSO_4$ ³³	Zigzag chains(ii)	1.560(4)	1.448(2)	2.657		

Table 3.10(continued)

$(\text{CH}_3\text{COH}_2)\text{HSO}_4$ ⁴⁰	Infinite chains(iii)	1.443(2)	2.567
$[\text{Co}(\text{NH}_3)_6]^{2+}$	Acyclic dimers	1.554	1.451
$(\text{HSO}_4)_3(\text{SO}_4)$ ^{36, 37}			
$\text{Na}_3(\text{HSO}_4)_4\text{SO}_4$ ³⁸	Acyclic dimers	1.527	1.474
$(\text{NH}_4)_3(\text{HSO}_4)_4\text{SO}_4$ ³⁹	Acyclic dimers	1.518	1.450
			1.40
			2.434
			2.540
			177
			180

(i) Hydrogen is disordered

(ii) Infinite zigzag chains linked by hydrogen bonds from H_3O^+ ions to form infinite double layers.

(iii) Infinite chains are connected to each other by hydrogen bonds through $(\text{CH}_3\text{COH}_2)^+$ ions to form double layers.

distances, as can be seen from Table 3.10, are amongst the shortest so far reported for the $\text{H}_2\text{SO}_4/\text{HSO}_4/\text{SO}_4$ system. Especially in cyclic dimers, e.g. K ,²⁸⁻³⁰ $\beta\text{-Na}$ ²⁶), the O.....O distances are considerably longer, and hence the hydrogen bonds substantially weaker. Only one O.....O distance, shorter than the present short one, namely in the acyclic dimer, $\text{Na}_3\text{H}(\text{SO}_4)_2$,³⁸ has been reported in this system.

In three of these bisulphate derivatives, N-H...O hydrogen bonding from the cation to the anion was observed (see Table 3.11).

Table 3.11: N-H...O hydrogen bonds from the cation to the anion.

	N-H...O (Å)	H...O (Å)	N-H...O°
1) Present structure	2.936-3.157	1.806-2.110	102.0-102.9
2) NH_4HSO_4 ³²	3.04-3.13		
3) $(\text{NH}_4)_3\text{H}(\text{SO}_4)_2$ ³⁹	2.86-3.12	2.13-2.51	116-162
4) $\text{Co}(\text{NH}_3)\text{complex}$ ^{36,37}	2.80-3.18	1.95-2.64	92-168

It can be seen that the N-H...O hydrogen bonds of the present structure belong among the shorter ones in the above examples. Hence, one can come to the conclusion that the hydrogen bonds in $\text{TAABH}_2(\text{HSO}_4)_2$ are strong, indeed stronger than most such bonds in comparable structural types.

3.3.3 $\text{TAABH}_2(\text{BF}_4)_2$

This compound was the first of this set of three to be investigated, but required the knowledge of the picrate and the bisulphate structures for a satisfactory interpretation of its data.

The compound $\text{TAABH}_2(\text{BF}_4)_2$ has the structure, with a crystallographic two-fold symmetry imposed on the molecule, shown in Figure 3.4, which also shows the numbering scheme used, together with the important bond lengths and angles. The complete lists of bond length and angles for this structure are given in Tables 3.12 and 3.13. The ORTEP drawings of the structure are in Drawing 3.3.

It can be seen from Figure 3.4 that this result too, agrees well with the structure proposed by Busch and co-workers for this type of $(\text{TAABH}_2)^{2+}$ salt (see section 3.3.1). On the other hand the poor data set, and the disorder of the BF_4 ion (see section 3.2.3) do not permit precise bond distances and angles to be derived, nor any certainty about the actual bond orders and the hydrogen positions in structure (a) in Diagram 3.3.

The evidence in favour of structure (a) in Diagram 3.3 is as follows:

The bond lengths	$\text{C}(1)-\text{N}(2) = 1.440(9) \text{ \AA}$
	$\text{C}(9)-\text{N}(2) = 1.452(9) \text{ \AA}$
	$\text{N}(1)-\text{C}(2) = 1.418(9) \text{ \AA}$
	$\text{C}(1)-\text{C}(14') = 1.451(10) \text{ \AA}$

have a single bond character which is expected from the formulation (a).

The bond length $\text{C}(8)-\text{N}(2) = 1.318(9) \text{ \AA}$ is short enough to be considered as a double bond, but high e.s.d. values make it difficult to derive significant conclusions. Some electron density, suggesting a hydrogen atom, is observed near the C(1) atom at a distance of 1.14 \AA . [But see also evidence against structure (a) in the following section.]

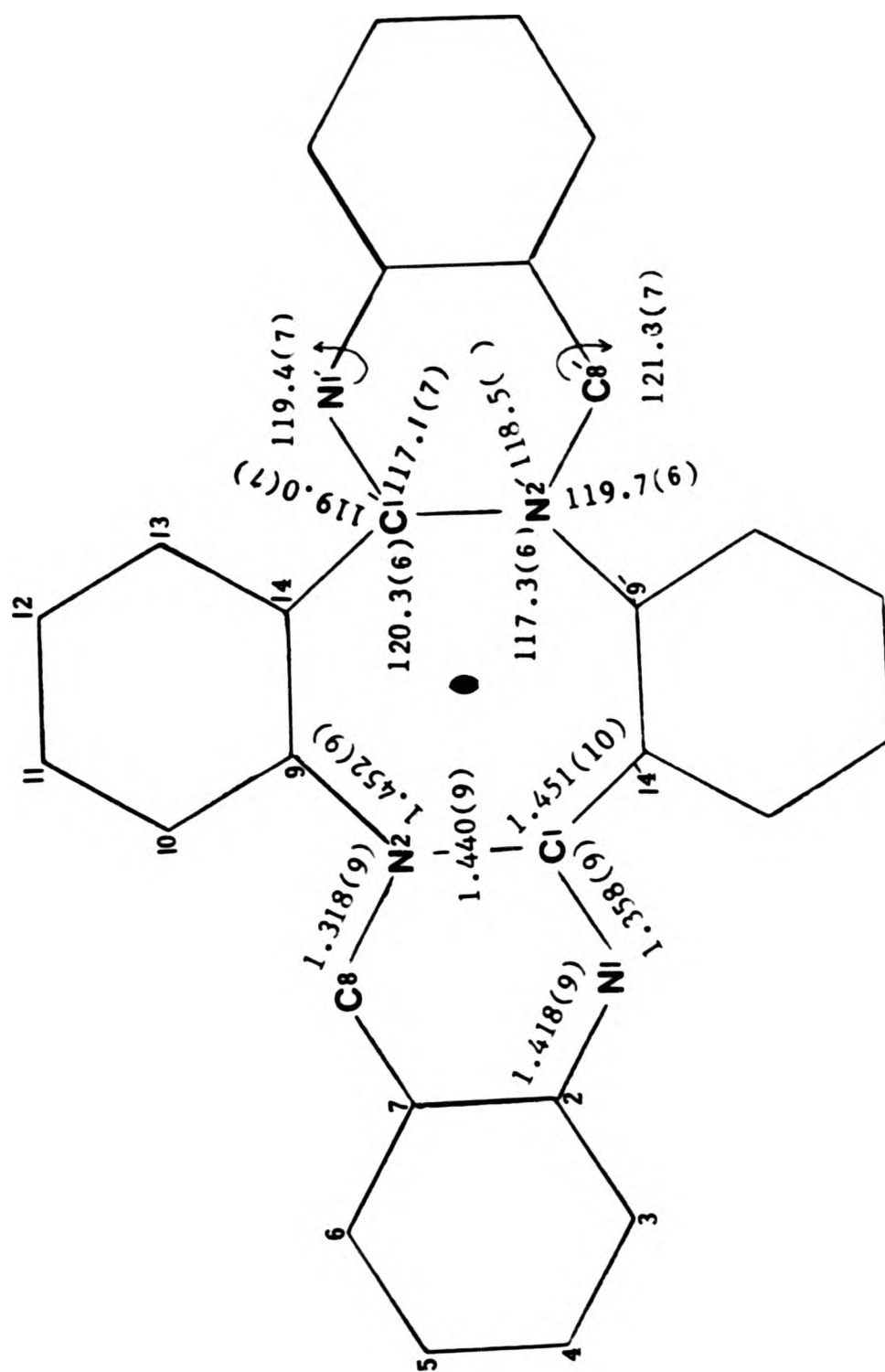


Figure 3.4

The evidence against structure (a) is as follows:

Bond angles around C(1) (to carbon and nitrogen atoms) as well as around N(2) indicate near planarity. Both sums of bond angles appear to be equivalent at $\sim 356^\circ$. Electron density, possibly suggesting a hydrogen atom, at a distance of 1.42 Å from N(2), remains unexplained. The existence of a hydrogen atom on C(1) would not be possible, however, as an almost planar carbon atom could not accommodate a hydrogen atom in a perpendicular relationship.

The bond length N(1)-C(1) = 1.358(9) Å is not in the range of C-N single bonds, and such a single bond would be necessary for structure (a). Again, the high e.s.d. values militate against firm conclusions being drawn about the above-mentioned points.

However, these points might be reconciled with structure (a), if statistical disorder is assumed (see below), as explained above for the HSO₄ salt (section 3.3.2).

Alternatively, one might consider whether a tautomer of structure (a) could explain better the observed bond lengths and angles.

The resonance forms of a tautomer, (T), of structure (a) are shown in Diagram 3.16.

With the formulation (T), we could explain the observed planarity around C(1) as well as around N(2). However, this is the only point in favour of the above formulation.

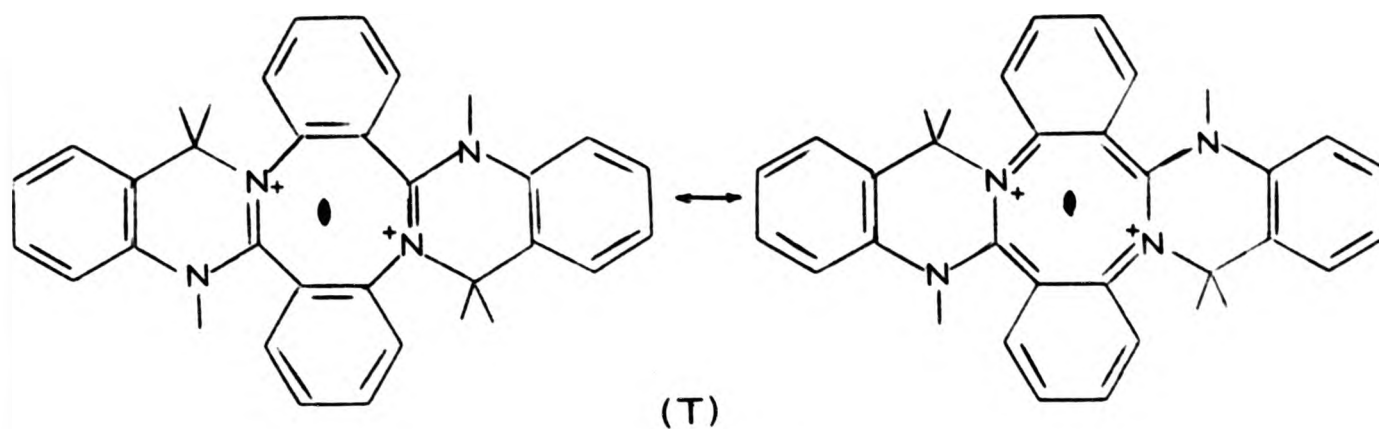


Diagram 3.16

The evidence against the formulation (T) is as follows:

Only one hydrogen atom was observed on the C(8) atom, as well as a possible hydrogen atom near C(1). With formulation (T) one would expect to observe 2 hydrogen atoms on C(8) with a tetrahedral C(7)-C(8)-N(2) angle and no hydrogen on the C(1) atom. The observed C(7)-C(8)-N(2) angle is $121.3(7)^\circ$ from which sp^2 -hybridization can be deduced for C(8). The bond lengths N(2)-C(1), N(2)-C(9), and C(1)-C(14') would be expected to be intermediate between that of a single and a double bond. The observed 3 bond lengths 1.440(9), 1.452(9), and 1.451(9) Å respectively for the above, however, have a single bond character. With the formulation (T) the bond lengths N(2)-C(8) and C(1)-N(1) would be expected to have single bond character. The observed values for these bonds are C(1)-N(1) = 1.358(9) and C(8)-N(2) = 1.318(8) Å, which show considerable double bond character.

Hence formulation (T) can be dismissed as highly unlikely.

The most persuasive explanation of the experimental data suggests the following. Isolated units of the cation have the structure proposed by Busch and co-workers¹. The reason why the observed bond lengths and angles differ from the ones expected for this formulation, is because

there is statistical disorder of the cation (as was observed in the HSO_4 salt), in addition to disorder in the BF_4 ion.

When statistical disorder was assumed (see section 3.2.3) the structure refined further, and the R-factor dropped from 0.077 to 0.067 while the e.s.d. values were somewhat improved. The important bond length and angles obtained for the disordered model are shown in Figure 3.5.

The evidence in favour of formulation (a+b) in Diagram 3.14.

The bond length $\text{N}(2)-\text{C}(1) = 1.477(10) \text{ \AA}$ has a single bond character. Bond lengths $\text{C}(1)-\text{C}(14')$ and $\text{N}(2)-\text{C}(9)$ of $1.435(8)$ and $1.468(8) \text{ \AA}$ respectively also have a single bond character and they are equal to each other, within the experimental error. The $\text{C}(8)-\text{N}(2)$ and $\text{N}(1)-\text{C}(1)$ bond lengths are also equal to each other within the experimental error, which would have been expected from the formulation (a+b). They could also be considered to have a character intermediate between that of a single and a double bond, although the observed values of $1.337(9)$, $1.336(8) \text{ \AA}$ are somewhat closer to the latter. The bond lengths $\text{C}(7)-\text{C}(8) = 1.384(8)$ and $\text{C}(2)-\text{N}(1) = 1.372(8) \text{ \AA}$ are also equal to each other within the experimental error as expected from the formulation (a+b). The sum of the angles around $\text{N}(2)$ and $\text{C}(1)$ are $356.1(9)^\circ$ and $355.8(9)^\circ$ respectively, which are equal to each other within the experimental error. The average value of 355.9° differs 4.1° from planarity as expected from the above formulation.

All the data hitherto discussed favour the disordered model. On the basis of this model we would expect to find half a hydrogen atom each at

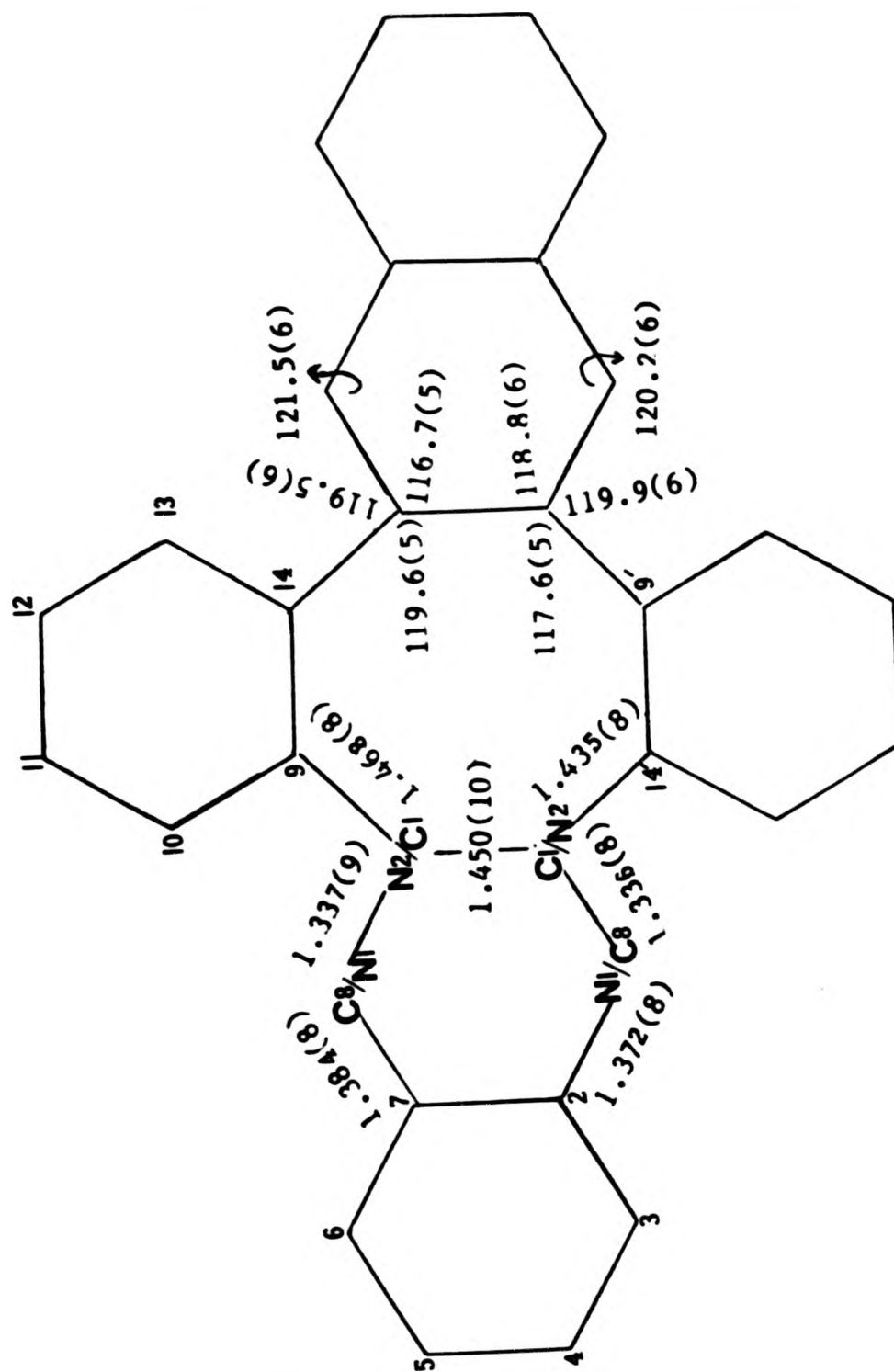


Figure 3.5

equivalent distances from the C(1)/N(2) and N(2)/C(1) sites. We would expect these to be at approximately 1.08 \AA from the actual position of the carbon atom. This is displaced through the averaging process. The average position of the C/N atom was found to be 0.165 \AA above the plane of the three connected atoms. In the $\text{TAABH}_2(\text{PICRATE})_2$ salt, which has an ordered structure (see section 3.3.1), the C(1) atom is 0.398 \AA above the plane of the three connected atoms. Hence, one would expect to find electron density near the C(1)/N(2) and N(2)/C(1) sites at a distance of $0.398 - 0.165 + 1.08 = 1.313 \text{ \AA}$. From the data of the ordered model, electron density was observed at 1.14 \AA from C(1) and 1.42 \AA from N(2), which is unexplained. A similar behaviour is observed in the disordered model, i.e. at 1.27 and 1.41 \AA respectively. This peak at 1.27 \AA from C(1) was assumed to be the H(1) position and it was included in the refinement; the R-factor converged at 0.067, $R_w = 0.071$. The peak at 1.41 \AA remains unexplained.

The disordered BF_4 counter-ion resolved into two components (see section 3.2.3). The bond lengths and angles are given in Tables 3.12 and 3.13.

Both components of the BF_4 ion have reasonable, although distorted, tetrahedral configuration. The average bond lengths and angles are given below.

$$\text{B-F(1)} = 1.332(12) \text{ \AA}$$

$$\text{B-F(2)} = 1.319(8) \text{ \AA}$$

$$\text{B-F(3)} = 1.316(7) \text{ \AA}$$

$$\text{B-F(4)} = 1.306(11) \text{ \AA}$$

$$\text{Mean: } 1.318 \text{ \AA}$$

$$F(1)-B-F(2) = 108.5(6)^\circ$$

$$F(2)-B-F(4) = 106.8(7)^\circ$$

$$F(4)-B-F(3) = 107.5(7)^\circ$$

$$F(3)-B-F(1) = 109.5(7)^\circ$$

$$F(1)-B-F(4) = 114.0(9)^\circ$$

$$F(2)-B-F(3) = 108.5(11)^\circ$$

$$\text{Mean: } 108.1^\circ$$

The average F-B-F bond angles are in agreement with those of other workers.^{41,42} The B-F bond lengths (1.318 Å average) of the present structure appear, however, to be much shorter than previously reported values (1.41 Å) for tetrahedral boron;⁴¹⁻⁴³ they are close to values (1.31 Å) for trigonal planar boron.⁴⁴

The fluorine atoms F(4a) and F(2b) are pointing towards the N(1)/C(8) and C(8)/N(1) atom sites respectively. The distances F(4a).....N(1)/C(8) and F(2b).....C(8)/N(1) are 3.026 and 2.899 Å respectively (see Diagram 3.17 and section 3.4).

X-ray crystallographic investigations of N-H...F hydrogen bonds are not very numerous. The majority have been published in the last dozen years. They are, on the whole, fairly accurate structure determinations and are reasonably well documented.

The structures of ammonium fluorides and of related fluorine-containing compounds, e.g. $N_2H_6F_2$ and NH_4HF_2 , differ markedly from related compounds, where either the ammonium ion is replaced by an alkali metal ion, or the fluorine-containing anion is replaced by one

containing another halide.⁴³ Thus, for instance, NH_4F has a totally different crystal structure compared to those of the other ammonium halides NH_4X ($\text{X} = \text{Cl}, \text{Br}, \text{I}$), which are, in turn, closely related, and NH_4HF_2 has a structure very different from those of the alkali metal bifluorides, e.g. KHF_2 .⁴³ This difference in structure in itself has been attributed to N-H...F hydrogen bonding, both nitrogen and fluorine being prone to this type of interaction. Further evidence comes from the N-H...F distances, as well as, where available, the H...F distances. Examples of compounds with N-H...F hydrogen bonds, including the present structure, together with the geometries of these, are given in Table 3.14.

Table 3.14 Examples of N-H...F hydrogen bonds

Example	N-H...F (Å)	H...F (Å)	N-H...F (°)
1) Present structure	2.899	1.915	149.8
2) NH_4F ⁴⁵	2.707-2.709		
3) NH_4HF_2 ⁴⁶	2.797-3.106		
4) NH_4BF_4 ⁴²	2.930-3.446	2.16-2.50	122.4-171.6
5) $\text{H}_3\text{N-BF}_3$ ⁴⁷	2.98 -3.15		
6) $(\text{NH}_4)_2\text{SiF}_6$ (cubic) ⁴⁸	2.996	2.075	155
7) $(\text{NH}_4)_2\text{BeF}_4$ ⁴⁹	2.785-3.094	1.93-2.51	122 -171
8) $(\text{NH}_4)_2\text{VF}_4\text{O}$ ⁵⁰	2.825-3.196		
9) $(\text{NH}_4)_2\text{Ni}(\text{BeF}_4)_2 \cdot 6\text{H}_2\text{O}$ ⁵¹	2.777-3.022		
10) $\text{N}_2\text{H}_6\text{F}_2$ ⁵²	2.62		
11) $\text{N}_2\text{H}_6\text{SiF}_6$ ⁵³	2.714-2.945	1.881-2.299	122.2-169.3
12) $\text{N}_2\text{H}_6\text{TiF}_6$ ⁵⁴	2.612-3.070		
13) $\text{N}_2\text{H}_6\text{ZrF}_6$ ⁵⁵	2.62 -2.85		
14) $(\text{N}_2\text{H}_6)_2\text{F}_2(\text{TiF}_6)$ ⁵⁶	2.568-2.765		

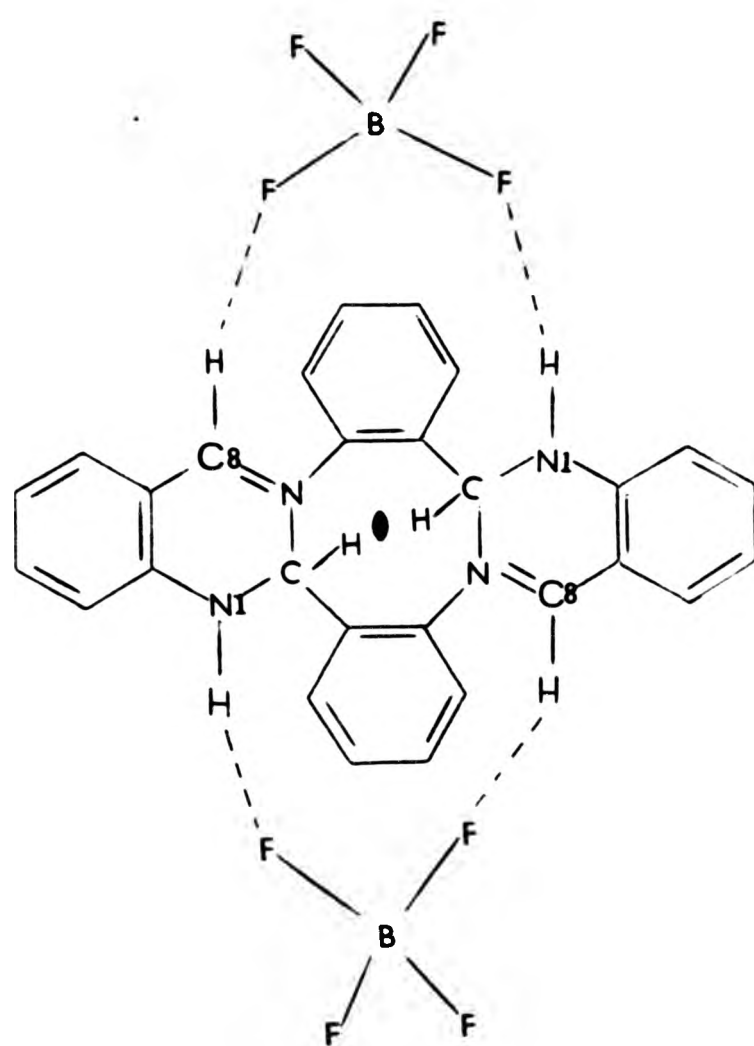


Diagram 3.17

Table 3.12 Bond lengths (\AA) for $\text{TAABH}_2(\text{BF}_4)_2$

N(1) -C(1)	1.336(8)	N(1) -Nc(1)	1.335(8)
N(1) -C(2)	1.370(8)	Cn(1) -C(1)	1.335(8)
Cn(1) -Nc(1)	1.336(8)	Cn(1) -C(2)	1.372(8)
N(2) -C(1)	1.450(10)	N(2) -Nc(1)	1.447(10)
N(2) -C(8)	1.337(9)	N(2) -Nc(8)	1.337(9)
N(2) -C(14b)	1.468(8)	Cn(2) -C(1)	1.447(10)
Cn(2) -Nc(1)	1.450(10)	Cn(2) -C(8)	1.336(9)
Cn(2) -Nc(8)	1.336(9)	Cn(2) -C(14b)	1.468(8)
C(1) -C(9)	1.435(8)	Nc(1) -C(9)	1.435(8)
C(2) -C(3)	1.420(9)	C(2) -C(7)	1.429(10)
C(3) -C(4)	1.359(10)	C(4) -C(5)	1.398(14)
C(5) -C(6)	1.398(11)	C(6) -C(7)	1.396(9)
C(7) -C(8)	1.384(8)	C(7) -Nc(8)	1.384(8)
C(9) -C(10)	1.383(8)	C(9) -C(14)	1.398(6)
C(10) -C(11)	1.393(10)	C(11) -C(12)	1.365(8)
C(12) -C(13)	1.362(10)	C(13) -C(14)	1.386(9)
B -F(1a)	1.317(13)	B -F(1b)	1.341(21)
B -F(2a)	1.325(10)	B -F(2b)	1.305(13)
B -F(3b)	1.388(18)	B -F(3a)	1.244(15)
B -F(4b)	1.211(22)	B -F(4a)	1.398(10)
F(1a) -F(1b)	.635(18)	F(1b) -F(3a)	1.80(3)
F(2a) -F(2b)	.848(19)	F(2a) -F(4b)	1.543(19)
F(2b) -F(3a)	1.658(17)	F(3b) -F(3a)	.714(15)
F(3b) -F(4a)	1.702(18)	F(4b) -F(4a)	.817(19)

Table 3.13: Bond angles ($^{\circ}$) for $\text{TAABH}_2(\text{BF}_4)_2$

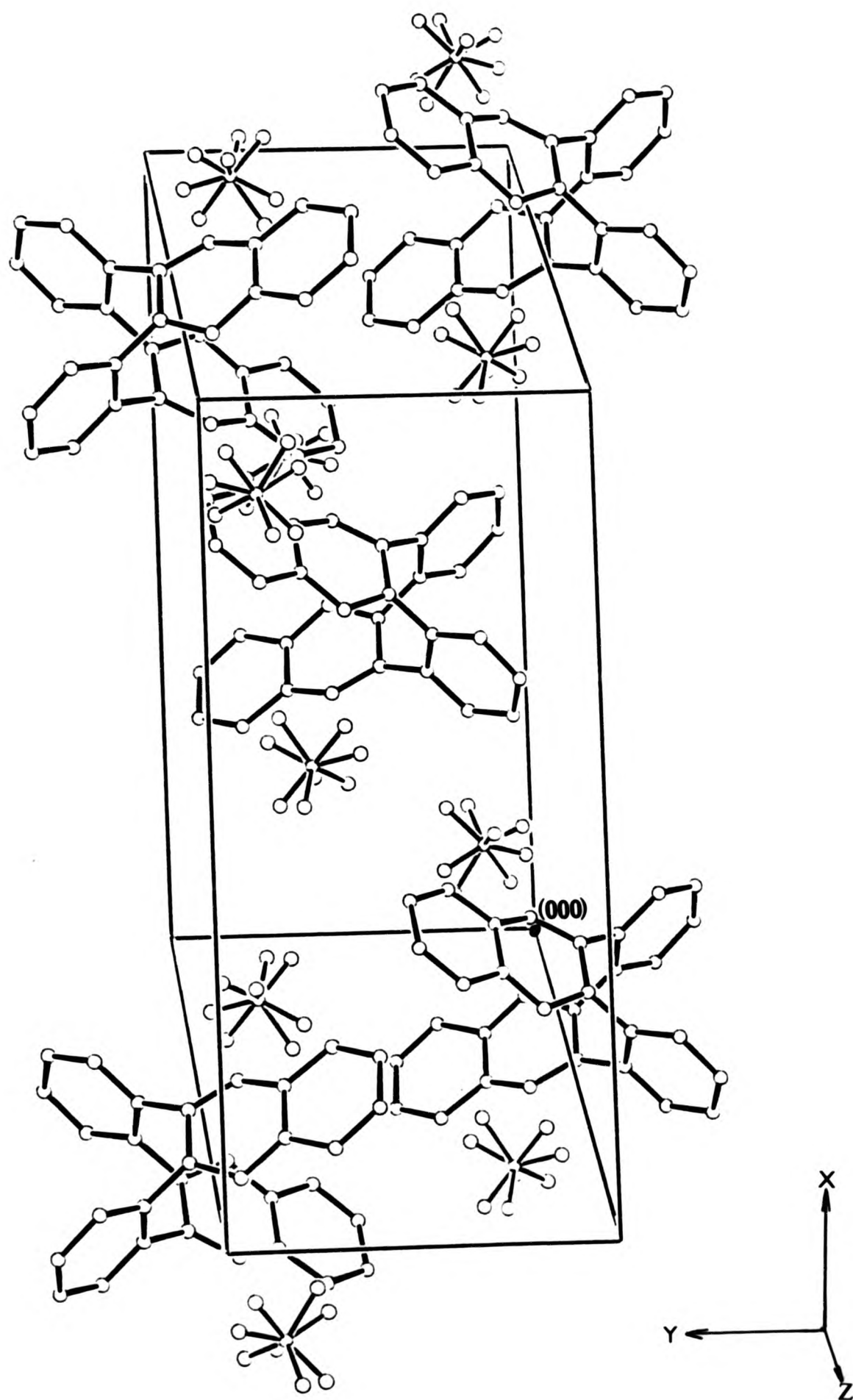
Nc(1) -N(1) -C(1)	0.0(1)	C(2) -N(1) -C(1)	121.5(6)
C(2) -N(1) -Nc(1)	121.5(6)	Nc(1) -Cn(1) -C(1)	0.0(1)
C(2) -Cn(1) -C(1)	121.5(6)	C(2) -Cn(1) -Nc(1)	121.5(6)
Nc(1) -N(2) -C(1)	0.0(1)	C(8) -N(2) -C(1)	118.8(6)
C(8) -N(2) -Nc(1)	118.8(6)	Nc(8) -N(2) -C(1)	118.8(6)
Nc(8) -N(2) -Nc(1)	118.8(6)	Nc(8) -N(2) -C(8)	0.0(1)
C(14b)-N(2) -C(1)	117.6(5)	C(14b)-N(2) -Nc(1)	117.6(5)
C(14b)-N(2) -C(8)	119.9(6)	C(14b)-N(2) -Nc(8)	119.9(6)
Nc(1) -Cn(2) -C(1)	0.0(1)	C(8) -Cn(2) -C(1)	118.8(6)
C(8) -Cn(2) -Nc(1)	118.8(6)	Nc(8) -Cn(2) -C(1)	118.8(6)
Nc(8) -Cn(2) -Nc(1)	118.8(6)	Nc(8) -Cn(2) -C(8)	0.0(1)
C(14b)-Cn(2) -C(1)	117.6(5)	C(14b)-Cn(2) -Nc(1)	117.6(5)
C(14b)-Cn(2) -C(8)	119.9(6)	C(14b)-Cn(2) -Nc(8)	119.9(6)
Cn(1) -C(1) -N(1)	0.0(1)	N(2) -C(1) -N(1)	116.7(5)
N(2) -C(1) -Cn(1)	116.7(5)	Cn(2) -C(1) -N(1)	116.7(5)
Cn(2) -C(1) -Cn(1)	116.7(5)	Cn(2) -C(1) -N(2)	0.0(1)
C(9) -C(1) -N(1)	119.5(6)	C(9) -C(1) -Cn(1)	119.5(6)
C(9) -C(1) -N(2)	119.6(5)	C(9) -C(1) -Cn(2)	119.6(5)
Cn(1) -Nc(1) -N(1)	0.0(1)	N(2) -Nc(1) -N(1)	116.7(5)
N(2) -Nc(1) -Cn(1)	116.7(5)	Cn(2) -Nc(1) -N(1)	116.7(5)
Cn(2) -Nc(1) -Cn(1)	116.7(5)	Cn(2) -Nc(1) -N(2)	0.0(1)
C(9) -Nc(1) -N(1)	119.5(6)	C(9) -Nc(1) -Cn(1)	119.5(6)
C(9) -Nc(1) -N(2)	119.6(5)	C(9) -Nc(1) -Cn(2)	119.6(5)
Cn(1) -C(2) -N(1)	0.0(1)	C(3) -C(2) -N(1)	122.6(7)
C(3) -C(2) -Cn(1)	122.6(7)	C(7) -C(2) -N(1)	117.8(6)

Table 3.13: continued

C(7) -C(2) -Cn(1)	117.8(6)	C(7) -C(2) -C(3)	119.3(6)
C(4) -C(3) -C(2)	119.4(8)	C(5) -C(4) -C(3)	122.2(7)
C(6) -C(5) -C(4)	119.2(7)	C(7) -C(6) -C(5)	120.5(8)
C(6) -C(7) -C(2)	119.2(6)	C(8) -C(7) -C(2)	116.9(5)
C(8) -C(7) -C(6)	123.6(7)	Nc(8) -C(7) -C(2)	116.9(5)
Nc(8) -C(7) -C(6)	123.6(7)	Nc(8) -C(7) -C(8)	0.0(1)
Cn(2) -C(8) -N(2)	0.0(1)	C(7) -C(8) -N(2)	120.2(6)
C(7) -C(8) -Cn(2)	120.2(6)	Cn(2) -Nc(8) -N(2)	0.0(1)
C(7) -Nc(8) -N(2)	120.2(6)	C(7) -Nc(8) -Cn(2)	120.2(6)
Nc(1) -C(9) -C(1)	0.0(1)	C(10) -C(9) -C(1)	119.9(4)
C(10) -C(9) -Nc(1)	119.9(4)	C(14) -C(9) -C(1)	121.4(5)
C(14) -C(9) -Nc(1)	121.4(5)	C(14) -C(9) -C(10)	118.7(5)
C(11) -C(10) -C(9)	119.9(5)	C(12) -C(11) -C(10)	120.8(6)
C(13) -C(12) -C(11)	120.0(6)	C(14) -C(13) -C(12)	120.5(5)
C(13) -C(14) -C(9)	120.1(5)	Cn(2) -C(14b) -N(2)	0.0(1)
F(1b) -B -F(1a)	27.6(8)	F(2a) -B -F(1a)	109.7(8)
F(2a) -B -F(1b)	116.4(8)	F(2b) -B -F(1a)	119.9(9)
F(2b) -B -F(1b)	107(1)	F(2b) -B -F(2a)	37.6(9)
F(3b) -B -F(1a)	123(1)	F(3b) -B -F(1b)	106(1)
F(3b) -B -F(2a)	126(1)	F(3b) -B -F(2b)	100(1)
F(3a) -B -F(1a)	114(1)	F(3a) -B -F(1b)	88(1)
F(3a) -B -F(2a)	117.2(9)	F(3a) -B -F(2b)	81(1)
F(3a) -B -F(3b)	30.9(8)	F(4b) -B -F(1a)	96(1)
F(4b) -B -F(1b)	124(2)	F(4b) -B -F(2a)	75(1)
F(4b) -B -F(2b)	109(1)	F(4b) -B -F(3b)	109(1)
F(4b) -B -F(3a)	138(1)	F(4a) -B -F(1a)	104.6(7)
F(4a) -B -F(1b)	124(1)	F(4a) -B -F(2a)	104.2(7)
F(4a) -B -F(2b)	128(1)	F(4a) -B -F(3b)	75.3(8)

Table 3.13: continued

F(4a) -B	-F(3a)	106.2(8)	F(4a) -B	-F(4b)	35.6(9)
F(1b) -F(1a) -B		78(2)	F(1a) -F(1b) -B		74(2)
F(3a) -F(1b) -B		43.7(8)	F(3a) -F(1b) -F(1a)		115(2)
F(2b) -F(2a) -B		69.9(9)	F(4b) -F(2a) -B		49.2(9)
F(4b) -F(2a) -F(2b)		115(1)	F(2a) -F(2b) -B		72.5(9)
F(3a) -F(2b) -B		47.9(8)	F(3a) -F(2b) -F(2a)		119(1)
F(3a) -F(3b) -B		63(1)	F(4a) -F(3b) -B		52.6(7)
F(4a) -F(3b) -F(3a)		116(2)	F(1b) -F(3a) -B		48.1(9)
F(2b) -F(3a) -B		51.0(7)	F(2b) -F(3a) -F(1b)		76.1(9)
F(3b) -F(3a) -B		86(2)	F(3b) -F(3a) -F(1b)		112(2)
F(3b) -F(3a) -F(2b)		115(2)	F(2a) -F(4b) -B		56.0(9)
F(4a) -F(4b) -B		85(2)	F(4a) -F(4b) -F(2a)		129(2)
F(3b) -F(4a) -B		52.1(6)	F(4b) -F(4a) -B		60(1)
F(4b) -F(4a) -F(3b)		109(2)			



Drawing 3.3b

3.4 A COMPARISON OF THE STRUCTURES OF THE TAAB SALTS (PICRATE,
HSO₄, AND BF₄)

Hydrogen bonds of five types were observed either with certainty, or at least with a high degree of probability, in the above three TAAB salts. These types are given in Table 3.15 together with their dimensions.

Table 3.15 Hydrogen bonds in TAAB salts

Type of H-bond	Anion of TAAB salt	X-H...Y(Å)	H...Y(Å)	X-H...Y(°)
O-H...O	HSO ₄	2.466	1.621	149.0
		2.506	1.703	139.1
N-H...O	Picrate	2.889	2.040	143.8
	HSO ₄	2.936	1.806	102.9
N-H...F	BF ₄	2.899	1.915	149.8
C-H...O	Picrate	3.119	2.183	168.9
	HSO ₄	3.157	2.110	102.0
C-H...F	BF ₄	3.026	1.993	162.2

As mentioned earlier, of the above three structures, only that of the picrate is ordered. Here the assignment of N-H...O and C-H...O contacts (2.889 and 3.119 Å respectively) are unambiguous. In the HSO₄ and BF₄ salts, disorder is observed in the cation as well as in the anions. Two distinct contacts for C/N-H...O in the HSO₄ salt (2.947 and 3.160 Å), as well as for C/N-H...F in the BF₄ salt (2.899 and 3.026 Å), were observed. In the case of the HSO₄ derivative the assignment, by

analogy to that of the picrate is quite simple as the values are close in these two salts. As N-H...O bonds are generally stronger, and therefore shorter, than otherwise similar C-H...O bonds, it seems likely that a similar relationship applies also to N-H...F and C-H...F bonds, and the assignments of the longer and the shorter distances for the BF_4 salt were made on this assumption. The two experimentally-observed values are, however, close to each other. The shorter one (2.899 \AA) comes close to reported N-H...F hydrogen bond values (see section 3.3.3, Table 3.14). Whilst a number of N-H...F hydrogen bonds have been previously observed, the present structure may well represent the first example of a C-H...F hydrogen bond. The geometry is eminently reasonable, and as the C-H...O hydrogen bond in the picrate salt is the shortest one (3.119 \AA) reported by X-ray crystallography with a large C-H...O angle of 168.9° , and hydrogen bonding is also strong in the bisulphate salt (see section 3.3.2), the structural situation seems very suitable for a chelated pair of hydrogen bonds in these salts. The argument is strengthened by recent observations of C-H...Cl hydrogen bonds.^{57,58} Most, but not all, of these are to Cl^- ions. In the BF_4 ion each F atom would have only a $1/4$ negative charge. As fluorine is, however, much more prone to hydrogen bonding than chlorine, and as the BF_4 ion has been observed to hydrogen bond in NH_4BF_4 ,⁴² the postulate of a C-H...F hydrogen bond in the BF_4 salt seems well justified.

In all of these three structures, two atoms with lone pairs of electrons (O,F) approach to close proximity and in an acceptable geometry to the NH and to the CH groups of the cation, forming a doubly hydrogen bridged chelated structure at each half of the cation. This is shown diagrammatically in Diagram 3.18.

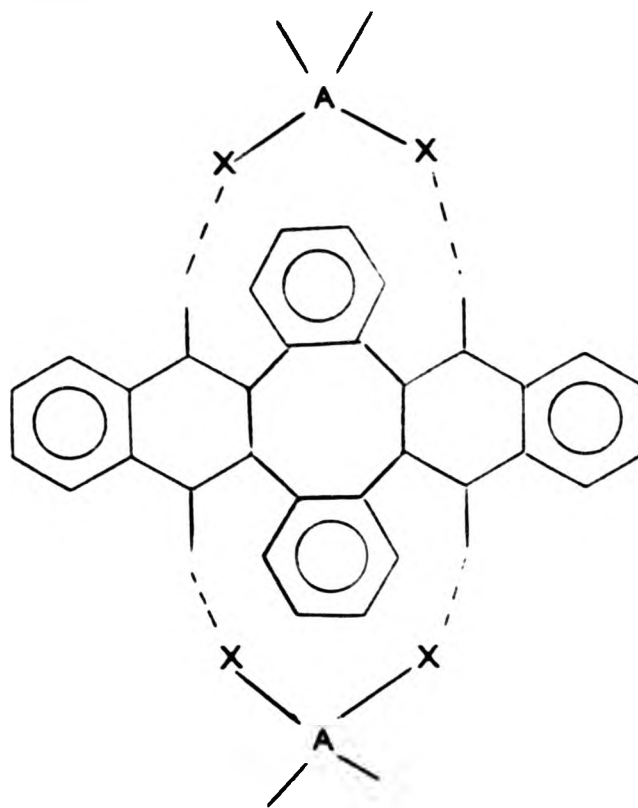


Diagram 3.18

Chelation, in general, is known to enhance the stability of a complex system containing one or more chelate rings, as compared to the stability of a system which is as similar as possible without containing these rings.⁵⁹

OH and NH hydrogen bonds to oxygen are well established.⁶⁰ Similar bonds to fluorine are documented^{44,61} (see also section 3.3.3). CH hydrogen bonds to oxygen have been advanced for about twenty years,⁶² although these were by no mean universally accepted. The recent careful analysis of neutron diffraction data by Taylor and Kennard,⁵⁷ and by Jeffrey and Maluszynska,⁵⁸ places the existence of these bonds now beyond reasonable doubt.

In the three structures of TAAB salts described above, each exhibits some peculiarity of its own. Two of these, the BF_4 and the HSO_4 salt are disordered, the picrate salt is ordered. Taking the ordered structure first (see Diagram 3.8), we observe that the phenolic oxygen atom of the picrate ion forms a strong hydrogen bond to the NH group of

N(1), and another, somewhat weaker, hydrogen bond from a nitro group oxygen, O(1), to the CH group, C(8). The structural situation, with a doubly bonded nitrogen atom carrying a positive charge next to the CH group in question, makes this, according to Taylor and Kennard's⁵⁷ analysis a particularly favourable situation. This is borne out by the fact that the CH hydrogen bond reported here is the shortest one on record and the C-H...O bond angle the largest.

In the HSO_4 salt the structure is disordered and we effectively see the average of the CH/NH sites. Again, the distances and the geometries of the approach of the HSO_4 oxygen atoms indicate strong hydrogen bonding (see Diagram 3.15). Over and above the hydrogen bonding between the cation and the anion, there is also strong O-H...O hydrogen bonding between two HSO_4 units. The overall effect is a macromolecular chain structure held together by hydrogen bonding, and this accounts for the insolubility of this salt in non-hydroxylic solvents.

In the BF_4 salt the fluorine atoms approach within a reasonable distance and geometry to the disordered NH/CH sites (see Diagram 3.17). Two NH/CH...F distances are observed, of which one, at 2.899 \AA , agrees well with previously reported N-H...F values (see section 3.3.3).

All the three counter-ions have a unit negative charge. In the picrate this will be largely localised on the phenolic oxygen atom, whilst in the HSO_4 and BF_4 ions, it will be distributed over 3 or 4 equivalent sites respectively, and thus the net charge density will be lower than that on the phenolic oxygen atom on the picrate ion. NH hydrogen bonds are much stronger than CH hydrogen bonds. It may well be

that some change in bond length associated with the mean of the C(8)-N(2) and N(1)-C(1) bond lengths is related to the strength of the hydrogen bond of the NH group. According to the arguments developed above, the hydrogen bond from the phenolic oxygen atom should be the strongest. The greater the strength of this bond the greater the possibility of mesomeric release of electrons which will ultimately affect the C(8)-N(2) bond length (see Diagram 3.4). It will be shown in section 4.4, which deals with the condensation products of AA, that a nitrogen bonded to hydrogen is more effective in such a mesomeric effect than one which is only bonded to carbon atoms.

We have argued that the electron release will tend to reduce the double bond character of this bond and hence increase its length. If, as we suggest, the HSO₄ and the BF₄ ions form weaker hydrogen bonds to the NH group, the mesomeric effect will be reduced, the C(8)-N(2) bond will have more double bond character and, therefore, will be shortened. As both structures are disordered the overall effect will be shortened average C(8)-N(2) and N(1)-C(1) bonds. The average bond lengths and angles for the three structures are shown in Diagram 3.19.

On comparing bond lengths, the same trends are apparent in all three structures. Only one significant difference in bond length is observed: the C(8)-N(2) and C(1)-N(1) mean bond length in the HSO₄ salt is significantly shorter than the corresponding mean bond length in the picrate, suggesting, as argued above, a somewhat greater double bond character for the C(8)-N(2) bond. Although statistically not significant, a trend, similar to that observed in the HSO₄ salt, can be seen in the BF₄ salt.

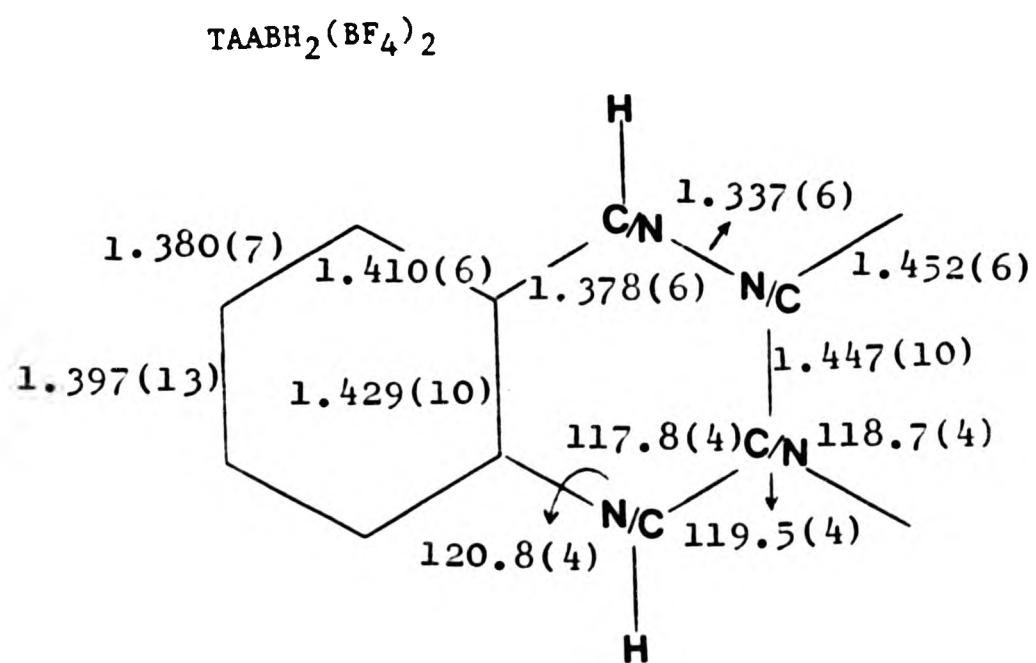
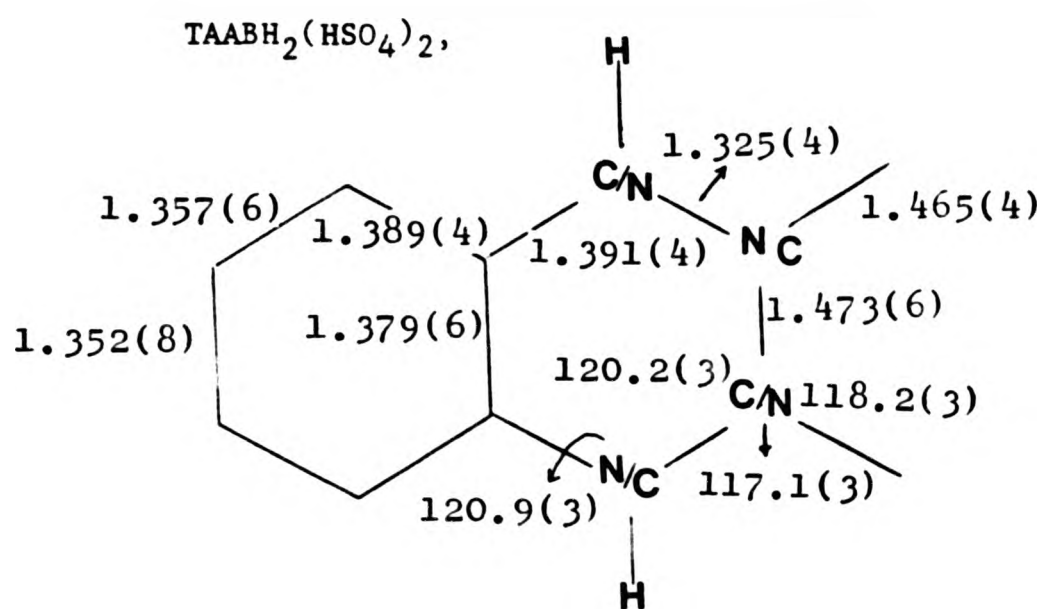
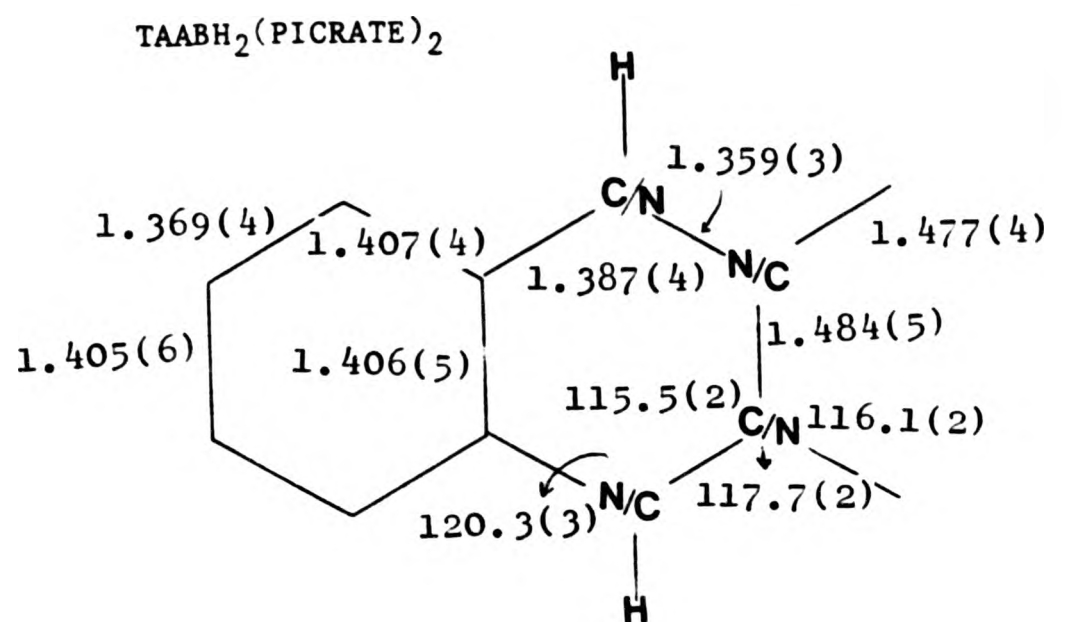


Diagram 3.19

The bond angles around the bridge-head C/N sites are significantly larger for the HSO_4 and BF_4 salts than in the picrate salt. The mean sums of the bond angles per C/N bridge-head site are 355.5, 356.0, and 349.3° respectively for the HSO_4 , BF_4 and picrate salts. As the nitrogen atom is planar in the picrate, the above data suggest a somewhat more flattened carbon atom in the HSO_4 and BF_4 salts than in the picrate.

The TAABH_2 cation lacks mirror symmetry. Its mirror image is not superimposable. Both enantiomers are present in the crystal. In the picrate salt these occur in an ordered array as the phenolic oxygen atom shows a preference to hydrogen bond to the N-H site. Therefore the nitro group oxygen atom has to bond at the C-H site. In the HSO_4 and BF_4 salts both electron donor sites are equivalent, and therefore hydrogen bonding does not favour the ordered over the disordered cation arrangement. Bilirubin⁶³, a neutral hydrogen bonded molecule, also gives rise to a disordered structure due to the two enantiomers occupying each others sites.

One point remains to be made in the comparison of the above three structures. The picrate ion is the only one where the atoms with the lone pairs involved in the hydrogen bonding are not equivalent. This structure is ordered. In the other two salts, the HSO_4 and the BF_4 , the two lone pair donor sites are equivalent and these structures are disordered. This observation may well be significant.

REFERENCES

1. J.S. Skuratowicz, I. L. Madden, and D. H. Busch, Inorg. Chem., 1977, 16, 1721.
2. J. O. Lundgren and I. Olovsson, in "The Hydrogen Bond", Edts., P. Schuster, G. Zundel, and C. Sandorfy, North Holland, Amsterdam, New York, Oxford, 1976, Ch. 10.
3. J. D. Goddard and T. Norris, Inorg. Nucl. Chem. Letts., 1978, 14, 211.
4. A. Caron, G. J. Palenik, E. Goldish, and J. Donohue, Acta Cryst., 1964, 17, 102.
5. B. Kamenar, B. Kaitner, V. Katovic, and D. H. Busch, Inorg. Chem., 1979, 18, 815.
6. R. Radhakrishnan and S. Raghunathan, Acta Cryst., 1982, B38, 326.
7. M. J. S. Dewar, "Hyperconjugation", The Ronald Press Co., New York, 1962, Ch. 3; M. J. S. Dewar and H. N. Schmeising, Tetrahedron, 1959, 5, 166; 1960, 11, 196.
8. J. Elguero, A. R. Katritzky, B. S. El-Osta, R. L. Harlow, and S. H. Simonsen, J. Chem. Soc. Perkin I, 1976, 312.
9. P. A. Tucker, A. Hoekstra, J. M. Ten Cate, and A. Vos, Acta Cryst., 1975, B31, 733.
10. J. N. Brown and L. M. Trefonas, Acta Cryst., 1973, B29, 237.
11. T. Ottersen, C. Christophersen, and S. Treppendahl, Acta Chem. Scand., 1975, A29, 45.
12. G. M. Sheldrick and J. Trotter, Acta Cryst., 1978, B34, 3122.
13. L. Pauling, "The Nature of the Chemical Bond", 3rd Edn., Cornell University Press, Ithaca, New York, 1960, p. 237.
14. R. J. Kurland and E. B. Wilson, Jr., J. Chem. Phys., 1957, 27, 585.

15. ref. 13, p. 282.
16. J. B. Bernstein, H. Regev, and F. H. Herbstein, Acta Cryst., 1980, B36, 1170.
17. B. Jensen, Acta Chem. Scand., 1975, B29, 115.
18. K. Maarlmann-Moe, Acta Cryst., 1969, B25, 1452.
19. U. Thewalt and C. E. Bugg, Acta Cryst., 1972, B28, 82.
20. D. L. Hughes, C. L. Mortimer, and M. R. Truter, Inorg. Chim. Acta, 1978, 28, 83.
21. B. Jensen, Acta Chem. Scand., 1975, B29, 891.
22. F. H. Herbstein and M. Kaftary, Acta Cryst., 1976, B32, 387.
23. F. Seidel, Ber., 1927, 60, 314.
24. S. G. McGeachin, Can. J. Chem., 1966, 44, 2323.
25. C. Pascard-Billy, Acta Cryst., 1965, 18, 829.
26. E. J. Sonneveld and J. W. Visser, Acta Cryst., 1978, B34, 643.
27. Idem, ibid., 1979, B35, 1975.
28. L. H. Loopstra and C. MacGillavry, Acta Cryst., 1958, 11, 349.
29. D. W. J. Cruikshank, Acta Cryst., 1964, 17, 682.
30. F. A. Cotton, B. A. Frenz, and D. L. Hunter, Acta Cryst., 1975, B31, 302.
31. J. P. Ashmore and H. E. Petch, Can. J. Phys., 1975, 53, 2694.
32. R. J. Nelmes, Acta Cryst., 1971, B27, 272.
33. I. Taesler and I. Olovsson, Acta Cryst., 1968, B24, 299.
34. G. E. Pringle and T. A. Broadbent, Acta Cryst., 1965, 19, 426.
35. S. Grimvall, Acta Chem. Scand., 1971, 25, 3213.
36. W. P. Schaefer and R. E. Marsh, Acta Cryst., 1966, 21, 735.
37. W. P. Schaefer, S. E. Ealick, and R. E. Marsh, Acta Cryst., 1981, B37, 34.
38. M. Catti, G. Ferraris, and G. Ivaldi, Acta Cryst., 1979, B35, 525.

39. S. Suzuki and Y. Makita, Acta Cryst., 1978, B34, 732.
40. P.-G. Jonsson and I. Olovsson, Acta Cryst., 1968, B24, 559.
41. Von E. Hohne and L. Kutschabsky, Z. anorg. Chem., 1966, 344, 279.
42. A. P. Caron and J. L. Ragle, Acta Cryst., 1971, B27, 1102.
43. A. F. Wells, "Structural Inorganic Chemistry", 4th Edn., Clarendon Press, Oxford, 1975, pp. 835-836.
44. ref. 43, pp. 301-321.
45. B. Morosin, Acta Cryst., 1970, B26, 1635.
46. T. R. R. McDonald, Acta Cryst., 1960, 13, 113.
47. J. L. Hoard, S. Geller, and W. M. Cashin, Acta Cryst., 1951, 4, 396.
48. E. O. Schlemper, W. C. Hamilton, and J. J. Rush, J. Chem. Phys., 1966, 44, 2499.
49. A. Garg and R. C. Srivastava, Acta Cryst., 1979, B35, 1429.
50. P. Bukovec and L. Golic, Acta Cryst., 1980, B36, 1925.
51. H. Montgomery, Acta Cryst., 1980, B36, 2121.
52. M. L. Kronberg and D. Harker, J. Chem. Phys., 1942, 10, 309.
53. B. Frlec, D. Gantar, L. Golic, and I. Leban, Acta Cryst., 1980, B36, 1917.
54. B. Kojic-Prodic, B. Matkovic, and S. Scavnicar, Acta Cryst., 1971, B27, 635.
55. E. Kojic-Prodic, S. Scavnicar, and B. Matkovic, Acta Cryst., 1971, B27, 638.
56. L. Golic, V. Kaucic, and B. Kojic-Prodic, Acta Cryst., 1980, B36, 659.
57. R. Taylor and O. Kennard, J. Am. Chem. Soc., 1982, in the press and personal communication.
58. G. A. Jeffrey and H. Maluszynska, Int. J. Biol. Macromol., 1982,

- in the press and personal communication.
59. F. A. Cotton and G. Wilkinson, "Advanced Inorganic Chemistry", 4th Edn., John Wiley and Sons, New York, London, Chichester, Brisbane, Toronto, 1980, p. 71.
 60. I. Olovsson and P.-G. Jonsson, ref. 2, Ch. 4.
 61. W. C. Hamilton and J. A. Ibers, "Hydrogen Bonding in Solids", Benjamin, New York, 1968.
 62. D. J. Sutor, Nature, 1962, 195, 68; J. Chem Soc., 1963, 1105.
 63. R. Bonnett, J. E. Davies, M. B. Hursthouse, and G. M. Sheldrick, Proc. Roy. Soc. Lond., 1978, B202, 294.

CHAPTER 4

STRUCTURAL INVESTIGATIONS OF THE SELF-CONDENSATION PRODUCTS OF
ANTHRANILIC ACID (AA)

4.1 METHOD OF PREPARATION

The trimeric and tetrameric condensation products of AA were prepared by the method as reported in reference 1.

Solvent free crystals of AA TETRAMER were obtained from acetonitrile.

AA TETRAMER

	C	H	N
Analysis: Found	74.8	4.1	13.1
Calculated	76.4	3.6	12.7

AA TRIMER on recrystallisation from chloroform gave crystals stable at room temperature containing one molecule of chloroform per trimer molecule.

AA TRIMER. CHCl_3

	C	H	N
Analysis: Found	60.1	3.4	9.5
Calculated	57.6	3.05	9.2

By contrast although trimer gave also well-shaped crystals from

acetonitrile and ethyl acetate, these were only stable in contact with the mother-liquor. The crystals of the former were sealed into a Lindemann tube together with some mother-liquor and were found on crystallographic investigation to contain one molecule of acetonitrile and one molecule of water per trimer molecule.

AA TRIMER. $\text{CH}_3\text{CN}\cdot\text{H}_2\text{O}$

	C	H	N
Analysis: Found	69.4	4.3	15.15
Calculated	69.3	4.5	14.1

4.2 DATA COLLECTION AND STRUCTURE SOLUTION OF AA DERIVATIVES

4.2.1 DATA COLLECTION AND STRUCTURE SOLUTION OF AA TETRAMER

Details of the data collection and of crystal data are summarised in Tables 4.1 and 4.2.

Data reduction applied to the raw data consisting of 3668 reflections, resulted in 1311 unique reflections with $I > 3\sigma(I)$. The following systematic absences were observed.

h00	N.C.	h0l	$l=2n+1$
0k0	$k=2n+1$	0kl	N.C.
00l	N.C.	hk0	N.C.

From the volume of the unit cell, assuming that there are 4 molecules in the unit cell, the density was calculated, $D_c = 1.395 \text{ g/cm}^3$. The measured density is 1.381 g/cm^3 . From the above conditions the space group was uniquely defined as $P2_1/c$. An automatic

Table 4.1: Crystal data of anthranilic acid condensation products

	AA TETRAMER	AA TRIMER. CHCl_3	AA TRIMER. $\text{CH}_3\text{CN} \cdot \text{H}_2\text{O}$
Formula	$\text{C}_{28}\text{H}_{16}\text{N}_4\text{O}_2$	$\text{C}_{21}\text{H}_{13}\text{N}_3\text{O}_2 \cdot \text{CHCl}_3$	$\text{C}_{21}\text{H}_{13}\text{N}_3\text{O}_2 \cdot \text{CH}_3\text{N} \cdot \text{H}_2\text{O}$
Molecular weight	440	339+119=458	339+41+18=398
Crystal system	Monoclinic	Triclinic	Monoclinic
Space group	$\text{P}2_1/c$	$\bar{P}1$	$\text{P}2_1/c$
a (Å)	14.708(3)	11.278(3)	10.252(3)(6)
b (Å)	8.618(2)	10.781(3)	13.055(3)
c (Å)	17.484(4)	8.917(2)	16.088(4)
α (°)	90.00	95.62(3)	90.00
β (°)	109.15(4)	102.25(4)	106.21(4)
γ (°)	90.00	82.71(3)	90.00
Volume (Å ³)	2093.5	1047.8	2067.6
D_c (g/cm ³)	1.395	1.451	1.278
D_m (g/cm ³)	1.381	1.443	1.301
Z	4	2	4
F(000)	912	468	832
$\mu(\text{Mo-K}\alpha)$ (cm ⁻¹)	0.52	4.07	0.52

Table 4.2: Data collection and structure solution details of
anthranilic acid condensation products

	AA TETRAMER	AA TRIMER.CHCl ₃	AA TRIMER.CH ₃ CN.H ₂ O
Crystal size (mm)	0.36x0.24x0.25	0.32x0.21x0.33	0.48x0.44x0.43
Crystal colour	Pale yellow	Pale yellow	Colourless
Shape	Thin plates	Cubic	Cubic plates
BMO	1	1	1
SMO	1	1	1
Scan width (°)	0.9	0.9	0.8
θ-range (°)	3-30	3-30	3-30
Reflections meas.	3668	3691	2866
Unique data set	1311	2230	1502
Least-squares	209	276	277
parameters			
Data/parameter	6.3	8.0	5.5
Shift/e.s.d.	0.004	0.002	0.007
Weighting scheme	1/[σ ² (F)]	1/[σ ² (F)]	1/[σ ² (F)]
Max. electron	0.47	0.52	0.43
dens. residue e/Å ³			
R	0.056	0.063	0.057
R _w	0.053	0.068	0.054

centrosymmetric direct method was applied to the data. No solution was obtained. A tangent map was calculated with $E \geq 1.3$. 495 Reflections gave 7 path breaks. Two new origins were selected taking care that they have the same parity as in the E-map. 4 Multisolutions were introduced. The map with the lowest value of R_a gave the solution. All the non-hydrogen atoms (34) were located from this map. When these atoms were included, 12 cycles of difference Fourier and blocked full matrix least squares refinement calculations led to the location of 12 of the 16 hydrogen atoms. At this stage the refinement converged at $R = 0.087$. The atoms were blocked as follows: block 1 half the molecule, atoms with label (a); block 2 the other half of the molecule, atoms with label (b) (Diagram 4.1).

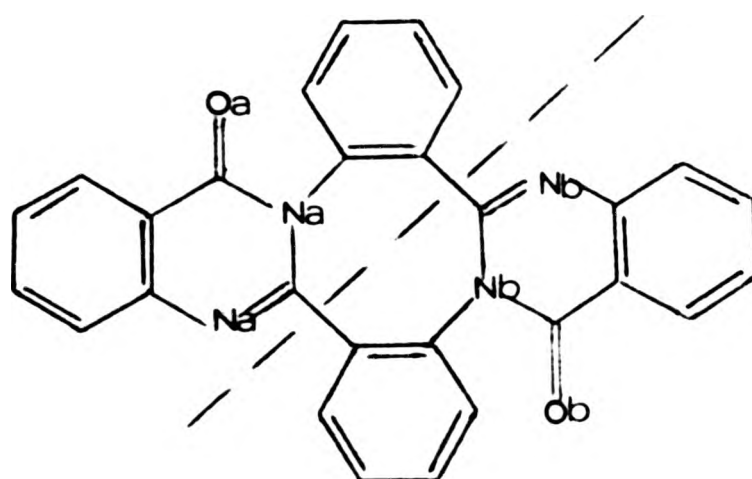


Diagram 4.1

12 Hydrogen atoms were included at their found positions. 8 Cycles of difference Fourier and blocked full matrix least squares refinement calculations led to the location of the last 4 hydrogen atoms with $R = 0.074$. In the next 10 cycles the two oxygen and four nitrogen atoms were refined with anisotropic thermal vibration parameters, and the last 4 hydrogen atoms were included in their found positions. The refinement

converged at $R = 0.058$. All the hydrogen atoms were placed at geometrically calculated positions with $C-H = 1.08 \text{ \AA}$, and 10 cycles of difference Fourier and full matrix least squares refinement calculations led to $R = 0.056$ and $R_w = 0.053$. The refinement was stopped when the calculated parameter shift/e.s.d. ratio fell to a maximum of 0.004. The highest residual electron density of 0.47 e/\AA^3 was observed near C(6b).

$$0.47 < \Delta\rho < -0.48$$

4.2.2 DATA COLLECTION AND STRUCTURE SOLUTION OF AA TRIMER. CHCl_3

Data collection and crystal data are in Tables 4.1 and 4.2.

Data reduction applied to the raw data consisting of 3691 reflections resulted in 2230 unique reflections with $I > 3\sigma(I)$. No systematic absences were observed, as expected for triclinic crystal system, with the possibility of the 2 space groups $P1$ or $P\bar{1}$. From the volume of the unit cell, assuming that there are 2 molecules in the unit cell, the density was calculated, $D_c = 1.451 \text{ g/cm}^3$. The measured density is $D_m = 1.443 \text{ g/cm}^3$.

First, the centrosymmetric automatic direct method was applied to solve the structure in the $P\bar{1}$ space group. 2 using E-values > 1.3 expanded to 241 signs using 1993 relations. No direct solution was obtained. The minimum E-value was varied, but still no solution was obtained. Therefore a tangent map was calculated. New origins and multisolutions were selected manually, taking care that the origins had

the same parity as in the E-maps. With $E \geq 1.4$, 450 reflections were used in the tangent map. The map ranked 9th in order of $R_{\bar{G}}$ values gave a recognisable solution. The 10 highest and 9 lower peaks were selected as non-hydrogen atoms. When these 19 non-hydrogen atoms (out of 26) were included, difference Fourier and 4 cycles of full matrix least squares refinement calculations led to $R = 0.51$, and the remaining 7 non-hydrogen atoms were located. Successive difference Fourier and full matrix least squares refinement calculations led to the location of CHCl_3 with $R = 0.45$. The refinement was continued using blocked full matrix refinement, where the atoms were grouped as follows: block 1 all non-hydrogen atoms, except the ones in the chloroform; block 2 chloroform. At this stage the refinement converged at $R = 0.23$. In the next cycles all the non-hydrogen atoms were refined with anisotropic thermal parameters, which led to the location of all 13 hydrogen atoms with $R = 0.083$. All observed hydrogen atom co-ordinates were included and for refinement allowed to ride on their respective carbon atom co-ordinates with site occupancy and temperature factors free. The refinement was stopped when the calculated parameter shift/e.s.d. ratio fell to a maximum of 0.002. The final $R = 0.063$, $R_w = 0.068$. The highest residual electron density of $0.52 \text{ e}/\text{\AA}^3$ was observed near the chloroform molecule.

$$0.52 < \Delta\rho < -0.56$$

4.2.3 DATA COLLECTION AND STRUCTURE SOLUTION OF AA TRIMER. $\text{CH}_3\text{CN} \cdot \text{H}_2\text{O}$

Several single crystals were mounted in subsequently sealed Lindemann tubes, as they rapidly decomposed when free from

mother-liquor. This is probably due to the loss of solvent, trapped in the crystal lattice.

The data collection and crystal data are in Tables 4.1 and 4.2.

Data reduction applied to the raw data consisting of 2866 reflections resulted in 1502 unique reflections with $I > 3 \sigma(I)$. The following systematic absences were observed.

h00	N.C.	h01	$l = 2n + 1$
0k0	$k = 2n + 1$	0kl	N.C.
00l	N.C.	hk0	N.C.

From the volume of the unit cell, assuming that there are 4 molecules in the unit cell, the density was calculated $D_c = 1.278 \text{ g/cm}^3$. The measured density is 1.301 g/cm^3 . The somewhat larger error than usual is due to the ready decomposition of these crystals. From the above conditions the space group was uniquely defined as $P2_1/c$. No solution was obtained with the automatic direct method. A convergence map was calculated with $E \gg 1.5$. 417 Reflections gave 6 path breaks. 3 New origins were selected manually taking care that they had the same parity as in the E-map. 3 Multisolutions were introduced. The map ranked 3rd in order of R_{σ} values, gave a recognisable solution. 25 Non-hydrogen atoms out of 26 (main molecule) were located. When these 25 atoms were included 5 cycles of difference Fourier and blocked full matrix least squares refinement calculations led to the location of the last non-hydrogen atom of the main molecule and the non-hydrogen atoms of acetonitrile with $R = 0.20$. The atoms were blocked as follows: block

1, 1st half of the main molecule; block 2 2nd half of the main molecule (Diagram 4.2).

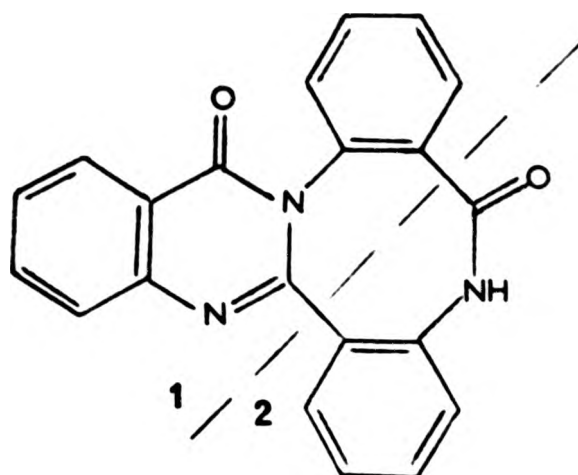


Diagram 4.2

In the next 12 cycles, with 29 non-hydrogen atoms, blocked full matrix least squares refinement converged at $R = 0.15$. The third block in these cycles was the acetonitrile molecule. When all the oxygen and the nitrogen atoms, and the carbon atoms of acetonitrile were refined with anisotropic thermal parameters and all the hydrogen atoms of the main molecule placed geometrically ($C-H = 1.08 \text{ \AA}$), 12 cycles of least squares refinement led to $R = 0.14$. 1 More peak appeared, which was assumed to be the oxygen atom of a water molecule. The oxygen atom was included in the next 8 cycles of blocked full matrix least squares refinement calculations, with the 4th block being the oxygen atom. This led to the location of 2 hydrogen atoms, one near the oxygen atom of the water molecule, the other near the carbon atom of the acetonitrile molecule. This led to $R = 0.095$. When the oxygen atom was refined with anisotropic thermal parameters 8 cycles of refinement converged at $R = 0.087$. The second hydrogen of the water molecule was located. In the final 8 cycles of the refinement the three hydrogen atoms of

acetonitrile were placed geometrically, the hydrogen atoms of the water molecule were included into the refinement at their found locations and allowed to ride on the oxygen atom co-ordinates with the site occupancy factors free and temperature factors common. The refinement converged at $R = 0.057$, $R_w = 0.054$. The refinement was stopped when the calculated parameter shift/e.s.d. ratio fell to a maximum of 0.007. The highest residual electron density of $0.43 \text{ e}/\text{\AA}^3$ was observed near the H(12) atom.

$$0.43 < \Delta\rho < -0.41$$

4.3 DISCUSSION OF AA DERIVATIVES

4.3.1 AA TETRAMER

The tetrameric condensation product of AA, AA TETRAMER, has the structure shown in Figure 4.1, which also shows important average bond length and angles. The bond length and angle data are given in Tables 4.3 and 4.4. The ORTEP drawing for this structure are in Drawing 4.1.

The whole molecule can be described as having a double saddle-shape, as observed for the $\text{TAABH}_2(\text{PICRATE})_2$ salt, but here there is no crystallographically imposed symmetry. One pair of opposite benzene rings 1, 2 (see Figure 4.1 and Table 4.5) are folding down, the other pair, 7, 14, are folding up with respect to the central eight-membered ring. The above feature gives the eight-membered ring a boat conformation. The molecule is folded by 7° along the C(8b),N(1b) line, but there is no corresponding fold along C(8a),N(1a). The remaining

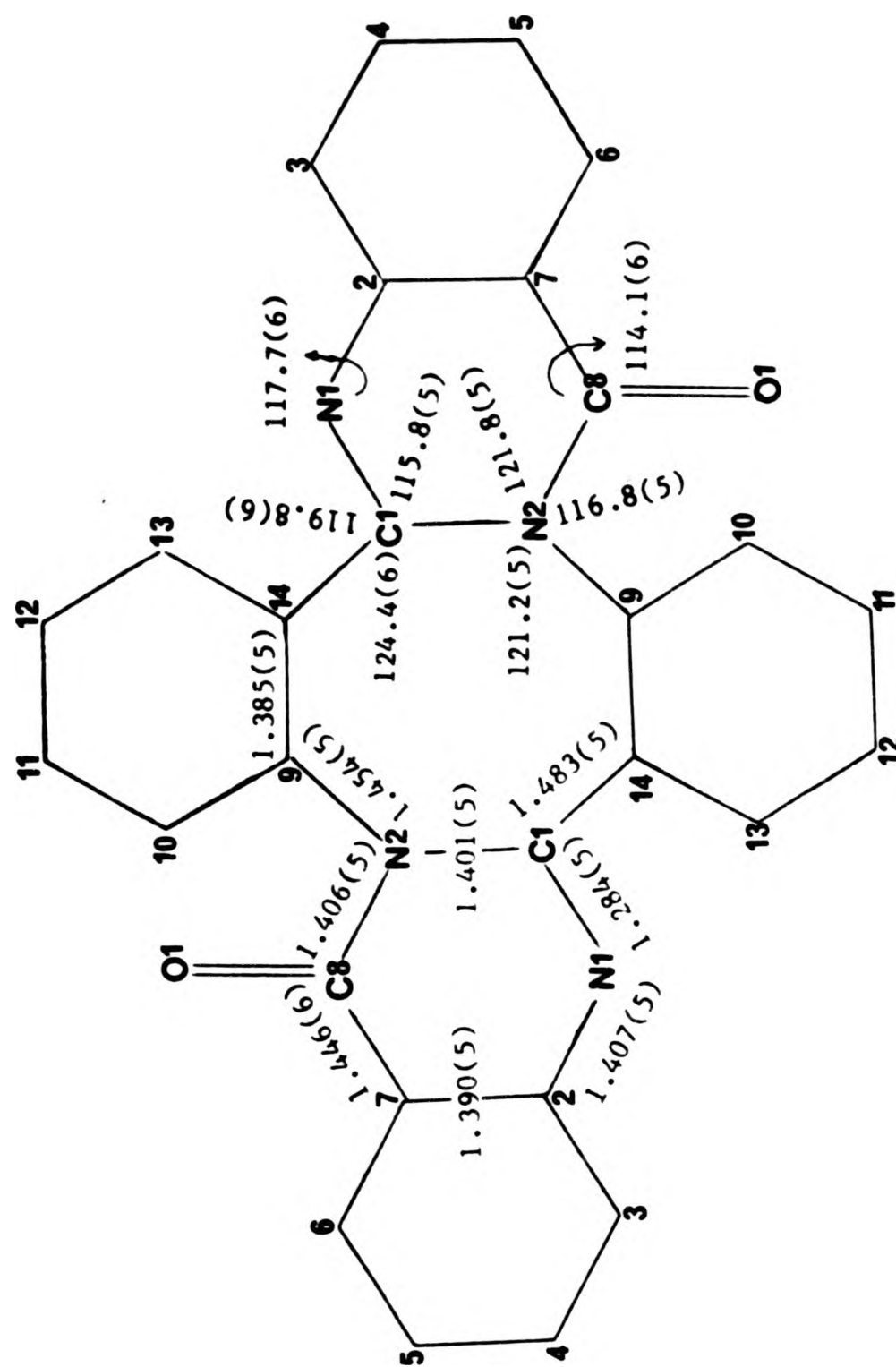
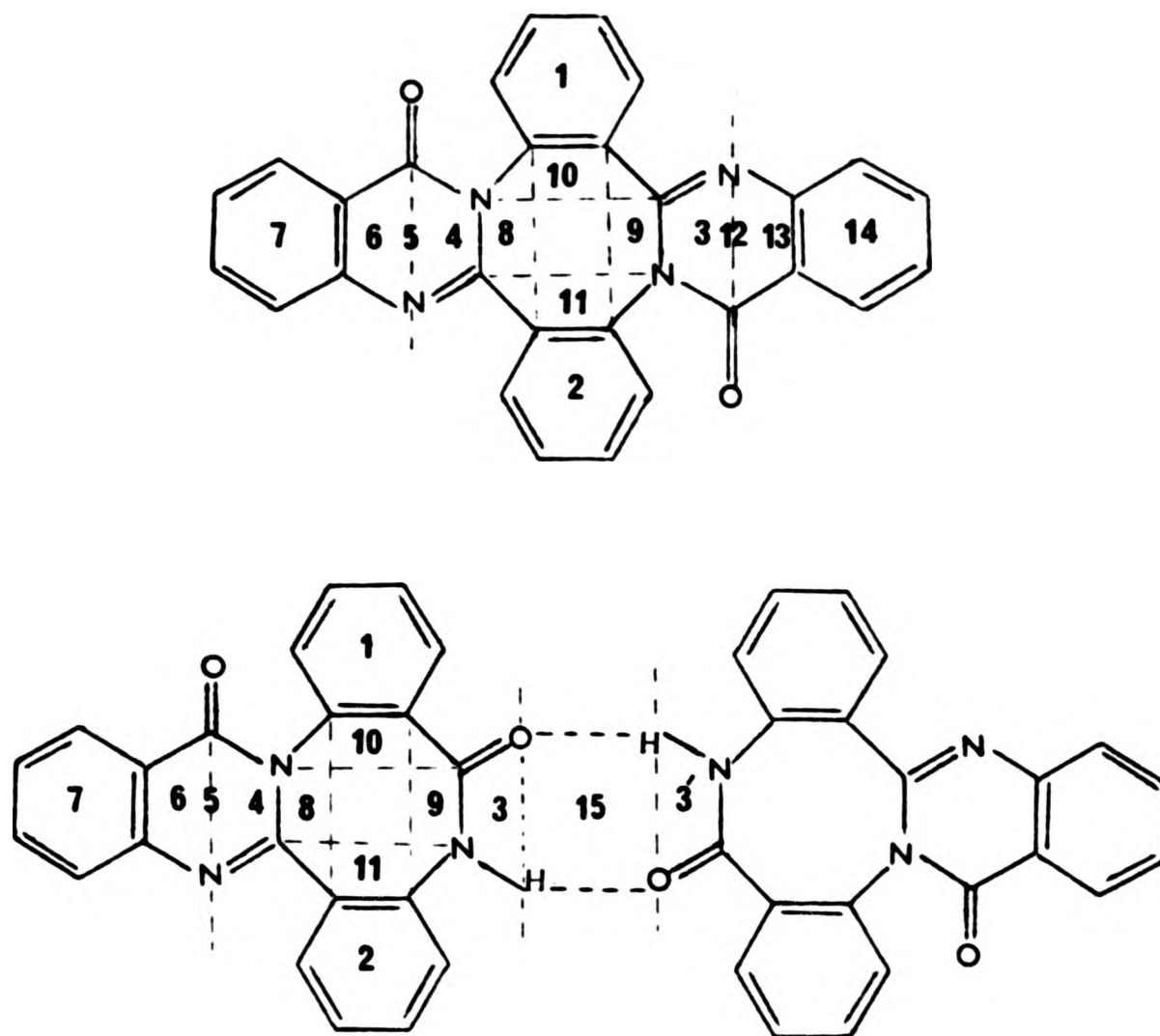


Figure 4.1

Table 4.5 : Angles between the planes in AA derivatives



Planes	TETRAMER Angle ^o	TRIMER.CHCl ₃ Angle ^o	TRIMER.CH ₃ CN.H ₂ O Angle ^o
1-2	73	79	67
3-4	75	83	74
6-15(6-13 TAAB)	71	84	79
4-8, 3-9	3,1	2	3
3-7(7-14 TAAB)	66	83	72
8-9	72	75	70
10-11	68	74	68
1-4	66	60	67
2-4	70	74	77
1-3		76	70
2-3		58	69

Table 4.3: Bond lengths (Å) for AA TETRAMER

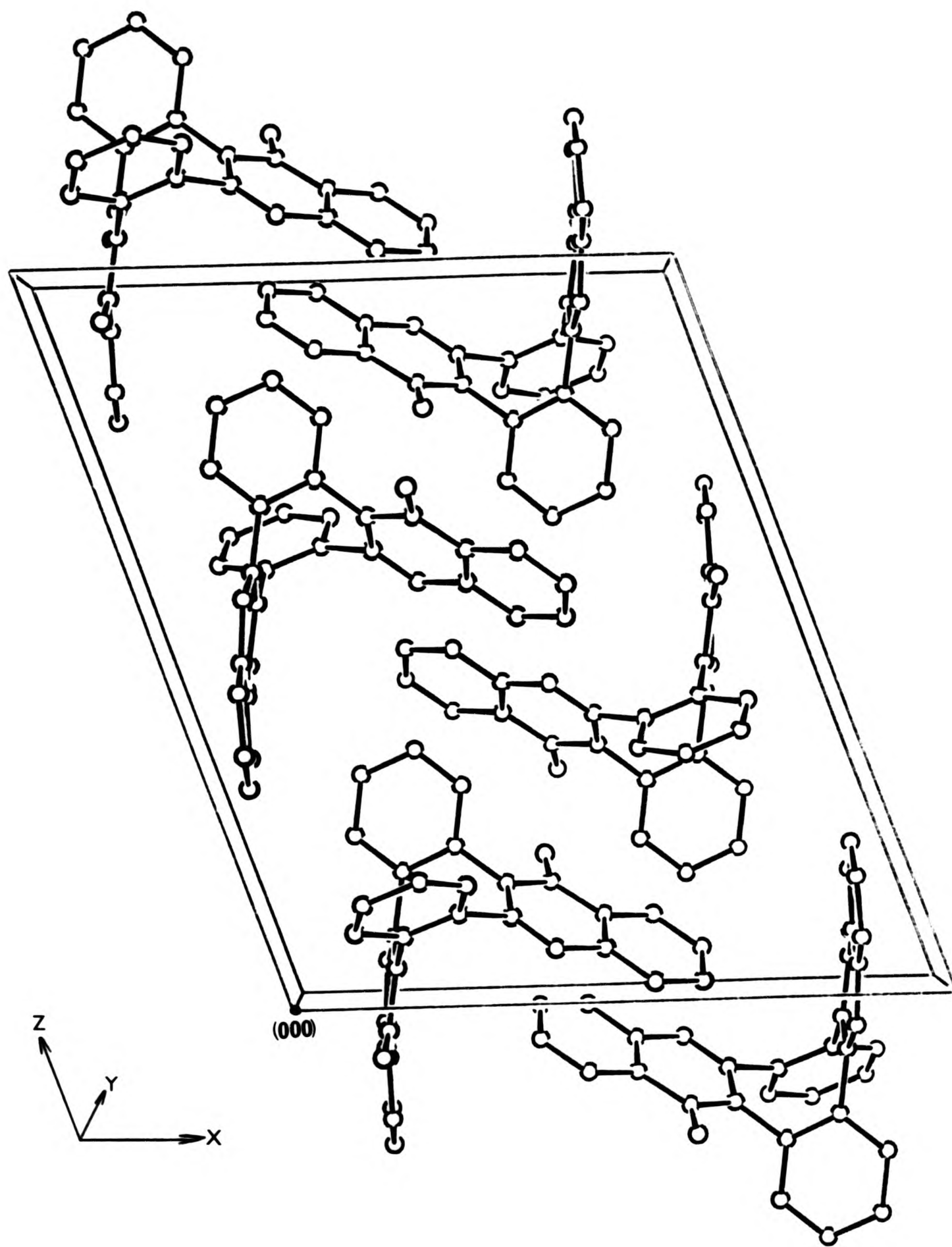
O(1a) -C(8a)	1.233(7)	N(1a) -C(1a)	1.281(7)
N(1a) -C(2a)	1.413(7)	N(2a) -C(1a)	1.402(7)
N(2a) -C(8a)	1.403(7)	N(2a) -C(9a)	1.452(7)
C(1a) -C(14b)	1.487(8)	C(2a) -C(3a)	1.400(8)
C(2a) -C(7a)	1.391(8)	C(3a) -C(4a)	1.373(9)
C(4a) -C(5a)	1.392(9)	C(5a) -C(6a)	1.370(9)
C(6a) -C(7a)	1.414(9)	C(7a) -C(8a)	1.457(8)
C(9a) -C(10a)	1.377(8)	C(9a) -C(14a)	1.384(8)
C(10a) -C(11a)	1.383(8)	C(11a) -C(12a)	1.389(9)
C(12a) -C(13a)	1.393(9)	C(13a) -C(14a)	1.401(8)
C(14a) -C(1b)	1.478(8)	O(1b) -C(8b)	1.235(8)
N(1b) -C(1b)	1.287(8)	N(1b) -C(2b)	1.401(7)
N(2b) -C(1b)	1.399(8)	N(2b) -C(8b)	1.408(8)
N(2b) -C(9b)	1.455(8)	C(2b) -C(3b)	1.405(9)
C(2b) -C(7b)	1.389(8)	C(3b) -C(4b)	1.379(10)
C(4b) -C(5b)	1.389(10)	C(5b) -C(6b)	1.386(9)
C(6b) -C(7b)	1.389(9)	C(7b) -C(8b)	1.435(9)
C(9b) -C(10b)	1.379(8)	C(9b) -C(14b)	1.387(8)
C(10b) -C(11b)	1.397(9)	C(11b) -C(12b)	1.390(9)
C(12b) -C(13b)	1.382(9)	C(13b) -C(14b)	1.398(8)

Table 4.4: Bond angles ($^{\circ}$) for AA TETRAMER

C(2a) -N(1a) -C(1a)	117.7(6)	C(8a) -N(2a) -C(1a)	121.8(5)
C(9a) -N(2a) -C(1a)	121.2(5)	C(9a) -N(2a) -C(8a)	116.8(5)
N(2a) -C(1a) -N(1a)	124.4(6)	C(14b)-C(1a) -N(1a)	119.8(6)
C(14b)-C(1a) -N(2a)	115.8(5)	C(3a) -C(2a) -N(1a)	117.8(6)
C(7a) -C(2a) -N(1a)	121.8(6)	C(7a) -C(2a) -C(3a)	120.4(7)
C(4a) -C(3a) -C(2a)	119.0(7)	C(5a) -C(4a) -C(3a)	121.2(7)
C(6a) -C(5a) -C(4a)	120.5(7)	C(7a) -C(6a) -C(5a)	119.3(7)
C(6a) -C(7a) -C(2a)	119.6(6)	C(8a) -C(7a) -C(2a)	120.1(6)
C(8a) -C(7a) -C(6a)	120.2(7)	N(2a) -C(8a) -O(1a)	120.8(6)
C(7a) -C(8a) -O(1a)	125.1(7)	C(7a) -C(8a) -N(2a)	114.1(6)
C(10a)-C(9a) -N(2a)	119.2(6)	C(14a)-C(9a) -N(2a)	119.3(6)
C(14a)-C(9a) -C(10a)	121.3(6)	C(11a)-C(10a)-C(9a)	120.1(6)
C(12a)-C(11a)-C(10a)	119.8(7)	C(13a)-C(12a)-C(11a)	120.1(7)
C(14a)-C(13a)-C(12a)	120.0(7)	C(13a)-C(14a)-C(9a)	118.8(6)
C(1b) -C(14a)-C(9a)	122.4(6)	C(1b) -C(14a)-C(13a)	118.8(6)
C(2b) -N(1b) -C(1b)	117.2(6)	C(8b) -N(2b) -C(1b)	121.1(6)
C(9b) -N(2b) -C(1b)	120.7(5)	C(9b) -N(2b) -C(8b)	118.1(6)
N(1b) -C(1b) -C(14a)	118.4(6)	N(2b) -C(1b) -C(14a)	117.2(6)
N(2b) -C(1b) -N(1b)	124.4(6)	C(3b) -C(2b) -N(1b)	117.3(7)
C(7b) -C(2b) -N(1b)	122.1(7)	C(7b) -C(2b) -C(3b)	120.5(6)
C(4b) -C(3b) -C(2b)	119.2(8)	C(5b) -C(4b) -C(3b)	120.5(8)
C(6b) -C(5b) -C(4b)	119.9(7)	C(7b) -C(6b) -C(5b)	120.5(7)

table 4.4: continued

C(6b) -C(7b) -C(2b)	119.3(7)	C(8b) -C(7b) -C(2b)	120.3(6)
C(8b) -C(7b) -C(6b)	120.4(7)	N(2b) -C(8b) -O(1b)	120.3(7)
C(7b) -C(8b) -O(1b)	125.7(7)	C(7b) -C(8b) -N(2b)	114.1(7)
C(10b)-C(9b) -N(2b)	119.2(6)	C(14b)-C(9b) -N(2b)	118.6(6)
C(14b)-C(9b) -C(10b)	122.2(7)	C(11b)-C(10b)-C(9b)	118.7(7)
C(12b)-C(11b)-C(10b)	120.4(7)	C(13b)-C(12b)-C(11b)	119.7(7)
C(14b)-C(13b)-C(12b)	120.9(7)	C(9b) -C(14b)-C(1a)	123.7(6)
C(13b)-C(14b)-C(1a)	118.1(6)	C(13b)-C(14b)-C(9b)	118.2(6)



Drawing 4.1

rings are all individually planar. Ring 7 is coplanar with the fused six-membered heterocyclic ring, whilst 14 makes a 6° angle with the corresponding mean plane of the adjacent heterocycle, thus making the two halves of the molecule not exactly equal. The angle between rings 1 and 2 is 73° , that between 7 and 14 is 66° . Except for these folds, the bond lengths and angles in each half of the molecule (a and b) are very similar (see Tables 4.3 and 4.4).

The discussion will be based on the average values of the (a) and (b) halves of the molecule (Diagram 4.1), to facilitate comparison with the TAAB salts, which have crystallographic two-fold symmetry.

The results indicate that the bonding can be best represented by contributions from the resonance structures shown in Diagram 4.3.

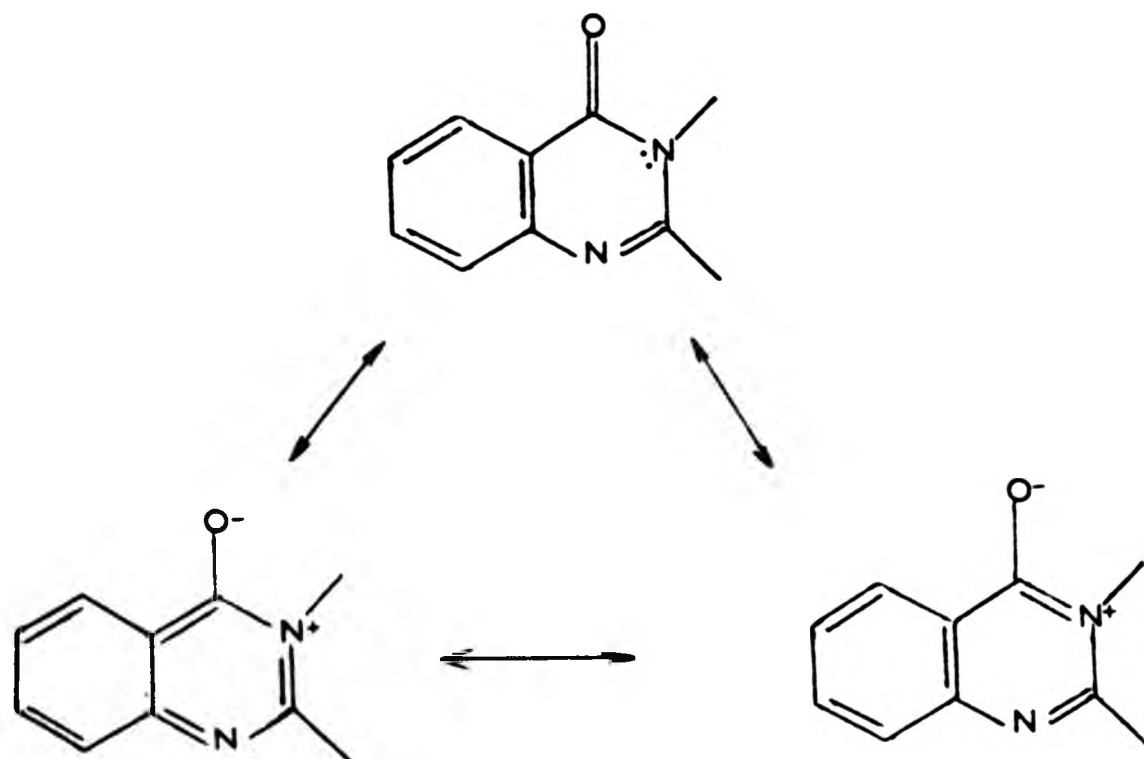


Diagram 4.3

The bonding around all the atoms appears to be trigonal planar (sp^2 -hybridisation). There is one very short bond, $C(1)-N(1) = 1.284(5) \text{ \AA}$. It is in the region expected for carbon-nitrogen double bonds (see section 3.3.1).

From a simple valency formulation, as published by other authors,^{2,3} the $N(2)$ atoms should be sp^3 -hybridised, i.e. pyramidal. The evidence presented here shows that they are trigonal planar. In addition, the $N(2)-C(1)$ and $N(2)-C(8)$ bond lengths are short, $1.400(5)$ and $1.405(6) \text{ \AA}$ respectively. They have values somewhat between that of a single and that of a double bond. This is probably due to the back-donation of the lone pairs of electrons on the $N(2)$ atoms towards the $C(1)$ and $C(8)$ atoms, giving rise to canonical forms as shown in Diagram 4.3.

The bond length data suggests that this back-donation is equal in amount in both directions. Similar examples where this back-donation is possible, resulting in short bond lengths, are given in section 3.3.1.

In the eight-membered ring the bond $N(2)-C(9)$ is $1.453(5) \text{ \AA}$, whereas in the six-membered ring $N(1)-C(2)$ is $1.407(5) \text{ \AA}$. They are significantly different, although both bonds are between sp^2 -hybridised nitrogen and sp^2 -hybridised carbon atoms. This is probably again due to the back-donation of the lone pairs on the $N(1)$ atoms towards the $C(2)$ atoms. The double bond character of $N(1)-C(2)$ is of about the same order as that between $N(2)-C(8)$ and $N(2)-C(1)$. These three bonds are significantly shorter than $N(2)-C(9)$.

The bond lengths $C(1)-C(14) = 1.483(6) \text{ \AA}$ and $C(7)-C(8) = 1.446(6) \text{ \AA}$

are just about significantly different.

All these bonds are between sp^2 -hybridised carbon atoms. (See later discussion about a comparison between this molecule and the TAAB salts, section 4.4).

4.3.2 AA TRIMER. $CHCl_3$

The stable crystals of the trimeric condensation product of AA, AA TRIMER. $CHCl_3$, have the structure shown in Figure 4.2 with important bond lengths and angles. The bond length and angle data are given in Tables 4.6 and 4.7. The ORTEP drawings of the structure is given in Drawing 4.2. The shape of the molecule, as in the AA TETRAMER, can be described as double saddle- shape. One pair of opposite benzene rings 1, 2 (Table 4.5) are folding down, the other benzene ring 7 and the plane of the N(3),C(15),O(2),H(N3) atoms (plane 3) are folding up with respect to the central eight-membered ring. This feature gives to the eight-membered ring a boat conformation as in the AA TETRAMER. The angle between the first two benzene rings is 79° and between the second set of planes 83° . The benzene ring 7 is coplanar with the adjacent heterocyclic ring.

As in the AA TETRAMER, contributions from quinonoid resonance forms rationalise the observed data on bond lengths and angles. The bond length N(1)-C(1) = 1.292(5) Å is that expected for a double bond between sp^2 -hybridised carbon and nitrogen atoms.

As in the AA TETRAMER the N(2) atom would be expected to be pyramidal. The data shows that it is trigonal planar. In addition the

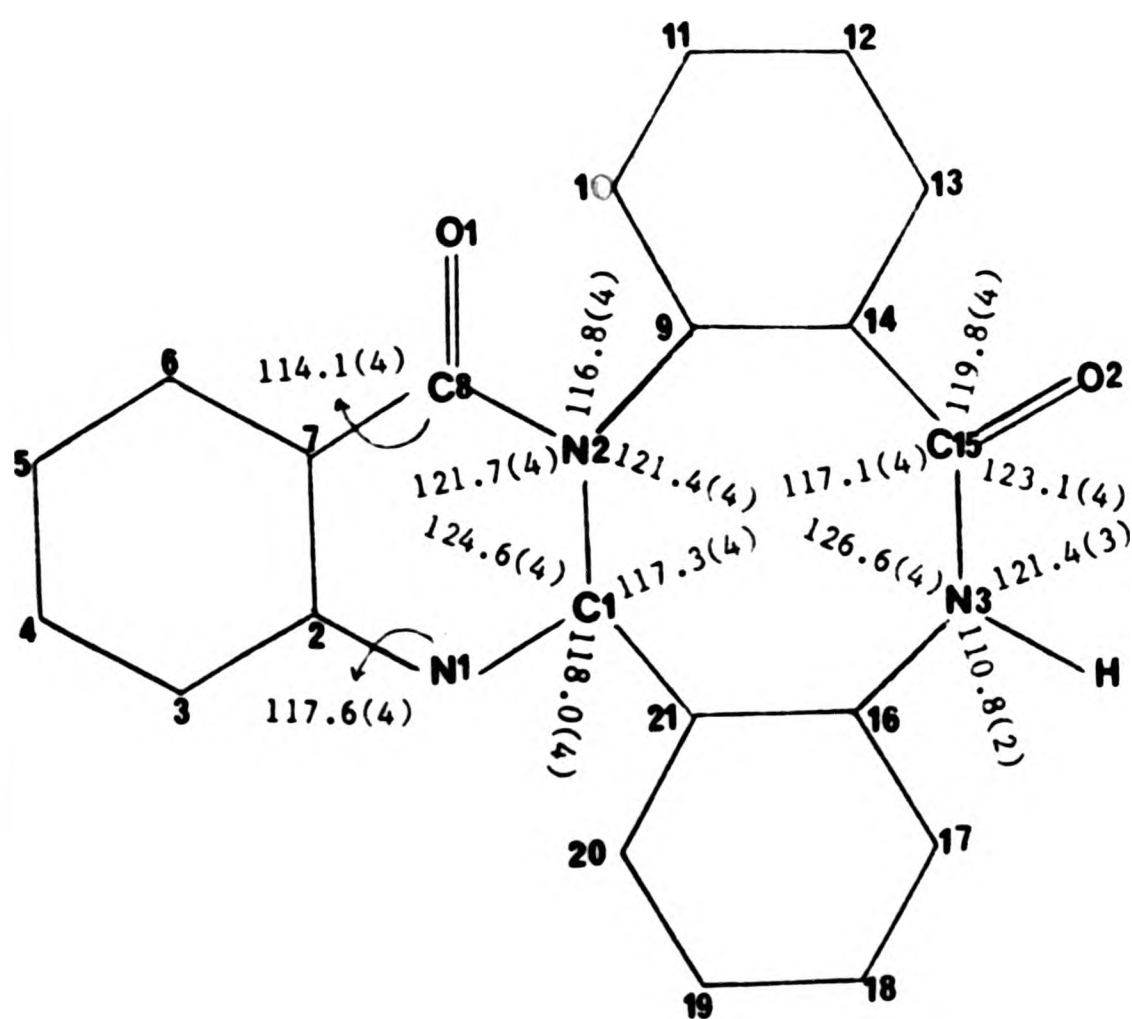
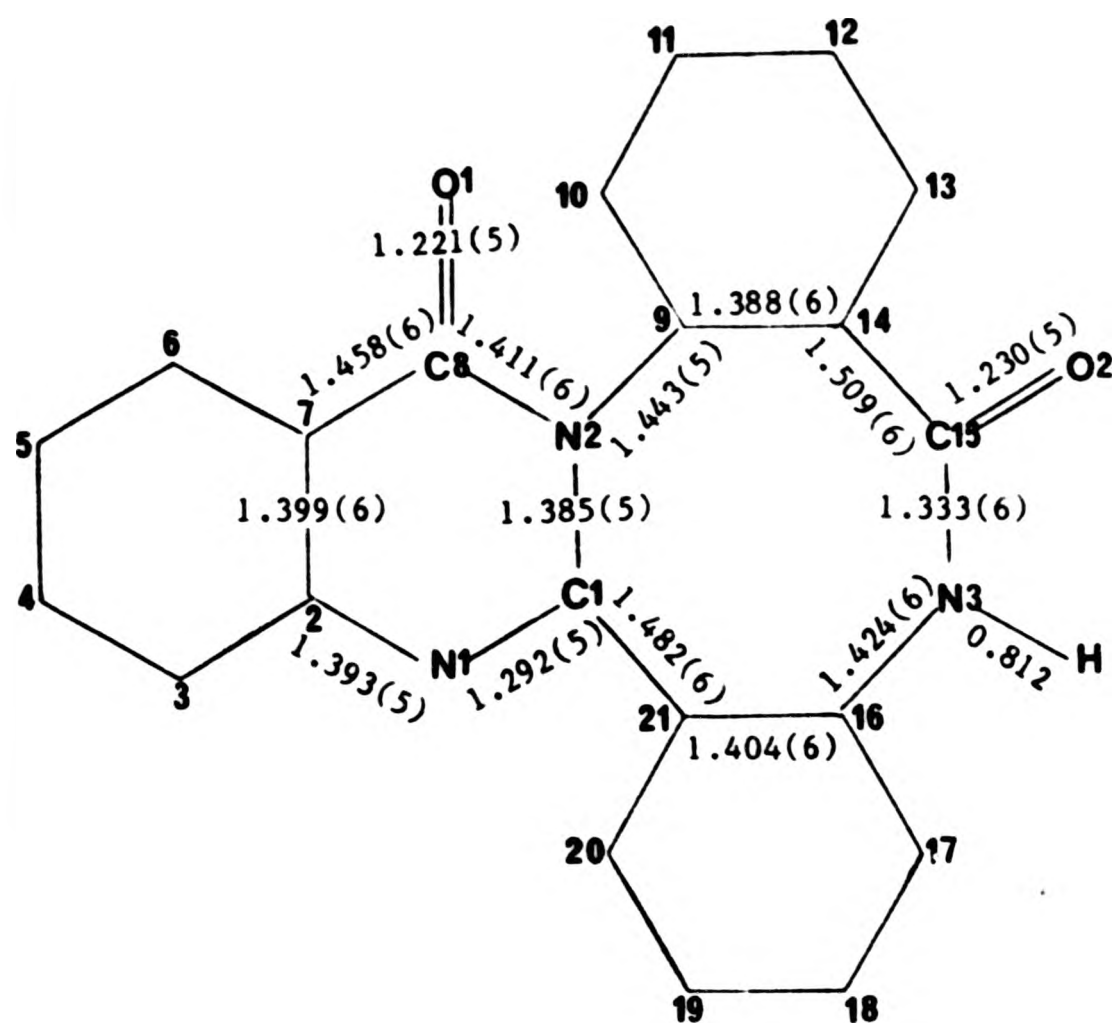


Figure 4.2

Table 4.6: Bond lengths (Å) for AA TRIMER.CCl₃

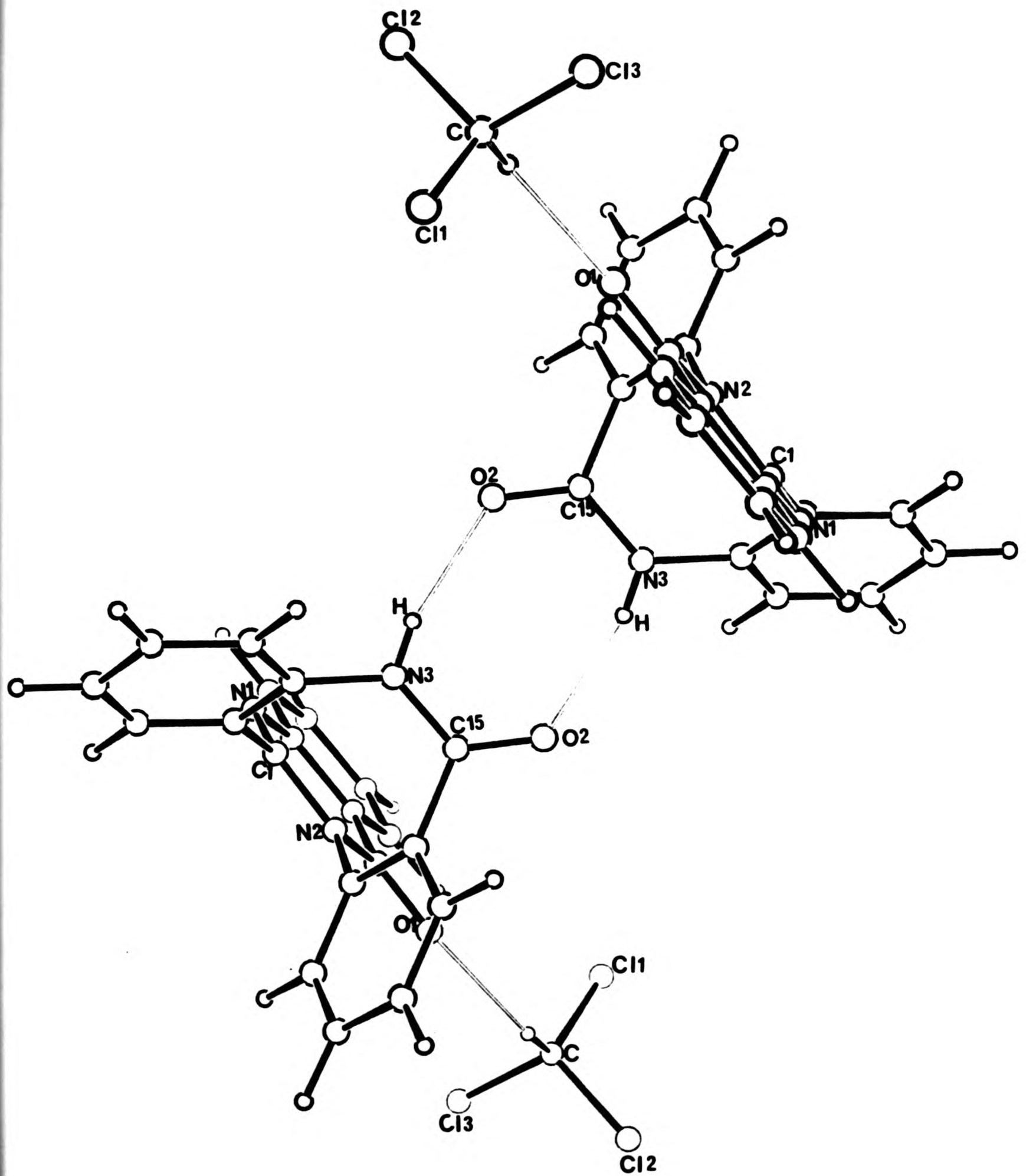
O(1)	-C(8)	1.221(5)	O(2)	-C(15)	1.230(5)
N(1)	-C(1)	1.292(5)	N(1)	-C(2)	1.393(5)
N(2)	-C(1)	1.385(5)	N(2)	-C(8)	1.411(6)
N(2)	-C(9)	1.443(5)	N(3)	-C(15)	1.333(6)
N(3)	-C(16)	1.424(6)	C(1)	-C(21)	1.482(6)
C(2)	-C(3)	1.413(6)	C(2)	-C(7)	1.399(6)
C(3)	-C(4)	1.378(7)	C(4)	-C(5)	1.386(7)
C(5)	-C(6)	1.376(7)	C(6)	-C(7)	1.399(6)
C(7)	-C(8)	1.458(6)	C(9)	-C(10)	1.381(6)
C(9)	-C(14)	1.388(6)	C(10)	-C(11)	1.404(7)
C(11)	-C(12)	1.375(8)	C(12)	-C(13)	1.381(7)
C(13)	-C(14)	1.395(6)	C(14)	-C(15)	1.509(6)
C(16)	-C(17)	1.386(6)	C(16)	-C(21)	1.404(6)
C(17)	-C(18)	1.376(7)	C(18)	-C(19)	1.380(7)
C(19)	-C(20)	1.382(7)	C(20)	-C(21)	1.386(6)
C	-Cl(1)	1.716(6)	C	-Cl(2)	1.734(6)
C	-Cl(3)	1.750(6)	C	-H	1.223
N(3)	-H(N3)	0.812			

Table 4.7: Bond angles ($^{\circ}$) for AA TRIMER. CHCl_3

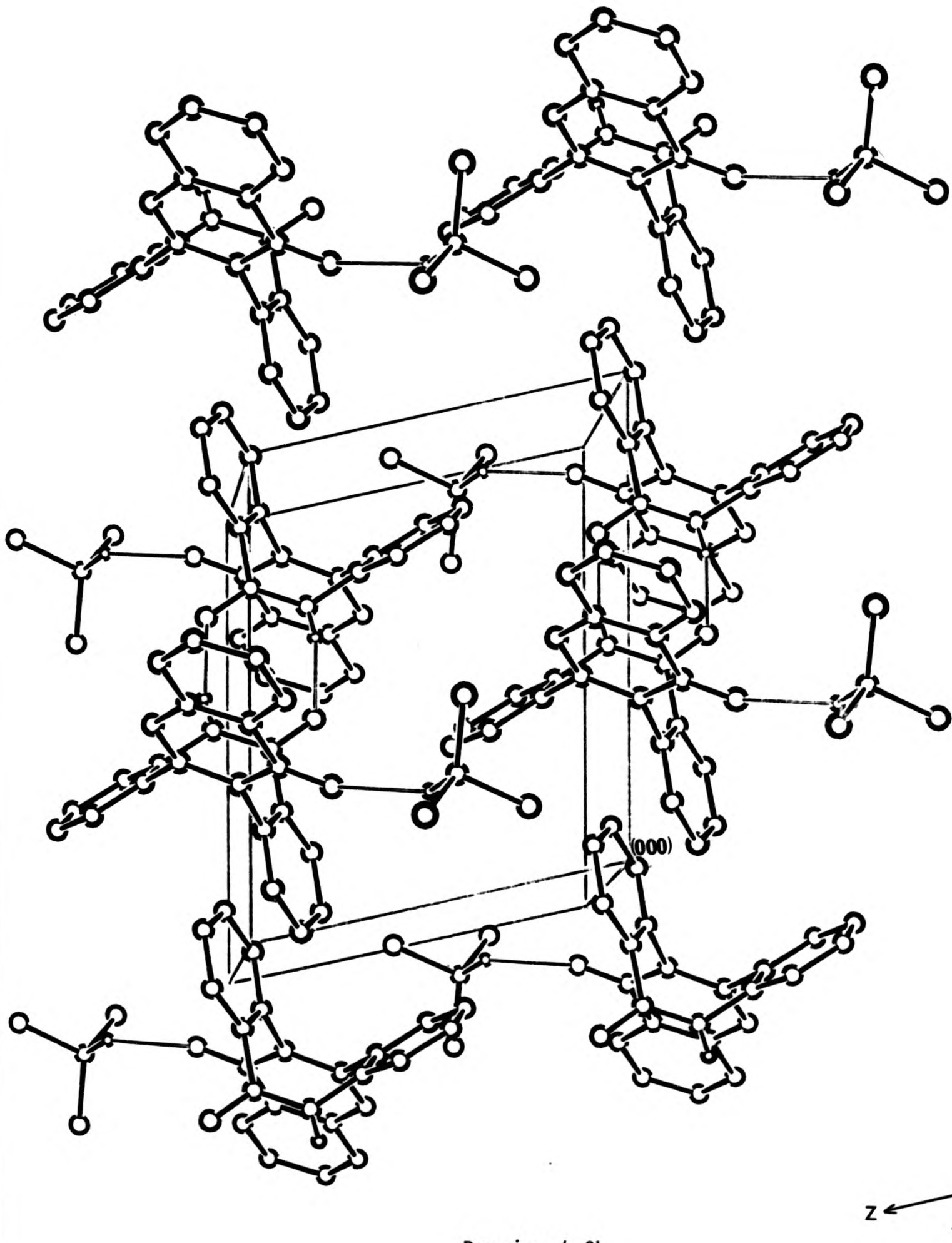
C(2) -N(1) -C(1)	117.6(4)	C(8) -N(2) -C(1)	121.7(4)
C(9) -N(2) -C(1)	121.4(4)	C(9) -N(2) -C(8)	116.8(4)
C(16) -N(3) -C(15)	126.6(4)	N(2) -C(1) -N(1)	124.6(4)
C(21) -C(1) -N(1)	118.0(4)	C(21) -C(1) -N(2)	117.3(4)
C(3) -C(2) -N(1)	118.2(4)	C(7) -C(2) -N(1)	122.4(4)
C(7) -C(2) -C(3)	119.4(4)	C(4) -C(3) -C(2)	118.8(5)
C(5) -C(4) -C(3)	121.8(5)	C(6) -C(5) -C(4)	119.8(5)
C(7) -C(6) -C(5)	120.1(5)	C(6) -C(7) -C(2)	120.1(4)
C(8) -C(7) -C(2)	119.5(4)	C(8) -C(7) -C(6)	120.3(4)
N(2) -C(8) -O(1)	120.8(4)	C(7) -C(8) -O(1)	125.1(4)
C(7) -C(8) -N(2)	114.1(4)	C(10) -C(9) -N(2)	118.9(4)
C(14) -C(9) -N(2)	120.3(4)	C(14) -C(9) -C(10)	120.6(4)
C(11) -C(10) -C(9)	119.4(5)	C(12) -C(11) -C(10)	119.6(5)
C(13) -C(12) -C(11)	121.0(5)	C(14) -C(13) -C(12)	119.5(5)
C(13) -C(14) -C(9)	119.7(4)	C(15) -C(14) -C(9)	122.8(4)
C(15) -C(14) -C(13)	117.5(4)	N(3) -C(15) -O(2)	123.1(4)
C(14) -C(15) -O(2)	119.8(4)	C(14) -C(15) -N(3)	117.1(4)
C(17) -C(16) -N(3)	120.0(4)	C(21) -C(16) -N(3)	120.6(4)
C(21) -C(16) -C(17)	119.4(4)	C(18) -C(17) -C(16)	120.7(5)
C(19) -C(18) -C(17)	120.2(5)	C(20) -C(19) -C(18)	119.9(5)
C(21) -C(20) -C(19)	120.7(5)	C(16) -C(21) -C(1)	120.9(4)
C(20) -C(21) -C(1)	119.8(4)	C(20) -C(21) -C(16)	119.2(4)

table 4.7: continued

C1(2) -C	-C1(1)	110.9(3)	C1(3) -C	-C1(1)	109.8(3)
C1(3) -C	-C1(2)	111.9(3)	C1(1) -C	-H	105.3(2)
C1(2) -C	-H	122.5(2)	C1(3) -C	-H	95.1(2)
C(15) -N(3)	-H(N3)	121.4(3)	C(16) -N(3)	-H(N3)	110.8(2)



Drawing 4.2a



Drawing 4.2b

N(2)-C(1) and N(2)-C(8) bond lengths are short. They are 1.385(5) and 1.411(6) Å respectively. They are not significantly different from each other and have a character in between that of a single and that of a double bond. This is again possibly due to the back-donation of the lone pair on the N(2) atom towards the C(1) and C(8) atoms as explained in the discussion section on the AA TETRAMER.

The N(3) atom is not part of a fused ring and it is almost coplanar with its three bonding partners. The sum of the angles around it is 358.8°. The adjacent carbon atom C(15) is also planar. Both the N(3) and C(15) atoms are sp^2 -hybridised. This due to the contributions from the canonical resonance forms (A) and (B) of Diagram 4.4, which also accounts for a carbon-nitrogen distance very much shortened from that expected for a carbon-nitrogen single bond. The carbon-oxygen bond is of the right length when compared to that in other amides (see section 3.3.1).

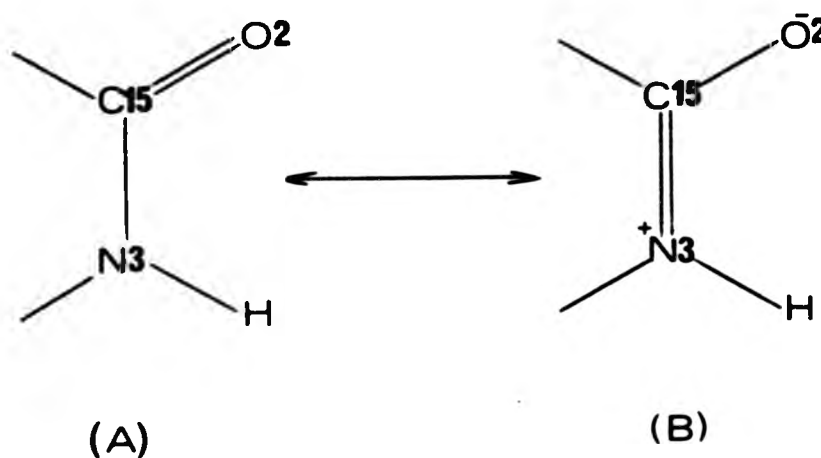


Diagram 4.4

The bond length N(3)-C(15) = 1.333(6) Å is significantly shorter than that of C(1)-N(2) = 1.385(5) Å. This is probably due to the back-donation of the lone pair on the N(3) atom mainly towards C(15)

[and possibly also, but to a lesser extent, to C(16)] being further re-inforced by the hydrogen bonding. This links two molecules of trimer into a dimer unit through the N(3), O(2) atoms. Accompanying the shortening of the bond length N(3)-C(15), an enlarged bond angle of C(16)-N(2)-C(15) = $126.6(4)^\circ$ is observed. This angle is significantly larger than that of C(1)-N(2)-C(9) = $121.4(4)^\circ$.

The bond length C(14)-C(15) = $1.495(6) \text{ \AA}$ is significantly longer than that of C(7)-C(8) = $1.446(7) \text{ \AA}$, although both bonds are between a benzene ring carbon and a carbonyl carbon, both being sp^2 -hybridised atoms. Furthermore the O(2) atom is involved in hydrogen bonding to give dimer units of the AA TRIMER. The O(1) atom is involved in another hydrogen bond with a chloroform molecule. In addition the bond length C(2)-N(1) = $1.393(5) \text{ \AA}$ is significantly shorter than N(2)-C(9) = $1.448(6) \text{ \AA}$. These bonds are between sp^2 -hybridised nitrogen atoms and benzene rings carbon atoms.

The dimer units of the AA TRIMER, with the chloroform hydrogen bonding, are shown in Diagram 4.5.

The O(2).....N(3) hydrogen bond distance is 2.855 \AA with the O(2)...H(3) distance 2.061 \AA . These are expected values for N-H...O hydrogen bonds (see section 1.3). The bond angles C(15)-O(2)-H(3) and O(2)-H(3)-N(3) are 130.1° and 165.4° respectively. The new eight-membered ring formed by the above hydrogen bonds is planar. The angles between this plane and that of planes 7 and 7' are 83° and 97° respectively (see Diagram 4.5 and Table 4.5.)

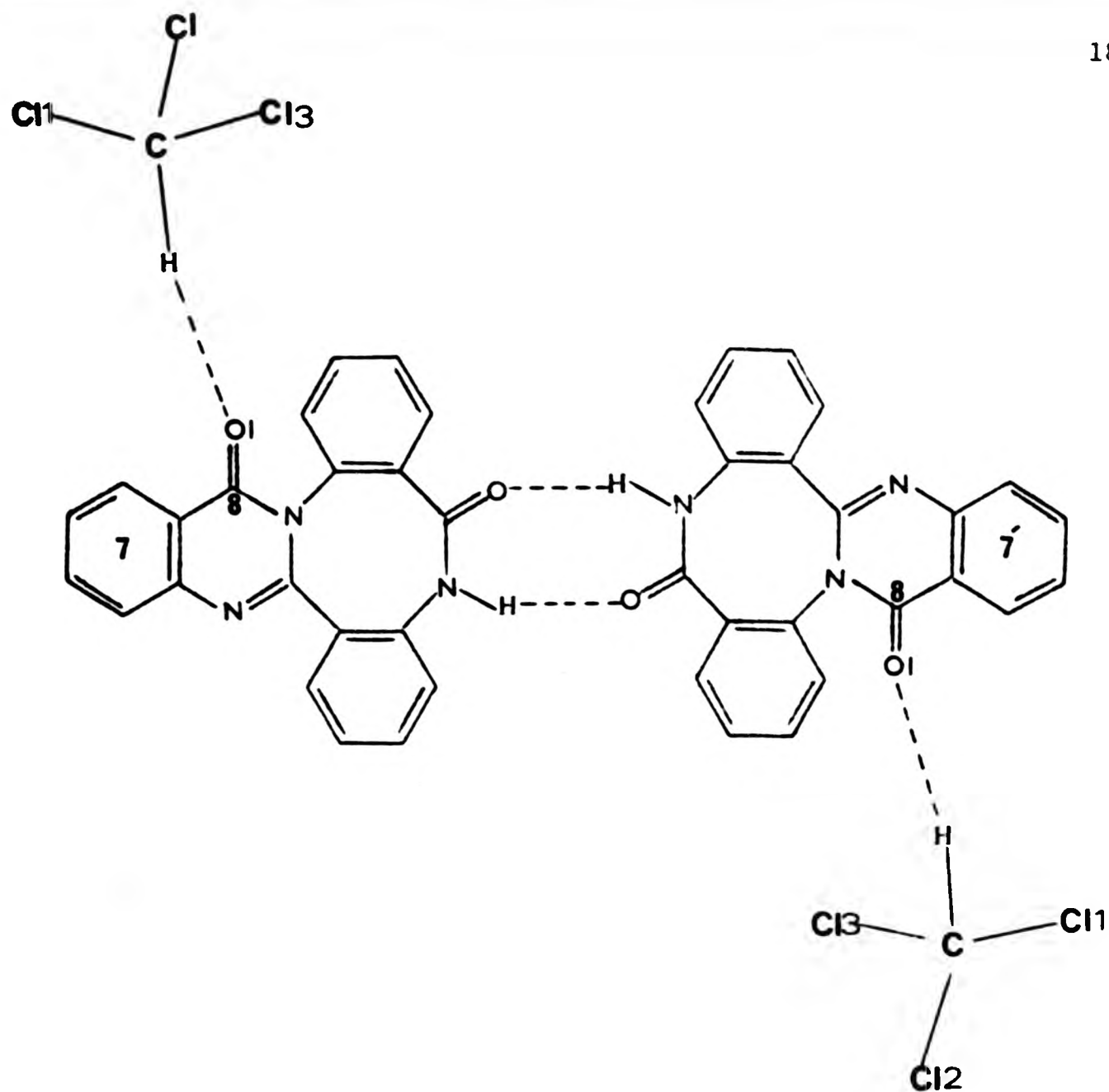


Diagram 4.5

Each trimer unit is hydrogen bonded through O(1) to a chloroform molecule. The O(1).....C distance is 3.350 Å with the O(1).....H distance 2.319 Å. These values are in agreement with previously reported chloroform hydrogen bonds (see section 1.3). The bond angles C(8)-O(1)...H and O(1)...H-C are 151.9° and 140.1° respectively.

4.3.3 AA TRIMER·CH₃CN·H₂O

The unstable crystals of this solvate of the trimeric condensation product of AA, has the structure shown in Figure 4.3, which also shows the important bond lengths and angles. The bond length and angle data

are given in Tables 4.8 and 4.9. For convenience the same numbering scheme is used in all condensation products of AA. The ORTEP drawings for this molecule are given in Drawing 4.3. The overall shape of the molecule is almost exactly the same as in the chloroform solvate of the AA TRIMER, i.e. double saddle-shape. Rings 1 and 2 are folding down and the planes 7 and 3 are folding up with respect to the central eight-membered ring, which has a boat conformation. The angle between the planes 1 and 2 is 67° and that between 7 and 3 is 72° . The benzene ring 7 is coplanar with the adjacent heterocyclic ring. (See Table 4.5)

All the bond lengths and angles are very similar to those in the AA TRIMER. CHCl_3 (see Tables 4.6 and 4.7) except that the bond angles around the N(3) atom in this molecule add up to 359.8° , whilst in the former one they come to 358.8° . This suggests a greater degree of planarity in the latter.

As in the AA TRIMER. CHCl_3 , the O(2) atom is involved in hydrogen bonding, N-H...O, to give dimer units of the AA TRIMER. Neither the acetonitrile nor the water molecule, trapped in the crystal lattice, are involved in any hydrogen bonding. Hence this accounts for the tendency of these crystals to disintegrate with loss of solvent.

The hydrogen bonded dimeric unit of AA TRIMER. $\text{CH}_3\text{CN} \cdot \text{H}_2\text{O}$ is shown in Diagram 4.6.

The O(2).....N(3) distance is 2.870 \AA with the O(2)...H(3) distance = 1.865 \AA . These distances indicate a strong hydrogen bond compared to values reported in the literature (see section 1.3). The

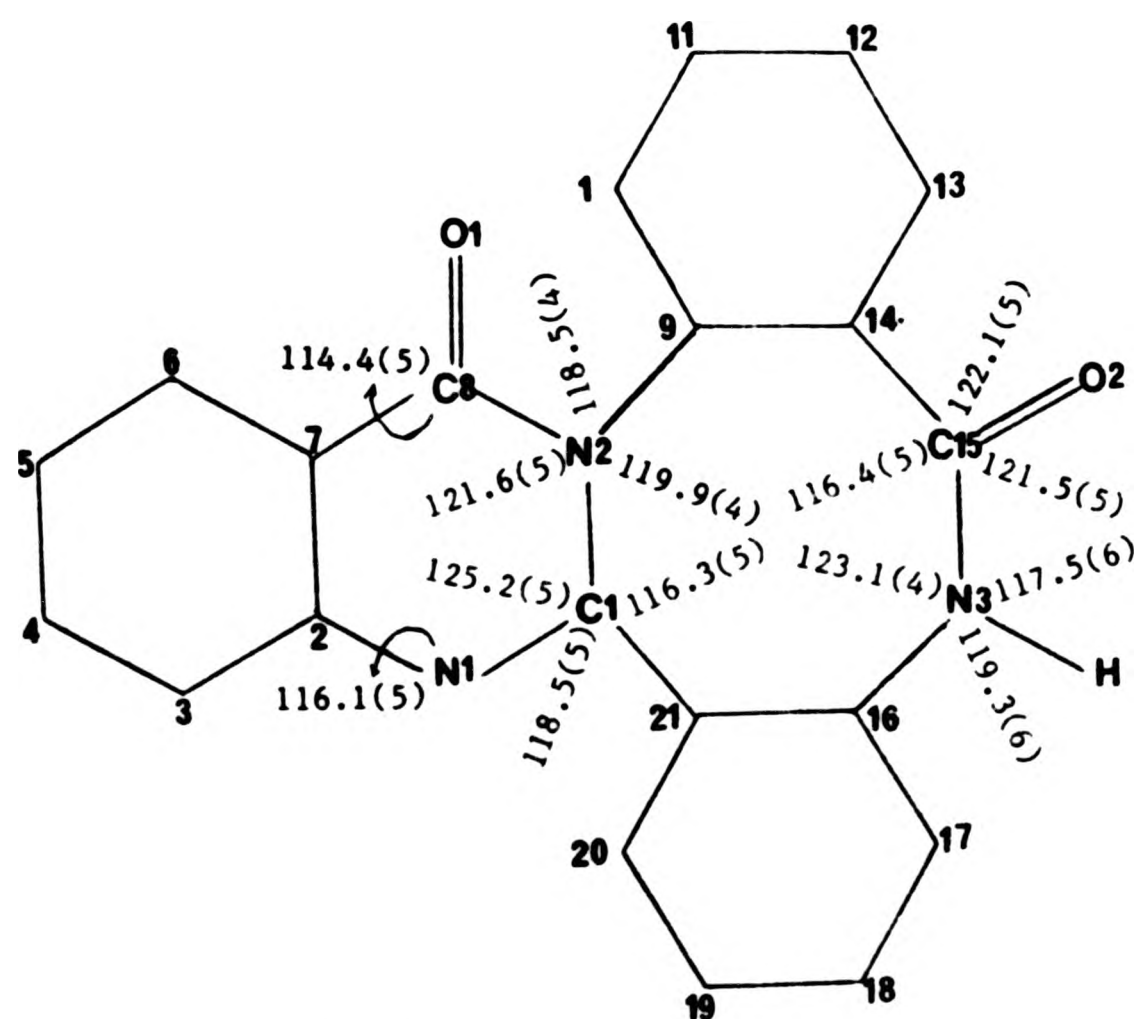
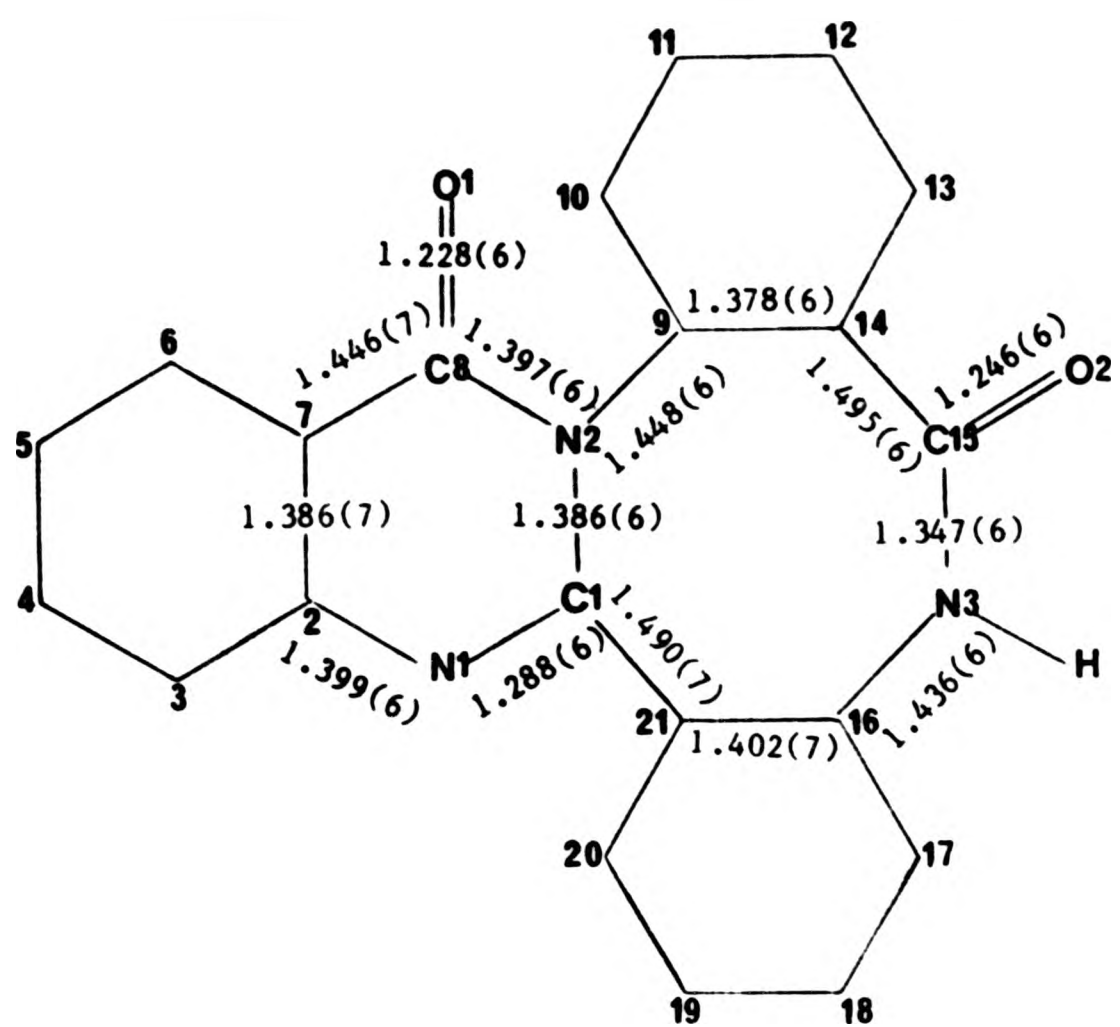


Figure 4.3

Table 4.8: Bond lengths (\AA) for AA TRIMER. $\text{CH}_3\text{CN}\cdot\text{H}_2\text{O}$

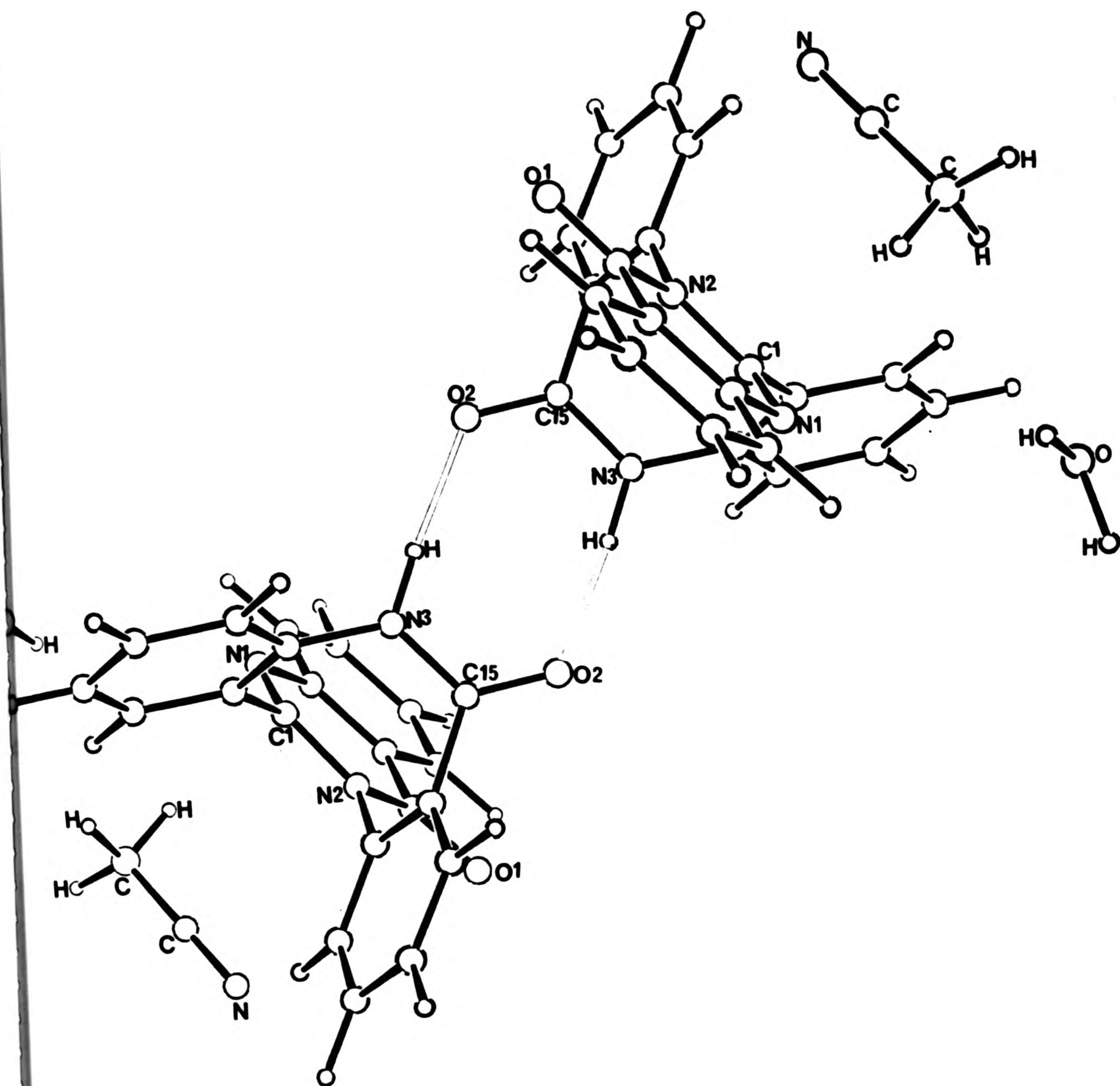
O(1)	-C(8)	1.228(6)	O(2)	-C(15)	1.246(6)
N(1)	-C(1)	1.288(6)	N(1)	-C(2)	1.399(6)
N(2)	-C(1)	1.386(6)	N(2)	-C(8)	1.397(6)
N(2)	-C(9)	1.448(6)	N(3)	-C(15)	1.347(6)
N(3)	-C(16)	1.436(6)	C(1)	-C(21)	1.490(7)
C(2)	-C(3)	1.411(7)	C(2)	-C(7)	1.386(7)
C(3)	-C(4)	1.384(8)	C(4)	-C(5)	1.391(8)
C(5)	-C(6)	1.379(7)	C(6)	-C(7)	1.405(7)
C(7)	-C(8)	1.446(7)	C(9)	-C(10)	1.383(6)
C(9)	-C(14)	1.378(6)	C(10)	-C(11)	1.394(7)
C(11)	-C(12)	1.383(7)	C(12)	-C(13)	1.376(7)
C(13)	-C(14)	1.389(6)	C(14)	-C(15)	1.495(6)
C(16)	-C(17)	1.385(7)	C(16)	-C(21)	1.402(7)
C(17)	-C(18)	1.382(7)	C(18)	-C(19)	1.380(7)
C(19)	-C(20)	1.388(7)	C(20)	-C(21)	1.386(7)
C(a)	-C(b)	1.414(11)	C(b)	-N	1.146(11)
C(a)	-H(a1)	1.079	C(a)	-H(a2)	1.080
C(a)	-H(a3)	1.080	O	-H(w1)	1.159
O	-H(w2)	1.132			

Table 4.9: Bond angles ($^{\circ}$) for AA TRIMER. $\text{CH}_3\text{CN}\cdot\text{H}_2\text{O}$

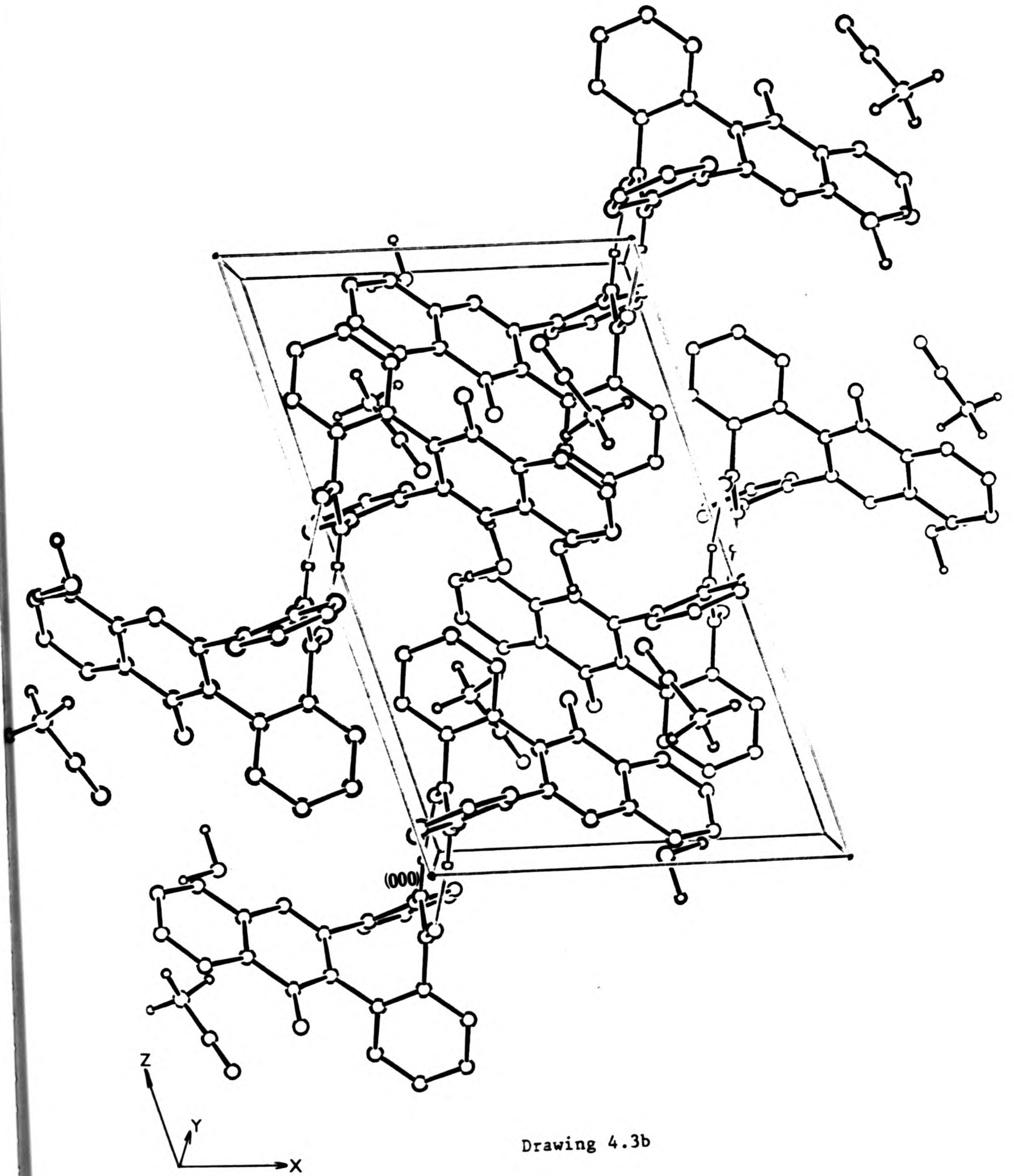
C(2) -N(1) -C(1)	116.1(5)	C(8) -N(2) -C(1)	121.6(5)
C(9) -N(2) -C(1)	119.9(4)	C(9) -N(2) -C(8)	118.5(4)
C(16) -N(3) -C(15)	123.1(4)	N(2) -C(1) -N(1)	125.2(5)
C(21) -C(1) -N(1)	118.5(5)	C(21) -C(1) -N(2)	116.3(5)
C(3) -C(2) -N(1)	117.5(6)	C(7) -C(2) -N(1)	123.2(5)
C(7) -C(2) -C(3)	119.3(6)	C(4) -C(3) -C(2)	119.8(6)
C(5) -C(4) -C(3)	120.2(6)	C(6) -C(5) -C(4)	120.9(6)
C(7) -C(6) -C(5)	119.1(6)	C(6) -C(7) -C(2)	120.7(5)
C(8) -C(7) -C(2)	119.4(5)	C(8) -C(7) -C(6)	119.8(5)
N(2) -C(8) -O(1)	119.9(5)	C(7) -C(8) -O(1)	125.7(6)
C(7) -C(8) -N(2)	114.4(5)	C(10) -C(9) -N(2)	118.8(5)
C(14) -C(9) -N(2)	120.1(4)	C(14) -C(9) -C(10)	121.1(5)
C(11) -C(10) -C(9)	118.9(5)	C(12) -C(11) -C(10)	120.1(5)
C(13) -C(12) -C(11)	120.4(5)	C(14) -C(13) -C(12)	119.9(5)
C(13) -C(14) -C(9)	119.6(5)	C(15) -C(14) -C(9)	119.7(5)
C(15) -C(14) -C(13)	120.6(5)	N(3) -C(15) -O(2)	121.5(5)
C(14) -C(15) -O(2)	122.1(5)	C(14) -C(15) -N(3)	116.4(5)
C(17) -C(16) -N(3)	119.3(5)	C(21) -C(16) -N(3)	120.2(5)
C(21) -C(16) -C(17)	120.5(5)	C(18) -C(17) -C(16)	119.3(6)
C(19) -C(18) -C(17)	120.9(6)	C(20) -C(19) -C(18)	119.9(6)
C(21) -C(20) -C(19)	120.2(6)	C(16) -C(21) -C(1)	120.4(5)
C(20) -C(21) -C(1)	120.4(5)	C(20) -C(21) -C(16)	119.2(5)

table 4.9: continued

N	-C(b)	-C(a)	178(1)	C(b)	-C(a)	-H(a1)	102.8(6)
C(b)	-C(a)	-H(a2)	107.9(5)	C(b)	-C(a)	-H(a3)	117.4(5)
H(a1)	-C(a)	-H(a2)	109.4	H(a2)	-C(a)	-H(a3)	109.4
H(a1)	-C(a)	-H(a3)	109.4	H(w1)	-0	-H(w2)	96.1



Drawing 4.3a



Drawing 4.3b

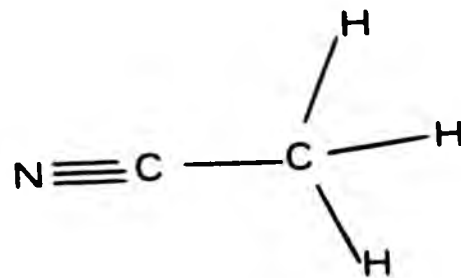
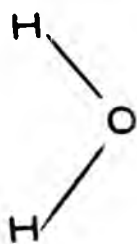
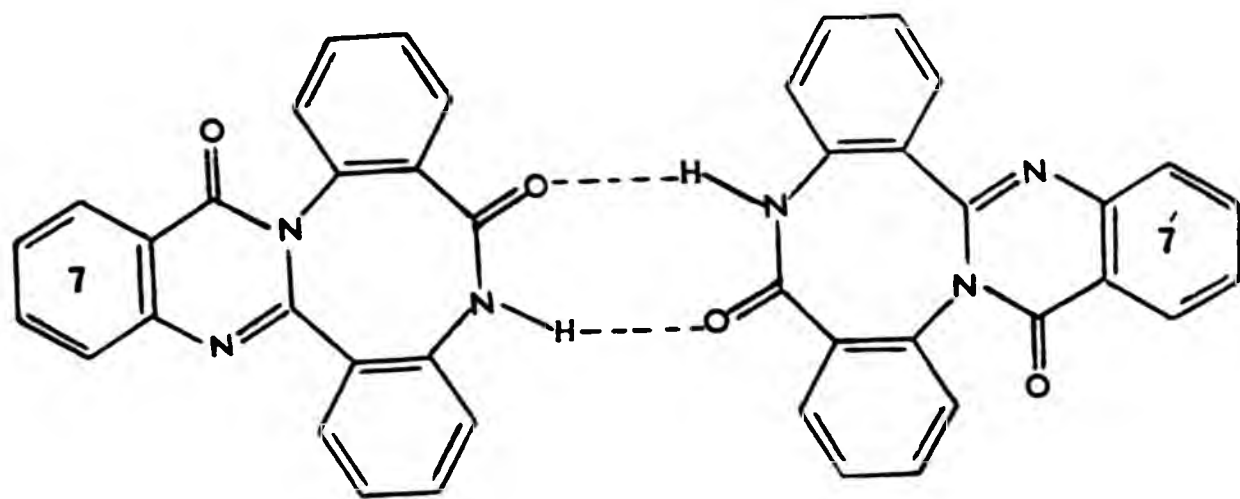
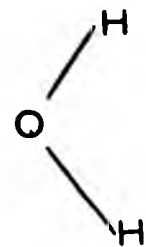
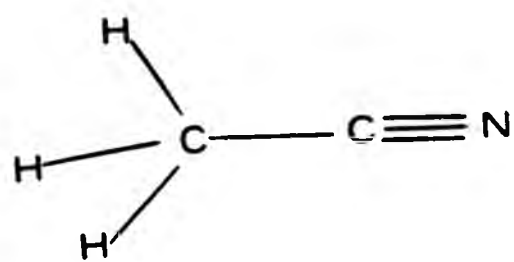


Diagram 4.6

bond angles C(15)-O(2)-H(N3) and O(2)-H(3)-N(3) are 124.9° and 173.5° respectively. The eight-membered ring formed by the hydrogen bonds is planar. The angles between this plane and those of planes 7 and 7' are 72.°

4.4 COMPARISON OF AA STRUCTURES

If we consider the two trimer structures the corresponding bond lengths and angles within them are not significantly different. The two trimer structures differ from that of the tetramer only on that side of the 8-membered ring, where intermolecular hydrogen bonding occurs.

In all the three structures of AA condensation products the lone pairs of electrons on the N(2) atoms are delocalised in approximately equal amounts towards C(1) and C(8), but not to any significant extent towards C(9). In the trimer structures there is also little or no delocalisation from N(3) towards C(16). The bond N(3)-C(15) [1.340(4) Å](av) is significantly shorter than that for N(2)-C(1) [1.385(4) Å](av). The former delocalisation, [N(3)-C(15)], occurs only in one direction, and is probably further enhanced by the fact that N(3)-H(N3) and O(2) form dimeric units through intermolecular hydrogen bonding. In all three AA structures N(2)-C(9) [1.448(3) Å](av) and where appropriate N(3)-C(16) [1.430(4) Å](av) are significantly longer than N(1)-C(2) [1.399(3) Å](av). Similarly C(1)-C(14) [1.483(5) Å](av) in the tetramer and C(1)-C(21) [1.486(5) Å](av) and C(14)-C(15) [1.502(4) Å](av) in the trimer structures are significantly longer than C(7)-C(8) [1.450(4) Å](av). All of the above bonds are between sp²-hybridised atoms. The longer set of bonds N(2)-C(9), N(3)-C(16) as well as C(1)-C(14), C(1)-C(21) and C(14)-C(15) have the adjacent benzo rings (see Table 4.5) twisted at angles from 58° to 77° degrees with respect to the planes through N(1), C(1), N(2), C(8) (plane 4) and H(N3), N(3), C(15), O(2) (plane 3). This will substantially reduce, possibly even eliminate, any π-interaction which is possible in the shorter bonds mentioned above.

In all the three AA structures a double saddle-shape is observed, if one considers the hydrogen bonded dimerisation as the fourth part of the double saddle in the trimer structures.

4.5 COMPARISON OF AA DERIVATIVES WITH $\text{TAABH}_2(\text{PICRATE})_2$

It can be seen that the $\text{N}(2)-\text{C}(1)$ distance [1.484(5) Å] in the picrate salt is significantly longer than the corresponding bond distances in the AA structures [1.401(5), 1.385(5) and 1.386(6) Å for AA TETRAMER, AA TRIMER. CHCl_3 , and AA TRIMER. $\text{CH}_3\text{CN} \cdot \text{H}_2\text{O}$ respectively]. The first mentioned of these is a single bond, whereas the other three have significant double bond character. In all four crystal structures the carbon-nitrogen double bond, $\text{C}(8)-\text{N}(2)$ in the picrate salt [1.301(4) Å] and $\text{C}(1)-\text{N}(1)$ in the three AA structures [1.284(5), 1.292(5) and 1.288(6) Å respectively as above], are in the expected range (see section 3.3.1) with possibly the first of these marginally on the long side.

It will be noted that in the picrate salt $\text{C}(8)-\text{C}(7)$ [1.407(5) Å] and $\text{N}(1)-\text{C}(2)$ [1.367(5) Å] are on the short side for single bonds and indeed suggest a bond order of ~ 1.5 . A similar observation, although to a somewhat lesser extent applies to the three AA structures. The relevant values are 1.446(6) and 1.407(5), 1.458(6) and 1.393(5), 1.446(7) and 1.399(6) Å respectively as above.

A rationalisation for these findings is, as pointed out earlier, to invoke contributions from the mesomeric resonance forms shown in Diagram 3.4 for $\text{TAABH}_2(\text{PICRATE})_2$ (see section 3.3.1).

This suggestion is reinforced by the observed $\text{C}(5)-\text{C}(6)$ [1.363(6) Å] and $\text{C}(3)-\text{C}(4)$ [1.375(6) Å] bond distances in the picrate salt, which are shorter than the other bonds in the benzene ring. This type of quinonoid resonance forms seems to make some contributions, although to

a lesser extent, in the AA structures (see Diagram 4.7).

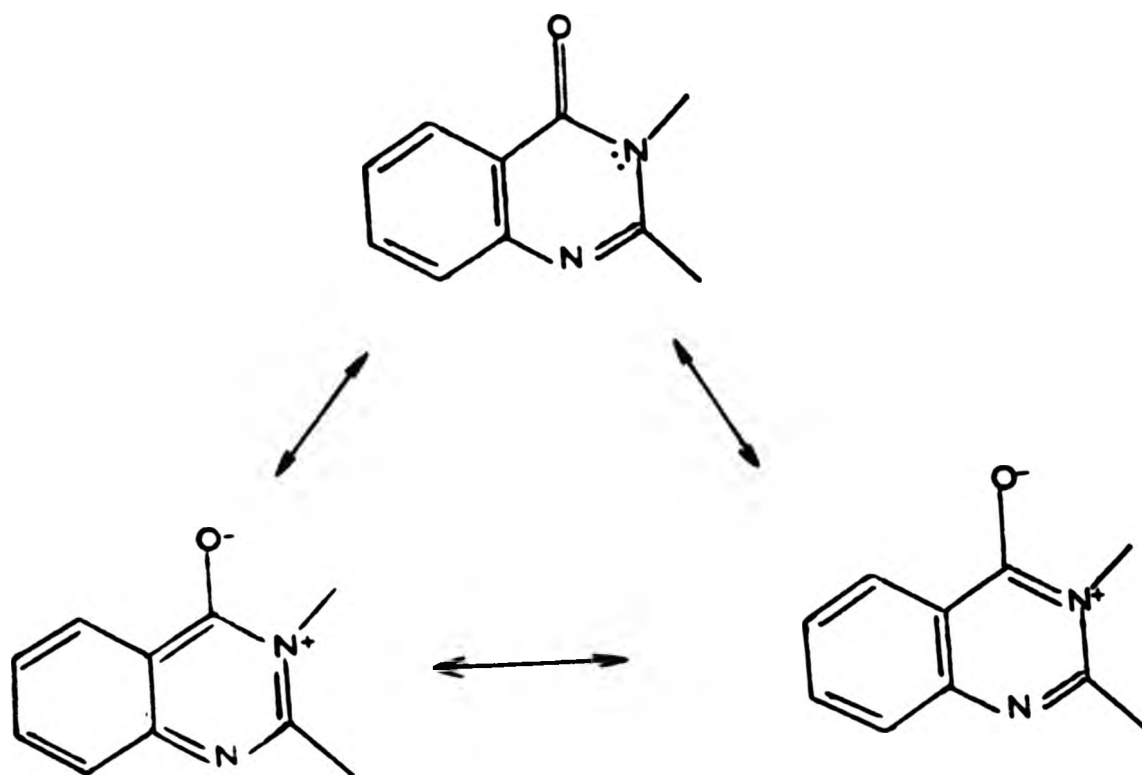


Diagram 4.7

It seems feasible that the NH hydrogen bonding in the picrate salt is responsible for enhancing this resonance contribution. This suggestion is re-inforced by the greater shortening of N(3)-C(15) [1.333(6), 1.347(6) Å] bonds in the AA TRIMER structures compared to those of N(2)-C(1) [1.385(5), 1.386(6) Å].

We have seen earlier that the benzo rings 1 and 2 (see section 3.3.1) in $\text{TAABH}_2(\text{PICRATE})_2$ are orthogonal (82 and 89 degrees respectively) to the heterocyclic segment 4; this prevents any conjugative interaction between them. The bonds are thus pure single

bonds without any π -component. In the AA structures the corresponding angles are between 58 to 77 degrees (Table 4.5), again reducing such a π -interaction to small or negligible proportions. A comparison of the relevant bond lengths is given in Table 4.10. A comparison of the angles between the relevant planes can be obtained by inspecting Tables 3.5 and 4.5.

It can be seen from Table 4.10, that there are no significant differences between C(1)-C(14) and C(1)-C(21). When the C(1)-C(21) and C(1)-C(14) bond lengths are averaged over the three AA structures the value 1.485(3) Å is obtained. When the averaging process includes also the C(14)-C(15) bonds the value is 1.491(3) Å. Neither of these average values is meaningfully different from the value of 1.491(5) Å for C(1)-C(14) in the picrate salt, where the bond is however between two carbon atoms which are formally sp^3 - and sp^2 -hybridised, again without any π -contribution.

By contrast the bond C(1)-N(2) in the picrate 1.485(5) Å has a value close to that generally accepted for a bond between an sp^3 -hybridised carbon atom and a 4-covalent nitrogen atom [1.479(5) Å].⁴

Again as it can be seen from Table 4.10, there are no significant differences in length for the bonds N(2)-C(9) which average to 1.448(3) Å. If the bonds N(3)-C(16) are included in the averaging process a value of 1.440(2) Å is obtained. The bond N(2)-C(9) in the picrate salt has a length of 1.463(5) Å. It is not significantly different from the first average value and barely significantly longer than the second.

Table 4.10: Comparison of bond lengths in $\text{TAABH}_2(\text{PICRATE})_2$ and

Bond	AA derivatives			
	TAABH_2 $(\text{PICRATE})_2$	AA TETRAMER	AA TRIMER $\cdot\text{CHCl}_3$	AA TRIMER $\cdot\text{CH}_3\text{CN}\cdot\text{H}_2\text{O}$
C(1)-C(14B)(21)	1.491(5)	1.483(5)	1.482(6)	1.490(7)
C(1)-N(2)	1.484(5)	1.401(5)	1.385(5)	1.386(6)
C(1)-N(1)	1.417(5)	1.284(5)	1.292(5)	1.288(6)
N(1)-C(2)	1.367(5)	1.407(5)	1.393(5)	1.399(6)
C(2)-C(7)	1.406(5)	1.390(5)	1.399(6)	1.386(7)
C(2)-C(3)	1.402(5)	1.402(6)	1.413(6)	1.411(7)
C(3)-C(4)	1.375(6)	1.376(6)	1.378(7)	1.384(8)
C(4)-C(5)	1.405(6)	1.390(6)	1.386(7)	1.391(7)
C(5)-C(6)	1.363(6)	1.378(6)	1.376(7)	1.379(7)
C(6)-C(7)	1.412(5)	1.401(6)	1.399(6)	1.405(7)
C(7)-C(8)	1.407(5)	1.446(6)	1.458(6)	1.446(7)
C(8)-N(2)	1.301(4)	1.406(5)	1.411(6)	1.397(6)
N(2)-C(9)	1.463(5)	1.454(5)	1.443(5)	1.448(6)
C(9)-C(14)		1.385(5)	1.388(6)	1.378(6)
C(8)-O(1)		1.233(5)	1.221(5)	1.228(6)
C(15)-O(2)			1.230(5)	1.246(6)
C(14)-C(15)			1.509(6)	1.495(6)
C(15)-N(3)			1.333(6)	1.347(6)
N(3)-C(16)			1.424(6)	1.436(6)
C(16)-C(21)			1.404(6)	1.402(7)
C(21)-C(1)			1.482(6)	1.490(7)

The interpretation of the bond length between N(1) and C(1) 1.418(5) Å, in the picrate salt, presents some problems. The sum of the bond angles around N(1) is 354.0 degrees. Although not a very accurate value, because of the possible error in locating the hydrogen atom, it indicates that the nitrogen atom has a geometry deviating from planarity towards pyramidality. The nitrogen atom can therefore be considered to exhibit a hybridisation between sp^3 and sp^2 . One would therefore expect a bond length for N(1)-C(1) to be of the same order as between C(1) and N(2) or perhaps marginally longer. Instead a bond shortening of approximately 0.07 Å is observed. The C(1) carbon atom, judging from its bond length, appears to show an extra-ordinary behaviour. It behaves like an sp^3 -hybridised carbon atom towards N(2), 1.485(5) Å, and like an sp^2 -hybridised carbon atom towards C(14), 1.491(5) Å. The bond C(1)-N(1), 1.418(5) Å is short enough to be commensurate with a bond between sp^2 -hybridised carbon and sp^2 -hybridised nitrogen atoms with some double bond character.

It remains to consider the angles between different planes in the TAAB salts and the AA products. All these molecules have a double saddle-shape. There are however significant differences between the TAAB salts, on the one hand, and the AA derivatives, on the other, as well as variations within each class of compounds.

In the following discussion all the atoms defining each least squares plane lie in that plane. The angles quoted are those between the normals of the planes.

Thus the angles between the planes 3 and 4 (see Tables 3.5 and 4.5)

for the AA derivatives ($74-83^\circ$) are very much larger than those for the TAAB salts ($16-27^\circ$) (Table 3.5). Similarly the angles between planes 4 and 8 (as well as planes 3 and 9) are very small in the AA derivatives ($1-3^\circ$) compared to those in the TAAB salts ($22-27^\circ$). These two sets of angles mentioned above cause a step in the profile taken along the long axis of the cation in the TAAB salts (see Diagram 4.8).

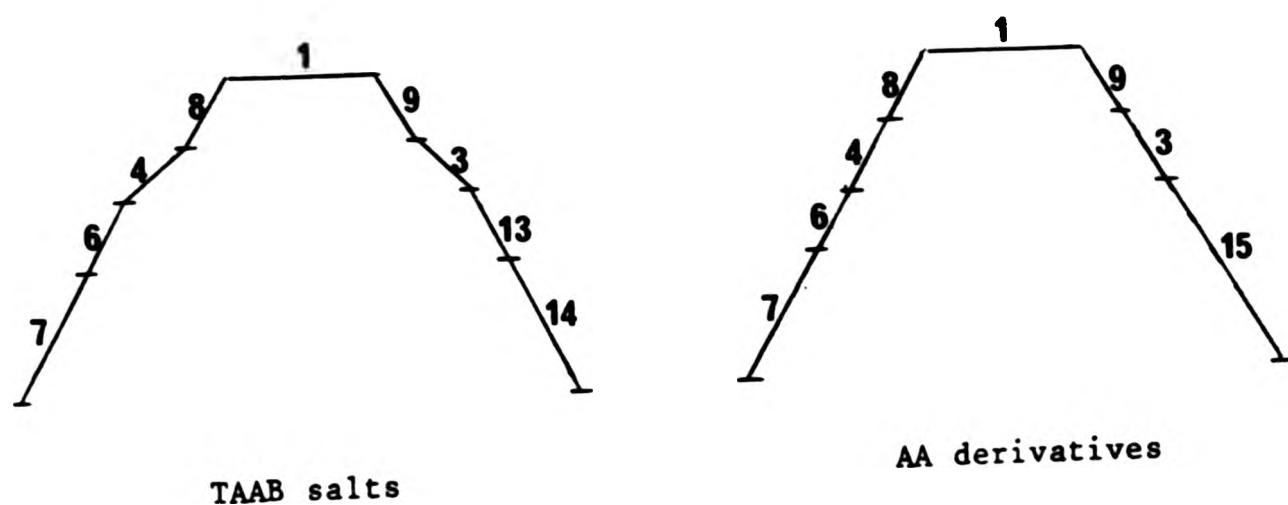


Diagram 4.8

No such step is apparent for the AA derivatives, nor for either sets of compounds for the profile along the short axis. Such major differences are not observed between planes 8 and 9, 6 and 13(15). Similarly the angles between planes 1 and 2 and between planes 10 and 11 are similar. The overall effect is to give a gross similar shape to all the compounds discussed in this section.

A somewhat lesser variation in angles between the planes 1 and 2 ($65-79^\circ$) along the short axis profile, than the variation between 6 and 13(15) ($60-84^\circ$) along the long axis profile is observed. Along both profiles the angles between the planes of the TAAB salts are somewhat

smaller than those of the AA structures, making the cations somewhat flatter than the AA derivatives. The variations within the TAAB salts are less than those amongst the AA structures.

All the structures discussed, barring the AA TETRAMER, are involved in some sort of hydrogen bonding. The AA TRIMER. CHCl_3 exhibits the largest angles between planes 1 and 2, as well as between 6 and 13(15), i.e. has the most folded structure. This molecule, apart from intermolecular hydrogen bonding leading to dimerisation, has another hydrogen bond from its second carbonyl group to the chloroform molecule. It may be worthwhile to mention in passing that the hydrogen bonding of a chloroform molecule in $\text{Cu}(\text{salen})$ affects significantly its structure, when compared to that of the unsolvated complex (see section 1.2.4)

REFERENCES

1. A. Chatterjee and M. Ganguly, J. Org. Chem., 1968, 33, 3358.
2. T. Ottersen, C. Christophersen, and S. Treppendahl, Acta Chem. Scand., 1975, A29, 45.
3. J. Elguero, A. R. Katritzky, S. El-Osta, R. L. Harlow, and S. H. Simonsen, J. Chem. Soc. Perkin I, 1976, 312.
4. "Interatomic Distances Supplement", Edt., L. E. Sutton, Special Publication 18, The Chemical Society, London, 1965, p. S19s.

CHAPTER 5

STRUCTURAL INVESTIGATION OF $\text{Cu}(\text{TAABH}_2)$

5.1 METHOD OF PREPARATION

The crystals of the above compound were kindly supplied by Drs. Goddard and Norris.¹

5.2 DATA COLLECTION AND STRUCTURE SOLUTION

Details of data collection and crystal data are summarized in Tables 5.1 and 5.2.

Data reduction applied to the raw data, consisting of 1748 reflections, resulted in 603 unique reflections with $I > 3\sigma(I)$. The following systematic absences were observed.

h00	$h = 2n + 1$	hk0	N.C.
0k0	N.C.	h0l	$h = 2n + 1$
00l	$l = 2n + 1$	0kl	$l = 2n + 1$

Assuming that there are 4 molecules in the unit cell, the density was calculated. $D_c = 1.442 \text{ g/cm}^3$. The measured density, $D_m = 1.436 \text{ g/cm}^3$, is in good agreement with the calculated one. From

Table 5.1: Crystal data of Cu(TAABH₂)

Formula	CuC ₂₈ H ₂₂ N ₄
Molecular weight	478
Crystal system	Orthorhombic
Space group	Pca2 ₁
a (Å)	23.558(6)
b (Å)	11.979(5)
c (Å)	7.789(3)
α (°)	90.00
β (°)	90.00
γ (°)	90.00
Volume (Å ³)	2198.1
D _c (g/cm ³)	1.442
D _m (g/cm ³)	1.436
Z	4
F(000)	988
μ(Mo-Kα) (cm ⁻¹)	9.78

Table 5.2: Data collection and structure solution details of
Cu(TAABH₂)

Crystal size (mm)	0.22x0.29x0.13
Crystal colour	Reddish black
Shape	Elongated plates
BMO	1
SMO	1
Scan width (°)	1.0
θ-range (°)	3-30
Reflections measured	1748
Unique data set	603
Least-squares parameters	89
Data/parameter	6.7
Shift/e.s.d.	0.01
Weighting scheme	$1/[\sigma^2(F)+F^2]$
Max. electron density residue e/Å ³	0.46
R	0.067
R _w	0.067

the above conditions two space groups are possible: $Pca2_1$ and $Pbcm$. Both space groups have been investigated. The Patterson vectors for the two space groups were calculated and these vectors were compared with the vectors given from the Patterson synthesis. The space group $Pca2_1$ has 4 equivalent positions. Therefore there is one formula unit in each of the equivalent positions, and $1/4$ of the unit cell is the asymmetric unit.

$Pca2_1$ equivalent positions

- 1) x, y, z
- 2) $-x, -y, 1/2 + z$
- 3) $1/2 - x, y, 1/2 + z$
- 4) $1/2 + x, -y, z$

Patterson vectors for $Pca2_1$	Height
1) $\pm (2x, 2y, 1/2)$	1
2) $\pm (1/2 - 2x, 0, 1/2)$	1
3) $\pm (1/2, 2y, 0)$	1

Observed first 6 peaks from the Patterson map

	U	V	W	Height	Assignment
1)	0.5	0.388	0	326	$1/2, 2y, 0$
2)	0.287	0.0	0.5	246	$1/2 - 2x, 0, 1/2$
3)	0.0	0.157	0.0	169	
4)	0.5	0.0	0.0	154	
5)	0.5	0.217	0.0	152	
6)	0.215	0.392	0.5	142	$2x, 2y, 1/2$

From (6) $2x = 0.125$ $2y = 0.392$

$$\begin{aligned} \text{From (2)} \quad 1/2 - 2x &= 0.287 \\ 2x &= 0.213 \end{aligned}$$

$$\text{From (1)} \quad 2y = 0.388$$

$$\begin{aligned} x &= (0.213 + 0.215)/4 & y &= (0.392 + 0.388)/4 \\ x &= 0.107 & y &= 0.195 \end{aligned}$$

The position of the Cu atom is $x = 0.107$, $y = 0.195$, and z will be chosen arbitrarily.

For the space group $Pca2_1$, the z -co-ordinate of copper could take any value, but for the $Pbcm$ (centrosymmetric) space group the z -value must be 0.25, when h and k are interchanged. To clarify this space group problem, the copper atom was assumed to be at $x = 0.107$, $y = 0.195$ as found, and $z = 0.25$, as it would be in $Pbcm$, as well as in the $Pca2_1$ space group.

Using phases calculated from the copper atom position, deduced above, Fourier maps were calculated for both space groups. A benzene ring was located in each case. Using the phases calculated from the copper atom, and the found positions of the benzene ring, difference Fourier and full matrix least squares refinement calculations were done in both space groups. Only the non-centric one, $Pca2_1$, refined well, down to $R = 0.33$ and 15 more non-hydrogen atoms, apart from Cu and the first benzene, ring were located.

The remaining non-hydrogen atoms were found from successive difference Fourier maps. The copper atom was refined with anisotropic

thermal parameters. The hydrogen atom co-ordinates were estimated geometrically (assuming C-H = 1.08 Å) and for the refinement allowed to ride on their respective carbon atom co-ordinates. Due to the insufficient data (603 reflections) the phenyl rings were refined as rigid bodies with C-C = 1.395 Å. The refinement was stopped, when the calculated parameter shift/e.s.d. ratio fell to a maximum of 0.01.

The final R-value was 0.067, $R_w = 0.067$. The final difference Fourier map showed the mean amplitude of,

$$0.46 > \Delta\sigma > -0.40$$

The highest residual electron density of 0.46 e/Å³ was observed near the C(17) atom.

5.3 DISCUSSION OF CU(TAABH₂)

5.3.1 DESCRIPTION OF THE STRUCTURE

The compound Cu(TAABH₂) has the structure shown in Figure 5.1, which also shows the numbering scheme used for this molecule together with the important bond lengths and angles. The complete data for bond lengths and angles are in Tables 5.3 and 5.4. The ORTEP drawings of this molecule are in Drawing 5.1.

The molecule has the structure shown in Figure 5.1. It adopts a double saddle-shape with the angles between opposite pairs of benzene rings, 1 and 2, 3 and 4 being 68° and 26° respectively.

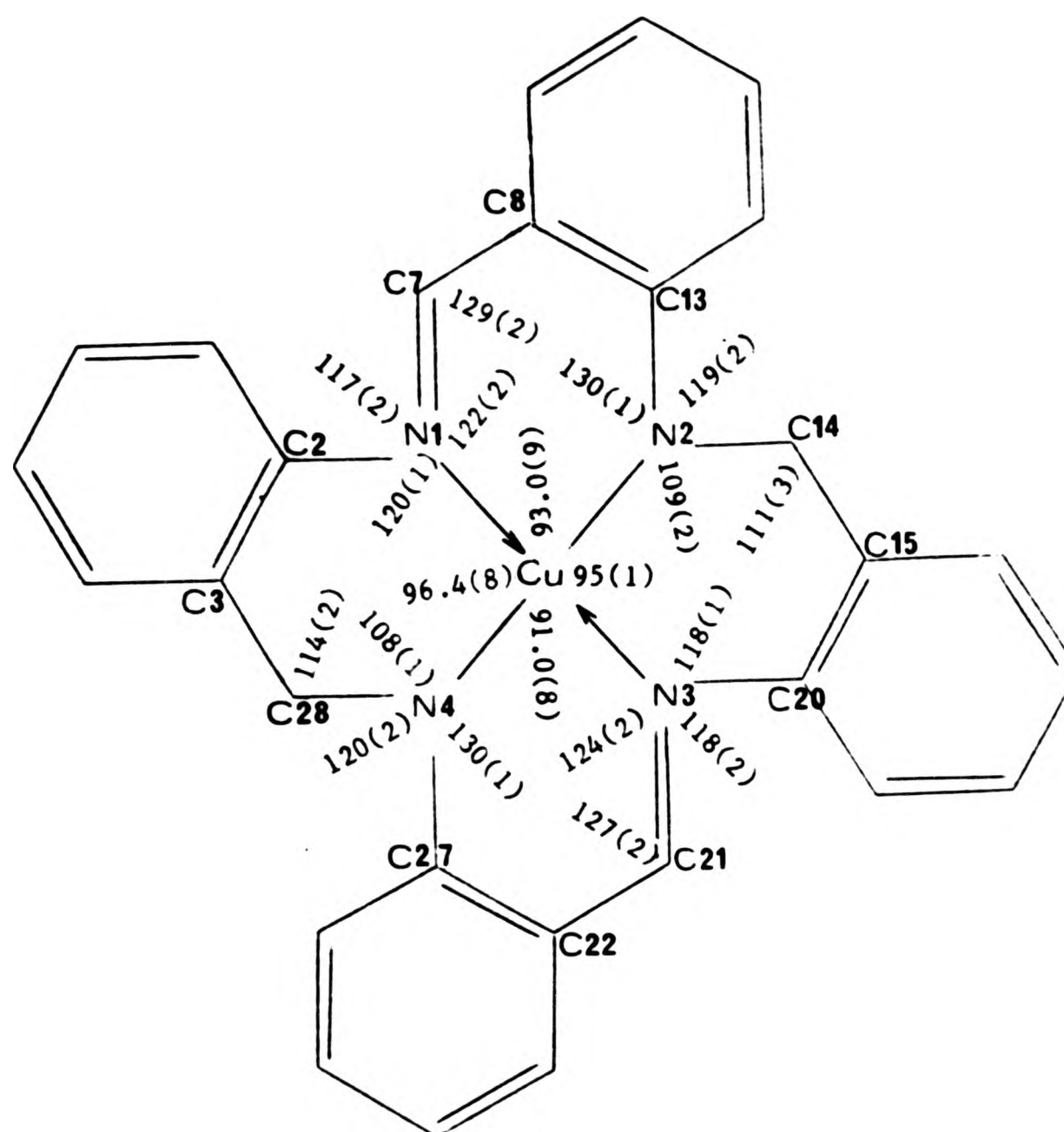


Figure 5.1b

Table 5.3: Bond lengths (Å) Cu(TAABH₂)

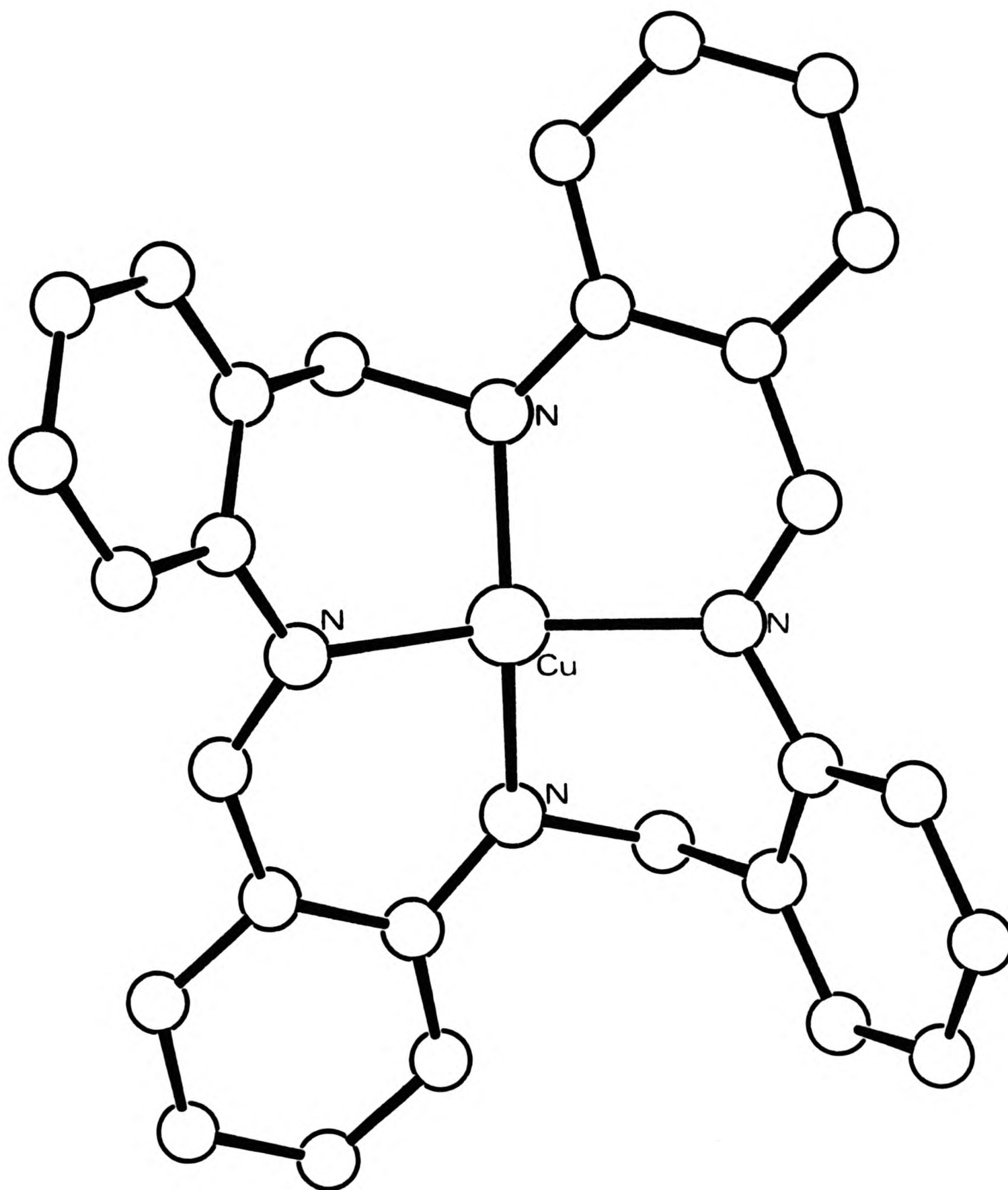
Cu	-N(1)	1.990(17)	Cu	-N(2)	1.943(16)
Cu	-N(3)	2.036(19)	Cu	-N(4)	1.913(18)
Cu	-C(28)	2.77(3)	C(1)	-C(2)	1.395
C(1)	-C(6)	1.395	C(2)	-C(3)	1.395
C(2)	-N(1)	1.389(23)	C(3)	-C(4)	1.395
C(3)	-C(28)	1.45(3)	C(4)	-C(5)	1.395
C(5)	-C(6)	1.395(1)	N(1)	-C(7)	1.268(24)
C(7)	-C(8)	1.435(24)	C(9)	-C(10)	1.395
C(10)	-C(11)	1.395	C(11)	-C(12)	1.395
C(12)	-C(13)	1.395	C(13)	-C(8)	1.395
C(13)	-N(2)	1.371(22)	C(15)	-C(14)	1.54(3)
N(2)	-C(14)	1.50(3)	C(16)	-C(17)	1.395
C(16)	-C(15)	1.395	C(17)	-C(18)	1.395
C(18)	-C(19)	1.395	C(19)	-C(20)	1.395
C(20)	-C(15)	1.395	C(20)	-N(3)	1.439(23)
N(3)	-C(21)	1.294(25)	C(21)	-C(22)	1.42(3)
N(4)	-C(27)	1.377(24)	C(22)	-C(27)	1.395
N(4)	-C(28)	1.51(3)	C(22)	-C(23)	1.395
C(23)	-C(24)	1.395	C(24)	-C(25)	1.395
C(25)	-C(26)	1.395	C(26)	-C(27)	1.395

Table 5.4: Bond angles ($^{\circ}$) Cu(TAABH₂)

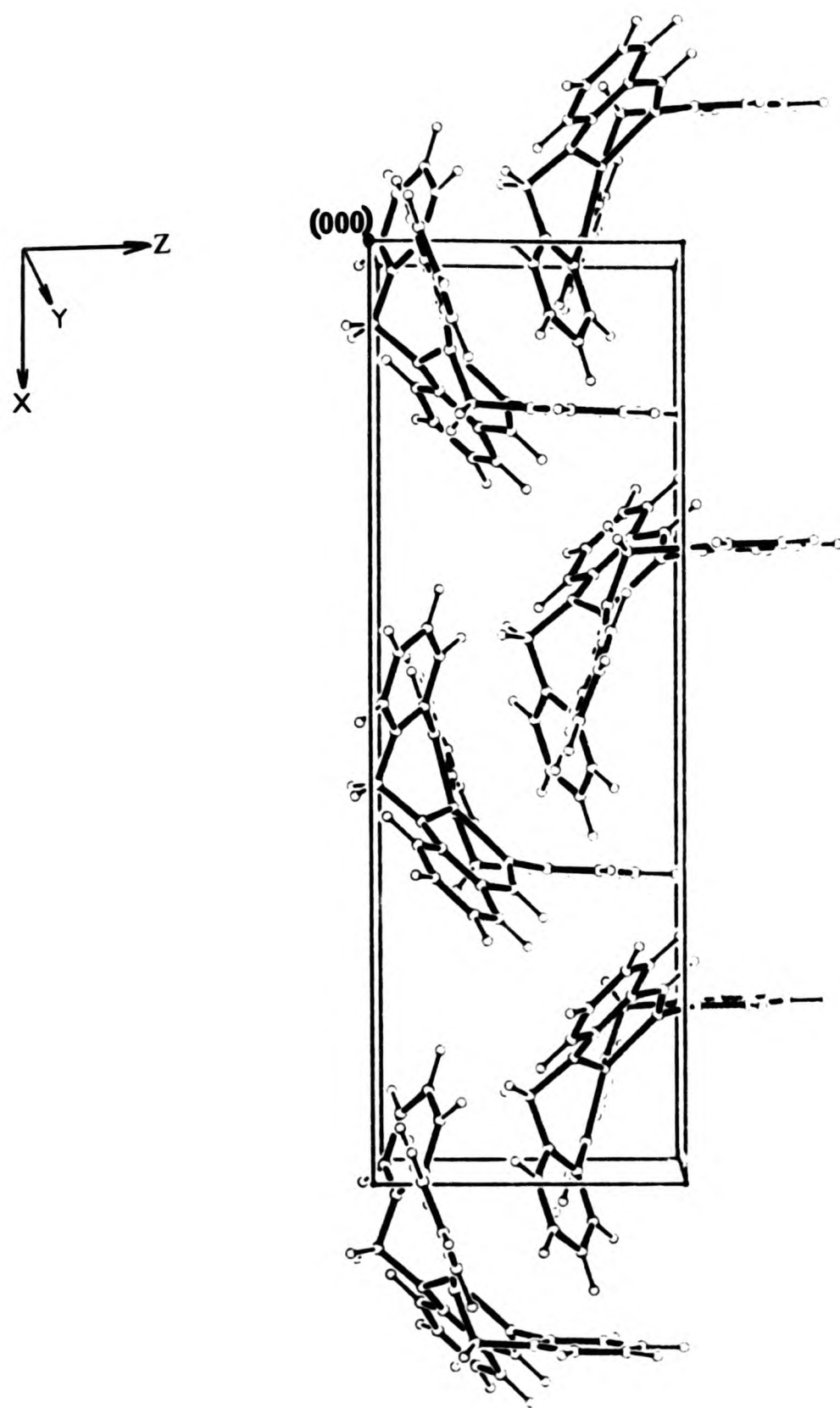
N(2) -Cu -N(1)	93.0(9)	N(3) -Cu -N(1)	148.5(7)
N(3) -Cu -N(2)	95(1)	N(4) -Cu -N(1)	96.4(8)
N(4) -Cu -N(2)	152(1)	N(4) -Cu -N(3)	91.0(8)
C(28) -Cu -N(1)	68.4(7)	C(28) -Cu -N(2)	136(1)
C(28) -Cu -N(3)	122.3(8)	C(28) -Cu -N(4)	31.3(8)
C(6) -C(1) -C(2)	120.0(1)	C(3) -C(2) -C(1)	120.0(1)
N(1) -C(2) -C(1)	120.8(9)	N(1) -C(2) -C(3)	119.1(9)
C(4) -C(3) -C(2)	120.0(1)	C(5) -C(4) -C(3)	120.0(1)
C(28) -C(3) -C(2)	118(1)	C(28) -C(3) -C(4)	122(1)
C(6) -C(5) -C(4)	120.0(1)	C(5) -C(6) -C(1)	120.0(1)
C(2) -N(1) -Cu	120(1)	C(7) -N(1) -Cu	122(2)
C(7) -N(1) -C(2)	117(2)	(8) -C(7) -N(1)	129(2)
C(8) -C(9) -C(10)	120.0(1)	C(11) -C(10) -C(9)	120.0(1)
C(12) -C(11) -C(10)	120.0(1)	C(13) -C(12) -C(11)	120.0(1)
C(8) -C(13) -C(12)	120.0(1)	N(2) -C(13) -C(12)	122(1)
N(2) -C(13) -C(8)	117(1)	C(13) -C(8) -C(9)	120.0(1)
C(9) -C(8) -C(7)	112(1)	C(13) -C(8) -C(7)	127(1)
C(13) -N(2) -Cu	130(1)	C(14) -N(2) -Cu	109(2)
C(14) -N(2) -C(13)	119(2)	C(15) -C(16) -C(17)	120.0(1)

Table 5.4 continued

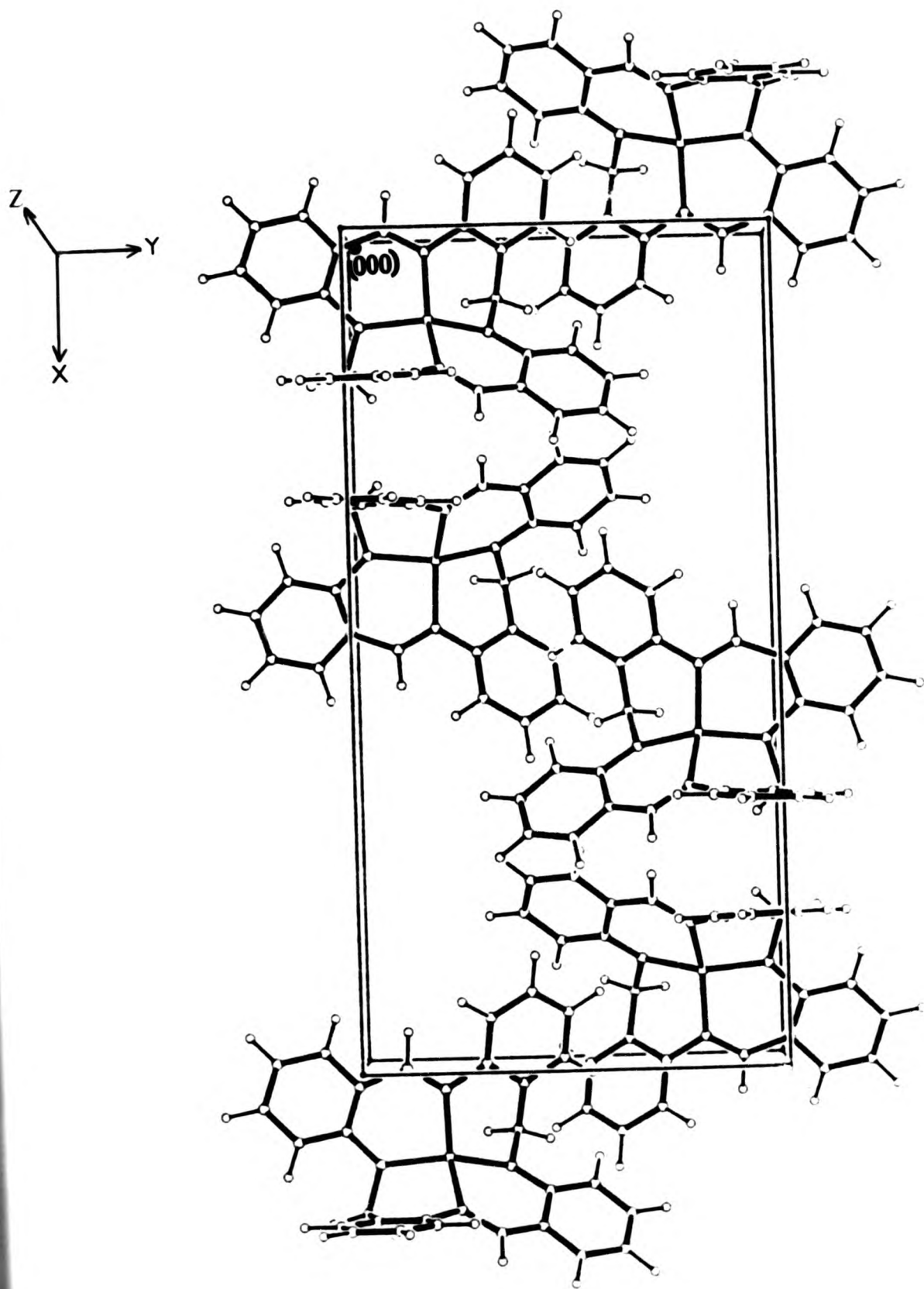
C(18) -C(17) -C(16)	120.0(1)	C(19) -C(18) -C(17)	120.0(1)
C(20) -C(19) -C(18)	120.0(1)	C(15) -C(20) -C(19)	120.0(1)
N(3) -C(20) -C(19)	121.2(9)	N(3) -C(20) -C(15)	118.6(9)
C(20) -C(15) -C(16)	120.0(1)	C(20) -N(3) -Cu	118(1)
C(14) -C(15) -C(16)	124(1)	C(14) -C(15) -C(20)	116(1)
C(21) -N(3) -Cu	124(2)	C(21) -N(3) -C(20)	118(2)
C(22) -C(21) -N(3)	127(2)	C(27) -N(4) -Cu	130(1)
C(28) -N(4) -Cu	108(1)	C(28) -N(4) -C(27)	120(2)
C(15) -C(14) -N(2)	111(3)	C(27) -C(22) -C(23)	120.0(1)
C(23) -C(22) -C(21)	113(1)	C(27) -C(22) -C(21)	126(1)
C(24) -C(23) -C(22)	120.0(1)	C(25) -C(24) -C(23)	120.0(1)
C(26) -C(25) -C(24)	120.0(1)	C(27) -C(26) -C(25)	120.0(1)
C(22) -C(27) -N(4)	119(1)	C(26) -C(27) -N(4)	121(1)
C(26) -C(27) -C(22)	120.0(1)	C(3) -C(28) -Cu	96(1)
N(4) -C(28) -Cu	41(1)	N(4) -C(28) -C(3)	114(2)



Drawing 5.1a



Drawing 5.1b



Drawing 5.1c

One half of this saddle is slightly (68°), the other half very much flatter (26°), than the corresponding parts of the TAAB salts and of the AA derivatives (65-79 and 60-84 $^\circ$ respectively) (see section 4.5).

The free ligand, TAABH₄, although isolated, has not had its structure determined by X-ray crystallography. One would expect its imine and amine nitrogen atoms to be respectively sp²- and sp³-hybridised.

The copper atom is 4-co-ordinate, and located on the best plane of the four nitrogen atoms. The imine nitrogen atoms N(1), N(3) and the anionic nitrogen atoms N(2), N(4) are displaced by +0.5 and -0.5 Å respectively, from that best plane. This gives to the copper atom a distorted square planar configuration, with a distortion towards a tetrahedron.

This distortion of the co-ordination sphere of copper, towards a tetrahedral structure is in line with other work. Tricyclic and tetracyclic systems of copper, with ring size arrangements 6-,6-,6 and 6-,6-,6-,6 tend towards a tetrahedral shape, whilst 6-,5-,6- and 6-,5-,6-,5-arrangements tend to be square planar or nearly so (see chapter 8).

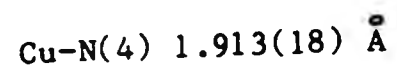
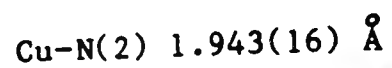
The imine nitrogen-copper distances are

Cu-N(1) 1.990(17) Å

Cu-N(3) 2.036(19) Å

[Cu-N(imine)] average 2.013(13) Å

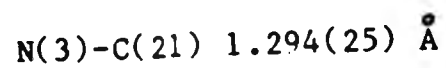
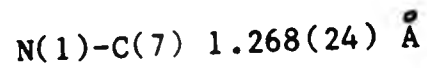
The anionic nitrogen-copper distances are



It can be seen that the average [Cu-N(imine)] bond length is significantly longer than the average [Cu-N(anionic)] bond length, probably, because the Cu ion interacts in the former with a neutral, and in the latter with a negatively charged atom, the latter attraction being the more powerful one.

The imine nitrogen atoms N(1) and N(3) are found to be approximately 0.06 and 0.03 Å displaced from the planes of Cu, C(2), C(7) and Cu, C(20), C(21) respectively. Therefore they are approximately sp²-hybridised. The anionic nitrogen atoms N(2) and N(4) are approximately 0.10 and 0.14 Å displaced from the planes of Cu, C(14), C(13) and Cu, C(27), C(28) respectively. For an sp³-hybridised atom the deviation would be expected to be 0.6-0.7 Å. The average sum of the bond angles around N(2) and N(4) is 358.1°. Therefore the best description of hybridisation is approximately sp².

The bond lengths



are very short, showing the expected double bond character (see section 3.3.1).

The bond lengths

N(2)-C(14) 1.500(30) Å

N(4)-C(28) 1.510(30) Å

are longer than the previous ones, [N(1)-C(7) and N(3)-C(21)], and have the expected single bond character. C(14) and C(28) are sp^3 -hybridised.

Finally the bond lengths

N(2)-C(13) 1.371(22) Å

N(4)-C(27) 1.377(24) Å

average N-C 1.374(16) Å

N(1)-C(2) 1.389(23) Å

N(3)-C(20) 1.439(23) Å

average N-C 1.414(16) Å

show that the average value of the latter bonds, N(1)-C(2), N(3)-C(20), is somewhat longer than that of the former ones, N(2)-C(13), N(4)-C(27). The difference, although expected on chemical grounds (see section 5.3.2), is, however, not statistically significant, the non-centric space group and the relative paucity of reflections giving rise to rather high e.s.d. values.

5.3.2 COMPARISON OF THE STRUCTURE OF THE COPPER AND RELATED

TAABH₄ DERIVATIVES

Four X-ray crystallographic investigations have been reported for

metal complexes of TAAB and its derivatives.²⁻⁴ These are:

I) Charged species of MTAAB

a) $[\text{Ni}(\text{TAAB})(\text{H}_2\text{O})\text{I}]\text{I}^2$ and b) $[\text{Ni}(\text{TAAB})](\text{BF}_4)_2^2$

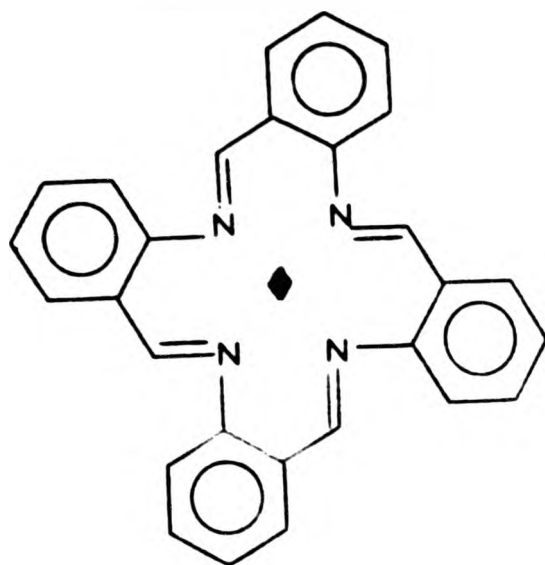
and II) neutral species of TAABH_4 metal complexes

a) $\text{Ni}[\text{TAAB}(\text{CH}_2\text{COCH}_3)_2]^3$ and b) $\{\text{Fe}[\text{TAAB}(\text{OCH}_3)_2]\}_2\text{O}^4$

The $\text{Cu}(\text{TAABH}_2)$ complex, which has been discussed in the previous section falls into the second class.

The structure determination of the class I compounds, due to the packing disorder in the cations, were poor. The results were even worse in the second compound $[\text{Ni}(\text{TAAB})](\text{BF}_4)_2$, due to the added effect of the tumbling of the BF_4 counter-ion. The R-factors were 10.9 and 14.1% respectively for compounds (a) and (b), and the e.s.d. values were very high. In compound (a) Ni is 6-co-ordinate, to four nitrogen atoms, the water molecule, and one iodide ion. The other iodide ion is the counter-ion. In compound (b) the Ni atom is only 4-co-ordinate (to the four nitrogen atoms) with the BF_4 ions well separated from the cation. The average bond lengths for four-fold symmetry related sections of both compounds are given in Diagram 5.1.

The structure determination of class II compounds: (a) $\text{Ni}[\text{TAAB}(\text{CH}_2\text{COCH}_3)_2]$ and (b) $\{\text{Fe}[\text{TAAB}(\text{OCH}_3)_2]\}_2\text{O}$ show both to be ordered and the R-factors are 6.0 and 5.8% respectively. The Ni atom is co-ordinated to four nitrogen atoms, whilst the Fe atom is 5-co-ordinate, the fifth co-ordination position being occupied by the oxo-bridge. The average bond lengths for 2-fold symmetry related sections of both compounds, together with the one, $\text{Cu}(\text{TAABH}_2)$, reported in this Thesis, are given in Diagram 5.2.



TAAB

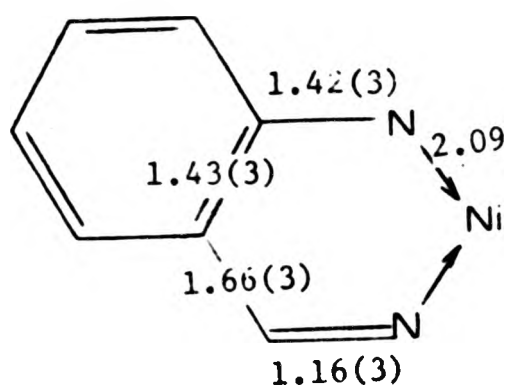
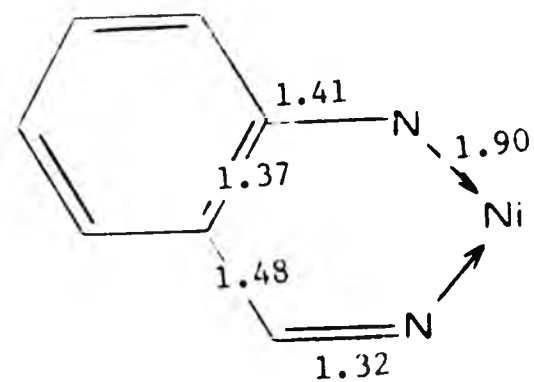
 $[\text{Ni}(\text{TAAB})(\text{H}_2\text{O})]\text{I}$  $[\text{Ni}(\text{TAAB})](\text{BF}_4)_2$

Diagram 5.1

A comparison of the copper complex reported here with the neutral Ni and Fe complexes, for both of which rather accurate structural data are available, shows that bond length differences in all three structures have the same pattern. Therefore, although in the copper complex the difference in the last mentioned C-N bond lengths (see section 5.3.1) [1.374(16) and 1.414(16) Å] is not statistically significant, it can nevertheless be considered as real.

The structural Diagram 5.2 needs, however, some modification. The

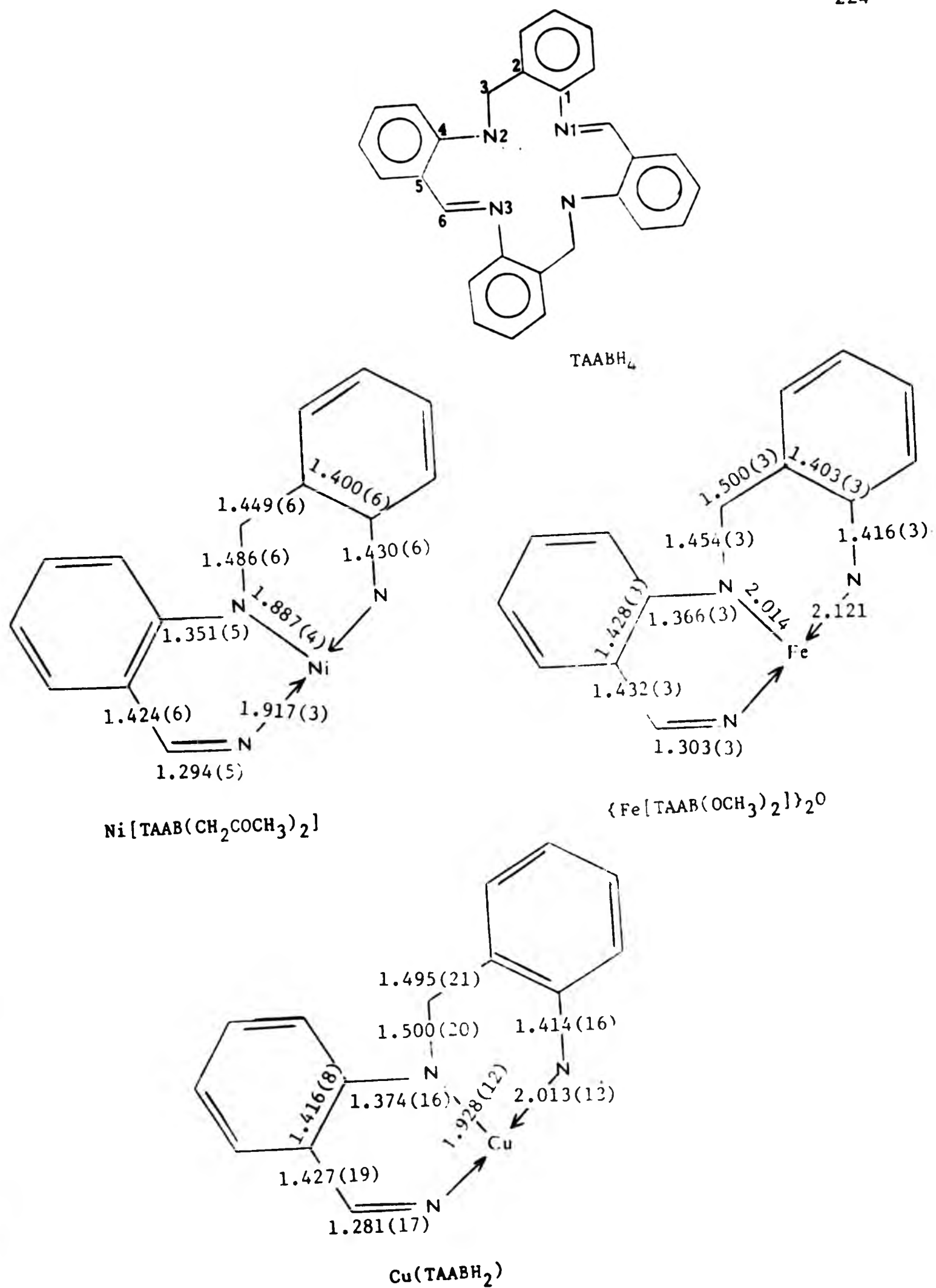


Diagram 5.2

bonds C(5)-C(6) are too short for a single bond, (1.424-1.432). Dewar⁵ gives a value of 1.485 Å for a pure sp^2-sp^2 -bond without any π -character. We have observed earlier, in the sections on AA condensation products (4.4 and 4.5), a similar value (to that of Dewar's) of 1.483(6) Å for C(1)-C(14) and for the analogous N(2)-C(9) bond a value of 1.453(5) Å. The bonds N(1)-C(1) (1.414-1.430 Å), and especially N(2)-C(4) (1.351-1.374 Å) in these metal complexes, are significantly shorter than the above value. The assumption of a significant contribution from o-quinonoid resonance forms (see Diagram 5.3) can explain these observed bond lengths. A similar suggestion has been made for the $TAABH_2(PICRATE)_2$ salt (section 3.3.1) and the AA structures (sections 4.4 and 4.5), and has been discussed in some detail there.

It is most helpful to interpret the resonance forms of the copper compound, in conjunction with the more accurate data of the Fe and Ni derivatives. There is a slight lengthening of the N(3)-C(6) (see Diagram 5.2) over that normally accepted for a C=N bond. The shortening of N(1)-C(1) [and the more pronounced effect of this kind in N(2)-C(4)], as well as the shortening of the carbon-carbon bond C(5)-C(6) [compared to that of a similar bond without any π -character (1.485 Å)], suggest that contributions from resonance forms (A), (B) and (C) all play a part. As the paucity of the data enforced rigid body refinement of the benzene rings, data for bond lengths and angles changes in these benzene rings are lacking, and hence the light these may throw on the contributions of the various resonance forms.

The angles at the metal atoms in the TAAB and $TAABH_4$ metal

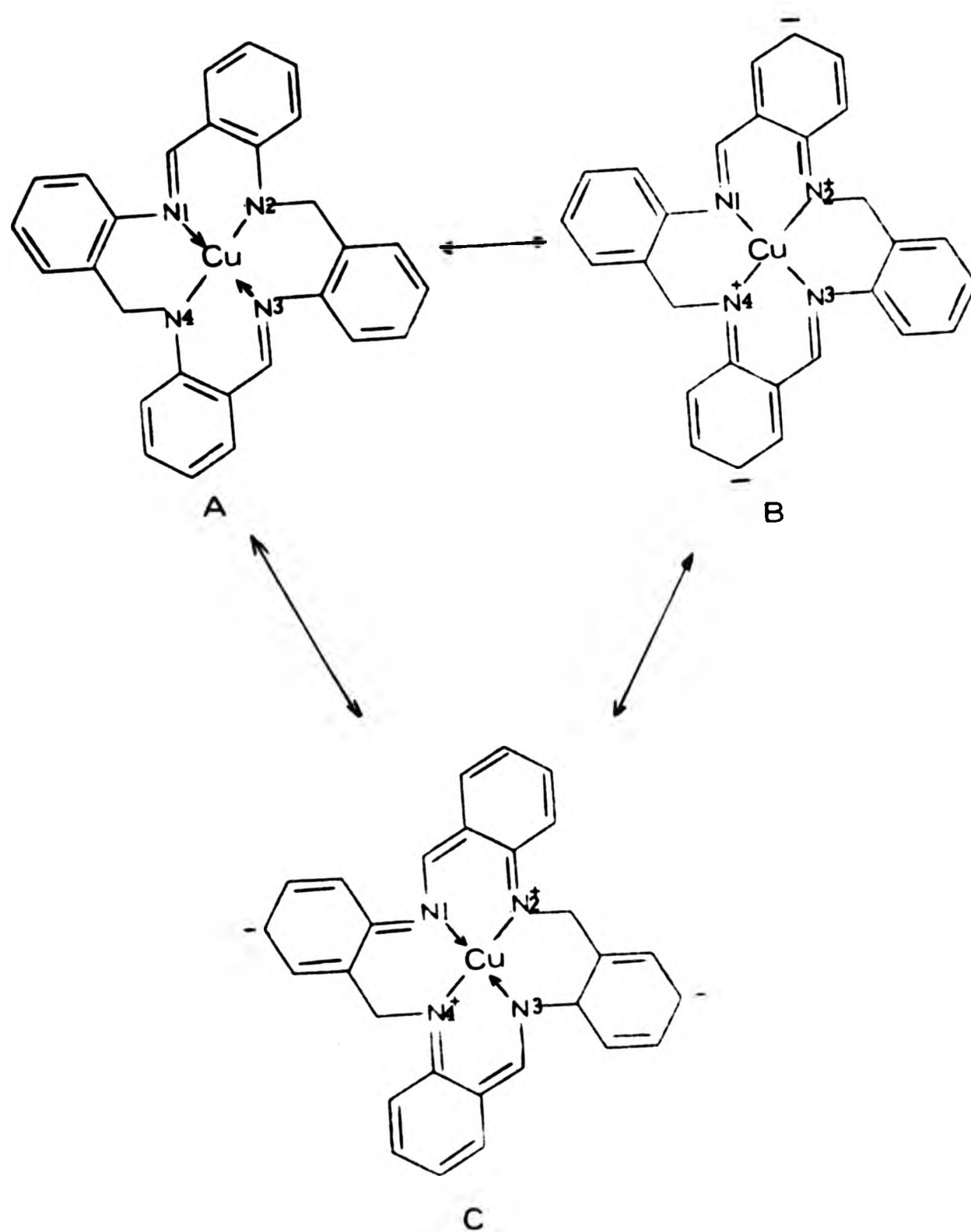


Diagram 5.3

derivatives are close to 90° (Diagrams 5.4 and 5.5).

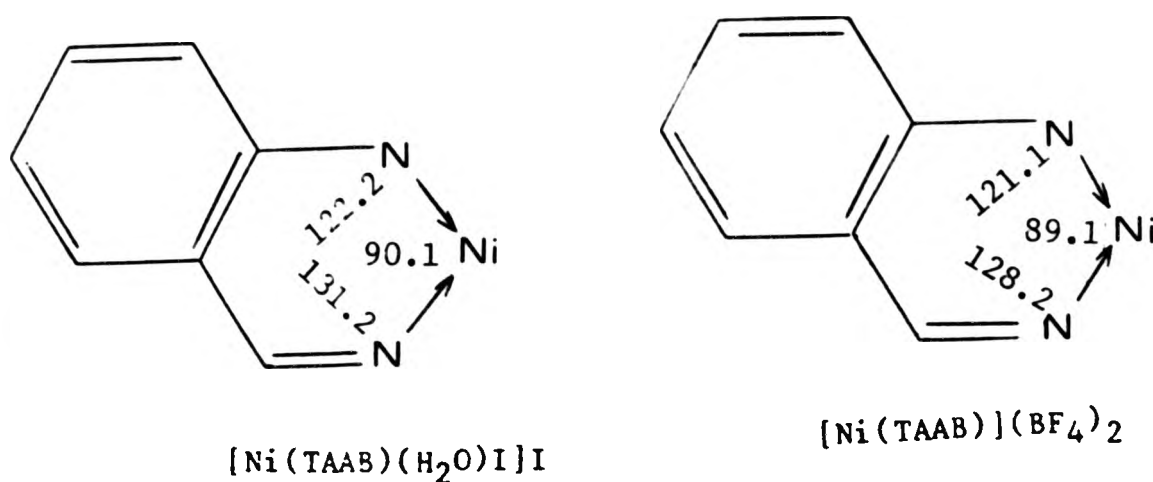


Diagram 5.4

In $\text{Cu}(\text{TAABH}_2)$, the rings, containing $\text{C}=\text{N}$ bonds are almost planar, whilst the formally saturated rings adopt a twisted boat conformation. On comparing the three TAABH_4 derivatives (Diagram 5.5), it is noted that the angles which the saturated rings make with the metal atoms are larger than the corresponding ones in the unsaturated ones. A possible contributing factor to this phenomenon, is that the larger bond angle of the unsaturated imine nitrogen atom, enforces a smaller angle at the metal atom.

The sums of the bond angles around the two types of nitrogen atoms in the iron complex are less than 360° . (Both are 357.9° .) This is undoubtedly due to the iron atom being significantly above the plane of the four nitrogen atoms, a common structural feature of 5-co-ordinate Fe complexes of this type (see Table 8.5).

As the Fe^{3+} ion has a smaller ionic radius (0.53 \AA) than that of the

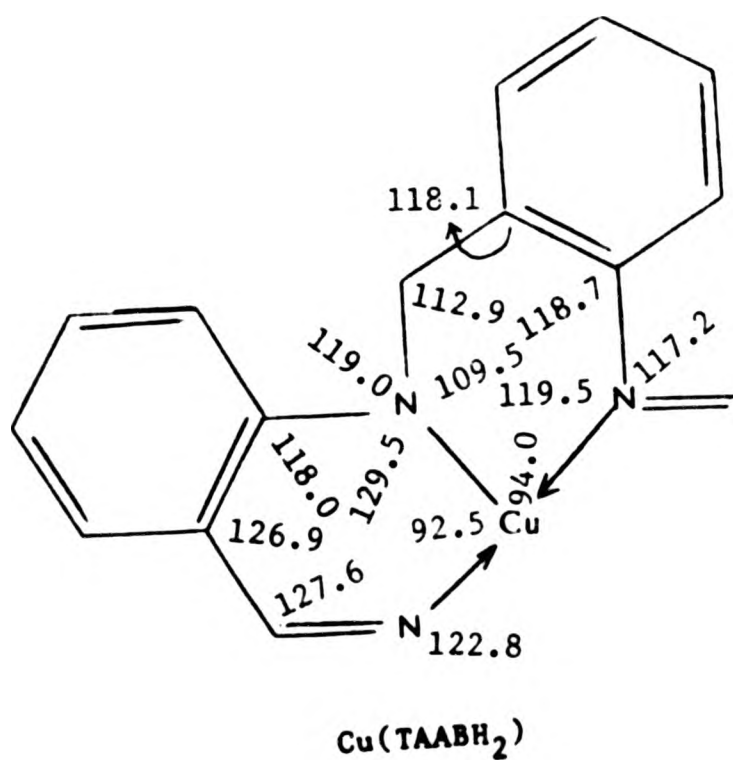
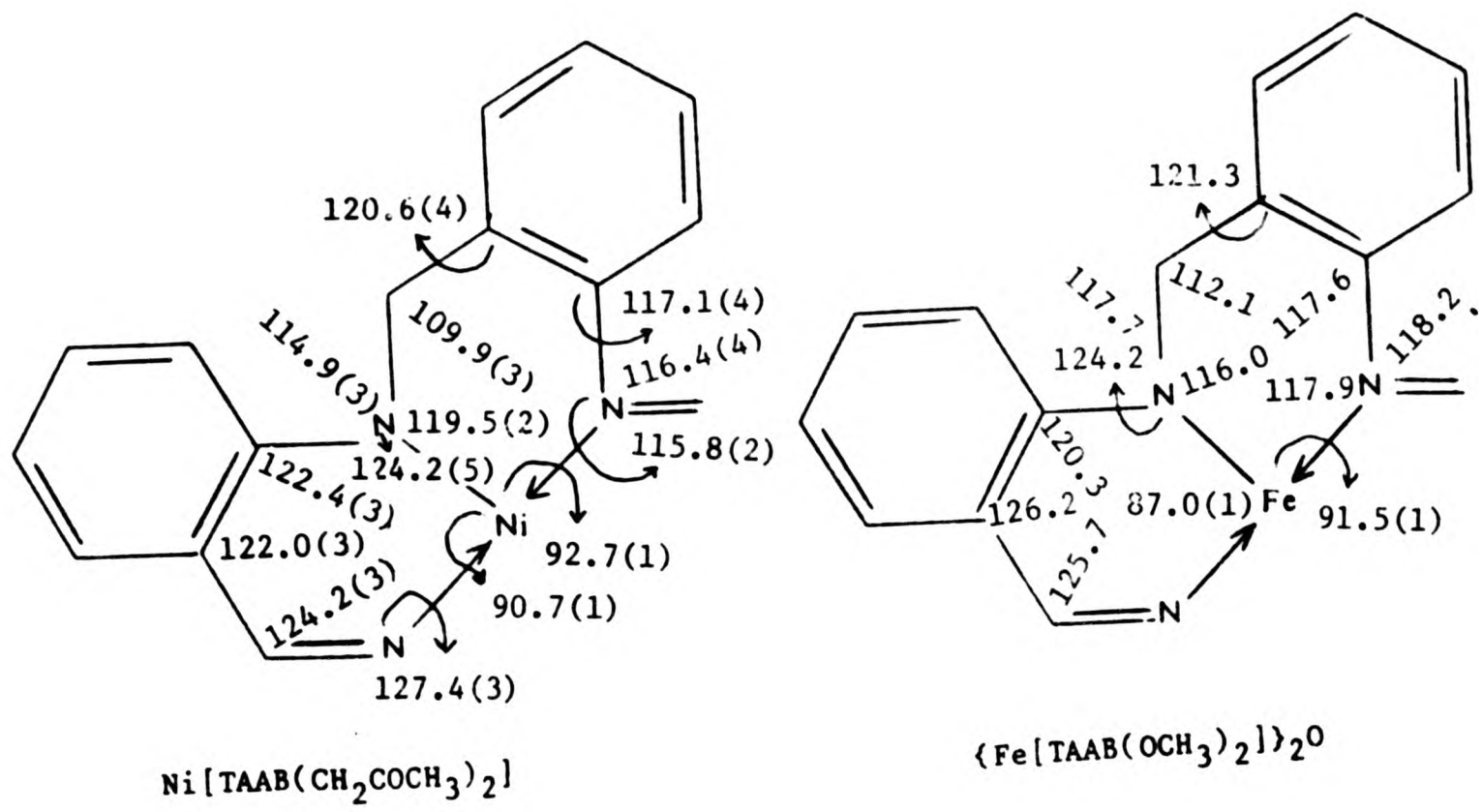
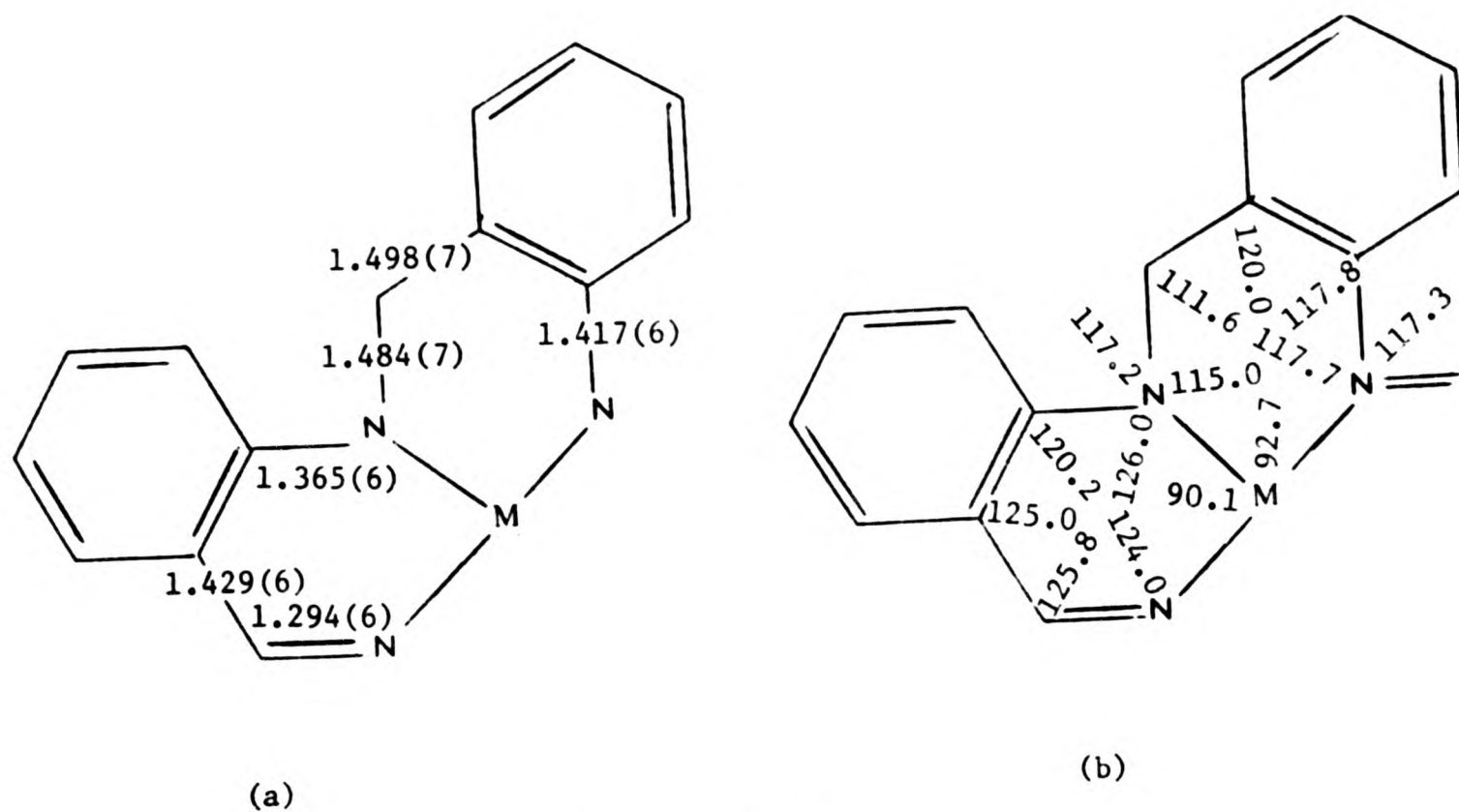


Diagram 5.5

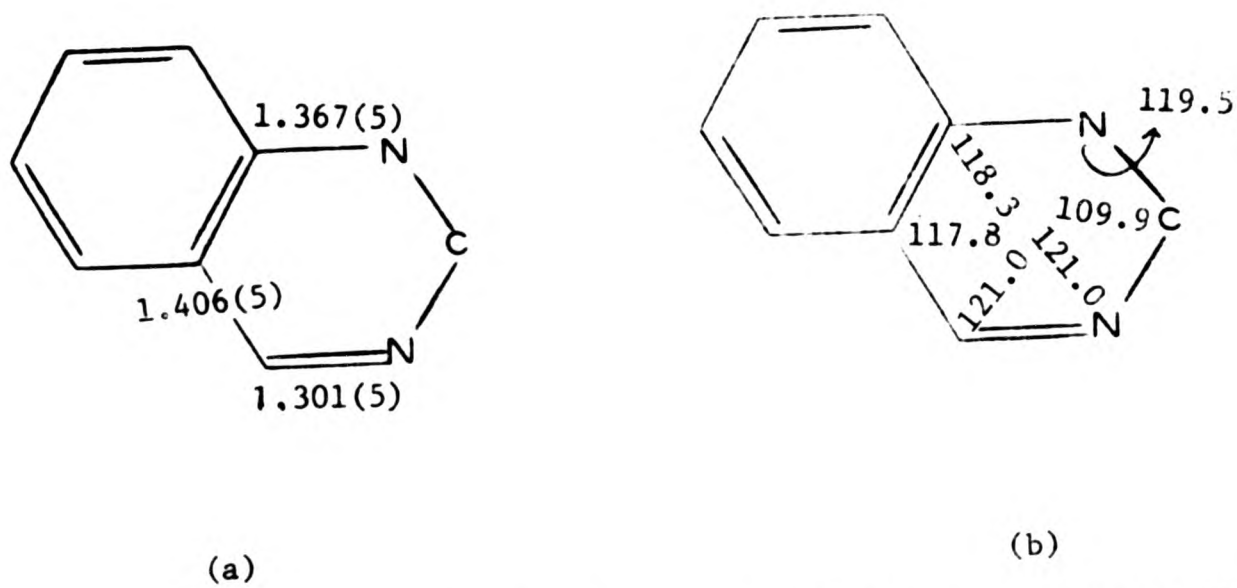
Cu^{2+} ion (0.72 \AA),⁶ size factors cannot be the reason why the iron atom is above the plane of the four nitrogen atoms whilst the copper atom is within that plane.

On comparing the relevant five-atom segments of the TAABH_4 metal derivatives with the those of $\text{TAABH}_2(\text{PICRATE})_2$ salt, by excluding the metal atom of the former and the carbon atom (fused to the 8-membered ring) of the latter, very close similarities in bond lengths are observed (see Diagram 5.6). Both heterocycles have a similar, almost planar, shape, that of the $\text{TAABH}_2(\text{PICRATE})_2$ salt being slightly less so, because of the fold of 22° along C(8)-N(1). However bond angles differ markedly. The angle at the metal atom is a right angle, whilst that at the above mentioned carbon atom is a tetrahedral one. The remaining bond angles are uniformly somewhat larger in the metal derivatives than in the picrate salt (Diagram 5.6).



M = Ni, Fe, Cu

Average bond lengths (a) and angles (b) of three TAABH₄ metal complexes



Bond lengths (a) and angles (b) of the relevant segment of TAABH₂(PICRATE)₂

Diagram 5.6

REFERENCES

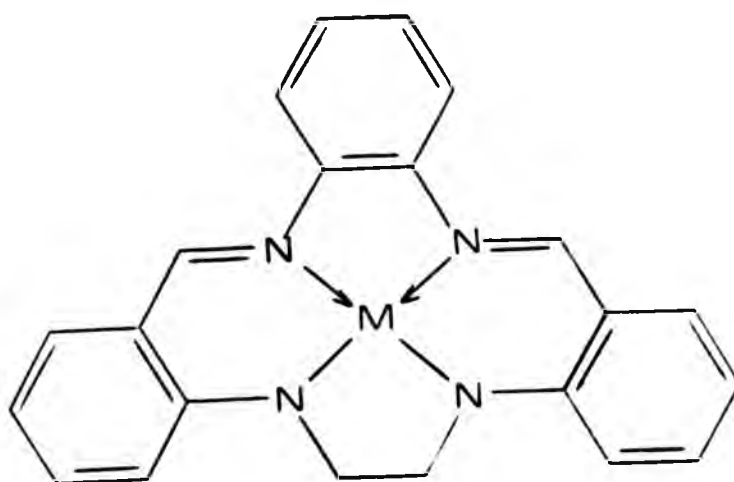
1. J. D. Goddard and T. Norris, Inorg. Nucl. Chem. Letts., 1978, 14, 211.
2. S. W. Hawkinson and E. B. Fleischer, Inorg. Chem., 1969, 8, 2402.
3. B. Kamenar, B. Kaitner, V. Katovic, and D. H. Busch, Inorg. Chem., 1979, 18, 815.
4. B. Kamenar and B. Kaitner, in "Structural Studies on Molecules of Biological Interest", Edts. G. Dodson, J. P. Glusker, and D. Sayre, Oxford University Press, 1981, p. 123.
5. M. J. S. Dewar, "Hyperconjugation", The Ronald Press Co., New York, 1962, ch. 3; M. J. S. Dewar and H. N. Schmeising, Tetrahedron, 1959, 5, 166; 1960, 11, 196.
6. F. A. Cotton and G. Wilkinson, "Advanced Inorganic Chemistry", 4th Edn. John Wiley Sons, New York, Chichester, Brisbane, Toronto, 1980, p. 14.

CHAPTER 6

STRUCTURAL INVESTIGATIONS OF METAL COMPLEXES OF LIGAND
OXIDISED TETRA-AZAMACROCYCLES

6.1 METHOD OF PREPARATION

During studies of 14-membered tetra-azamacrocyclic ligands and their metal complexes, R. Peters of this Department prepared several derivatives of (1) (Diagram 6.1).



a: M = Fe-OAc

b: M = Cu

c: M = Co

Diagram 6.1

When 1(a) was dissolved for recrystallization in dimethylformamide and held at 80 C° for 6 hours, the solution deposited black needles. X-ray crystallographic investigations of this compound, unexpectedly showed that the ethane bridge between the anilino nitrogen atoms had been oxygenated (forming an α, β -diketo group).¹ In certain cases related

Co(II), Ni(II) and Cu(II) complexes with trimethylene bridges have been observed² to undergo dehydrogenation in the presence of O₂, but oxygenation of the above type has not previously been reported.

The unexpected oxygenation of this iron compound had aroused interest within this Department. The copper complex of the same ligand underwent a similar oxygenation reaction,¹ when it was dissolved in dimethylformamide and held at 100 C° for 18 hours. The same compound was also obtained from ligands, in which the oxamido unit had been incorporated. An X-ray crystal structure investigation was carried out on the copper complex (section 6.2.2), which was prepared by R. Peters² by the second method.

In view of the interest in metal complexes of macrocyclic diketo derivatives it was thought to be desirable to determine the structure of the FREE LIGAND. A. Greenwood of this Department attempted to prepare it in the presence of zinc salts, and a crystal structure investigation was carried out by the author of this Thesis (section 6.2.3).

6.2 DATA COLLECTION AND STRUCTURE SOLUTION OF METAL COMPLEXES OF LIGAND OXIDISED TETRA-AZAMACROCYCLES

6.2.1 DATA COLLECTION AND STRUCTURE SOLUTION OF μ -OXO-BIS(17,18,19,20- TETRAHYDRO-18,19-DIOXOTRIBENZO[e,i,m][1,4,8,11]TETRA-AZACYCLO TETRADECINATO(2-)IRON(III)), FeDIKETO

Details of data collection and crystal data are summarized in Tables 6.1 and 6.2.

Data reduction applied to the raw data consisting of 2074 reflections, resulted in 1911 unique reflections with $I > 3\sigma(I)$. The following systematic absences were observed.

h00	N.C.	h0l	$l = 2n + 1$
001	N.C.	hk0	N.C.
0k0	$k = 2n + 1$	0kl	N.C.

Assuming that there are 4 molecules in the unit cell the density was calculated, $D_c = 1.428 \text{ g/cm}^3$. The measured density ($D_m = 1.400 \text{ g/cm}^3$) is not in agreement with the calculated one due to the solvent DMF, whose presence was found crystallographically later on.

From the above conditions the space group was unequivocally deduced as $P2_1/c$. The iron atoms were located using Patterson syntheses as explained below.

There are 4 equivalent positions in the space group $P2_1/c$. Hence there is one molecule at each of the equivalent positions and $1/4$ of the unit cell is the asymmetric unit. Two iron atoms in one molecule need to be located.

$P2_1/c$ equivalent positions

- 1) x, y, z
- 2) $-x, -y, -z$
- 3) $-x, 1/2+y, 1/2-z$

Details of data collection and crystal data are summarized in Tables 6.1 and 6.2.

Data reduction applied to the raw data consisting of 2074 reflections, resulted in 1911 unique reflections with $I > 3\sigma(I)$. The following systematic absences were observed.

h00	N.C.	h0l	$l = 2n + 1$
00l	N.C.	hk0	N.C.
0k0	$k = 2n + 1$	0kl	N.C.

Assuming that there are 4 molecules in the unit cell the density was calculated, $D_c = 1.428 \text{ g/cm}^3$. The measured density ($D_m = 1.400 \text{ g/cm}^3$) is not in agreement with the calculated one due to the solvent DMF, whose presence was found crystallographically later on.

From the above conditions the space group was unequivocally deduced as $P2_1/c$. The iron atoms were located using Patterson syntheses as explained below.

There are 4 equivalent positions in the space group $P2_1/c$. Hence there is one molecule at each of the equivalent positions and $1/4$ of the unit cell is the asymmetric unit. Two iron atoms in one molecule need to be located.

$P2_1/c$ equivalent positions

- 1) x, y, z
- 2) $-x, -y, -z$
- 3) $-x, 1/2+y, 1/2-z$

Table 6.1: Crystal data of ligand oxidised tetra-azamacrocyclic metal complexes and of a related free ligand

	FeDIKETO	CuDIKETO	FREE LIGAND
Formula	$\text{Fe}_2\text{C}_{44}\text{H}_{28}\text{N}_8\text{O}_5 + 2/3\text{DMF}$	$\text{CuC}_{22}\text{H}_{14}\text{N}_4\text{O}_2$	$\text{C}_{28}\text{H}_{22}\text{N}_6\text{O}_2$
Molecular weight	860.5+49	430	476
Crystal system	Monoclinic	Monoclinic	Orthorhombic
Space group	$P2_1/c$	$P2_1/n$	$Pca2_1$
a (Å)	10.819(3)	14.920(4)	23.076(7)
b (Å)	26.738(7)	15.918(3)	6.709(1)
c (Å)	14.910(4)	7.224(1)	15.036(3)
α (°)	90.00	90.00	90.00
β (°)	101.82(3)	95.03(3)	90.00
γ (°)	90.00	90.00	90.00
Volume (Å ³)	4221.7	1709.1	2327.8
D_c (g/cm ³)	1.430	1.668	1.357
D_m (g/cm ³)	1.477	1.631	1.327
Z	4	4	4
F(000)	1872	876	1000
$\mu(\text{Mo-K}\alpha)$ (cm ⁻¹)	6.92	12.60	0.52

Table 6.2: Data collection and structure solution of ligand oxidised
tetra-azamacrocyclic metal complexes and of a related
free ligand

	FeDIKETO	CuDIKETO	FREE LIGAND
Crystal size (mm)	0.16x0.22x0.24	0.32x0.25x0.14	0.12x0.22x0.31
Crystal colour	Black	Burgundy	Pale yellow
Shape	rod-like	cubic	platelets
BMO	1	2	1
SMO	2	2	1
Scan width (°)	0.82	0.80	1.20
θ -range (°)	3-30	3-30	3-30
Reflections meas.	1973	3407	2126
Unique data set	1912	3162	619
Least-squares parameters	341	301	141
Data/parameter	5.6	10.5	4.3
Shift/e.s.d.	0.3	0.05	
Weighting scheme	$1/[\sigma^2(F)+F^2]$	$1/[\sigma^2(F)+F^2]$	
Max. electron dens. residue $e/\text{\AA}^3$	0.52	0.62	
R	0.063	0.33	
R_w	0.062	0.33	

4) $x, 1/2-y, 1/2+z$ Patterson vectors for $P2_1/c$ Height

1) $\pm[2x$	$2y$	$2z]$	1
2) $\pm[2x$	$-1/2$	$-1/2+2z]$	2
3) $\pm[0$	$-1/2+2y$	$-1/2]$	2

Unique Patterson vectors for 2 equal heavy atoms for $P2_1/c$

1)	$2x_1$	$2y_1$	$2z_1$
2)	$2x_1$	$-1/2$	$-1/2+2z_1$
3)	0	$-1/2+2y_1$	$-1/2$
4)	$2x_2$	$2y_2$	$2z_2$
5)	$2x_2$	$-1/2$	$-1/2+2z_2$
6)	0	$-1/2+2y_2$	$-1/2$
7)	x_1-x_2	y_1-y_2	z_1-z_2
8)	x_1+x_2	y_1+y_2	z_1+z_2
9)	x_1+x_2	$y_1-y_2-1/2$	$z_1-1/2+z_2$
10)	x_1-x_2	$y_1+y_2-1/2$	$z_1-1/2-z_2$

First 10 peaks + 2 from the Patterson map

	U	V	W	Assignment		
1)	0.0	0.322	0.500	0	$1/2-2y_1$	$1/2$
				0	$1/2-2y_2$	$1/2$
2)	0.206	0.0	0.216	x_1-x_2	y_1-y_2	z_1-z_2
3)	0.386	0.500	0.062	x_1+x_2	$y_1-y_2-1/2$	$z_1+z_2-1/2$
4)	-0.206	0.322	0.286	x_2-x_1	$1/2-2y$	$1/2-z_1+z_2$
5)	-0.402	0.500	0.277	$2x_2$	$1/2$	$-1/2+2z_2$
6)	-0.177	0.500	0.154	$2x_1$	$1/2$	$-1/2+2z_1$
7)	-0.389	0.178	0.435	x_1+x_2	y_1+y_2	z_1+z_2
8)	0.361	0.0	0.143			
9)	0.383	0.051	0.137			

$$10) \quad -0.096 \quad 0.078 \quad 0.040$$

$$26) \quad 0.187 \quad 0.181 \quad 0.350 \quad 2x1 \quad 2y1 \quad 2z1$$

$$27) \quad 0.398 \quad 0.177 \quad 0.217 \quad 2x2 \quad 2y2 \quad 2z2$$

In the Patterson map there is only one peak, which corresponds to the two Patterson vectors.

$$3) \quad 0.0 \quad 0.322 \quad 0.500 \quad 0 \quad 1/2-2y1 \quad 1/2$$

$$\quad \quad \quad \quad \quad \quad \quad \quad 0 \quad 1/2-2y2 \quad 1/2$$

$$1/2-2y1 = 0.322$$

$$2y1 = 0.5-0.322$$

$$2y1 = 0.178$$

$$y1 = y2 = 0.089$$

$$2y = 0.178 \text{ could be either}$$

$$y1+y2 = 0.178 \text{ or } 2y1 = 0.178 \text{ or } 2y2 = 0.178$$

Since the $2x$, $2y$, $2z$ type of vector is half the height of the $x1+x2$, $y1+y2$, $z1+z2$ type of vector in the Patterson map, one expects to find 3 vectors with the same value: two of these of the same height, and the third one twice the height of the first two.

These three vectors are: one, as peak 7, whose height is 157, and the other two, further down in the list as peaks 26 and 27, whose heights are 75 and 74 respectively, which almost satisfy the required condition $75.2 = 150$, ~ 157 , and $74.2 = 148$, ~ 157 .

- 26) 0.187 0.181 0.350 2x 2y 2z type
 27) 0.398 0.177 0.217

Since there is only one peak, 0, 0.322, 0.500, where $0.322 = 1/2 - 2y$ or $0.322 = 1/2 - y_1 - y_2$, the 10th Patterson vector was assigned as peak 4 in the Patterson map.

- 10) -0.206 0.322 0.286 $x_1 - x_2$ $y_1 + y_2 - 1/2$ $z_1 - z_2 - 1/2$
 $x_2 - x_1$ $1/2 - 2y_2$ $1/2 - z_1 + z_2$

$$0.5 - z_1 + z_2 = 0.286$$

$$z_1 - z_2 = 0.5 - 0.286$$

$$= 0.214$$

Since $y_1 - y_2 = 0$ and $z_1 - z_2 = 0.214$, one can assign the Patterson vector 7) $x_1 - x_2$, $y_1 - y_2$, $z_1 - z_2$ as peak 2 in the Patterson map.

Therefore the assignments up this point are:

- | | | | | | | |
|----|--------|-------|-------|-------------|--------------|-------------------|
| A) | 0 | 0.322 | 0.500 | 0 | $1/2 - 2y_1$ | $1/2$ |
| | | | | 0 | $1/2 - 2y_2$ | $1/2$ |
| B) | -0.206 | 0.322 | 0.286 | $x_2 - x_1$ | $1/2 - 2y$ | $1/2 - z_1 + z_2$ |
| C) | 0.206 | 0.0 | 0.216 | $x_1 - x_2$ | $y_1 - y_2$ | $z_1 - z_2$ |
| D) | 0.187 | 0.181 | 0.350 | $2x_1$ | $2y_1$ | $2z_1$ |
| E) | 0.398 | 0.177 | 0.217 | $2x_2$ | $2y_2$ | $2z_2$ |
| F) | -0.389 | 0.178 | 0.435 | $x_1 + x_2$ | $y_1 + y_2$ | $z_1 + z_2$ |

$$C+F \text{ gives } 2x_1 \quad 2y_1 \quad 2z_1$$

$$C-F \text{ gives } 2x_2 \quad 2y_2 \quad 2z_2$$

Hence the former is assigned to D, the latter to E.

If C) 0.206 0.0 0.216 is kept unchanged 0.206 0.0 0.216
 and F) -0.389 0.178 0.435 becomes 0.611 0.178 0.435

Then C+F = 0.817 0.178 0.651 (2x1 2y1 2z1)
 and C-F = -0.405 -0.178 -0.219 (-2x2 -2y2 -2z2)

Hence the above vectors D and F should be given the following values;

D) 0.813 0.181 0.650 (2x1 2y1 2z1)
 F) 0.611 0.178 0.435 (x1+x2 y1+y2 z1+z2)

Therefore the co-ordinates of the iron atoms are

x1 = 0.407 x2 = 0.202
 y1 = 0.089 y2 = 0.089
 z1 = 0.325 z2 = 0.111

Using the phases calculated from the two iron atom positions deduced above, successive difference Fourier and full matrix least-squares refinement calculations led to the location of;

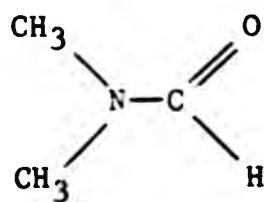
- 1) Initially 42 of the 57 non-hydrogen atoms.
- 2) After one further cycle the remaining non-hydrogen atoms and 9 of the 28 of the hydrogen atoms.

At this stage 4 more peaks appeared in the map which were too high to be assigned as hydrogen atoms. These new peaks were assumed to be carbon atoms. When these were refined as carbon atoms, the length of the presumed C-C bond became very short, and the U-values were inconsistent with the other U-values of carbon atoms in the molecule.

Hence the assignment of these 4 peaks was changed to oxygen atoms since the C=O distance is known to be rather short. At this stage in addition to the above 4 peaks, a further 4 new peaks were observed. These were, by contrast, not connected to the main molecule. One of these appeared to be not connected to any other atom. Hence it was assumed to be an oxygen atom. The other three atoms were connected to each other. Therefore at this stage of refinement there were two possible interpretations for these molecules trapped in the crystal lattice.

- 1) Water and Dimethylamine [H₂O + CH₃-NH-CH₃]
 or 2) Water and Ethanol [H₂O + H-O-CH₂-CH₃]

The former assumption was tested first and the highest of the three peaks was assigned as a nitrogen atom and the other two as carbon atoms. After further refinement some additional peaks appeared around the above ones, and one of these was high enough to be considered as a carbon atom. The oxygen atom which had appeared in the early stages of refinement to be unconnected to any other atom, was now seen to be connected to the small molecule trapped in the lattice. Hence this molecule seemed likely to be N,N'-dimethylformamide.



Successive refinement confirmed, that this was indeed the case with a site occupation factor of 0.67.

The iron atoms were refined with anisotropic thermal parameters. Blocked full matrix refinement was carried out during the final stages

of refinement, where the atoms were grouped as follows: group 1, one half of the dimer and the DMF molecule. Group 2, the other half of the dimer together with the bridging oxygen atom. The hydrogen atom co-ordinates were estimated geometrically (assuming C-H = 1.08 Å) and for refinement allowed to ride on their respective carbon atoms. The refinement was stopped when the calculated parameter shift/e.s.d. ratio fell to a maximum of 0.3. The final R value was 0.063 with $R_w = 0.062$. The final difference Fourier map showed the mean amplitudes of

$$0.52 > \Delta\rho > -0.40$$

The highest residual electron density of 0.52 e/Å³ was observed near the Fe(1) atom.

6.2.2 DATA COLLECTION AND STRUCTURE SOLUTION OF 17,18,19,20-
TETRAHYDRO-18,19-DIOXOTRIBENZO[e,i,m][1,4,8,11]TETRA-AZACYCLO
TETRADECINATO(2-)COPPER(II), CuDIKETO

Details of data collection and of the crystal data are summarized in Tables 6.1 and 6.2. Data reduction applied to the raw data consisting of 3407 reflections, resulted in 3162 unique reflections with $I > 3\sigma(I)$. The following systematic absences were observed:

h00	$h = 2n + 1$	h01	$h + 1 = 2n + 1$
001	$l = 2n + 1$	0k1	N.C.
0k0	$k = 2n + 1$	hk0	N.C.

Assuming that there are 4 molecules in the unit cell the density was calculated, $D_c = 1.668 \text{ g/cm}^3$. The measured density is $D_m = 1.631 \text{ g/cm}^3$,

and agrees well with the calculated one. From the above conditions the space group is uniquely deduced as $P2_1/n$. Since the space group $P2_1/n$ has 4 equivalent positions, there is one molecule in each of the equivalent positions and $1/4$ of the unit cell is the asymmetric unit.

To locate the copper atom the Patterson map was calculated:

$P2_1/n$ equivalent positions

1)	x	y	z
2)	-x	-y	-z
3)	-x+1/2	1/2+y	1/2-z
4)	x-1/2	1/2-y	1/2+z

Patterson vectors			height	
1)	$\pm(2x$	$2y$	$2z)$	1
2)	$\pm(2x-1/2$	$-1/2$	$2z-1/2)$	2
3)	$\pm(1/2$	$2y-1/2$	$1/2$	2

The asymmetric part of the unit cell contains 1 formula unit having 1 copper atom.

The first 3 Patterson peaks from the Patterson map are:

	U	V	W	height	assignment		
1)	0.500	0.362	0.500	344	1/2	2y-1/2	-1/2
2)	0.557	0.500	0.159	312	2x-1/2	-1/2	2z-1/2
3)	0.941	0.140	0.346	202	2x	2y	2z

From vector 1 $2y - 1/2 = 0.362$ $y = 0.431$
 vector 3 can be written as 0.059 0.860 0.654

From vector 3 $2y = 0.860$ $y = 0.430$
 $2x = 0.059$ $x = 0.030$
 $2z = 0.654$ $z = 0.327$

From vector 2 $2x - 1/2 = 0.557$ $x = 0.029$
 $2z - 1/2 = 0.159$ $z = 0.328$

Therefore the co-ordinates of the copper atom are:

$$\begin{aligned} x &= 0.030 \\ y &= 0.430 \\ z &= 0.328 \end{aligned}$$

Using phases calculated from the copper atom position deduced above, successive Fourier and full matrix least squares refinement calculations led to the location of:

- 1) Initially 28 of the 29 non-hydrogen atoms
- 2) After one further cycle, the last non-hydrogen atom and 13 of the 14 hydrogen atoms

All non-hydrogen atoms were refined with anisotropic thermal parameters and this gave the position of the last hydrogen atom. At this stage refinement converged at $R = 0.047$. Blocked full matrix refinement was carried out in further cycles, where the atoms were

From vector 1 $2y-1/2 = 0.362$ $y = 0.431$
 vector 3 can be written as 0.059 0.860 0.654

From vector 3 $2y = 0.860$ $y = 0.430$
 $2x = 0.059$ $x = 0.030$
 $2z = 0.654$ $z = 0.327$

From vector 2 $2x-1/2 = 0.557$ $x = 0.029$
 $2z-1/2 = 0.159$ $z = 0.328$

Therefore the co-ordinates of the copper atom are:

$$\begin{aligned} x &= 0.030 \\ y &= 0.430 \\ z &= 0.328 \end{aligned}$$

Using phases calculated from the copper atom position deduced above, successive Fourier and full matrix least squares refinement calculations led to the location of:

- 1) Initially 28 of the 29 non-hydrogen atoms
- 2) After one further cycle, the last non-hydrogen atom and 13 of the 14 hydrogen atoms

All non-hydrogen atoms were refined with anisotropic thermal parameters and this gave the position of the last hydrogen atom. At this stage refinement converged at $R = 0.047$. Blocked full matrix refinement was carried out in further cycles, where the atoms were

grouped as follows: Group 1 Cu and all the non-hydrogen atoms in one half of the molecule, group 2 the non-hydrogen atoms of the other half of the molecule, group 3 all the hydrogen atoms. There was no constraint on the hydrogen atoms. They were refined with isotropic temperature factors. The refinement was stopped when the calculated parameter shift/e.s.d. ratio fell to a maximum of 0.05.

The final R-value was 0.033 ($R_w = 0.033$). The final difference Fourier map showed the mean amplitude of

$$0.62 > \Delta\rho > -0.61 \text{ e/\AA}^3.$$

The highest residual electron density of 0.62 e/\AA^3 was observed near the Cu atom.

6.2.3 DATA COLLECTION AND STRUCTURE SOLUTION OF FREE LIGAND

Details of data collection and available crystal data are summarised in Tables 6.1 and 6.2. Data reduction applied to 2126 reflections resulted in 619 unique reflections with $I > 3\sigma(I)$. The following systematic absences were observed.

h00	$h = 2n + 1$	hk0	N.C.
0k0	N.C.	h0l	$h = 2n + 1$
00l	$l = 2n + 1$	0kl	$l = 2n + 1$

Assuming that there are four molecules in the unit cell, the density was calculated, $D_c = 1.357 \text{ g/cm}^3$. The measured density, $D_m = 1.327$

g/cm^3 . From the above conditions two space groups are possible: $\text{Pca}2_1$ and Pbcm (when h and k are interchanged). The centric space group Pbcm , when a centrosymmetric direct method is applied, gave no solution. Examination of the convergence (path ways of the all triplet relationships) showed that for the $\text{Pca}2_1$ space group, data $hk0$ was restricted in phase to 0 and 180 . Using the SHELX centrosymmetric direct method (Chapter 2) only with $hk0$ data, the phase permutations for 14 reflections on $E\text{-value} \geq 0.75$ for the solutions of highest combined figure of merit were then passed onto the tangent noncentric direct method procedure. These fixed phases together with one origin, one enantiomorph, and two multisolutions were included into the tangent map. This map using $E\text{-values} \geq 1.15$ showed that the 18th map ranked in order of $R_0\text{-values}$ gave a recognisable solution. All the non-hydrogen atoms (32) were located. 8 Cycles of least squares refinement and difference Fourier calculations gave $R = 0.12$. When all the non-hydrogen atoms were refined with anisotropic thermal parameters 10 cycles of Fourier difference and least squares refinement calculations gave $R = 0.07$. The bond lengths and angles were very unreasonable and very high correlations were observed. Further attempts to solve the structure in the centric space group were unsuccessful and the structure solution was abandoned at this stage.

6.3 DISCUSSION

6.3.1 FeDIKETO

The compound FeDIKETO, has the structure shown in Figure 6.1, which also gives the numbering scheme used for this molecule together with the averaged important bond lengths and angles. The complete data for bond lengths and angles are given in Tables 6.3 and 6.4. The ORTEP drawings for this structure are in Drawing 6.1. A preliminary report on this structure has been published.¹

The two halves of the molecule have closely similar structures. The iron atoms Fe(1) and Fe(2) have approximately square pyramidal co-ordination geometries (lying 0.64 and 0.65 Å respectively above the mean planes of the N₄ donor sets) and are significantly closer to the oxamido nitrogen atoms [1.994(7) Å] than to the o-phenylene nitrogen atoms [2.085(7) Å]. The distance between the two iron atoms is 3.469(3) Å. The oxamido groups are inclined at 27° and 26° to the N₄ co-ordination planes about Fe(1) and Fe(2) respectively, and the iron atoms lie very close to the planes of the oxamido groups.

Most of the atoms in the 14-membered inner great ring lie close to the N₄ co-ordination plane. The exceptions are the two carbon atoms of the o-phenylene group, which are close (0.05 Å) to the N₄ plane in the macrocycle containing Fe(1), but are appreciably below it (0.24 Å) in the other. There are other, smaller, differences in conformation between the two macrocycles, which may be attributed to packing constraints imposed by the solvent molecule. The angle and bond lengths in the μ-oxo-bridge [151(1)° and 1.777(8) and 1.758(9) Å] fall centrally within the range of values (139-175° and 1.76-1.79 Å) observed in related 5-co-ordinate FeIII complexes (see chapter 8).

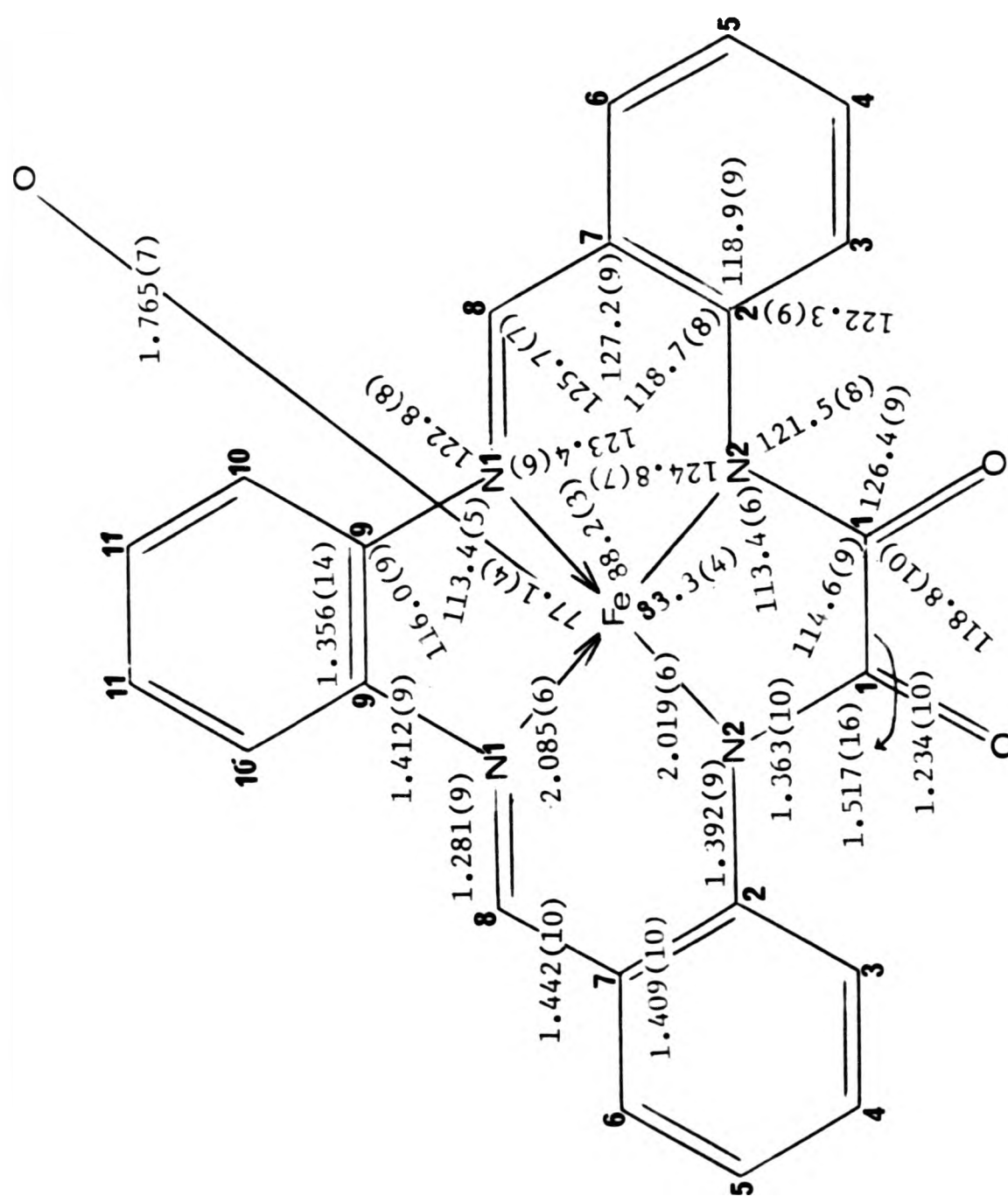


Figure 6.1

Table 6.3 Bond lengths (Å) for FeDIKETO

Fe(1) -Fe(2)	3.469(3)	Fe(1) -O(2)	1.767(10)
Fe(1) -N(2b)	1.987(14)	Fe(1) -N(2a)	2.008(13)
Fe(1) -N(1a)	2.058(14)	Fe(1) -N(1b)	2.116(12)
Fe(2) -O(2)	1.764(10)	Fe(2) -N(2d)	1.994(13)
Fe(2) -N(2c)	2.007(12)	Fe(2) -N(1c)	2.097(12)
Fe(2) -N(1d)	2.069(13)	N(2b) -C(2b)	1.420(20)
N(2b) -C(1b)	1.371(21)	N(2a) -C(1a)	1.367(22)
N(2a) -C(2a)	1.371(19)	N(1a) -C(8a)	1.257(18)
N(1a) -C(9a)	1.419(17)	N(1b) -C(9b)	1.395(18)
N(1b) -C(8b)	1.317(18)	N(2d) -C(2d)	1.360(18)
N(2d) -C(1d)	1.342(19)	N(2c) -C(1c)	1.372(19)
N(2c) -C(2c)	1.417(18)	N(1c) -C(8c)	1.277(18)
N(1c) -C(9c)	1.421(17)	N(1d) -C(9d)	1.415(18)
N(1d) -C(8d)	1.274(17)	C(1a) -C(1b)	1.516(24)
C(1a) -O(1a)	1.256(21)	C(2a) -C(3a)	1.446(21)
C(2a) -C(7a)	1.384(21)	C(3a) -C(4a)	1.368(20)
C(4a) -C(5a)	1.313(22)	C(5a) -C(6a)	1.425(22)
C(6a) -C(7a)	1.460(21)	C(7a) -C(8a)	1.457(21)
C(9a) -C(10a)	1.422(20)	C(9a) -C(9b)	1.356(19)
C(10a) -C(11a)	1.402(21)	C(11a) -C(11b)	1.399(21)
C(11b) -C(10b)	1.340(21)	C(10b) -C(9b)	1.413(20)
C(8b) -C(7b)	1.408(21)	C(7b) -C(6b)	1.449(22)
C(7b) -C(2b)	1.426(22)	C(6b) -C(5b)	1.404(23)
C(5b) -C(4b)	1.312(23)	C(4b) -C(3b)	1.390(23)
C(3b) -C(2b)	1.399(23)	C(1b) -O(1b)	1.220(20)

Table 6.3 continued

C(1c) -C(1d)	1.519(21)	C(1c) -O(1c)	1.210(18)
C(2c) -C(3c)	1.394(19)	C(2c) -C(7c)	1.417(20)
C(3c) -C(4c)	1.425(21)	C(4c) -C(5c)	1.375(20)
C(5c) -C(6c)	1.393(21)	C(6c) -C(7c)	1.419(21)
C(7c) -C(8c)	1.452(20)	C(9c) -C(10c)	1.402(19)
C(9c) -C(9d)	1.357(20)	C(10c)-C(11c)	1.403(20)
C(11c)-C(11d)	1.377(21)	C(11d)-C(10d)	1.384(20)
C(10d)-C(9d)	1.424(20)	C(8d) -C(7d)	1.453(20)
C(7d) -C(6d)	1.452(21)	C(7d) -C(2d)	1.411(20)
C(6d) -C(5d)	1.414(22)	C(5d) -C(4d)	1.411(23)
C(4d) -C(3d)	1.375(22)	C(3d) -C(2d)	1.409(20)
C(1d) -O(1d)	1.250(18)	O -C(3)	1.14(3)
N -C(1)	1.38(3)	N -C(2)	1.37(3)
N -C(3)	1.26(3)		

Table 6.4: Bond angles ($^{\circ}$) for FeDIKETO

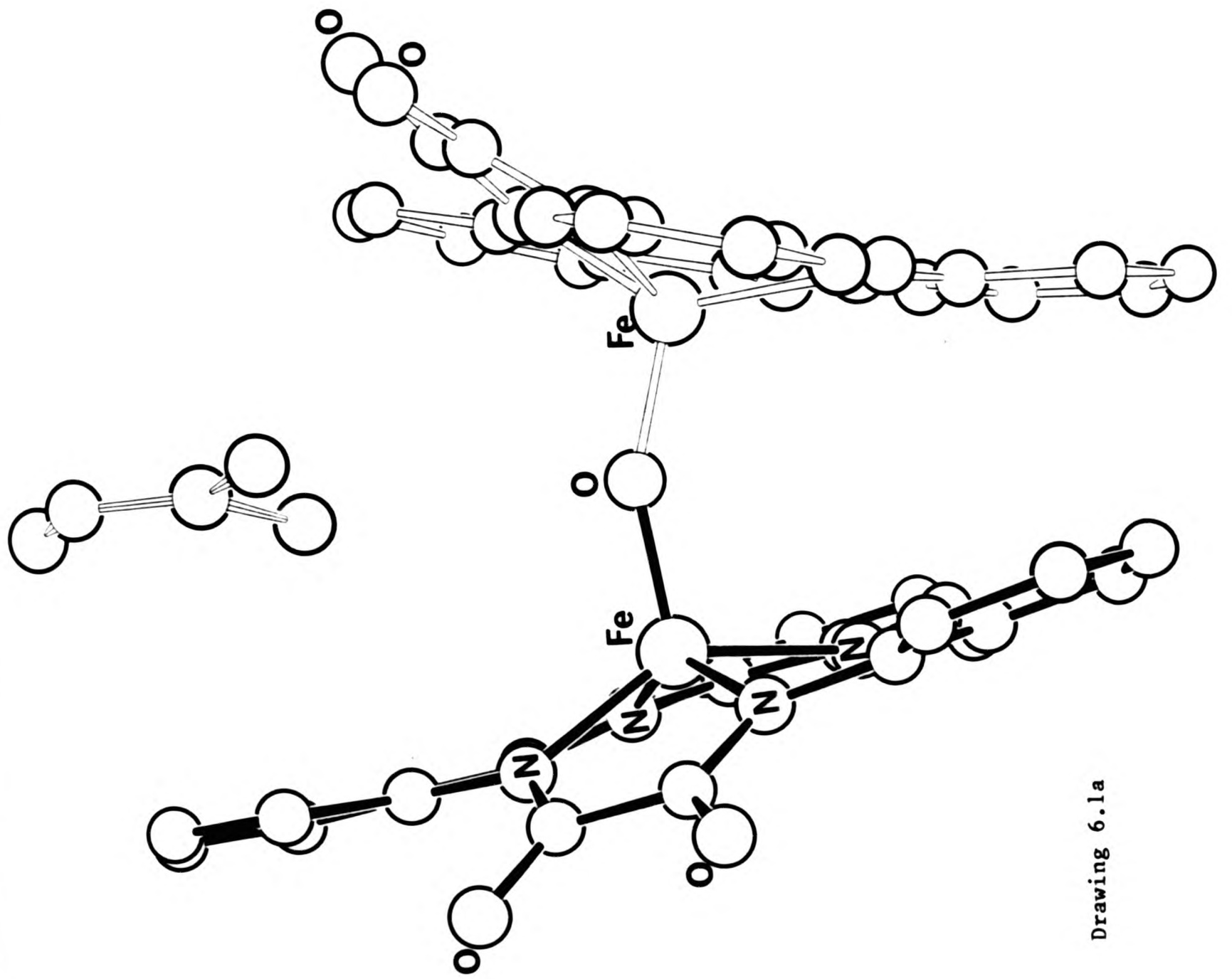
O(2) -Fe(1) -Fe(2)	11.5(3)	N(2b) -Fe(1) -Fe(2)	105.5(4)
N(2b) -Fe(1) -O(2)	110.4(5)	N(2a) -Fe(1) -Fe(2)	126.7(4)
N(2a) -Fe(1) -O(2)	116.1(5)	N(2a) -Fe(1) -N(2b)	83.1(6)
N(1a) -Fe(1) -Fe(2)	107.9(4)	N(1a) -Fe(1) -O(2)	105.0(5)
N(1a) -Fe(1) -N(2b)	143.8(5)	N(1a) -Fe(1) -N(2a)	88.2(5)
N(1b) -Fe(1) -Fe(2)	90.0(3)	N(1b) -Fe(1) -O(2)	100.3(4)
N(1b) -Fe(1) -N(2b)	89.6(6)	N(1b) -Fe(1) -N(2a)	143.2(5)
N(1b) -Fe(1) -N(1a)	76.7(5)	O(2) -Fe(2) -Fe(1)	11.5(3)
N(2d) -Fe(2) -Fe(1)	114.9(4)	N(2d) -Fe(2) -O(2)	109.6(5)
N(2c) -Fe(2) -Fe(1)	120.6(4)	N(2c) -Fe(2) -O(2)	110.8(5)
N(2c) -Fe(2) -N(2d)	83.6(5)	N(1c) -Fe(2) -Fe(1)	99.5(3)
N(1c) -Fe(2) -O(2)	106.0(5)	N(1c) -Fe(2) -N(2d)	144.2(5)
N(1c) -Fe(2) -N(2c)	87.5(5)	N(1d) -Fe(2) -Fe(1)	97.8(4)
N(1d) -Fe(2) -O(2)	108.2(5)	N(1d) -Fe(2) -N(2d)	87.7(5)
N(1d) -Fe(2) -N(2c)	140.7(5)	N(1d) -Fe(2) -N(1c)	77.5(5)
Fe(2) -O(2) -Fe(1)	157.0(6)	C(2b) -N(2b) -Fe(1)	124(1)
C(1b) -N(2b) -Fe(1)	115(1)	C(1b) -N(2b) -C(2b)	121(2)
C(1a) -N(2a) -Fe(1)	113(1)	C(2a) -N(2a) -Fe(1)	125(1)
C(2a) -N(2a) -C(1a)	122(1)	C(8a) -N(1a) -Fe(1)	123(1)
C(9a) -N(1a) -Fe(1)	113(1)	C(9a) -N(1a) -C(8a)	123(2)
C(9b) -N(1b) -Fe(1)	112(1)	C(8b) -N(1b) -Fe(1)	123(1)
C(8b) -N(1b) -C(9b)	124(1)	C(2d) -N(2d) -Fe(2)	125(1)
C(1d) -N(2d) -Fe(2)	112(1)	C(1d) -N(2d) -C(2d)	123(2)
C(1c) -N(2c) -Fe(2)	114(1)	C(2c) -N(2c) -Fe(2)	126(1)
C(2c) -N(2c) -C(1c)	120(1)	C(8c) -N(1c) -Fe(2)	123(1)

Table 6.4: continued

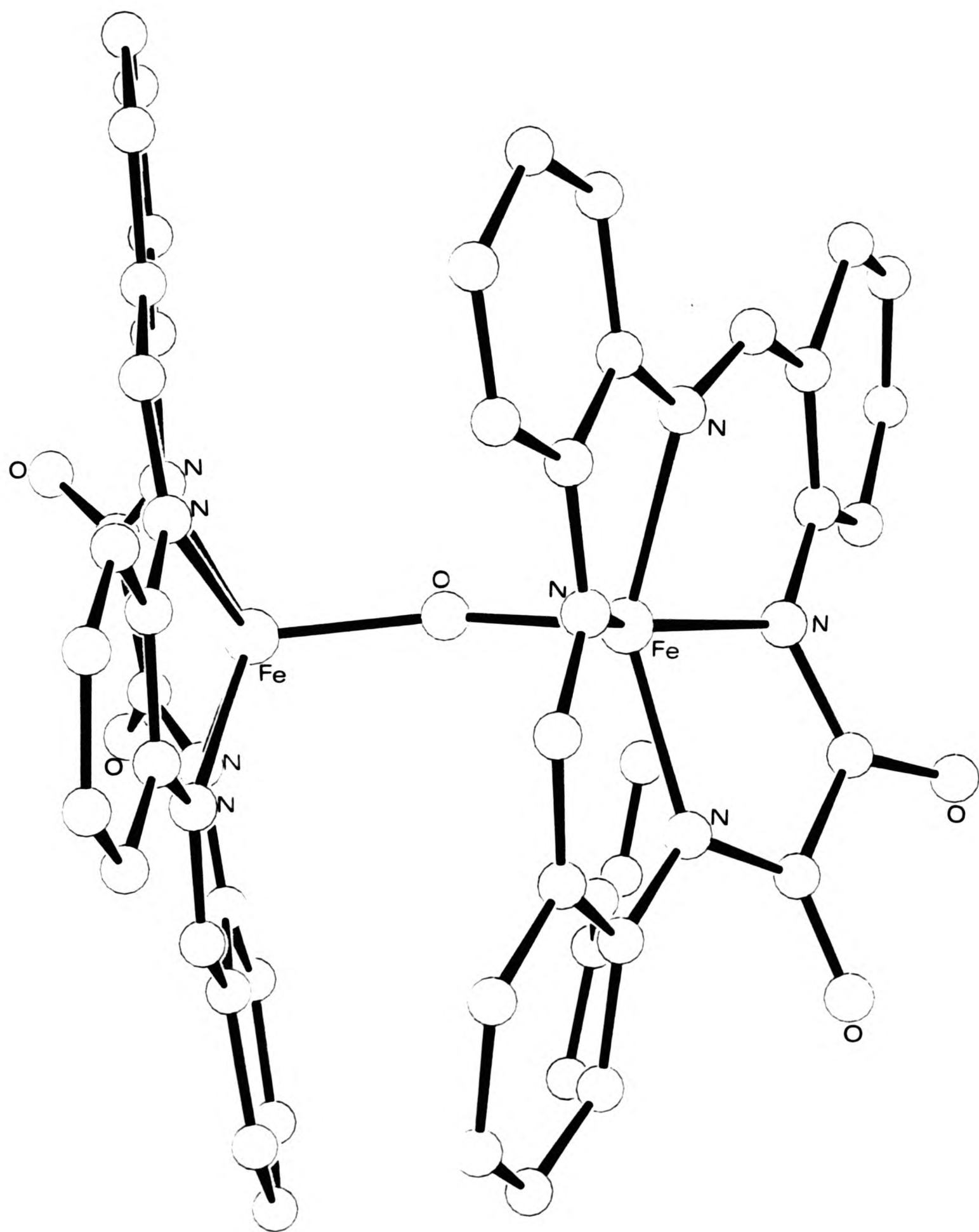
C(9c) -N(1c) -Fe(2)	113(1)	C(9c) -N(1c) -C(8c)	124(1)
C(9d) -N(1d) -Fe(2)	115(1)	C(8d) -N(1d) -Fe(2)	125(1)
C(8d) -N(1d) -C(9d)	120(1)	C(1b) -C(1a) -N(2a)	115(2)
O(1a) -C(1a) -N(2a)	126(2)	O(1a) -C(1a) -C(1b)	118(2)
C(3a) -C(2a) -N(2a)	122(2)	C(7a) -C(2a) -N(2a)	120(2)
C(7a) -C(2a) -C(3a)	118(2)	C(4a) -C(3a) -C(2a)	118(2)
C(5a) -C(4a) -C(3a)	125(2)	C(6a) -C(5a) -C(4a)	121(2)
C(7a) -C(6a) -C(5a)	115(2)	C(6a) -C(7a) -C(2a)	123(2)
C(8a) -C(7a) -C(2a)	124(2)	C(8a) -C(7a) -C(6a)	113(2)
C(7a) -C(8a) -N(1a)	129(2)	C(10a) -C(9a) -N(1a)	123(2)
C(9b) -C(9a) -N(1a)	116(1)	C(9b) -C(9a) -C(10a)	121(2)
C(11a) -C(10a) -C(9a)	117(2)	C(11b) -C(11a) -C(10a)	119(2)
C(10b) -C(11b) -C(11a)	124(2)	C(9b) -C(10b) -C(11b)	117(2)
C(9a) -C(9b) -N(1b)	116(1)	C(10b) -C(9b) -N(1b)	123(2)
C(10b) -C(9b) -C(9a)	121(2)	C(7b) -C(8b) -N(1b)	124(2)
C(6b) -C(7b) -C(8b)	113(2)	C(2b) -C(7b) -C(8b)	131(2)
C(2b) -C(7b) -C(6b)	115(2)	C(5b) -C(6b) -C(7b)	120(2)
C(4b) -C(5b) -C(6b)	122(2)	C(3b) -C(4b) -C(5b)	121(2)
C(2b) -C(3b) -C(4b)	120(2)	C(7b) -C(2b) -N(2b)	117(2)
C(3b) -C(2b) -N(2b)	122(2)	C(3b) -C(2b) -C(7b)	121(2)
C(1a) -C(1b) -N(2b)	113(2)	O(1b) -C(1b) -N(2b)	126(2)
O(1b) -C(1b) -C(1a)	121(2)	C(1d) -C(1c) -N(2c)	112(2)
O(1c) -C(1c) -N(2c)	127(2)	O(1c) -C(1c) -C(1d)	120(2)
C(3c) -C(2c) -N(2c)	121(2)	C(7c) -C(2c) -N(2c)	119(2)
C(7c) -C(2c) -C(3c)	120(2)	C(4c) -C(3c) -C(2c)	119(2)
C(5c) -C(4c) -C(3c)	121(2)	C(6c) -C(5c) -C(4c)	121(2)
C(7c) -C(6c) -C(5c)	119(2)	C(6c) -C(7c) -C(2c)	120(2)
C(8c) -C(7c) -C(2c)	126(2)	C(8c) -C(7c) -C(6c)	114(2)

Table 6.4: continued

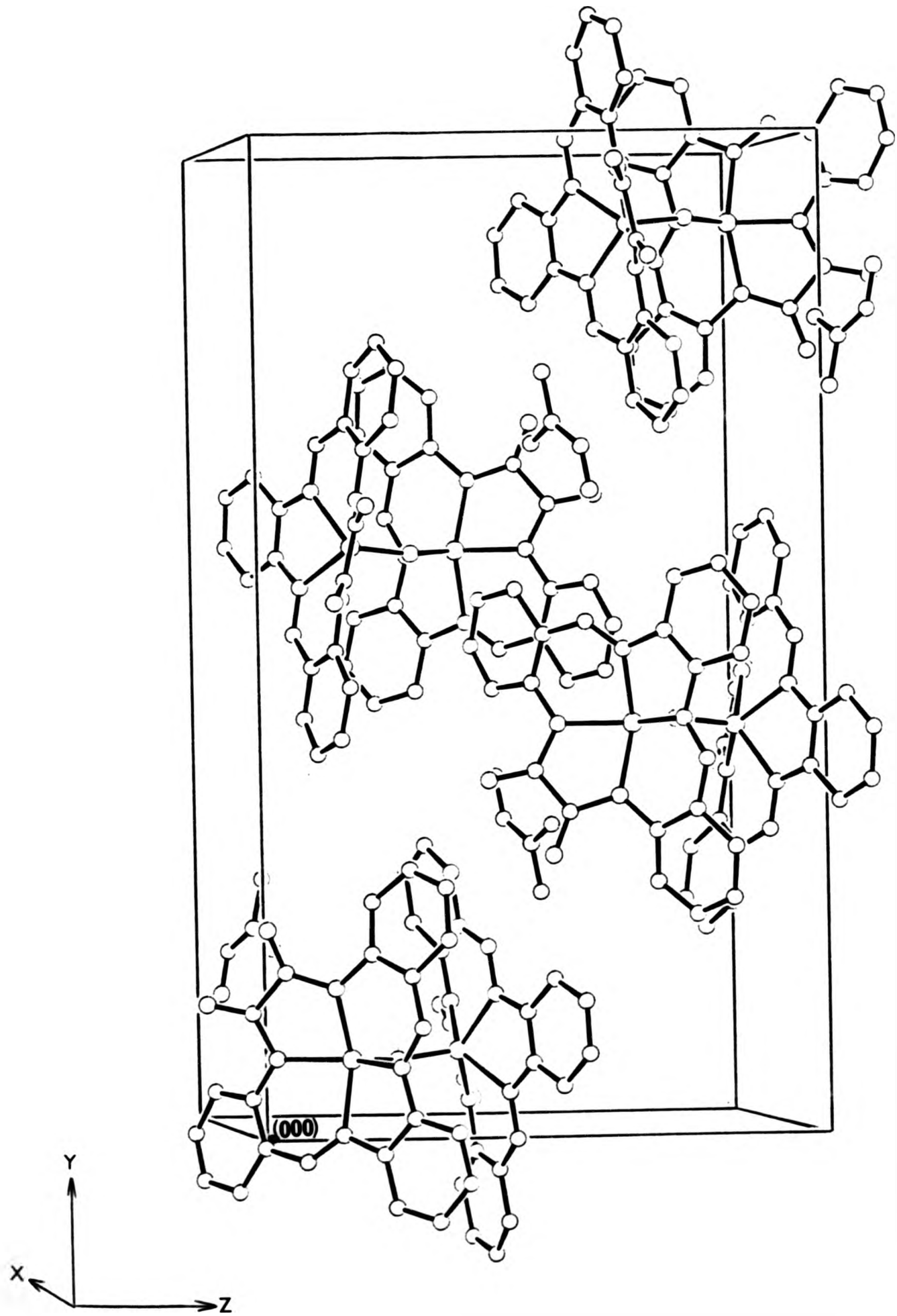
C(7c) -C(8c) -N(1c)	127(2)	C(10c)-C(9c) -N(1c)	122(1)
C(9d) -C(9c) -N(1c)	116(1)	C(9d) -C(9c) -C(10c)	121(2)
C(11c)-C(10c)-C(9c)	118(2)	C(11d)-C(11c)-C(10c)	121(2)
C(10d)-C(11d)-C(11c)	120(2)	C(9d) -C(10d)-C(11d)	119(2)
C(9c) -C(9d) -N(1d)	116(1)	C(10d)-C(9d) -N(1d)	124(1)
C(10d)-C(9d) -C(9c)	120(2)	C(7d) -C(8d) -N(1d)	123(2)
C(6d) -C(7d) -C(8d)	111(2)	C(2d) -C(7d) -C(8d)	128(2)
C(2d) -C(7d) -C(6d)	121(2)	C(5d) -C(6d) -C(7d)	119(2)
C(4d) -C(5d) -C(6d)	119(2)	C(3d) -C(4d) -C(5d)	121(2)
C(2d) -C(3d) -C(4d)	123(2)	C(7d) -C(2d) -N(2d)	119(2)
C(3d) -C(2d) -N(2d)	124(2)	C(3d) -C(2d) -C(7d)	117(2)
C(1c) -C(1d) -N(2d)	118(2)	O(1d) -C(1d) -N(2d)	127(2)
O(1d) -C(1d) -C(1c)	115(2)	C(2) -N -C(1)	111(2)
C(3) -N -C(1)	125(3)	C(3) -N -C(2)	123(3)
N -C(3) -O	125(4)		



Drawing 6.1a



Drawing 6.1b



Drawing 6.1c

μ -oxo-bridged iron compounds will be discussed later together with the brominated iron(salen) derivative (see chapter 8).

6.3.2 CuDIKETO

The CuDIKETO has the structure shown in Figure 6.2, which also gives the numbering scheme together with the important averaged bond lengths and angles. The bond length and angle data for the complete structure are in Tables 6.5 and 6.6. The ORTEP drawings are in Drawing 6.2.

The copper atom is 4-co-ordinate and located 0.02 \AA below the best plane of the four nitrogen atoms. The nitrogen atoms are located on that plane. The copper atom has a square planar co-ordination. The rings incorporating the copper atom are 6-,5-,6-,5-membered. This arrangement favours a square planar structure (see section 1.2.4). The plane of the diketo group is tilted 13 degrees from the CuN_4 plane.

The whole molecule, except for the diketo group, is almost planar with $+0.1 \text{ \AA}$ deviations of the C(4b), C(3b), C(10b) and C(11b) atoms from the co-ordination plane. The carbon and oxygen atoms of the two keto groups are $0.2, 0.2$ and $0.4, 0.5 \text{ \AA}$ respectively above that plane.

The average copper-imine nitrogen bond length $\text{Cu-N}(1) = 1.946(1) \text{ \AA}$ is equal to the average copper-anilino nitrogen bond length $\text{Cu-N}(2) = 1.941(1) \text{ \AA}$. In $\text{Cu}(\text{TAABH}_2)$ (section 5.2) the copper-imine nitrogen bonds are longer than the copper-anilino nitrogen bonds, for reasons outlined there. In the present structure electron density on the anilino nitrogen atoms is syphoned off by the electron-withdrawing

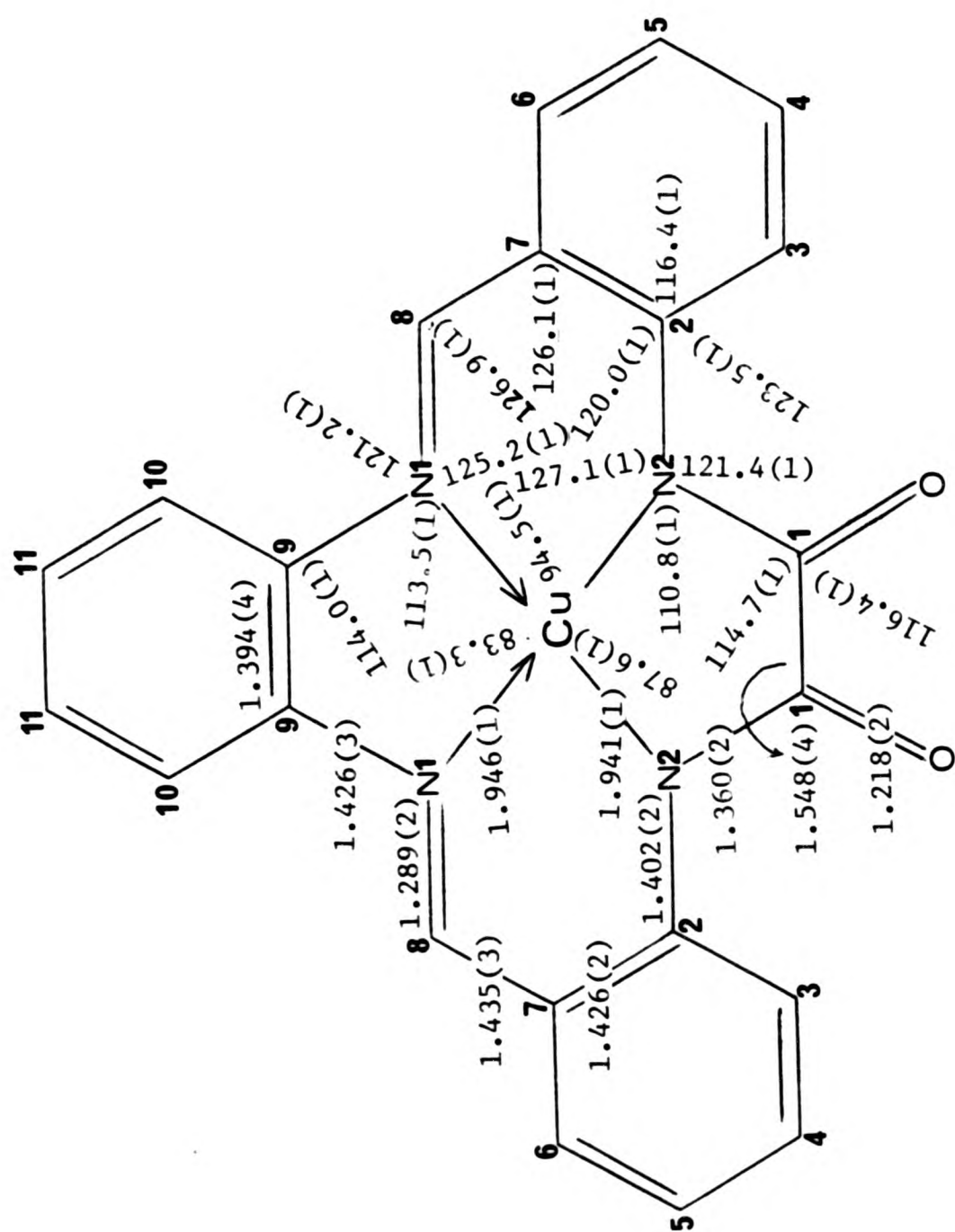


Figure 6.2

Table 6.5 Bond lengths (Å) for CuDIKETO

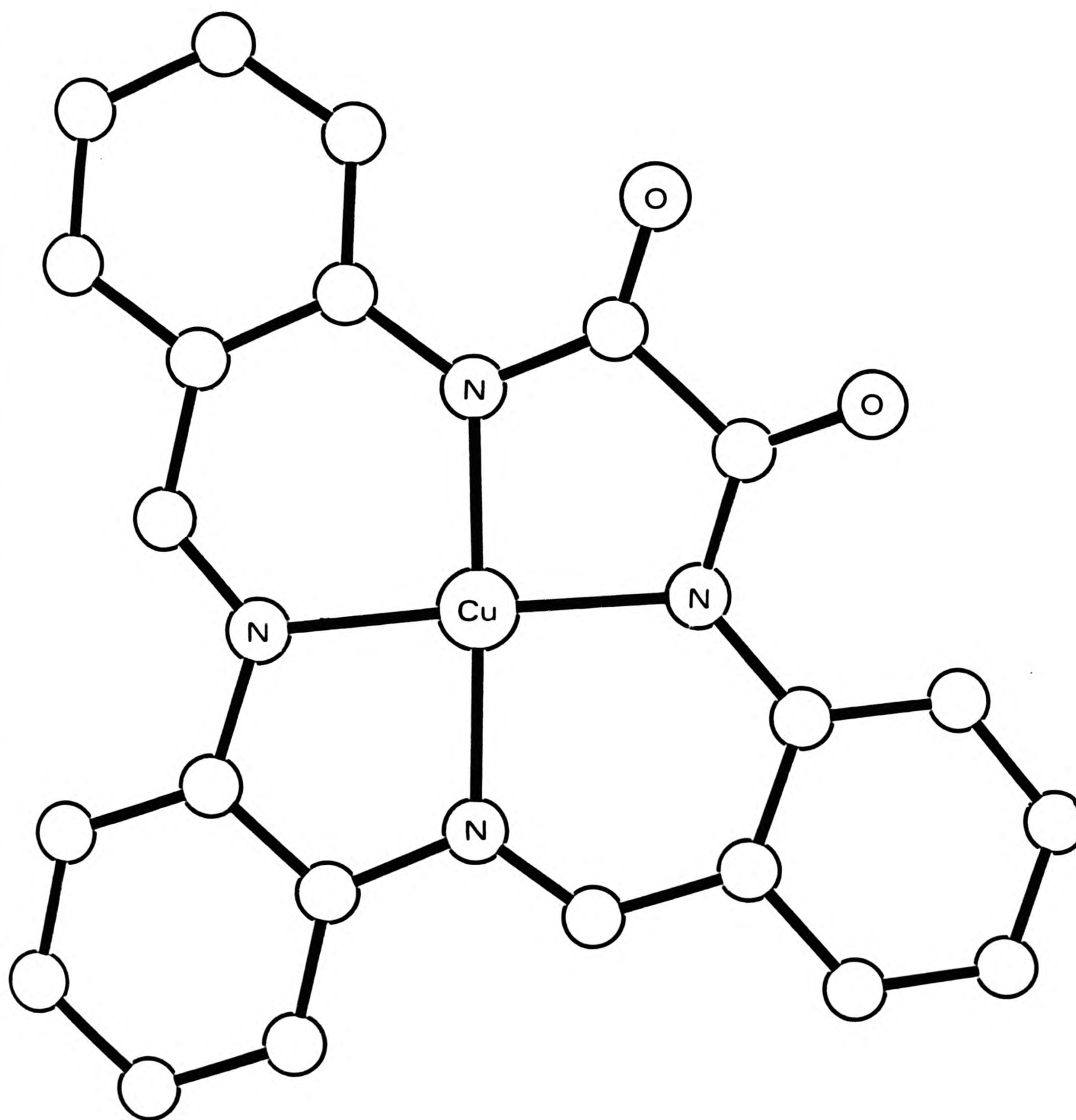
Cu	-N(2a)	1.947(2)	Cu	-N(1a)	1.947(2)
Cu	-N(2b)	1.936(2)	Cu	-N(1b)	1.946(2)
N(2a)	-C(1a)	1.363(3)	N(2a)	-C(2a)	1.401(3)
N(1a)	-C(8a)	1.286(3)	N(1a)	-C(9a)	1.429(3)
N(2b)	-C(2b)	1.404(3)	N(2b)	-C(1b)	1.358(3)
N(1b)	-C(9b)	1.423(3)	N(1b)	-C(8b)	1.292(3)
O(1a)	-C(1a)	1.215(3)	O(1b)	-C(1b)	1.222(3)
C(1a)	-C(1b)	1.548(4)	C(2a)	-C(3a)	1.405(4)
C(2a)	-C(7a)	1.427(4)	C(3a)	-C(4a)	1.387(4)
C(4a)	-C(5a)	1.377(5)	C(5a)	-C(6a)	1.357(4)
C(6a)	-C(7a)	1.410(4)	C(7a)	-C(8a)	1.439(4)
C(9a)	-C(10a)	1.392(4)	C(9a)	-C(9b)	1.394(4)
C(10a)	-C(11a)	1.375(5)	C(11a)	-C(11b)	1.371(5)
C(11b)	-C(10b)	1.362(4)	C(10b)	-C(9b)	1.391(4)
C(8b)	-C(7b)	1.432(3)	C(7b)	-C(6b)	1.414(4)
C(7b)	-C(2b)	1.426(3)	C(6b)	-C(5b)	1.360(4)
C(5b)	-C(4b)	1.389(5)	C(4b)	-C(3b)	1.372(4)
C(3b)	-C(2b)	1.404(4)			

Table 6.6 Bond angles ($^{\circ}$) for CuDIKETO

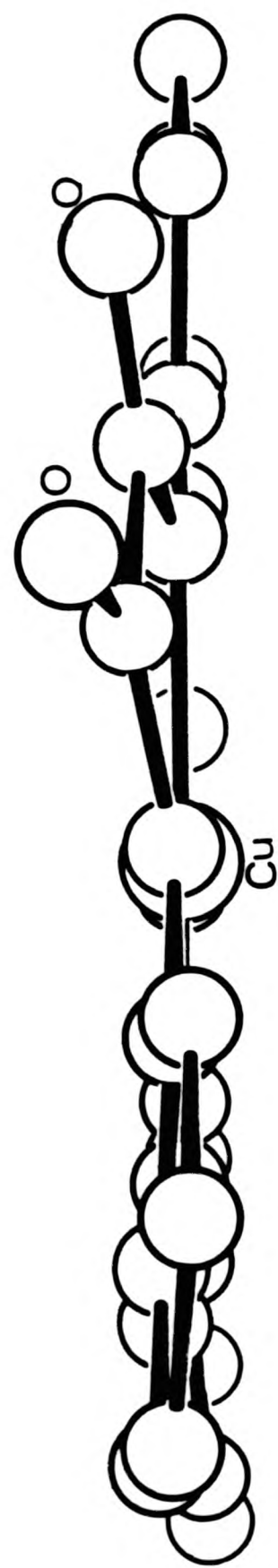
N(1a) -Cu -N(2a)	94.6(1)	N(2b) -Cu -N(2a)	87.6(1)
N(2b) -Cu -N(1a)	177.5(1)	N(1b) -Cu -N(2a)	177.6(1)
N(1b) -Cu -N(1a)	83.3(1)	N(1b) -Cu -N(2b)	94.4(1)
C(1a) -N(2a) -Cu	110.9(2)		
C(2a) -N(2a) -Cu	127.2(2)	C(2a) -N(2a) -C(1a)	121.3(2)
C(8a) -N(1a) -Cu	125.0(2)	C(9a) -N(1a) -Cu	113.4(2)
C(9a) -N(1a) -C(8a)	121.6(2)	C(2b) -N(2b) -Cu	127.0(2)
C(1b) -N(2b) -Cu	110.7(2)	C(1b) -N(2b) -C(2b)	121.5(2)
C(9b) -N(1b) -Cu	113.7(2)	C(8b) -N(1b) -Cu	125.4(2)
C(8b) -N(1b) -C(9b)	120.8(2)		
O(1a) -C(1a) -Cu	169.7(2)	O(1a) -C(1a) -N(2a)	129.3(3)
C(1b) -C(1a) -Cu	73.0(1)	C(1b) -C(1a) -N(2a)	114.4(2)
C(1b) -C(1a) -O(1a)	116.3(2)	C(3a) -C(2a) -N(2a)	123.7(2)
C(7a) -C(2a) -N(2a)	119.8(2)	C(7a) -C(2a) -C(3a)	116.5(2)
C(4a) -C(3a) -C(2a)	121.8(3)	C(5a) -C(4a) -C(3a)	121.0(3)
C(6a) -C(5a) -C(4a)	118.8(3)	C(7a) -C(6a) -C(5a)	122.4(3)
C(6a) -C(7a) -C(2a)	119.3(3)	C(8a) -C(7a) -C(2a)	126.3(2)
C(8a) -C(7a) -C(6a)	114.4(3)	C(7a) -C(8a) -N(1a)	127.2(2)
C(10a) -C(9a) -N(1a)	125.7(3)	C(9b) -C(9a) -N(1a)	114.8(2)
C(9b) -C(9a) -C(10a)	119.6(2)	C(11a) -C(10a) -C(9a)	118.9(3)
C(11b) -C(11a) -C(10a)	121.5(3)	C(10b) -C(11b) -C(11a)	120.0(3)

table 6.6 continued

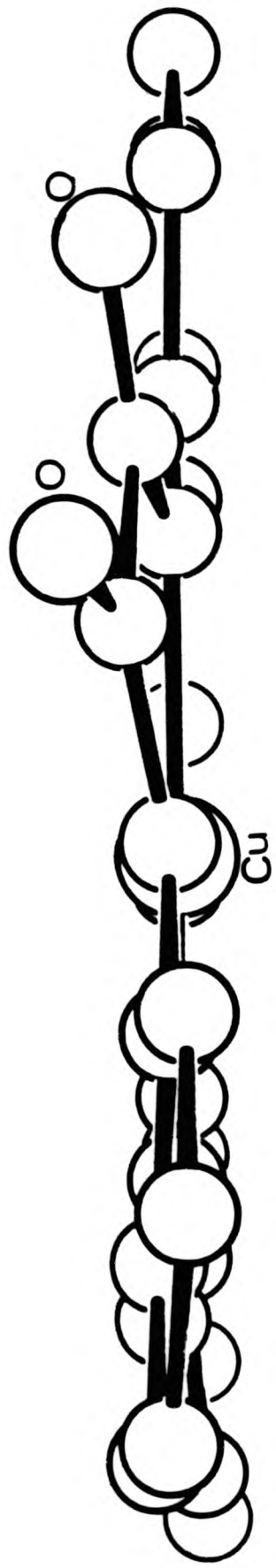
C(9b) -C(10b)-C(11b)	120.1(3)	C(9a) -C(9b) -N(1b)	114.7(2)
C(10b)-C(9b) -N(1b)	125.5(2)	C(10b)-C(9b) -C(9a)	119.8(2)
C(7b) -C(8b) -N(1b)	126.6(2)	C(6b) -C(7b) -C(8b)	114.3(2)
C(2b) -C(7b) -C(8b)	126.0(2)	C(2b) -C(7b) -C(6b)	119.6(2)
C(5b) -C(6b) -C(7b)	122.2(3)	C(4b) -C(5b) -C(6b)	118.3(3)
C(3b) -C(4b) -C(5b)	121.3(3)	C(2b) -C(3b) -C(4b)	122.3(3)
C(7b) -C(2b) -N(2b)	120.3(2)	C(3b) -C(2b) -N(2b)	123.4(2)
C(3b) -C(2b) -C(7b)	116.3(2)	N(2b) -C(1b) -Cu	41.6(1)
O(1b) -C(1b) -Cu	165.7(2)	O(1b) -C(1b) -N(2b)	128.2(3)
C(1a) -C(1b) -Cu	74.1(1)	C(1a) -C(1b) -N(2b)	115.1(2)
C(1a) -C(1b) -O(1b)	116.6(2)		



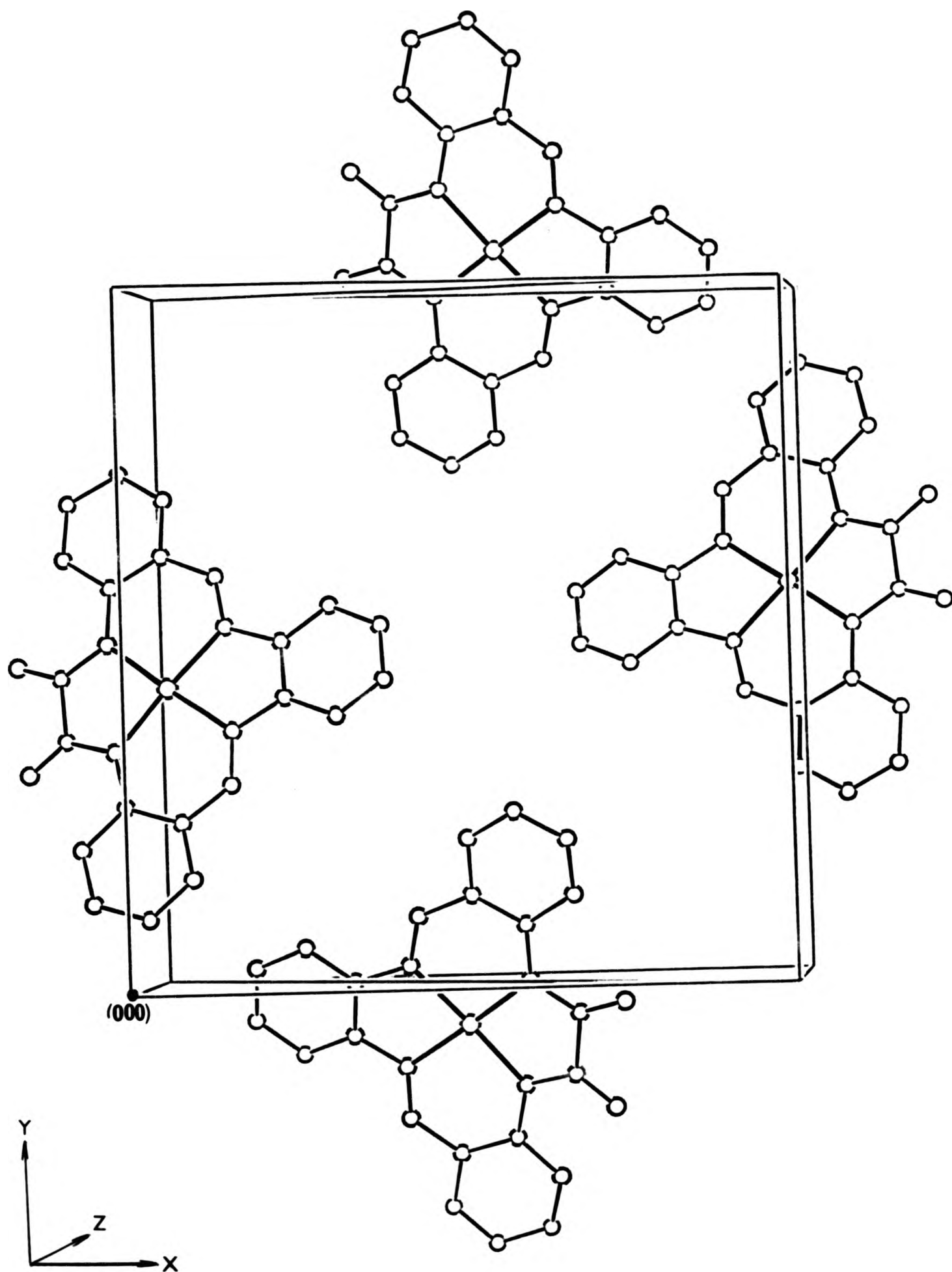
Drawing 6.2a



Drawing 6.2b



Drawing 6.2b



Drawing 6.2c

carbonyl groups. In addition, as the rings around the Cu atom in this compound are 6-,5-,6-,5-membered, whilst in Cu(TAABH₂) they are 6-,6-,6-,6-membered, possibly a somewhat more favourable steric condition for close approach of the ligand atoms to the metal may prevail in CuDIKETO. It is conceivable that the combination of these two effects make these chemically non-equivalent bonds equal in length in this compound.

Each nitrogen atom is coplanar within 0.1 Å with the three atoms to which it is bonded. This trigonal planar structure suggests sp²-hybridisation. This is borne out by the bond lengths.

The bonds

$$C(8b)-N(1b) = 1.292(3) \text{ \AA}$$

$$C(8a)-N(1a) = 1.286(3) \text{ \AA}$$

show double bond character (see section 3.3.1), which is expected from the method of synthesis, whilst the bond lengths

$$C(2b)-N(2b) = 1.404 \text{ \AA}$$

$$C(2a)-N(2a) = 1.401(3) \text{ \AA}$$

are in between those found for double and single bonds.

The bond C(1a)-C(1b) has a value of 1.548(4) Å, which is long for an sp²-sp²-hybridised carbon-carbon bond.

The two chemically equivalent halves do not show significant

differences, although they are crystallographically independent.

6.3.3 FREE LIGAND

The FREE LIGAND has the unexpected acyclic structure shown in Figure 6.3. It is not possible to discuss the bond lengths and angles in any detail. The only significant result obtained from this investigation, is the knowledge that the structure is acyclic, with an extra o-phenylene diamine unit in the molecule, that the carbonyl groups have a trans-relationship, and that probably hydrogen bonding occurs. The ORTEP drawing for this molecule is in Drawing 6.3.

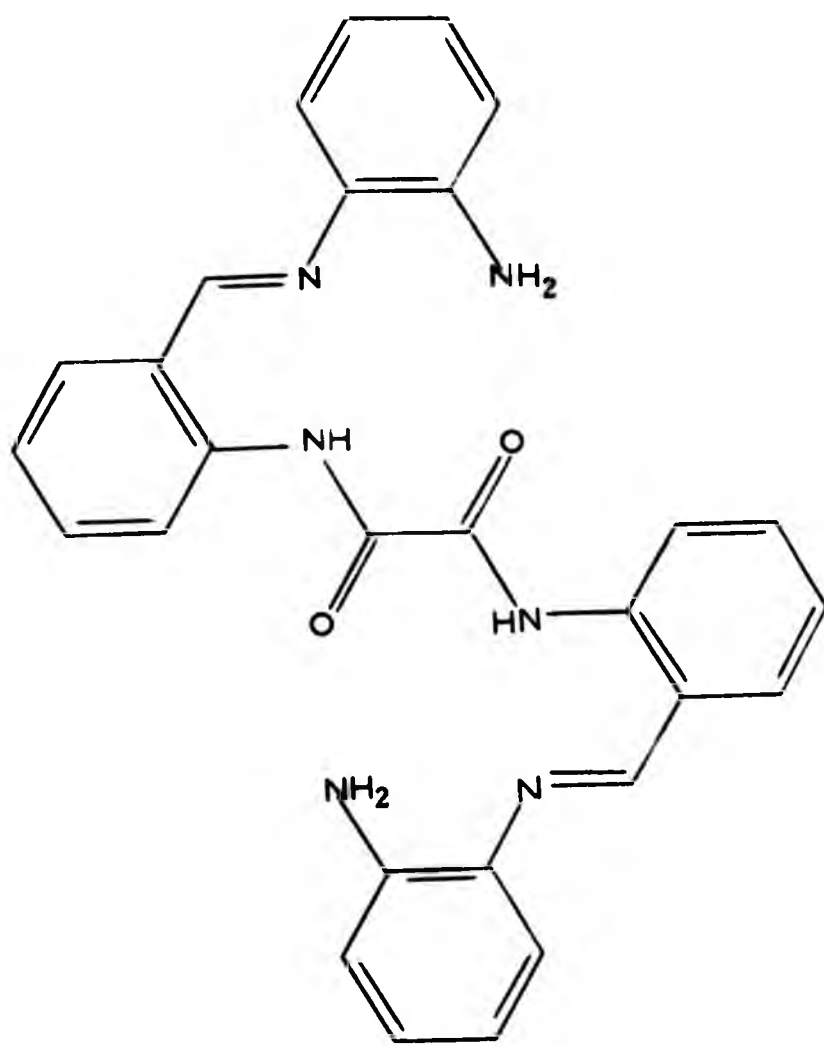
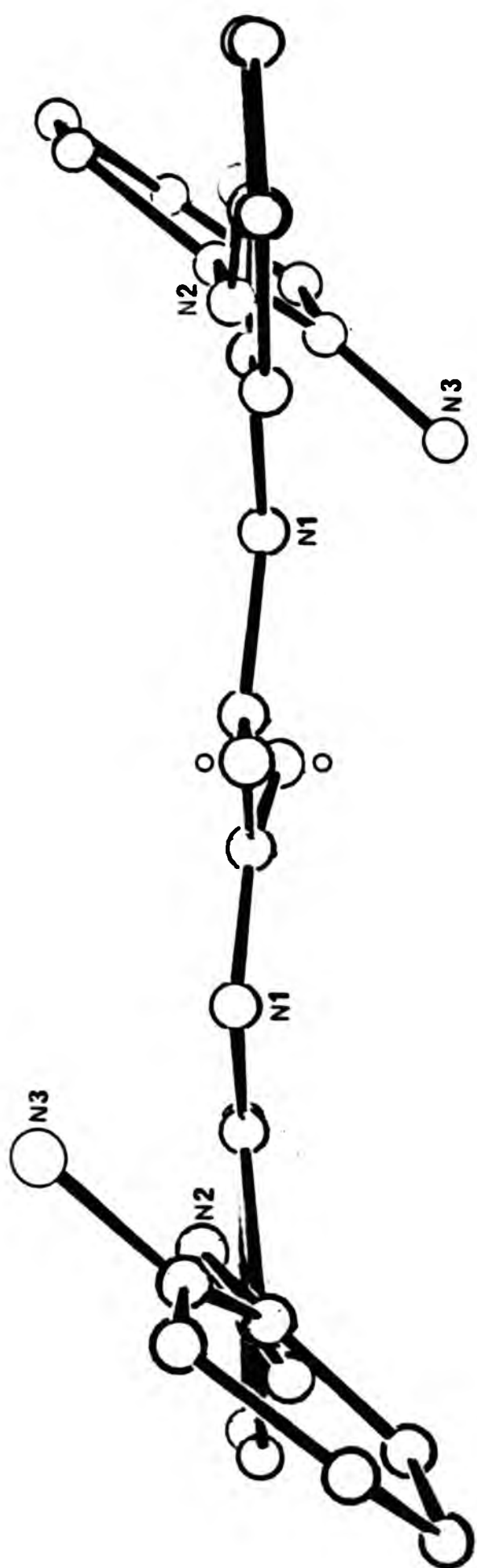
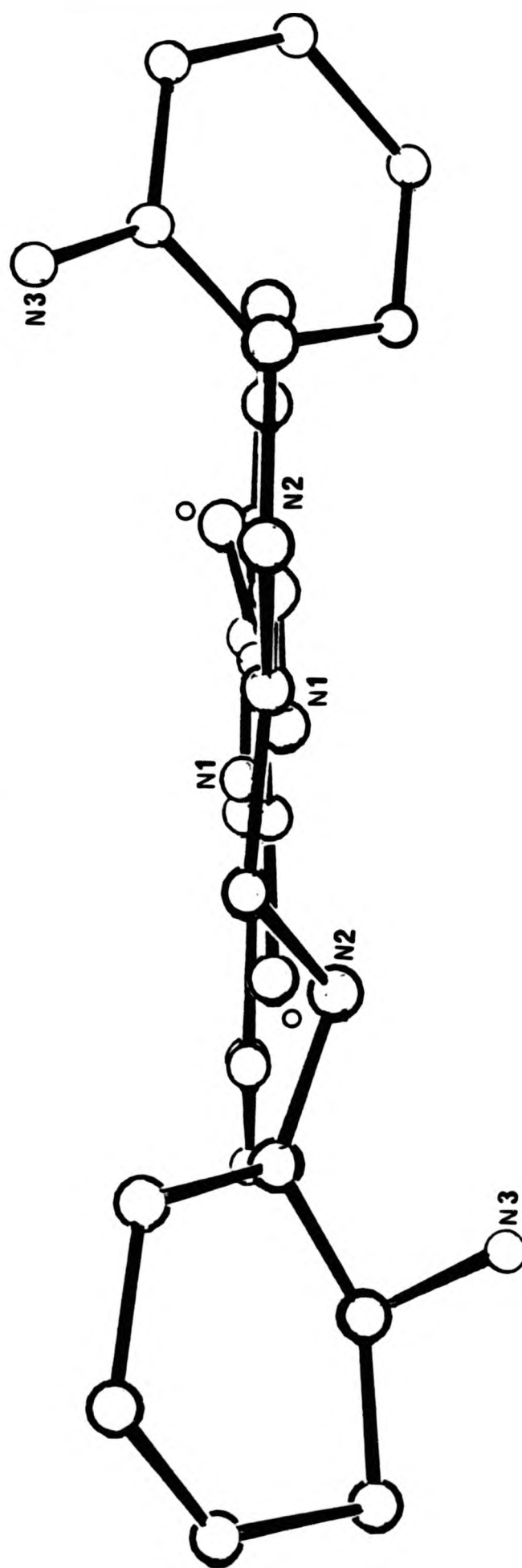


Figure 6.3



Drawing 6.3a



Drawing 6.3b

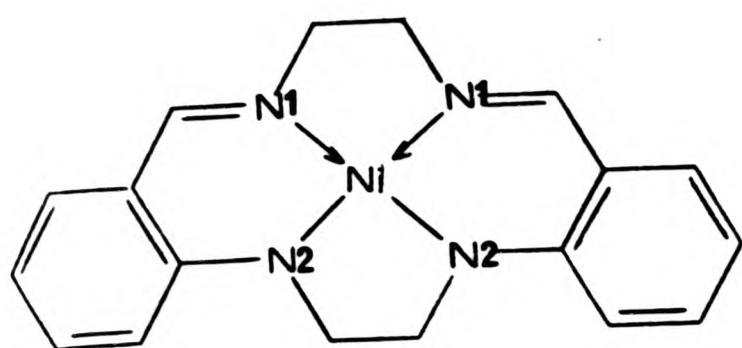
6.3.4 COMPARISON BETWEEN METAL COMPLEXES OF LIGAND OXIDISED

TETRA-AZAMACROCYCLES

During studies on metal complexes of 14-membered tetra-azamacrocyclic ligands, Maslen and co-workers³ prepared compound (I). When this was recrystallised from dimethylformamide, DMF, they observed two kinds of crystals. The bulk sample, compound (I), was needle-shaped; the second one, compound (II), found as a minor impurity, consisted of prismatic crystals. The rationalisation for obtaining compound (II) is the same as for obtaining compounds (III) and (IV). In the case of compounds (III) and (IV) the reaction stops after the oxygenation of the ethylene bridge. In compound (I) the newly formed α, β -diketo group (probably formed on oxygenation of the ethylene bridge) reacts with an excess of the reagent, ethylene diamine, to form compound (II). A preliminary report of the novel oxygenation reaction of the iron compound has been published.¹ It seems likely that all the α, β -diketo groups in these metal complexes can react further with ethylene diamine. Whether this occurs, or not, will depend on whether the oxygenation of the ethylene bridge occurs in the presence or the absence of the diamine.

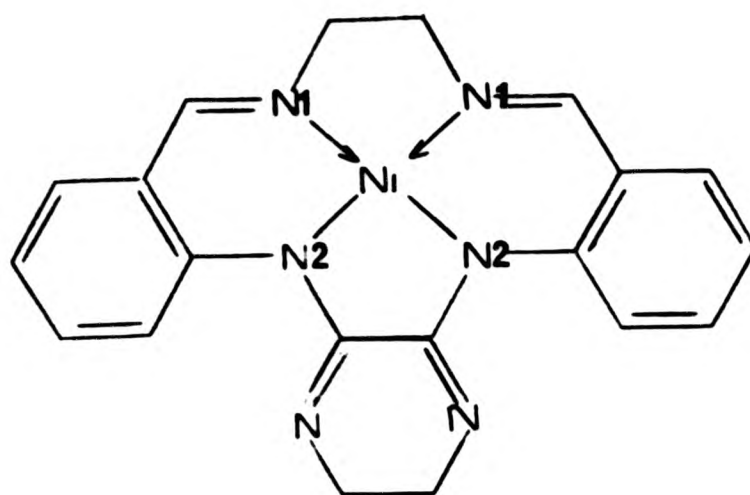
In both nickel compounds (I) and (II), the nickel atom is in the N_4 co-ordination plane. The same is the case for the copper atom in compound (IV). In compound (III), however, the iron atom is 0.66 \AA above the plane of the four nitrogen atoms.

All four complexes (Diagram 6.2) have two chemically different types of nitrogen atoms. However, only in the iron compound does this



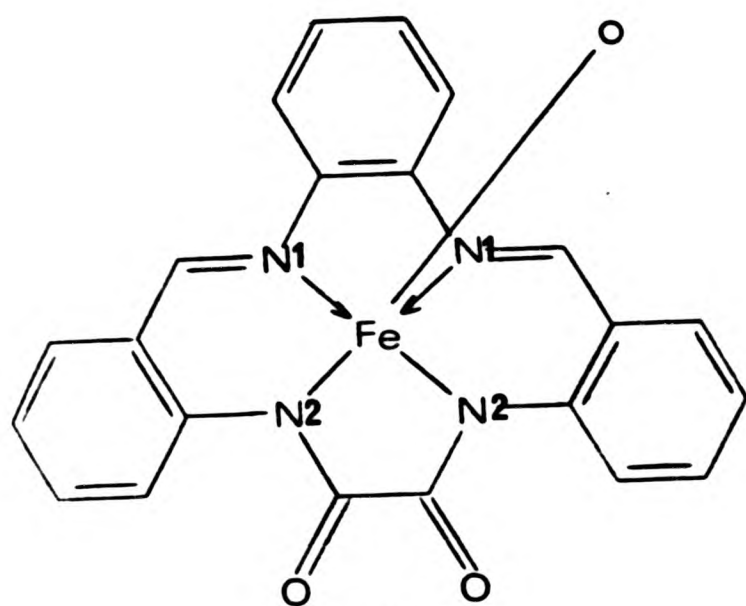
(I)

$$\begin{aligned}\text{Ni-N(1)} &= 1.844(4) \\ \text{Ni-N(2)} &= 1.850(4)\end{aligned}$$



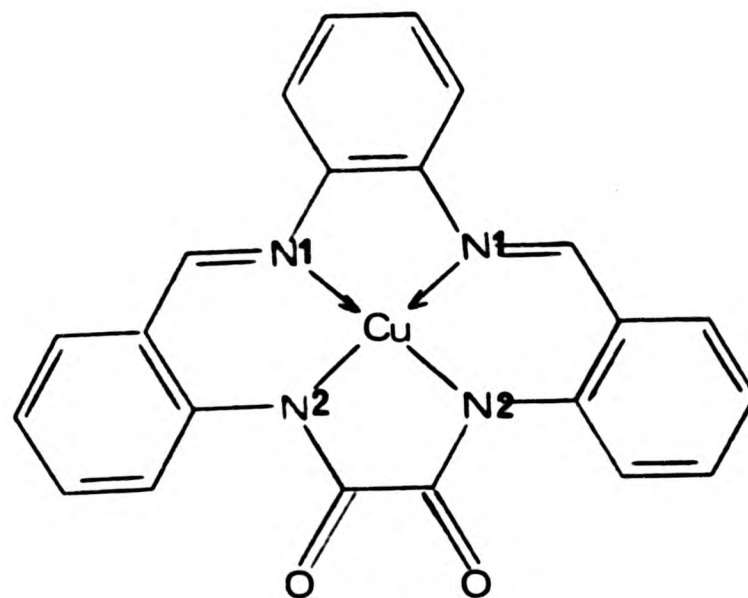
(II)

$$\begin{aligned}\text{Ni-N(1)} &= 1.853(4) \\ \text{Ni-N(2)} &= 1.860(4)\end{aligned}$$



(III)

$$\begin{aligned}\text{Fe-N(1)} &= 2.085(7) \\ \text{Fe-N(2)} &= 1.994(7)\end{aligned}$$



(IV)

$$\begin{aligned}\text{Cu-N(2)} &= 1.941(1) \\ \text{Cu-N(1)} &= 1.949(1)\end{aligned}$$

Diagram 6.2

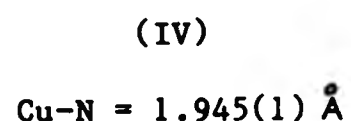
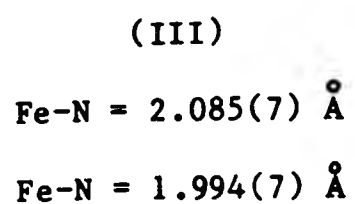
manifest itself in two different metal-nitrogen bond lengths (see Chapter 8).

(I)

$$\text{Ni-N} = 1.847(3) \text{ \AA}$$

(II)

$$\text{Ni-N} = 1.856(3) \text{ \AA}$$



The angles around the metal atoms show some similarities. In all four structures the angles N(1)-M-N(2) are larger than those of N(1)-M-N(1) and of N(2)-M-N(2). In structures (I) and (II) the latter two angles are equal or nearly so, whilst in compounds (III) and (IV) the N(1)-M-N(1) angles are significantly smaller than the N(2)-M-N(2) angles.

In structures (III) and (IV) the diketo group is tilted from the N_4 co-ordination plane by 25 and 13° respectively, whilst in structure (II) the relevant segment of the molecule tilts 30° from the N_4 co-ordination plane.

In three of the above-mentioned compounds (II, III, and IV) the lone pairs on the N(2) atoms back-donate in almost equal amounts towards the C(1) and C(2) atoms. Therefore contributions from resonance forms (Diagram 6.3), where N(2) is doubly bonded to C(1) as well as C(2), must be considered.

The N(2)-C(2) and N(2)-C(1) bond lengths are short for their kind. They are 1.390(7) and 1.380(7), 1.385(11) and 1.359(12), 1.400(2) and 1.362(2) Å respectively for the compounds (II), (III) and (IV). As a result the endocyclic angles at C(2) in the benzene rings are small. They are 116.1(5), 118.5(8) and 116.3(2)° respectively for the compounds (II), (III) and (IV).

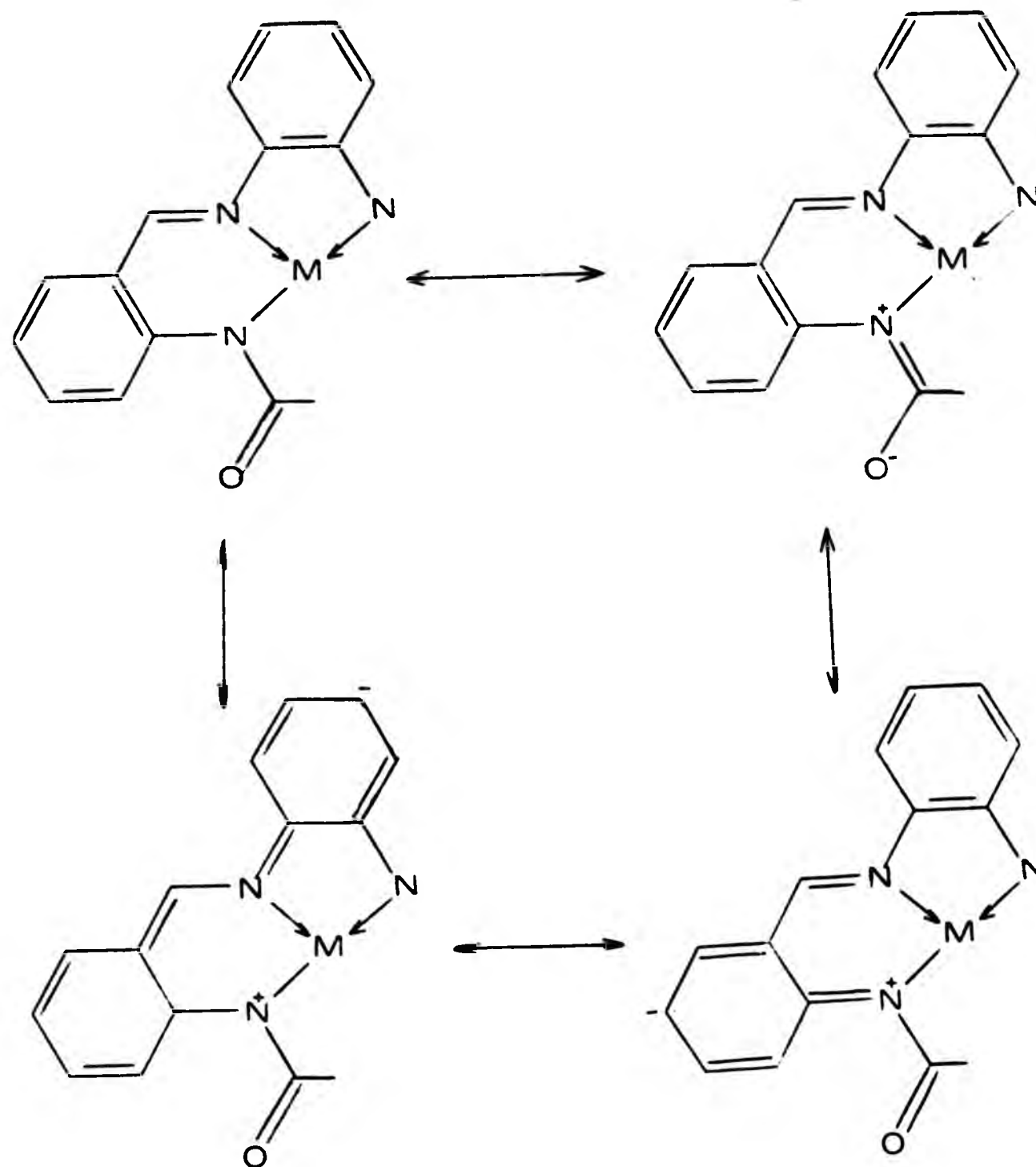


Diagram 6.3

In compound (I), however, the lone pair on the N(2) atom can only delocalise in one direction, namely towards C(2) (Diagram 6.4). Hence C(2)-N(2) becomes even shorter [1.340(7) Å] (see section 4.4), and the angle at C(2) in the benzene ring is even smaller [114.4(8)°] than in the other three compounds. Correspondingly N(2)-C(1) is in the expected range [1.462(7) Å] for carbon-nitrogen single bonds.

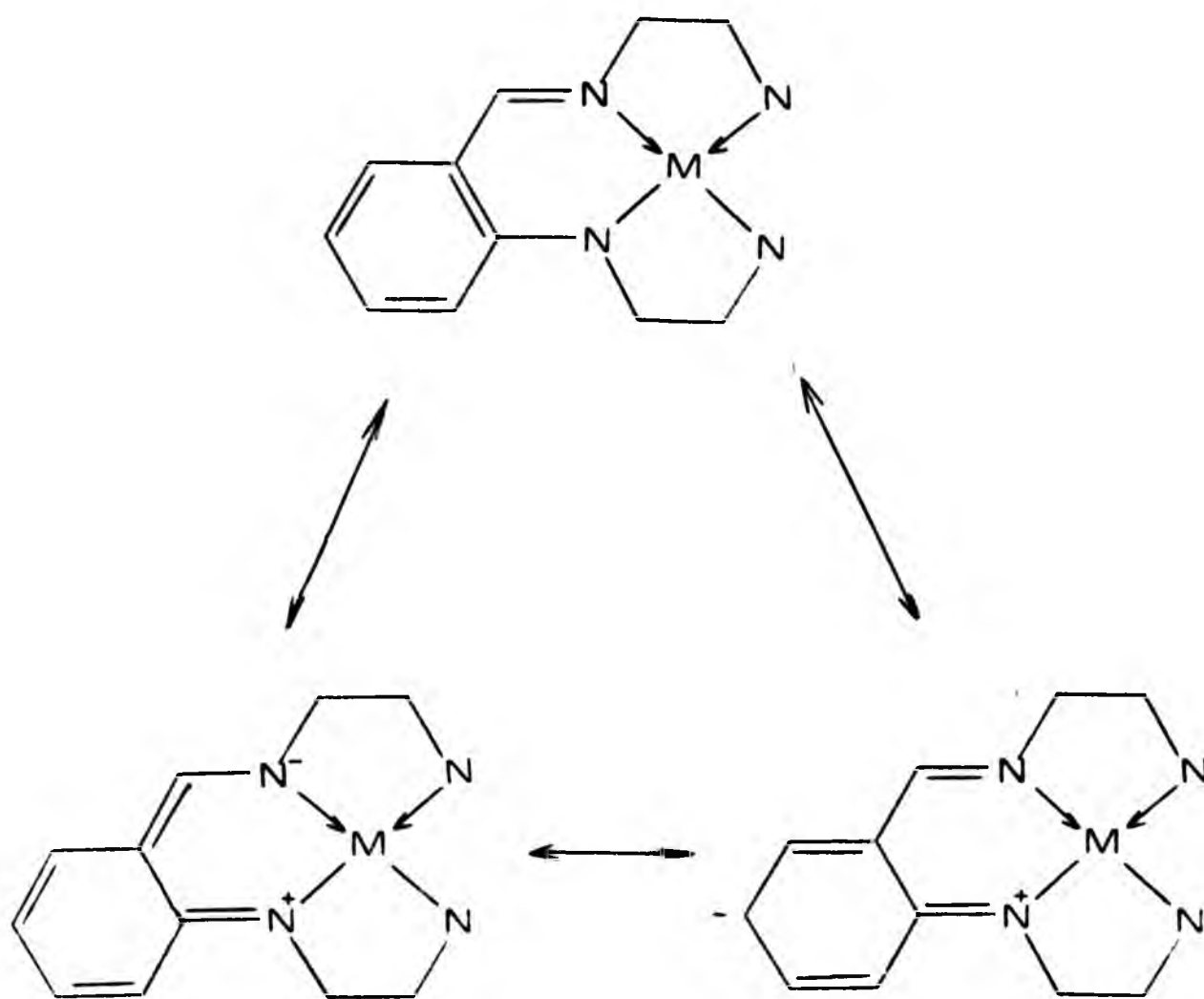


Diagram 6.4

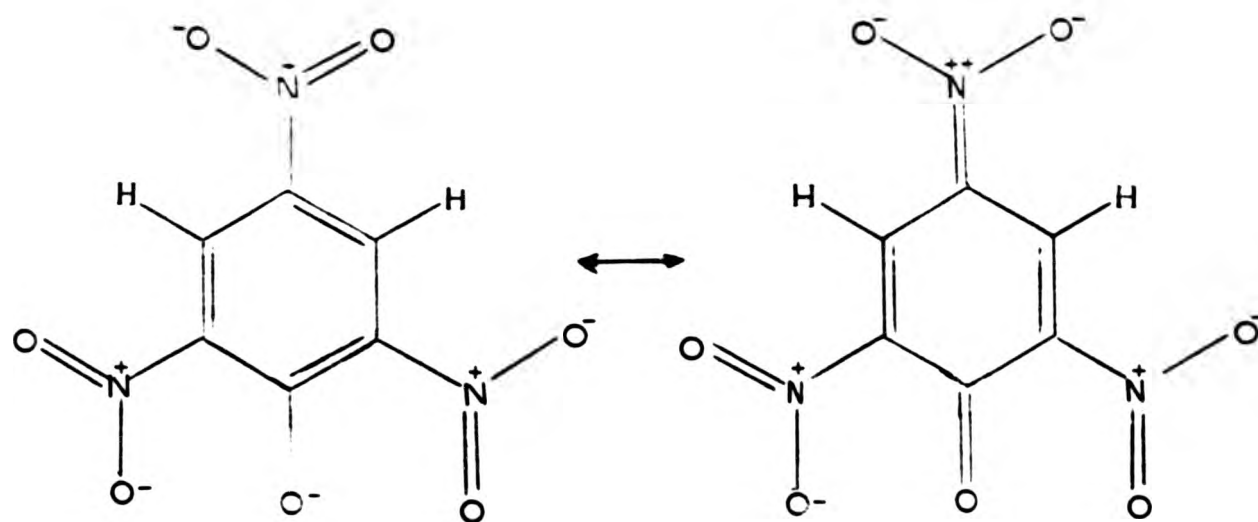
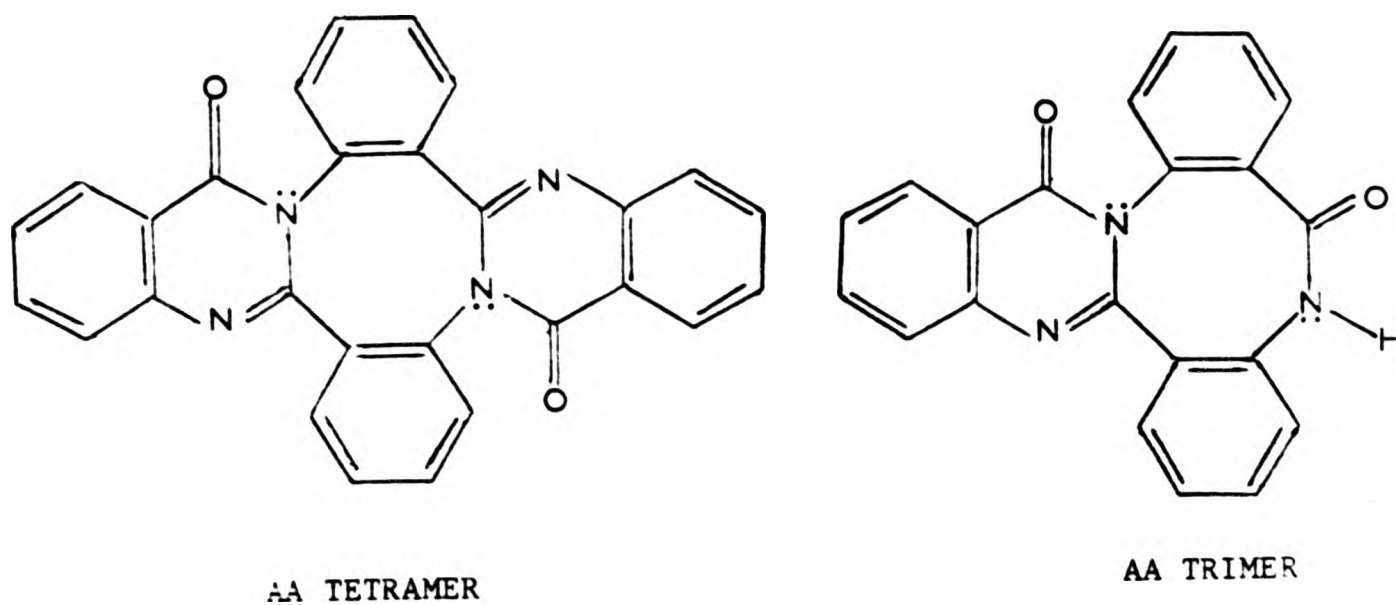
This is a situation similar to that observed in the condensation products of AA and in the $\text{TAABH}_2(\text{PICRATE})_2$ salt, as shown in Diagram 6.5. In the AA TETRAMER and AA TRIMER the lone pairs on the N(2) atoms delocalise in equal amounts in both directions towards C(1) and C(8), hence making both these bonds short for their kind [average bond length $1.399(2) \text{ \AA}$]. In the AA TRIMER the lone pair on N(3) delocalises only in one direction, towards C(15), making this bond much shorter [$\text{N}(3)-\text{C}(15)_{\text{av}} = 1.340(4) \text{ \AA}$] than the previous ones mentioned.

These values agree well with the average result of the above metal complexes, when the nitrogen lone pair is delocalised over two bonds [1.379(3) Å], or over one bond [1.340(7) Å], respectively.

In the picrate counter-ion too, lone pair delocalisation (this time from the oxygen atom) is also observed. This results in a short carbon-oxygen bond, O(7)-C(6), 1.243(4) Å and a small endocyclic bond angle at C(6) 111.1(3)°.

In the Cu complex the angle C(7)-C(2)-C(3) has an average value of 116.4°, whilst the angle C(10b)-C(9b)-C(9a) has an average value of 119.7°. Comparison with the picrate ion (see section 3.3.1) and the theoretical discussion by Domenicano and Vaciago⁴ suggest that quinonoid resonance forms involving the former benzo ring, but not the latter, are important. The corresponding values for the Fe complex are 119.1 and 120.7°. This structure is less accurate, the values less convincing, but, nevertheless, they still point in the same direction as in the Cu derivative.

The carbon-carbon bond between the two carbonyl groups is long for two sp²-hybridised carbon atoms. Such a bond without any π-contribution should be 1.485 Å (see section 3.3.1). The values observed for the FeIII complex [1.517(16) Å], and especially for the CuII complex [1.548(4) Å] greatly exceed this. In the case of the former, high e.s.d. values limit discussion. In the case of the copper complex, however, there is little doubt that the bond length compares with that for a pure Csp³-Csp³ bond, e. g. 1.5445 Å in diamond.⁵ The same source⁶ gives a value of 1.49 ± 0.01 Å for the carbon-carbon bond between two



Picrate counter-ion of $\text{TAABH}_2(\text{PICRATE})_2$ salt

Diagram 6.5

carbonyl groups. The examples are, however, very limited. A search of the Cambridge Data File revealed 122 structures with this type of bond. Bond lengths range from 1.451 to 1.588 Å, with a mean of 1.545(22) Å. When the search was restricted to α,β -diamides, only 8 structures were found, whose bond lengths ranged from 1.486 to 1.549 Å, with a mean of

1.527(21) Å. Hence the average value, for this type of bond, according to recent work is long, and the structures reported here, fit into this pattern.

An interesting extension of this work was to investigate the structure of the free diketo ligand, FREE LIGAND, of the above two metal complexes. Colleagues in this Department attempted its synthesis in the presence of zinc salts, but were uncertain, when passing these crystals to the author for X-ray crystallographic investigation, whether it was the free macrocycle or its zinc complex. Crystallographic investigations showed them to be neither. The compound in question is an acyclic free ligand, containing six nitrogen atoms and two carbonyl oxygen atoms. The molecule contains one *o*-phenylene diamine residue in excess of that required for the macrocyclic structure. In contrast to the metal complexes, the two carbonyl groups here are trans to one another. This is undoubtedly due to the presence of hydrogen bonds. It has been shown in two other acyclic free ligand structures,⁷ that the ligand prefers to adopt an extended configuration, rather than one tending to a cyclic one. It has been suggested, that this configuration is preferred, to minimize lone pair-lone pair repulsions between the nitrogen atoms. Free ligands of this type can cause difficulties in their crystal structure determinations. A tetra-azacyclohexadecene, investigated by Sheldrick and Trotter⁸ bears this out. Conventional direct methods failed to give an encouraging molecular fragment, and more complex methods for structure determination had to be employed. Even with this, the refinement converged with an R-factor of 12% and the e.s.d. values were high.

Similar, but even greater problems were encountered with bilirubin,⁹ where disorder compounded the problems. Bilirubin is a ring-opened product of heme. The initial oxidative ring opening gives biliverdin, which then on reduction forms bilirubin. The gross structure of biliverdin appears to be somewhat similar to that of heme, whilst that of bilirubin has involved a rotation of dipyrrolyl units around the CH₂ bond. This is not feasible in the olefinic structure of biliverdin. The structure of bilirubin has also its two carbonyl groups in a trans-arrangement. This conformation is stabilized by six hydrogen bonds, two O-H...O and four N-H...O. The structure of the FREE LIGAND reported here shows some similarities to this.

REFERENCES

1. S. Gözen, R. Peters, P. G. Owston, and P. A. Tasker, J. Chem. Soc. Chem. Comm., 1980, 1199.
2. For references see ref. 1
3. E. N. Maslen, L. M. Engelhardt, and A. H. White, J. Chem. Soc. Dalton, 1974, 1799.
4. A. Domenicano and A. Vaciago, Acta Cryst., 1979, B35, 1382.
5. "Interatomic Distances Supplement", Edt. L. E. Sutton, Special Publication 18, The Chemical Society, London, 1965, p. S14s.
6. Ref. 5, p. S15s.
7. P. G. Owston, R. Peters, E. Ramsamy, P. A. Tasker, and J. Trotter, J. Chem. Soc. Chem. Comm., 1980, 1218.
8. G. M. Sheldrick and J. Trotter, Acta Cryst., 1978, B34, 3122.
9. R. Bonnett, J. E. Davies, M. B. Hursthouse, and G. M. Sheldrick, Proc. Roy. Soc. Lond., 1978, B202, 249.

CHAPTER 7

STRUCTURAL INVESTIGATIONS OF METAL COMPLEXES OF DIBROMINATED SCHIFF BASES

7.1 METHOD OF PREPARATION

The compounds were prepared and characterised by R. Peters.¹

7.2 DATA COLLECTION AND STRUCTURE SOLUTION OF COPPER AND IRON COMPLEXES
OF DIBROMINATED SCHIFF BASES7.2.1 DATA COLLECTION AND STRUCTURE SOLUTION OF Cu(DIBrSALEN)
N,N'-ETHYLENEBIS[5-BROMO-2-HYDROXYBENZYLIDENEIMINATO(1-)]COPPER(II)

Details of the data collection and of the crystal data are summarised in Tables 7.1 and 7.2.

After the data collection 488 azimuthal absorption scan data from 19 independent reflections were collected.

Data reduction applied to the raw data consisting of 3175 reflections, resulted in 2233 unique reflections with $I > 3\sigma(I)$. No systematic absences were observed, which was expected since the space

Table 7.1: Crystal data of brominated Schiff bases

	Cu(diBrsalen)	Fe(diBrsalof)
Formula	$\text{CuC}_{16}\text{H}_{12}\text{N}_2\text{O}_2\text{Br}_2$	$\text{Fe}_2\text{C}_{40}\text{H}_{24}\text{N}_4\text{O}_5\text{Br}_4$
Molecular weight	487	2144
Crystal system	Triclinic	Triclinic
Space group	$\bar{P}1$	$\bar{P}1$
a (Å)	8.341(1)	11.311(2)
b (Å)	9.696(2)	12.709(3)
c (Å)	11.164(3)	13.518(3)
α (°)	116.59(1)	106.17(1)
β (°)	77.03(1)	86.60(1)
γ (°)	101.72(2)	97.42(1)
Volume (Å ³)	781.4	1850.2
D_c (g/cm ³)	2.07	1.923
D_m (g/cm ³)	2.01	1.908
Z	2	2
F(000)	474	1000
$\mu(\text{Mo-K}\alpha)$ (cm ⁻¹)	63.89	50.19

Table 7.2: Data collection and structure solution details of
dibrominated Schiff bases

	Cu(diBrsalen)	Fe(diBrsalof)
Crystal size (mm)	0.50x0.40x0.08	0.13x0.32x0.40
Crystal colour	Smoky-grey	Deep red
Shape	Rectangular rods	Chunky blocks
BMO	2	2
SMO	2	2
Scan width (°)	0.76	0.86
θ -range (°)	3-30	3-30
Reflections measured	3175	3468
Unique data set	2233	3066
Least-squares	171	397
parameters		
Data/parameter	13.0	7.7
Shift/e.s.d.	0.08	0.01
Weighting scheme	$1/[\sigma^2(F)+F^2]$	$1/[\sigma^2(F)+F^2]$
Max. electron dens.	0.71	0.68
residue $e/\text{\AA}^3$		
R	0.035	0.052
R_w	0.037	0.050

group is triclinic, with the possibility of two space groups $P1$ and $P\bar{1}$.

Assuming that there were 2 molecules in the unit cell the density was calculated, $D_c = 2.07 \text{ g/cm}^3$. The measured density, $D_m = 2.01 \text{ g/cm}^3$, agrees very well with the calculated one.

The $P\bar{1}$ space group was first investigated. Since the $P\bar{1}$ space group has two equivalent positions the asymmetric unit is half of the unit cell and each molecule occupies one equivalent position. Hence the heavy atoms in one molecule need to be located. In this case the heavy atoms are two bromine atoms and one copper atom. These atoms were located using the Patterson synthesis.

$P\bar{1}$ equivalent positions

- 1) $x \quad y \quad z$
- 2) $-x \quad -y \quad -z$

Patterson vector for $P\bar{1}$

- 1) $2x \quad 2y \quad 2z$

Unique Patterson vectors for 3 heavy atoms for $P\bar{1}$

			Height	
1)	$\pm(2x_1$	$2y_1$	$2z_1)$	1
2)	$\pm(x_1-x_2$	y_1-y_2	$z_1-z_2)$	2
3)	$\pm(x_1+x_2$	y_1+y_2	$z_1+z_2)$	2
4)	$\pm(x_1-x_3$	y_1-y_3	$z_1-z_3)$	2
5)	$\pm(x_1+x_3$	y_1+y_3	$z_1+z_3)$	2
6)	$\pm(2x_2$	$2y_2$	$2z_2)$	1

7) $\pm(x_2-x_3$	y_2-y_3	$z_2-z_3)$	2
8) $\pm(x_2+x_3$	y_2+y_3	$z_2+z_3)$	2
9) $\pm(2x_3$	$2y_3$	$2z_3)$	1

$2x_1$	$2y_1$	$2z_1$
$2x_2$	$2y_2$	$2z_2$
$2x_3$	$2y_3$	$2z_3$

The heights of these three vectors will be half the height of the other six vectors, because these three occur only once and the other six occur twice. Hence one should expect to find 3 sets of 4 vectors, which when added and subtracted should give 2 different sets of vectors which can be assigned as $2x$ $2y$ $2z$.

First 10 peaks from Patterson map

	U	V	W	height	Assignment		
1)	0.500	0.500	0.500	474	x_1+x_3	y_1+y_3	z_1+z_3
2)	0.806	0.313	0.938	336	x_2-x_3	y_2-y_3	z_2-z_3
3)	0.299	0.406	0.179	334	x_2+x_3	y_2+y_3	z_2+z_3
4)	0.229	0.093	0.319	302	x_1-x_2	y_1-y_2	z_1-z_2
5)	0.570	0.221	0.622	295	x_1-x_3	y_1-y_3	z_1-z_3
6)	0.923	0.278	0.880	291	$2x_1$	$2y_1$	$2z_1$
					$-2x_3$	$-2y_3$	$-2z_3$
7)	0.729	0.180	0.558	283	x_1+x_2	y_1+y_2	z_1+z_2
8)	0.500	0.094	0.239	144	$2x_2$	$2y_2$	$2z_2$
9)	0.985	0.295	0.220	124			
10)	0.243	0.256	0.060	107			

First set of four vectors from Patterson map:

7) 0.729 0.180 0.558

4) 0.229 0.093 0.319

4+7 gives 0.958 0.273 0.887 which is except for the U-value
almost the same as peak 6.

6) 0.923 0.278 0.880

4-7 gives 0.500 0.087 0.239 which is almost the same as peak 8.

8) 0.500 0.094 0.239

The first set of four vectors

Assignment

7) 0.729 0.180 0.558

x_1+x_2 y_1+y_2 z_1+z_2

4) 0.229 0.093 0.319

x_1-x_2 y_1-y_2 z_1-z_2

6) 0.958 0.273 0.877

$2x_1$ $2y_1$ $2z_1$

8) 0.500 0.087 0.239

$2x_2$ $2y_2$ $2z_2$

Second set of four vectors from Patterson map:

3) 0.299 0.406 0.179

x_2+x_3 y_2+y_3 z_1+z_3

2) 0.806 0.313 0.938

x_2-x_3 y_2-y_3 z_2-z_3

When these two vectors are added or subtracted, one of the results
should be the same as the one found from the first set. So these two
vectors should be adjusted accordingly.

2) 0.194 -0.313 0.062 x_2-x_3 y_2-y_3 z_2-z_3
 3) 0.299 0.406 0.179 x_2+x_3 y_2+y_3 z_2+z_3
 2+3 gives 0.493 0.093 0.241 which is almost the same as peak 8.

8) 0.500 0.094 0.239 $2x_2$ $2y_2$ $2z_2$

3-2 gives 0.105 0.719 0.117 which must be assigned as $2x_3$ $2y_3$ $2z_3$.

One should be able to find this vector (obtained by subtraction) in the Patterson peaks.

Vector 0.105 0.719 0.117 could be rewritten as
 -0.895 -0.281 -0.883 or
 0.895 0.281 0.883 which is roughly peak 6.

Peak 6 0.923 0.278 0.880 has already been assigned as $2x_1$ $2y_1$ $2z_1$ and now it should also be assigned as $2x_3$ $2y_3$ $2z_3$ vector. This means that Patterson peak 6, should not be used to find the position of the heavy atoms, because the $2x_1$ $2y_1$ $2z_1$ and $2x_3$ $2y_3$ $2z_3$ vectors are overlapping and the true maximum is occurring between the two maxima.

To prove this, one should take both the $2x_1$ $2y_1$ $2z_1$ and $2x_3$ $2y_3$ $2z_3$ vectors, add them, and take the average. The result should give the overlapping maximum i.e. peak 6.

$2x_1$	$2y_1$	$2z_1$	0.958	0.273	0.880
$2x_3$	$2y_3$	$2z_3$	0.895	0.281	0.883
		Add	1.853	0.554	1.763
and take the average			0.926	0.277	0.881

This vector is almost exactly the same as peak 6, as was expected.

Hence,

2)	0.194	-0.313	0.062	x_2-x_3	y_2-y_3	z_2-z_3
3)	0.299	0.406	0.179	x_2+x_3	y_2+y_3	z_2+z_3
8)	0.493	0.093	0.241	$2x_2$	$2y_2$	$2z_2$
6)	0.105	0.719	0.117	$2x_3$	$2y_3$	$2z_3$

The third set of four vectors from the Patterson map:

5) 0.570 0.221 0.622 can be written as

5)	0.430	-0.221	0.378
1)	0.500	0.500	0.500

5 + 1 gives 0.930 0.279 0.878 which is roughly peak 6.

6) 0.923 0.278 0.880

1 - 5 gives 0.070 0.721 0.122 which is roughly peak -6.

-6) 0.077 0.722 0.120

Hence,

5)	0.430	-0.221	0.378	x_1-x_3	y_1-y_3	z_1-z_3
1)	0.500	0.500	0.500	x_1+x_3	y_1+y_3	z_1+z_3
6)	0.930	0.279	0.878	$2x_1$	$2y_1$	$2z_1$
-6)	0.070	0.721	0.122	$2x_3$	$2y_3$	$2z_3$

Therefore,

$$\begin{aligned} 2x_1 &= (0.958 + 0.930)/2 = 0.944 & x_1 &= 0.472 \\ 2y_1 &= (0.279 + 0.273)/2 = 0.276 & y_1 &= 0.138 \\ 2z_1 &= (0.877 + 0.878)/2 = 0.877 & z_1 &= 0.438 \end{aligned}$$

$$\begin{aligned} 2x_2 &= (0.500 + 0.493)/2 = 0.496 & x_2 &= 0.248 \\ 2y_2 &= (0.093 + 0.094)/2 = 0.093 & y_2 &= 0.046 \\ 2z_2 &= (0.239 + 0.241)/2 = 0.240 & z_2 &= 0.120 \end{aligned}$$

$$\begin{aligned} 2x_3 &= (0.105 + 0.070)/2 = 0.087 & x_3 &= 0.043 \\ 2y_3 &= (0.719 + 0.721)/2 = 0.720 & y_3 &= 0.360 \\ 2z_3 &= (0.117 + 0.122)/2 = 0.119 & z_3 &= 0.059 \end{aligned}$$

These positions are assigned to two bromine atoms and one copper atom.

Using the phases calculated from 2 bromine atoms and 1 copper atom positions, successive difference Fourier and full matrix least squares refinement calculations led to the location of

- 1) Initially 17 out of 20 non-hydrogen atoms
- 2) After one cycle, the remaining non-hydrogen atoms and 11 out of 12 hydrogen atoms
- 3) The next cycle of refinement led to the location of the last hydrogen atom

All bromine, copper, nitrogen and oxygen atoms were refined with anisotropic thermal parameters. Full matrix refinement was carried out during the refinement. There was no constraint on the hydrogen atoms. They were refined in three different groups with a common isotropic temperature factor. Group 1 all aliphatic hydrogen atoms; group 2 all other hydrogen atoms in one half of the molecule; group 3 all other hydrogen atoms in the other half of the molecule. The isotropic temperature factors were 0.035, 0.039, and 0.050 Å² respectively. At this stage refinement converged at 0.042.

An absorption correction was applied to the data collected. Transmission factors ranged from 0.661 to 1.000 for the full data set, with a merging R-factor based on equivalent reflections calculated as 0.045 before correction, and 0.019 after correction.

The refinement was stopped when the calculated parameter shift/e.s.d. ratio fell to a maximum of 0.08.

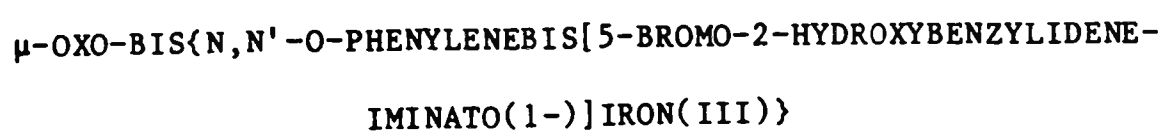
The R-value after the absorption correction was 0.035, $R_w = 0.037$.

The final difference Fourier map showed the mean amplitude of

$$0.71 > \Delta\rho > 0.42 \text{ e/\AA}^3$$

The highest residual electron density of 0.71 e/Å³ was observed near atom Br(a).

7.2.2 DATA COLLECTION AND STRUCTURE SOLUTION OF Fe(diBrsalof)



Details of data collection and crystal data are summarized in Tables 7.1 and 7.2.

Data reduction applied to the raw data consisting of 3468 reflections resulted in 3066 unique reflections. No systematic absences were observed, which was expected since the crystal system is triclinic with the possibility of two space group $P1$ and $P\bar{1}$. Assuming that there were two molecules in the unit cell the density was calculated, $D_c = 1.923 \text{ g/cm}^3$. The measured density, $D_m = 1.908 \text{ g/cm}^3$ agrees with the calculated one.

First the Patterson map for the triclinic crystal system was calculated and the $P\bar{1}$ space group was investigated. Since $P\bar{1}$ has two equivalent positions the asymmetric unit is half of the unit cell and each molecule occupies one equivalent position. Hence the heavy atoms in one molecule, namely 4 bromine and 2 iron atoms, need to be located. Patterson vectors calculated for $P\bar{1}$ were not consistent with the map. Therefore it was decided that the space group is $P1$, with one equivalent position and two molecules occupying that position together. In this case the asymmetric unit is the whole of the unit cell and all the heavy atoms in the unit cell, namely 8 bromine and 4 iron atoms, need to be located. These atoms were located from the Patterson synthesis as shown below.

P1 equivalent positions

1) x y z

Patterson vectors for P1

1) x y z

Unique Patterson vectors for 12 heavy atoms for P1

1) ±[x1-x2	y1-y2	z1-z2]
3) ±[x1-x3	y1-y3	z1-z3]
4) ±[x1-x4	y1-y4	z1-z4]
5) ±[x1-x5	y1-y5	z1-z5]
6) ±[x1-x6	y1-y6	z1-z6]
7) ±[x1-x8	y1-y8	z1-z8]
8) ±[x1-x9	y1-y9	z1-z9]
9) ±[x1-x10	y1-y10	z1-z10]
10) ±[x1-x11	y1-y11	z1-z11]
11) ±[x1-x12	y1-y12	z1-z12]
12) ±[x2-x3	y2-y3	z2-z3]
13) ±[x2-x4	y2-y4	z2-z4]
14) ±[x2-x5	y2-y5	z2-z5]
15) ±[x2-x6	y2-y6	z2-z6]
16) ±[x2-x7	y2-y7	z2-z7]
17) ±[x2-x8	y2-y8	z2-z8]
18) ±[x2-x9	y2-y9	z2-z9]
19) ±[x2-x10	y2-y10	z2-z10]
20) ±[x2-x11	y2-y11	z2-z11]
21) ±[x2-x12	y2-y12	z2-z12]
22) ±[x3-x4	y3-y4	z3-z4]

23)±[x3-x5	y3-y5	z3-z5]
24)±[x3-x6	y3-y6	z3-z6]
25)±[x3-x7	y3-y7	z3-z7]
26)±[x3-x8	y3-y8	z3-z8]
27)±[x3-x9	y3-y9	z3-z9]
28)±[x3-x10	y3-y10	z3-z10]
29)±[x3-x11	y3-y11	z3-z11]
30)±[x3-x12	y3-y12	z3-z12]
31)±[x4-x5	y4-y5	z4-z5]
32)±[x4-x6	y4-y6	z4-z6]
33)±[x4-x7	y4-y7	z4-z7]
34)±[x4-x8	y4-y8	z4-z8]
35)±[x4-x9	y4-y9	z4-z9]
36)±[x4-x10	y4-y10	z4-z10]
37)±[x4-x11	y4-y11	z4-z11]
38)±[x4-x12	y4-y12	z4-z12]
39)±[x5-x6	y5-y6	z5-z6]
40)±[x5-x7	y5-y7	z5-z7]
41)±[x5-x8	y5-y8	z5-z8]
42)±[x5-x9	y5-y9	z5-z9]
43)±[x5-x10	y5-y10	z5-z10]
44)±[x5-x11	y5-y11	z5-z11]
45)±[x5-x12	y5-y12	z5-z11]
45)±[x6-x7	y6-y7	z6-z7]
47)±[x6-x8	y6-y8	z6-z8]
48)±[x6-x9	y6-y9	z6-z9]
49)±[x6-x10	y6-y10	z6-z10]
50)±[x6-x11	y6-y11	z6-z11]

51)±[x6-x12	y6-y12	z6-z12]
52)±[x7-x8	y7-y8	z7-z8]
53)±[x7-x9	y7-y9	z7-z9]
54)±[x7-x10	y7-y10	z7-z10]
55)±[x7-x11	y7-y11	z7-z11]
56)±[x7-x12	y7-y12	z7-z12]
57)±[x8-x9	y8-y9	z8-z9]
58)±[x8-x10	y8-y10	z8-z10]
59)±[x8-x11	y8-y11	z8-z11]
60)±[x8-x12	y8-y12	z8-z12]
61)±[x9-x10	y9-y10	z9-z10]
62)±[x9-x11	y9-y11	z9-z11]
63)±[x9-x12	y9-y12	z9-z12]
64)±[x10-x11	y10-y11	z10-z11]
65)±[x10-x12	y10-y12	z10-z12]
66)±[x11-x12	y11-y12	z11-z12]

Since the space group is P1, it was assumed that one of the atoms is at the (0,0,0) position. In this case Br(a) was assumed to be at $x_1 = 0$, $y_1 = 0$, and $z_1 = 0$.) Therefore the vectors involving the x_1 , y_1 , and z_1 values should be easily detected, since the $(x_1-x_2, y_1-y_2, z_1-z_2)$ vectors would be $(-x_2, -y_2, -z_2)$. Therefore the first 11 vectors were selected, assuming that they are

- 1) -x2 -y2 -z2
- 2) -x3 -y3 -z3
- 3) -x4 -y4 -z4

$$11) \quad -x_{12} \quad -y_{12} \quad -z_{12}$$

Each of these vectors was tested by subtracting from the other 10 vectors. If the assignment was correct for the first vector, the subtraction results of the next 10 vectors from the first, would give 10 new vectors in the Patterson map in the form of

$$1) \quad x_2-x_3 \quad y_2-y_3 \quad z_2-z_3$$

$$2) \quad x_2-x_4 \quad y_2-y_4 \quad z_2-z_4$$

$$3) \quad x_2-x_5 \quad y_2-y_5 \quad z_2-z_5$$

$$10) \quad x_2-x_{12} \quad y_2-y_{12} \quad z_2-z_{12}$$

If the assignment was correct for the second vector, the subtraction results of the next 9 vectors from the second, would give 9 new vectors in the Patterson map in the form of

$$1) \quad x_3-x_4 \quad y_3-y_4 \quad z_3-z_4$$

$$2) \quad x_3-x_5 \quad y_3-y_5 \quad z_3-z_5$$

$$3) \quad x_3-x_6 \quad y_3-y_6 \quad z_3-z_6$$

$$9) \quad x_3-x_{12} \quad y_3-y_{12} \quad z_3-z_{12}$$

In the same way, if the assignment was correct for the rest, the subtractions would give 8 new vectors for the 3rd, 7 new vectors for 4th, 6 new vectors for the 5th, and so on.

From the first 11 vectors selected, those which did not give any new

vectors (as a result of subtraction) in the Patterson map, were assumed, that they were not $-x$, $-y$, $-z$ type of vectors. From the Patterson map new peaks were assumed to be of the type wanted and they were tested in the same manner. This process continued until the vectors were all assigned.

The first 40 peaks from the Patterson map:

1)	0.777	0.226	0.933	=	-0.223	0.226	-0.067	x_1-x_2, x_5-x_6
					-0.777	-0.226	0.067	$x_{11}-x_{12}$
					0.221	-0.226	0.067	x_4-x_9
2)	0.951	0.473	0.044	=	0.049	0.527	-0.044	$x_1-x_9, x_2-x_4,$
								x_6-x_{11}
					-0.951	0.527	-0.044	x_5-x_{12}
3)	0.755	0.237	0.478	=	-0.225	0.237	0.478	x_1-x_3
					0.225	-0.237	0.528	x_1-x_7
					0.225	0.763	-0.478	x_8-x_{11}
					0.775	0.236	-0.528	$x_{10}-x_{11}$
4)	0.017	0.011	0.555	=	0.017	0.011	0.555	x_2-x_3
					0.017	0.011	-0.445	$x_{10}-x_{12}$
5)	0.535	0.160	0.143	=	0.535	0.160	0.143	$x_1-x_5, x_2-x_6,$
								x_4-x_{11}
					-0.465	0.160	0.143	x_9-x_{12}
6)	0.705	0.068	0.964	=	0.295	0.932	0.036	x_1-x_{11}
					0.295	-0.068	0.036	x_3-x_8
					-0.705	-0.068	0.036	x_7-x_{10}
7)	0.960	0.477	0.585	=	0.040	0.519	-0.585	x_3-x_4
					-0.960	0.519	0.415	x_5-x_{10}
8)	0.239	0.296	0.476	=	0.239	0.296	-0.524	x_3-x_9

				-0.741	0.296	0.476	x6-x10
9)	0.692	0.061	0.414 =	0.308	-0.061	0.586	x2-x8
				-0.692	-0.061	-0.414	x7-x12
10)	0.080	0.165	0.510 =	0.080	0.165	0.510	x1-x8
				0.080	0.165	-0.490	x7-x11
11)	0.243	0.410	0.616 =	0.243	-0.590	0.616	x4-x8
				-0.243	0.590	0.384	x5-x7
12)	0.516	0.368	0.814 =	0.484	-0.368	0.186	x4-x6
				-0.484	0.368	-0.186	x5-x9
13)	0.159	0.246	0.104 =	-0.165	0.758	-0.103	x1-x4, x5-x11
14)	0.959	0.363	0.440 =	-0.041	0.363	0.440	x6-x7
				-0.041	0.363	-0.560	x8-x9
15)	0.481	0.480	0.411 =	0.519	0.520	0.589	x2-x7
				-0.481	0.520	-0.411	x8-x12
16)	0.515	0.158	0.604 =	0.515	0.158	-0.396	x3-x6
				-0.485	0.158	0.604	x9-x10
17)	-0.007	0.012	0.173				
18)	0.315	0.389	0.073 =	0.315	0.389	0.073	x1-x6
19)	0.265	0.305	0.026 =	0.265	0.305	0.026	x2-x9
				-0.735	0.305	0.026	x6-x12
20)	0.505	0.487	0.960 =	0.495	0.513	0.040	x3-x7
				-0.505	0.513	0.040	x8-x10
21)	0.412	0.310	0.900 =	-0.412	0.690	0.100	x1-x12
				0.588	0.690	0.100	x2-x11
22)	0.448	-0.004	0.622 =	0.448	-0.004	0.622	x4-x7
				-0.448	0.004	0.378	x5-x8
23)	0.272	0.077	0.343 =	0.728	-0.077	-0.343	x3-x5
				-0.272	-0.077	0.657	x4-x10

24)	0.445	0.318	0.448 =	-0.445	0.682	0.552	x1-x10
				0.555	0.682	-0.448	x3-x11
24)	0.225	0.237	0.576 =	-0.225	-0.237	0.424	x6-x8
				-0.225	-0.237	-0.573	x7-x9
26)	0.809	0.456	0.639 =	-0.191	0.456	0.614	x2-x10
				-0.191	0.456	-0.386	x3-x12
27)	0.252	0.061	0.789 =	0.748	-0.061	0.210	x2-x5
				-0.252	-0.061	0.210	x4-x12
28)	0.756	0.219	0.081				
29)	0.157	0.238	0.654				
30)	0.093	0.154	0.898				
31)	0.772	0.241	0.687				
32)	0.678	0.062	0.124				
33)	0.759	0.232	0.267				
34)	0.842	0.467	0.175 =	-0.158	0.467	0.175	x2-x12
35)	0.191	0.261	0.786				
36)	0.184	0.253	0.874				
37)	0.283	0.345	0.374				
38)	0.677	0.048	0.294				
39)	0.685	0.402	0.241 =	0.685	-0.598	0.245	x4-x5

Therefore

x1 = 0	x2 = 0.223	x3 = 0.225
y1 = 0	y2 = -0.226	y3 = -0.237
z1 = 0	z2 = 0.067	z3 = -0.478
x4 = 0.165	x5 = -0.535	x6 = -0.315
y4 = -0.758	y5 = -0.160	z6 = -0.389
z4 = 0.103	z5 = -0.143	z6 = -0.073

$$x_7 = -0.225 \quad x_8 = -0.080 \quad x_9 = -0.049$$

$$y_7 = 0.237 \quad y_8 = -0.165 \quad y_9 = -0.527$$

$$z_7 = -0.528 \quad z_8 = -0.518 \quad z_9 = -0.044$$

$$x_{10} = 0.445 \quad x_{11} = -0.295 \quad x_{12} = 0.412$$

$$y_{10} = -0.682 \quad y_{11} = -0.932 \quad y_{12} = -0.960$$

$$z_{10} = -0.552 \quad z_{11} = -0.036 \quad z_{12} = -0.100$$

Using the phases calculated from 8 bromine and 4 iron atom positions, successive difference Fourier and full matrix least squares refinement calculations led to the location of

- 1) Initially 56 of the 110 non-hydrogen atoms
- 2) After one further cycle 11 more non-hydrogen atoms
- 3) One more cycle yielded the location of the remaining non-hydrogen atoms and 23 of the 48 hydrogen atoms.

All bromine and iron atoms were refined with anisotropic thermal parameters. Blocked full matrix refinement was carried out during the early stages of refinement where the atoms were grouped as follows: Group 1 first molecule, half of the dimer including the bridging oxygen atom; group 2 the second half of the dimer; group 3, second molecule half of the dimer including the bridging oxygen atom; group 4, second half of second molecule.

An absorption correction was applied to the data collected. Transmission factors ranged from 0.478 to 0.990 for the full data set.

The refinement was continued using blocked cascade least squares calculations, this being the only program available for refinement for over 100 atoms. The hydrogen atom co-ordinates were estimated geometrically (assuming C-H = 1.08 Å) and for refinement allowed to ride on their respective carbon atom co-ordinates. The refinement was stopped when the calculated parameter shift/e.s.d. ratio fell to a maximum of 0.001. The final R-value was 0.044 ($R_w = 0.044$).

To be certain about the structure being non-centric, the mid-points of the corresponding atoms between the two independent molecules were calculated. They all appeared to have approximately the same mid-point (0.12 0.11 -0.39), suggesting the existence of centrosymmetry. It seemed that these two independent molecules have a centrosymmetry at (0 0 -1/2). The new positions for all bromine, iron, nitrogen, and oxygen atoms, for both molecules, were calculated assuming their mid-points to lie at (0 0 -1/2) (or in other words assuming that they have centrosymmetry at this point). A difference Fourier map was calculated with the new positions calculated for four bromine, two iron, four nitrogen, and five oxygen atoms of one molecule, assuming that the other molecule will be generated by this mid-point. 6 Cycles of full matrix least squares refinement calculations led to $R = 0.30$. All the 40 carbon atoms were located. A further 9 cycles of Fourier difference and least squares refinement calculations, assigning to four bromine, two iron, and the bridging oxygen atoms anisotropic thermal parameters, with all 40 carbon atoms included, gave $R = 0.07$. 19 Of the 24 hydrogen atoms were located. During the next 6 cycles of Fourier difference and full matrix least squares refinement calculations, all the remaining atoms, except C(2), C(3), C(7), C(8), and C(9), were refined with

anisotropic thermal parameters. This led to $R = 0.057$. For the next 6 cycles of least squares refinement calculations, all the hydrogen atom co-ordinates were estimated geometrically (assuming $C-H = 1.08 \text{ \AA}$) and for refinement allowed to ride on their respective carbon atom co-ordinates. The refinement was stopped when the calculated parameter shift/e.s.d. ratio fell to a maximum of 0.01. The R-value was 0.052 ($R_w = 0.050$).

The final difference Fourier map showed the mean amplitudes of

$$0.68 > \Delta\rho > 0.73 \text{ e/\AA}^3$$

The highest residual electron density of 0.68 e/\AA^3 was observed near atom Fe(1).

7.3 DESCRIPTION OF STRUCTURES

7.3.1 Cu(DIBrSALEN)

The compound Cu(diBrsalen) has the structure shown in Figure 7.1 which shows the important bond lengths and angles together with the numbering scheme. The complete data for bond lengths and angles are given in Tables 7.3 and 7.4. The ORTEP drawings are in Drawing 7.1.

The molecular framework (excluding the atoms C(9a), C(9b) and Cu) consists of two planes, one each either side of the imaginary line D (Diagram 7.1). If one draws a line along the axis Br(a) and Br(b) the two planes show a rotation of 30° around this line with respect to each other.

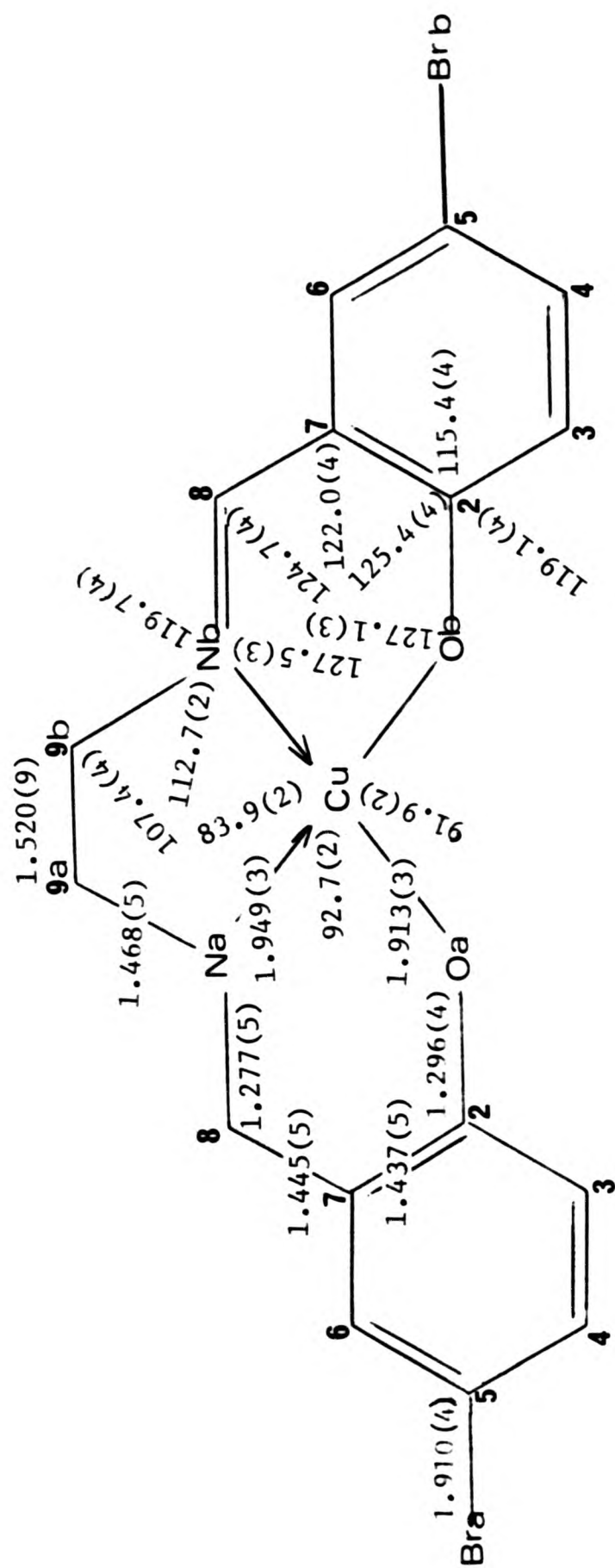


Figure 7.1

Table 7.3: Bond lengths (Å) for Cu(DIBrSALEN)

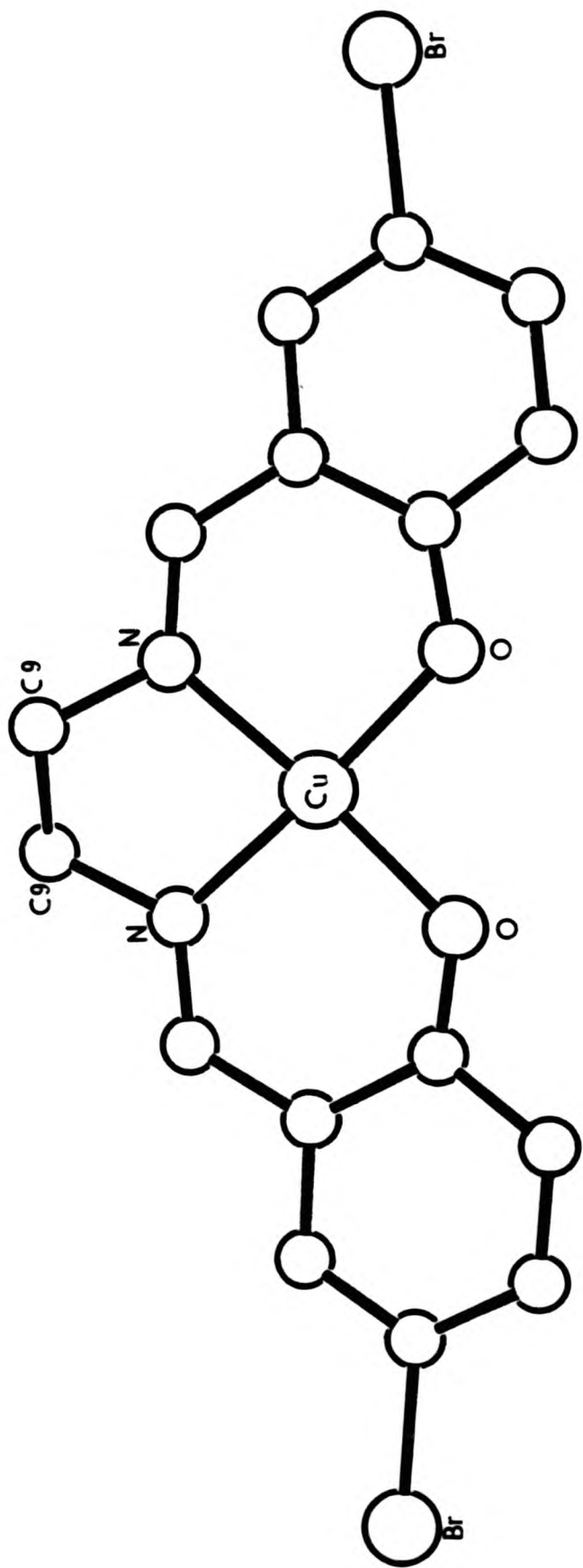
Br(a) -C(5a)	1.905(6)	Cu -Na	1.948(4)
Cu -Nb	1.951(4)	Cu -Oa	1.918(3)
Cu -Ob	1.909(4)	Br(b) -C(5b)	1.915(5)
Na -C(8a)	1.275(7)	Na -C(9a)	1.469(7)
Nb -C(9b)	1.468(7)	Nb -C(8b)	1.279(7)
Oa -C(2a)	1.287(6)	Ob -C(2b)	1.305(7)
C(2a) -C(3a)	1.434(7)	C(2a) -C(7a)	1.443(7)
C(3a) -C(4a)	1.366(8)	C(4a) -C(5a)	1.415(8)
C(5a) -C(6a)	1.353(8)	C(6a) -C(7a)	1.411(8)
C(7a) -C(8a)	1.443(8)	C(9a) -C(9b)	1.520(9)
C(8b) -C(7b)	1.447(7)	C(7b) -C(6b)	1.405(7)
C(7b) -C(2b)	1.431(7)	C(6b) -C(5b)	1.351(8)
C(5b) -C(4b)	1.393(8)	C(4b) -C(3b)	1.372(9)
C(3b) -C(2b)	1.432(8)		
C(3a) -H(3a)	.77(6)	C(4a) -H(4a)	1.03(5)
C(6a) -H(6a)	.72(6)	C(7a) -H(6a)	1.82(6)
C(8a) -H(8a)	.93(6)	C(9a) -H(9a1)	1.06(6)
C(9a) -H(9a2)	1.20(5)	C(9b) -H(9b1)	.83(6)
C(9b) -H(9b2)	1.02(6)	C(8b) -H(8b)	1.06(7)
C(6b) -H(6b)	1.00(7)	C(4b) -H(4b)	1.02(7)
C(3b) -H(3b)	.86(7)		

Table 7.4: Bond angles ($^{\circ}$) for Cu(DIBrSALEN)

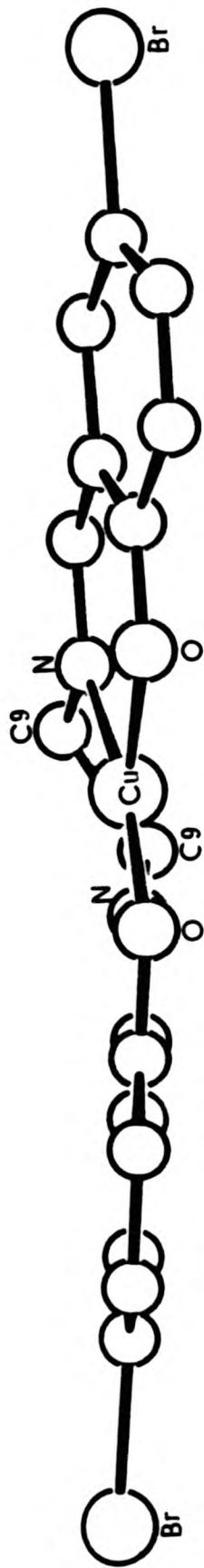
Nb	-Cu	-Na	83.9(2)	Oa	-Cu	-Na	92.8(2)
Oa	-Cu	-Nb	170.4(2)	Ob	-Cu	-Na	171.5(2)
Ob	-Cu	-Nb	92.6(2)	Ob	-Cu	-Oa	91.9(2)
C(8a)	-Na	-Cu	127.4(4)	C(9a)	-Na	-Cu	112.8(3)
C(9a)	-Na	-C(8a)	119.7(5)	C(9b)	-Nb	-Cu	112.6(4)
C(8b)	-Nb	-Cu	127.6(4)	C(8b)	-Nb	-C(9b)	119.8(5)
C(2a)	-Oa	-Cu	127.4(3)	C(2b)	-Ob	-Cu	126.7(4)
C(3a)	-C(2a)	-Oa	120.1(5)	C(7a)	-C(2a)	-Oa	125.1(5)
C(7a)	-C(2a)	-C(3a)	114.8(5)	C(4a)	-C(3a)	-C(2a)	123.5(6)
C(5a)	-C(4a)	-C(3a)	119.3(6)	C(4a)	-C(5a)	-Br(a)	119.4(4)
C(6a)	-C(5a)	-Br(a)	120.2(4)	C(6a)	-C(5a)	-C(4a)	120.3(5)
C(7a)	-C(6a)	-C(5a)	121.3(6)	C(6a)	-C(7a)	-C(2a)	120.6(5)
C(8a)	-C(7a)	-C(2a)	122.2(5)	C(8a)	-C(7a)	-C(6a)	117.2(5)
C(7a)	-C(8a)	-Na	124.8(5)	C(9b)	-C(9a)	-Na	108.1(5)
C(9a)	-C(9b)	-Nb	106.7(5)	C(7b)	-C(8b)	-Nb	124.6(5)
C(6b)	-C(7b)	-C(8b)	117.9(5)	C(2b)	-C(7b)	-C(8b)	121.8(5)
C(2b)	-C(7b)	-C(6b)	120.3(5)	C(5b)	-C(6b)	-C(7b)	120.8(5)
C(6b)	-C(5b)	-Br(b)	118.9(4)	C(4b)	-C(5b)	-Br(b)	119.9(4)
C(4b)	-C(5b)	-C(6b)	121.2(5)	C(3b)	-C(4b)	-C(5b)	119.5(6)
C(2b)	-C(3b)	-C(4b)	122.1(6)	C(7b)	-C(2b)	-Ob	125.7(5)
C(3b)	-C(2b)	-Ob	118.2(5)	C(3b)	-C(2b)	-C(7b)	116.0(5)

table 7.4: continued

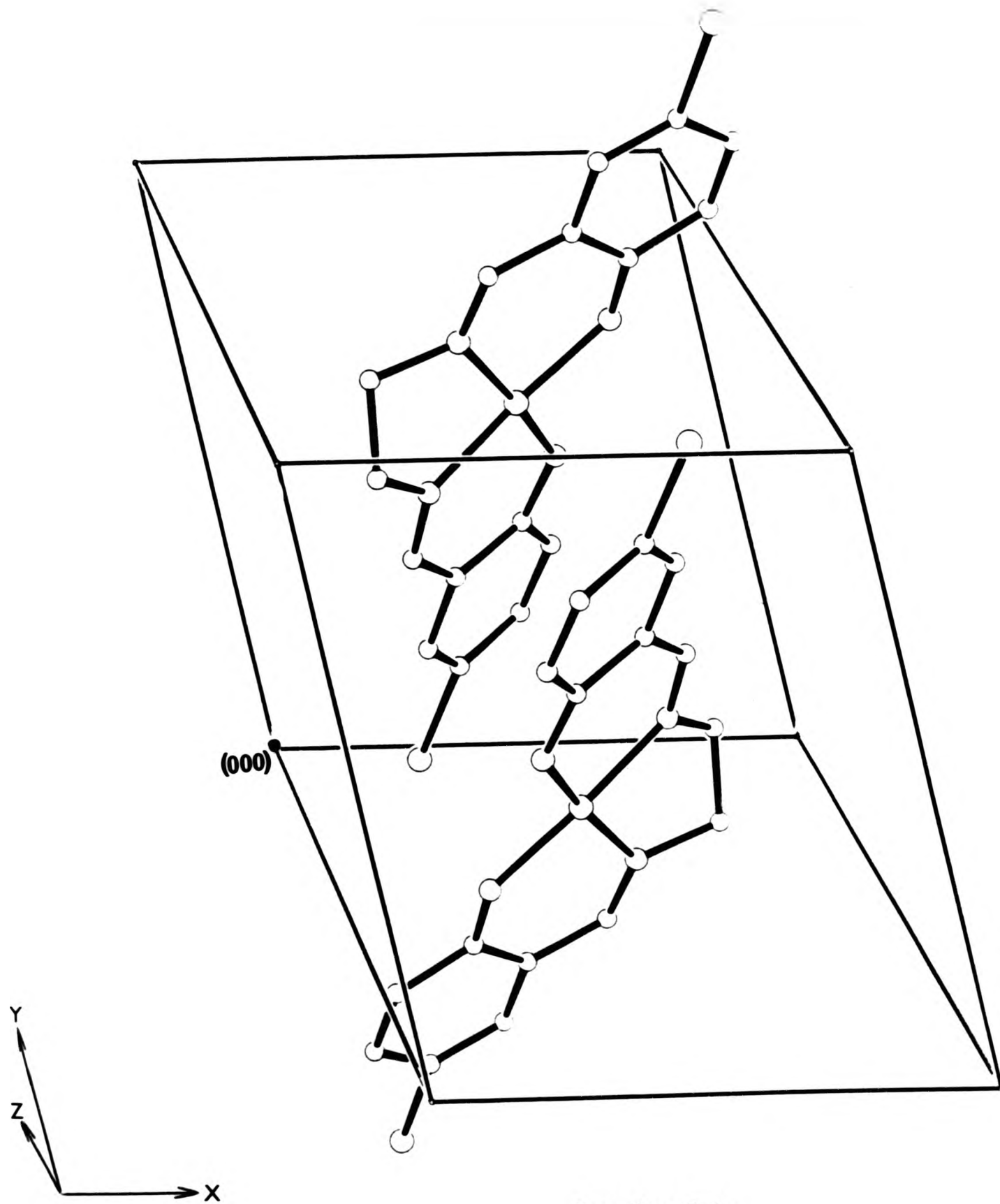
H(3a) -C(3a) -C(2a)	109(5)	H(3a) -C(3a) -C(4a)	127(5)
H(4a) -C(4a) -C(3a)	118(3)	H(4a) -C(4a) -C(5a)	122(3)
H(6a) -C(6a) -C(5a)	125(5)	H(6a) -C(6a) -C(7a)	113(5)
H(6a) -C(7a) -C(2a)	141(2)	H(6a) -C(7a) -C(6a)	21(2)
H(6a) -C(7a) -C(8a)	96(2)	H(8a) -C(8a) -Na	111(3)
H(8a) -C(8a) -C(7a)	124(3)	H(9a1)-C(9a) -Na	114(3)
H(9a1)-C(9a) -C(9b)	104(3)	H(9a2)-C(9a) -Na	112(3)
H(9a2)-C(9a) -C(9b)	100(3)	H(9a2)-C(9a) -H(9a1)	116(4)
H(9b1)-C(9b) -Nb	98(4)	H(9b1)-C(9b) -C(9a)	110(4)
H(9b2)-C(9b) -Nb	104(3)	H(9b2)-C(9b) -C(9a)	111(3)
H(9b2)-C(9b) -H(9b1)	123(5)	H(8b) -C(8b) -Nb	115(4)
H(8b) -C(8b) -C(7b)	121(4)	H(6b) -C(6b) -C(7b)	118(4)
H(6b) -C(6b) -C(5b)	122(4)	H(4b) -C(4b) -C(5b)	128(4)
H(4b) -C(4b) -C(3b)	113(4)	H(3b) -C(3b) -C(4b)	125(5)
H(3b) -C(3b) -C(2b)	107(5)	C(7a) -H(6a) -C(6a)	45(4)



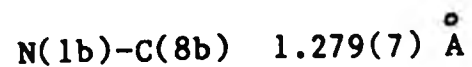
Drawing 7.1a



Drawing 7.1b

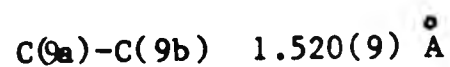


Drawing 7.1c



show the expected double bond character (see section 3.3.1).

The bond length



shows a single bond character which is also expected since both C(9a) and C(9b) are sp^3 -hybridised.

The two chemically equivalent halves do not show any significant differences, although they are crystallographically independent.

7.3.2 Fe(DIBrSALOF)

Fe(diBrsalof) has the structure shown in Figure 7.2, which also shows the numbering scheme together with the important bond lengths and angles. The complete data for bond lengths and angles are in Tables 7.5 and 7.6. The ORTEP drawings for this structure are in Drawing 7.2.

It can be seen that this compound has a μ -oxo-bridge. The two halves of the molecule are chemically equivalent, but crystallographically independent, and show no significant differences.

The Fe(1) and Fe(2) atoms are 5-co-ordinate with square pyramidal configurations. These Fe atoms are located 0.56 and $-0.54 \overset{\circ}{\text{A}}$ away from the best plane of O(1a), O(1b), N(1a), N(1b) and O(1c), O(1d), N(1c), N(1d) respectively. The oxygen and nitrogen atoms lie in their best

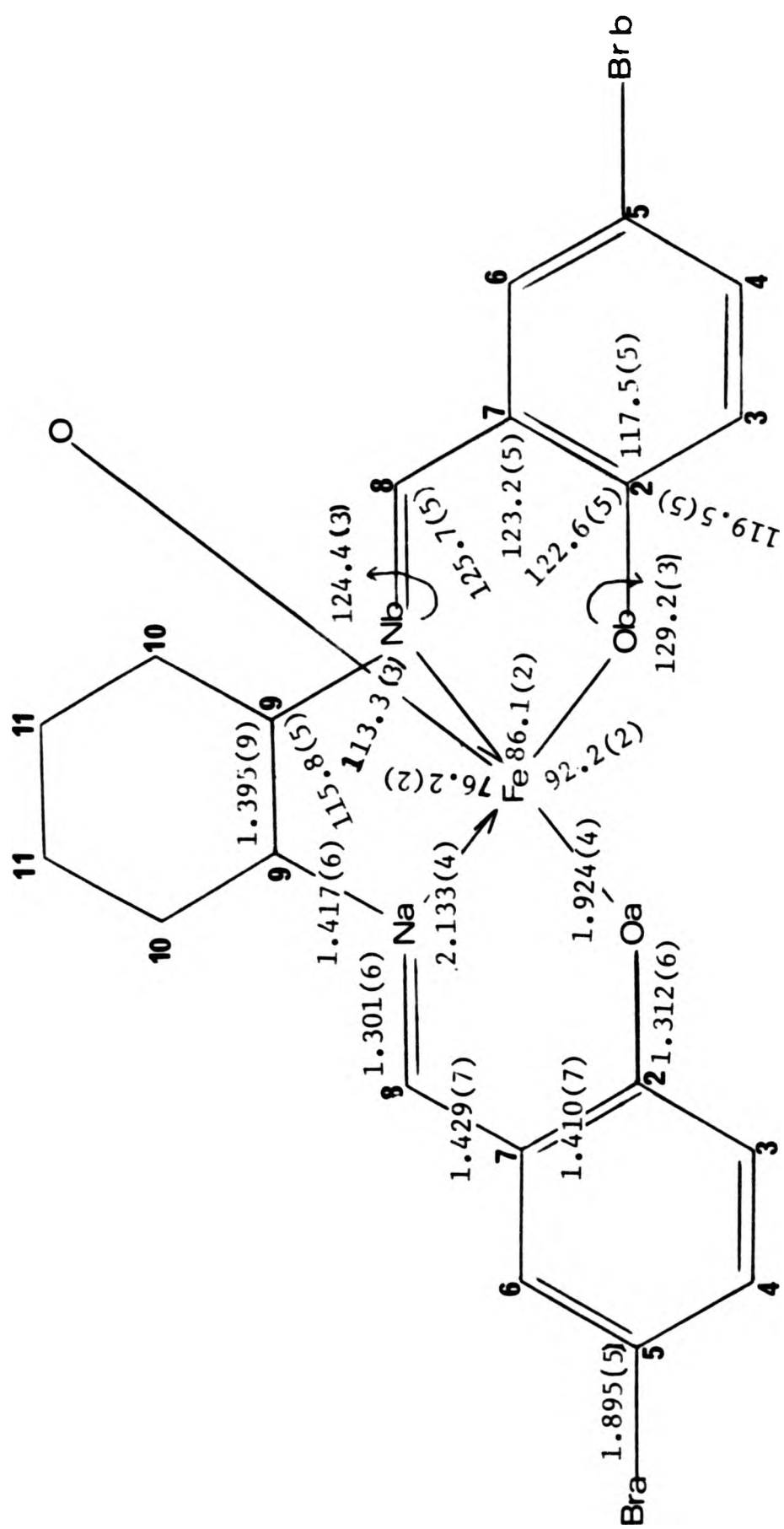


Table 7.5: Bond lengths (Å) for Fe(DIBrSALOF)

O(1) -Fe(1)	1.765(7)	O(1) -Fe(2)	1.774(7)
Fe(1) -N(1a)	2.123(7)	Fe(1) -N(1b)	2.145(8)
Fe(1) -O(1a)	1.932(7)	Fe(1) -O(1b)	1.915(7)
Fe(2) -N(1c)	2.134(8)	Fe(2) -N(1d)	2.133(8)
Fe(2) -O(1c)	1.921(6)	Fe(2) -O(1d)	1.930(6)
Br(a) -C(5a)	1.902(12)	Br(b) -C(5b)	1.896(12)
Br(c) -C(5c)	1.888(9)	Br(d) -C(5d)	1.896(9)
N(1a) -C(8a)	1.319(14)	N(1a) -C(9a)	1.420(11)
N(1b) -C(9b)	1.415(11)	N(1b) -C(8b)	1.299(14)
N(1c) -C(8c)	1.304(11)	N(1c) -C(9c)	1.396(13)
N(1d) -C(9d)	1.438(13)	N(1d) -C(8d)	1.279(11)
O(1a) -C(2a)	1.300(13)	O(1b) -C(2b)	1.294(14)
O(1c) -C(2c)	1.336(10)	O(1d) -C(2d)	1.315(10)
C(2a) -C(3a)	1.413(14)	C(2a) -C(7a)	1.414(12)
C(3a) -C(4a)	1.341(16)	C(4a) -C(5a)	1.389(13)
C(5a) -C(6a)	1.377(14)	C(6a) -C(7a)	1.417(15)
C(7a) -C(8a)	1.426(13)	C(9a) -C(10a)	1.371(12)
C(9a) -C(9b)	1.400(15)	C(10a) -C(11a)	1.404(13)
C(11a) -C(11b)	1.371(16)	C(11b) -C(10b)	1.358(13)
C(10b) -C(9b)	1.419(13)	C(8b) -C(7b)	1.407(12)
C(7b) -C(6b)	1.406(15)	C(7b) -C(2b)	1.428(13)
C(6b) -C(5b)	1.368(13)	C(5b) -C(4b)	1.399(14)
C(4b) -C(3b)	1.368(16)	C(3b) -C(2b)	1.402(13)
C(2c) -C(3c)	1.374(14)	C(2c) -C(7c)	1.428(14)
C(3c) -C(4c)	1.372(13)	C(4c) -C(5c)	1.377(16)

Table 7.5: continued

C(5c) -C(6c)	1.353(16)	C(6c) -C(7c)	1.409(12)
C(7c) -C(8c)	1.412(13)	C(9c) -C(10c)	1.415(15)
C(9c) -C(9d)	1.389(12)	C(10c)-C(11c)	1.371(17)
C(11c)-C(11d)	1.377(14)	C(11d)-C(10d)	1.392(16)
C(10d)-C(9d)	1.382(15)	C(8d) -C(7d)	1.464(14)
C(7d) -C(6d)	1.390(12)	C(7d) -C(2d)	1.392(14)
C(6d) -C(5d)	1.396(15)	C(5d) -C(4d)	1.365(16)
C(4d) -C(3d)	1.374(12)	C(3d) -C(2d)	1.416(14)

Table 7.6: Bond angles ($^{\circ}$) for Fe(DIBrSALOF)

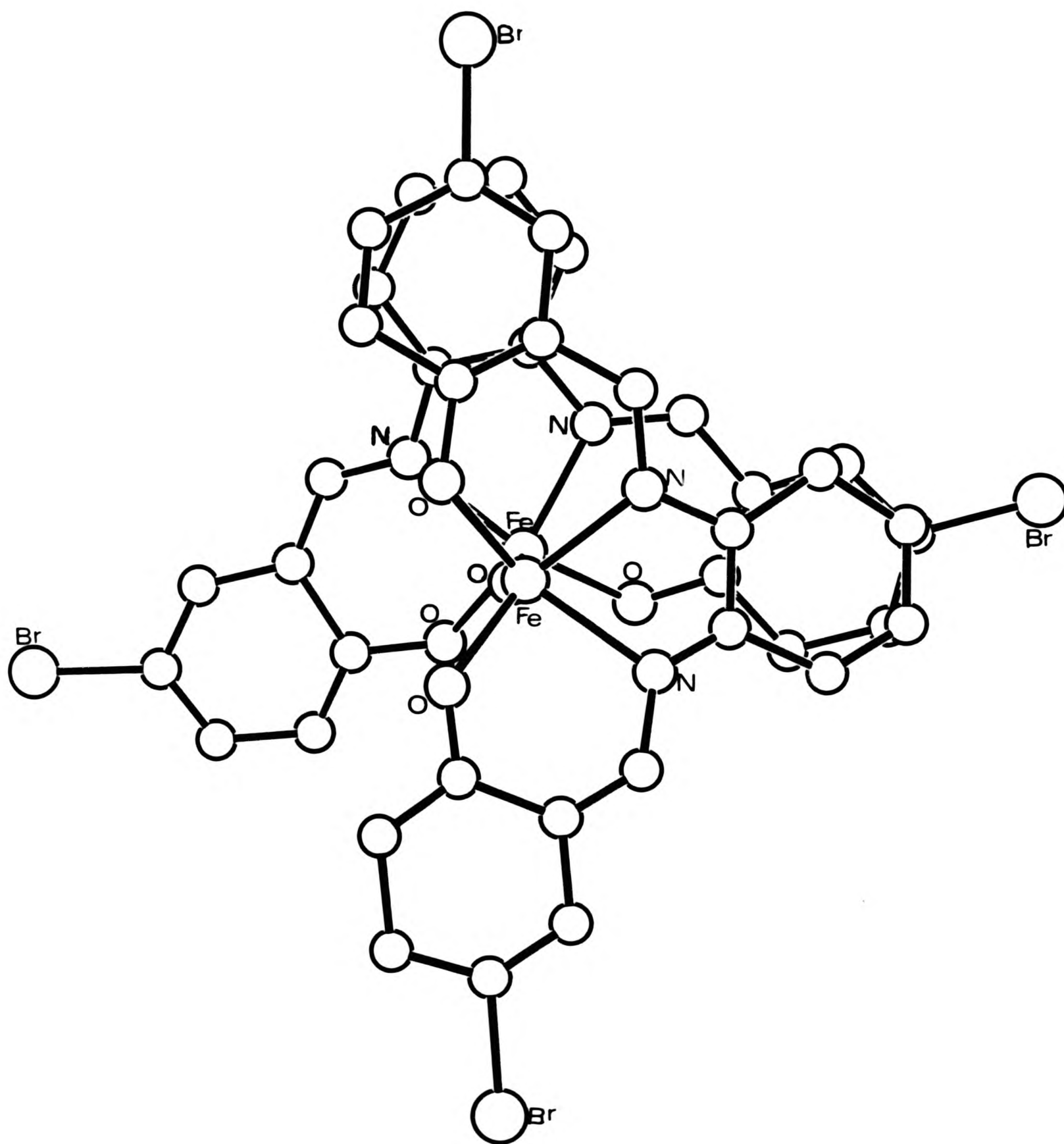
Fe(2) -O(1) -Fe(1)	165.8(4)	N(1a) -Fe(1) -O(1)	102.0(3)
N(1b) -Fe(1) -O(1)	100.9(3)	N(1b) -Fe(1) -N(1a)	75.9(3)
O(1a) -Fe(1) -O(1)	110.2(3)	O(1a) -Fe(1) -N(1a)	86.8(3)
O(1a) -Fe(1) -N(1b)	147.0(3)	O(1b) -Fe(1) -O(1)	110.9(3)
O(1b) -Fe(1) -N(1a)	145.0(3)	O(1b) -Fe(1) -N(1b)	86.3(3)
O(1b) -Fe(1) -O(1a)	92.7(3)	N(1c) -Fe(2) -O(1)	102.0(3)
N(1d) -Fe(2) -O(1)	104.5(3)	N(1d) -Fe(2) -N(1c)	76.5(3)
O(1c) -Fe(2) -O(1)	109.2(3)	O(1c) -Fe(2) -N(1c)	87.1(3)
O(1c) -Fe(2) -N(1d)	144.9(3)	O(1d) -Fe(2) -O(1)	109.7(3)
O(1d) -Fe(2) -N(1c)	146.7(3)	O(1d) -Fe(2) -N(1d)	85.9(3)
O(1d) -Fe(2) -O(1c)	91.7(3)	C(8a) -N(1a) -Fe(1)	124.3(6)
C(9a) -N(1a) -Fe(1)	114.1(6)	C(9a) -N(1a) -C(8a)	120.5(7)
C(9b) -N(1b) -Fe(1)	111.9(7)	C(8b) -N(1b) -Fe(1)	124.3(6)
C(8b) -N(1b) -C(9b)	123.5(8)	C(8c) -N(1c) -Fe(2)	123.9(7)
C(9c) -N(1c) -Fe(2)	114.0(5)	C(9c) -N(1c) -C(8c)	121.9(8)
C(9d) -N(1d) -Fe(2)	113.5(5)	C(8d) -N(1d) -Fe(2)	125.2(7)
C(8d) -N(1d) -C(9d)	121.0(8)	C(2a) -O(1a) -Fe(1)	129.7(6)
C(2b) -O(1b) -Fe(1)	131.7(6)	C(2c) -O(1c) -Fe(2)	127.6(6)
C(2d) -O(1d) -Fe(2)	130.0(6)	C(3a) -C(2a) -O(1a)	120.1(8)
C(7a) -C(2a) -O(1a)	122.4(9)	C(7a) -C(2a) -C(3a)	117(1)
C(4a) -C(3a) -C(2a)	121.6(8)	C(5a) -C(4a) -C(3a)	121.3(9)
C(4a) -C(5a) -Br(a)	120.9(8)	C(6a) -C(5a) -Br(a)	119.1(7)
C(6a) -C(5a) -C(4a)	120(1)	C(7a) -C(6a) -C(5a)	119.6(8)
C(6a) -C(7a) -C(2a)	119.9(9)	C(8a) -C(7a) -C(2a)	124.4(9)
C(8a) -C(7a) -C(6a)	115.7(8)	C(7a) -C(8a) -N(1a)	124.7(8)

Table 7.6: continued

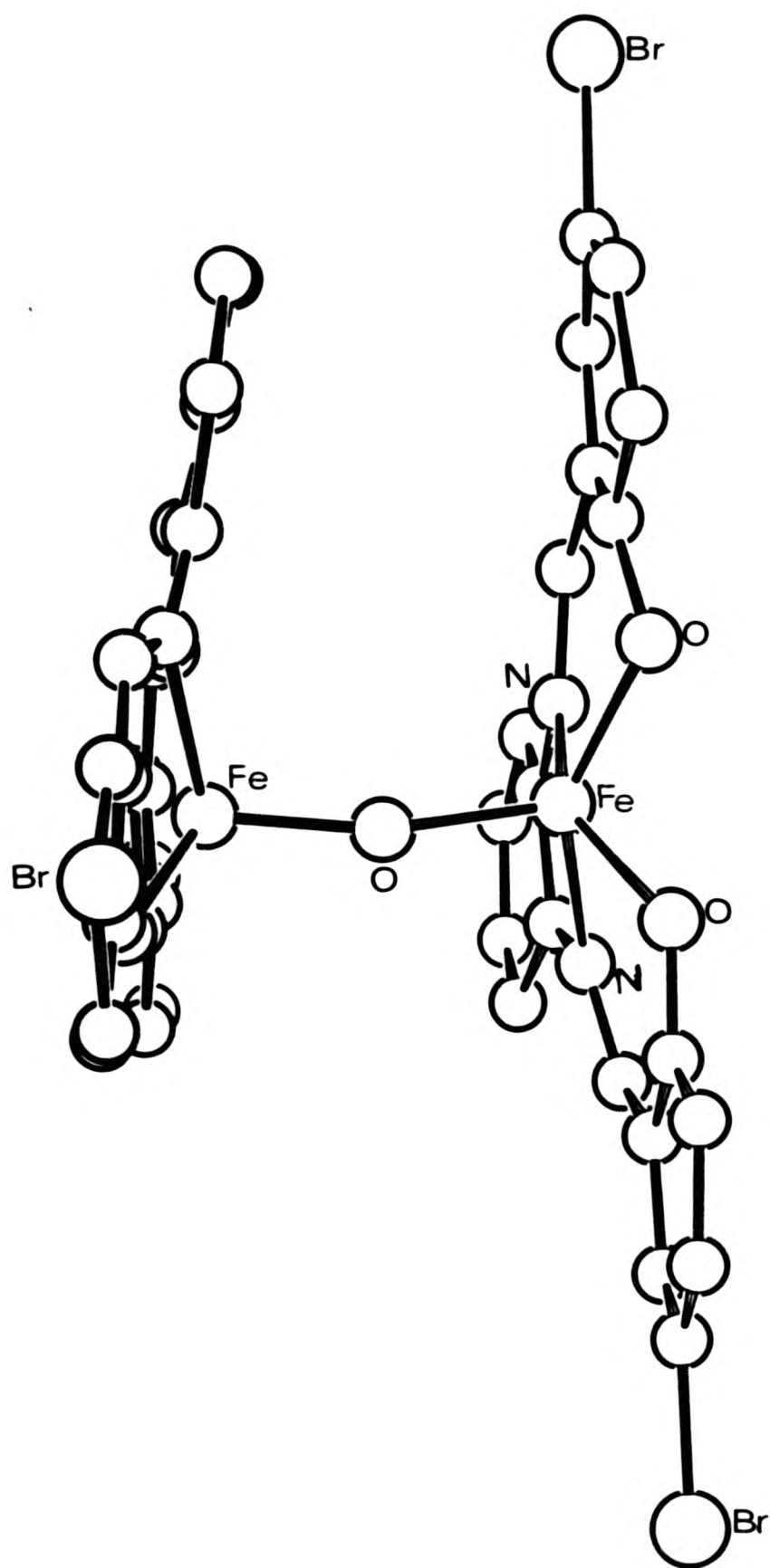
C(10a)-C(9a) -N(1a)	126.7(9)	C(9b) -C(9a) -N(1a)	114.2(7)
C(9b) -C(9a) -C(10a)	119.0(8)	C(11a)-C(10a)-C(9a)	122(1)
C(11b)-C(11a)-C(10a)	117.6(9)	C(10b)-C(11b)-C(11a)	123.4(9)
C(9b) -C(10b)-C(11b)	118(1)	C(9a) -C(9b) -N(1b)	117.1(8)
C(10b)-C(9b) -N(1b)	123.1(9)	C(10b)-C(9b) -C(9a)	119.7(8)
C(7b) -C(8b) -N(1b)	126.0(9)	C(6b) -C(7b) -C(8b)	117.3(8)
C(2b) -C(7b) -C(8b)	123(1)	C(2b) -C(7b) -C(6b)	119.3(8)
C(5b) -C(6b) -C(7b)	121.1(9)	C(6b) -C(5b) -Br(b)	121.4(8)
C(4b) -C(5b) -Br(b)	118.1(8)	C(4b) -C(5b) -C(6b)	120(1)
C(3b) -C(4b) -C(5b)	118.8(9)	C(2b) -C(3b) -C(4b)	123.3(9)
C(7b) -C(2b) -O(1b)	122.5(8)	C(3b) -C(2b) -O(1b)	120.5(9)
C(3b) -C(2b) -C(7b)	117(1)	C(3c) -C(2c) -O(1c)	120.2(9)
C(7c) -C(2c) -O(1c)	122.2(8)	C(7c) -C(2c) -C(3c)	117.6(8)
C(4c) -C(3c) -C(2c)	122(1)	C(5c) -C(4c) -C(3c)	120(1)
C(4c) -C(5c) -Br(c)	120.6(8)	C(6c) -C(5c) -Br(c)	119.3(8)
C(6c) -C(5c) -C(4c)	120.1(9)	C(7c) -C(6c) -C(5c)	121(1)
C(6c) -C(7c) -C(2c)	118.9(9)	C(8c) -C(7c) -C(2c)	123.7(8)
C(8c) -C(7c) -C(6c)	117.4(9)	C(7c) -C(8c) -N(1c)	126(1)
C(10c)-C(9c) -N(1c)	124.3(8)	C(9d) -C(9c) -N(1c)	117.1(8)
C(9d) -C(9c) -C(10c)	118.7(9)	C(11c)-C(10c)-C(9c)	118.9(9)
C(11d)-C(11c)-C(10c)	122(1)	C(10d)-C(11d)-C(11c)	119(1)
C(9d) -C(10d)-C(11d)	119.4(9)	C(9c) -C(9d) -N(1d)	115.4(8)
C(10d)-C(9d) -N(1d)	123.2(8)	C(10d)-C(9d) -C(9c)	121.4(9)
C(7d) -C(8d) -N(1d)	125.7(9)	C(6d) -C(7d) -C(8d)	117.3(9)
C(2d) -C(7d) -C(8d)	122.0(8)	C(2d) -C(7d) -C(6d)	120.7(9)
C(5d) -C(6d) -C(7d)	120(1)	C(6d) -C(5d) -Br(d)	119.7(8)
C(4d) -C(5d) -Br(d)	120.3(7)	C(4d) -C(5d) -C(6d)	120.0(8)
C(3d) -C(4d) -C(5d)	121(1)	C(2d) -C(3d) -C(4d)	120.8(9)

Table 7.6: continued

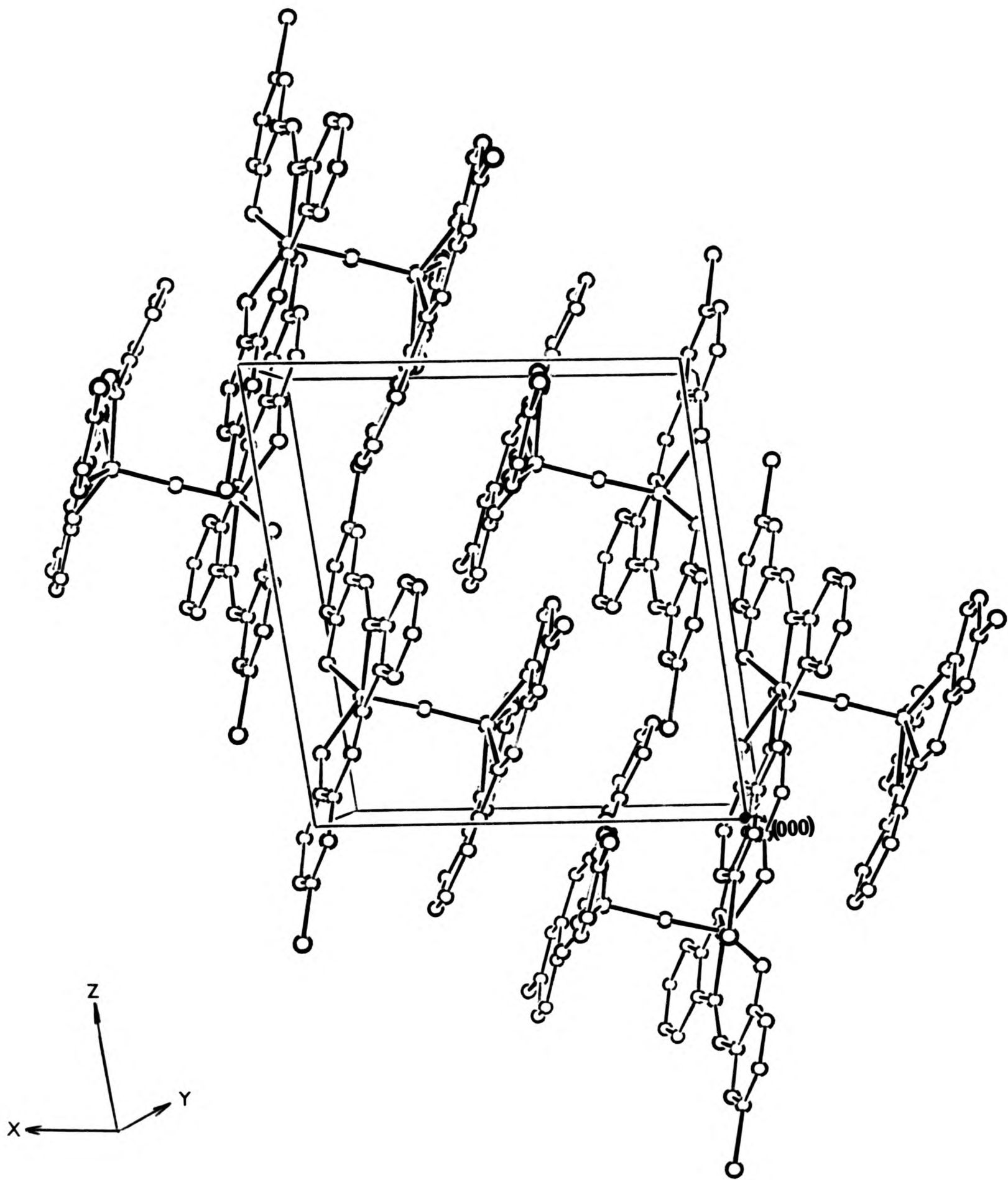
C(7d) -C(2d) -O(1d)	124.0(9)	C(3d) -C(2d) -O(1d)	118.2(9)
C(3d) -C(2d) -C(7d)	117.9(8)		



Drawing 7.2a



Drawing 7.2b



Drawing 7.2c

planes.

The angles and bond lengths of the μ -oxo-bridge 164.9° (average) and $1.787(7) \text{ \AA}$ (average) fall centrally within the range of values ($139-180^\circ$ and $1.76-1.80 \text{ \AA}$) observed in related 5-co-ordinate Fe(III) complexes.² (See also Table 8.4.)

In each half of the dimer the two bromine atoms are on an axis occupying the two extreme ends of the ligand. The axes of the two ligands make an angle of $\sim 90^\circ$ with each other.

The average bond length

Fe-N $2.133(4) \text{ \AA}$

is longer than the average bond length

Fe-O $1.924(4) \text{ \AA}$

7.4 COMPARISON OF THE STRUCTURES OF THE BROMINATED SCHIFF BASE METAL COMPLEXES

It will be useful to discuss the two brominated Schiff base complexes together, as they have some, but not all, structural features in common. As the crystal structure determination of the copper complex is rather more accurate than that of the iron compound, the former will be discussed in somewhat greater detail.

As mentioned in section 1.2.4, the structures of Cu(salen),

unsolvated and solvated, have been investigated, as have been other related derivatives with modified substituents on the imine nitrogen atoms. No structure has as yet been reported with modifications in the benzo ring. R. Peters¹ of this Department investigated the bromination of Cu(salen) and prepared a dibromo derivative of unknown structure. This compound was investigated as part of the present study. The copper complex is found to be unsolvated and monomeric, with the bromine atoms in para-positions relative to the phenolic oxygen atoms. It has been mentioned earlier in this Thesis, in connection with $\text{TAABH}_2(\text{PICRATE})_2$, that bond length and angle data suggest considerable back-donation from the lone pairs of the phenolic oxygen atom towards the benzene ring. This delocalisation will be less, though still pronounced, in neutral phenolic derivatives (Diagram 7.2).

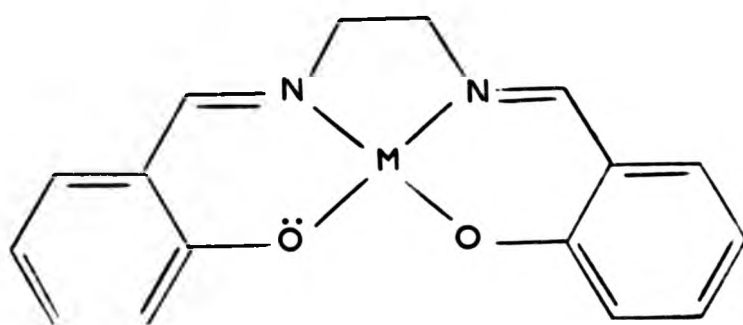


Diagram 7.2

This implies activation of the benzene ring towards electrophilic substitution and a p-derivative is in accord with this. The copper-oxygen bond distances of 1.913(2) Å (average) are somewhat shorter than the copper-nitrogen bond lengths 1.949(3) Å (average), in line with most other findings (Table 7.7).

The geometry of the immediate co-ordination sphere of copper in this

compound is compared with some related ones in Table 7.7. The values reported for the present structure fall centrally within the range described in this Table. The N(a)-Cu-O(b) angle (Figure 7.1) deviates slightly from 180° being 171° . The angle N-Cu-N in the 5-membered ring is smaller [$83.9(2)^\circ$] than that of N-Cu-O [$92.6(1)^\circ$] in the 6-membered ring, as observed in other structures (see Chapter 8).

Table 7.7: The geometry around the copper atom in Schiff base complexes

Compound	Cu-O Å	Cu-N Å	N-Cu-N $^\circ$	N-Cu-O $^\circ$
Present structure	1.913(2)	1.950(3)	83.9(2)	92.6(1)
Cu(salen)tu ³	1.890(4)	1.931(4)	84.8(2)	94.0(1)
Cu(salof)tu ³	1.896(3)	1.954(3)	84.2(1)	94.3(1)
Cu(salen).p-nitrophenol ⁴	1.896	1.916	82.7	94.8
Cu(salen).chloroform ⁵	1.91	1.94	84.7	92.4
Cu(salen) ⁶	1.97	2.01	82.0	92.5

As in earlier sections on TAAB salts (section 3.3.1), AA derivatives (section 4.4), and other metal complexes (sections 5.3 and 6.3), one conventional valence bond formula is not sufficient to describe the structure, and quinonoid resonance forms have to be invoked.

In both structures the C-O bond is short 1.296(4) Å (Cu) and 1.312(6) Å (Fe), and the adjacent internal bond angles in the benzo ring are small, C(7)-C(2)-C(3) = $115.4(4)^\circ$ (Cu), $117.5(5)^\circ$ (Fe), indicative

according to Domenicano and Vaciago⁷ of π -conjugation in the C-O bond. Domenicano and Vaciago⁷ discussed this π -conjugation and its effect on the geometry of the benzene ring with special reference to the tetraphenyl borate ion, which is shown in Diagram 7.3 together with the relevant segments of the present two structures.

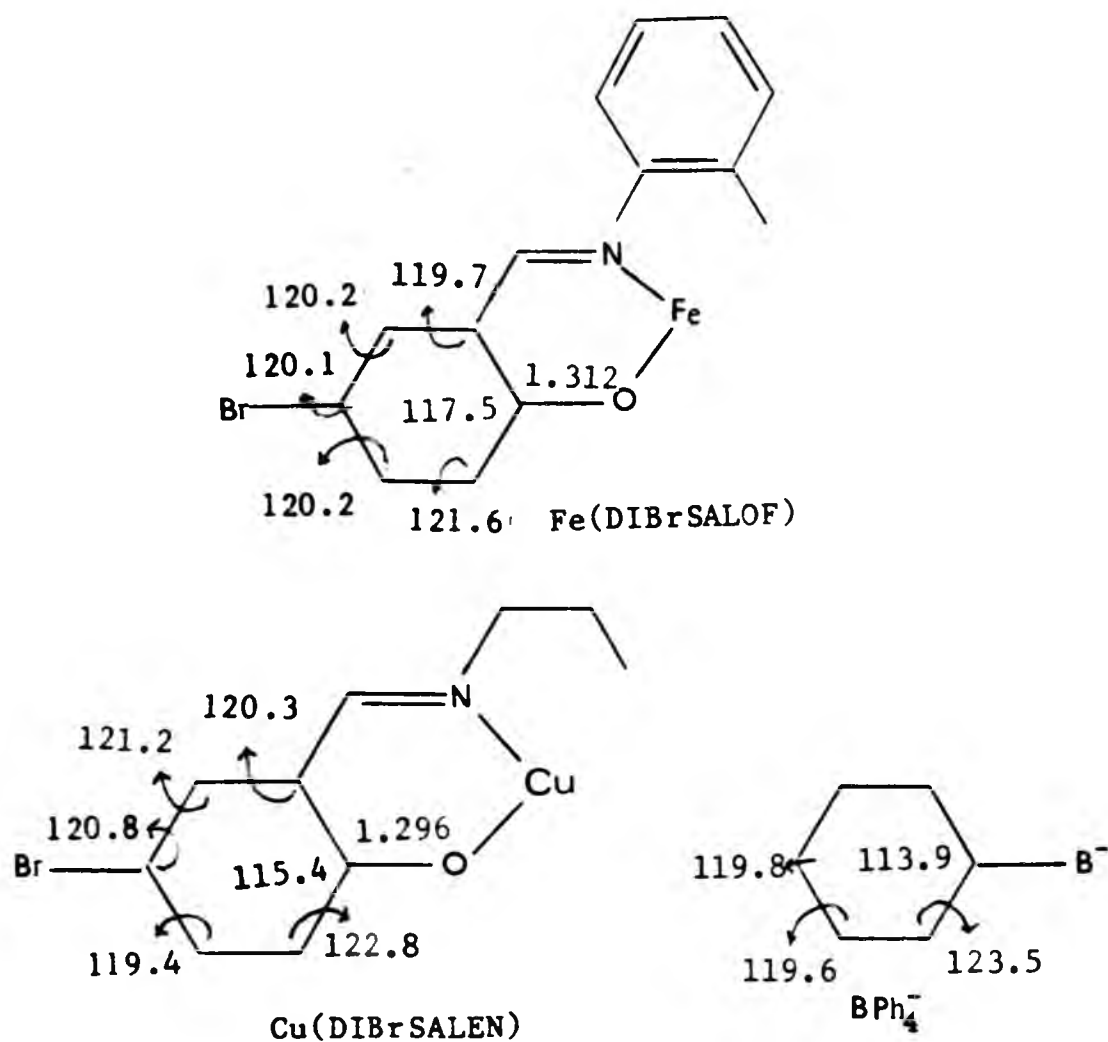


Diagram 7.3

In the copper compound the bonds $C(3)-C(4) = 1.369(6)$ Å and $C(5)-C(6) = 1.352(6)$ Å are significantly shorter than the other bonds in that ring, this being some evidence for a contribution from resonance form (B) (see Diagram 7.4).

The bond $C(7)-C(8) = 1.445(5)$ Å is, however, somewhat shorter than the value of 1.485 Å for bonds of this type⁸ without any π -conjugation.

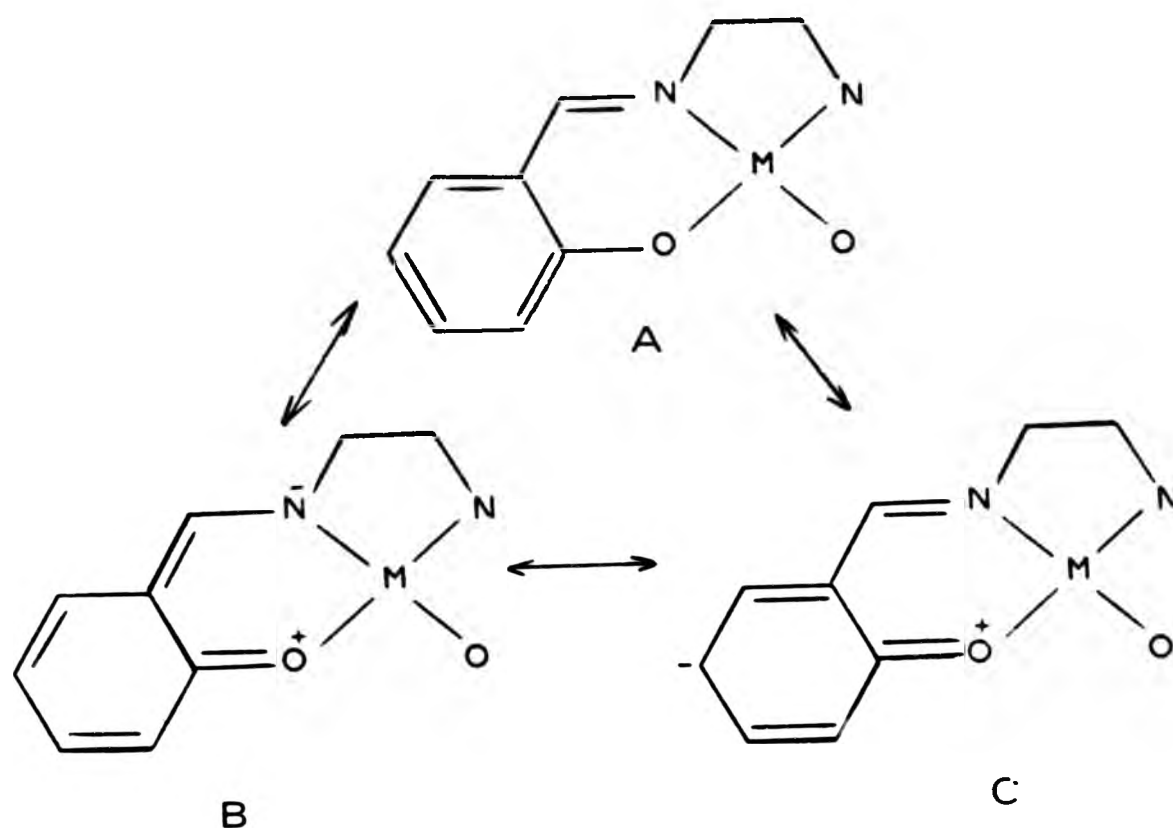


Diagram 7.4

However it is not as short as the corresponding bond in the iron complex and hence resonance form (C) will make also a contribution. The bond $C(8)-N(1) = 1.277(5) \text{ \AA}$ is somewhat shorter in the copper complex than the corresponding bond in the iron complex $1.301(6) \text{ \AA}$, which is in line with the previous observation.

In the iron complex the bonds $C(7)-C(8) = 1.429(7) \text{ \AA}$ and $N(1)-C(9) = 1.417(6) \text{ \AA}$ are both short for sp^2-sp^2 -bonds without π -conjugation and hence resonance form (B) (see Diagram 7.5) must be important for this compound.

The C-O bond length and the adjacent internal benzene ring bond angle indicate that the electron drift involved in the resonance forms (B) and (C) (Diagrams 7.4 and 7.5) is not as pronounced as in the picrate ion $C-O = 1.241 \text{ \AA}$, $C(1)-C(5)-C(6)$ bond angle 111° (see Tables 3.3 and 3.4 in section 3.3.1) and of the same order of magnitude as in

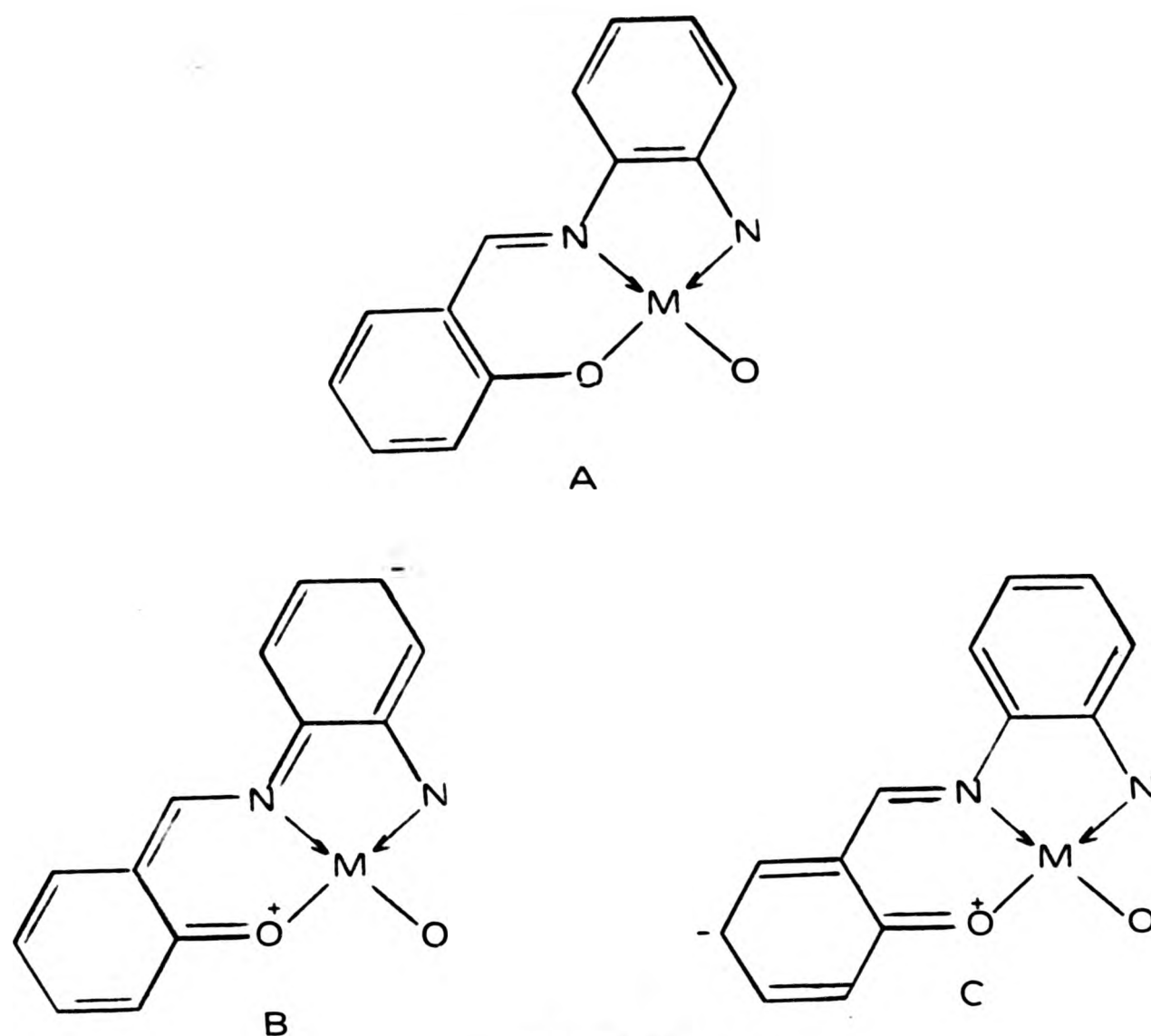


Diagram 7.5

picric acid $C-O = 1.324 \text{ \AA}$, bond angle $C(1)-C(5)-C(6) 115.5^\circ$ (see Tables 3.3 and 3.4 in section 3.3.1). This back-conjugation in picric acid is rather more pronounced than in other phenols, $C-O = 1.36 \text{ \AA}$.⁹ Undoubtedly the electron-withdrawing power of the three nitro groups in picric acid is responsible for this.

REFERENCES

1. R. Peters, Ph. D. Thesis, CNAAs, 1981.
2. B. Kamenar and B. Kaitner, in "Structural Studies on Molecules of Biological Interest", G. Dodson, J. Glusker, and D. Sayre, Edts., Oxford University Press, 1981, p. 123.
3. M. B. Ferrari, G. G. Fava, and C. Pelizzi, *Acta Cryst.*, 1976, B32, 901.
4. E. N. Baker, D. Hall, and T. N. Waters, *J. Chem. Soc. (A)*, 1970, 400.
5. *Idem*, *ibid.*, p. 405
6. D. Hall and T. N. Waters, *J. Chem. Soc.*, 1960, 2644.
7. A. Domenicano and A. Vaciago, *Acta Cryst.*, 1979, B35, 1382.
8. M. J. S. Dewar, "Hyperconjugation", The Ronald Press Co., New York, 1962, ch. 3; M. J. S. Dewar and H. N. Schmeising, *Tetrahedron*, 1959, 5, 166; 1960, 11, 196.
9. "Interatomic Distances Supplement", Edt. L. E. Sutton, Special Publication 18, The Chemical Society, London, 1965, p. S20s.

CHAPTER 8

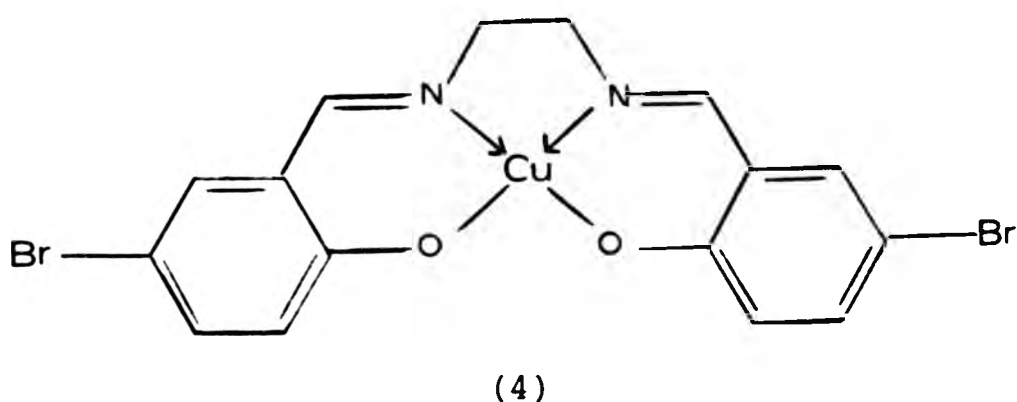
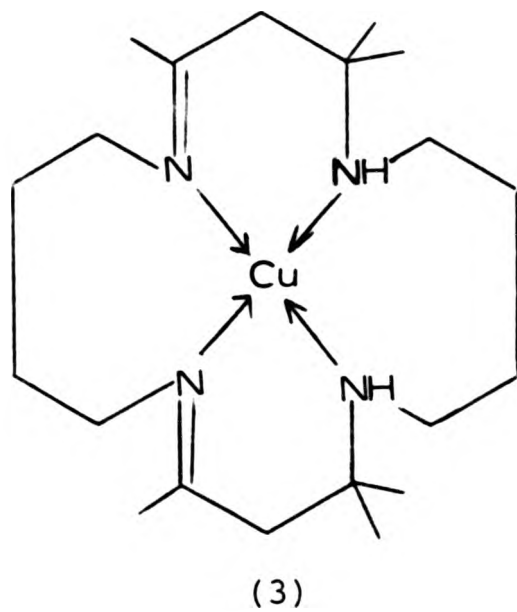
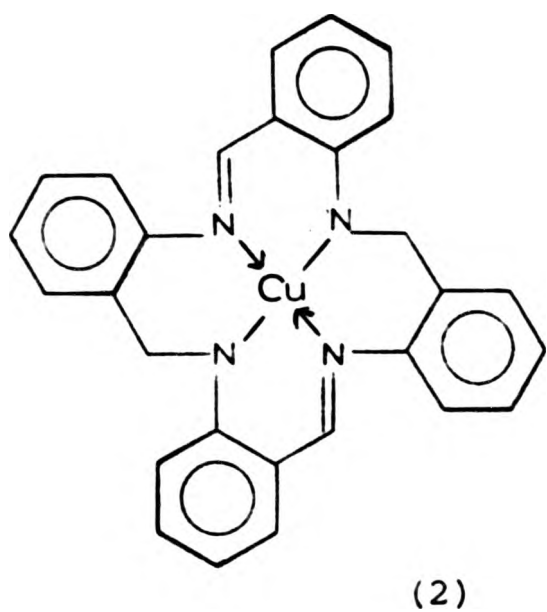
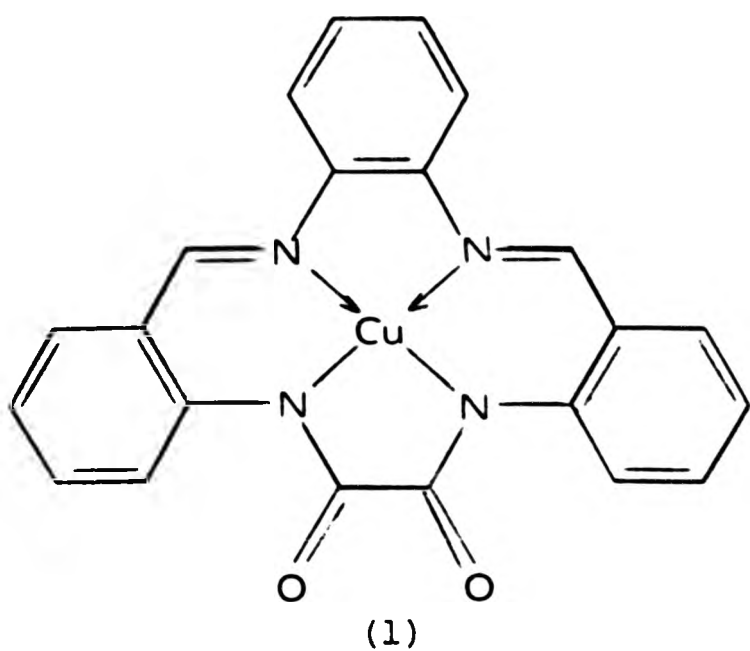
A COMPARISON OF THE METAL COMPLEXES DESCRIBED IN THIS THESIS

The three copper complexes, which have been investigated in the present study, all have the copper atom 4-co-ordinate. No other donor atom approaches to the copper atom closer than 3.5 Å.

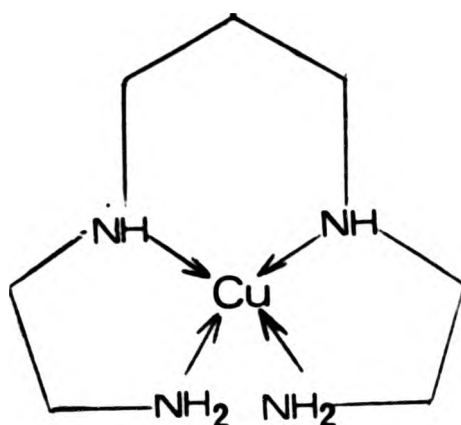
CuDIKETO, (1), and Cu(TAABH₂), (2), together with the structure, (3), reported by Martell,¹ make up a set of 14-, 16-, and 18-membered tetra-azamacrocyclic complexes. The 14-membered ring complex, CuDIKETO, (1), has a structure, where the copper atom is almost square planar (see Table 8.1). In contrast to this, in the other two compounds, (2,3), the copper atom is considerably distorted towards the tetrahedral arrangement, with that in Cu(TAABH₂), (2), marginally more so than that in the structure reported by Martell, (3). In the above three compounds, the metal containing rings have arrangements 6-,5-,6-,5 for CuDIKETO, (1), 6-,6-,6-,6 for Cu(TAABH₂), (2), and 6-,7-,6-,7 for the structure due to Martell, (3). In Cu(diBrsalen), (4), reported in this Thesis (see section 7.3), the three metal-containing rings have a 6-,5-,6-arrangement and they relate to those in the CuDIKETO, (1), structure. It is noteworthy, that in compound (4), the distortion from planarity, although somewhat greater than that in CuDIKETO, (1), is not as pronounced as in the Cu(TAABH₂), (2), and Martell structures, (3), probably because the 6-,5-,6-,5-arrangement makes lesser steric demands than the other two.

Table 8.1: Comparison of the copper complexes reported in this Thesis

Complex	$\widehat{N(1)-Cu-N(2)}^\circ$	$\widehat{N(2)-Cu-N(3)}^\circ$	$\widehat{N(3)-Cu-N(4)}^\circ$	$\widehat{N(4)-Cu-N(1)}^\circ$	$\widehat{N(1)-Cu-N(3)}^\circ$	$\widehat{N(2)-Cu-N(4)}^\circ$	Reference
CuDIKETO	87.7(1)	94.6(2)	83.3(1)	94.4(1)	177.4(1)	177.6(1)	Chapter 6
Cu(TAABH ₂)	93.0(9)	95.0(10)	91.0(8)	96.4(8)	148.5(7)	152.0(10)	Chapter 5
Cu-Martell	93.3(2)	90.7(2)	90.1(2)	97.5(2)	154.6(2)	152.7(2)	1
	$\widehat{N(1a)-Cu-N(1b)}^\circ$	$\widehat{O(1a)-Cu-O(1b)}^\circ$	$\widehat{N(1a)-Cu-O(1a)}^\circ$	$\widehat{N(1b)-Cu-O(1b)}^\circ$	$\widehat{N(1a)-Cu-O(1b)}^\circ$	$\widehat{N(1b)-Cu-O(1a)}^\circ$	
Cu(diBrsalen)	83.9(2)	91.9(2)	92.8(2)	92.6(2)	171.5(2)	170.4(2)	Chapter 7



In the $\text{Cu}(2,3,2\text{-tet})(\text{ClO}_4)_2$ structure, (5),² again a 5-,6-,5-ring system occurs. Angles at opposite nitrogen atoms again indicate almost complete planarity, and thus, the two long apical bonds to perchlorate ions, hardly affect the stereochemistry. Indeed, the excellent table prepared by Fawcett et al.,² dealing with 6-co-ordinate copper derivatives, allows some insight under which conditions deviations from



(5)

a square planar stereochemistry occurs (see Table 8.2). Those compounds, in Table 8.2, where the two halves of the tetra-aza donor set, are independent, bidentate ligand molecules, give rise to only two metal-containing ring sets. All the 5- and 6-membered ring systems summarized (see Table 8.2), give planar CuN_4 units. In the same table, four sets of fused tricyclic ring systems are compared. The 5-,5-,5- the 6-,6-,6- and the 6-,7-,6-arrangements deviate considerably from planarity, whilst the 5-,6-,5- is almost square planar. The fused tricyclic $\text{Cu}(\text{salen})$ structure has a 6-,5-,6-arrangement and seems to fit in well with the 5-,6-,5-structure reported here, both having alternating 5-,6-arrangements. The fused tetracyclic systems discussed here, have a planar CuN_4 set in the 5-,6-,5-,6-arrangement, (1) whilst the 6-,6-,6-,6- and 6-,7-,6-,7-analogues (2,3) tend towards a tetrahedral structure of the CuN_4 unit.

The above generalization, relating ring size arrangement and copper stereochemistry, applies when the ligands make only small steric demands. There are indications, that bulky substituents on the ligands, particularly if these are in close proximity to one another, can substantially affect the stereochemistry.

Table 8.2: Stereochemistry of some cyclic tetra-aza copper derivatives

Complex	Cu-N (Å)	N-Cu-N°			Cu-L (Å)
		5-ring	6-ring	<u>trans</u>	
Cu(2,2,2-tet)(SCN) ₂ (A)	2.008(7)	84.6(3)		154.0	2.607(2)
	2.030(5)	84.3(2)		161.0	
		87.7(3)			
Cu(2,3,2-tet)(ClO ₄) ₂ (B)	2.016(6)	85.3(2)	93.9(2)	176.4(3)	2.667(5)
	2.032(6)	85.2(2)		178.5(4)	2.527(5)
Cu(3,4,3-tet)(ClO ₄) ₂ (C)	2.008(8)		94.6	159.3	
	2.062(8)		91.1	172.7	
Cu(3,3,3-tet)(ClO ₄) ₂ (D)	2.02(2)		92.7(7)	159.4(7)	
	2.04(2)		97.7(7)	169.4(7)	
			85.3(7)		
Cu(cyclam)(ClO ₄) ₂ (E)	2.02(2)	86.0(2)	94.0(2)	180	2.57
	2.02(4)				
Cu[H ₂ N(CH ₂) ₂ ⁻ CH(NH ₂)CH ₃] ₂ (chair form a)	(Fa) 2.027(7)		93.3(2)	180	2.676(10)
	-2.031(7)				
	same compound (chair form b)	(Fb) 2.018(6)		88.9(3)	180
Cu[H ₂ N(CH ₂) ₃ ⁻ NH ₂] ₂ (NO ₂) ₂ (G)	2.028(6)		86.8(2)	180	2.655(8)
	-2.048(6)				

Table 8.2(continued)

$\text{Cu(en)}_2(\text{BF}_4)_2$	(H)	2.02(1)	86.4(5)	180	2.56(1)
		-2.03(1)			
$\text{Cu}(\text{CH}_3\text{NHCH}_2\text{CH}_2\text{NH}_2)_2$	(I)	2.004(5)			
$(\text{ClO}_4)_2$		-2.066(5)	84.6(2)	180	2.575(6)
$\text{Cu(Pn)}_2(\text{ClO}_4)_2$	(J)	2.01(3)			
		-2.03(3)	86.0	180	2.61(2)

The copper-nitrogen bond can be visualized, to be formed in the above complexes, between the positively charged copper ion and the lone pair of electrons on a nitrogen atom; this atom can be either neutral or anionic. A neutral nitrogen atom will be trigonal planar, if it is of the imine type, but pyramidal, if it is of the amine type. The anionic nitrogen atom can be considered to be derived from the amine type by loss of a proton, and thus will have a pyramidal character. One might expect, different metal-nitrogen bonds, depending on which type of nitrogen atoms (described above), are involved. In the CuDIKETO structure, (1), all the nitrogen atoms are found to be trigonal planar, and the Cu-N distances are found to be almost equal in length. The two bonds from the imine linkages of the Schiff base, and the two, adjacent to the diketo group, are closely similar, because of the nitrogen lone pair delocalisation towards the adjacent benzo ring, as well as to the carbonyl group. The former, is derived from a neutral nitrogen atom, the latter from an anionic one, and the complex, overall, has no charge. In Cu(TAABH₂), (2), two significantly different Cu-N bond lengths are observed. The ones, from the neutral imine type of nitrogen atoms, are significantly longer than those from the negatively charged amine nitrogen atoms. All four nitrogen atoms are 3-co-ordinate. The two imine nitrogen atoms are trigonal planar, whilst the two amine nitrogen atoms differ slightly from this. The sums of the bond angles around these nitrogen atoms are 359.8 and 358.7° respectively. Here, in contrast to the CuDIKETO structure, (1), delocalisation of the lone pairs of the amine nitrogen atoms is only towards the benzo ring. This can be demonstrated from the observed values of the bond lengths and the sums of the bond angles. Again, overall, the complex carries no charge. In the structure of the copper complex reported by Martell, (3), there

are again two different Cu-N bond lengths, and all the four nitrogen atoms are neutral. Two are 3-co-ordinate, of the imine type, and two 4-co-ordinate, of the amine type. As this ligand does not neutralize any charge on the copper atom, the resulting complex is cationic. The Cu-N bonds from the tetrahedral nitrogen atoms are the longer ones. This is in line with the generalization proposed by Curtis.³ The reason is undoubtedly the same as for carbon atoms, bonds from sp^3 -hybridised atoms being longer than those from sp^2 -hybridised ones (see Chapter 3).

In the 14-membered $\text{Cu}(\text{cyclam})^{2+}$ structure⁴ (see Table 8.2), there is only one type of Cu-N bond. All the Cu-N bonds are based on neutral, pyramidal amine nitrogen atoms. These nitrogen atoms have some of the most pyramidal structures encountered in the present discussion, as they are flanked by saturated carbon atoms, which prevent nitrogen lone pair delocalisation. In this case too, the ligand being neutral, the resultant complex is cationic.

Both iron compounds investigated in this study, have Fe-N bond lengths consistent with high spin compounds (see Table 8.3). The parameters for the FeDIKETO complex, (6), are somewhat in between those of $[\text{Fe}(\text{TPP})]_2\text{O}$, (7)⁵, and $[\text{Fe}(\text{C}_{22}\text{H}_{22}\text{N}_4)]_2\text{O}\cdot\text{CH}_3\text{CN}$, (8).⁶ In both of these structures only one Fe-N distance was observed, in contrast to the FeDIKETO derivative, (6), (see section 6.3.1) reported here, where the two pairs of chemically different nitrogen atoms, give rise to two sets of significantly different Fe-N bond lengths.

$\text{Fe}(\text{diBrsalof})$, (9), (see section 7.3.2) has similar parameters to the DIKETO derivative, (6), reported here. The Fe-O-Fe angle is,

Table 8.3: Fe-N(equatorial) bond lengths and spin states of some iron complexes*

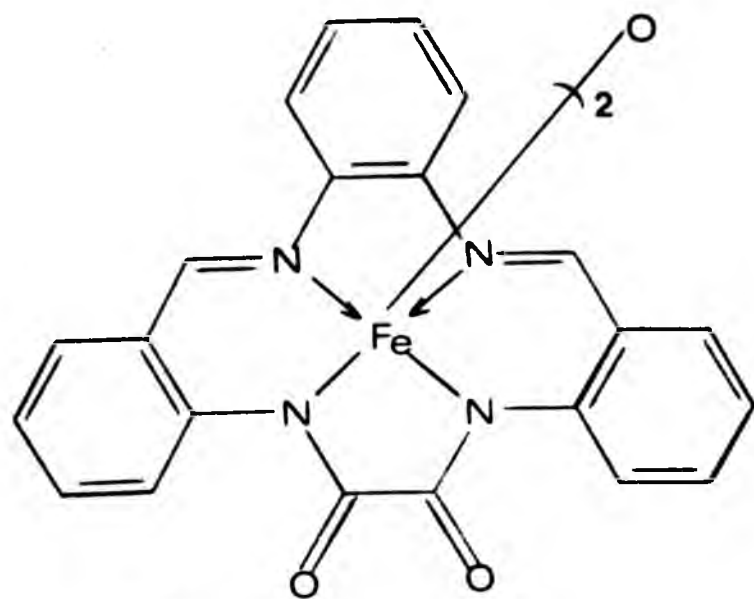
Complex	Co-ord. of Fe	Fe-N (Å)	d (Å)	Spin state
Fe(diBrsalof)	5	2.133(4)	0.54	
FeDIKETO	5	2.039(5)	0.64	
[Fe(TAAB)(OCH ₃) ₂] ₂ O	5	2.067	0.50	high
[Fe(TPP)] ₂ O	5	2.087	0.50	high
[Fe(TPP)] ₂ N	5	1.991	0.32	low(?)
MeOFeMeso	5	2.073	0.455	high or int.
Chlorohemin	5	2.062	0.475	high or int.
Fe(TPP)Cl	5	2.049	0.383	high
Fe(TPP)Br	5	2.069	0.49	high
Fe(TPP)I	5	2.066	0.46	high
Fe(TPP)ClO ₄	5	1.997	0.27	mixed
Fe(PPIXDME)(SC ₆ H ₄ -p-NO ₂)	5	2.064	0.434	high
[Fe(TPP)(Im) ₂]Cl·CH ₃ OH	6	1.989	0.009	low
[Fe(1-Me-Im) ₂ (PPIX)]·CH ₃ OH· H ₂ O	6	1.990	0.011	low
Fe(OEP)(ClO ₄)·2EtOH	6	2.034	0.008	high or int.
[Fe(TPP)(OH ₂) ₂]ClO ₄ ·2THF	6	2.041	0.000	high or mixed
Fe(TPP)[C(CN) ₃]	6	1.995	0.000	int.
[Fe(TMSO) ₂ (TPP)]ClO ₄	6	2.045	0.000	high

* Data for all compounds, except those reported in this Thesis, from ref. 12; Etio = etioporphyrin; Deut = 2,4-diacetyldeuteroporphyrin-IX dimethyl ester; TPP = tetraphenylporphyrin; Meso = mesoporphyrin-IX dimethyl ester; PPIX = protoporphyrin IX; DME = dimethyl ester;

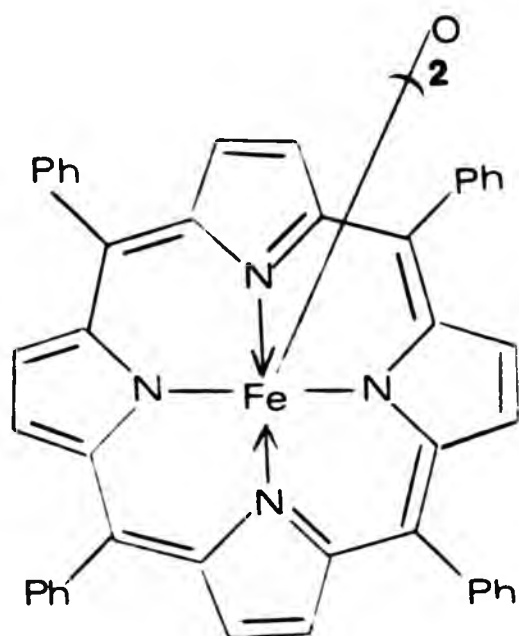
IM = imidazole; 1-Me-IM = methylimidazole; OEP = octaethylporphyrin;

TMSO = tetramethylene sulphoxide.

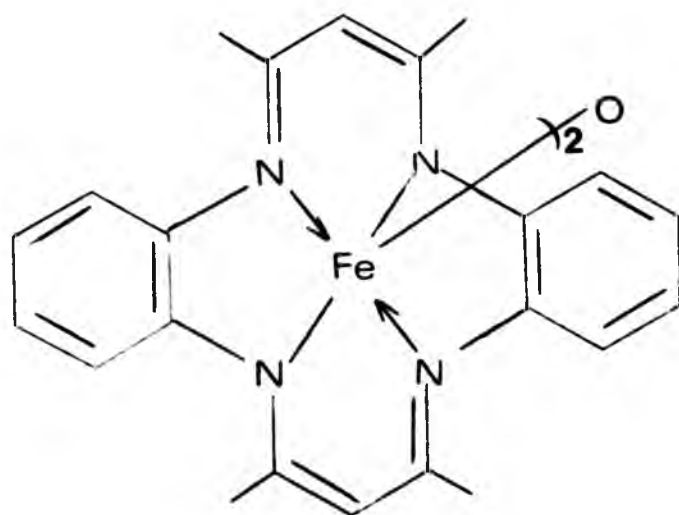
d = displacement of iron atom from the plane defined by the four
nitrogen atom donor set.



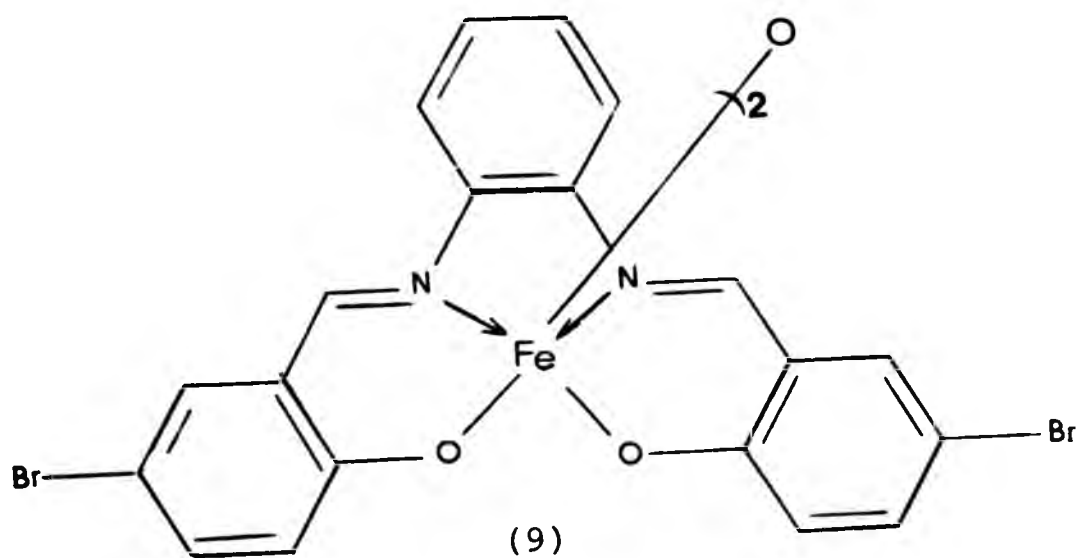
(6)



(7)



(8)



(9)

however, considerably longer than that in $\text{Fe}(\text{salen})$, (10),⁷⁻⁹ and nearer to those derivatives, with bulky substituents on the nitrogen atoms, such as: $[\text{Fe}(\text{N-p-chlorophenyl-sal})_2]_2\text{O}$, (11a),¹⁰ and $[\text{Fe}(\text{N-n-propyl-sal})_2]_2\text{O}$, (11b).¹¹ Table 8.4 gives geometries of some

μ -oxo-bridged iron complexes from the literature together with the two reported in this Thesis.

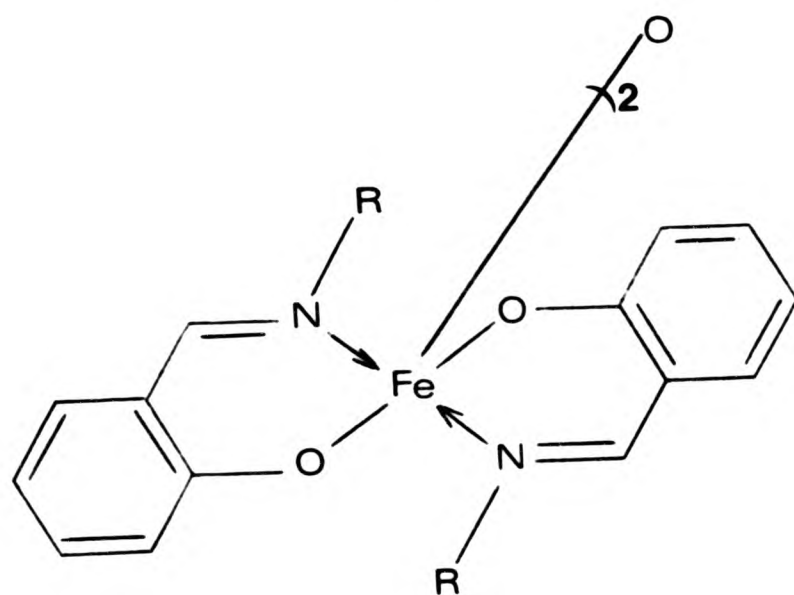
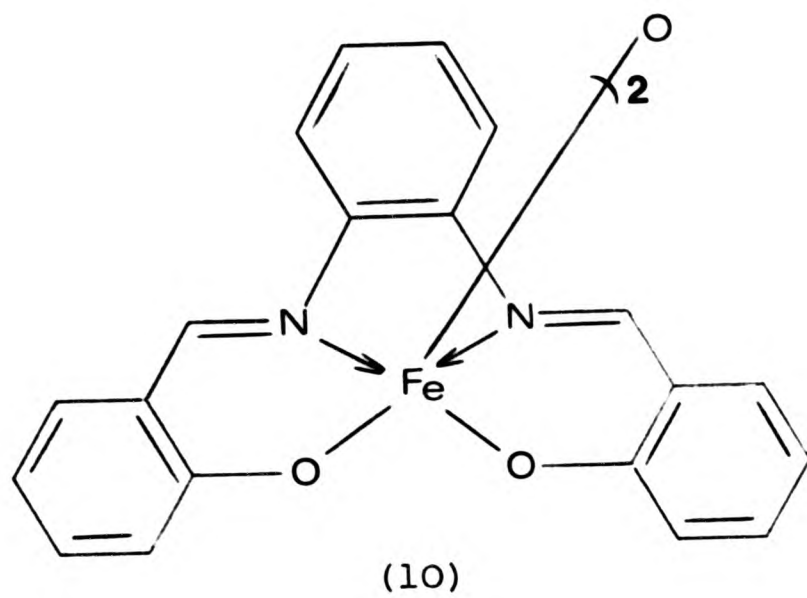


Table 8.4: Geometries of some μ -oxo-bridged iron complexes

Complex	Fe-O(b) (\AA)	Fe-L (\AA)	Co-ord. of Fe	$\widehat{\text{Fe-O-Fe}}$ ($^\circ$)	Fe.....Fe (\AA)	d (\AA)
(pyH) ₂ [FeCl ₃] ₂ O·py	1.755	2.213(Cl)	4	155.6	3.43	
Fe(diBrsalof)	1.774(5)	2.133(4)(N)	5	165.8	3.51	0.54
		1.924(4)(O)				
FeDIKETO	1.767(5)	2.039(5)(N)	5	157.0	3.46	0.64
[Fe(TAAB)(OCH ₃) ₂] ₂ O	1.777	2.067(N)	5	176.0	3.55	0.50
[Fe(TPP)] ₂ O	1.763	2.087(N)	5	174.5	3.53	0.50
[Fe(sal-N-p-chlorophenyl) ₂] ₂ O	1.760	2.16(N)	5	175.0	3.53	0.53
		1.89(O)				
[Fe(salen)] ₂ O·2py	1.80	2.087(N)	5	139.1	3.36	0.56
		1.918(O)				
[Fe(N-n-propyl-sal) ₂] ₂ O	1.77	2.14(N)	5	164	3.51	0.53
		1.93(O)				
[Fe(salen)] ₂ O	1.78	2.12(N)	5	144.6	3.39	0.58
		1.92(O)				
[Fe(2-Mequin) ₂] ₂ O·CHCl ₃	1.780	2.190(N)	5	151.6	3.45	0.64
		1.918(O)				
[Fe(salen)] ₂ O·CH ₂ Cl ₂	1.794	2.105(N)	5	142.2	3.40	0.56
		1.923(O)				

Table 8.4 (continued)

$[\text{Fe}(\text{C}_{22}\text{H}_{22}\text{N}_4)_2] \cdot \text{O} \cdot \text{CH}_3\text{CN}$	1.792	2.054(N)	5	142.8	3.40	0.698
$[\text{Fe}(\text{OOC})_2\text{pyCl}(\text{H}_2\text{O})_2] \cdot 2\text{O} \cdot 4\text{H}_2\text{O}$	1.773	2.094(O)	6	180	3.55	0.17 [Fe(1)] 0.0 [Fe(2)]
		2.056(OH ₂)				
		2.105(N)				
$[\text{Fe}(\text{TEPA})]_2\text{O} \cdot \text{I}_4$	1.77	2.33(N)	6	172	3.53	0.33
		2.12(N)				
$(\text{enH})_2[\text{Fe}(\text{HEDTA})]_2 \cdot 0.6\text{H}_2\text{O}$	1.79	2.25(N)	6	165.0	3.56	0.36
		2.03(O)				
$[\text{FeB}(\text{H}_2)]_2\text{O}(\text{ClO}_4)_4$	1.80	2.20(N)	7	178	3.6	

* Data for all compounds, except those reported in this Thesis, from ref. 12;

O(b) = bridging oxygen atom; L = ligand; (OOC)₂pyCl = 4-chloro-2,6-pyridinecarboxylate;

TPP = tetraphenylporphyrin; sal = salicylaldehyde; 2-Mequin = 8-hydroxy-2-methylquinolate;

salen = N,N'-ethylenebis(salicylidene-iminate); TEPA = tetraethylenepenta-amine;

HEDTA = N-hydroxyethyl-ethylenediaminetriacetate;

B = 2,13-dimethyl-3,6,9,12,18-penta-azabicyclo[12,3,1]-octadeca-1(18),2,12,14,16-pentaene;

$\text{C}_{22}\text{H}_{22}\text{N}_4$ = [7,16-dihydro-6,8,15,17-tetramethyl]-dibenzo[b,i][1,4,8,11]tetra-azacyclotetradecinate;

d = displacement of the iron atom from the plane defined by the equatorial donor atoms.

REFERENCES

1. J. W. L. Martin, J. H. Timmons, A. E. Martell, P. Rudolf, A. Clearfield, J. Chem. Soc. Chem. Comm., 1979, 999.
2. T. G. Fawcett, S. M. Rudich, B. H. Toby, R. A. Lalacette, J. A. Potenza, and H. J. Schugar, Inorg. Chem., 1980, 19, 940.
3. N. F. Curtis, Coord. Chem. Rev., 1968, 3, 3.
4. P. A. Tasker and L. Sklar, J. Cryst. Mol. Struct., 1975, 5, 329.
5. A. B. Hoffman, D. M. Collins, V. W. Day, E. B. Fleischer, T. S. Srivastava, and J. L. Hoard, J. Am. Chem. Soc., 1972, 94, 3620.
6. M. C. Weiss and V. L. Goedken, Inorg. Chem., 1979, 18, 819.
7. F. E. Mabbs, V. N. McLachlan, D. McFadden, and A. T. McPhail, J. Chem. Soc. Dalton, 1973, 2016.
8. J. E. Davies and B. M. Gatehouse, Acta Cryst., 1973, B29, 1934.
9. P. Coggan, A. T. McPhail, F. E. Mabbs, and V. N. McLachlan, J. Chem. Soc. (A), 1971, 1014.
10. J. E. Davies and B. M. Gatehouse, Acta Cryst., 1973, B29, 2651.
11. J. E. Davies and B. M. Gatehouse, Cryst. Struct. Commun., 1972, 1, 115.
12. B. Kamenar, and B. Kaitner, in "Structural Studies on Molecules of Biological Interest", Edts., G. Dodson, J. Glusker, and D. Sayre, Oxford University Press, 1981, p. 123.

CHAPTER 9

SUMMARY, CONCLUSIONS AND SCOPE FOR FUTURE WORK

X-ray crystallographic investigations of twelve structures are reported in this Thesis. Of these twelve, nine are ordered and two disordered. The data set for the twelfth is too poor for anything more than an outline structure.

Hydrogen bonding was observed in six structures, and its effect on structure forms one of the main themes of this Thesis. As some more unusual types of hydrogen bonds, C-H...O, N-H...F and C-H...F, were encountered in this work, the literature was surveyed for these types and the present findings placed into context.

Hydrogen bonding plays a key role in stabilising the cation structure of the TAAF salts investigated. The possibility that non-equivalent electron donor sites in the anion may give rise to ordered cation structures is mentioned.

Another main theme is the inadequacy of a single valence bond formulation to describe the results obtained in this work. Resonance forms, mainly ortho-quininoid (see Diagram 9.1), must be invoked for all these structures. The third main theme, which affects all compounds described in this Thesis, as well as others studied by the author,¹ is

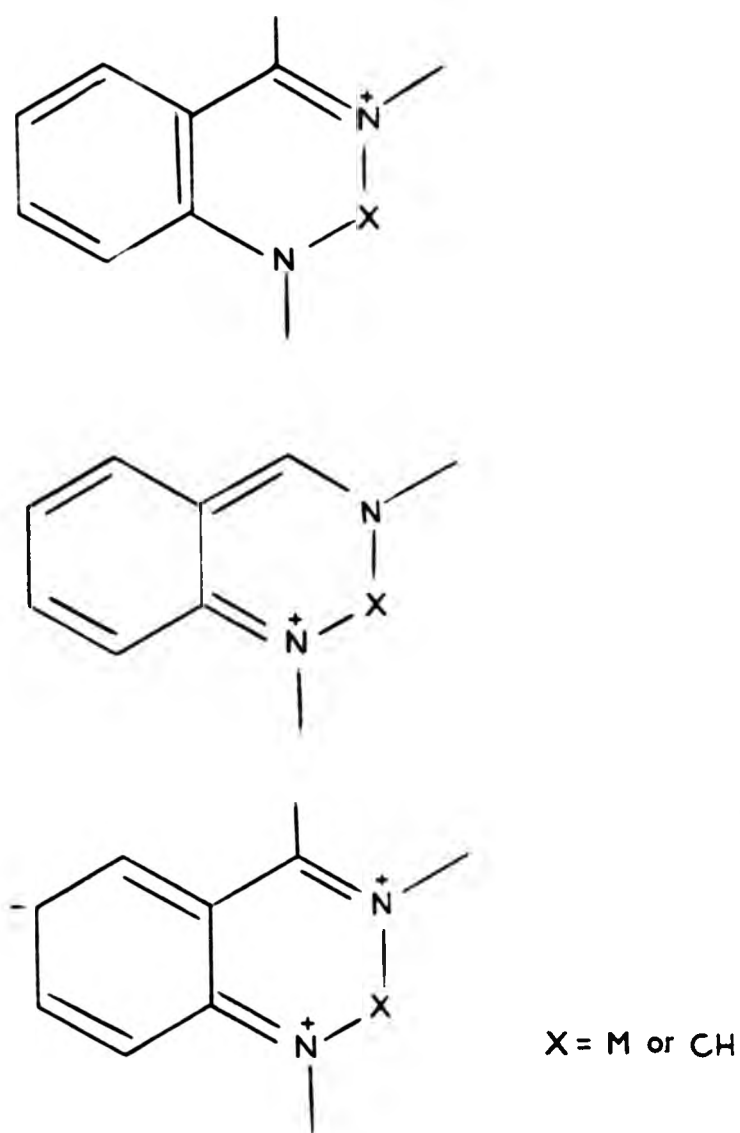
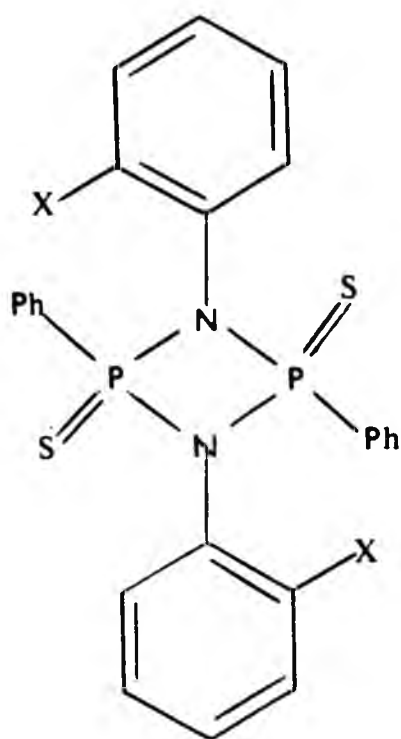


Diagram 9.1

the versatile role of nitrogen in heterocyclic compounds. The bond lengths of this atom to its ring neighbours, as well as to its exocyclic substituent, are markedly dependent on whether any π -bonding involving the nitrogen atom can occur. Such interactions are, of course, functions of conformation, and hence conformation and bond length are intimately linked.

An example of this is represented by the structures of some N-phenylcyclophosph(v)azanes¹ (Diagram 9.2). If the phenyl group is co-planar with the 4-membered P-N ring, π -conjugation can occur, and the bond is short [1.418(3)(9.2a) and 1.423(4) Å(9.2b)]. If the aromatic



- (a) X = H
- (b) X = OMe
- (c) X = Me

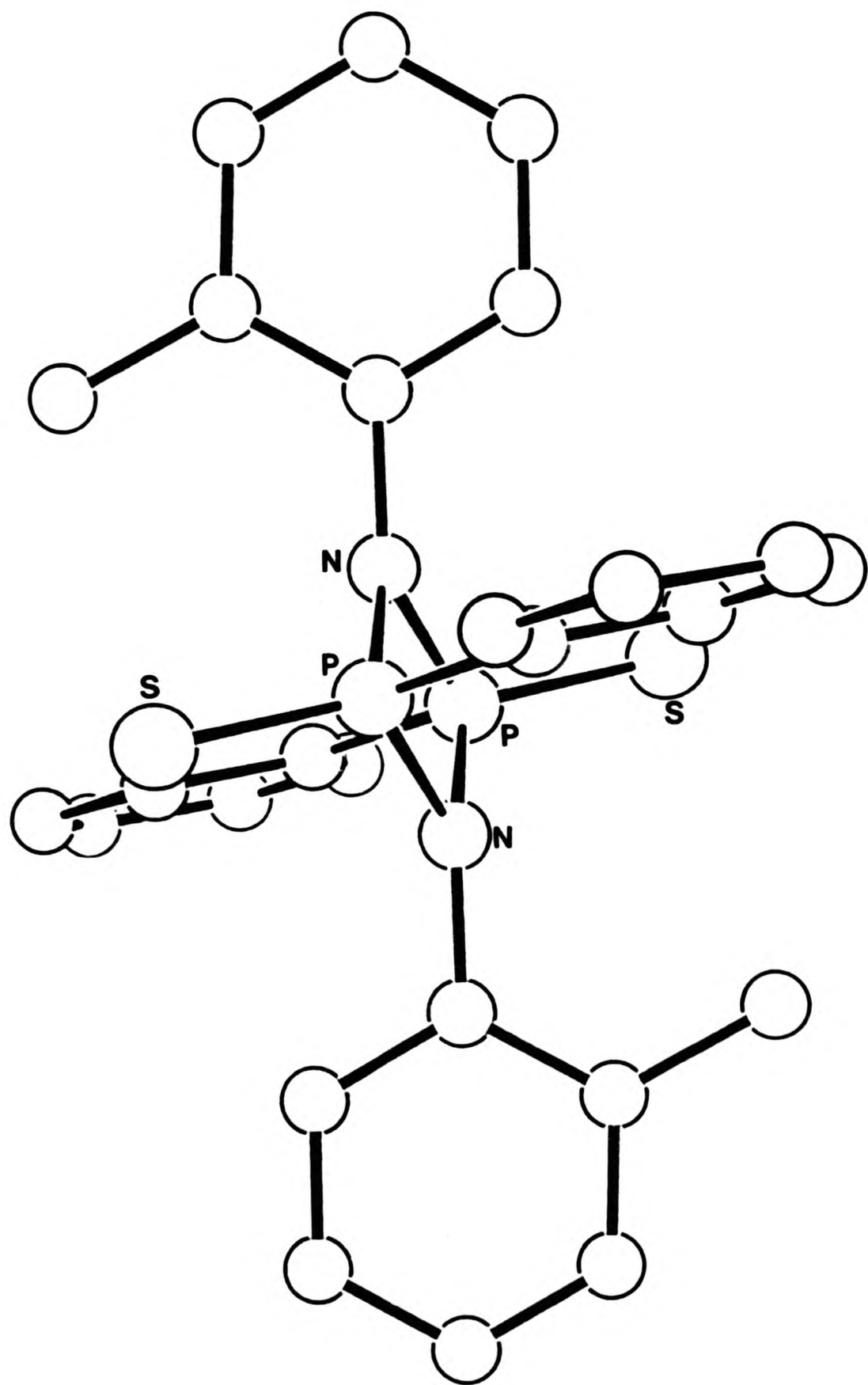
Diagram 9.2

group is twisted around the C-N bond, so as to decrease, or to eliminate, any π -interaction, this bond is lengthened to 1.440(3) Å(9.2c). ORTEP drawings of the two structures investigated by the author are given in Drawings 9.1 and 9.2.

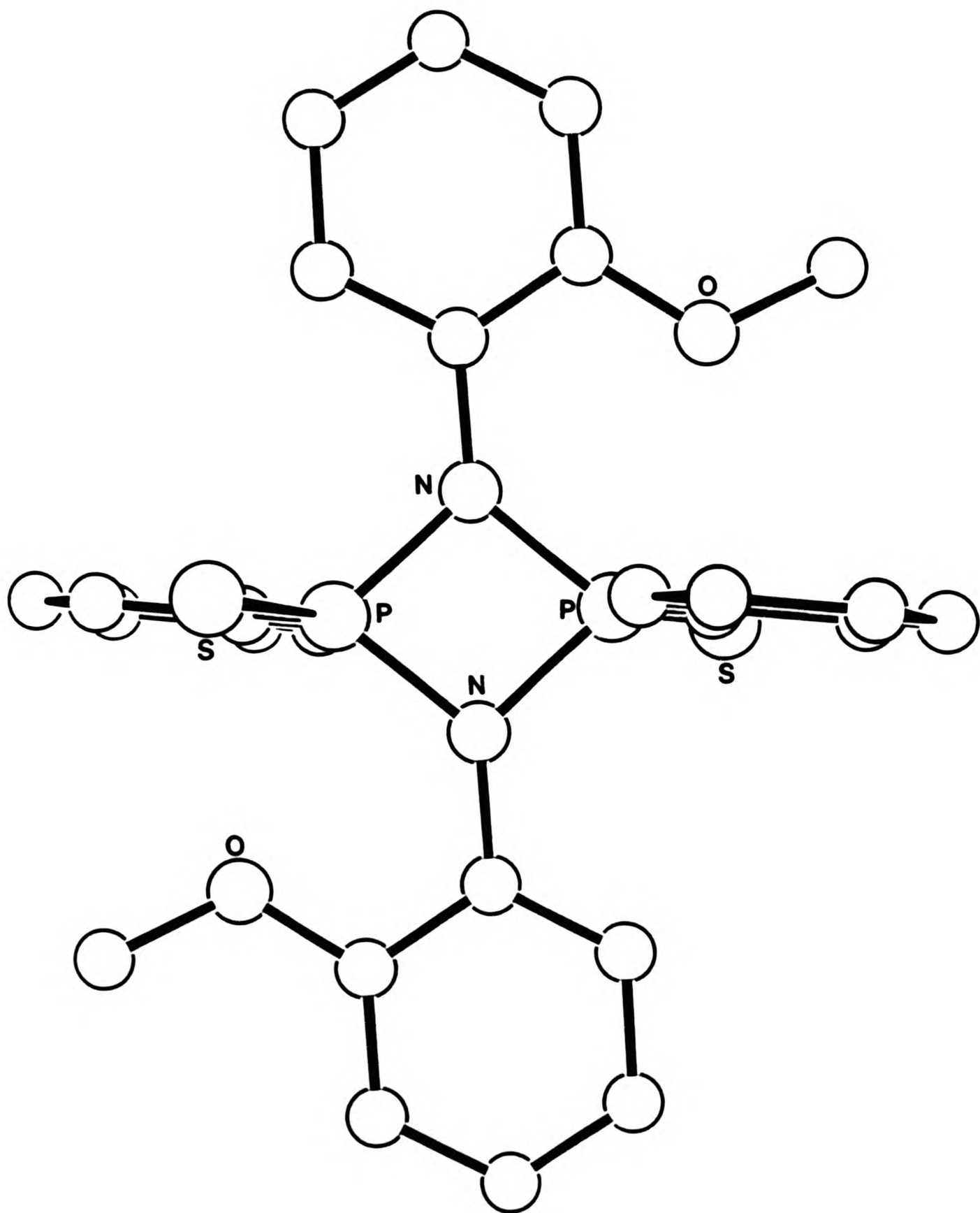
The work described here has answered some questions, but, in the nature of scientific inquiry, it has raised others.

Controversies in the literature about the nature and structure of the self-condensation products of ortho-aminobenzaldehyde² and anthranilic acid have been resolved.

The questions raised include the structural implications if hydrogen bonding is prevented, e. g. if the active NH in the TAAB salts and in the AA TRIMER is replaced by NMe (see Diagram 9.3).



Drawing 9.1



Drawing 9.2

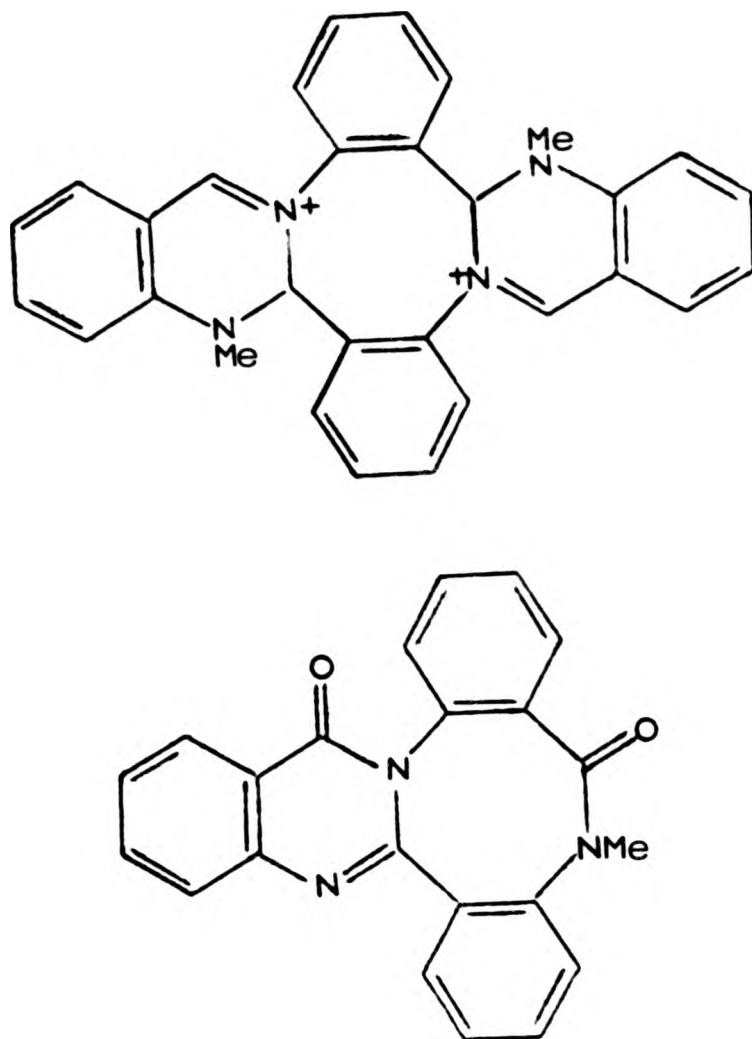


Diagram 9.3

Another intriguing question pertains to the nature of the counter-ion in TAAB salts, and its effect, if any, on order-disorder problems. All the anions studied: picrate, bisulphate and tetrafluoroborate (this Thesis), and trifluoromethylsulphonate³, have two or more electron donor sites. The hypothesis made in this Thesis that two non-equivalent sites give rise to ordered, and equivalent ones to disordered structures of the cation, should be tested. What would be the effect on structure, if the anion has no electron donor sites, e. g. the tetraphenylborate, or only one site, e. g. the chloride or bromide? It is noteworthy that these halide salts are always reported as hydrates.

Five complexes based on the metal ions CuII and FeIII are reported

here, and, together with another FeIII derivative reported in the literature⁴ represent three pairs. One pair is based on the ligand TAABH₄. To systematise this group, further structural investigations on complexes of these two ions with TAAB and with TAABH₈ would be needed.

The structures of the free ligands themselves, TAABH₄ (both isomeric forms which have been reported) and TAABH₈, should prove interesting. The up-to-now unknown TAAB (1) has four imine bonds, donor lone pairs on four nitrogen atoms, and would be macrocyclic (if one could obtain it), as it cannot isomerise into a polycycle (as does TAABH₂²⁺ and TAABH₄), unless highly strained 4-membered rings are formed. In the case of the TAABH₂²⁺ cation, this has been shown to exist in the polycyclic form (2), not in the macrocyclic one (3) (Chapter 3). TAABH₄ has a metastable macrocyclic isomer (4), which converts into the stable polycyclic form (5). TAABH₈ exists only as the macrocyclic isomer (6). In this system, TAAB/TAABH₂²⁺/TAABH₄/TAABH₈, we have a subtle interplay of several different effects: lone pair repulsion, hydrogen bonding, and C=N unsaturation, which can give rise to isomeric polycycles. It is likely that detailed structural data, obtained by X-ray crystallography, may help to provide an understanding of this system.

Rewarding also would be structural investigations on the so-called hydrates, TAAB.H₂O and TRI.H₂O, and their relationships to the metal derivatives, MTAAB, and the salts, TAABH₂(X)₂.

Further work on modified Cu(salen) derivatives may reveal under which structural conditions dimer formation can and cannot occur.

REFERENCES

1. P. G. Owston, L. S. Shaw (née Gözen), R. A. Shaw, and D. A. Watkins, J. Chem. Soc. Chem. Comm., 1982, 16.
2. P. G. Owston, L. S. Shaw (née Gözen), and P. A. Tasker, J. Chem. Soc. Chem. Comm., 1982, 17.
3. J. S. Skuratovicz, I. L. Madden, and D. H. Busch, Inorg. Chem., 1977, 16, 1721.
4. B. Kamenar and B. Kaitner, in "Structural Studies on Molecules of Biological Interest", G. Dodson, J. Glusker, and D. Sayre, Edts., Oxford University Press, 1981, p. 123.

APPENDIX 1

Table 1.1: Fractional atomic coordinates and thermal parameters (\AA^2)
for $\text{TAABH}_2(\text{PICRATE})_2$

Atom	x	y	z	Uiso or Ueq
N(1)	0.2591(1)	0.5887(3)	0.0400(3)	0.048(2)
N(2)	0.1880(1)	0.4770(4)	0.1421(3)	0.047(2)
C(1)	0.2345(2)	0.4550(4)	0.0649(4)	0.040(2)
C(2)	0.2205(2)	0.7036(4)	-0.0007(4)	0.041(2)
C(3)	0.2357(2)	0.8209(4)	-0.0731(5)	0.055(3)
C(4)	0.1955(2)	0.9345(5)	-0.1087(5)	0.064(3)
C(5)	0.1409(2)	0.9381(5)	-0.0690(6)	0.069(4)
C(6)	0.1267(2)	0.8271(5)	0.0059(5)	0.065(3)
C(7)	0.1663(2)	0.7072(4)	0.0408(4)	0.043(2)
C(8)	0.1566(2)	0.5955(4)	0.1281(4)	0.039(2)
C(9)	0.3222(2)	0.3589(4)	0.2694(4)	0.040(2)
C(10)	0.3690(2)	0.2646(5)	0.3255(4)	0.053(3)
C(11)	0.3777(2)	0.1514(5)	0.2414(5)	0.061(3)
C(12)	0.3389(2)	0.1333(5)	0.1035(5)	0.059(3)
C(13)	0.2912(2)	0.2315(4)	0.0477(4)	0.046(3)
C(14)	0.2826(2)	0.3455(4)	0.1296(4)	0.038(2)
Cp(1)	0.0119(2)	0.4318(4)	0.3274(4)	0.040(2)
Cp(2)	-0.0281(2)	0.3317(4)	0.3508(4)	0.044(2)
Cp(3)	-0.0087(2)	0.2474(4)	0.4737(5)	0.049(3)
Cp(4)	0.0490(2)	0.2641(4)	0.5722(4)	0.046(3)
Cp(5)	0.0877(2)	0.3683(4)	0.5509(4)	0.038(2)
Cp(6)	0.0737(2)	0.4609(4)	0.4247(4)	0.039(2)

Table 1.1: continued

Np(a)	-0.0121(2)	0.5196(4)	0.1994(4)	0.053(2)
Np(b)	-0.0515(2)	0.1432(4)	0.5014(5)	0.067(3)
Np(c)	0.1455(2)	0.3835(5)	0.6654(4)	0.051(2)
O(1)	0.0227(1)	0.5871(4)	0.1521(4)	0.103(3)
O(2)	-0.0680(1)	0.5264(4)	0.1436(3)	0.070(2)
O(3)	-0.1029(2)	0.1300(4)	0.4141(4)	0.091(3)
O(4)	-0.0335(2)	0.0744(4)	0.6149(4)	0.092(3)
O(5)	0.1652(1)	0.2797(4)	0.7433(3)	0.072(2)
O(6)	0.1715(1)	0.5000(4)	0.6818(3)	0.067(2)
O(7)	0.1093(1)	0.5537(3)	0.4039(3)	0.052(2)

Table 1.2: Fractional atomic coordinates for the hydrogen atoms
for TAABH₂(PICRATE)₂

Atom	x	y	z	
Hn(1)	0.297(1)	0.561(1)	0.017(1)	0.08(1)
H(1)	0.207(1)	0.417(1)	-0.033(1)	0.08(1)
H(3)	0.278(1)	0.822(1)	-0.101(1)	0.08(1)
H(4)	0.206(1)	1.023(1)	-0.168(1)	0.08(1)
H(5)	0.110(1)	1.029(1)	-0.098(1)	0.08(1)
H(6)	0.085(1)	0.831(1)	0.039(1)	0.08(1)
H(8)	0.118(1)	0.582(1)	0.143(1)	0.08(1)
H(10)	0.399(1)	0.278(1)	0.434(1)	0.08(1)
H(11)	0.415(1)	0.077(1)	0.284(1)	0.08(1)
H(12)	0.345(1)	0.044(1)	0.039(1)	0.08(1)
H(13)	0.261(1)	0.218(1)	-0.060(1)	0.08(1)
Hp(2)	-0.074(1)	0.318(1)	0.275(1)	0.08(1)
Hp(4)	0.064(1)	0.195(1)	0.665(1)	0.08(1)

Table 1.3: Anisotropic thermal parameters (\AA^2)
for TAABH₂(PICRATE)₂

Atom	U11	U22	U33	U23	U13	U12
N(1)	0.044(2)	0.050(2)	0.049(2)	0.008(2)	0.020(2)	0.010(2)
N(2)	0.041(2)	0.057(2)	0.042(2)	0.013(2)	0.016(2)	0.005(2)
C(1)	0.037(2)	0.038(2)	0.044(2)	0.002(2)	0.018(2)	0.004(2)
C(2)	0.044(2)	0.042(3)	0.036(2)	-0.003(2)	0.007(2)	0.002(2)
C(3)	0.068(3)	0.044(3)	0.054(3)	0.008(2)	0.019(2)	-0.004(2)
C(4)	0.092(4)	0.042(3)	0.060(3)	0.005(3)	0.013(3)	-0.003(3)
C(5)	0.079(4)	0.040(3)	0.087(4)	0.005(3)	0.006(3)	0.016(3)
C(6)	0.062(3)	0.049(3)	0.084(4)	-0.000(3)	0.019(3)	0.016(2)
C(7)	0.046(2)	0.040(3)	0.044(2)	0.000(2)	0.008(2)	0.004(2)
C(8)	0.025(2)	0.043(2)	0.048(3)	-0.002(2)	-0.000(2)	0.002(2)
C(9)	0.037(2)	0.045(3)	0.039(2)	-0.008(2)	0.016(2)	0.002(2)
C(10)	0.043(2)	0.069(3)	0.048(3)	0.010(3)	0.014(2)	0.013(2)
C(11)	0.052(3)	0.054(3)	0.076(4)	0.013(3)	0.022(3)	0.020(2)

Table 1.3: continued

C(12)	0.065(3)	0.040(3)	0.073(3)	-0.008(3)	0.030(3)	0.003(2)
C(13)	0.047(2)	0.045(3)	0.047(3)	-0.007(2)	0.018(2)	-0.002(2)
C(14)	0.038(2)	0.039(2)	0.037(2)	-0.001(2)	0.016(2)	-0.002(2)
Cp(1)	0.040(2)	0.047(2)	0.034(2)	0.001(2)	0.012(2)	0.002(2)
Cp(2)	0.041(2)	0.045(3)	0.046(3)	-0.011(2)	0.012(2)	-0.006(2)
Cp(3)	0.054(3)	0.042(3)	0.052(3)	-0.001(2)	0.019(2)	-0.009(2)
Cp(4)	0.050(3)	0.043(3)	0.044(2)	-0.001(2)	0.012(2)	0.008(2)
Cp(5)	0.034(2)	0.045(2)	0.034(2)	-0.002(2)	0.006(2)	0.002(2)
Cp(6)	0.036(2)	0.042(2)	0.038(2)	-0.002(2)	0.016(2)	0.006(2)
Np(a)	0.040(2)	0.075(3)	0.044(2)	0.007(2)	0.012(2)	-0.002(2)
Np(b)	0.075(3)	0.056(3)	0.071(3)	0.001(2)	0.025(3)	-0.017(2)
Np(c)	0.046(2)	0.070(3)	0.038(2)	-0.001(2)	0.013(2)	0.002(2)
O(1)	0.051(2)	0.164(4)	0.093(3)	0.072(3)	0.011(2)	-0.011(2)

Table 1.3: continued

0(2)	0.039(2)	0.116(3)	0.053(2)	0.019(2)	-0.001(1)	-0.003(2)
0(3)	0.077(2)	0.103(3)	0.092(3)	0.006(2)	0.010(2)	-0.047(2)
0(4)	0.099(3)	0.080(3)	0.096(3)	0.027(2)	0.031(2)	-0.022(2)
0(5)	0.073(2)	0.088(2)	0.056(2)	0.020(2)	-0.003(2)	0.016(2)
0(6)	0.054(2)	0.095(3)	0.053(2)	0.002(2)	0.003(1)	-0.027(2)
0(7)	0.042(2)	0.059(2)	0.056(2)	0.006(2)	0.020(1)	-0.007(1)

Table 1.4: Intermolecular distances (Å) for TAABH₂(PICRATE)₂

			S	a	b	c
N(2)	...N(1)	3.15	2	0.0	0.0	0.0
C(8)	...N(1)	3.23	2	0.0	0.0	0.0
O(6)	...N(1)	3.15	2	0.0	0.0	0.0
O(7)	...N(1)	2.89	2	0.0	0.0	0.0
Cp(6)	...Hn(1)	2.98	2	0.0	0.0	0.0
Np(c)	...Hn(1)	3.01	2	0.0	0.0	0.0
O(6)	...Hn(1)	2.34	2	0.0	0.0	0.0
O(7)	...Hn(1)	2.04	2	0.0	0.0	0.0
O(2)	...N(2)	3.26	-1	0.0	1.0	0.0
N(2)	...N(2)	2.97	2	0.0	0.0	0.0
C(1)	...N(2)	2.88	2	0.0	0.0	0.0
C(9)	...N(2)	1.46	2	0.0	0.0	0.0
C(10)	...N(2)	2.44	2	0.0	0.0	0.0
H(10)	...N(2)	2.65	2	0.0	0.0	0.0
C(14)	...N(2)	2.46	2	0.0	0.0	0.0
C(1)	...C(1)	3.47	2	0.0	0.0	0.0
C(9)	...C(1)	2.52	2	0.0	0.0	0.0
C(10)	...C(1)	3.37	2	0.0	0.0	0.0
C(14)	...C(1)	3.28	2	0.0	0.0	0.0
Np(c)	...H(1)	2.87	1	0.0	0.0	1.0
O(5)	...H(1)	2.46	1	0.0	0.0	1.0
O(6)	...H(1)	2.77	1	0.0	0.0	1.0

Symmetry code S 1 = x, y, z
 -1 = -x, -y, -z
 2 = 0.5-x, y, 0.5-z
 -2 = 0.5+x, -y, 0.5+z

2nd atom is related to the first one at x, y, z, by the transformation
 S, with a, b, c, added respectively

table 1.4: continued

C(9)	...H(1)	2.89	2	0.0	0.0	0.0
O(3)	...H(3)	2.69	-2	0.0	1.0	1.0
H(13)	...C(4)	3.00	1	0.0	-1.0	0.0
O(3)	...C(4)	3.15	-1	0.0	1.0	0.0
O(5)	...H(4)	2.62	1	0.0	-1.0	1.0
O(3)	...C(5)	3.28	-1	0.0	1.0	0.0
Hp(2)	...C(6)	2.98	-1	0.0	1.0	0.0
O(2)	...C(7)	3.25	-1	0.0	1.0	0.0
O(2)	...C(8)	3.03	-1	0.0	1.0	0.0
C(9)	...C(8)	2.41	2	0.0	0.0	0.0
C(10)	...C(8)	3.20	2	0.0	0.0	0.0
C(14)	...C(8)	3.32	2	0.0	0.0	0.0
O(2)	...H(8)	2.87	-1	0.0	1.0	0.0
C(9)	...H(8)	2.50	2	0.0	0.0	0.0
C(10)	...H(8)	2.98	2	0.0	0.0	0.0
C(9)	...C(9)	3.19	2	0.0	0.0	0.0
C(14)	...C(9)	2.84	2	0.0	0.0	0.0
O(7)	...C(9)	3.19	2	0.0	0.0	0.0
O(2)	...H(10)	2.68	-2	0.0	1.0	0.0
O(4)	...C(11)	3.40	-2	0.0	0.0	1.0
O(4)	...H(11)	2.69	-2	0.0	0.0	1.0
Cp(5)	...C(12)	3.37	2	0.0	0.0	0.0
O(3)	...H(12)	2.53	-2	0.0	0.0	1.0
O(4)	...H(12)	2.85	-2	0.0	0.0	1.0
Cp(5)	...C(13)	3.42	2	0.0	0.0	0.0

Table 1.4 continued

Np(c) ...C(13)	3.19	2	0.0	0.0	0.0
O(5) ...C(13)	3.31	2	0.0	0.0	0.0
O(5) ...H(13)	2.49	1	0.0	0.0	1.0
O(5) ...H(13)	2.85	2	0.0	0.0	0.0
C(14) ...C(14)	3.13	2	0.0	0.0	0.0
O(7) ...C(14)	3.22	2	0.0	0.0	0.0
Cp(4) ...Cp(1)	3.43	-1	0.0	1.0	1.0
Cp(5) ...Cp(1)	3.41	-1	0.0	1.0	1.0
Cp(5) ...Cp(2)	3.38	-1	0.0	1.0	1.0
Cp(6) ...Cp(2)	3.32	-1	0.0	1.0	1.0
O(6) ...Hp(2)	2.92	-1	0.0	1.0	1.0
Cp(6) ...Cp(3)	3.39	-1	0.0	1.0	1.0
O(4) ...Cp(3)	3.35	-1	0.0	0.0	1.0
Np(a) ...Cp(4)	3.30	-1	0.0	1.0	1.0
O(2) ...Cp(4)	3.32	-1	0.0	1.0	1.0
O(2) ...Cp(5)	3.30	-1	0.0	1.0	1.0
O(4) ...Np(b)	3.24	-1	0.0	0.0	1.0
O(7) ...Np(b)	3.37	-1	0.0	1.0	1.0
O(2) ...Np(c)	3.04	-1	0.0	1.0	1.0
O(1) ...O(1)	3.27	-1	0.0	1.0	0.0
O(5) ...O(2)	3.29	-1	0.0	1.0	1.0
O(6) ...O(2)	3.30	-1	0.0	1.0	1.0

Table 1.5: Intramolecular distances (Å) for TAABH₂(PICRATE)₂

N(2) ...N(1)	2.38	H(1) ...N(1)	2.00
C(3) ...N(1)	2.42	H(3) ...N(1)	2.68
C(7) ...N(1)	2.38	C(8) ...N(1)	2.71
C(9) ...N(1)	3.12	C(13) ...N(1)	3.41
C(14) ...N(1)	2.44	C(1) ...Hn(1)	1.90
C(2) ...Hn(1)	2.15	C(3) ...Hn(1)	2.80
C(9) ...Hn(1)	3.02	C(14) ...Hn(1)	2.37
H(1) ...N(2)	1.96	C(2) ...N(2)	2.76
C(7) ...N(2)	2.36	H(8) ...N(2)	1.88
C(9) ...N(2)	3.13	C(14) ...N(2)	2.51
C(2) ...C(1)	2.41	C(7) ...C(1)	2.79
C(8) ...C(1)	2.43	C(9) ...C(1)	2.52
C(13) ...C(1)	2.49	H(13) ...C(1)	2.68
C(2) ...H(1)	2.71	C(7) ...H(1)	3.02
C(8) ...H(1)	2.76	C(13) ...H(1)	2.53
C(14) ...H(1)	2.07	H(3) ...C(2)	2.16
C(4) ...C(2)	2.39	C(5) ...C(2)	2.79
C(6) ...C(2)	2.44	C(8) ...C(2)	2.41
H(4) ...C(3)	2.12	C(5) ...C(3)	2.43
C(6) ...C(3)	2.81	C(7) ...C(3)	2.43
C(4) ...H(3)	2.14	H(5) ...C(4)	2.16
C(6) ...C(4)	2.40	C(7) ...C(4)	2.77

Table 1.5: continued

C(5) ...H(4)	2.15	H(6) ...C(5)	2.12
C(7) ...C(5)	2.40	C(6) ...H(5)	2.12
C(8) ...C(6)	2.47	H(8) ...C(6)	2.69

C(7) ...H(6)	2.17	C(8) ...H(6)	2.72
H(8) ...C(7)	2.06	O(1) ...C(8)	3.12
O(7) ...C(8)	3.21	O(1) ...H(8)	2.18
O(7) ...H(8)	2.62	H(10) ...C(9)	2.12
C(11) ...C(9)	2.37	C(12) ...C(9)	2.75
C(13) ...C(9)	2.38	H(11) ...C(10)	2.14
C(12) ...C(10)	2.41	C(13) ...C(10)	2.77
C(14) ...C(10)	2.41	C(11) ...H(10)	2.15
H(12) ...C(11)	2.14	C(13) ...C(11)	2.40
C(14) ...C(11)	2.78	C(12) ...H(11)	2.13
H(13) ...C(12)	2.15	C(14) ...C(12)	2.41
C(13) ...H(12)	2.16	C(14) ...H(13)	2.13
Hp(2) ...Cp(1)	2.13	Cp(3) ...Cp(1)	2.37
Cp(4) ...Cp(1)	2.77	Cp(5) ...Cp(1)	2.41
O(1) ...Cp(1)	2.31	O(2) ...Cp(1)	2.31
O(7) ...Cp(1)	2.40	Cp(4) ...Cp(2)	2.42
Cp(5) ...Cp(2)	2.78	Cp(6) ...Cp(2)	2.51
Np(a) ...Cp(2)	2.39	Np(b) ...Cp(2)	2.45
O(2) ...Cp(2)	2.67	O(3) ...Cp(2)	2.73

Table 1.5: continued

Cp(3) ...Hp(2)	2.16	Np(a) ...Hp(2)	2.58
Np(b) ...Hp(2)	2.67	O(2) ...Hp(2)	2.36
O(3) ...Hp(2)	2.43	Hp(4) ...Cp(3)	2.14
Cp(5) ...Cp(3)	2.37	Cp(6) ...Cp(3)	2.87
O(3) ...Cp(3)	2.31	O(4) ...Cp(3)	2.30
Cp(6) ...Cp(4)	2.50	Np(b) ...Cp(4)	2.45
Np(c) ...Cp(4)	2.38	O(4) ...Cp(4)	2.70
O(5) ...Cp(4)	2.67	Cp(5) ...Hp(4)	2.13
Np(b) ...Hp(4)	2.67	Np(c) ...Hp(4)	2.56

O(4) ...Hp(4)	2.39	O(5) ...Hp(4)	2.34
O(5) ...Cp(5)	2.31	O(6) ...Cp(5)	2.30
O(7) ...Cp(5)	2.39	Np(a) ...Cp(6)	2.52
Np(c) ...Cp(6)	2.53	O(1) ...Cp(6)	2.82
O(6) ...Cp(6)	2.83	O(7) ...Np(a)	2.90
O(7) ...Np(c)	2.91	O(2) ...O(1)	2.11
O(7) ...O(1)	2.67	O(4) ...O(3)	2.18
O(6) ...O(5)	2.16	O(7) ...O(6)	2.70

Table 1.6: Fractional atomic coordinates and thermal parameters(\AA^2)
for $\text{TAABH}_2(\text{HSO}_4)_2$

Atom	x	y	z	Uiso or Ueq
C(11)	0.0568(3)	-0.1867(4)	0.0507(4)	0.058(2)
C(10)	0.1023(3)	-0.1228(4)	0.1648(5)	0.058(2)
C(9)	0.1480(3)	-0.1858(3)	0.2786(4)	0.043(2)
C(1)	0.1974(2)	-0.1161(4)	0.3974(4)	0.056(2)
N(2c1)	0.1974(2)	-0.1161(4)	0.3974(4)	0.056(2)
N(1)	0.1534(2)	-0.0950(3)	0.5276(4)	0.050(2)
C(8n1)	0.1534(2)	-0.0950(3)	0.5276(4)	0.050(2)
C(7)	0.2005(2)	-0.0299(3)	0.6419(4)	0.046(2)
C(6)	0.1528(3)	0.0257(5)	0.7614(5)	0.078(3)
C(5)	0.2018(3)	0.0820(4)	0.8735(4)	0.068(3)
S	0.09889(10)	0.25000	0.35240(17)	0.0492(8)
O(1a)	0.0396(15)	0.1537(16)	0.3087(13)	0.105(9)
O(1b)	0.0459(10)	0.1372(13)	0.3868(10)	0.084(6)
O(2)	0.1610(4)	0.2172(8)	0.4805(5)	0.070(5)
O(3)	0.1625(4)	0.2075(5)	0.2244(5)	0.075(5)

Table 1.7: Fractional atomic coordinates for the hydrogen atoms
for $\text{TAABH}_2(\text{HSO}_4)_2$

Atom	x	y	z
H(11)	-0.0250	0.1438	1.0222
H(10)	-0.1049	0.0329	0.8444
H(6)	-0.0889	-0.0208	0.2403
H(5)	-0.1657	-0.1227	0.0543
Hs(2)	0.2197	0.2500	0.5059
Hs(3)	0.2302	0.2372	0.2163

Table 1.8: Anisotropic thermal parameters (\AA^2) TAABH₂(HSO₄)₂

Atom	U11	U22	U33	U23	U13	U12
C(11)	0.055(2)	0.067(3)	0.052(2)	0.008(2)	-0.014(2)	0.011(2)
C(10)	0.058(2)	0.043(2)	0.072(3)	-0.001(2)	-0.017(2)	0.010(2)
C(9)	0.040(2)	0.048(2)	0.040(2)	-0.006(2)	-0.001(2)	0.007(2)
C(1)	0.043(2)	0.076(3)	0.049(2)	-0.025(2)	-0.007(2)	0.016(2)
N(2c1)	0.043(2)	0.076(3)	0.049(2)	-0.025(2)	-0.007(2)	0.016(2)
N(1)	0.054(2)	0.051(2)	0.046(2)	-0.012(2)	0.009(2)	-0.004(2)
C(8n1)	0.054(2)	0.051(2)	0.046(2)	-0.012(2)	0.009(2)	-0.004(2)
C(7)	0.051(2)	0.047(2)	0.040(2)	-0.003(2)	0.004(2)	-0.003(2)
C(6)	0.066(3)	0.103(4)	0.066(3)	-0.030(3)	0.020(3)	-0.015(3)
C(5)	0.087(3)	0.074(3)	0.045(2)	-0.012(2)	0.013(2)	-0.009(2)
S	0.039(1)	0.048(1)	0.060(1)	0.000(1)	0.002(1)	0.000(1)
O(1a)	0.133(9)	0.062(8)	0.120(11)	-0.014(8)	-0.039(10)	-0.040(7)
O(1b)	0.076(5)	0.057(5)	0.119(8)	0.008(6)	-0.005(7)	-0.023(4)
O(2)	0.064(3)	0.095(10)	0.052(3)	0.027(4)	-0.005(3)	0.000(4)
O(3)	0.057(3)	0.111(8)	0.057(3)	-0.034(3)	0.011(3)	-0.024(3)

Table 1.9: Intermolecular distances (\AA) for $\text{TAABH}_2(\text{HSO}_4)_2$

		S	a	b	c
H(11) ...C(11)	.91	-1	0.0	0.0	1.0
H(10) ...C(11)	2.02	-1	0.0	0.0	1.0
C(10) ...C(11)	2.38	3	0.0	-1.0	0.0
C(9) ...C(11)	2.76	3	0.0	-1.0	0.0
H(11) ...C(11)	1.99	-3	0.0	1.0	1.0
H(11) ...C(10)	1.99	-1	0.0	0.0	1.0
H(10) ...C(10)	.97	-1	0.0	0.0	1.0
C(1) ...C(10)	3.48	2	0.0	0.0	0.0
C(10) ...C(10)	2.75	3	0.0	-1.0	0.0
C(9) ...C(10)	2.39	3	0.0	-1.0	0.0
H(10) ...C(9)	2.07	-1	0.0	0.0	1.0
C(9) ...C(9)	2.85	2	0.0	0.0	0.0
C(1) ...C(9)	2.52	2	0.0	0.0	0.0
N(2c1)...C(9)	2.52	2	0.0	0.0	0.0
C(1) ...C(9)	2.48	3	0.0	-1.0	0.0
N(2c1)...C(9)	2.48	3	0.0	-1.0	0.0
N(1) ...C(9)	3.24	3	0.0	-1.0	0.0
C(8n1)...C(9)	3.24	3	0.0	-1.0	0.0
C(9) ...C(9)	3.17	4	0.0	-1.0	0.0
C(1) ...C(9)	3.22	4	0.0	-1.0	0.0
N(2c1)...C(9)	3.22	4	0.0	-1.0	0.0
H(10) ...C(1)	2.66	-1	0.0	0.0	1.0
N(2c1)...C(1)	1.47	2	0.0	0.0	0.0
N(1) ...C(1)	2.40	2	0.0	0.0	0.0
C(8n1)...C(1)	2.40	2	0.0	0.0	0.0

Table 1.9: continued

C(7) ...C(1)	2.76	2	0.0	0.0	0.0
C(1) ...C(1)	2.89	3	0.0	-1.0	0.0
N(2c1)...C(1)	2.89	3	0.0	-1.0	0.0
N(1) ...C(1)	3.38	3	0.0	-1.0	0.0
C(8n1)...C(1)	3.38	3	0.0	-1.0	0.0
C(1) ...C(1)	3.24	4	0.0	-1.0	0.0
N(2c1)...C(1)	3.24	4	0.0	-1.0	0.0
H(10) ...N(2c1)	2.66	-1	0.0	0.0	1.0
N(1) ...N(2c1)	2.40	2	0.0	0.0	0.0
C(8n1)...N(2c1)	2.40	2	0.0	0.0	0.0
C(7) ...N(2c1)	2.76	2	0.0	0.0	0.0
N(2c1)...N(2c1)	2.89	3	0.0	-1.0	0.0
N(1) ...N(2c1)	3.38	3	0.0	-1.0	0.0
C(8n1)...N(2c1)	3.38	3	0.0	-1.0	0.0
N(2c1)...N(2c1)	3.24	4	0.0	-1.0	0.0
O(1a) ...N(1)	3.13	-1	0.0	0.0	1.0
O(1b) ...N(1)	2.93	-1	0.0	0.0	1.0
H(6) ...N(1)	2.57	-1	0.0	0.0	1.0
N(1) ...N(1)	2.71	2	0.0	0.0	0.0
C(8n1)...N(1)	2.71	2	0.0	0.0	0.0
C(7) ...N(1)	2.39	2	0.0	0.0	0.0
N(1) ...N(1)	3.34	3	0.0	-1.0	0.0
C(8n1)...N(1)	3.34	3	0.0	-1.0	0.0
O(1a) ...C(8n1)	3.13	-1	0.0	0.0	1.0
O(1b) ...C(8n1)	2.93	-1	0.0	0.0	1.0
H(6) ...C(8n1)	2.57	-1	0.0	0.0	1.0
C(8n1)...C(8n1)	2.71	2	0.0	0.0	0.0
C(7) ...C(8n1)	2.39	2	0.0	0.0	0.0

Table 1.9: continued

C(8n1)...C(8n1)	3.34	3	0.0	-1.0	0.0
H(6) ...C(7)	1.96	-1	0.0	0.0	1.0
C(6) ...C(7)	2.39	2	0.0	0.0	0.0
C(5) ...C(7)	2.75	2	0.0	0.0	0.0
O(1a) ...C(6)	3.37	-1	0.0	0.0	1.0
H(6) ...C(6)	.90	-1	0.0	0.0	1.0
H(5) ...C(6)	1.95	-1	0.0	0.0	1.0
C(6) ...C(6)	2.72	2	0.0	0.0	0.0
C(5) ...C(6)	2.34	2	0.0	0.0	0.0
H(6) ...C(5)	1.99	-1	0.0	0.0	1.0
H(5) ...C(5)	.93	-1	0.0	0.0	1.0
H(5) ...C(5)	2.01	-2	0.0	0.0	1.0
O(2) ...S	3.57	2	0.0	0.0	0.0
O(3) ...S	3.56	2	0.0	0.0	0.0
Hs(2) ...S	2.88	2	0.0	0.0	0.0
Hs(3) ...S	2.68	2	0.0	0.0	0.0
H(11) ...O(1a)	2.70	1	0.0	0.0	1.0
H(10) ...O(1a)	2.59	-1	0.0	0.0	1.0
O(1a) ...O(1a)	2.08	3	0.0	0.0	0.0
O(1b) ...O(1a)	2.36	3	0.0	0.0	0.0
O(2) ...O(1a)	2.68	3	0.0	0.0	0.0
O(3) ...O(1a)	2.40	3	0.0	0.0	0.0
H(10) ...O(1b)	2.87	-1	0.0	0.0	1.0
O(1b) ...O(1b)	2.43	3	0.0	0.0	0.0
O(2) ...O(1b)	2.40	3	0.0	0.0	0.0
O(3) ...O(1b)	2.75	3	0.0	0.0	0.0
Hs(2) ...O(1b)	2.92	3	0.0	0.0	0.0
O(2) ...O(2)	2.49	2	0.0	0.0	0.0

Table 1.9: continued

Hs(2) ...0(2)	1.72	2	0.0	0.0	0.0
Hs(3) ...0(2)	2.81	2	0.0	0.0	0.0
O(3) ...0(2)	2.41	3	0.0	0.0	0.0
Hs(2) ...0(2)	.92	3	0.0	0.0	0.0
Hs(3) ...0(2)	2.59	3	0.0	0.0	0.0
O(2) ...0(2)	2.59	4	0.0	0.0	0.0
Hs(2) ...0(2)	1.72	4	0.0	0.0	0.0
Hs(3) ...0(2)	2.84	4	0.0	0.0	0.0
H(10) ...0(3)	2.78	-1	0.0	0.0	1.0
H(5) ...0(3)	2.64	-1	0.0	0.0	0.0
O(3) ...0(3)	2.45	2	0.0	0.0	0.0
Hs(3) ...0(3)	1.54	2	0.0	0.0	0.0
Hs(2) ...0(3)	2.66	3	0.0	0.0	0.0
Hs(3) ...0(3)	1.12	3	0.0	0.0	0.0
O(3) ...0(3)	2.62	4	0.0	0.0	0.0
Hs(3) ...0(3)	1.62	4	0.0	0.0	0.0

Symmetry code S	1	=	x ,	y ,	z
	- 1	=	-x ,	-y ,	-z
	2	=	$\frac{1}{2}$ -x ,	y ,	z
	- 2	=	$\frac{1}{2}$ +x ,	-y ,	z
	3	=	x ,	$\frac{1}{2}$ -y ,	z
	- 3	=	-x ,	$\frac{1}{2}$ +y ,	-z
	4	=	$\frac{1}{2}$ -x ,	$\frac{1}{2}$ -y ,	z
	- 4	=	$\frac{1}{2}$ +x ,	$\frac{1}{2}$ +y ,	-z

The 2nd atom is related to the first one at x,y,z by the transformation S, with a,b,c added respectively.

Table 1.10: Intramolecular distances (\AA) for $\text{TAABH}_2(\text{HSO}_4)_2$

C(9) ...C(11)	2.39	C(1) ...C(10)	2.46
N(2c1)...C(10)	2.46	N(1) ...C(10)	3.31
C(8n1)...C(10)	3.31	O(1a) ...C(10)	3.36
H(6) ...C(10)	2.97	N(1) ...C(9)	2.42
C(8n1)...C(9)	2.42	C(7) ...C(1)	2.36
C(7) ...N(2c1)	2.36	C(6) ...N(1)	2.45
O(1b) ...N(1)	3.18	C(6) ...C(8n1)	2.45
O(1b) ...C(8n1)	3.18	O(2) ...C(8n1)	3.40
C(5) ...C(7)	2.38	O(2) ...C(7)	3.08
O(2) ...C(6)	3.24	Hs(2) ...S	2.17
Hs(3) ...S	2.20	O(2) ...O(1a)	2.38
O(3) ...O(1a)	1.96	H(6) ...O(1a)	2.67
Hs(3) ...O(1a)	2.93	O(2) ...O(1b)	2.01
O(3) ...O(1b)	2.31	H(6) ...O(1b)	2.86
Hs(2) ...O(1b)	2.92	O(3) ...O(2)	2.28
Hs(3) ...O(2)	2.55	Hs(2) ...O(3)	2.66

Table 1.11: Fractional atomic coordinates and thermal parameters (\AA^2)
for $\text{TAABH}_2(\text{BF}_4)_2$

Atom	x	y	z	Uiso or Ueq
N(1)	0.0431(3)	0.0564(6)	0.3868(3)	0.061(3)
Cn(1)	0.0431(3)	0.0564(6)	0.3868(3)	0.061(3)
N(2)	0.0928(3)	-0.0637(7)	0.3031(3)	0.083(4)
Cn(2)	0.0928(3)	-0.0637(7)	0.3031(3)	0.083(4)
C(1)	0.0486(3)	-0.0708(6)	0.3501(3)	0.074(4)
Nc(1)	0.0486(3)	-0.0708(6)	0.3501(3)	0.074(4)
C(2)	0.0963(3)	0.1697(7)	0.4052(3)	0.061(4)
C(3)	0.1046(3)	0.2865(7)	0.4627(4)	0.075(4)
C(4)	0.1549(4)	0.4010(8)	0.4737(4)	0.084(5)
C(5)	0.1956(4)	0.4134(7)	0.4266(5)	0.079(5)
C(6)	0.1870(4)	0.3013(8)	0.3684(4)	0.083(5)
C(7)	0.1387(3)	0.1780(7)	0.3576(3)	0.062(4)
C(8)	0.1236(3)	0.0679(7)	0.2975(3)	0.062(3)
Nc(8)	0.1236(3)	0.0679(7)	0.2975(3)	0.062(3)
C(9)	-0.0087(3)	-0.1862(6)	0.3317(3)	0.056(3)
C(10)	0.0045(3)	-0.3037(7)	0.3870(3)	0.070(4)
C(11)	-0.0528(4)	-0.4113(7)	0.3713(4)	0.086(5)
C(12)	-0.1219(4)	-0.4029(7)	0.3014(4)	0.081(5)
C(13)	-0.1346(3)	-0.2908(8)	0.2450(4)	0.075(4)
C(14)	-0.0790(3)	-0.1812(7)	0.2594(3)	0.070(4)
B	0.1459(4)	0.1541(10)	0.1039(5)	0.068(5)
F(1a)	0.1789(3)	0.1859(7)	0.0557(4)	0.107(5)
F(1b)	0.1837(7)	0.2468(17)	0.0759(11)	0.191(14)
F(2a)	0.1887(3)	0.0551(7)	0.1615(4)	0.106(5)
F(2b)	0.1882(6)	0.1388(21)	0.1841(7)	0.174(12)

Table 1.11: continued

F(3b)	0.0855(6)	0.2385(17)	0.1036(11)	0.209(13)
F(3a)	0.1236(7)	0.2671(10)	0.1279(8)	0.270(12)
F(4b)	0.1213(10)	0.0318(24)	0.0738(14)	0.232(19)
F(4a)	0.0793(3)	0.0738(9)	0.0525(4)	0.121(5)
C(14b)	0.0790(3)	-0.1812(7)	0.2406(3)	0.050(**)

Table 1.12: Fractional atomic coordinates for the hydrogen atoms
for $\text{TAABH}_2(\text{BF}_4)_2$

Atom	x	y	z
H(1)	0.1159	-0.1097	0.4032
H(3)	0.0724	0.2830	0.4990
H(4)	0.1636	0.4857	0.5205
H(5)	0.2331	0.5086	0.4349
H(6)	0.2167	0.3108	0.3304
H(8)	0.1403	0.0569	0.2480
H(10)	0.0591	-0.3121	0.4425
H(11)	-0.0426	-0.5014	0.4152
H(12)	-0.1663	-0.4863	0.2901
H(13)	-0.1888	-0.2867	0.1877
Hn(1)	0.0086	0.0754	0.4184
Hn(2)	0.1515	-0.1079	0.3686

Table 1.13: Anisotropic thermal parameters (\AA^2) for $\text{TAABH}_2(\text{BF}_4)_2$

Atom	U11	U22	U33	U23	U13	U12
N(1)	0.050(3)	0.065(3)	0.068(3)	-0.015(3)	0.027(3)	-0.017(3)
Cn(1)	0.050(3)	0.065(3)	0.068(3)	-0.015(3)	0.027(3)	-0.017(3)
N(2)	0.075(4)	0.077(4)	0.097(4)	-0.021(4)	0.057(3)	-0.017(3)
Cn(2)	0.075(4)	0.077(4)	0.097(4)	-0.021(4)	0.057(3)	-0.017(3)
C(1)	0.081(4)	0.066(4)	0.074(3)	-0.011(3)	0.050(3)	-0.018(3)
Nc(1)	0.081(4)	0.066(4)	0.074(3)	-0.011(3)	0.050(3)	-0.018(3)
C(2)	0.050(3)	0.074(4)	0.060(4)	0.001(3)	0.018(3)	-0.003(3)
C(3)	0.075(4)	0.057(4)	0.095(5)	-0.025(4)	0.035(4)	-0.021(3)
C(4)	0.082(5)	0.087(5)	0.083(5)	-0.013(4)	0.016(4)	0.008(4)
C(5)	0.080(5)	0.069(5)	0.088(5)	0.013(4)	0.013(4)	-0.010(4)
C(6)	0.079(4)	0.090(5)	0.081(5)	0.017(4)	0.032(4)	-0.027(4)
C(7)	0.055(3)	0.073(4)	0.057(4)	0.018(3)	0.019(3)	0.002(3)
C(8)	0.069(3)	0.065(4)	0.051(3)	-0.001(3)	0.024(3)	-0.009(3)

Table 1.13: continued

Nc(8)	0.069(3)	0.065(4)	0.051(3)	-0.001(3)	0.024(3)	-0.009(3)
C(9)	0.055(3)	0.059(4)	0.053(3)	-0.004(3)	0.027(3)	-0.013(3)
C(10)	0.076(4)	0.081(4)	0.054(4)	0.004(3)	0.026(3)	-0.013(4)
C(11)	0.108(5)	0.083(5)	0.068(4)	0.001(4)	0.044(4)	-0.028(4)
C(12)	0.077(4)	0.088(5)	0.078(4)	-0.013(4)	0.039(4)	-0.030(4)
C(13)	0.057(4)	0.107(5)	0.061(4)	-0.004(4)	0.020(3)	-0.031(4)
C(14)	0.058(4)	0.089(5)	0.062(4)	0.011(4)	0.034(3)	0.006(4)
B	0.060(4)	0.078(5)	0.067(5)	-0.006(4)	0.022(4)	0.008(4)
F(1a)	0.089(4)	0.124(5)	0.107(4)	0.047(4)	0.073(4)	0.029(4)
F(1b)	0.103(9)	0.177(13)	0.294(20)	0.166(14)	0.035(11)	-0.027(9)
F(2a)	0.080(4)	0.139(6)	0.101(4)	0.074(4)	0.036(3)	0.031(4)
F(2b)	0.083(7)	0.364(22)	0.076(8)	-0.028(11)	0.026(7)	-0.064(11)
F(3b)	0.089(7)	0.185(12)	0.352(20)	0.140(14)	0.153(11)	0.073(8)
F(3a)	0.308(13)	0.118(7)	0.384(16)	-0.109(9)	0.262(13)	-0.014(8)
F(4b)	0.169(15)	0.203(17)	0.326(25)	-0.144(19)	0.062(16)	0.022(14)
F(4a)	0.082(4)	0.200(8)	0.081(4)	-0.013(5)	0.021(4)	-0.053(5)

Table 1.14: Intermolecular distances (\AA) for $\text{TAABH}_2(\text{BF}_4)_2$

		S	a	b	c
Cn(2) ...N(1)	3.41	2	0.0	0.0	0.0
C(8) ...N(1)	3.43	2	0.0	0.0	0.0
C(14b)...N(1)	3.23	2	0.0	0.0	0.0
F(3b) ...N(1)	3.04	2	0.0	0.0	0.0
F(4a) ...N(1)	3.03	2	0.0	0.0	0.0
F(4b) ...N(1)	3.10	-2	0.0	0.0	0.0
F(4a) ...N(1)	2.97	-2	0.0	0.0	0.0
N(2) ...Cn(1)	3.41	2	0.0	0.0	0.0
Cn(2) ...Cn(1)	3.41	2	0.0	0.0	0.0
C(8) ...Cn(1)	3.43	2	0.0	0.0	0.0
Nc(8) ...Cn(1)	3.43	2	0.0	0.0	0.0
C(14b)...Cn(1)	3.23	2	0.0	0.0	0.0
F(3b) ...Cn(1)	3.04	2	0.0	0.0	0.0
F(4a) ...Cn(1)	3.03	2	0.0	0.0	0.0
F(4b) ...Cn(1)	3.10	-2	0.0	0.0	0.0
F(4a) ...Cn(1)	2.97	-2	0.0	0.0	0.0
N(2) ...N(2)	3.22	2	0.0	0.0	0.0
Cn(2) ...N(2)	3.22	2	0.0	0.0	0.0
C(1) ...N(2)	2.88	2	0.0	0.0	0.0
Nc(1) ...N(2)	2.88	2	0.0	0.0	0.0
C(9) ...N(2)	2.48	2	0.0	0.0	0.0
C(13) ...N(2)	2.47	2	0.0	0.0	0.0
C(14) ...N(2)	1.47	2	0.0	0.0	0.0
C(14b)...N(2)	3.23	2	0.0	0.0	0.0
H(13) ...N(2)	2.67	2	0.0	0.0	0.0

Table 1.14: continued

Cn(2) ...Cn(2)	3.22	2	0.0	0.0	0.0
C(1) ...Cn(2)	2.88	2	0.0	0.0	0.0
Nc(1) ...Cn(2)	2.88	2	0.0	0.0	0.0
C(9) ...Cn(2)	2.48	2	0.0	0.0	0.0
C(13) ...Cn(2)	2.47	2	0.0	0.0	0.0
C(14) ...Cn(2)	1.47	2	0.0	0.0	0.0
C(14b)...Cn(2)	3.23	2	0.0	0.0	0.0
H(13) ...Cn(2)	2.67	2	0.0	0.0	0.0
C(1) ...C(1)	3.22	2	0.0	0.0	0.0
Nc(1) ...C(1)	3.22	2	0.0	0.0	0.0
C(8) ...C(1)	3.42	2	0.0	0.0	0.0
Nc(8) ...C(1)	3.42	2	0.0	0.0	0.0
C(9) ...C(1)	3.17	2	0.0	0.0	0.0
C(13) ...C(1)	3.47	2	0.0	0.0	0.0
C(14) ...C(1)	2.49	2	0.0	0.0	0.0
C(14b)...C(1)	2.47	2	0.0	0.0	0.0
Nc(1) ...Nc(1)	3.22	2	0.0	0.0	0.0
C(8) ...Nc(1)	3.42	2	0.0	0.0	0.0
C(9) ...Nc(1)	3.17	2	0.0	0.0	0.0
C(14) ...Nc(1)	2.49	2	0.0	0.0	0.0
C(14b)...Nc(1)	2.47	2	0.0	0.0	0.0
F(4b) ...C(2)	3.36	-2	0.0	0.0	0.0
F(3b) ...C(3)	3.35	2	0.0	0.0	0.0
F(4b) ...C(3)	3.39	-2	0.0	0.0	0.0
H(10) ...C(4)	3.05	1	0.0	-1.0	0.0
F(1a) ...C(5)	3.34	2	0.5	-0.5	0.0
C(9) ...C(8)	3.28	2	0.0	0.0	0.0
C(13) ...C(8)	3.30	2	0.0	0.0	0.0

Table 1.14: continued

C(14) ...C(8)	2.43	2	0.0	0.0	0.0
C(9) ...Nc(8)	3.28	2	0.0	0.0	0.0
C(13) ...Nc(8)	3.30	2	0.0	0.0	0.0
C(14) ...Nc(8)	2.43	2	0.0	0.0	0.0
C(9) ...C(9)	3.10	2	0.0	0.0	0.0
C(14) ...C(9)	2.84	2	0.0	0.0	0.0
C(14b)...C(9)	1.40	2	0.0	0.0	0.0
H(3) ...C(10)	3.03	-1	0.0	0.0	1.0
C(14b)...C(10)	2.39	2	0.0	0.0	0.0
F(4a) ...C(10)	3.35	-2	0.0	0.0	0.0
H(3) ...C(11)	2.77	-1	0.0	0.0	1.0
C(14b)...C(11)	2.75	2	0.0	0.0	0.0
F(3b) ...C(11)	3.24	2	0.0	1.0	0.0
F(3a) ...C(11)	3.17	2	0.0	1.0	0.0
C(14b)...C(12)	2.39	2	0.0	0.0	0.0
F(3a) ...C(12)	3.20	2	0.0	1.0	0.0
F(2b) ...C(12)	3.34	1	0.5	0.5	0.0
C(14b)...C(13)	1.39	2	0.0	0.0	0.0
Hn(2) ...C(13)	2.51	2	0.0	0.0	0.0
F(2a) ...C(13)	3.35	1	0.5	0.5	0.0
F(2b) ...C(13)	3.16	1	0.5	0.5	0.0
C(14) ...C(14)	3.23	2	0.0	0.0	0.0
H(1) ...C(14)	2.75	2	0.0	0.0	0.0
H(8) ...C(14)	2.40	2	0.0	0.0	0.0
Hn(2) ...C(14)	2.19	2	0.0	0.0	0.0
C(14b)...C(14b)	3.23	2	0.0	0.0	0.0
H(13) ...C(14b)	2.14	2	0.0	0.0	0.0
Hn(1) ...B	2.92	2	0.0	0.0	0.0

Table 1.14: continued

H(10) ...B	2.97	-2	0.0	0.0	1.0
H(13) ...B	2.91	1	-0.5	-0.5	0.0
H(5) ...B	3.02	2	0.5	0.5	0.0
H(1) ...F(1a)	2.54	-2	0.0	0.0	1.0
H(4) ...F(1a)	2.97	-2	0.0	1.0	1.0
H(10) ...F(1a)	2.56	-2	0.0	0.0	1.0
H(13) ...F(1a)	2.60	1	-0.5	-0.5	0.0
H(5) ...F(1a)	2.27	2	0.5	0.5	0.0
H(4) ...F(1b)	2.54	-2	0.0	1.0	1.0
H(10) ...F(1b)	2.59	-2	0.0	0.0	1.0
H(13) ...F(1b)	2.40	1	-0.5	-0.5	0.0
H(5) ...F(1b)	2.72	2	0.5	0.5	0.0
H(12) ...F(2a)	2.74	1	-0.5	-0.5	0.0
H(13) ...F(2a)	2.61	1	-0.5	-0.5	0.0
H(5) ...F(2a)	2.80	2	0.5	0.5	0.0
H(6) ...F(2a)	2.80	2	0.5	0.5	0.0
H(12) ...F(2b)	2.82	1	-0.5	-0.5	0.0
H(13) ...F(2b)	2.45	1	-0.5	-0.5	0.0
H(3) ...F(3b)	2.80	2	0.0	0.0	0.0
H(11) ...F(3b)	2.43	2	0.0	-1.0	0.0
Hn(1) ...F(3b)	2.22	2	0.0	0.0	0.0
H(10) ...F(3b)	2.78	-2	0.0	0.0	1.0
H(11) ...F(3a)	2.49	2	0.0	-1.0	0.0
H(12) ...F(3a)	2.56	2	0.0	-1.0	0.0
Hn(1) ...F(3a)	2.87	2	0.0	0.0	0.0
Hn(1) ...F(4b)	2.61	2	0.0	0.0	0.0
Hn(1) ...F(4b)	2.82	-2	0.0	0.0	1.0
H(5) ...F(4b)	2.90	2	0.5	0.5	0.0

Table 1.14: continued

F(4a) ...F(4a)	3.08	-1	0.0	0.0	0.0
Hn(1) ...F(4a)	1.99	2	0.0	0.0	0.0
H(10) ...F(4a)	2.80	-2	0.0	0.0	1.0
Hn(1) ...F(4a)	2.54	-2	0.0	0.0	1.0

Symmetry code S	1	=	x,	y,	z
	- 1	=	-x,	-y,	-z
	2	=	-x,	y,	$\frac{1}{2}-z$
	- 2	=	x,	-y,	$\frac{1}{2}+z$

The 2nd atom is related to the first one at x,y,z by the transformation S, with a,b,c, added respectively.

Table 1.15: Intramolecular distances (Å) for TAABH₂(BF₄)₂

N(2) ...N(1)	2.37	Cn(2) ...N(1)	2.37
C(3) ...N(1)	2.45	C(7) ...N(1)	2.40
C(8) ...N(1)	2.69	Nc(8) ...N(1)	2.69
C(9) ...N(1)	2.40	C(10) ...N(1)	3.28
C(14) ...N(1)	3.23	H(1) ...N(1)	1.97
H(3) ...N(1)	2.72	Hn(2) ...N(1)	2.69
N(2) ...Cn(1)	2.37	Cn(2) ...Cn(1)	2.37
C(3) ...Cn(1)	2.45	C(7) ...Cn(1)	2.40
C(8) ...Cn(1)	2.69	Nc(8) ...Cn(1)	2.69
C(9) ...Cn(1)	2.40	C(10) ...Cn(1)	3.28
C(14) ...Cn(1)	3.23	H(1) ...Cn(1)	1.97
H(3) ...Cn(1)	2.72	Hn(2) ...Cn(1)	2.69
C(2) ...N(2)	2.75	C(7) ...N(2)	2.36
C(9) ...N(2)	2.49	C(14) ...N(2)	3.23
H(1) ...N(2)	1.70	H(8) ...N(2)	1.95
C(2) ...Cn(2)	2.75	C(7) ...Cn(2)	2.36
C(9) ...Cn(2)	2.49	C(10) ...Cn(2)	3.47
C(14) ...Cn(2)	3.23	H(1) ...Cn(2)	1.70
H(8) ...Cn(2)	1.95	C(2) ...C(1)	2.36
C(7) ...C(1)	2.78	C(8) ...C(1)	2.40
Nc(8) ...C(1)	2.40	C(10) ...C(1)	2.44
C(14) ...C(1)	2.47	C(14b) ...C(1)	2.49
H(10) ...C(1)	2.66	Hn(1) ...C(1)	2.15
Hn(2) ...C(1)	1.90	C(2) ...Nc(1)	2.36
C(7) ...Nc(1)	2.78	C(8) ...Nc(1)	2.40

Table 1.15: continued

Nc(8) ...Nc(1)	2.40	C(10) ...Nc(1)	2.44
C(14) ...Nc(1)	2.47	C(14b)...Nc(1)	2.49
H(10) ...Nc(1)	2.66	Hn(1) ...Nc(1)	2.15
Hn(2) ...Nc(1)	1.90	C(4) ...C(2)	2.40
C(5) ...C(2)	2.80	C(6) ...C(2)	2.44
C(8) ...C(2)	2.40	Nc(8) ...C(2)	2.40
H(1) ...C(2)	2.51	H(3) ...C(2)	2.18
Hn(1) ...C(2)	2.00	Hn(2) ...C(2)	2.88
C(5) ...C(3)	2.41	C(6) ...C(3)	2.81
C(7) ...C(3)	2.46	H(4) ...C(3)	2.11
Hn(1) ...C(3)	2.50	C(6) ...C(4)	2.41
C(7) ...C(4)	2.79	H(3) ...C(4)	2.12
H(5) ...C(4)	2.16	C(7) ...C(5)	2.43
H(4) ...C(5)	2.14	H(6) ...C(5)	2.15
C(8) ...C(6)	2.45	Nc(8) ...C(6)	2.45
H(5) ...C(6)	2.16	H(8) ...C(6)	2.91
H(1) ...C(7)	2.78	H(6) ...C(7)	2.14
H(8) ...C(7)	2.26	Hn(2) ...C(7)	2.55
C(14b)...C(8)	2.43	F(2a) ...C(8)	3.22
F(2b) ...C(8)	2.90	H(1) ...C(8)	2.52
H(6) ...C(8)	2.70	Hn(2) ...C(8)	1.93
C(14b)...Nc(8)	2.43	F(2a) ...Nc(8)	3.22
F(2b) ...Nc(8)	2.90	H(1) ...Nc(8)	2.52
H(6) ...Nc(8)	2.70	Hn(2) ...Nc(8)	1.93
C(11) ...C(9)	2.40	C(12) ...C(9)	2.78
C(13) ...C(9)	2.41	C(14b)...C(9)	2.84
H(1) ...C(9)	2.27	H(10) ...C(9)	2.14
Hn(1) ...C(9)	2.73	Hn(2) ...C(9)	2.95

Table 1.15: continued

C(12) ...C(10)	2.40	C(13) ...C(10)	2.76
C(14) ...C(10)	2.39	H(1) ...C(10)	2.67
H(11) ...C(10)	2.14	C(13) ...C(11)	2.36
C(14) ...C(11)	2.75	H(10) ...C(11)	2.15
H(12) ...C(11)	2.13	C(14) ...C(12)	2.39
H(11) ...C(12)	2.12	H(13) ...C(12)	2.13
H(12) ...C(13)	2.12	C(14b)...C(14)	3.23
H(13) ...C(14)	2.14	H(1) ...C(14b)	2.75
H(8) ...C(14b)	2.40	Hn(2) ...C(14b)	2.19
H(8) ...B	2.78	F(2a) ...F(1a)	2.16
F(2b) ...F(1a)	2.27	F(3b) ...F(1a)	2.37
F(3a) ...F(1a)	2.15	F(4b) ...F(1a)	1.88
F(4a) ...F(1a)	2.15	F(2a) ...F(1b)	2.27
F(2b) ...F(1b)	2.13	F(3b) ...F(1b)	2.17
F(4b) ...F(1b)	2.25	F(4a) ...F(1b)	2.42
F(3b) ...F(2a)	2.42	F(3a) ...F(2a)	2.19
F(4a) ...F(2a)	2.15	H(8) ...F(2a)	2.14
F(3b) ...F(2b)	2.06	F(4b) ...F(2b)	2.05
F(4a) ...F(2b)	2.43	H(6) ...F(2b)	2.87
H(8) ...F(2b)	1.91	F(4b) ...F(3b)	2.11
H(8) ...F(3b)	2.82	F(4b) ...F(3a)	2.30
F(4a) ...F(3a)	2.12	H(8) ...F(3a)	2.76

APPENDIX 2

Table 2.1: Fractional atomic coordinates and thermal parameters (\AA)
for AA TETRAMER.

Atom	x	y	z	Uiso or Ueq
O(1a)	0.4647(3)	-0.0641(5)	0.6934(3)	0.056(3)
N(1a)	0.4280(4)	0.3491(6)	0.5710(3)	0.037(3)
N(2a)	0.3883(4)	0.1700(6)	0.6582(3)	0.034(3)
C(4a)	0.6323(5)	0.1957(9)	0.5185(4)	0.054(5)
C(5a)	0.6506(5)	0.0560(9)	0.5609(4)	0.062(6)
C(11a)	0.3259(5)	0.0934(8)	0.8440(4)	0.047(5)
C(12a)	0.2296(6)	0.0520(8)	0.8113(4)	0.055(5)
O(1b)	0.1047(3)	0.3759(5)	0.4309(3)	0.054(3)
N(1b)	0.1603(4)	-0.0364(6)	0.5529(3)	0.039(4)
N(2b)	0.1730(4)	0.2381(6)	0.5480(3)	0.038(4)
C(4b)	0.0769(5)	-0.1859(10)	0.3457(5)	0.061(6)
C(5b)	0.0622(5)	-0.0499(11)	0.3007(5)	0.060(6)
C(11b)	0.1644(6)	0.6241(8)	0.6407(4)	0.053(5)
C(12b)	0.2616(6)	0.6615(8)	0.6708(4)	0.055(5)
C(1a)	0.3771(5)	0.3096(8)	0.6149(4)	0.036(2)
C(2a)	0.5023(4)	0.2475(8)	0.5684(4)	0.035(2)
C(3a)	0.5585(5)	0.2909(8)	0.5209(4)	0.042(2)
C(6a)	0.5958(5)	0.0114(9)	0.6071(4)	0.051(2)
C(7a)	0.5196(5)	0.1079(8)	0.6107(4)	0.040(2)
C(8a)	0.4584(5)	0.0603(8)	0.6573(4)	0.039(2)
C(9a)	0.3319(4)	0.1372(7)	0.7107(4)	0.030(2)
C(10a)	0.3768(5)	0.1349(8)	0.7933(4)	0.043(2)

table 2.1: continued

C(13a)	0.1843(5)	0.0536(7)	0.7277(4)	0.044(2)
C(14a)	0.2360(4)	0.0968(7)	0.6766(4)	0.034(2)
C(1b)	0.1865(5)	0.0952(8)	0.5881(4)	0.037(2)
C(2b)	0.1214(5)	-0.0358(8)	0.4682(4)	0.042(2)
C(3b)	0.1034(5)	-0.1804(10)	0.4290(5)	0.059(2)
C(6b)	0.0774(5)	0.0926(9)	0.3396(4)	0.053(2)
C(7b)	0.1073(5)	0.1007(8)	0.4236(4)	0.039(2)
C(8b)	0.1256(5)	0.2481(9)	0.4638(5)	0.046(2)
C(9b)	0.2034(4)	0.3818(8)	0.5929(4)	0.034(2)
C(10b)	0.1345(5)	0.4828(8)	0.6013(4)	0.045(2)
C(13b)	0.3291(5)	0.5576(8)	0.6619(4)	0.044(2)

Table 2.2: Fractional atomic coordinates for the hydrogen atoms for AA TETRAMER

Atom	x	y	z
H(3a)	0.5439	0.3977	0.4867
H(4a)	0.6770	0.2297	0.4832
H(5a)	0.7084	-0.0176	0.5573
H(6a)	0.6106	-0.0965	0.6403
H(10a)	0.4520	0.1656	0.8185
H(11a)	0.3608	0.0932	0.9088
H(12a)	0.1898	0.0185	0.8507
H(13a)	0.1094	0.0215	0.7023
H(3b)	0.1103	-0.2860	0.4637
H(4b)	0.0674	-0.2967	0.3153
H(5b)	0.0389	-0.0552	0.2354
H(6b)	0.0660	0.1981	0.3044
H(10b)	0.0591	0.4533	0.5778
H(11b)	0.1116	0.7048	0.6479
H(12b)	0.2843	0.7712	0.7009
H(13b)	0.4047	0.5866	0.6857

Table 2.3: Anisotropic thermal parameters (\AA^2) for AA TETRAMER

Atom	U11	U22	U33	U23	U13	U12
O(1a)	0.061(3)	0.042(3)	0.065(3)	0.020(3)	0.029(3)	0.015(3)
N(1a)	0.038(3)	0.033(3)	0.041(3)	0.006(3)	0.021(3)	0.009(3)
N(2a)	0.039(3)	0.028(3)	0.036(3)	0.004(3)	0.018(3)	0.007(3)
C(4a)	0.044(5)	0.059(5)	0.058(5)	0.002(5)	0.030(4)	-0.003(4)
C(5a)	0.055(5)	0.054(5)	0.077(6)	0.017(5)	0.039(5)	0.021(4)
C(11a)	0.059(5)	0.039(5)	0.043(5)	0.003(4)	0.016(4)	-0.000(4)
C(12a)	0.068(6)	0.044(5)	0.052(5)	0.004(4)	0.038(5)	0.004(4)
O(1b)	0.061(3)	0.049(3)	0.053(3)	0.012(3)	0.016(3)	0.011(3)
N(1b)	0.040(4)	0.037(4)	0.041(4)	0.003(3)	0.007(3)	-0.001(3)
N(2b)	0.037(3)	0.039(4)	0.038(4)	0.007(3)	0.007(3)	0.003(3)
C(4b)	0.059(6)	0.064(6)	0.059(6)	-0.017(5)	-0.003(4)	0.011(5)
C(5b)	0.037(5)	0.097(7)	0.045(5)	-0.008(5)	0.005(4)	0.009(5)
C(11b)	0.059(5)	0.042(5)	0.059(5)	0.007(4)	0.032(4)	0.015(4)
C(12b)	0.060(6)	0.039(5)	0.065(5)	-0.009(4)	0.026(5)	0.006(5)

Table 2.4: Intermolecular distances (\AA) for AA TETRAMER

		S	a	b	c
H(10a)...O(1a)	2.67	2	1.0	0.0	1.0
H(13b)...O(1a)	2.68	2	1.0	0.0	1.0
H(3a) ...N(1a)	2.50	-1	1.0	1.0	1.0
H(11a)...N(1a)	2.73	-2	0.0	1.0	1.0
H(11a)...C(3a)	2.96	2	1.0	-1.0	1.0
C(2b) ...H(5a)	2.72	-1	1.0	0.0	1.0
C(7b) ...H(5a)	2.72	-1	1.0	0.0	1.0
C(10a)...H(6a)	2.57	2	1.0	0.0	1.0
C(11a)...H(6a)	2.81	2	1.0	0.0	1.0
H(13b)...C(8a)	2.83	2	1.0	0.0	1.0
O(1b) ...H(12a)	2.35	-2	0.0	1.0	0.0
H(12b)...C(13a)	2.96	1	0.0	1.0	0.0
C(4b) ...H(13a)	2.95	-1	0.0	0.0	1.0
C(5b) ...H(13a)	2.52	-1	0.0	0.0	1.0
C(6b) ...H(13a)	2.78	-1	0.0	0.0	1.0
H(12b)...C(14a)	2.89	1	0.0	1.0	0.0
H(3b) ...O(1b)	2.97	1	0.0	-1.0	0.0
H(10b)...O(1b)	2.78	-1	0.0	1.0	1.0
H(6b) ...C(4b)	2.95	2	0.0	0.0	0.0
C(6b) ...H(4b)	3.00	2	0.0	0.0	0.0
C(11b)...H(5b)	2.92	-2	0.0	1.0	1.0

Symmetry code S 1 = x, y, z
 -1 = -x, -y, -z
 2 = -x, 1/2+y, 1/2-z
 -2 = x, 1/2-y, 1/2+z

2nd atom is related to the first one at x, y, z by the transformation S, with a, b, c added respectively.

Table 2.5: Intramolecular distances (Å) for AA TETRAMER

N(2a) ...O(1a)	2.29	C(6a) ...O(1a)	2.89
H(6a) ...O(1a)	2.62	C(7a) ...O(1a)	2.39
C(9a) ...O(1a)	2.70	N(2a) ...N(1a)	2.37
C(3a) ...N(1a)	2.41	H(3a) ...N(1a)	2.63
C(7a) ...N(1a)	2.45	C(8a) ...N(1a)	2.87
H(13b)...N(1a)	2.96	C(14b)...N(1a)	2.40
C(2a) ...N(2a)	2.73	C(7a) ...N(2a)	2.40
C(10a)...N(2a)	2.44	H(10a)...N(2a)	2.65
C(14a)...N(2a)	2.45	C(1b) ...N(2a)	2.89
C(14b)...N(2a)	2.45	C(2a) ...C(1a)	2.31
C(7a) ...C(1a)	2.74	C(8a) ...C(1a)	2.45
C(9a) ...C(1a)	2.49	N(2b) ...C(1a)	2.91
C(9b) ...C(1a)	2.53	C(13b)...C(1a)	2.47
H(13b)...C(1a)	2.66	H(3a) ...C(2a)	2.16
C(4a) ...C(2a)	2.39	C(5a) ...C(2a)	2.77
C(6a) ...C(2a)	2.43	C(8a) ...C(2a)	2.47
H(4a) ...C(3a)	2.12	C(5a) ...C(3a)	2.41
C(6a) ...C(3a)	2.80	C(7a) ...C(3a)	2.42
C(4a) ...H(3a)	2.13	H(5a) ...C(4a)	2.14
C(6a) ...C(4a)	2.40	C(7a) ...C(4a)	2.77
C(5a) ...H(4a)	2.14	H(6a) ...C(5a)	2.13
C(7a) ...C(5a)	2.40	C(6a) ...H(5a)	2.12

table 2.5: continued

C(8a) ...C(6a)	2.49	C(7a) ...H(6a)	2.17
C(8a) ...H(6a)	2.71	C(9a) ...C(8a)	2.43
H(10a)...C(8a)	2.99	H(10a)...C(9a)	2.13
C(11a)...C(9a)	2.39	C(12a)...C(9a)	2.76
C(13a)...C(9a)	2.40	C(1b) ...C(9a)	2.51
C(14b)...C(9a)	2.81	H(11a)...C(10a)	2.14
C(12a)...C(10a)	2.40	C(13a)...C(10a)	2.77
C(14a)...C(10a)	2.41	C(11a)...H(10a)	2.14
H(12a)...C(11a)	2.14	C(13a)...C(11a)	2.41
C(14a)...C(11a)	2.79	C(12a)...H(11a)	2.15
H(13a)...C(12a)	2.15	C(14a)...C(12a)	2.42
C(13a)...H(12a)	2.15	C(1b) ...C(13a)	2.48
C(14a)...H(13a)	2.15	N(1b) ...H(13a)	2.99
C(1b) ...H(13a)	2.68	N(1b) ...C(14a)	2.38
N(2b) ...C(14a)	2.46	C(9b) ...C(14a)	2.82
N(2b) ...O(1b)	2.29	C(6b) ...O(1b)	2.87
H(6b) ...O(1b)	2.59	C(7b) ...O(1b)	2.38
C(9b) ...O(1b)	2.73	H(10b)...O(1b)	2.94
N(2b) ...N(1b)	2.38	C(3b) ...N(1b)	2.40
H(3b) ...N(1b)	2.62	C(7b) ...N(1b)	2.44
C(8b) ...N(1b)	2.86	C(2b) ...N(2b)	2.72
C(7b) ...N(2b)	2.38	C(10b)...N(2b)	2.44

table 2.5: continued

H(10b)...N(2b)	2.66	C(14b)...N(2b)	2.44
C(2b) ...C(1b)	2.29	C(7b) ...C(1b)	2.73
C(8b) ...C(1b)	2.44	C(9b) ...C(1b)	2.48
H(3b) ...C(2b)	2.16	C(4b) ...C(2b)	2.40
C(5b) ...C(2b)	2.77	C(6b) ...C(2b)	2.40
C(8b) ...C(2b)	2.45	H(4b) ...C(3b)	2.13
C(5b) ...C(3b)	2.40	C(6b) ...C(3b)	2.78
C(7b) ...C(3b)	2.43	C(4b) ...H(3b)	2.14
H(5b) ...C(4b)	2.14	C(6b) ...C(4b)	2.40
C(7b) ...C(4b)	2.78	C(5b) ...H(4b)	2.14
H(6b) ...C(5b)	2.14	C(7b) ...C(5b)	2.41
C(6b) ...H(5b)	2.14	C(8b) ...C(6b)	2.45
C(7b) ...H(6b)	2.14	C(8b) ...H(6b)	2.67
C(9b) ...C(8b)	2.46	H(10b)...C(9b)	2.14
C(11b)...C(9b)	2.39	C(12b)...C(9b)	2.76
C(13b)...C(9b)	2.39	H(11b)...C(10b)	2.15
C(12b)...C(10b)	2.42	C(13b)...C(10b)	2.78
C(14b)...C(10b)	2.42	C(11b)...H(10b)	2.16
H(12b)...C(11b)	2.15	C(13b)...C(11b)	2.40
C(14b)...C(11b)	2.79	C(12b)...H(11b)	2.14
H(13b)...C(12b)	2.13	C(14b)...C(12b)	2.42
C(13b)...H(12b)	2.14	C(14b)...H(13b)	2.15

Table 2.6: Fractional atomic coordinates and thermal parameters (\AA^2)
for AA TRIMER. CHCl_3

Atom	x	y	z	Uiso or Ueq
O(1)	0.1922(3)	-0.0531(3)	-0.1457(4)	0.065(2)
O(2)	0.3712(2)	-0.4550(3)	-0.1332(3)	0.052(2)
N(1)	0.3888(3)	-0.0874(3)	0.2918(4)	0.045(2)
N(2)	0.2442(3)	-0.1562(3)	0.0756(4)	0.039(2)
N(3)	0.3881(3)	-0.4213(3)	0.1234(4)	0.025(2)
C(1)	0.3134(3)	-0.1656(4)	0.2231(5)	0.040(2)
C(2)	0.4027(4)	0.0122(4)	0.2109(5)	0.043(2)
C(3)	0.4848(4)	0.0984(4)	0.2847(6)	0.050(2)
C(4)	0.5004(4)	0.1968(4)	0.2055(6)	0.062(3)
C(5)	0.4387(4)	0.2123(4)	0.0555(6)	0.057(3)
C(6)	0.3587(4)	0.1285(4)	-0.0174(6)	0.053(3)
C(7)	0.3394(4)	0.0285(4)	0.0601(5)	0.043(2)
C(8)	0.2531(4)	-0.0592(4)	-0.0155(5)	0.046(2)
C(9)	0.1558(3)	-0.2426(4)	0.0101(5)	0.041(2)
C(10)	0.0330(4)	-0.2006(4)	-0.0077(5)	0.052(3)
C(11)	-0.0537(4)	-0.2803(5)	-0.0834(6)	0.066(3)
C(12)	-0.0154(5)	-0.3973(5)	-0.1434(6)	0.067(3)
C(13)	0.1072(4)	-0.4401(4)	-0.1242(5)	0.053(3)
C(14)	0.1937(3)	-0.3629(4)	-0.0446(4)	0.040(2)
C(15)	0.3263(4)	-0.4158(4)	-0.0212(5)	0.044(2)
C(16)	0.3390(3)	-0.3961(4)	0.2592(5)	0.040(2)
C(17)	0.3345(4)	-0.4931(4)	0.3483(5)	0.055(3)

table 2.6: continued

c(18)	0.2909(4)	-0.4696(5)	0.4824(6)	0.061(3)
c(19)	0.2489(4)	-0.3491(5)	0.5282(5)	0.057(3)
c(20)	0.2542(4)	-0.2510(4)	0.4418(5)	0.050(3)
c(21)	0.2991(3)	-0.2729(4)	0.3073(5)	0.040(2)
c	0.1480(5)	-0.8683(5)	-0.4379(6)	0.072(3)
c1(1)	0.0717(1)	-0.7455(2)	-0.3472(3)	0.133(1)
c1(2)	0.2905(1)	-0.8324(1)	-0.4526(2)	0.113(1)
c1(3)	0.0593(2)	-0.9090(1)	-0.6179(2)	0.113(1)

Table 2.7: Fractional atomic coordinates for the hydrogen atoms for AA TRIMER. CHCl_3

Atom	x	y	z
H(N3)	0.4579	-0.4545	0.1432
H(3)	0.5346	0.0874	0.4011
H(4)	0.5625	0.2634	0.2618
H(5)	0.4532	0.2900	-0.0037
H(6)	0.3111	0.1399	-0.1346
H(10)	0.0039	-0.1074	0.0364
H(11)	-0.1500	-0.2499	-0.0949
H(12)	-0.0822	-0.4569	-0.2060
H(13)	0.1360	-0.5326	-0.1709
H(17)	0.3653	-0.5881	0.3121
H(18)	0.2896	-0.5459	0.5518
H(19)	0.2120	-0.3312	0.6316
H(20)	0.2230	-0.1565	0.4792
H	0.1341	-0.9617	-0.3787

Table 2.8: Anisotropic thermal parameters (\AA^2) for AA TRIMER. CHCl_3

Atom	U11	U22	U33	U23	U13	U12
O(1)	0.072(2)	0.070(2)	0.055(2)	0.026(1)	-0.013(2)	-0.028(1)
O(2)	0.055(2)	0.060(2)	0.043(1)	0.003(1)	0.012(1)	0.002(1)
N(1)	0.052(2)	0.042(2)	0.044(2)	0.005(1)	0.005(1)	-0.008(1)
N(2)	0.041(2)	0.037(2)	0.040(2)	0.008(1)	0.006(1)	-0.007(1)
N(3)	0.027(2)	0.025(2)	0.024(2)	0.006(1)	0.003(1)	0.003(1)
C(1)	0.040(2)	0.038(2)	0.041(2)	0.002(2)	0.006(2)	-0.006(2)
C(2)	0.047(2)	0.034(2)	0.049(2)	0.002(2)	0.012(2)	-0.005(2)
C(3)	0.054(3)	0.040(2)	0.056(3)	0.002(2)	0.011(2)	-0.011(2)
C(4)	0.061(3)	0.054(3)	0.073(4)	-0.002(2)	0.013(2)	-0.014(2)
C(5)	0.058(3)	0.046(3)	0.069(3)	0.012(2)	0.015(2)	-0.012(2)
C(6)	0.054(3)	0.048(3)	0.057(3)	0.012(2)	0.010(2)	-0.006(2)
C(7)	0.046(2)	0.036(2)	0.046(2)	0.007(2)	0.008(2)	-0.005(2)
C(8)	0.046(2)	0.045(2)	0.047(3)	0.010(2)	0.007(2)	-0.003(2)

table 2.8: continued

C(9)	0.037(2)	0.045(2)	0.043(2)	0.010(2)	0.003(2)	-0.008(2)
C(10)	0.045(2)	0.052(3)	0.061(3)	0.019(2)	0.009(2)	-0.002(2)
C(11)	0.043(3)	0.082(4)	0.081(4)	0.031(3)	0.002(2)	-0.014(3)
C(12)	0.056(3)	0.077(4)	0.069(3)	0.006(3)	-0.003(2)	-0.034(3)
C(13)	0.054(3)	0.050(3)	0.057(3)	0.004(2)	0.004(2)	-0.021(2)
C(14)	0.040(2)	0.046(2)	0.035(2)	0.006(2)	0.007(2)	-0.010(2)
C(15)	0.051(2)	0.032(2)	0.052(3)	0.005(2)	0.015(2)	-0.009(2)
C(16)	0.040(2)	0.037(2)	0.043(2)	0.009(2)	0.001(2)	-0.005(2)
C(17)	0.065(3)	0.049(3)	0.051(3)	0.013(2)	0.007(2)	-0.005(2)
C(18)	0.076(3)	0.060(3)	0.051(3)	0.022(2)	0.012(2)	-0.014(2)
C(19)	0.063(3)	0.075(3)	0.040(2)	0.015(2)	0.015(2)	-0.012(2)
C(20)	0.054(3)	0.055(3)	0.043(2)	0.004(2)	0.014(2)	-0.006(2)
C(21)	0.039(2)	0.044(2)	0.038(2)	0.007(2)	0.004(2)	-0.008(2)

table 2.8: continued

C	0.090(4)	0.064(3)	0.064(3)	0.002(3)	0.014(3)	-0.017(3)
C1(1)	0.084(1)	0.160(2)	0.174(2)	-0.077(1)	0.029(1)	0.003(1)
C1(2)	0.094(1)	0.124(1)	0.124(1)	0.019(1)	0.051(1)	-0.003(1)
C1(3)	0.214(2)	0.112(1)	0.060(1)	0.013(1)	-0.016(1)	-0.070(1)

Table 2.9: Intermolecular distances (\AA) for AA TRIMER. CHCl_3

			S	a	b	c
H	...O(1)	2.32	1	0.0	-1.0	0.0
H(10)	...O(1)	2.91	-1	0.0	0.0	0.0
H(18)	...O(2)	2.88	1	0.0	0.0	1.0
H(19)	...O(2)	2.78	1	0.0	0.0	1.0
N(3)	...O(2)	2.85	-1	1.0	-1.0	0.0
H(N3)	...O(2)	2.06	-1	1.0	-1.0	0.0
H(4)	...O(2)	2.71	-1	1.0	0.0	0.0
H(5)	...O(2)	2.83	-1	1.0	0.0	0.0
H(3)	...N(1)	2.69	-1	1.0	0.0	1.0
H(5)	...N(3)	2.84	-1	1.0	0.0	0.0
H(17)	...C(4)	2.81	1	0.0	-1.0	0.0
C(19)	...H(4)	2.71	-1	1.0	0.0	1.0
C(20)	...H(4)	2.99	-1	1.0	0.0	1.0
C(15)	...H(5)	2.94	-1	1.0	0.0	0.0
H(11)	...C(6)	2.87	-1	0.0	0.0	0.0
C	...H(6)	2.93	1	0.0	-1.0	0.0
Cl(2)	...H(6)	2.84	1	0.0	-1.0	0.0
C(17)	...H(12)	2.95	-1	0.0	-1.0	0.0
H(19)	...C(14)	2.99	1	0.0	0.0	1.0
Cl(3)	...H	2.73	-1	0.0	-2.0	-1.0

Symmetry code 1 = x, y, z

-1 = -x, -y, -z

2nd atom is related to the first one at x,y,z by the transformation

S, with a, b, c, added to x, y, z, respectively.

Table 2.10: Intramolecular distances (Å) for AA TRIMER.CHCl₃

N(2) ...O(1)	2.29	C(6) ...O(1)	2.87
H(6) ...O(1)	2.60	C(7) ...O(1)	2.38
C(9) ...O(1)	2.70	N(3) ...O(2)	2.25
H(N3) ...O(2)	2.45	C(13) ...O(2)	2.98
H(13) ...O(2)	2.82	C(14) ...O(2)	2.37
N(2) ...N(1)	2.37	C(3) ...N(1)	2.41
H(3) ...N(1)	2.64	C(7) ...N(1)	2.45
C(8) ...N(1)	2.87	H(20) ...N(1)	2.96
C(21) ...N(1)	2.38	C(2) ...N(2)	2.72
C(7) ...N(2)	2.41	C(10) ...N(2)	2.43
H(10) ...N(2)	2.65	C(14) ...N(2)	2.46
C(15) ...N(2)	2.94	C(21) ...N(2)	2.45
C(1) ...N(3)	2.89	C(14) ...N(3)	2.43
C(17) ...N(3)	2.43	H(17) ...N(3)	2.65
C(21) ...N(3)	2.46	C(15) ...H(N3)	1.89
C(16) ...H(N3)	1.87	C(17) ...H(N3)	2.61
C(21) ...H(N3)	2.97	C(2) ...C(1)	2.30
C(7) ...C(1)	2.74	C(8) ...C(1)	2.44
C(9) ...C(1)	2.47	C(16) ...C(1)	2.51
C(20) ...C(1)	2.48	H(20) ...C(1)	2.68
H(3) ...C(2)	2.17	C(4) ...C(2)	2.40
C(5) ...C(2)	2.79	C(6) ...C(2)	2.42

table 2.10; continued

C(8) ...C(2)	2.47	H(4) ...C(3)	2.13
C(5) ...C(3)	2.41	C(6) ...C(3)	2.79
C(7) ...C(3)	2.43	C(4) ...H(3)	2.14
H(5) ...C(4)	2.14	C(6) ...C(4)	2.39
C(7) ...C(4)	2.76	C(5) ...H(4)	2.13
H(6) ...C(5)	2.13	C(7) ...C(5)	2.40
C(6) ...H(5)	2.13	C(8) ...C(6)	2.48
C(7) ...H(6)	2.15	C(8) ...H(6)	2.69
C(9) ...C(8)	2.43	H(10) ...C(9)	2.14
C(11) ...C(9)	2.40	C(12) ...C(9)	2.76
C(13) ...C(9)	2.41	C(15) ...C(9)	2.54
C(21) ...C(9)	2.82	H(11) ...C(10)	2.16
C(12) ...C(10)	2.40	C(13) ...C(10)	2.78
C(14) ...C(10)	2.41	C(11) ...H(10)	2.16
H(12) ...C(11)	2.13	C(13) ...C(11)	2.40
C(14) ...C(11)	2.78	C(12) ...H(11)	2.13
H(13) ...C(12)	2.14	C(14) ...C(12)	2.40
C(13) ...H(12)	2.13	C(15) ...C(13)	2.48
C(14) ...H(13)	2.15	C(15) ...H(13)	2.67
C1(1) ...H(13)	2.74	C(16) ...C(14)	2.88
C(16) ...C(15)	2.46	H(17) ...C(16)	2.14
C(18) ...C(16)	2.40	C(19) ...C(16)	2.78

table 2.10; continued

C(20) ...C(16)	2.41	H(18) ...C(17)	2.13
C(19) ...C(17)	2.39	C(20) ...C(17)	2.76
C(21) ...C(17)	2.41	C(18) ...H(17)	2.13
H(19) ...C(18)	2.14	C(20) ...C(18)	2.39
C(21) ...C(18)	2.78	C(19) ...H(18)	2.13
H(20) ...C(19)	2.13	C(21) ...C(19)	2.41
C(20) ...H(19)	2.14	C(21) ...H(20)	2.14
C1(1) ...H	2.35	C1(2) ...H	2.60
C1(3) ...H	2.22	C1(2) ...C1(1)	2.84
C1(3) ...C1(1)	2.84	C1(3) ...C1(2)	2.89

Table 2.11: Fractional atomic coordinates and thermal parameters (\AA^2)
for AA TRIMER. $\text{CH}_3\text{CN}\cdot\text{H}_2\text{O}$

Atom	x	y	z	Uiso or Ueq
O(1)	0.5294(4)	-0.0142(3)	0.2389(3)	0.074(3)
O(2)	0.9421(3)	-0.0406(3)	0.3904(2)	0.043(2)
N(1)	0.5752(4)	0.1990(3)	0.4311(3)	0.044(3)
N(2)	0.6390(4)	0.1227(3)	0.3143(2)	0.037(3)
N(3)	0.9290(4)	0.1201(3)	0.4402(2)	0.035(3)
C(1)	0.6535(5)	0.1926(4)	0.3811(3)	0.036(3)
C(2)	0.4713(5)	0.1262(5)	0.4176(3)	0.044(4)
C(3)	0.3859(6)	0.1296(5)	0.4728(4)	0.057(4)
C(4)	0.2853(6)	0.0565(6)	0.4647(4)	0.066(5)
C(5)	0.2666(6)	-0.0188(6)	0.4013(4)	0.069(5)
C(6)	0.3482(6)	-0.0228(5)	0.3462(4)	0.053(4)
C(7)	0.4510(5)	0.0509(4)	0.3546(3)	0.041(3)
C(8)	0.5379(6)	0.0477(5)	0.2976(3)	0.047(4)
C(9)	0.7270(5)	0.1287(4)	0.2580(3)	0.036(3)
C(10)	0.6768(6)	0.1713(4)	0.1766(3)	0.048(4)
C(11)	0.7619(7)	0.1780(4)	0.1226(3)	0.056(4)
C(12)	0.8932(7)	0.1408(4)	0.1501(4)	0.060(4)
C(13)	0.9414(6)	0.0976(4)	0.2309(3)	0.048(4)
C(14)	0.8580(5)	0.0919(4)	0.2856(3)	0.034(3)
C(15)	0.9115(5)	0.0513(4)	0.3756(3)	0.034(3)
C(16)	0.9041(5)	0.2277(4)	0.4255(3)	0.034(3)
C(17)	1.0130(6)	0.2947(4)	0.4421(3)	0.041(4)

table 2.11: continued

C(18)	0.9890(7)	0.3982(4)	0.4270(4)	0.054(4)
C(19)	0.8583(7)	0.4354(4)	0.3969(3)	0.056(4)
C(20)	0.7489(6)	0.3686(4)	0.3818(3)	0.046(4)
C(21)	0.7706(5)	0.2644(4)	0.3955(3)	0.033(3)
C(a)	0.2270(9)	0.3094(6)	0.2737(5)	0.103(7)
C(b)	0.2702(11)	0.2593(9)	0.2080(7)	0.119(9)
N	0.3007(12)	0.2177(9)	0.1536(7)	0.192(11)
O	0.4228(11)	0.4524(6)	0.4862(6)	0.248(12)

Table 2.12: Fractional atomic coordinates for the hydrogen atoms
for AA TRIMER. $\text{CH}_3\text{CN}\cdot\text{H}_2\text{O}$

Atom	x	y	z
H(N3)	0.9687	0.0945	0.5012
H(3)	0.3988	0.1891	0.5211
H(4)	0.2213	0.0579	0.5079
H(5)	0.1870	-0.0749	0.3951
H(6)	0.3332	-0.0816	0.2973
H(10)	0.5736	0.1990	0.1552
H(11)	0.7251	0.2123	0.0593
H(12)	0.9584	0.1455	0.1078
H(13)	1.0439	0.0683	0.2518
H(17)	1.1156	0.2664	0.4667
H(18)	1.0738	0.4505	0.4388
H(19)	0.8413	0.5164	0.3852
H(20)	0.6466	0.3979	0.3592
H(a1)	0.3113	0.3593	0.3027
H(a2)	0.2175	0.2523	0.3202
H(a3)	0.1347	0.3539	0.2539
H(w1)	0.3294	0.3985	0.4720
H(w2)	0.4248	0.4704	0.5554

Table 2.13: Anisotropic thermal parameters (\AA^2) for AA TRIMER. $\text{CH}_3\text{CN.H}_2\text{O}$

Atom	U11	U22	U33	U23	U13	U12
O(1)	0.061(3)	0.088(3)	0.073(3)	-0.036(3)	0.026(2)	-0.026(2)
O(2)	0.051(2)	0.038(2)	0.041(2)	0.000(2)	0.008(2)	0.003(2)
N(1)	0.037(3)	0.056(3)	0.041(3)	0.001(2)	0.015(2)	0.001(3)
N(2)	0.030(3)	0.048(3)	0.032(2)	-0.007(2)	0.006(2)	-0.006(2)
N(3)	0.040(3)	0.036(3)	0.029(2)	0.004(2)	0.009(2)	0.002(2)
C(1)	0.039(4)	0.037(3)	0.032(3)	0.001(3)	0.005(3)	0.003(3)
C(2)	0.029(3)	0.060(4)	0.043(4)	0.006(3)	0.007(3)	0.002(3)
C(3)	0.046(4)	0.068(4)	0.056(4)	0.010(3)	0.025(3)	0.011(4)
C(4)	0.044(4)	0.091(6)	0.063(4)	0.025(4)	0.022(4)	0.009(4)
C(5)	0.038(4)	0.093(6)	0.077(5)	0.021(4)	0.017(4)	-0.008(4)
C(6)	0.041(4)	0.060(4)	0.058(4)	0.002(3)	0.006(3)	-0.008(3)
C(7)	0.030(3)	0.057(4)	0.037(3)	0.003(3)	0.004(3)	-0.008(3)
C(8)	0.040(4)	0.060(4)	0.042(4)	-0.011(3)	0.008(3)	-0.002(3)

table 2.13: continued

C(9)	0.038(3)	0.044(3)	0.027(3)	0.002(3)	0.011(3)	-0.001(3)
C(10)	0.052(4)	0.056(4)	0.036(3)	-0.003(3)	0.009(3)	0.002(3)
C(11)	0.087(5)	0.057(4)	0.023(3)	0.008(3)	0.014(3)	0.011(4)
C(12)	0.077(5)	0.060(4)	0.041(4)	0.006(3)	0.033(3)	0.009(4)
C(13)	0.055(4)	0.044(4)	0.045(4)	0.001(3)	0.026(3)	0.006(3)
C(14)	0.040(3)	0.034(3)	0.029(3)	-0.003(2)	0.010(3)	-0.002(3)
C(15)	0.029(3)	0.040(3)	0.033(3)	0.002(3)	0.007(2)	-0.003(3)
C(16)	0.038(3)	0.039(3)	0.024(3)	-0.001(2)	0.011(3)	-0.008(3)
C(17)	0.040(4)	0.045(4)	0.039(3)	-0.005(3)	0.006(3)	-0.010(3)
C(18)	0.056(4)	0.041(4)	0.064(4)	-0.005(3)	0.020(3)	-0.012(3)
C(19)	0.078(5)	0.032(4)	0.056(4)	-0.002(3)	0.029(4)	-0.000(4)
C(20)	0.054(4)	0.048(4)	0.038(3)	0.004(3)	0.015(3)	0.005(3)
C(21)	0.041(4)	0.036(3)	0.023(3)	-0.001(2)	0.010(3)	0.002(3)

table 2.13: continued

C(a)	0.123(8)	0.092(6)	0.093(7)	0.022(5)	0.041(6)	0.011(5)
C(b)	0.114(9)	0.116(9)	0.126(10)	0.034(8)	0.044(8)	0.035(7)
N	0.182(10)	0.204(12)	0.191(11)	0.011(8)	0.078(9)	0.059(8)
O	0.410(18)	0.206(11)	0.130(7)	0.033(8)	0.093(10)	0.166(10)

Table 2.14: Intermolecular distances (Å) for AA TRIMER.CH₃CN.H₂O

			S	a	b	c
H(20) ...O(1)	2.34	2	1.0	0.0	0.0	
H(a1) ...O(1)	2.54	2	1.0	0.0	0.0	
H(w2) ...O(1)	2.90	-2	0.0	1.0	1.0	
H(5) ...O(2)	2.53	1	-1.0	0.0	0.0	
N(3) ...O(2)	2.87	-1	2.0	0.0	1.0	
Hn(3) ...O(2)	1.86	-1	2.0	0.0	1.0	
H(4) ...O(2)	2.66	-1	1.0	0.0	1.0	
H(a3) ...O(2)	2.62	2	1.0	0.0	0.0	
H(11) ...N(1)	2.49	-2	0.0	1.0	0.0	
H(4) ...N(3)	3.00	1	-1.0	0.0	0.0	
C(15) ...Hn(3)	2.78	-1	2.0	0.0	1.0	
N ...H(3)	2.87	-2	0.0	1.0	0.0	
C(15) ...H(4)	2.97	-1	1.0	0.0	1.0	
C(20) ...H(6)	2.84	2	1.0	0.0	0.0	
C(21) ...H(11)	2.82	-2	0.0	1.0	1.0	
H(18) ...C(12)	2.93	2	2.0	0.0	0.0	
C(17) ...H(12)	2.98	-2	0.0	1.0	1.0	
C(19) ...H(18)	2.94	-1	2.0	1.0	1.0	
N ...H(19)	2.98	2	1.0	-1.0	0.0	
O ...O	1.96	-1	1.0	1.0	1.0	
H(w2) ...O	2.12	-1	1.0	1.0	1.0	
Symmetry code S	1 =	x,	y,	z		
	-1 =	-x,	-y,	-z		
	2 =	-x,	1/2+y,	1/2-z		
	-2 =	x,	1/2-y,	1/2+z		

2nd atom related to the first one at x, y, z by the transformation

S with a, b, c added to x, y, z respectively.

Table 2.15: Intramolecular distances (Å) for AA TRIMER. $\text{CH}_3\text{CN}\cdot\text{H}_2\text{O}$

N(2) ...O(1)	2.27	C(6) ...O(1)	2.87
H(6) ...O(1)	2.60	C(7) ...O(1)	2.38
C(9) ...O(1)	2.71	N(3) ...O(2)	2.26
Hn(3) ...O(2)	2.47	C(14) ...O(2)	2.40
N(2) ...N(1)	2.37	C(3) ...N(1)	2.40
H(3) ...N(1)	2.62	C(7) ...N(1)	2.45
C(8) ...N(1)	2.86	C(21) ...N(1)	2.39
C(2) ...N(2)	2.71	C(7) ...N(2)	2.39
C(10) ...N(2)	2.44	H(10) ...N(2)	2.65
C(14) ...N(2)	2.45	C(15) ...N(2)	2.85
C(21) ...N(2)	2.44	C(1) ...N(3)	2.88
C(14) ...N(3)	2.42	C(17) ...N(3)	2.43
H(17) ...N(3)	2.65	C(21) ...N(3)	2.46
C(15) ...Hn(3)	2.02	C(16) ...Hn(3)	2.12
C(17) ...Hn(3)	2.86	C(2) ...C(1)	2.28
C(7) ...C(1)	2.72	C(8) ...C(1)	2.43
C(9) ...C(1)	2.45	C(16) ...C(1)	2.51
C(20) ...C(1)	2.50	H(20) ...C(1)	2.70
H(3) ...C(2)	2.16	C(4) ...C(2)	2.42
C(5) ...C(2)	2.78	C(6) ...C(2)	2.43
C(8) ...C(2)	2.44	H(4) ...C(3)	2.14
C(5) ...C(3)	2.41	C(6) ...C(3)	2.79

table 2.15: continued

C(7) ...C(3)	2.41	C(4) ...H(3)	2.14
H(5) ...C(4)	2.14	C(6) ...C(4)	2.41
C(7) ...C(4)	2.78	C(5) ...H(4)	2.15
H(6) ...C(5)	2.14	C(7) ...C(5)	2.40
C(6) ...H(5)	2.13	C(8) ...C(6)	2.47
C(7) ...H(6)	2.16	C(8) ...H(6)	2.69
C(9) ...C(8)	2.44	H(10) ...C(9)	2.15
C(11) ...C(9)	2.39	C(12) ...C(9)	2.75
C(13) ...C(9)	2.39	C(15) ...C(9)	2.49
C(21) ...C(9)	2.77	H(11) ...C(10)	2.15
C(12) ...C(10)	2.41	C(13) ...C(10)	2.78
C(14) ...C(10)	2.41	C(11) ...H(10)	2.15
N ...H(10)	2.80	H(12) ...C(11)	2.14
C(13) ...C(11)	2.39	C(14) ...C(11)	2.77
C(12) ...H(11)	2.14	H(13) ...C(12)	2.13
C(14) ...C(12)	2.39	C(13) ...H(12)	2.13
C(15) ...C(13)	2.50	C(14) ...H(13)	2.14
C(15) ...H(13)	2.71	C(16) ...C(14)	2.80
C(16) ...C(15)	2.45	H(17) ...C(16)	2.14
C(18) ...C(16)	2.39	C(19) ...C(16)	2.77
C(20) ...C(16)	2.41	H(18) ...C(17)	2.13
C(19) ...C(17)	2.40	C(20) ...C(17)	2.78

table 2.15: continued

C(21) ...C(17)	2.42	C(18) ...H(17)	2.14
H(19) ...C(18)	2.14	C(20) ...C(18)	2.40
C(21) ...C(18)	2.77	C(19) ...H(18)	2.13
H(20) ...C(19)	2.14	C(21) ...C(19)	2.41
C(20) ...H(19)	2.14	C(21) ...H(20)	2.14
N ...C(a)	2.56	C(b) ...H(a1)	1.96
C(b) ...H(a2)	2.03	C(b) ...H(a3)	2.14

APPENDIX 3

Table 3.1: Fractional atomic coordinates and thermal parameters(\AA^2)
for Cu(TAABH₂)

Atom	x	y	z	Uiso or Ueq
Cu	0.10624(12)	0.19435(25)	0.25000	0.0437(16)
C(1)	-0.0614(6)	0.2982(11)	0.2082(20)	0.031(6)
C(2)	-0.0052(6)	0.2860(11)	0.1549(20)	0.033(7)
C(3)	0.0211(6)	0.3712(11)	0.0625(20)	0.036(7)
C(4)	-0.0087(6)	0.4686(11)	0.0233(20)	0.036(8)
C(5)	-0.0649(6)	0.4807(11)	0.0767(20)	0.063(9)
C(6)	-0.0913(6)	0.3955(11)	0.1691(20)	0.057(9)
N(1)	0.0244(7)	0.1880(16)	0.1868(22)	0.032(6)
C(7)	-0.0004(11)	0.0967(19)	0.1533(36)	0.041(8)
C(9)	-0.0209(5)	-0.0953(13)	0.1365(22)	0.036(8)
C(10)	-0.0090(5)	-0.2083(13)	0.1598(22)	0.048(8)
C(11)	0.0437(5)	-0.2413(13)	0.2238(22)	0.056(8)
C(12)	0.0845(5)	-0.1612(13)	0.2645(22)	0.044(7)
C(13)	0.0726(5)	-0.0481(13)	0.2411(22)	0.040(7)
C(8)	0.0199(5)	-0.0151(13)	0.1772(22)	0.018(7)
N(2)	0.1135(8)	0.0328(13)	0.2549(52)	0.046(5)
C(16)	0.1788(6)	-0.0580(11)	0.6390(26)	0.068(11)
C(17)	0.1804(6)	-0.0296(11)	0.8127(26)	0.060(11)
C(18)	0.1789(6)	0.0823(11)	0.8618(26)	0.053(9)
C(19)	0.1759(6)	0.1659(11)	0.7374(26)	0.054(8)
C(20)	0.1743(6)	0.1375(11)	0.5638(26)	0.046(8)

table 1.3: continued

C(15)	0.1758(6)	0.0255(11)	0.5146(26)	0.023(7)
N(3)	0.1663(7)	0.2210(14)	0.4333(27)	0.031(6)
C(21)	0.1949(10)	0.3128(20)	0.4475(37)	0.049(8)
N(4)	0.1213(7)	0.3370(14)	0.1495(26)	0.034(6)
C(14)	0.1712(12)	0.0023(24)	0.3211(36)	0.059(10)
C(22)	0.1904(8)	0.4096(11)	0.3439(25)	0.052(9)
C(23)	0.2252(8)	0.4970(11)	0.3975(25)	0.060(9)
C(24)	0.2201(8)	0.6021(11)	0.3218(25)	0.060(9)
C(25)	0.1802(8)	0.6197(11)	0.1924(25)	0.042(8)
C(26)	0.1453(8)	0.5323(11)	0.1388(25)	0.038(8)
C(27)	0.1504(8)	0.4272(11)	0.2145(25)	0.054(9)
C(28)	0.0790(9)	0.3540(22)	0.0055(40)	0.055(9)

Table 3.2: Fractional atomic coordinates for the Cu(TAABH₂)
hydrogen atoms

Atom	x	y	z
H(1)	-0.0819	0.2322	0.2798
H(4)	0.0117	0.5345	-0.0482
H(5)	-0.0880	0.5561	0.0464
H(6)	-0.1348	0.4049	0.2104
H(7)	-0.0423	0.1041	0.0982
H(9)	-0.0617	-0.0697	0.0870
H(10)	-0.0406	-0.2703	0.1284
H(11)	0.0529	-0.3288	0.2419
H(12)	0.1253	-0.1867	0.3140
H(16)	0.1799	-0.1447	0.6009
H(17)	0.1827	-0.0943	0.9090
H(18)	0.1801	0.1043	0.9963
H(19)	0.1747	0.2525	0.7755
H(21)	0.2259	0.3160	0.5496
H(14a)	0.1781	-0.0856	0.2993
H(14b)	0.2032	0.0499	0.2537
H(23)	0.2562	0.4834	0.4977
H(24)	0.2471	0.6698	0.3633
H(25)	0.1762	0.7010	0.1338
H(26)	0.1144	0.5459	0.0386
H(28a)	0.0800	0.2818	-0.0776
H(28b)	0.0919	0.4270	-0.0659
H(28a)	0.0800	0.2818	-0.0776
H(28b)	0.0919	0.4270	-0.0659

Table 3.3: Anisotropic thermal parameters (\AA^2) Cu(TAABH₂)

Atom	U11	U22	U33	U23	U13	U12
Cu	0.033(1)	0.060(2)	0.038(2)	0.003(4)	-0.018(3)	0.001(2)

Table 3.4: Intermolecular distances (Å) Cu(TAABH₂)

			S	a	b	c
C(18) ...Cu	3.72	1	0.0	0.0	1.0	
H(18) ...Cu	2.85	1	0.0	0.0	1.0	
C(9) ...Cu	3.81	2	0.0	0.0	-1.0	
C(10) ...Cu	3.93	2	0.0	0.0	-1.0	
H(9) ...Cu	3.20	2	0.0	0.0	-1.0	
H(10) ...Cu	3.45	2	0.0	0.0	-1.0	
H(4) ...C(1)	3.00	2	0.0	1.0	-1.0	
C(11) ...C(3)	3.42	2	0.0	0.0	0.0	
H(11) ...C(4)	2.95	2	0.0	0.0	0.0	
H(10) ...C(5)	3.06	1	0.0	-1.0	0.0	
H(28b)...C(5)	3.06	2	0.0	1.0	-1.0	
H(28b)...C(5)	3.06	2	0.0	1.0	-1.0	
H(4) ...C(6)	3.01	2	0.0	1.0	-1.0	
H(26) ...C(6)	3.01	2	0.0	1.0	-1.0	
H(28b)...C(6)	2.96	2	0.0	1.0	-1.0	
H(28b)...C(6)	2.96	2	0.0	1.0	-1.0	
C(21) ...H(5)	3.07	2	0.0	1.0	0.0	
C(22) ...H(5)	2.91	2	0.0	1.0	0.0	
C(27) ...H(5)	2.98	2	0.0	1.0	0.0	
C(12) ...H(7)	2.87	2	0.0	0.0	0.0	
C(13) ...H(7)	2.95	2	0.0	0.0	0.0	
H(28a)...C(10)	2.78	2	0.0	0.0	-1.0	
H(28a)...C(10)	2.78	2	0.0	0.0	-1.0	
H(25) ...C(12)	2.90	1	0.0	1.0	0.0	
H(9) ...C(13)	3.05	2	0.0	0.0	-1.0	

table 3.4: continued

N(2) ...H(9)	2.89	2	0.0	0.0	0.0
C(20) ...H(9)	2.78	2	0.0	0.0	0.0
C(15) ...H(9)	2.80	2	0.0	0.0	0.0
C(26) ...H(11)	2.86	1	0.0	1.0	0.0
C(25) ...H(12)	2.82	1	0.0	1.0	0.0
H(18) ...N(2)	2.69	1	0.0	0.0	1.0
H(14b)...C(17)	2.94	3	0.0	0.0	-1.0
H(14b)...C(18)	2.93	3	0.0	0.0	-1.0
H(28a)...C(19)	3.02	1	0.0	0.0	-1.0
H(28a)...C(19)	3.02	1	0.0	0.0	-1.0
C(14) ...H(18)	2.82	1	0.0	0.0	-1.0
H(23) ...C(24)	2.95	3	0.0	0.0	0.0
H(23) ...C(25)	2.69	3	0.0	0.0	0.0
H(23) ...C(26)	2.63	3	0.0	0.0	0.0
H(23) ...C(27)	2.85	3	0.0	0.0	0.0

Symmetry code S	1	=	x ,	y ,	z
	2	=	-x ,	-y ,	$\frac{1}{2}+z$
	3	=	$\frac{1}{2}-x$,	y ,	$\frac{1}{2}+z$

The 2nd atom is related to the first one at x,y,z by the transformation S, with a,b,c added to x,y,z respectively.

Table 3.5: Intramolecular distances (Å) Cu(TAABH₂)

C(2) ...Cu	2.94	C(3) ...Cu	3.26
C(7) ...Cu	2.87	C(20) ...Cu	3.00
C(13) ...Cu	3.01	C(8) ...Cu	3.28
C(15) ...Cu	3.32	C(27) ...Cu	2.99
C(21) ...Cu	2.96	C(14) ...Cu	2.82
H(14b) ...Cu	2.87	C(22) ...Cu	3.33
H(28a) ...Cu	2.83	H(28a) ...Cu	2.83
C(3) ...C(1)	2.42	C(4) ...C(1)	2.79
C(5) ...C(1)	2.42	C(7) ...C(2)	2.27
H(6) ...C(1)	2.15	N(1) ...C(1)	2.42
C(7) ...C(1)	2.84	H(7) ...C(1)	2.52
C(4) ...C(2)	2.42	C(5) ...C(2)	2.79
C(6) ...C(2)	2.42	H(1) ...C(2)	2.15
H(7) ...C(2)	2.39	H(4) ...C(3)	2.15
N(4) ...C(2)	3.04	C(28) ...C(2)	2.44
H(28a) ...C(2)	2.70	H(28a) ...C(2)	2.70
C(5) ...C(3)	2.42	C(6) ...C(3)	2.79
N(1) ...C(3)	2.40	C(7) ...C(3)	3.40
N(4) ...C(3)	2.49	C(27) ...C(3)	3.34
H(26) ...C(3)	3.04	C(6) ...C(4)	2.42
H(28a) ...C(3)	2.06	H(28b) ...C(3)	2.06

table 3.5: continued

H(28a)...C(3)	2.06	H(28b)...C(3)	2.06
H(5) ...C(4)	2.15	H(26) ...C(4)	3.05
C(28) ...C(4)	2.48	H(28b)...C(4)	2.52
H(28b)...C(4)	2.52	H(4) ...C(5)	2.15
H(6) ...C(5)	2.15	H(1) ...C(6)	2.15
H(5) ...C(6)	2.15	N(2) ...N(1)	2.85
N(1) ...H(1)	2.66	C(7) ...H(1)	2.70
C(28) ...H(4)	2.71	H(7) ...N(1)	1.99
C(13) ...N(1)	3.08	C(8) ...N(1)	2.44
N(4) ...N(1)	2.91	C(28) ...N(1)	2.76
H(28a)...N(1)	2.69	H(28a)...N(1)	2.69
C(9) ...C(7)	2.35	C(13) ...C(7)	2.54
H(9) ...C(7)	2.51	H(10) ...C(9)	2.15
N(2) ...C(7)	2.90	C(9) ...H(7)	2.46
C(8) ...H(7)	2.14	C(11) ...C(9)	2.42
C(12) ...C(9)	2.79	C(13) ...C(9)	2.42
C(12) ...C(10)	2.42	C(13) ...C(10)	2.79
C(8) ...C(10)	2.42	H(9) ...C(10)	2.15

table 3.5: continued

H(11) ...C(10)	2.15	C(13) ...C(11)	2.42
C(8) ...C(11)	2.79	H(10) ...C(11)	2.15
H(12) ...C(11)	2.15	C(8) ...C(12)	2.42
H(11) ...C(12)	2.15	N(2) ...C(12)	2.42
C(14) ...C(12)	2.86	H(14a)...C(12)	2.40
H(12) ...C(13)	2.15	C(15) ...C(13)	3.35
C(14) ...C(13)	2.48	H(14a)...C(13)	2.56
H(9) ...C(8)	2.15	N(2) ...C(8)	2.36
N(2) ...H(12)	2.68	C(14) ...H(12)	2.51
C(20) ...N(2)	3.07	C(15) ...N(2)	2.50
N(3) ...N(2)	2.93	C(14) ..C(16)	2.59
H(14a)...N(2)	2.11	H(14b)...N(2)	2.12
C(18) ...C(16)	2.42	C(19) ...C(16)	2.79
C(20) ...C(16)	2.42	H(17) ...C(16)	2.15
H(14a)...C(16)	2.67	C(19) ...C(17)	2.42
C(20) ...C(17)	2.79	C(15) ...C(17)	2.42
H(16) ...C(17)	2.15	H(18) ...C(17)	2.15
C(20) ...C(18)	2.42	C(15) ...C(18)	2.79
H(17) ...C(18)	2.15	H(19) ...C(18)	2.15
C(15) ...C(19)	2.42	H(18) ...C(19)	2.15

Table 3.5: continued

N(3) ...C(19)	2.47	H(19) ...C(20)	2.15
C(21) ...C(19)	2.90	H(21) ...C(19)	2.60
C(21) ...C(20)	2.34	H(21) ...C(20)	2.46
C(14) ...C(20)	2.49	H(14b) ...C(20)	2.72
H(16) ...C(15)	2.15	N(3) ...C(15)	2.44
H(14a) ...C(15)	2.14	H(14b) ...C(15)	2.15
C(14) ...H(16)	2.81	N(3) ...H(19)	2.70
C(21) ...H(19)	2.70	N(4) ...C(21)	2.91
H(21) ...N(3)	2.02	N(4) ...N(3)	2.82
C(14) ...N(3)	2.76	H(14b) ...N(3)	2.63
C(22) ...N(3)	2.43	C(27) ...N(3)	3.02
C(23) ...C(21)	2.35	C(27) ...C(21)	2.50
H(23) ...C(21)	2.53	H(26) ...N(4)	2.65
C(22) ...H(21)	2.13	C(23) ...H(21)	2.47
C(22) ...N(4)	2.39	C(26) ...N(4)	2.41
H(28a) ...N(4)	2.12	H(28b) ...N(4)	2.11
H(28a) ...N(4)	2.12	H(28b) ...N(4)	2.11
C(24) ...C(22)	2.42	C(25) ...C(22)	2.79
C(26) ...C(22)	2.42	H(23) ...C(22)	2.15
C(25) ...C(23)	2.42		

table 3.5: continued

C(26) ...C(23)	2.79	C(27) ...C(23)	2.42
H(24) ...C(23)	2.15	C(28) ...C(26)	2.84
C(26) ...C(24)	2.42	C(27) ...C(24)	2.79
H(23) ...C(24)	2.15	H(25) ...C(24)	2.15
C(27) ...C(25)	2.42	H(24) ...C(25)	2.15
H(26) ...C(25)	2.15	H(25) ...C(26)	2.15
H(28b)...C(26)	2.39	H(28b)...C(26)	2.39
H(26) ...C(27)	2.15	H(28b)...C(27)	2.58
C(28) ...C(27)	2.50	H(28b)...C(27)	2.58
C(28) ...H(26)	2.46		

APPENDIX 4

Table 4.1: Fractional atomic coordinates and thermal parameters
for FeDIKETO

Atom	x	y	z	Uiso or Ueq
Fe(1)	-0.2944(2)	0.0868(1)	0.1107(1)	0.048(2)
Fe(2)	-0.0934(2)	0.0907(1)	0.3235(1)	0.044(2)
O(2)	-0.1695(8)	0.0837(4)	0.2077(6)	0.050(7)
N(2b)	-0.3387(13)	0.1576(5)	0.0788(9)	0.056(10)
N(2a)	-0.2444(12)	0.0867(6)	-0.0118(8)	0.056(9)
N(1a)	-0.3537(12)	0.0141(5)	0.0861(9)	0.053(10)
N(1b)	-0.4514(11)	0.0818(5)	0.1747(8)	0.046(9)
N(2d)	0.0537(12)	0.1367(5)	0.3321(8)	0.045(10)
N(2c)	0.0406(12)	0.0384(5)	0.3597(8)	0.044(9)
N(1c)	-0.2029(12)	0.0509(5)	0.4000(8)	0.048(9)
N(1d)	-0.1836(12)	0.1472(5)	0.3800(8)	0.047(10)
O(1a)	-0.2427(14)	0.1414(5)	-0.1335(9)	0.106(12)
O(1b)	-0.3306(16)	0.2152(5)	-0.0353(10)	0.124(14)
O(1c)	0.2585(11)	0.0344(4)	0.4008(8)	0.066(9)
O(1d)	0.2705(11)	0.1290(5)	0.3453(10)	0.099(11)
C(1a)	-0.2589(18)	0.1324(8)	-0.0541(15)	0.071(6)
C(2a)	-0.1938(17)	0.0466(7)	-0.0488(12)	0.058(5)
C(3a)	-0.0997(16)	0.0522(7)	-0.1043(12)	0.070(6)
C(4a)	-0.0522(17)	0.0096(7)	-0.1354(12)	0.069(6)
C(5a)	-0.0928(17)	-0.0360(8)	-0.1261(13)	0.077(6)
C(6a)	-0.1872(16)	-0.0457(7)	-0.0743(12)	0.070(6)
C(7a)	-0.2314(16)	-0.0015(6)	-0.0325(11)	0.052(5)
C(8a)	-0.3177(17)	-0.0132(7)	0.0278(12)	0.061(6)
C(9a)	-0.4296(15)	-0.0034(6)	0.1467(11)	0.045(5)
C(10a)	-0.4454(15)	-0.0551(6)	0.1639(12)	0.061(5)

Table 4.1: continued

C(11a)	-0.5208(16)	-0.0674(7)	0.2267(12)	0.068(6)
C(11b)	-0.5687(16)	-0.0290(7)	0.2735(12)	0.066(6)
C(10b)	-0.5549(15)	0.0197(7)	0.2567(11)	0.056(5)
C(9b)	-0.4803(15)	0.0324(7)	0.1926(11)	0.047(5)
C(8b)	-0.5030(15)	0.1213(7)	0.2050(11)	0.053(5)
C(7b)	-0.4644(16)	0.1708(7)	0.1938(12)	0.060(5)
C(6b)	-0.5139(18)	0.2064(7)	0.2507(13)	0.078(6)
C(5b)	-0.4762(18)	0.2567(8)	0.2528(14)	0.085(7)
C(4b)	-0.3996(18)	0.2735(8)	0.2019(13)	0.085(7)
C(3b)	-0.3524(17)	0.2420(8)	0.1428(13)	0.078(6)
C(2b)	-0.3863(18)	0.1914(7)	0.1369(13)	0.066(6)
C(1b)	-0.3145(18)	0.1730(8)	-0.0036(15)	0.068(6)
C(1c)	0.1614(19)	0.0565(7)	0.3704(12)	0.054(5)
C(2c)	0.0191(16)	-0.0134(7)	0.3691(11)	0.051(5)
C(3c)	0.1079(15)	-0.0488(6)	0.3552(11)	0.054(5)
C(4c)	0.0843(16)	-0.1003(7)	0.3695(11)	0.064(6)
C(5c)	-0.0245(17)	-0.1152(7)	0.3958(12)	0.073(6)
C(6c)	-0.1163(17)	-0.0806(7)	0.4074(12)	0.072(6)
C(7c)	-0.0935(15)	-0.0290(6)	0.3955(10)	0.045(5)
C(8c)	-0.1924(18)	0.0038(7)	0.4139(12)	0.066(6)
C(9c)	-0.2960(14)	0.0809(6)	0.4286(10)	0.037(4)
C(10c)	-0.3923(15)	0.0601(7)	0.4669(11)	0.060(5)
C(11c)	-0.4752(15)	0.0927(7)	0.4992(11)	0.063(5)
C(11d)	-0.4592(16)	0.1437(7)	0.4965(11)	0.060(5)
C(10d)	-0.3655(15)	0.1639(6)	0.4569(11)	0.056(5)
C(9d)	-0.2831(15)	0.1312(6)	0.4217(11)	0.041(5)
C(8d)	-0.1646(15)	0.1938(7)	0.3713(11)	0.046(5)
C(7d)	-0.0599(16)	0.2131(6)	0.3342(11)	0.055(5)

Table 4.1: continued

C(6d)	-0.0718(17)	0.2667(7)	0.3192(12)	0.071(6)
C(5d)	0.0247(19)	0.2926(8)	0.2874(13)	0.088(7)
C(4d)	0.1279(19)	0.2655(8)	0.2681(13)	0.087(7)
C(3d)	0.1351(16)	0.2145(7)	0.2805(11)	0.064(6)
C(2d)	0.0456(16)	0.1868(7)	0.3164(11)	0.051(5)
C(1d)	0.1639(18)	0.1119(7)	0.3479(12)	0.053(5)
O	0.3046(20)	0.1416(9)	-0.0412(14)	0.100(7)
N	0.2379(23)	0.2084(9)	0.0103(16)	0.066(7)
C(1)	0.2476(25)	0.2588(12)	0.0294(21)	0.088(10)
C(2)	0.1301(28)	0.1885(11)	0.0310(18)	0.083(10)
C(3)	0.3123(32)	0.1835(13)	-0.0271(22)	0.095(11)

Table 4.2: Fractional atomic coordinates for the hydrogen atoms
for FeDIKETO

Atom	x	y	z
H(3a)	-0.0681	0.0887	-0.1209
H(4a)	0.0256	0.0138	-0.1700
H(5a)	-0.0546	-0.0667	-0.1589
H(6a)	-0.2232	-0.0827	-0.0663
H(8a)	-0.3557	-0.0507	0.0216
H(10a)	-0.4012	-0.0837	0.1299
H(11a)	-0.5414	-0.1060	0.2389
H(11b)	-0.6199	-0.0392	0.3258
H(10b)	-0.5988	0.0481	0.2910
H(8b)	-0.5790	0.1153	0.2408
H(6b)	-0.5792	0.1942	0.2921
H(5b)	-0.5123	0.2824	0.2971
H(4b)	-0.3725	0.3124	0.2062
H(3b)	-0.2893	0.2565	0.1016
H(3c)	0.1934	-0.0373	0.3341
H(4c)	0.1525	-0.1280	0.3590
H(5c)	-0.0389	-0.1543	0.4084
H(6c)	-0.2037	-0.0928	0.4245
H(8c)	-0.2652	-0.0137	0.4429
H(10c)	-0.4026	0.0201	0.4711
H(11c)	-0.5525	0.0775	0.5262
H(11d)	-0.5198	0.1681	0.5260
H(10d)	-0.3550	0.2040	0.4526
H(8d)	-0.2295	0.2201	0.3916
H(6d)	-0.1534	0.2865	0.3322

Table 4.2: continued

H(5d)	0.0190	0.3327	0.2776
H(4d)	0.2022	0.2850	0.2440
H(3d)	0.2131	0.1947	0.2617
H(11)	0.3046	0.2330	-0.0005
H(12)	0.3005	0.2715	0.0949
H(13)	0.2229	0.2905	-0.0156
H(21)	0.1426	0.1587	0.0808
H(22)	0.0373	0.2047	0.0254
H(23)	0.2010	0.2169	0.0525
H(3)	0.3880	0.2036	-0.0482

Table 4.3: Anisotropic thermal parameters (\AA^2) for FeDIKETO

Atom	U11	U22	U33	U23	U13	U12
Fe(1)	0.049(2)	0.060(2)	0.035(2)	0.006(2)	0.015(1)	0.001(2)
Fe(2)	0.044(2)	0.052(2)	0.037(2)	-0.001(2)	0.012(1)	0.006(2)
O(2)	0.042(7)	0.067(8)	0.041(7)	0.009(7)	0.014(5)	-0.001(7)
N(2b)	0.073(11)	0.048(10)	0.049(10)	0.012(8)	0.015(8)	-0.004(8)
N(2a)	0.082(11)	0.044(9)	0.043(9)	0.009(10)	0.010(8)	-0.008(10)
N(1a)	0.048(9)	0.068(11)	0.043(9)	0.003(8)	0.034(7)	0.010(8)
N(1b)	0.037(8)	0.051(10)	0.051(9)	-0.015(8)	0.004(7)	0.006(8)
N(2d)	0.050(10)	0.045(10)	0.041(9)	0.004(7)	0.005(7)	0.012(8)
N(2c)	0.053(10)	0.048(10)	0.031(8)	-0.003(7)	0.008(7)	0.007(8)
N(1c)	0.051(10)	0.057(10)	0.035(9)	0.003(8)	0.022(7)	-0.004(9)
N(1d)	0.049(10)	0.052(10)	0.039(9)	0.002(8)	0.012(7)	0.002(8)
O(1a)	0.168(15)	0.087(11)	0.062(10)	0.015(8)	0.045(10)	-0.032(10)
O(1b)	0.215(18)	0.071(11)	0.087(11)	0.023(9)	0.033(11)	0.010(11)

Table 4.3: continued

O(1c)	0.050(8)	0.071(9)	0.078(9)	0.008(8)	0.012(7)	0.014(7)
O(1d)	0.043(9)	0.077(10)	0.178(15)	0.039(10)	0.024(9)	0.008(8)

Table 4.4: Intermolecular distances (Å) for FeDIKETO

			S	a	b	c
H(5a) ...Fe(1)	3.74	-1	0.0	0.0	0.0	
H(4a) ...Fe(2)	3.78	-1	0.0	0.0	0.0	
C(5a) ...Fe(2)	4.16	-1	0.0	0.0	0.0	
H(5a) ...Fe(2)	3.26	-1	0.0	0.0	0.0	
C(5c) ...Fe(2)	4.17	-1	0.0	0.0	1.0	
C(6c) ...Fe(2)	4.19	-1	0.0	0.0	1.0	
H(5a) ...O(2)	2.71	-1	0.0	0.0	0.0	
C(3c) ...C(4a)	3.38	-1	0.0	0.0	0.0	
C(2c) ...H(4a)	2.91	-1	0.0	0.0	0.0	
C(3c) ...H(4a)	2.99	-1	0.0	0.0	0.0	
C(1d) ...H(5a)	3.07	-1	0.0	0.0	0.0	
H(21) ...C(6a)	3.06	-1	0.0	0.0	0.0	
O ...H(6a)	2.53	-1	0.0	0.0	0.0	
C(2) ...H(6a)	3.01	-1	0.0	0.0	0.0	
C(9a) ...C(8a)	3.40	-1	-1.0	0.0	0.0	
O ...H(8a)	2.50	-1	0.0	0.0	0.0	
O ...H(10a)	2.41	-1	0.0	0.0	0.0	
O(1a) ...C(11a)	3.31	-1	-1.0	0.0	0.0	
O(1a) ...H(11a)	2.71	-1	-1.0	0.0	0.0	
H(3c) ...C(11b)	2.91	1	1.0	0.0	0.0	
O(1c) ...C(11b)	3.38	1	1.0	0.0	0.0	
C(3c) ...H(11b)	3.08	1	1.0	0.0	0.0	
O(1c) ...H(11b)	2.73	1	1.0	0.0	0.0	
C(11c)...H(11b)	2.97	-1	-1.0	0.0	1.0	
O(1c) ...C(10b)	3.26	1	1.0	0.0	0.0	

Table 4.4: continued

C(1c) ...H(10b)	3.07	1	1.0	0.0	0.0
O(1c) ...H(10b)	2.50	1	1.0	0.0	0.0
O(1d) ...H(10b)	2.79	1	1.0	0.0	0.0
O(1d) ...H(8b)	2.50	1	1.0	0.0	0.0
H(3d) ...C(6b)	3.01	1	1.0	0.0	0.0
O(1d) ...H(6b)	2.62	1	1.0	0.0	0.0
H(12) ...C(5b)	3.03	1	1.0	0.0	0.0
O(1b) ...C(5b)	3.32	-2	0.0	1.0	0.0
O(1b) ...H(5b)	2.85	-2	0.0	1.0	0.0
O(1a) ...H(4b)	2.80	-2	0.0	1.0	0.0
C(10d)...H(3b)	3.02	-2	0.0	1.0	1.0
H(8c) ...C(1c)	3.01	-1	0.0	0.0	1.0
C(8c) ...C(2c)	3.40	-1	0.0	0.0	1.0
C(9c) ...C(4c)	3.43	-1	0.0	0.0	1.0
H(5d) ...C(4c)	2.88	2	0.0	0.0	0.0
H(5d) ...C(5c)	2.95	2	0.0	0.0	0.0
O(1c) ...C(8c)	3.16	-1	0.0	0.0	1.0
O(1c) ...H(8c)	2.38	-1	0.0	0.0	1.0
O(1c) ...C(10c)	3.35	-1	0.0	0.0	1.0
O(1c) ...H(10c)	2.64	-1	0.0	0.0	1.0
O(1c) ...C(11c)	3.34	1	1.0	0.0	0.0
O(1d) ...C(11c)	3.35	1	1.0	0.0	0.0
O(1c) ...H(11c)	2.73	1	1.0	0.0	0.0
O(1d) ...C(11d)	3.33	1	1.0	0.0	0.0
O(1b) ...C(10d)	3.25	-2	0.0	1.0	0.0
O(1b) ...H(10d)	2.18	-2	0.0	1.0	0.0
O(1b) ...H(8d)	2.42	-2	0.0	1.0	0.0
O(1a) ...C(6d)	3.24	-2	0.0	1.0	0.0

Table 4.4: continued

O(1a) ...H(6d)	2.26	-2	0.0	1.0	0.0
H(13) ...C(3d)	3.00	-2	0.0	1.0	0.0
H(13) ...C(2d)	2.89	-2	0.0	1.0	0.0

The symmetry code S is the same as in appendix 2 page 25

Table 4.5: Intramolecular distances (\AA) for FeDIKETO

C(1a) ...Fe(1)	2.84	C(2a) ...Fe(1)	3.01
C(7a) ...Fe(1)	3.35	C(8a) ...Fe(1)	2.94
C(9a) ...Fe(1)	2.93	C(9b) ...Fe(1)	2.94
C(8b) ...Fe(1)	3.04	C(7b) ...Fe(1)	3.30
C(3b) ...Fe(1)	4.24	C(2b) ...Fe(1)	3.02
C(1b) ...Fe(1)	2.85	O(1a) ...Fe(1)	4.07
O(1b) ...Fe(1)	4.04	N(1b) ...Fe(2)	4.06
C(1c) ...Fe(2)	2.85	C(2c) ...Fe(2)	3.06
C(7c) ...Fe(2)	3.38	C(8c) ...Fe(2)	2.99
C(9c) ...Fe(2)	2.96	C(9d) ...Fe(2)	2.96
C(8d) ...Fe(2)	2.99	C(7d) ...Fe(2)	3.29
C(2d) ...Fe(2)	2.99	C(1d) ...Fe(2)	2.79
O(1c) ...Fe(2)	4.04	O(1d) ...Fe(2)	4.02
N(2b) ...O(2)	3.09	N(2a) ...O(2)	3.21
N(1a) ...O(2)	3.04	N(1b) ...O(2)	2.99
N(2d) ...O(2)	3.07	N(2c) ...O(2)	3.11
N(1c) ...O(2)	3.09	N(1d) ...O(2)	3.11
N(2a) ...N(2b)	2.65	N(1b) ...N(2b)	2.89
C(1a) ...N(2b)	2.41	C(8b) ...N(2b)	3.00
C(7b) ...N(2b)	2.42	C(3b) ...N(2b)	2.47
H(3b) ...N(2b)	2.71	O(1b) ...N(2b)	2.31
N(1a) ...N(2a)	2.83	C(3a) ...N(2a)	2.47
H(3a) ...N(2a)	2.75	C(7a) ...N(2a)	2.39
C(8a) ...N(2a)	2.88	C(1b) ...N(2a)	2.44
O(1a) ...N(2a)	2.33	N(1b) ...N(1a)	2.59

Table 4.5: continued

C(2a) ...N(1a)	3.04	C(7a) ...N(1a)	2.45
H(8a) ...N(1a)	1.98	C(10a)...N(1a)	2.49
H(10a)...N(1a)	2.77	C(9b) ...N(1a)	2.35
C(9a) ...N(1b)	2.34	C(10b)...N(1b)	2.46
H(10b)...N(1b)	2.74	H(8b) ...N(1b)	2.06
C(7b) ...N(1b)	2.40	C(2b) ...N(1b)	3.09
N(2c) ...N(2d)	2.67	N(1d) ...N(2d)	2.82
C(1c) ...N(2d)	2.45	C(8d) ...N(2d)	2.97
C(7d) ...N(2d)	2.39	C(3d) ...N(2d)	2.44
H(3d) ...N(2d)	2.69	O(1d) ...N(2d)	2.32
N(1c) ...N(2c)	2.84	C(3c) ...N(2c)	2.45
H(3c) ...N(2c)	2.69	C(7c) ...N(2c)	2.44
C(8c) ...N(2c)	2.95	C(1d) ...N(2c)	2.40
O(1c) ...N(2c)	2.31	N(1d) ...N(1c)	2.61
C(2c) ...N(1c)	3.06	C(7c) ...N(1c)	2.45
H(8c) ...N(1c)	2.01	C(10c)...N(1c)	2.47
H(10c)...N(1c)	2.72	C(9d) ...N(1c)	2.36
C(9c) ...N(1d)	2.35	C(10d)...N(1d)	2.51
H(10d)...N(1d)	2.78	H(8d) ...N(1d)	2.03
C(7d) ...N(1d)	2.40	C(2d) ...N(1d)	3.02
C(2a) ...C(1a)	2.40	C(3a) ...C(1a)	2.94
H(3a) ...C(1a)	2.73	O(1b) ...C(1a)	2.38
H(3a) ...C(2a)	2.21	C(4a) ...C(2a)	2.41
C(5a) ...C(2a)	2.81	C(6a) ...C(2a)	2.50
C(8a) ...C(2a)	2.51	O(1a) ...C(2a)	2.83
H(4a) ...C(3a)	2.10	C(5a) ...C(3a)	2.38
C(6a) ...C(3a)	2.85	C(7a) ...C(3a)	2.42
O(1a) ...C(3a)	2.83	C(4a) ...H(3a)	2.14

Table 4.5: continued

O(1a) ...H(3a)	2.33	H(5a) ...C(4a)	2.07
C(6a) ...C(4a)	2.39	C(7a) ...C(4a)	2.72
C(5a) ...H(4a)	2.05	H(6a) ...C(5a)	2.21
C(7a) ...C(5a)	2.43	C(6a) ...H(5a)	2.17
C(8a) ...C(6a)	2.44	H(8a) ...C(6a)	2.54
C(7a) ...H(6a)	2.24	C(8a) ...H(6a)	2.66
H(8a) ...C(7a)	2.15	C(9a) ...C(8a)	2.36
C(10a)...C(8a)	2.90	H(10a)...C(8a)	2.69
C(9a) ...H(8a)	2.51	C(10a)...H(8a)	2.51
H(10a)...C(9a)	2.19	C(11a)...C(9a)	2.41
C(11b)...C(9a)	2.73	C(10b)...C(9a)	2.41
H(11a)...C(10a)	2.16	C(11b)...C(10a)	2.41
C(10b)...C(10a)	2.83	C(9b) ...C(10a)	2.42
C(11a)...H(10a)	2.17	H(11b)...C(11a)	2.13
C(10b)...C(11a)	2.41	C(9b) ...C(11a)	2.77
C(11b)...H(11a)	2.16	H(10b)...C(11b)	2.11
C(9b) ...C(11b)	2.35	C(10b)...H(11b)	2.08
C(8b) ...C(10b)	2.91	H(8b) ...C(10b)	2.57
C(10c)...C(10b)	3.44	C(9b) ...H(10b)	2.18
C(8b) ...H(10b)	2.66	C(8b) ...C(9b)	2.40
H(8b) ...C(9b)	2.62	C(6b) ...C(8b)	2.39
H(6b) ...C(8b)	2.57	C(2b) ...C(8b)	2.58
C(7b) ...H(8b)	2.14	C(6b) ...H(8b)	2.53
H(6b) ...C(7b)	2.20	C(5b) ...C(7b)	2.47
C(4b) ...C(7b)	2.83	C(3b) ...C(7b)	2.46
H(5b) ...C(6b)	2.15	C(4b) ...C(6b)	2.38
C(3b) ...C(6b)	2.78	C(2b) ...C(6b)	2.43
C(10d)...C(6b)	3.36	C(5b) ...H(6b)	2.16

Table 4.5: continued

H(4b) ...C(5b)	2.07	C(3b) ...C(5b)	2.35
C(2b) ...C(5b)	2.77	C(4b) ...H(5b)	2.06
H(3b) ...C(4b)	2.15	C(2b) ...C(4b)	2.41
H(6d) ...C(4b)	2.98	C(3b) ...H(4b)	2.14
C(1b) ...C(3b)	2.95	O(1b) ...C(3b)	2.81
C(2b) ...H(3b)	2.15	C(1b) ...H(3b)	2.71
O(1b) ...H(3b)	2.28	C(1b) ...C(2b)	2.43
O(1b) ...C(2b)	2.83	O(1a) ...C(1b)	2.38
C(2c) ...C(1c)	2.42	C(3c) ...C(1c)	2.87
H(3c) ...C(1c)	2.60	O(1d) ...C(1c)	2.34
H(3c) ...C(2c)	2.16	C(4c) ...C(2c)	2.43
C(5c) ...C(2c)	2.80	C(6c) ...C(2c)	2.46
C(8c) ...C(2c)	2.55	O(1c) ...C(2c)	2.84
H(4c) ...C(3c)	2.17	C(5c) ...C(3c)	2.44
C(6c) ...C(3c)	2.83	C(7c) ...C(3c)	2.43
O(1c) ...C(3c)	2.76	C(4c) ...H(3c)	2.18
O(1c) ...H(3c)	2.21	H(5c) ...C(4c)	2.13
C(6c) ...C(4c)	2.41	C(7c) ...C(4c)	2.79
C(5c) ...H(4c)	2.13	H(6c) ...C(5c)	2.15
C(7c) ...C(5c)	2.42	C(6c) ...H(5c)	2.14
C(8c) ...C(6c)	2.41	H(8c) ...C(6c)	2.53
C(7c) ...H(6c)	2.18	C(8c) ...H(6c)	2.59
H(8c) ...C(7c)	2.16	C(9c) ...C(8c)	2.38
C(10c) ...C(8c)	2.88	H(10c) ...C(8c)	2.62
C(9c) ...H(8c)	2.56	C(10c) ...H(8c)	2.47
H(10c) ...C(9c)	2.16	C(11c) ...C(9c)	2.41
C(11d) ...C(9c)	2.77	C(10d) ...C(9c)	2.41
H(11c) ...C(10c)	2.15	C(11d) ...C(10c)	2.42

Table 4.5: continued

C(10d)...C(10c)	2.80	C(9d) ...C(10c)	2.41
C(11c)...H(10c)	2.17	H(11d)...C(11c)	2.13
C(10d)...C(11c)	2.40	C(9d) ...C(11c)	2.78
C(11d)...H(11c)	2.13	H(10d)...C(11d)	2.14
C(9d) ...C(11d)	2.42	C(10d)...H(11d)	2.14
C(8d) ...C(10d)	2.85	H(8d) ...C(10d)	2.44
C(9d) ...H(10d)	2.18	C(8d) ...H(10d)	2.61
C(8d) ...C(9d)	2.32	H(8d) ...C(9d)	2.51
C(6d) ...C(8d)	2.39	H(6d) ...C(8d)	2.55
C(2d) ...C(8d)	2.58	C(7d) ...H(8d)	2.19
C(6d) ...H(8d)	2.53	H(6d) ...C(7d)	2.21
C(5d) ...C(7d)	2.47	C(4d) ...C(7d)	2.81
C(3d) ...C(7d)	2.41	H(5d) ...C(6d)	2.17
C(4d) ...C(6d)	2.44	C(3d) ...C(6d)	2.80
C(2d) ...C(6d)	2.49	C(5d) ...H(6d)	2.17
H(4d) ...C(5d)	2.16	C(3d) ...C(5d)	2.42
C(2d) ...C(5d)	2.87	C(4d) ...H(5d)	2.17
H(3d) ...C(4d)	2.12	C(2d) ...C(4d)	2.45
C(3d) ...H(4d)	2.13	C(1d) ...C(3d)	2.92
O(1d) ...C(3d)	2.78	C(2d) ...H(3d)	2.14
C(1d) ...H(3d)	2.67	O(1d) ...H(3d)	2.17
C(1d) ...C(2d)	2.37	O(1d) ...C(2d)	2.84
O(1c) ...C(1d)	2.37	O(1b) ...O(1a)	2.74
O(1d) ...O(1c)	2.67	N ...O	2.13
C(1) ...O	3.40	H(11) ...O	2.52
C(2) ...O	2.67	H(21) ...O	2.81
H(23) ...O	2.81	H(3) ...O	1.90
H(12) ...N	2.13	H(13) ...N	2.23

Table 4.5: continued

H(21) ...N	2.09	H(22) ...N	2.23
H(3) ...N	2.00	C(2) ...C(1)	2.27
H(21) ...C(1)	3.07	H(22) ...C(1)	2.69
C(3) ...C(1)	2.34	H(3) ...C(1)	2.56
C(2) ...H(11)	2.36	C(2) ...H(12)	2.92
C(3) ...H(12)	2.99	C(2) ...H(13)	3.03
C(3) ...H(13)	3.04	C(3) ...C(2)	2.31
C(3) ...H(21)	2.76	C(3) ...H(23)	2.06

Table 4.6: Fractional atomic coordinates and thermal parameters (\AA^2)
for CuDIKETO

Atom	x	y	z	Uiso or Ueq
Cu	0.47171(2)	-0.06893(2)	0.17120(4)	0.0354(2)
N(2a)	0.5725(1)	-0.0040(1)	0.2850(3)	0.039(1)
N(1a)	0.3833(1)	0.0191(1)	0.1992(3)	0.041(1)
N(2b)	0.5554(1)	-0.1601(1)	0.1442(3)	0.038(1)
N(1b)	0.3676(1)	-0.1312(1)	0.0635(3)	0.038(1)
O(1a)	0.7201(1)	-0.0358(1)	0.3955(3)	0.067(1)
O(1b)	0.6980(1)	-0.1923(1)	0.2807(4)	0.080(1)
C(1a)	0.6475(2)	-0.0529(2)	0.3149(4)	0.043(1)
C(2a)	0.5704(2)	0.0781(1)	0.3542(3)	0.041(1)
C(3a)	0.6469(2)	0.1212(2)	0.4312(4)	0.053(2)
C(4a)	0.6419(2)	0.2026(2)	0.4984(4)	0.061(2)
C(5a)	0.5611(2)	0.2446(2)	0.4915(4)	0.060(2)
C(6a)	0.4860(2)	0.2057(2)	0.4144(4)	0.055(2)
C(7a)	0.4874(2)	0.1230(2)	0.3447(4)	0.045(1)
C(8a)	0.4011(2)	0.0921(2)	0.2696(4)	0.047(1)
C(9a)	0.2941(1)	-0.0037(2)	0.1285(4)	0.045(1)
C(10a)	0.2182(2)	0.0471(2)	0.1290(6)	0.070(2)
C(11a)	0.1373(2)	0.0173(2)	0.0496(7)	0.083(2)
C(11b)	0.1300(2)	-0.0608(2)	-0.0304(6)	0.071(2)
C(10b)	0.2034(2)	-0.1116(2)	-0.0288(5)	0.056(2)
C(9b)	0.2861(1)	-0.0843(2)	0.0529(4)	0.042(1)
C(8b)	0.3681(2)	-0.2087(2)	0.0106(4)	0.042(1)

table 4.6: continued

c(7b)	0.4452(2)	-0.2622(1)	0.0086(3)	0.040(1)
c(6b)	0.4264(2)	-0.3428(2)	-0.0676(4)	0.052(2)
c(5b)	0.4925(2)	-0.3994(2)	-0.0931(5)	0.063(2)
c(4b)	0.5810(2)	-0.3766(2)	-0.0416(5)	0.068(2)
c(3b)	0.6019(2)	-0.2995(2)	0.0354(4)	0.056(2)
c(2b)	0.5358(2)	-0.2395(2)	0.0659(4)	0.041(1)
c(1b)	0.6359(1)	-0.1438(2)	0.2403(4)	0.046(1)

Table 4.7 Fractional atomic coordinates for the CuDIKETO
hydrogen atoms

Atom	x	y	z
H(3a)	0.7009	0.0948	0.4410
H(4a)	0.6970	0.2243	0.5550
H(5a)	0.5574	0.2979	0.5417
H(6a)	0.4323	0.2291	0.4065
H(8a)	0.3585	0.1295	0.2776
H(10a)	0.2221	0.0988	0.2079
H(11a)	0.0871	0.0482	0.0587
H(11b)	0.0737	-0.0859	-0.0806
H(10b)	0.1988	-0.1639	-0.0781
H(8b)	0.3125	-0.2350	-0.0301
H(6b)	0.3701	-0.3560	-0.0950
H(5b)	0.4741	-0.4516	-0.1386
H(4b)	0.6214	-0.4132	-0.0691
H(3b)	0.6565	-0.2853	0.0671

Table 4.8 Anisotropic thermal parameters (\AA^2) for CuDIKETO

Atom	U11	U22	U33	U23	U13	U12
Cu	0.0281(1)	0.0370(2)	0.0410(2)	0.0045(1)	-0.0001(1)	0.0007(1)
N(2a)	0.034(1)	0.040(1)	0.043(1)	0.002(1)	0.002(1)	-0.003(1)
N(1a)	0.035(1)	0.039(1)	0.048(1)	0.008(1)	0.003(1)	0.002(1)
N(2b)	0.032(1)	0.039(1)	0.045(1)	0.002(1)	-0.003(1)	0.002(1)
N(1b)	0.030(1)	0.042(1)	0.042(1)	0.006(1)	-0.001(1)	0.002(1)
O(1a)	0.039(1)	0.069(1)	0.093(2)	-0.020(1)	-0.017(1)	0.001(1)
O(1b)	0.044(1)	0.053(1)	0.143(2)	-0.009(1)	-0.037(1)	0.012(1)
C(1a)	0.036(1)	0.051(1)	0.043(1)	0.002(1)	-0.000(1)	-0.002(1)
C(2a)	0.045(1)	0.043(1)	0.035(1)	0.004(1)	0.006(1)	-0.006(1)
C(3a)	0.053(2)	0.053(2)	0.054(2)	-0.004(1)	0.001(1)	-0.010(1)
C(4a)	0.069(2)	0.058(2)	0.054(2)	-0.007(1)	0.002(1)	-0.022(2)
C(5a)	0.085(2)	0.041(1)	0.054(2)	-0.006(1)	0.012(2)	-0.010(1)
C(6a)	0.068(2)	0.043(1)	0.053(2)	0.002(1)	0.013(1)	0.000(1)

Table 4.8 continued

C(7a)	0.054(1)	0.040(1)	0.041(1)	0.005(1)	0.009(1)	-0.004(1)
C(8a)	0.048(1)	0.039(1)	0.054(2)	0.007(1)	0.010(1)	0.007(1)
C(9a)	0.033(1)	0.045(1)	0.056(2)	0.010(1)	0.001(1)	0.005(1)
C(10a)	0.046(1)	0.048(2)	0.115(3)	0.001(2)	-0.001(2)	0.011(1)
C(11a)	0.037(1)	0.070(2)	0.142(4)	0.010(2)	-0.005(2)	0.019(1)
C(11b)	0.035(1)	0.068(2)	0.110(3)	0.007(2)	-0.009(2)	0.002(1)
C(10b)	0.035(1)	0.057(2)	0.075(2)	0.003(2)	-0.008(1)	0.001(1)
C(9b)	0.030(1)	0.048(1)	0.048(1)	0.011(1)	-0.000(1)	0.005(1)
C(8b)	0.037(1)	0.044(1)	0.046(1)	0.004(1)	-0.004(1)	-0.003(1)
C(7b)	0.039(1)	0.038(1)	0.042(1)	0.006(1)	-0.002(1)	0.001(1)
C(6b)	0.051(1)	0.045(1)	0.060(2)	-0.000(1)	-0.012(1)	-0.003(1)
C(5b)	0.073(2)	0.044(2)	0.073(2)	-0.008(2)	-0.016(2)	0.010(1)
C(4b)	0.064(2)	0.058(2)	0.083(2)	-0.012(2)	-0.015(2)	0.024(2)
C(3b)	0.043(1)	0.058(2)	0.066(2)	-0.007(1)	-0.008(1)	0.010(1)
C(2b)	0.038(1)	0.042(1)	0.042(1)	0.005(1)	-0.001(1)	0.003(1)
C(1b)	0.031(1)	0.046(1)	0.060(2)	0.006(1)	-0.002(1)	-0.001(1)

Table 4.9 Intermolecular distances (\AA) for CuDIKETO

			S	a	b	c
Cu	...Cu	3.47	-1	1.0	0.0	0.0
N(2a)	...Cu	3.50	-1	1.0	0.0	0.0
N(1a)	...Cu	3.67	-1	1.0	0.0	0.0
C(2a)	...Cu	3.54	-1	1.0	0.0	1.0
C(3a)	...Cu	3.60	-1	1.0	0.0	1.0
C(4a)	...Cu	3.72	-1	1.0	0.0	1.0
C(5a)	...Cu	3.77	-1	1.0	0.0	1.0
C(6a)	...Cu	3.71	-1	1.0	0.0	1.0
C(7a)	...Cu	3.60	-1	1.0	0.0	1.0
C(8a)	...Cu	3.87	-1	1.0	0.0	0.0
C(6a)	...N(2b)	3.38	-1	1.0	0.0	1.0
C(8a)	...N(2b)	3.30	-1	1.0	0.0	0.0
C(2a)	...N(1b)	3.34	-1	1.0	0.0	0.0
C(4a)	...N(1b)	3.38	-1	1.0	0.0	1.0
C(8a)	...O(1a)	3.27	-1	1.0	0.0	1.0
H(6b)	...O(1a)	2.82	-2	0.0	0.0	0.0
C(10b)	...O(1b)	3.41	-2	0.0	0.0	0.0
C(8b)	...O(1b)	3.31	-2	0.0	0.0	0.0
H(10b)	...O(1b)	2.51	-2	0.0	0.0	0.0
H(8b)	...O(1b)	2.39	-2	0.0	0.0	0.0
H(6b)	...O(1b)	2.75	-2	0.0	0.0	0.0
C(7a)	...C(1a)	3.49	-1	1.0	0.0	1.0
C(8a)	...C(1a)	3.21	-1	1.0	0.0	1.0
C(8b)	...C(3a)	3.47	-1	1.0	0.0	0.0
C(6b)	...C(5a)	3.46	-1	1.0	0.0	0.0

Table 4.9 continued

C(7b) ...C(6a)	3.43	-1	1.0	0.0	0.0
C(2b) ...C(6a)	3.50	-1	1.0	0.0	0.0
C(1b) ...C(6a)	3.36	-1	1.0	0.0	1.0
C(2b) ...C(7a)	3.49	-1	1.0	0.0	0.0
C(5b) ...C(5b)	3.47	-1	1.0	-1.0	0.0
H(5b) ...C(5b)	2.92	-1	1.0	-1.0	0.0

Symmetry code S	1	=	x ,	y ,	z
	2	=	-x ,	-y ,	-z
	3	=	$\frac{1}{2}-x$,	$\frac{1}{2}+y$,	$\frac{1}{2}-z$
	4	=	$\frac{1}{2}+x$,	$\frac{1}{2}-y$,	$\frac{1}{2}+z$

The 2nd atom is related to the first one at x,y,z by the transformation S, with a,b,c, added to x,y,z respectively.

Table 4.10 Intramolecular distances (Å) for CuDIKETO

O(1a) ...Cu	3.95	O(1b) ...Cu	3.93
C(2a) ...Cu	3.01	C(7a) ...Cu	3.30
C(8a) ...Cu	2.88	C(9a) ...Cu	2.84
C(9b) ...Cu	2.84	C(8b) ...Cu	2.89
C(7b) ...Cu	3.31	C(2b) ...Cu	3.00
N(1a) ...N(2a)	2.86	N(2b) ...N(2a)	2.69
O(1a) ...N(2a)	2.33	C(3a) ...N(2a)	2.47
C(7a) ...N(2a)	2.45	C(8a) ...N(2a)	2.97
C(1b) ...N(2a)	2.45	H(3a) ...N(2a)	2.65
N(1b) ...N(1a)	2.59	C(2a) ...N(1a)	3.06
C(7a) ...N(1a)	2.44	C(10a)...N(1a)	2.51
C(9b) ...N(1a)	2.38	H(8a) ...N(1a)	1.89
H(10a)...N(1a)	2.72	N(1b) ...N(2b)	2.85
O(1b) ...N(2b)	2.32	C(1a) ...N(2b)	2.45
C(8b) ...N(2b)	2.98	C(7b) ...N(2b)	2.46
C(3b) ...N(2b)	2.47	H(3b) ...N(2b)	2.59
C(9a) ...N(1b)	2.37	C(10b)...N(1b)	2.50
C(7b) ...N(1b)	2.43	C(2b) ...N(1b)	3.04
H(10b)...N(1b)	2.69	H(8b) ...N(1b)	1.94
O(1b) ...O(1a)	2.64	C(2a) ...O(1a)	2.87
C(3a) ...O(1a)	2.75	C(1b) ...O(1a)	2.35
H(3a) ...O(1a)	2.13	C(1a) ...O(1b)	2.36
C(3b) ...O(1b)	2.77	C(2b) ...O(1b)	2.86
H(3b) ...O(1b)	2.19	C(2a) ...C(1a)	2.41
C(3a) ...C(1a)	2.90	H(3a) ...C(1a)	2.62

Table 4.10 continued

C(4a) ...C(2a)	2.44	C(5a) ...C(2a)	2.84
C(6a) ...C(2a)	2.45	C(8a) ...C(2a)	2.56
H(3a) ...C(2a)	2.01	C(5a) ...C(3a)	2.41
C(6a) ...C(3a)	2.75	C(7a) ...C(3a)	2.41
H(4a) ...C(3a)	1.98	C(6a) ...C(4a)	2.35
C(7a) ...C(4a)	2.78	H(3a) ...C(4a)	1.99
H(5a) ...C(4a)	2.02	C(7a) ...C(5a)	2.43
H(4a) ...C(5a)	2.06	H(6a) ...C(5a)	1.98
C(8a) ...C(6a)	2.40	H(5a) ...C(6a)	1.99
H(8a) ...C(6a)	2.40	H(6a) ...C(7a)	1.95
H(8a) ...C(7a)	1.94	C(9a) ...C(8a)	2.37
C(10a) ...C(8a)	2.92	H(6a) ...C(8a)	2.42
H(10a) ...C(8a)	2.67	C(11a) ...C(9a)	2.38
C(11b) ...C(9a)	2.77	C(10b) ...C(9a)	2.41
H(8a) ...C(9a)	2.53	H(10a) ...C(9a)	2.06
C(11b) ...C(10a)	2.40	C(10b) ...C(10a)	2.77
C(9b) ...C(10a)	2.41	H(8a) ...C(10a)	2.62
H(11a) ...C(10a)	1.98	C(10b) ...C(11a)	2.37
C(9b) ...C(11a)	2.75	H(10a) ...C(11a)	2.08
H(11b) ...C(11a)	2.08	C(9b) ...C(11b)	2.38
H(11a) ...C(11b)	1.98	H(10b) ...C(11b)	1.98
C(8b) ...C(10b)	2.90	H(11b) ...C(10b)	1.98
H(8b) ...C(10b)	2.55	C(8b) ...C(9b)	2.36
H(10b) ...C(9b)	2.00	H(8b) ...C(9b)	2.51
C(6b) ...C(8b)	2.39	C(2b) ...C(8b)	2.55
H(10b) ...C(8b)	2.65	H(6b) ...C(8b)	2.47
C(5b) ...C(7b)	2.43	C(4b) ...C(7b)	2.77
C(3b) ...C(7b)	2.40	H(8b) ...C(7b)	2.02

Table 4.10: continued

H(6b) ...C(7b)	1.97	C(4b) ...C(6b)	2.36
C(3b) ...C(6b)	2.75	C(2b) ...C(6b)	2.45
H(8b) ...C(6b)	2.45	H(5b) ...C(6b)	1.96
C(3b) ...C(5b)	2.41	C(2b) ...C(5b)	2.84
H(6b) ...C(5b)	1.95	H(4b) ...C(5b)	1.93
C(2b) ...C(4b)	2.43	H(5b) ...C(4b)	2.07
H(3b) ...C(4b)	1.96	C(1b) ...C(3b)	2.91
H(4b) ...C(3b)	1.99	C(1b) ...C(2b)	2.41
H(3b) ...C(2b)	1.94	H(3b) ...C(1b)	2.61

APPENDIX 5

Table 5.1: Fractional atomic coordinates and thermal parameters (Å)
for Cu(DIBrSALEN)

Atom	x	y	z	Uiso or Ueq
Cu	0.48194(8)	0.13615(7)	0.43664(6)	0.0323(3)
Br(a)	0.74876(9)	0.95513(7)	0.87778(7)	0.0541(4)
Br(b)	0.05105(8)	-0.64023(6)	0.05838(7)	0.0482(4)
Na	0.6862(5)	0.2592(5)	0.3997(4)	0.033(2)
Nb	0.5869(5)	-0.0372(5)	0.2872(5)	0.036(2)
Oa	0.4061(4)	0.3074(4)	0.6000(4)	0.036(2)
Ob	0.2759(5)	0.0100(5)	0.4469(4)	0.041(2)
C(2a)	0.4850(6)	0.4434(6)	0.6558(5)	0.035(1)
C(3a)	0.4196(7)	0.5511(6)	0.7880(6)	0.040(1)
C(4a)	0.4951(7)	0.6979(7)	0.8533(6)	0.042(1)
C(5a)	0.6441(7)	0.7500(7)	0.7878(6)	0.041(1)
C(6a)	0.7140(7)	0.6536(7)	0.6638(6)	0.041(1)
C(7a)	0.6415(6)	0.4996(6)	0.5968(6)	0.037(1)
C(8a)	0.7332(7)	0.4014(6)	0.4709(6)	0.039(1)
C(9a)	0.7918(8)	0.1704(7)	0.2739(6)	0.043(1)
C(9b)	0.7657(8)	0.0021(7)	0.2537(7)	0.043(1)
C(8b)	0.5183(7)	-0.1741(6)	0.2214(6)	0.038(1)
C(7b)	0.3447(6)	-0.2272(6)	0.2483(5)	0.034(1)
C(6b)	0.2858(7)	-0.3784(6)	0.1622(6)	0.037(1)
C(5b)	0.1251(6)	-0.4350(6)	0.1818(5)	0.037(1)
C(4b)	0.0133(8)	-0.3466(7)	0.2889(6)	0.044(1)
C(3b)	0.0673(8)	-0.1994(7)	0.3766(6)	0.045(1)
C(2b)	0.2349(7)	-0.1309(6)	0.3593(6)	0.038(1)

Table 5.2: Fractional atomic coordinates for the hydrogen atoms
for Cu(DIBrSALEN)

Atom	x	y	z	
H(3a)	0.335(8)	0.515(7)	0.812(6)	0.04(1)
H(4a)	0.432(7)	0.771(6)	0.943(5)	0.04(1)
H(6a)	0.782(8)	0.677(7)	0.621(6)	0.04(1)
H(8a)	0.839(7)	0.432(6)	0.435(6)	0.04(1)
H(9a1)	0.920(7)	0.203(6)	0.277(6)	0.04(1)
H(9a2)	0.744(7)	0.156(6)	0.175(6)	0.04(1)
H(9b1)	0.796(7)	-0.005(6)	0.316(6)	0.04(1)
H(9b2)	0.794(7)	-0.071(7)	0.154(6)	0.04(1)
H(8b)	0.599(9)	-0.250(7)	0.143(7)	0.06(1)
H(6b)	0.367(9)	-0.442(8)	0.087(7)	0.06(1)
H(4b)	-0.109(9)	-0.378(8)	0.314(7)	0.06(1)
H(3b)	0.007(9)	-0.124(8)	0.420(7)	0.06(1)

Table 5.3: Anisotropic thermal parameters (\AA^2) for Cu(DIBrSALEN)

Atom	U11	U22	U33	U23	U13	U12
Cu	0.0324(3)	0.0332(3)	0.0314(3)	0.0089(2)	-0.0013(2)	0.0051(2)
Br(a)	0.0687(5)	0.0316(3)	0.0620(4)	0.0057(3)	-0.0150(3)	0.0068(3)
Br(b)	0.0552(4)	0.0327(3)	0.0567(4)	0.0106(3)	-0.0110(3)	0.0016(2)
Na	0.034(2)	0.033(2)	0.032(2)	0.009(2)	-0.002(2)	0.007(2)
Nb	0.030(2)	0.042(2)	0.037(2)	0.016(2)	0.001(2)	0.007(2)
Oa	0.038(2)	0.036(2)	0.034(2)	0.008(1)	0.000(2)	0.004(1)
Ob	0.039(2)	0.043(2)	0.041(2)	0.004(2)	0.004(2)	0.002(2)

Table 5.4: Intermolecular distances (Å) for Cu(DIBrSALEN)

		S	a	b	c
Br(b) ...Br(a)	4.12	1	-1.0	-2.0	-1.0
H(9a2)...Br(a)	3.00	1	0.0	-1.0	-1.0
H(9b2)...Br(a)	3.32	1	0.0	-1.0	-1.0
Cu ...Br(a)	4.05	-1	1.0	1.0	1.0
Br(b) ...Br(a)	4.14	-1	1.0	0.0	1.0
Ob ...Br(a)	3.84	-1	1.0	1.0	1.0
C(4a) ...Br(a)	3.93	-1	1.0	2.0	2.0
C(7b) ...Br(a)	3.77	-1	1.0	1.0	1.0
C(2b) ...Br(a)	3.70	-1	1.0	1.0	1.0
H(4a) ...Br(a)	2.97	-1	1.0	2.0	2.0
H(9a1)...Br(a)	3.19	-1	2.0	1.0	1.0
Cu ...Cu	3.59	-1	1.0	0.0	1.0
Nb ...Cu	3.52	-1	1.0	0.0	1.0
Ob ...Cu	3.43	-1	1.0	0.0	1.0
C(5a) ...Cu	3.57	-1	1.0	1.0	1.0
C(6a) ...Cu	3.51	-1	1.0	1.0	1.0
C(8b) ...Cu	3.67	-1	1.0	0.0	1.0
C(7b) ...Cu	3.77	-1	1.0	0.0	1.0
C(2b) ...Cu	3.65	-1	1.0	0.0	1.0
H(6a) ...Cu	3.45	-1	1.0	1.0	1.0
C(9a) ...Br(b)	3.72	1	1.0	1.0	0.0
H(9a1)...Br(b)	3.30	1	1.0	1.0	0.0

table 5.4: continued

H(9a2)...Br(b)	3.30	1	1.0	1.0	0.0
Br(b) ...Br(b)	3.80	-1	0.0	-1.0	0.0
C(5a) ...Br(b)	3.90	-1	1.0	0.0	1.0
C(5b) ...Br(b)	3.72	-1	0.0	-1.0	0.0
H(3a) ...Br(b)	3.44	-1	0.0	0.0	1.0
H(9b2)...Br(b)	3.05	-1	1.0	-1.0	0.0
H(8b) ...Br(b)	3.30	-1	1.0	-1.0	0.0
Ob ...Nb	3.30	-1	1.0	0.0	1.0
C(8b) ...Oa	3.04	-1	1.0	0.0	1.0
C(7b) ...Oa	3.35	-1	1.0	0.0	1.0
H(4b) ...Oa	2.56	-1	0.0	0.0	1.0
C(9b) ...Ob	3.33	-1	1.0	0.0	1.0
H(9b1)...Ob	2.60	-1	1.0	0.0	1.0
H(3b) ...Ob	2.65	-1	0.0	0.0	1.0
C(8a) ...C(2a)	3.43	-1	1.0	1.0	1.0
C(8b) ...C(2a)	3.44	-1	1.0	0.0	1.0
C(7b) ...C(2a)	3.38	-1	1.0	0.0	1.0
C(6b) ...C(2a)	3.40	-1	1.0	0.0	1.0
H(4b) ...C(2a)	3.04	-1	0.0	0.0	1.0
H(6b) ...C(3a)	3.07	-1	1.0	0.0	1.0
H(4b) ...C(3a)	2.94	-1	0.0	0.0	1.0
H(9a2)...C(4a)	2.81	-1	1.0	1.0	1.0
H(3b) ...C(3b)	3.03	-1	0.0	0.0	1.0
Symmetry code	S	1 = x,	y,	z	
		-1 = -x,	-y,	-z	

2nd atom is related to the first one at x, y, z, by the transformation
S with a, b, c, added to x, y, z respectively.

Table 5.5: Intramolecular distances (Å) for Cu(DIBrSALEN)

C(4a) ...Br(a)	2.88	C(6a) ...Br(a)	2.84
H(4a) ...Br(a)	3.01	H(6a) ...Br(a)	2.93
C(2a) ...Cu	2.89	C(7a) ...Cu	3.30
C(8a) ...Cu	2.91	C(9a) ...Cu	2.86
C(9b) ...Cu	2.86	C(8b) ...Cu	2.91
C(7b) ...Cu	3.31	C(2b) ...Cu	2.88
H(9a2)...Cu	3.29	H(9b1)...Cu	2.96
C(6b) ...Br(b)	2.83	C(4b) ...Br(b)	2.88
H(6b) ...Br(b)	2.92	H(4b) ...Br(b)	3.09
Nb ...Na	2.61	Oa ...Na	2.80
C(2a) ...Na	2.94	C(7a) ...Na	2.41
C(9b) ...Na	2.42	H(8a) ...Na	1.83
H(9a1)...Na	2.13	H(9a2)...Na	2.22
H(9b1)...Na	2.59	Ob ...Nb	2.79
C(9a) ...Nb	2.40	C(7b) ...Nb	2.41
C(2b) ...Nb	2.93	H(9a2)...Nb	2.68
H(9b1)...Nb	1.79	H(9b2)...Nb	1.98
H(8b) ...Nb	1.97	Ob ...Oa	2.75
C(3a) ...Oa	2.36	C(7a) ...Oa	2.42
C(8a) ...Oa	2.96	H(3a) ...Oa	2.37
C(8b) ...Ob	2.96	C(7b) ...Ob	2.44
C(3b) ...Ob	2.35	H(3b) ...Ob	2.36

table 5.5: continued

C(4a) ...C(2a)	2.47	C(5a) ...C(2a)	2.85
C(6a) ...C(2a)	2.48	C(8a) ...C(2a)	2.53
H(3a) ...C(2a)	1.84	C(5a) ...C(3a)	2.40
C(6a) ...C(3a)	2.77	C(7a) ...C(3a)	2.43
H(4a) ...C(3a)	2.06	C(6a) ...C(4a)	2.40
C(7a) ...C(4a)	2.80	H(3a) ...C(4a)	1.93
H(6a) ...C(4a)	3.07	C(7a) ...C(5a)	2.41
H(4a) ...C(5a)	2.15	H(6a) ...C(5a)	1.86
C(8a) ...C(6a)	2.44	H(8a) ...C(6a)	2.65
H(3a) ...C(7a)	3.07	H(8a) ...C(7a)	2.11
C(9a) ...C(8a)	2.38	H(6a) ...C(8a)	2.44
H(9a1)...C(8a)	2.60	H(8a) ...C(9a)	2.38
H(9b1)...C(9a)	1.96	H(9b2)...C(9a)	2.12
C(8b) ...C(9b)	2.38	H(9a1)...C(9b)	2.05
H(9a2)...C(9b)	2.10	H(8b) ...C(9b)	2.47
C(6b) ...C(8b)	2.44	C(2b) ...C(8b)	2.51
H(9b1)...C(8b)	2.68	H(9b2)...C(8b)	2.41
H(6b) ...C(8b)	2.57	C(5b) ...C(7b)	2.40
C(4b) ...C(7b)	2.79	C(3b) ...C(7b)	2.43
H(8b) ...C(7b)	2.19	H(6b) ...C(7b)	2.06
C(4b) ...C(6b)	2.39	C(3b) ...C(6b)	2.77
C(2b) ...C(6b)	2.46	H(8b) ...C(6b)	2.66

Table 5.6: Fractional atomic coordinates and thermal parameters (\AA^2)
for Fe(DIBrSALOF)

Atom	x	y	z	Uiso or Ueq
O(1)	-0.2502(5)	-0.2461(5)	-0.4965(5)	0.049(4)
Fe(1)	-0.39493(12)	-0.20831(10)	-0.49693(11)	0.0371(8)
Fe(2)	0.88720(12)	0.72138(10)	0.53706(10)	0.0373(8)
Br(a)	-0.64243(13)	-0.43151(10)	-0.06385(10)	0.0796(9)
Br(b)	-0.32567(14)	-0.04647(10)	-0.98848(10)	0.0799(10)
Br(c)	-0.15470(11)	-0.79816(9)	-0.88168(10)	0.0633(8)
Br(d)	0.08433(12)	0.26424(9)	-0.09192(10)	0.0662(8)
N(1a)	-0.4165(7)	-0.1107(6)	-0.3430(6)	0.039(5)
N(1b)	-0.3542(7)	-0.0419(6)	-0.5068(6)	0.040(5)
N(1c)	-0.1624(6)	-0.4381(6)	-0.4399(6)	0.039(5)
N(1d)	-0.1244(7)	-0.2464(6)	-0.2993(6)	0.039(5)
O(1a)	-0.5121(6)	-0.3176(5)	-0.4616(5)	0.050(5)
O(1b)	-0.4504(6)	-0.2426(5)	-0.6347(5)	0.053(5)
O(1c)	-0.0293(6)	-0.3508(5)	-0.5861(5)	0.046(4)
O(1d)	0.0037(6)	-0.1497(5)	-0.4390(5)	0.049(4)
C(4a)	-0.6086(9)	-0.4746(7)	-0.2833(8)	0.044(7)
C(5a)	-0.5961(9)	-0.3952(8)	-0.1890(9)	0.054(7)
C(6a)	-0.5510(8)	-0.2883(8)	-0.1855(8)	0.043(6)
C(10a)	-0.3247(9)	0.0667(8)	-0.2277(8)	0.046(7)
C(11a)	-0.2563(9)	0.1694(8)	-0.2170(8)	0.051(7)
C(11b)	-0.2211(10)	0.1991(8)	-0.3052(8)	0.054(7)
C(10b)	-0.2484(9)	0.1343(7)	-0.4012(8)	0.046(7)
C(6b)	-0.3461(8)	-0.0405(7)	-0.7753(7)	0.038(6)
C(5b)	-0.3637(9)	-0.1046(9)	-0.8741(8)	0.051(7)
C(4b)	-0.4092(9)	-0.2159(8)	-0.8934(8)	0.049(7)

Table 5.6: continued

C(4c)	-0.0626(9)	-0.5708(8)	-0.8226(8)	0.047(7)
C(5c)	-0.1152(9)	-0.6584(8)	-0.7881(9)	0.048(7)
C(6c)	-0.1414(8)	-0.6444(8)	-0.6867(8)	0.044(7)
C(10c)	-0.2719(9)	-0.5271(9)	-0.3140(9)	0.055(7)
C(11c)	-0.3060(9)	-0.5165(9)	-0.2130(9)	0.065(8)
C(11d)	-0.2822(10)	-0.4188(9)	-0.1374(9)	0.068(8)
C(10d)	-0.2231(9)	-0.3271(8)	-0.1639(8)	0.052(7)
C(6d)	-0.0050(9)	0.0386(8)	-0.1811(8)	0.050(7)
C(5d)	0.0534(9)	0.1343(8)	-0.2015(8)	0.044(7)
C(4d)	0.0875(9)	0.1341(8)	-0.3002(8)	0.045(7)
C(2a)	-0.5337(8)	-0.3408(8)	-0.3741(8)	0.040(2)
C(3a)	-0.5790(9)	-0.4492(8)	-0.3721(8)	0.045(3)
C(7a)	-0.5167(8)	-0.2603(7)	-0.2784(7)	0.038(2)
C(8a)	-0.4639(8)	-0.1496(8)	-0.2670(8)	0.041(2)
C(9a)	-0.3546(8)	-0.0026(7)	-0.3225(7)	0.037(2)
C(9b)	-0.3207(8)	0.0322(7)	-0.4107(7)	0.036(2)
C(8b)	-0.3502(8)	-0.0132(8)	-0.5921(7)	0.041(2)
C(7b)	-0.3732(8)	-0.0844(8)	-0.6909(7)	0.037(2)
C(3b)	-0.4368(9)	-0.2591(9)	-0.8118(8)	0.050(3)
C(2b)	-0.4210(9)	-0.1976(8)	-0.7088(8)	0.043(3)
C(2c)	-0.0601(8)	-0.4503(8)	-0.6503(7)	0.039(2)
C(3c)	-0.0342(9)	-0.4696(8)	-0.7540(8)	0.050(3)
C(7c)	-0.1181(8)	-0.5403(7)	-0.6151(7)	0.037(2)
C(8c)	-0.1588(8)	-0.5302(8)	-0.5124(7)	0.040(2)
C(9c)	-0.2064(8)	-0.4360(7)	-0.3408(7)	0.037(2)
C(9d)	-0.1864(8)	-0.3365(8)	-0.2650(7)	0.041(2)
C(8d)	-0.0902(8)	-0.1541(8)	-0.2350(8)	0.041(3)
C(7d)	-0.0266(8)	-0.0572(8)	-0.2610(7)	0.039(2)

Table 5.6: continued

c(3d)	0.0692(8)	0.0392(8)	-0.3795(8)	0.041(2)
c(2d)	0.0130(8)	-0.0600(8)	-0.3611(7)	0.039(2)

Table 5.7: Fractional atomic coordinates for the hydrogen atoms
for Fe(DIBrSALOF)

Atom	x	y	z
H(3a)	-0.5899	-0.5132	-0.4439
H(4a)	-0.6428	-0.5585	-0.2850
H(6a)	-0.5420	-0.2262	-0.1125
H(8a)	-0.4628	-0.0934	-0.1905
H(10a)	-0.3548	0.0417	-0.1594
H(11a)	-0.2322	0.2230	-0.1420
H(11b)	-0.1690	0.2782	-0.2980
H(10b)	-0.2159	0.1598	-0.4686
H(8b)	-0.3273	0.0734	-0.5865
H(6b)	-0.3110	0.0453	-0.7619
H(4b)	-0.4226	-0.2667	-0.9715
H(3b)	-0.4725	-0.3449	-0.8273
H(3c)	0.0101	-0.4029	-0.7824
H(4c)	-0.0437	-0.5816	-0.9039
H(6c)	-0.1807	-0.7140	-0.6602
H(8c)	-0.1900	-0.6057	-0.4922
H(10c)	-0.2947	-0.6038	-0.3721
H(11c)	-0.3531	-0.5870	-0.1921
H(11d)	-0.3092	-0.4135	-0.0583
H(10d)	-0.2060	-0.2493	-0.1059
H(8d)	-0.1101	-0.1471	-0.1544
H(6d)	-0.0333	0.0390	-0.1033
H(4d)	0.1295	0.2092	-0.3159
H(3d)	0.0979	0.0404	-0.4569

Table 5.8: Anisotropic thermal parameters (\AA^2) for Fe(DIBrSALOF)

Atom	U11	U22	U33	U23	U13	U12
O(1)	0.040(4)	0.048(4)	0.059(4)	0.025(4)	0.003(3)	0.012(3)
Fe(1)	0.037(1)	0.026(1)	0.047(1)	0.015(1)	0.002(1)	0.003(1)
Fe(2)	0.038(1)	0.028(1)	0.045(1)	0.016(1)	-0.002(1)	0.002(1)
Br(a)	0.100(1)	0.066(1)	0.073(1)	0.046(1)	-0.012(1)	-0.018(1)
Br(b)	0.133(1)	0.055(1)	0.051(1)	0.020(1)	-0.013(1)	-0.019(1)
Br(c)	0.074(1)	0.041(1)	0.075(1)	0.001(1)	-0.002(1)	0.002(1)
Br(d)	0.089(1)	0.043(1)	0.067(1)	0.003(1)	-0.002(1)	-0.004(1)
N(1a)	0.041(5)	0.023(4)	0.052(5)	0.006(4)	-0.003(4)	-0.005(4)
N(1b)	0.032(5)	0.037(5)	0.051(6)	0.014(4)	0.000(4)	0.009(4)
N(1c)	0.033(5)	0.035(5)	0.049(5)	0.015(4)	-0.010(4)	0.004(4)
N(1d)	0.044(5)	0.029(4)	0.043(5)	0.012(4)	0.001(4)	-0.001(4)
O(1a)	0.063(5)	0.039(4)	0.049(5)	0.012(3)	0.003(4)	-0.011(3)
O(1b)	0.052(5)	0.041(4)	0.066(5)	0.028(4)	-0.006(4)	-0.007(3)

Table 5.8: continued

O(1c)	0.043(4)	0.033(4)	0.064(5)	0.014(3)	0.001(4)	0.006(3)
O(1d)	0.058(5)	0.037(4)	0.051(4)	0.014(3)	0.005(4)	-0.012(3)
C(4a)	0.048(7)	0.024(5)	0.061(8)	0.003(5)	-0.015(6)	-0.001(5)
C(5a)	0.035(6)	0.051(7)	0.075(8)	0.043(6)	-0.006(6)	-0.002(5)
C(6a)	0.046(7)	0.036(6)	0.048(7)	0.019(5)	-0.002(5)	-0.001(5)
C(10a)	0.051(7)	0.043(6)	0.044(7)	0.011(5)	0.006(5)	0.004(5)
C(11a)	0.064(8)	0.034(6)	0.054(7)	0.002(5)	-0.013(6)	0.004(5)
C(11b)	0.070(8)	0.035(6)	0.057(8)	0.011(6)	0.004(6)	-0.003(6)
C(10b)	0.058(7)	0.032(6)	0.048(7)	0.020(5)	-0.005(6)	-0.005(5)
C(6b)	0.035(6)	0.032(5)	0.047(7)	0.012(5)	-0.001(5)	0.000(5)
C(5b)	0.048(7)	0.048(7)	0.057(7)	0.022(6)	-0.004(6)	0.004(5)
C(4b)	0.063(8)	0.044(6)	0.041(7)	0.006(5)	-0.016(6)	0.001(6)
C(4c)	0.045(7)	0.046(7)	0.051(7)	0.006(5)	0.001(5)	0.009(5)
C(5c)	0.049(7)	0.040(6)	0.055(8)	0.006(5)	-0.001(6)	0.010(5)
C(6c)	0.033(6)	0.037(6)	0.063(8)	0.013(5)	-0.003(6)	0.006(5)
C(10c)	0.048(7)	0.049(7)	0.067(8)	0.027(6)	-0.001(6)	0.002(5)

Table 5.8: continued

C(11c)	0.051(8)	0.056(7)	0.088(10)	0.037(7)	0.022(7)	0.005(6)
C(11d)	0.080(9)	0.061(8)	0.063(8)	0.038(7)	0.013(7)	0.018(7)
C(10d)	0.062(8)	0.043(6)	0.052(7)	0.017(5)	0.008(6)	0.002(6)
C(6d)	0.061(8)	0.044(7)	0.045(7)	0.007(5)	-0.002(6)	0.008(6)
C(5d)	0.047(7)	0.030(6)	0.055(7)	0.005(5)	-0.007(6)	0.003(5)
C(4d)	0.041(7)	0.041(6)	0.054(7)	0.012(5)	-0.005(5)	0.006(5)

Table 5.9 Intermolecular distances (Å) for Fe(DIBrSALOF)

			S	a	b	c
H(4d) ...O(1)	2.93	-1	0.0	0.0	-1.0	
Fe(2) ...Fe(1)	3.51	1	1.0	1.0	1.0	
H(3a) ...Fe(1)	3.39	-1	-1.0	-1.0	-1.0	
C(2c) ...Fe(2)	2.93	1	-1.0	-1.0	-1.0	
C(7c) ...Fe(2)	3.38	1	-1.0	-1.0	-1.0	
C(8c) ...Fe(2)	3.06	1	-1.0	-1.0	-1.0	
C(9c) ...Fe(2)	2.99	1	-1.0	-1.0	-1.0	
C(9d) ...Fe(2)	3.01	1	-1.0	-1.0	-1.0	
C(8d) ...Fe(2)	3.06	1	-1.0	-1.0	-1.0	
C(7d) ...Fe(2)	3.41	1	-1.0	-1.0	-1.0	
C(2d) ...Fe(2)	2.95	1	-1.0	-1.0	-1.0	
H(4d) ...Fe(2)	3.37	-1	1.0	1.0	0.0	
H(3d) ...Fe(2)	3.47	-1	1.0	1.0	0.0	
C(4b) ...Br(a)	3.89	1	0.0	0.0	-1.0	
H(4b) ...Br(a)	3.11	1	0.0	0.0	-1.0	
Br(c) ...Br(a)	4.18	-1	-1.0	-1.0	-1.0	
H(3b) ...Br(a)	3.21	-1	-1.0	-1.0	-1.0	
C(4c) ...Br(a)	3.76	-1	-1.0	-1.0	-1.0	
C(5c) ...Br(a)	3.94	-1	-1.0	-1.0	-1.0	
H(11c) ...Br(a)	3.40	-1	-1.0	-1.0	0.0	
C(11d) ...Br(a)	3.73	-1	-1.0	-1.0	0.0	
H(11d) ...Br(a)	2.89	-1	-1.0	-1.0	0.0	
Br(c) ...Br(b)	3.46	1	0.0	-1.0	0.0	
H(6a) ...Br(b)	3.31	1	0.0	0.0	1.0	
H(8a) ...Br(b)	3.09	1	0.0	0.0	1.0	

Table 5.9 continued

C(10a)...Br(b)	3.89	1	0.0	0.0	1.0
H(10a)...Br(b)	2.89	1	0.0	0.0	1.0
H(10d)...Br(b)	3.06	1	0.0	0.0	1.0
H(8d) ...Br(b)	3.34	1	0.0	0.0	1.0
Br(b) ...Br(b)	4.31	-1	-1.0	0.0	-2.0
Br(d) ...Br(c)	3.97	1	0.0	1.0	1.0
H(6b) ...Br(c)	3.20	1	0.0	1.0	0.0
H(6d) ...Br(c)	3.46	1	0.0	1.0	1.0
C(5a) ...Br(c)	3.88	-1	-1.0	-1.0	-1.0
C(6a) ...Br(c)	3.63	-1	-1.0	-1.0	-1.0
H(6a) ...Br(c)	3.49	-1	-1.0	-1.0	-1.0
C(8d) ...Br(c)	3.47	-1	0.0	-1.0	-1.0
H(8d) ...Br(c)	3.25	-1	0.0	-1.0	-1.0
C(7d) ...Br(c)	3.84	-1	0.0	-1.0	-1.0
H(4c) ...Br(d)	3.15	1	0.0	-1.0	-1.0
C(5b) ...Br(d)	3.91	-1	0.0	0.0	-1.0
C(4b) ...Br(d)	3.79	-1	0.0	0.0	-1.0
C(3c) ...Br(d)	3.88	-1	0.0	0.0	-1.0
H(3c) ...Br(d)	3.08	-1	0.0	0.0	-1.0
C(11d)...Br(d)	3.84	-1	0.0	0.0	0.0
H(11d)...Br(d)	3.38	-1	0.0	0.0	0.0
C(10d)...Br(d)	3.72	-1	0.0	0.0	0.0
H(10d)...Br(d)	3.14	-1	0.0	0.0	0.0
H(3d) ...N(1b)	2.91	-1	0.0	0.0	-1.0
C(7c) ...N(1c)	3.36	-1	0.0	-1.0	-1.0
C(6c) ...N(1d)	3.44	-1	0.0	-1.0	-1.0
H(3a) ...O(1a)	2.55	-1	-1.0	-1.0	-1.0
H(4a) ...O(1b)	2.78	-1	-1.0	-1.0	-1.0

Table 5.9 continued

H(11b)...O(1c)	2.86	-1	0.0	0.0	-1.0
C(8c) ...O(1c)	3.30	-1	0.0	-1.0	-1.0
H(8c) ...O(1c)	2.93	-1	0.0	-1.0	-1.0
H(4d) ...O(1c)	2.88	-1	0.0	0.0	-1.0
H(10b)...O(1d)	2.64	-1	0.0	0.0	-1.0
C(3d) ...O(1d)	3.34	-1	0.0	0.0	-1.0
H(3d) ...O(1d)	2.63	-1	0.0	0.0	-1.0
H(3a) ...C(2a)	3.03	-1	-1.0	-1.0	-1.0
H(3a) ...C(3a)	3.01	-1	-1.0	-1.0	-1.0
C(6c) ...C(3a)	3.49	-1	-1.0	-1.0	-1.0
C(7c) ...C(3a)	3.43	-1	-1.0	-1.0	-1.0
C(8c) ...C(3a)	3.38	-1	-1.0	-1.0	-1.0
C(6c) ...C(4a)	3.47	-1	-1.0	-1.0	-1.0
C(5c) ...C(5a)	3.47	-1	-1.0	-1.0	-1.0
C(6b) ...C(8a)	3.35	-1	-1.0	0.0	-1.0
H(6b) ...C(8a)	2.98	-1	-1.0	0.0	-1.0
C(6b) ...H(8a)	3.05	-1	-1.0	0.0	-1.0
C(7b) ...C(9a)	3.38	-1	-1.0	0.0	-1.0
C(10c)...H(11b)	2.93	1	0.0	-1.0	0.0
C(3d) ...C(8b)	3.23	-1	0.0	0.0	-1.0
H(3d) ...C(8b)	3.05	-1	0.0	0.0	-1.0
C(4d) ...C(7b)	3.36	-1	0.0	0.0	-1.0
C(11d)...H(4b)	3.04	1	0.0	0.0	1.0
H(11c)...C(3b)	2.88	-1	-1.0	-1.0	-1.0
C(11c)...H(3b)	2.99	-1	-1.0	-1.0	-1.0
C(8c) ...C(2c)	3.49	-1	0.0	-1.0	-1.0
C(9c) ...C(2c)	3.49	-1	0.0	-1.0	-1.0
H(3d) ...C(3d)	2.87	-1	0.0	0.0	-1.0
C(2d) ...H(3d)	2.91	-1	0.0	0.0	-1.0

The symmetry code is the same as in page 5.

Table 5.10: Intramolecular distances (Å) for Fe(DIBrSALOF)

N(1a) ...O(1)	3.03	N(1b) ...O(1)	3.02
N(1c) ...O(1)	3.05	N(1d) ...O(1)	3.10
O(1a) ...O(1)	3.03	O(1b) ...O(1)	3.03
O(1c) ...O(1)	3.01	O(1d) ...O(1)	3.03
C(2a) ...Fe(1)	2.94	C(7a) ...Fe(1)	3.38
C(8a) ...Fe(1)	3.07	C(9a) ...Fe(1)	3.00
C(9b) ...Fe(1)	2.98	C(8b) ...Fe(1)	3.07
C(7b) ...Fe(1)	3.40	C(2b) ...Fe(1)	2.94
C(4a) ...Br(a)	2.87	H(4a) ...Br(a)	2.97
C(6a) ...Br(a)	2.84	H(6a) ...Br(a)	2.94
C(6b) ...Br(b)	2.86	H(6b) ...Br(b)	2.97
C(4b) ...Br(b)	2.84	H(4b) ...Br(b)	2.94
C(4c) ...Br(c)	2.85	H(4c) ...Br(c)	2.96
C(6c) ...Br(c)	2.81	H(6c) ...Br(c)	2.90
C(6d) ...Br(d)	2.86	H(6d) ...Br(d)	2.96
C(4d) ...Br(d)	2.84	H(4d) ...Br(d)	2.94
N(1b) ...N(1a)	2.63	O(1a) ...N(1a)	2.79
C(2a) ...N(1a)	2.98	C(7a) ...N(1a)	2.43
H(8a) ...N(1a)	2.06	C(10a) ...N(1a)	2.49
H(10a) ...N(1a)	2.75	C(9b) ...N(1a)	2.37
O(1b) ...N(1b)	2.78	C(9a) ...N(1b)	2.40
C(10b) ...N(1b)	2.49	H(10b) ...N(1b)	2.76
H(8b) ...N(1b)	2.03	C(7b) ...N(1b)	2.41
C(2b) ...N(1b)	2.97	N(1d) ...N(1c)	2.64
O(1c) ...N(1c)	2.80	C(2c) ...N(1c)	2.98

Table 5.10: continued

C(7c) ...N(1c)	2.42	H(8c) ...N(1c)	2.04
C(10c)...N(1c)	2.49	H(10c)...N(1c)	2.76
C(9d) ...N(1c)	2.38	O(1d) ...N(1d)	2.77
C(9c) ...N(1d)	2.39	C(10d)...N(1d)	2.48
H(10d)...N(1d)	2.73	H(8d) ...N(1d)	2.02
C(7d) ...N(1d)	2.44	C(2d) ...N(1d)	2.95
O(1b) ...O(1a)	2.78	C(3a) ...O(1a)	2.35
H(3a) ...O(1a)	2.60	C(7a) ...O(1a)	2.38
C(8a) ...O(1a)	2.92	C(8b) ...O(1b)	2.90
C(7b) ...O(1b)	2.39	C(3b) ...O(1b)	2.34
H(3b) ...O(1b)	2.58	O(1d) ...O(1c)	2.76
C(3c) ...O(1c)	2.35	H(3c) ...O(1c)	2.58
C(7c) ...O(1c)	2.42	C(8c) ...O(1c)	2.93
C(8d) ...O(1d)	2.91	C(7d) ...O(1d)	2.39
C(3d) ...O(1d)	2.34	H(3d) ...O(1d)	2.58
H(3a) ...C(2a)	2.16	C(4a) ...C(2a)	2.41
C(5a) ...C(2a)	2.80	C(6a) ...C(2a)	2.45
C(8a) ...C(2a)	2.51	H(4a) ...C(3a)	2.09
C(5a) ...C(3a)	2.38	C(6a) ...C(3a)	2.78
C(7a) ...C(3a)	2.42	C(4a) ...H(3a)	2.09
C(6a) ...C(4a)	2.40	C(7a) ...C(4a)	2.77
C(5a) ...H(4a)	2.14	H(6a) ...C(5a)	2.13
C(7a) ...C(5a)	2.41	C(8a) ...C(6a)	2.41
H(8a) ...C(6a)	2.56	C(7a) ...H(6a)	2.17
C(8a) ...H(6a)	2.60	H(8a) ...C(7a)	2.15
C(9a) ...C(8a)	2.38	C(10a)...C(8a)	2.91
H(10a)...C(8a)	2.65	C(9a) ...H(8a)	2.56
C(10a)...H(8a)	2.55	H(10a)...C(9a)	2.12

Table 5.10: continued

C(11a)...C(9a)	2.42	C(11b)...C(9a)	2.76
C(10b)...C(9a)	2.44	H(11a)...C(10a)	2.17
C(11b)...C(10a)	2.37	C(10b)...C(10a)	2.77
C(9b) ...C(10a)	2.39	C(11a)...H(10a)	2.15
H(11b)...C(11a)	2.11	C(10b)...C(11a)	2.40
C(9b) ...C(11a)	2.79	C(11b)...H(11a)	2.14
H(10b)...C(11b)	2.12	C(9b) ...C(11b)	2.39
C(10b)...H(11b)	2.10	C(8b) ...C(10b)	2.93
H(8b) ...C(10b)	2.58	C(9b) ...H(10b)	2.18
C(8b) ...H(10b)	2.71	C(8b) ...C(9b)	2.39
H(8b) ...C(9b)	2.58	C(6b) ...C(8b)	2.40
H(6b) ...C(8b)	2.60	C(2b) ...C(8b)	2.50
C(7b) ...H(8b)	2.13	C(6b) ...H(8b)	2.57
H(6b) ...C(7b)	2.15	C(5b) ...C(7b)	2.41
C(4b) ...C(7b)	2.80	C(3b) ...C(7b)	2.41
C(4b) ...C(6b)	2.40	C(3b) ...C(6b)	2.75
C(2b) ...C(6b)	2.44	C(5b) ...H(6b)	2.12
H(4b) ...C(5b)	2.16	C(3b) ...C(5b)	2.38
C(2b) ...C(5b)	2.81	H(3b) ...C(4b)	2.11
C(2b) ...C(4b)	2.44	C(3b) ...H(4b)	2.13
C(2b) ...H(3b)	2.14	H(3c) ...C(2c)	2.12
C(4c) ...C(2c)	2.40	C(5c) ...C(2c)	2.80
C(6c) ...C(2c)	2.44	C(8c) ...C(2c)	2.50
H(4c) ...C(3c)	2.13	C(5c) ...C(3c)	2.38
C(6c) ...C(3c)	2.74	C(7c) ...C(3c)	2.40
C(4c) ...H(3c)	2.12	C(6c) ...C(4c)	2.37
C(7c) ...C(4c)	2.77	C(5c) ...H(4c)	2.13
H(6c) ...C(5c)	2.11	C(7c) ...C(5c)	2.40

Table 5.10: continued

C(8c) ...C(6c)	2.41	H(8c) ...C(6c)	2.58
C(7c) ...H(6c)	2.16	C(8c) ...H(6c)	2.61
H(8c) ...C(7c)	2.13	C(9c) ...C(8c)	2.36
C(10c)...C(8c)	2.89	H(10c)...C(8c)	2.66
C(9c) ...H(8c)	2.54	C(10c)...H(8c)	2.51
H(10c)...C(9c)	2.17	C(11c)...C(9c)	2.40
C(11d)...C(9c)	2.79	C(10d)...C(9c)	2.42
H(11c)...C(10c)	2.12	C(11d)...C(10c)	2.41
C(10d)...C(10c)	2.79	C(9d) ...C(10c)	2.41
C(11c)...H(10c)	2.13	H(11d)...C(11c)	2.14
C(10d)...C(11c)	2.39	C(9d) ...C(11c)	2.75
C(11d)...H(11c)	2.12	H(10d)...C(11d)	2.15
C(9d) ...C(11d)	2.40	C(10d)...H(11d)	2.15
C(8d) ...C(10d)	2.86	H(8d) ...C(10d)	2.45
C(9d) ...H(10d)	2.14	C(8d) ...H(10d)	2.59
C(8d) ...C(9d)	2.37	H(8d) ...C(9d)	2.53
C(6d) ...C(8d)	2.44	H(6d) ...C(8d)	2.63
C(2d) ...C(8d)	2.50	C(7d) ...H(8d)	2.18
C(6d) ...H(8d)	2.61	H(6d) ...C(7d)	2.15
C(5d) ...C(7d)	2.41	C(4d) ...C(7d)	2.77
C(3d) ...C(7d)	2.41	C(4d) ...C(6d)	2.39
C(3d) ...C(6d)	2.76	C(2d) ...C(6d)	2.42
C(5d) ...H(6d)	2.15	H(4d) ...C(5d)	2.12
C(3d) ...C(5d)	2.38	C(2d) ...C(5d)	2.80
H(3d) ...C(4d)	2.13	C(2d) ...C(4d)	2.43
C(3d) ...H(4d)	2.13	C(2d) ...H(3d)	2.16

SUPPLEMENTARY MATERIAL

**Oxygenation of a Co-ordinated Tetra-azamacrocyclic: The X-ray Structure
Determination of μ -Oxo-bis{17,18,19,20-tetrahydro-18,19-dioxotribenzo-
[e,i,m][1,4,8,11]tetra-azacyclotetradecinato(2-)}iron(III)}**

By SÜHEYLÂ GÖZEN, ROGER PETERS, PHILIP G. OWSTON,* and PETER A. TASKER
(Department of Chemistry, Polytechnic of North London, Holloway, London N7 8DB)

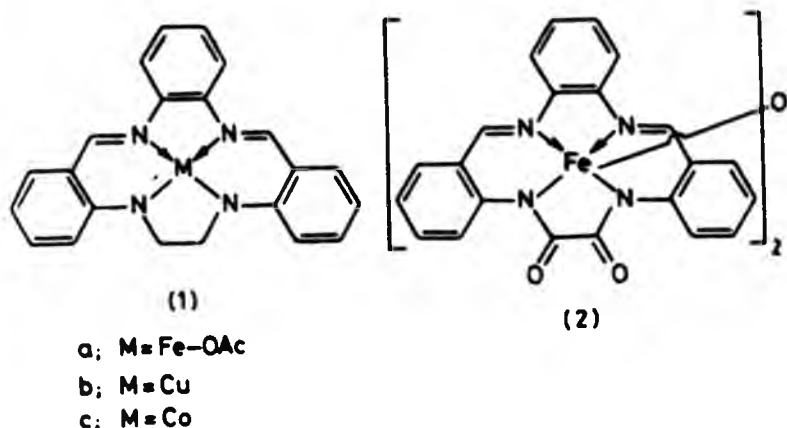
**Reprinted from the Journal of The Chemical Society
Chemical Communications 1980**

Oxygenation of a Co-ordinated Tetra-azamacrocyclic: The X-ray Structure Determination of μ -Oxo-bis{17,18,19,20-tetrahydro-18,19-dioxotribenzo-[e,i,m][1,4,8,11]tetra-azacyclotetradecinato(2-)}iron(III)}

By SÜHEYLÄ GÖZEN, ROGER PETERS, PHILIP G. OWSTON,* and PETER A. TASKER
(Department of Chemistry, Polytechnic of North London, Holloway, London N7 8DB)

Summary The -N-CH₂-CH₂-N- bridge in the neutral macrocyclic iron(III) complex (1a) is readily oxygenated to give a μ -oxo complex of the corresponding oxamido ligand.

DURING our studies¹ of tetra-aza macrocyclic ligands and their metal complexes, we have prepared the iron(III) complex (1a). When (1a) was dissolved in dimethylformamide and held at 80 °C for 6 h, the solution slowly deposited black



needles. These were examined by X-ray analysis† and shown to be the *NN*-dimethylformamide (DMF) solvate of the μ -oxo dimer (2) in which oxygenation of the ethane bridge between the anilino nitrogens has occurred. This reaction was unexpected; in certain cases related Co^{III}, Ni^{III}, and Cu^{III} complexes with a trimethylene bridge have been observed²

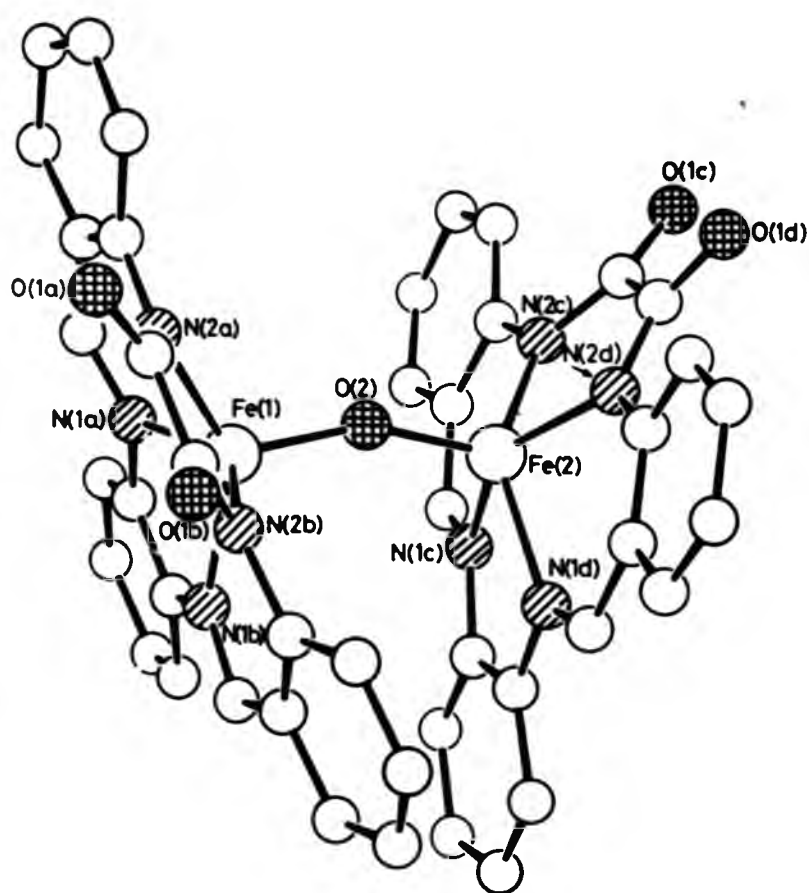


FIGURE. The structure of (2). Bond lengths Fe(1)-N(1a), 2.06(1); Fe(1)-N(1b), 2.11(1); Fe(1)-N(2a), 2.01(1); Fe(1)-N(2b), 1.98(1); Fe(1)-O(2), 1.777(8); Fe(2)-N(1c), 2.10(1); Fe(2)-N(1d), 2.07(1); Fe(2)-N(2c), 2.00(1); Fe(2)-N(2d), 1.99(1); Fe(2)-O(2), 1.758(9) Å.

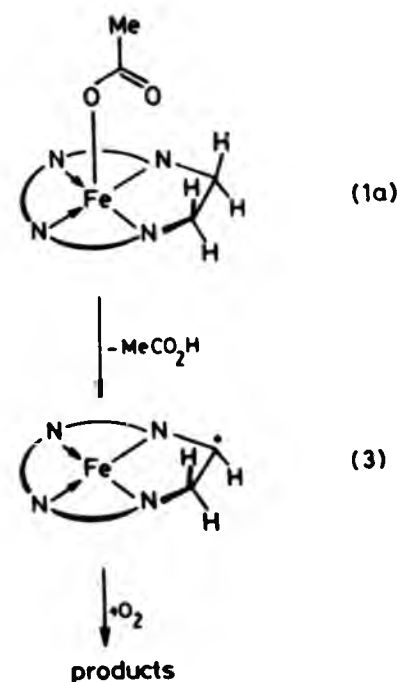
† *Crystal data*: [C₄₄H₃₈N₈O₂Fe₂](+0.67 DMF), *M* = 860.5 (+49.0), monoclinic, *P*2₁/*c*, *a* = 10.819(3), *b* = 26.738(7), *c* = 14.910(4) Å, β = 101.82(8)°, *U* = 4221.7 Å³, *Z* = 4, *D*_c = 1.43 g cm⁻³, μ (Mo-*K* α) = 6.92 cm⁻¹, *R* = 0.070 for 1911 data with *I*/ σ (*I*) > 3.0 obtained on a Philips PW1100 diffractometer. The structure was solved by Patterson methods and refined using isotropic thermal parameters except for the Fe atoms, with hydrogen atoms set with C-H = 1.08 Å; 0.52 > $\Delta\rho$ > -0.40 e Å⁻³. The atomic co-ordinates for this work are available on request from the Director of the Cambridge Crystallographic Data Centre, University Chemical Laboratory, Lensfield Road, Cambridge, CB2 1EW. Any request should be accompanied by the full literature citation for this communication.

‡ Certain Ni^{III} and Cu^{III} complexes analogous to (1) which contain a trimethylene link between the anilino nitrogen atoms are observed to undergo dehydrogenation (rather than oxygenation) with O₂ in reactions which appear to proceed *via* two-electron transfer followed by proton loss from a methylene group (ref. 2), rather than *via* the mechanism shown in the Scheme.

to undergo dehydrogenation in the presence of O₂, but oxygenation has not previously been reported.

The two halves of the molecule (Figure) have closely similar structures. The iron atoms Fe(1) and Fe(2) have approximately square-pyramidal co-ordination geometries (lying 0.64 and 0.65 Å above the mean planes of the N₄ donor sets) and are significantly closer to the oxamido nitrogens [2.00(1) Å] than to the other two nitrogens [2.09(1) Å]. The oxamido groups are inclined at 27 and 26° to the N₄ co-ordination planes about Fe(1) and Fe(2), and the iron atoms lie very close to the planes of the oxamido groups. Most of the atoms in the 14-membered inner great ring lie close to the N₄ co-ordination plane. The exceptions are the two carbon atoms attached to a benzene ring which are close (0.05 Å) to the N₄ plane in the macrocycle containing Fe(1) but appreciably below it (0.24 Å) in the other. There are other smaller differences in conformation between the two macrocycles which may be attributed to packing constraints imposed by the solvate molecule whose site was found, by X-ray analysis, to have an occupancy of 0.67. The angle and bond lengths of the μ -oxo bridge [157(1)° and 1.777(8) and 1.758(9) Å] fall centrally within the range of values (130–175° and 1.76–1.79 Å) observed³ in related five-co-ordinate iron(III) complexes.

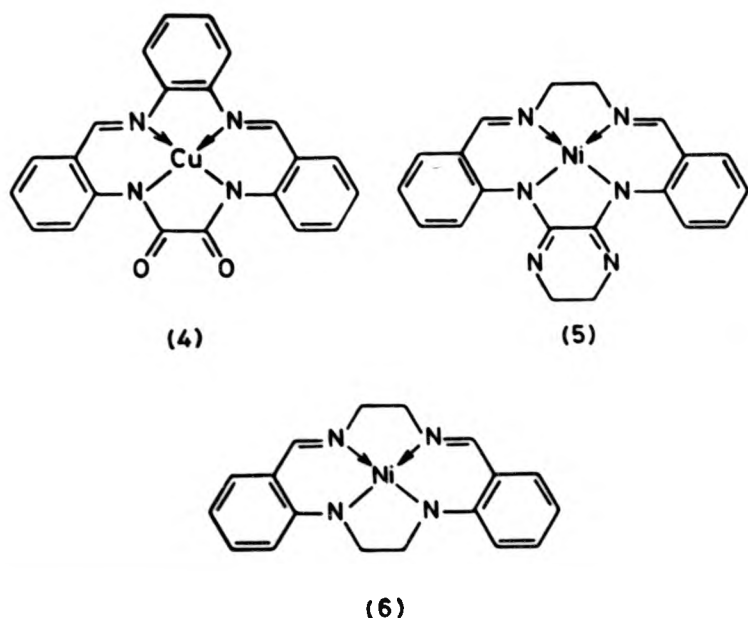
The mechanism of this facile oxygenation is under investigation, but in the light of recent work⁴ on base-induced ligand oxygenations of cobalt(III) complexes, a reasonable proposal (Scheme) for the initial step of the reaction involves the elimination of acetic acid to give an iron(II) complex of the ligand radical shown in (3).‡



SCHEME.

Structure
benzo-

macrocyclic ligands and
the iron(III) complex
dimethylformamide and
deposited black



Preliminary results suggest that other metal complexes of the ligand in (1) undergo similar oxygenation reactions, *e.g.* the Cu^{II} compound (1b) in DMF (100 °C/18 h) gives (4), which has previously⁵ been made from ligands in which the oxamido unit has been incorporated^{5,6} from a reaction sequence involving oxalyl dichloride. The related Co^{II} compound (1c) undergoes a more complex reaction with O₂, but i.r. spectra suggest that again an oxamido complex is present in the mixture of products obtained.

It seems likely that the compound (5), isolated⁷ by Maslen *et al.* during the preparation of (6), was formed by oxygenation of (6) to give an oxamide which then condensed with the excess of 1,2-diaminoethane which was present.

We thank the S.R.C. for a studentship (to R.P.) and for diffractometer equipment and computing facilities.

(Received, 24th September 1980; Com., 1053.)

¹ P. G. Owston, R. Peters, E. Ramsammy, P. A. Tasker, and J. Trotter, *J. Chem. Soc., Chem. Commun.*, 1980, accepted for publication; A. J. Greenwood, K. Henrick, P. G. Owston, and P. A. Tasker, *ibid.*, p. 88.

² D. St. C. Black, A. J. Hartshorn, M. Horner, and S. Hünig, *Aust. J. Chem.*, 1977, **30**, 2493.

³ A. B. Hoffman, D. M. Collins, V. W. Day, E. B. Fleischer, T. S. Srivastava, and J. L. Hoard, *J. Am. Chem. Soc.*, 1972, **94**, 3620; M. C. Weiss and V. L. Goedken, *Inorg. Chem.*, 1979, **18**, 819; P. Coggon, A. T. McPhail, F. E. Mabbs, and V. N. McLachlan, *J. Chem. Soc. (A)*, 1971, 1014; J. E. Davies and B. M. Gatehouse, *Acta Crystallogr., Sect. B*, 1973, **29**, 1934, 2651; M. Gerloch, E. D. McKenzie, and A. D. C. Towl, *J. Chem. Soc. (A)*, 1969, 2850.

⁴ J. A. Switzer and J. F. Endicott, *J. Am. Chem. Soc.*, 1980, **102**, 1181.

⁵ D. St. C. Black, C. H. Bos Vanderzalm, and A. J. Hartshorn, *Inorg. Nucl. Chem. Lett.*, 1976, **12**, 657.

⁶ C. Skötsch and E. Breitmaier, *Synthesis*, 1978, 680.

⁷ E. N. Maslen, L. M. Englehardt, and A. H. White, *J. Chem. Soc., Dalton Trans.*, 1974, 1799.

CHEM. COMM., 1980

metal complexes of
ation reactions, *e.g.*
0 °C/18 h) gives (4),
ligands in which the
from a reaction
The related Co^{II}
lex reaction with O₂,
oxamido complex is
ained.

, isolated⁷ by Maslen
formed by oxygena-
n condensed with the
present.
pip (to R.P.) and for
ng facilities.

er 1980; *Com.*, 1053.)

0, accepted for publi-

. *Soc.*, 1972, **94**, 3620;
McLachlan, *J. Chem.*
loch, E. D. McKenzie,

Two Different Modes of avoiding Steric Crowding in *ortho*-Substituted *N*-Phenylcyclophosph(v)azanes; X-Ray Crystal Structures of Two Derivatives†

Philip G. Owston,^a Leylâ S. Shaw^a (née Gözen), Robert A Shaw,^{b*} and David A. Watkins^b

^a*Department of Chemistry, The Polytechnic of North London, Holloway Road, London N7 8DB, U.K.*

^b*Department of Chemistry, Birkbeck College, University of London, Malet Street, London WC1 7HX, U.K.*

X-Ray structural analyses of the compounds [PhP(S)NC₆H₄X]₂, (1) (X = *o*-Me) and (2) (X = *o*-OMe), show that steric crowding is relieved in (1) by rotation about the C-N bond and in (2) by bending of this bond; the results are correlated with ³¹P chemical shift n.m.r. measurements in related substituted *N*-phenylcyclophosph(v)azanes.

Reprinted from the Journal of The Chemical Society
Chemical Communications 1982

Two Different Modes of avoiding Steric Crowding in *ortho*-Substituted *N*-Phenylcyclophosph(v)azanes; X-Ray Crystal Structures of Two Derivatives†

Philip G. Owston,^a Leylâ S. Shaw^a (née Gözen), Robert A Shaw,^{b*} and David A. Watkins^b

^aDepartment of Chemistry, The Polytechnic of North London, Holloway Road, London N7 8DB, U.K.

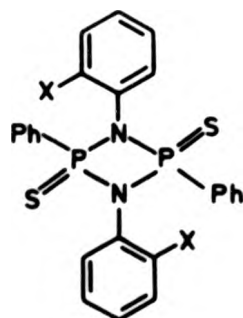
^bDepartment of Chemistry, Birkbeck College, University of London, Malet Street, London WC1 7HX, U.K.

X-Ray structural analyses of the compounds $[\text{PhP}(\text{S})\text{NC}_6\text{H}_4\text{X}]_2$, (1) ($\text{X} = o\text{-Me}$) and (2) ($\text{X} = o\text{-OMe}$), show that steric crowding is relieved in (1) by rotation about the C–N bond and in (2) by bending of this bond; the results are correlated with ^{31}P chemical shift n.m.r. measurements in related substituted *N*-phenylcyclophosph(v)azanes.

^{31}P N.m.r. chemical shifts do not indicate any pronounced *ortho*-effects in a series of substituted *N*-phenyl derivatives of $\text{P}(\text{S})\text{Cl}_2$ and $\text{PhP}(\text{S})\text{Cl}_2$, e.g. $\text{P}(\text{S})(\text{NHC}_6\text{H}_4\text{X})_2$ ($\text{X} = o\text{-}, m\text{-}, p\text{-Me}$, δ 43.6, 42.3, 43.9 p.p.m.; $\text{X} = o\text{-}, m\text{-}, p\text{-OMe}$, δ 46.6, 41.9, 46.3 p.p.m.) and $\text{PhP}(\text{S})(\text{NHC}_6\text{H}_4\text{X})_2$ ($\text{X} = o\text{-}, m\text{-}, p\text{-Me}$, δ 52.6, 51.5, 52.2 p.p.m.; $\text{X} = o\text{-}, m\text{-}, p\text{-OMe}$, δ 51.9, 51.4, 53.1 p.p.m.). In contrast, considerable chemical shift changes are observed in *ortho*-substituted *N*-phenylcyclophosph(v)azanes, viz. $[\text{PhP}(\text{S})\text{NC}_6\text{H}_4\text{X}]_2$ [$\text{X} = o\text{-}, m\text{-}, p\text{-Me}$, δ 77.1, 67.3, 68.1 p.p.m.; $\text{X} = o\text{-}, m\text{-}, p\text{-OMe}$, δ 72.9, 67.0, 70.8 p.p.m.).¹ Examples of preparative procedures are given elsewhere² (all compounds had satisfactory elemental analyses). The chemical shift data of the derivatives with $\text{X} = \text{Cl}, \text{Br}, \text{I}$, resemble those when $\text{X} = \text{Me}$, whilst the shifts for $\text{X} = \text{OEt}, \text{F}$, resemble those for $\text{X} = \text{OMe}$.¹ The other geometric isomer was detected in some reaction crude mixtures, but the shift difference between the isomers was in no case greater than 0.6 p.p.m.

X-Ray crystallographic investigations were undertaken for one member of each chemical shift type, δ 77 and 73 p.p.m., respectively [$\text{X} = o\text{-Me}$ (1) and $o\text{-OMe}$ (2)].

Crystal data: $[\text{PhP}(\text{S})\text{NC}_6\text{H}_4\text{-}o\text{-Me}]_2$ (1), m.p. 236–238 °C, $M = 490$, monoclinic, $a = 13.131(6)$, $b = 9.513(3)$, $c = 10.057(3)$ Å, $\beta = 96.09(6)^\circ$, $U = 1249.2$ Å³, space group $P2_1/n$, $Z = 2$, $D_c = 1.302$ g cm⁻³ [16 ± 2 °C, Mo- K_α radiation, $\lambda = 0.71069$ Å (graphite monochromator), $\mu = 3.08$ cm⁻¹], $F(000) = 512$. 2202 unique reflections in the range $\theta = 3\text{--}25^\circ$ were measured on a Philips PW1100 diffractometer, of which 1609 had $I > 3\sigma(I)$ and were used for structure solution by direct methods and for refinement (SHELX).³ The conventional R value is 0.034 with isotropic temperature factors for the hydrogen atoms and anisotropic factors for the heavier atoms. $[\text{PhP}(\text{S})\text{NC}_6\text{H}_4\text{-}o\text{-OMe}]_2$ (2), m.p. 239–240 °C, $M = 522$, triclinic, $a = 15.123(6)$, $b = 9.507(3)$, $c = 8.844(3)$ Å, $\alpha = 94.65(6)$, $\beta = 89.28(5)$, $\gamma = 88.51(5)^\circ$, $U = 1266.8$ Å³, space group $P\bar{1}$, $Z = 2$, $D_c = 1.368$ g cm⁻³ [16 ± 2 °C, Mo- K_α radiation, $\lambda = 0.71069$ Å (graphite monochromator), $\mu =$



- (1) $\text{X} = o\text{-Me}$
 (2) $\text{X} = o\text{-OMe}$
 (3) $\text{X} = \text{H}$

3.11 cm⁻¹], $F(000) = 544$. 4449 unique reflections in the range $\theta = 3\text{--}25^\circ$ were measured on a Philips PW100 diffractometer, of which 2759 had $I > 3\sigma(I)$ and were used in the analysis as for compound (1). The two molecules in the unit cell are crystallographically centrosymmetric and the asymmetric unit contains half of each molecule. The conventional R value is 0.036 with isotropic temperature factors for the hydrogen atoms and anisotropic factors for the heavier atoms.† ORTEP diagrams of compounds (1) and (2) are given in Figures 1 and 2, respectively.

Both compounds have a *trans*-structure and a planar four-membered (P–N)₂ ring, as observed for other compounds of this type.^{4–6} An earlier investigation⁴ of the parent *N*-phenyl derivative (3) ($\text{X} = \text{H}$) revealed that the *N*-phenyl group was almost coplanar with the (P–N)₂ ring (δ ^{31}P 67.1 p.p.m.).¹ In the *ortho*-tolyl derivative (1) the *N*-phenyl group is twisted by 74° about the C–N bond relative to the (P–N)₂ ring, thus drastically reducing or eliminating any possible $p_\pi\text{--}p_\pi$ interaction between the nitrogen lone-pair of electrons and the π -system of the phenyl group. The result is to confer some 'aliphatic character' on the bond to the *ortho*-tolyl group. This is confirmed by the lengthening of this C–N bond from 1.418(3) Å, observed in the *N*-Ph derivative, to 1.440(3) Å in

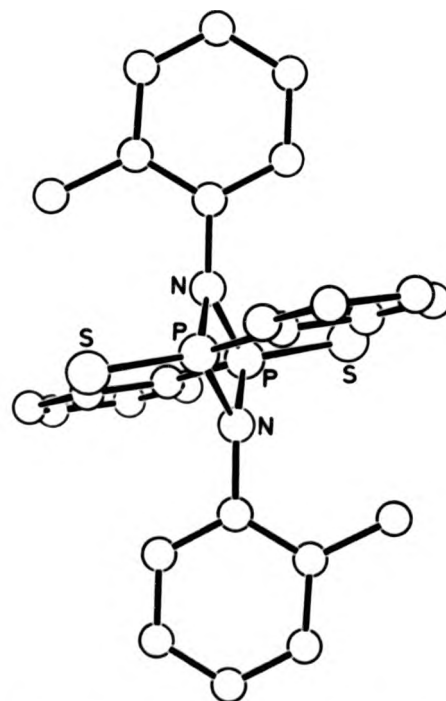


Figure 1. ORTEP drawing of $[\text{PhP}(\text{S})\text{NC}_6\text{H}_4\text{-}o\text{-Me}]_2$ (1).

† The atomic co-ordinates for this work are available on request from the Director of the Cambridge Crystallographic Data Centre, University Chemical Laboratory, Lensfield Road, Cambridge CB2 1EW. Any request should be accompanied by the full literature citation for this communication.

† Presented at the 3rd International Symposium on Inorganic Ring Systems, August 1981, Graz, Austria.

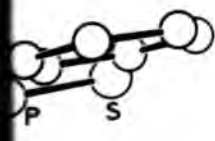
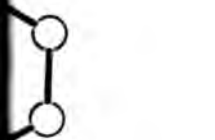
o-
tal

A. Watkins^b
7 8DB, U.K.
n WC1 7HX, U.K.

(2) (X = o-OMe),
by bending of this
substituted N-

unique reflections in the range
Philips PW100 diffractometer,
were used in the analysis as
molecules in the unit cell are
centric and the asymmetric unit
The conventional R value is
the factors for the hydrogen
the heavier atoms.† ORTEP
(2) are given in Figures 1 and

structure and a planar four-
ved for other compounds of
tion⁴ of the parent N-phenyl
that the N-phenyl group was
ring ($\delta^{31}\text{P}$ 67.1 p.p.m.).¹ In
the N-phenyl group is twisted
relative to the (P-N)₂ ring, thus
ing any possible p π -p π inter-
ne-pair of electrons and the
The result is to confer some
ad to the ortho-tolyl group.
ning of this C-N bond from
n derivative, to 1.440(3) Å in



[PhP(S)NC₆H₄-o-Me]₂ (1).

work are available on request
Crystallographic Data Centre,
7, Lensfield Road, Cambridge
be accompanied by the full
communication.

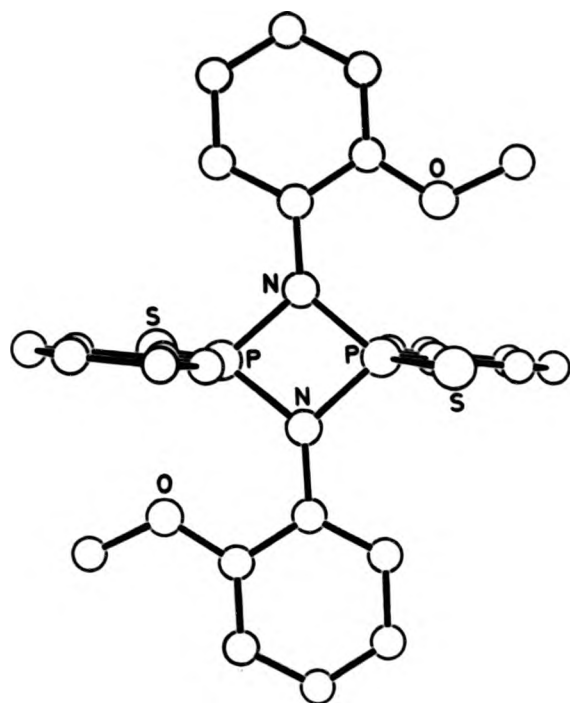


Figure 2. ORTEP drawing of [PhP(S)NC₆H₄-o-OMe]₂ (2).

the present structure. This value is closer to that observed for related aliphatic derivatives,^{5,6} e.g. in [PhP(S)NEt]₃ C-N = 1.463(9) Å,⁵ and is consistent with the observation that the chemical shifts of these two compounds are very similar, viz. $\delta^{31}\text{P}$ [PhP(S)NEt]₃ 76.3¹ and (1) δ 77.1 p.p.m.

In the ortho-methoxyphenyl-derivative (2) the molecule adopts another mode of avoiding steric crowding. The N-aryl ring is almost coplanar with the (P-N)₂ ring, with a C-N bond length of 1.423(4) Å, similar to the situation in the N-phenyl derivative. Steric crowding in this case is reduced by the bending of the C-N bond, leading to an increase in the P-N-C bond angle on the same side as the substituent. The difference, Δ , between the two P-N-C bond angles is close to zero, within experimental error, for the other compounds quoted; (3) 0.5°, (1) 1.0°, and [PhP(S)NEt]₃ 0.6°. In the ortho-methoxyphenyl compound (2), however, Δ is 5.5° (all angles and bond lengths quoted are mean values); the $\delta^{31}\text{P}$ chemical shift (δ 72.9 p.p.m.) is lower than in compound (1).

Table 1

X	(1) o-Me	(2) o-OMe	(3) H
$\delta^{31}\text{P}$ /p.p.m.	77.1	72.9	67.1
$\tau(\text{PNCC})/^\circ$	74.0	9.4	7.8
C-N/Å	1.440(3)	1.423(4)	1.418(3)
$\Delta \text{PNC}/^\circ$	1.0	5.5	0.5
Distance N-PPC plane/Å	0.143	0.020	0.022

It thus appears that two modes of avoiding the steric hindrance due to the ortho-substituent can occur and may be correlated with the $\delta^{31}\text{P}$ chemical shifts. We can conclude from the n.m.r. data (CDCl₃ solution) that bond-twisting occurs when X = o-Cl, Br, I, and bond-bending when X = o-OEt and F.

A detailed comparison of the structures of compounds (1), (2), and (3) (Table 1) shows that the C-N bond in (1) is significantly longer than in (2) or (3), and also that the nitrogen atom is significantly more pyramidal in (1) than in (2) or (3). We conclude that the hybridisation of the nitrogen atom in (2) and (3) is closer to sp³ than in (1) consistent with a lower p π -p π interaction in compound (1) caused by the observed bond rotation.

Received, 3rd August 1981; Com. 936

References

- P. J. Argent, Ph.D. thesis, London, 1978.
- P. J. Argent, D. Parker, R. A. Shaw, and M. Woods, *Inorg. Nucl. Chem. Lett.*, 1981, 17, 11.
- G. M. Sheldrick, University Chemical Laboratory, Cambridge, 1976.
- M. B. Peterson and A. J. Wagner, *J. Chem. Soc., Dalton Trans.*, 1973, 106.
- G. J. Bullen, J. S. Rutherford, and P. A. Tucker, *Acta Crystallogr., Sect. B*, 1973, 29, 1439.
- T. S. Cameron, C. K. Prout, and K. D. Howlett, *Acta Crystallogr., Sect. B*, 1975, 31, 2333.

The Self-condensation of *o*-Aminobenzaldehyde: the Polycyclic Structure of the Picrate Salt of the Diprotonated Tetra-anhydro Tetramer, 4b,5,15b,16-Tetrahydrodibenzo[3,4:7,8][1,5]diazocino-[2,1-*b*:6,5-*b*]diquinazoline-11,22-di-ium Picrate: X-Ray Crystal Structure

Philip G. Owston,* Leylâ S. Shaw (née Gözen), and Peter A. Tasker

Department of Chemistry, The Polytechnic of North London, Holloway, London N7 8DB, U.K.

An X-ray crystal structure determination shows that the diprotonated tetra-anhydro-tetramer of *o*-aminobenzaldehyde in the picrate salt, $[C_{28}H_{22}N_4][C_6H_2N_3O_7]_2$, has a heptacyclic structure (3), rather than that of the macrocyclic isomer (4), and appears to be stabilised by a strong N-H...O hydrogen bond and a short C-H...O interaction (C...O, 3.12 Å) to the picrate anions.

Reprinted from the Journal of The Chemical Society
Chemical Communications 1982

The Self-condensation of *o*-Aminobenzaldehyde: the Polycyclic Structure of the Picrate Salt of the Diprotonated Tetra-anhydro Tetramer, 4b,5,15b,16-Tetrahydrodibenzo[3,4:7,8][1,5]diazocino-[2,1-*b*:6,5-*b*]diquinazoline-11,22-di-ium Picrate: X-Ray Crystal Structure

Philip G. Owston,* Leylâ S. Shaw (née Gözen), and Peter A. Tasker

Department of Chemistry, The Polytechnic of North London, Holloway, London N7 8DB, U.K.

An X-ray crystal structure determination shows that the diprotonated tetra-anhydro-tetramer of *o*-aminobenzaldehyde in the picrate salt, $[C_{28}H_{22}N_4][C_6H_2N_3O_7]_2$, has a heptacyclic structure (3), rather than that of the macrocyclic isomer (4), and appears to be stabilised by a strong N-H...O hydrogen bond and a short C-H...O interaction (C...O, 3.12 Å) to the picrate anions.

The self-condensation of *o*-aminobenzaldehyde leads to a number of products,¹⁻⁴ which can be difficult to characterise because of their ready interconversion. The tetra-anhydro-tetramer, taab, (1), in particular has not been isolated, except as its derivatives, viz. as metal complexes,⁵ e.g. $[(taab)Ni(H_2O)]I$ (2), and as salts of strong acids, $[(taab)H_2]^+[X^-]_2$, for which the two isomeric structures (3) and (4) have been

proposed,^{4,6} as the hydrate, assigned^{5,6} structure (5), and as salts of this hydrate, thought⁶ to have the structure (6). The evidence for these structures is mainly spectroscopic except for the X-ray results⁵ for the metal complexes (2) and an incomplete analysis⁴ of the disordered salt $[(taab)H_2][CF_3SO_3]_2$. The protonated salts are labile in the presence of water, and the only non-aqueous solvents in which they are reasonably

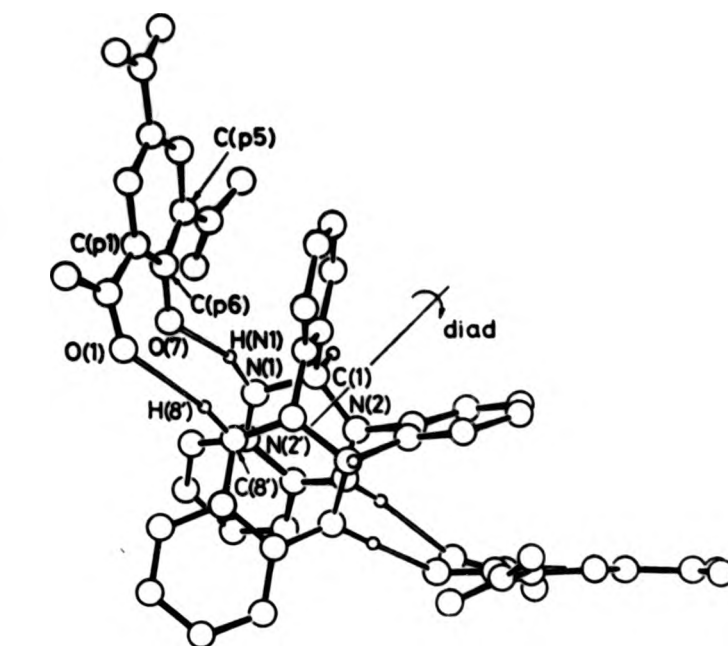
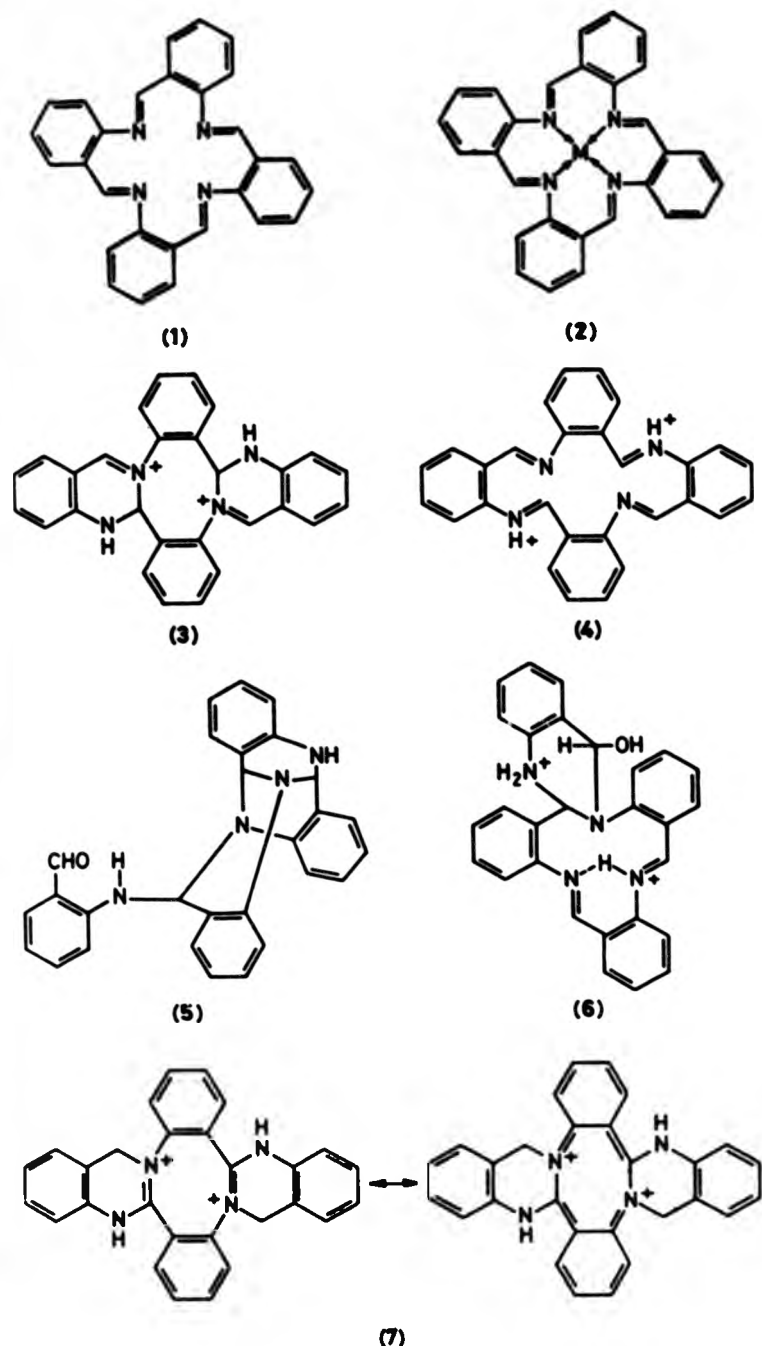


Figure 1. The conformation of $[(\text{taab})(\text{H}_2)]^{2+}$, showing hydrogen bonds to the picrate anions.

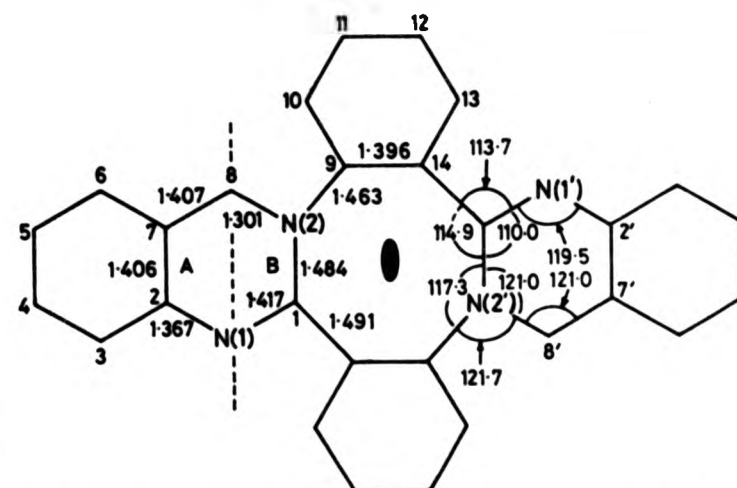


Figure 2. Selected bond lengths and angles in the dication $[(\text{taab})(\text{H}_2)]^{2+}$ (e.s.d.s are 0.005 Å and 0.3° respectively).

soluble are difficult to dehydrate thoroughly; spectroscopic and other observations made on solutions are therefore inconclusive. We have prepared a number of salts of taab and report here the crystal structure of $[(\text{taab})\text{H}_2]^{2+}[\text{picrate}]_2$ obtained from the condensation⁴ of *o*-aminobenzaldehyde in CH_3CN in the presence of picric acid.

Crystal data: $(\text{C}_{28}\text{H}_{22}\text{N}_4, 2\text{C}_6\text{H}_3\text{N}_3\text{O}_7)$ M (414 + 2 × 228), $F(000) = 896$, monoclinic, space group $P2_1/n$, $a = 22.694(6)$, $b = 9.344(3)$, $c = 9.765(3)$ Å, $\beta = 107.48(9)^\circ$, $Z = 2$, $D_c = 1.462$, $D_m = 1.471$ g/cm³, $\lambda(\text{Mo-K}\alpha) = 0.71069$ Å, $\mu = 0.72$ cm⁻¹, $R = 0.05$ for 1801 unique reflections with $I \geq 3\sigma(I)$. The intensities were measured using a Philips PW1100 diffractometer. The structure was solved by direct methods⁷ and Fourier synthesis, and was refined using anisotropic thermal parameters for all atoms other than hydrogen. All the hydrogen atoms were located from difference Fourier syntheses; for refinement the atoms H(1), H(8), and H(N1) were set in 'riding' positions on the carbon or nitrogen atom and the others were placed in calculated positions with C-H = 1.08 Å.†

† The atomic co-ordinates for this work are available on request from the Director of the Cambridge Crystallographic Data Centre, University Chemical Laboratory, Lensfield Road, Cambridge CB2 1EW. Any request should be accompanied by the full literature citation for this communication.

The title compound has the structure (3) for the $[(\text{taab})\text{H}_2]^{2+}$ ion, which has a diad axis of symmetry (Figure 1). The bond lengths and angles are consistent with the valence-bond isomer (3) with bond lengths for C(1)-N(2) and N(2)-C(8) (Figure 2) close to the values expected for single and double bonds respectively. Single hydrogen atoms were observed on C(1), C(8), and N(1), and bond angles show N(2) to be trigonal planar and C(1) to be approximately tetrahedral.‡ The central eight-membered ring has a 'boat conformation', and the molecule has a 'saddle-shaped' structure. The rings A and B are not coplanar, since there is a fold (22°) along the line C(8) ... N(1). The bond angles and distances in the picrate ion are closely similar to those in other structures,^{9,10} and show a similar pattern.§ The picrate anion is bonded to the

‡ The related BF_4^- salt,⁸ for which the e.s.d.s were approximately twice those for the picrate, shows a planarity around atoms C(1) and N(1) which would be consistent with a formulation as the tautomer (7). However, since the quality of the measurements precluded satisfactory location of the hydrogen atoms, and since the molecular configuration of the $[(\text{taab})\text{H}_2]^{2+}$ ion is very similar to that in the picrate salt, no firm conclusion is possible.

§ The carbon atom C(p6) bound to the phenolic oxygen has a short C-O bond (1.243 Å), much shorter than in picric acid, and two long C-C bonds (1.461, 1.464 Å); and the C(p5)-C(p6)-C(p1) angle is small (111°).

Cyclic hydro picric acid Crystal Structure

U.K.

er of structure (3), rather hydrogen bond

ed⁸ structure (5), and as have the structure (6). The ly spectroscopic except for complexes (2) and an incom- $[(\text{taab})\text{H}_2][\text{CF}_3\text{SO}_3]_2$. The presence of water, and the which they are reasonably

[(taab)H₂]²⁺ ion (Figure 1) by a relatively strong hydrogen bond O(7)...H(N1)-N(1), with O...N, 2.89; O...H, 2.04 Å; and O...H-N, 154°. There is also a close interionic contact O(1)...H(8')-C(8') with O...C, 3.12; O...H, 2.18 Å; and O...H-C, 169°, which could also be regarded as a hydrogen bond. It is considerably shorter than the C-H...O distances of 3.21–3.39 Å, with O...H-C angles of 162–144°, attributed¹¹ to hydrogen bonding; and¹ is a little shorter than the C-H...O distance of 3.16 Å between the picrate ion and picric acid found, but not specifically remarked upon, by Jensen.¹⁰ It is possible that these hydrogen bonds contribute significantly to the relative stability of the picrate salt and facilitate its isolation as a single tautomer (3), rather than a mixture of (3) and (7) which may account for disorder in an earlier attempt⁶ at structure determination. Ease of inter-conversion⁶ and relatively small differences in thermodynamic stabilities between (3), (4), and (7) suggest that the role of metal ions in *in situ* preparations of the metal complexes (2) is to act as a 'thermodynamic template'.¹²

We thank the S.R.C. for diffraction equipment and computing facilities, and Drs J. D. Goddard and T. Norris⁶ for samples of the BF₄⁻ salt.

Received, 23rd September 1981; Com. 1125

References

- 1 F. Seidel, *Ber. Dtsch. Chem. Ges.*, 1926, **59**, 1894; F. Seidel and W. Dick, *ibid.*, 1927, **60**, 2018; E. Bamberger, *ibid.*, 1927, **60**, 314.
- 2 S. G. McGeachin, *Can. J. Chem.*, 1966, **44**, 2323.
- 3 S. W. Hawkinson and E. B. Fleischer, *Inorg. Chem.*, 1969, **8**, 2402.
- 4 J. S. Skuratowicz, I. L. Madden, and D. H. Busch, *Inorg. Chem.*, 1977, **16**, 1721.
- 5 J. D. Goddard and T. Norris, *Inorg. Nucl. Chem. Lett.*, 1978, **14**, 211.
- 6 A. Albert and H. Yamamoto, *J. Chem. Soc. B*, 1966, 956.
- 7 G. M. Sheldrick, University Chemical Laboratory, Cambridge 1976.
- 8 J. D. Goddard, T. Norris, P. G. Owston, L. S. Shaw, and P. A. Tasker, unpublished work.
- 9 K. Maarimann-Moe, *Acta Crystallogr., Sect. B*, 1969, **25**, 452; B. Jensen, *Acta Chem. Scand., Ser. B*, 1975, **29**, 115; J. Bernstein, H. Regev, and F. H. Herbstein, *Acta Crystallogr., Sect. B*, 1980, **36**, 1170.
- 10 B. Jensen, *Acta Chem. Scand., Ser. B*, 1975, **29**, 891.
- 11 J. C. Calabrese, A. T. McPhail, and G. A. Sim, *J. Chem. Soc. B*, 1970, 282, 285; M. M. Mahmoud and S. C. Wallwork, *Acta Crystallogr., Sect. B*, 1979, **35**, 2370; D. Schomburg, *J. Am. Chem. Soc.*, 1980, **102**, 1055.
- 12 M. D. Rimken, R. I. Sheldon, W. G. Rohly, and K. B. Mertes, *J. Am. Chem. Soc.*, 1980, **102**, 4716 and references therein.

Attention is drawn to the fact that the copyright of this thesis rests with its author.

This copy of the thesis has been supplied on condition that anyone who consults it is understood to recognise that its copyright rests with its author and that no quotation from the thesis and no information derived from it may be published without the author's prior written consent.

I

D43422'82

END